REPORT UAG-83 PART II

WORLD DATA CENTER A
for
Solar-Terrestrial Physics

SOLAR-GEOPHYSICAL ACTIVITY REPORTS
for
September 7-24, 1977 and November 22, 1977

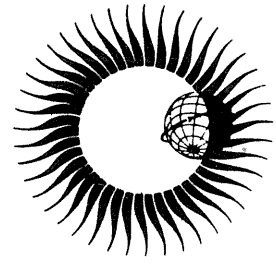

February 1982

WORLD DATA CENTER A
National Academy of Sciences
2101 Constitution Avenue, NW
Washington, D.C. 20418 USA

World Data Center A consists of the Coordination Office and the following seven Subcenters:

COORDINATION OFFICE
World Data Center A
National Academy of Sciences
2101 Constitution Avenue, NW
Washington, D.C. 20418 USA
[Telephone: (202) 334-3359]

GLACIOLOGY (Snow and Ice)
World Data Center A: Glaciology (Snow and Ice)
Cooperative Inst. for Research in Environmental Sciences
University of Colorado
Boulder, Colorado 80309 USA
[Telephone: (303) 492-5171]

METEOROLOGY (and Nuclear Radiation)
World Data Center A: Meteorology
National Climatic Center
Federal Building
Asheville, North Carolina 28801 USA
[Telephone: (704) 258-2850, ext. 381]

OCEANOGRAPHY
World Data Center A: Oceanography
National Oceanic and Atmospheric Administration
2001 Wisconsin Avenue, NW
Page Bldg. 1, Rm. 414
Washington, D.C. 20235 USA
[Telephone: (202) 634-7249]

ROCKETS AND SATELLITES
World Data Center A: Rockets and Satellites
Goddard Space Flight Center
Code 601
Greenbelt, Maryland 20771 USA
[Telephone: (301) 344-6695]

ROTATION OF THE EARTH
World Data Center A: Rotation of the Earth
U.S. Naval Observatory
Washington, D.C. 20390 USA
[Telephone (202) 254-4547]

SOLAR-TERRESTRIAL PHYSICS (Solar and Interplanetary Phenomena, Ionospheric Phenomena, Flare-Associated Events, Geomagnetic Variations, Aurora, Cosmic Rays, Airglow):

World Data Center A for Solar-Terrestrial Physics
Environmental Data and Information Service, NOAA, D63
325 Broadway
Boulder, Colorado 80303 USA
[Telephone: (303) 497-6323]

SOLID-EARTH GEOPHYSICS (Seismology, Tsunamis, Gravimetry, Earth Tides, Recent Movements of the Earth's Crust, Magnetic Measurements, Paleomagnetism and Archeomagnetism, Volcanology, Geothermics):

World Data Center A for Solid-Earth Geophysics
Environmental Data and Information Service, NOAA, D62
325 Broadway
Boulder, Colorado 80303 USA
[Telephone: (303) 497-6521]

World Data Centers conduct international exchange of geophysical observations in accordance with the principles set forth by the International Council of Scientific Unions. WDC-A is established in the United States under the auspices of the National Academy of Sciences. Communications regarding data interchange matters in general and World Data Center A as a whole should be addressed to World Data Center A, Coordination Office (see address above). Inquiries and communications concerning data in specific disciplines should be addressed to the appropriate subcenter listed above.

SUBSCRIPTION PRICE TO UAG REPORT SERIES: $40.00 a year; $23.00 additional for foreign mailing; single copy price varies. Checks and money orders should be made payable to the Department of Commerce, NOAA/NGSDC. Remittance and correspondence regarding subscriptions should be sent to the National Geophysical and Solar-Terrestrial Data Center, NOAA, D63, 325 Broadway, Boulder, Colorado 80303 USA.

WORLD DATA CENTER A
for
Solar-Terrestrial Physics

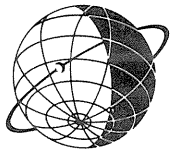

REPORT UAG-83 PART II

SOLAR-GEOPHYSICAL ACTIVITY REPORTS
for
September 7-24, 1977 and November 22, 1977

compiled by

John A. McKinnon and J. Virginia Lincoln
WDC-A for Solar-Terrestrial Physics
Boulder, Colorado 80303 USA

February 1982

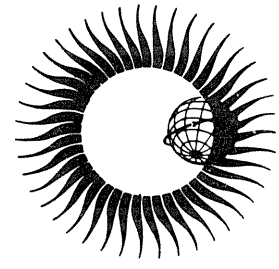

Published by World Data Center A for
Solar-Terrestrial Physics, NOAA, Boulder, Colorado
and printed by

U.S. DEPARTMENT OF COMMERCE
NATIONAL OCEANIC AND ATMOSPHERIC ADMINISTRATION
ENVIRONMENTAL DATA AND INFORMATION SERVICE
Boulder, Colorado, USA 80303

FORWORD

This exhaustive case study of an unusual period of solar-terrestrial activity (September and November 1977) is a truly cooperative international effort. It contains data reports from 116 individuals and groups throughout the world, giving details of the solar activity itself and its consequences in the interplanetary medium and the Earth's vicinity that far exceed those normally exchanged through the World Data Centers. The quantity of data contributed is amazing, yet it probably represents only a modest fraction of what exists. A by-product of this effort is its service as an index to (or perhaps more a reminder of) those groups that are active in monitoring and performing special experiments in the Solar-Terrestrial Physics (STP) disciplines.

The covered period excited the STP community for a number of reasons. It was the first period of outstanding STP activity since the 1976 solar cycle minimum. Of course, a solar minimum happens every 11 years and by itself is not exciting to any but the newest workers in the field, but this was a time of unusual activity for this (or any) stage of the solar cycle. There were two cosmic ray ground level events (GLEs) in September and one in November, with the November increase being the largest since 1960. The Sun was dominated by one active region, McMath 14943, which contained an old cycle spot group that Helen Dodson Prince had contemporaneously termed "ambiguous". The region was 2 days past the west limb when the second September GLE occurred, but the disk at that time was bland. There was therefore an opportunity to study in detail the major interplanetary and terrestrial effects of a solar activity situation that was not complicated, as it usually is, by several possible sources of enhanced solar radiation and particle emission. The phenomena seem to have been well observed and the November 22 events fortuitously came during a planned period of intensive observation, Interval Number 4 of the Study of Traveling Interplanetary Phenomena (STIP).

This was, in effect, a self-declared interval for special study; it was first suggested by Dodson Prince and then by the leaders of the STIP program of SCOSTEP. The plan for a special data compendium was endorsed by the MONSEE Steering Committee of SCOSTEP and a call for contributions was issued by the World Data Center A (WDC-A) for STP in January 1978. The response was literally overwhelming, to a degree that the editorial staff of WDC-A was swamped to the point of embarrassment. We take comfort in knowing that the phenomena were unique, at least thus far in our experiences with STP activity, and so the data reports should not become outdated.

This compilation has been a labor of love for John McKinnon and more recently for the retired long-time leader of WDC-A for STP, J. Virginia Lincoln. They have had much help from Helen Coffey and others in the technical editing of the data reports which were submitted in all variations of the English language. William Winkler, the chief editor for the Data Center, prepared the manuscript for publication, a not inconsiderable job. Others who have helped include Susan Godeaux and Carol Weathers. There has been welcome financial assistance from the U.S. Air Force Geophysical Laboratory. The delay in publication is regrettable, but some comfort can be taken that resources were indeed found in difficult times to complete the project and that the perseverance, especially of Miss Lincoln, prevailed. We think this project will have a lasting influence.

A.H. Shapley
Chair MONSEE Steering Committee
ICSU Scientific Committee on Solar-Terrestrial Physics

TABLE OF CONTENTS

Table of Contents (Continued)

Table of Contents (Continued)

Table of Contents (Continued)

Bremsstrahlung X-Ray Observations of Precipitating Electrons by Balloons Launched from Roberval, Canada (L≈4) on September 18 and 24, 1977

by

J.C. Siren, T.J. Rosenberg and D. Detrick
Institute for Physical Science and Technology
University of Maryland, College Park, MD 20742

X-ray detector-equipped balloons were launched from Roberval, Canada (48°31'N 72°16'W; MLT = UT-5h.) on September 18 and 24, 1977, bracketing the magnetic storm of September 20-21, 1977. As the scientific purpose of the balloon campaign was to investigate the wave-particle interactions that tend to occur during quieting intervals following magnetic activity [D.L. Carpenter, personal communication], no launches were made during the intense part of the storm. This report summarizes the X-ray data obtained from the two flights. Ground-based VLF, riometer and magnetometer data are mentioned as they pertain to the actual intervals of the flights. The X-ray instruments are identical to those described by Rosenberg et al. [1977], which should be consulted for more detailed information. A summary report of the available data has been submitted to World Data Center A, and is reproduced as Table 1. Sequential summaries of the more noteworthy observations are given in Table 2. Figure 1 shows time plots of the integral X-ray count rates (30-second averages) for the two flights.

TABLE 1. STATUS REPORT ON SPECIAL STP DATA

PROGRAM

F.4 Ballon Measurements

INSTRUMENTATION

X-Ray detector (scintillator crystal with pulse height analyzer)

PARAMETERS MEASURED

X-Ray: Count rates, 25 keV and 25-500 keV in seven differential channels

LOCATION OF MEASUREMENTS AND TIME OR TIME INTERVALS OF MEASUREMENTS

Roberval, Canada (48°31'N, 72°16'W)

2 Flights: 18 Sept. '77 0641-1539 UT X-ray
24 Sept. '77 0741-2020 UT X-ray

AMOUNT OF DATA AVAILABLE AND FORMAT

X-ray: 10 ms resolution, analog and digital tapes
Off-line digital tapes 1-s, 30-s averages
Plots of 30-s averaged data from complete flights

CONTACT THROUGH WHOM TO REQUEST DATA

Dr. T.J. Rosenberg
Institute for Physical Science and Technology
University of Maryland
College Park, MD 20742

TABLE 2. BALLOON FLIGHT LOGS

18 Sept. 1977

Time (UT)

0641	Launch
0830	Ceiling altitude-background count rate
0900	Whistlers triggering emissions. Magnetometer, riometer quiet.
1035	Whistlers at Siple.
1342	No transmissions received yet from Siple.
1353	Siple transmissions received at Roberval. (Continues with some fading until 1531.)
1539	Balloon cutdown. Balloon had drifted 257 km SW.

24 Sept. 1977

0738	Launch
0916	Count rate well above background.
0929	Ceiling altitude.
0940	Long-period count rate variations.
0950	5-10 sec period structure.
1043	Count rate decreasing. Riometer indicating absorption. Magnetometer indicating variations. VLF risers at Roberval and Siple.
1146-52	Small count rate increases.
1404-06	Count rate maximum.
1645-58	Small count rate increases.
1710-15	Count rate maxima. VLF quiet.
2020	Balloon cutdown. Baloon had drifted 385 km NE.

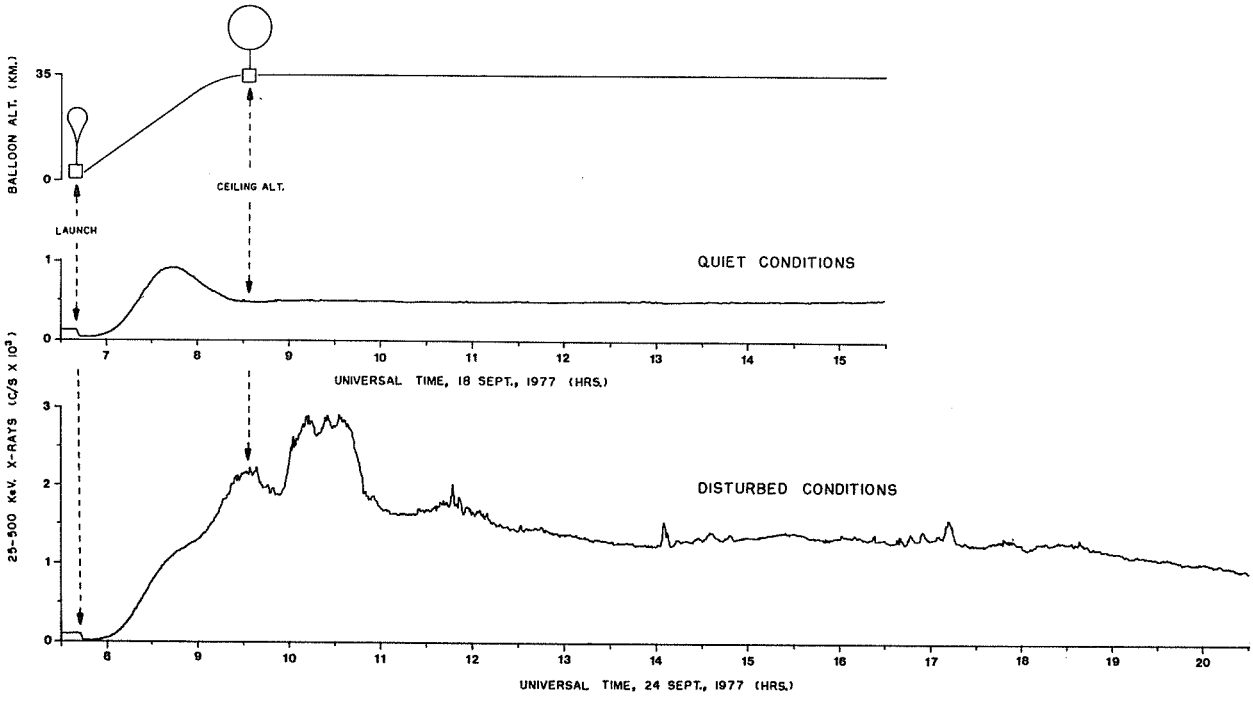

Fig. 1. Integral channel count rates.

In general the September 18 flight detected little other than steady cosmic ray background count rates in all differential channels and the integral channel. Limited, short-period positive excursions were observed briefly. No magnetometer or riometer activity occurred. However, VLF transmissions from Siple station at the conjugate point, and artificially stimulated emissions, were received at Roberval for about 2 hours beginning at 1353 UT. During this time the balloon was southwest of Roberval, in the sector from which Siple signals most often arrive [Leavitt et al., 1978]. However, there was no evident indication of any association of precipitation with the VLF emissions, possible indicating the wave-particle resonance involved electrons of energy less than the 25 keV instrumental threshold.

By contrast, the September 24 flight ascended into an event already in progress, as can be seen by comparison of the two flights' ascent curves. Count rates several times the background rate occurred in the differential channels, as well as the integral channel, prior to $\approx$ 1100 UT. Briefer count rate increases occurred at $\sim$ 2-3 h intervals subsequently. Riometers and magnetometer variations accompanied the initial count rate maximum. Much natural VLF activity (chorus and risers) was recorded at both Roberval and Siple but VLF transmissions from Siple were not received at Roberval.

REFERENCES

LEAVITT, M.K., D.L. CARPENTER, N.T. SEELY, R.R. PADDEN and J.H. DOOLITTLE — 1978 — Initial Results from a Tracking Receiver Direction Finder for Whistler Mode Signals, J. Geophys. Res. 83, 1601.

ROSENBERG, T.J., J.C. FOSTER, D.L. MATTHEWS, W.R. SHELDON and J.R. BENBROOK — 1977 — Microburst Electron Precipitation at L $\approx$ 4, J. Geophys. Res. 82, 177.

Ionospheric Effects of Proton Flares in September 1977 at Arkhangelsk and Gorky

by

V. V. Belikovich, E. A. Benediktov, L. V. Grishkevich,
E. F. Kozlov and N. I. Samorokin
Institute of Terrestrial Magnetism, the Ionosphere,
and Radio Wave Propagation
Academy of Sciences of the USSR
Gorky Scientific Research Radiophysical Institute

According to data published in *Solar-Geophysical Data* [1977a], on the 19th of September 1977 at 1028 UT a proton flare occurred causing different geophysical phenomena. This paper presents some riometer absorption observations both during the flare (SCNA) and some time after it (PCA and anomalous absorption). The riometer absorption was measured in two places simultaneously: at Arkhangelsk (N64.6 E40.5) and at Gorky (N56.1 E44.3). At Arkhangelsk the cosmic radiation level was recorded at 9, 13 and 25 MHz and at Gorky at 13 and 25 MHz.

The SCNA effect is clearly seen on all riometer records, and its development is shown in Figure 1. Curves 1-5 characterize anomalous absorption values during the flare and correspond to 9, 13 and 25 MHz measured at Arkhangelsk; and to 13 and 25 MHz measured at Gorky. Parts of the riometer records are shown as dotted lines. Since these measurements were greatly influenced by radio interference, they show only a tendency for anomalous absorption effects. In the same figure variations in the H component of the geomagnetic field relative to a diurnal variation determined by 5 magnetically quiet days (Arkhangelsk data) are given too. Figure 1 seems to present a typical magnetic crochet or solar flare effect. The maximum value of the anomalous absorption at 13 and 25 MHz at Arkhangelsk appears to be some 10% greater than that at Gorky for the same frequencies. The zenith angle (χ) of the Sun, however, was 65.5° at Arkhangelsk and 59.5° at Gorky. Such a relationship between the two zenith angles and the anomalous absorption values during SCNA events was noted before by Belikovich et al. [1977], and it seems to indicate a peculiar variation of ionospheric D-region parameters with latitude. In particular, the electron loss coefficient (Ψ) in the lower ionosphere may be considered a little less in the auroral zone than at mid-latitudes.

The duration of the SCNA effect at Gorky did not exceed an hour and a half, declining to a near-zero absorption level by 1200 UT. At Arkhangelsk the anomalous absorption declined as well after the flare until approximately 1245 UT. Then, it again began to increase. An increase in absorption following a flare is characteristic of the PCA phenomenon [Belikovich et al., 1969].

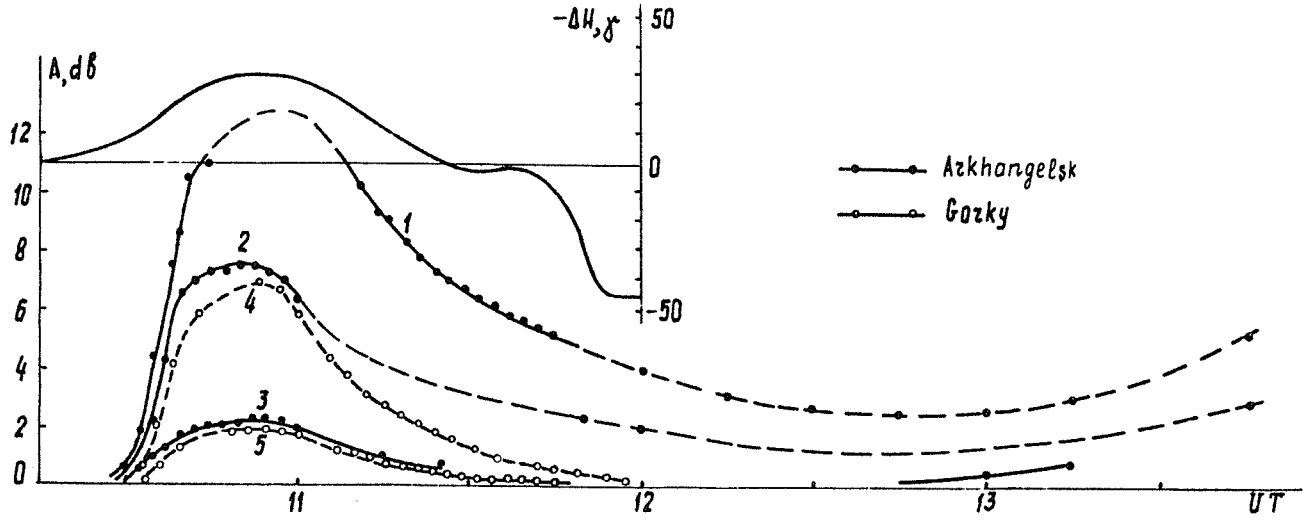

Fig. 1. Development of SCNA and magnetic crochet during the 3b flare of September 19, 1977 as observed at Arkhangelsk and Gorky, USSR. Curves 1, 2, and 3 represent absorption of 9, 13 and 25 MHz, respectively, measured at Arkhangelsk; curves 4 and 5 represent absorption at 13 and 25 MHz, respectively, measured at Gorky. The top unnumbered curve shows the variations in the Arkhangelsk H component of the geomagnetic field computed as the difference between the measured value and a diurnal curve determined from 5 magnetically quiet days.

Further absorption variations at 13 MHz together with H-intensity variations from September 19 to 27 are shown in Figure 2 (Arkhangelsk data). Each vertical line in Figure 2a indicates the difference between the maximum and minimum values of the anomalous absorption for a particular hour of observations. The length of each horizontal line along the x-axis corresponds to daylight hours. Hourly averaged values of the H-intensity in Figure 2b are connected by a broken line. The periodic dashed curve indicates a quiet H-intensity variation determined from 5 magnetically quiet days.

In the average the absorption was maximum on September 19 and 20 when PCA, anomalous absorption events, and a moderately severe geomagnetic storm occurred. For individual parts of the riometer records an index of absorption frequency dependence was calculated; its value appeared to be close to unity. This may be considered as an indirect confirmation that protons are of great importance in atmospheric ionization. After September 20 the average anomalous absorption decreased greatly, and in the evening of September 21, it was about 1 dB. On the same day at approximately 2000 UT, a new magnetic storm began during which the H-intensity varied up to 1000 nT. This storm was also accompanied by an increase auroral absorption on September 22 and 23.

It should be noted that between September 24 and 27 a rather considerable absorption was recorded, the maximum value of which at about local noon was 1-2 dB. During this period the magnetic field was quiet, with the exception of a short-term disturbance on the night of September 27. A clear dependence of the absorption value on the time of day (solar control) suggests that the riometers recorded a PCA phenomenon on these days. Another interpretation, however, of such diurnal variations in the anomalous absorption assumes that the electron loss coefficient (Ψ) in the lower ionosphere fell to 1/2 to 1/3 of its quiet-day value because the cluster ion concentration decreased.

As a final comment, observations published in *Solar-Geophysical Data* [1977b] described a weak proton flux enhancement detected by the NOAA satellite SMS-2 on November 22, 1977 during quiet geomagnetic field conditions. Arkhangelsk records contained no evidence of this event.

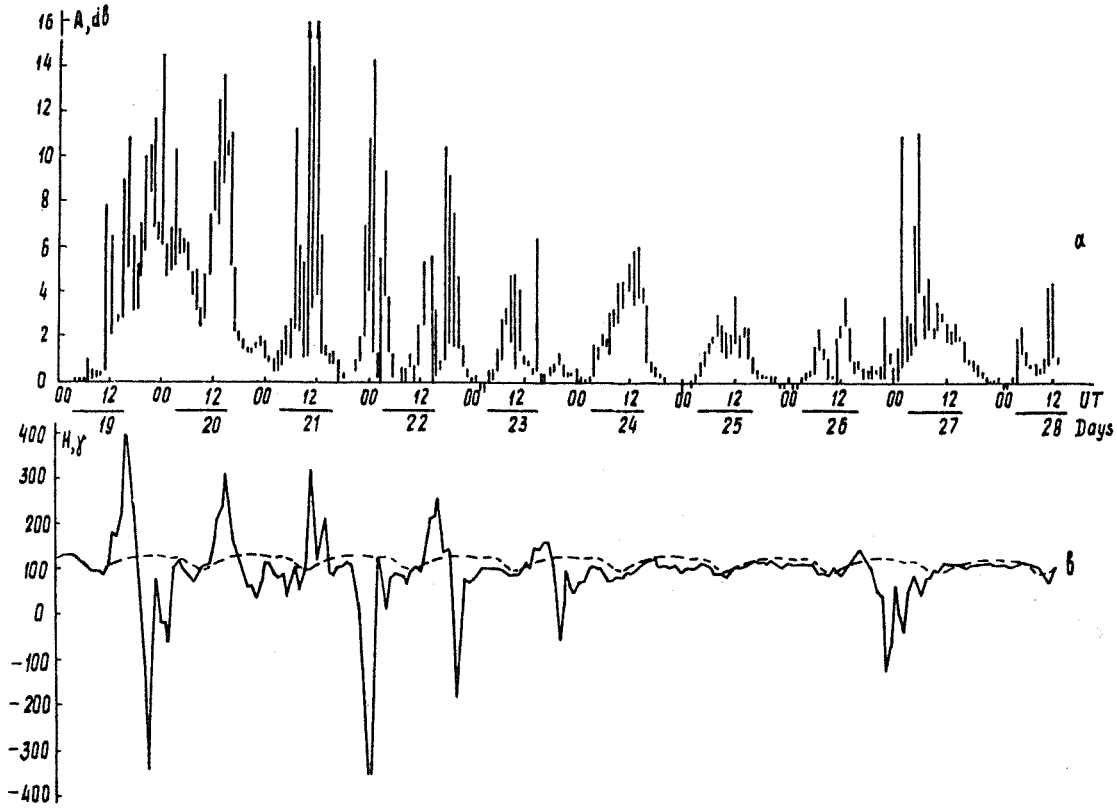

Fig. 2. (a) Daily 13 MHz absorption variation at Arkhangelsk for the September 19-28, 1977 period. Each vertical line indicates the difference between the maximum and minimum values of the anomalous absorption for a particular hour of observation. The length of each horizontal line along the x-axis corresponds to daylight hours. (b) Variations in the H-intensity at Arkhangelsk on September 19, 1977. The periodic dashed line connects hourly averaged values and indicates the quiet H-intensity variation determined from 5 magnetically quiet days.

REFERENCES

BELIKOVICH, V. V., BENEDIKTOV, E. A., and RAPOPORT, Z. Ts. 1969 PCA in July, August, and September 1966 according to Observations in the Auroral Zone, *Geomagnetizm i Aeronomiya, 9*, 666-673. (In Russian)

BELIKOVICH, V. V., BENEDIKTOV, E. A., and ITKINA, M. A. 1977 The Electron Loss Function in the D Region of the Ionosphere and Dependence of the Radio Wave Anomalous Absorption on the Zenith Angle of the Sun during Geomagnetic Disturbances, *Geomagnetizm i Aeronomiya, 17*, 427-432. (In Russian)

SGD 1977a *Solar-Geophysical Data*, 398 Part I, 11, October 1977, U. S. Department of Commerce (Boulder, Colorado, U.S.A. 80303).

SGD 1977b *Solar-Geophysical Data*, 400 Part I, 26, December 1977, U. S. Department of Commerce (Boulder, Colorado, U.S.A. 80303).

The Phenomena in the Ionosphere Associated with the Proton Flares on September 7-24 and November 22, 1977 According to the Data of the Sverdlovsk Station

by

V.F. Zakharchenko, A.S. Lakin, M.V. Levin, and T.V. Nikulnikova
Institute of Geophysics, the Urals Science Center
USSR Academy of Sciences, 91, Pervomaiskaya Str.
Sverdlovsk, USSR

The results obtained at the Sverdlovsk (Arty) ionospheric station (ϕ=56°26'N, λ=58°34'E) are presented for a detailed analysis of the geophysical events associated with the proton flares of September 7-24 and November 22, 1977.

Figure 1 shows the values of the lowest frequency at which echo traces were observed on the ionogram (f min) during September 1977. On September 19 at 1445 LT a sudden enhancement of f min (up to 5.9 MHz) was observed. It should be noted that the high values of f min continue for about half an hour followed by a slow return to the initial level. The duration of this disturbance is approximately 2 hours. It is in the usual form of sudden ionospheric disturbance caused by solar flares. A short-time absorption in the vicinity of a critical frequency of the F2 layer was observed on September 19 at 1445 LT.

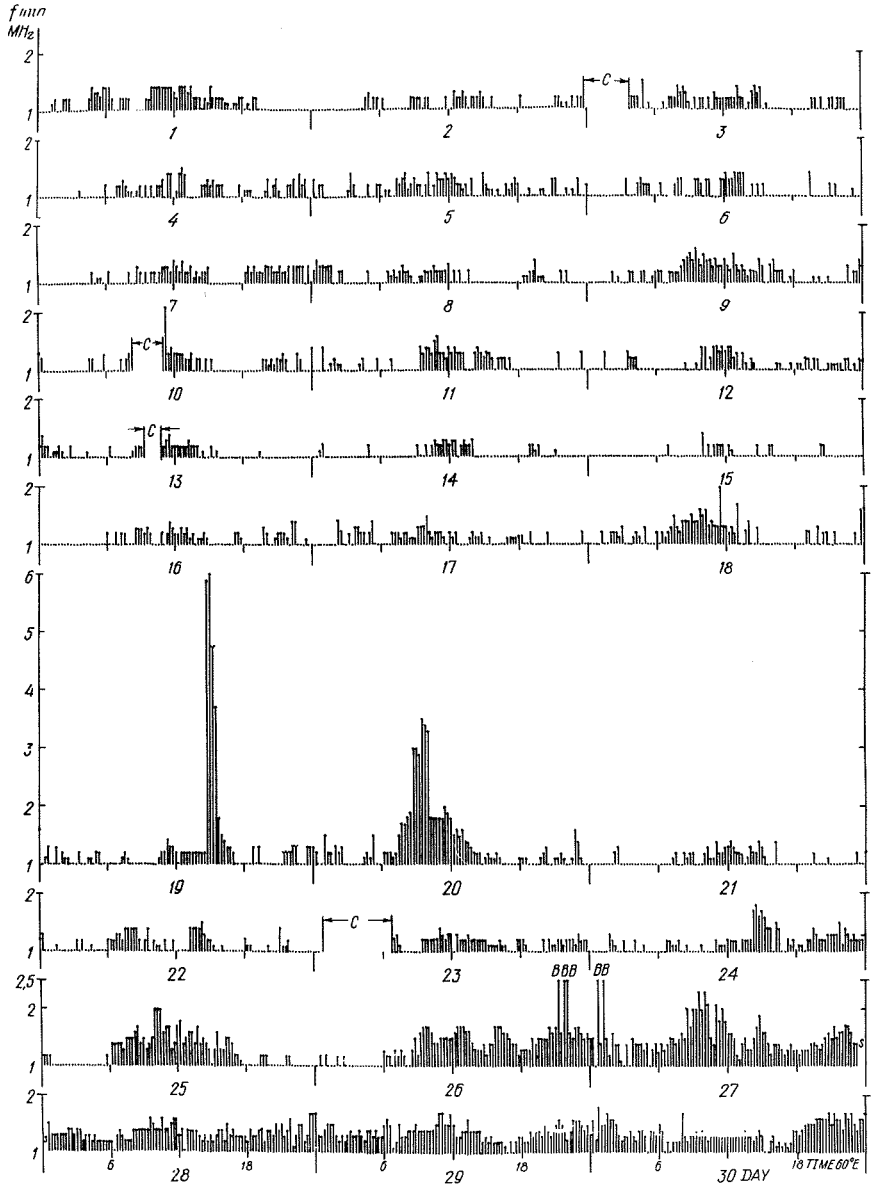

Fig. 1. fmin September 28-30, 1977 at Sverdlovsk (Arty)

An ionospheric disturbance with a gradual enhancement of f min took place on September 20 and lasted from 0730 to 1320 LT. The maximum value of f min (equal to 3.5 MHz) was registered at 0930 LT.

Abnormally high values of f min were also observed during the period of September 25-27, the short-lived black-out conditions taking place at frequencies up to 10 MHz on September 26 at 2115, 2145, 2200 LT and on September 27 at 0045, 0115 LT.

Figure 2 is the f plot during November 22, 1977. The solid line represents the median values of foF2 during the 10 universal magnetically quiet days in November. The results of vertical incidence sounding show the absorption present in the vicinity of the lower frequencies at 1100 and 1415 LT. The behavior of the critical frequency of the F2 layer is unusual. There is a small absorption near foF2 from 0715 to 1000 LT. At 1115 LT a sharp decrease of foF2 is observed. For 45 minutes foF2 decreased by 2.2 MHz. A drop of foF2 associated with solar flares was noted earlier [1971].

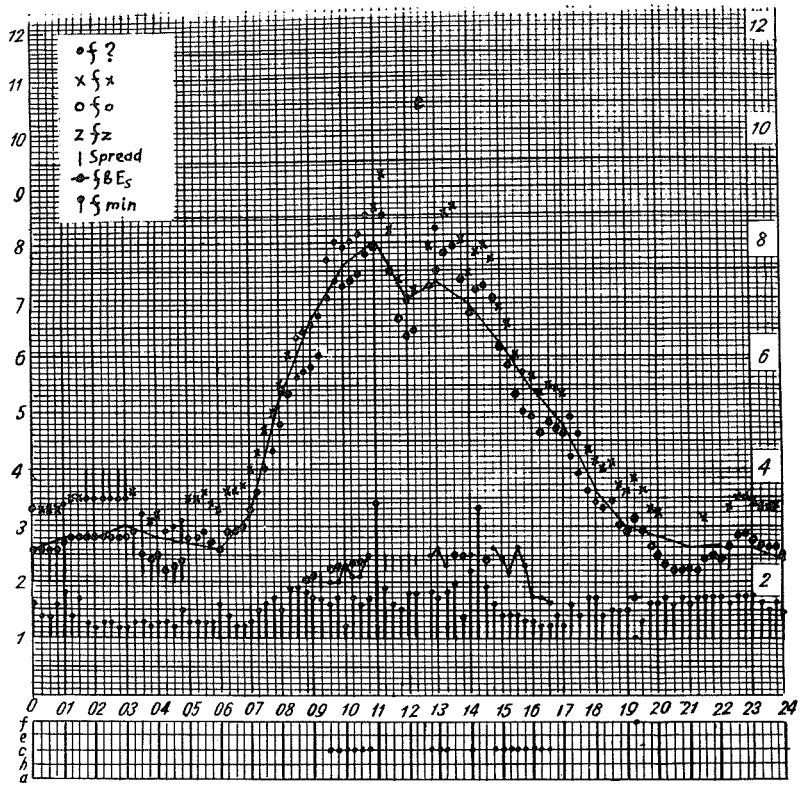

Fig. 2. f plot November 22, 1977 at Sverdlovsk (Arty)

References

THOME, G.D. and L.S. WAGNER 1971 Electron density enhancements in the E and F regions of the ionosphere during solar foares, J. Geophys. Res., 76, 6883-6895.

Polar Cap Absorption Events in September and November of 1977 by Riometer Data at the Soviet Arctic and Antarctic Stations

by

V.M. Driatsky, V.A. Ulyev and A.V. Shirochkov
The Antarctic and Arctic Research Institute
Leningrad, USSR

Introduction

In the present study we analyze PCA events which occurred in September and November 1977: Sept 9 - 11; Sept 16 - 19; Sept 19 - 22; Sept 24 - 28; and Nov 22 - 28. The analysis has been made according to the scheme used in our previous studies [see UAG-28]. The morphological features such as the general character of PCA variations, the noise storm, the day-night variation, the midday recovery, the sudden commencement absorption, the PCA latitudinal structure and the asymmetry absorption effect are examined in each PCA event.

The PCA mentioned above are designated as follows: PCA (1), PCA (2), PCA (3), PCA (4) and PCA (5). The absorption variations recorded during these PCA events are given in Figures 1-5. Dark lines under the time axis indicate periods when the Sun's zenith angle for the corresponding site exceeded 90°, vertical arrows on the time axis indicate time of local geographical noon. Solar flare characteristics are given in the upper part of each figure. The stations used in this study are at following corrected geomagnetic latitudes: ϕ = 82°N (NP-22), ϕ = 73.8°N (Heiss Island), ϕ = 70.3°N (Cape Zhelaniya), ϕ = 67.2°N (Dixon Island), ϕ = 63.9°N (Amderma), ϕ = 66.2°S (Novolasarevskaya), ϕ = 67.6°S (Molodezhnaya), ϕ = 76.8°S (Mirny), and ϕ = 84.3°S (Vostok).

The statement "station in the center of the polar cap" is used for the stations with ϕ>70° (NP - 22, Heiss Island, Mirny, Vostok), while the statement "stations in the auroral zone" is used for the stations with ϕ<70° (Cape Zhelaniya, Dixon Island, Amderma, Novolazarevskaya, Molodezhnaya).

The General Character of the PCA Events

The general character of the PCA event means the description of the main characteristics of the analyzed PCA (the time of commencement, maximum and end) by data of one of the stations in the center of the polar cap.

If the ionosphere vertically above the station was constantly in daylight during the PCA we estimated characteristics of the daytime PCA, if constantly in darkness, nighttime PCA. This situation was especially observed during the November PCA.

If there were changes in sunlit conditions (as in the September event), then we describe the characteristics of the daytime PCA event only.

PCA (1)

The time of onset and of the increasing phase of the PCA is difficult to describe because at this time the ionosphere over the stations was in darkness. The very smoothed maximum occurs on September 10 in the first part of the day. The decreasing phase is slow. This PCA ended on September 11. On the whole, such variations are typical of the PCA attributed to flares on the eastern side of the solar disk.

PCA (2)

The general characteristics of this PCA are as follows: Slow increase, smoothed maximum and slow decrease. This character for the PCA can be observed after flares occurring near the Sun's central meridian.

PCA (3)

This PCA has a rapid onset, a wide maximum with some peaks and a rather rapid decrease. This type of variation can be interpreted in this way: The absorption during this PCA is attributed to two fluxes of solar cosmic rays (SCR). One of them is the diffusive flux and the second is the trapped flux. The two intense flares that occurred on September 16 and 17 and the intensive flare on Sept 19 are attributed to the distortion of the interplanetary magnetic field (IMF) resulting in magnetic traps for SCR fluxes.

PCA (5)

The general features of the daytime variation (at the Vostok station) are as follows: A rapid onset, sharp maximum and gradual decrease. Such features are typical for the PCA events attributed to flares occurring on the western part of the solar disk and they reflect the diffusive mode of the SCR propagation in IMF. Two pecularities are the result of SCR generation and injection into space. The nighttime variation of this PCA (NP-22 variation), is essentially different from that of the daytime increase. It is more gradual, maximum magnitude is less and the whole duration is shorter than the corresponding characteristics of the daytime PCA. The maximum of the nighttime variation occurred 7 h later than the daytime one.

PCA (4)

Before this PCA no strong flares were on the visible side of the solar disk. This PCA could be associated with a flare behind the western limb of the Sun. The main features of this PCA are typical of PCA events, attributed to such flares: Rapid increase, sharp maximum and gradual decrease.

Noise Storm (SCNA)

A noise storm is registered on the riometer records as sharp short-time variations of the cosmic noise. Radio waves generated during the flare cause the noise storm--that is why we can register a noise storm only: 1) if the solar disk screens the radiowave propagation to the Earth, i.e., the flare occurs on the visible solar disk, 2) when the ionosphere vertically overhead is not screened by the Earth i.e., when the ionosphere vertically overhead is in sunlight.

PCA (1), PCA (2), PCA (4)

During these PCA events a noise storm was not registered because: (1) during PCA (1) and PCA (2) the ionosphere vertically overhead was not in sunlight and (2) the flare, attributed to PCA (4), occurred on the invisible solar disk.

PCA (3)

The noise storm was registered at all stations at the time near onset of the corresponding flare.

PCA (5)

The noise storm was registered only in the riometer records of the Southern Hemisphere stations. The noise storm occurs 10 min later than the PCA (5)-parent flare.

Day-night Variation

This effect becomes apparent at the stations where the ionosphere sunlit conditions vary from night (zenith angle is more than 90°) to day (zenith angle less than 90°). Under such conditions the absorption varies from small values at night to large values during the day. The difference is about 3 to 8 times. To estimate this effect "K" is used. K is the ratio of the daytime absorption to nighttime absorption [Driatsky, 1974].

PCA (1), PCA (2), PCA (3), PCA (4)

As shown in Figures 1, 2, 3 and 4, the day-night variation was present during all these PCA events in the absorption variations of all stations. We have calculated K because of the small absorption values during these PCA events during both night and day.

PCA (5)

During this PCA the day-night variation is registered only at the Southern Hemisphere stations: Mirny and Molodezhnaya. We did not calculate K for this PCA because during the night in the ionosphere over Mirny and Molodezhnaya there was total darkness (zenith angle was not more than 95°).

Sudden Commencement Absorption (SCA)

This effect is the increase over short-time period (some min or some h). This increase follows an SSC impulse registered in the geomagnetic data.

PCA (1), PCA (2), PCA (4)

During these PCA events an SSC impulse was not registered in the geomagnetic data. Thus it is obvious why the sudden commencement absorption effect was not registered in the riometer data.

PCA (3)

During this PCA the SSC impulse was not registered in the geomagnetic data. In the absorption variations there was no essential change in absorption which might be related to the impulse SSC. In the Southern Hemisphere after the SSC impulse, an absorption increase is observed which can be considered as an SCA effect. At the stations of the auroral zone the peak of this increase was registered 12 h after the SSC impulse and at the stations in the polar cap center - 4 h later.

PCA (5)

During this PCA the SSC impulse is registered in the geomagnetic data but a well pronounced change in the absorption characteristics is not evident in any of the examined variations.

Midday Recovery Effect

This effect is the absorption decrease lasting during several hours and its minimum falls on the local midday (before midday--at the stations of the Northern Hemisphere and after midday--at the stations of the Southern Hemisphere). As a rule the midday recovery is registered in those PCA events that are associated with the flares on the eastern part of the solar disk (sometimes those near the central meridian) or in those PCA events which are attributed to the trapped SCR [Ulyev, 1978].

PCA (1)

There are comparatively large values of auroral absorption at the stations in the auroral zone, so that we cannot decide if there is or if there is not a recovery effect during this PCA.

PCA (2)

In our opinion the absorption decrease on September 17 near local midday at Cape Zhelaniya, Amderma, Novolazarevskaya, Molodezhnaya and Mirny, is the result of the midday recovery effect. This decrease is first registered at the stations in the auroral zone.

Second, the decrease minimum as registered in the different hemispheres shows asymmetry of the high-latitude border. The causes of this asymmetry are not known.

PCA (3)

On September 20 at Dixon Island and Amderma at about 08 UT (local midday), a greater absorption decrease occurred which we interpret as the midday recovery.

From the point of view of the flare location (on the western part of the solar disk), the midday recovery appearance during this PCA is rather unusual because after such flares the midday recovery effect as a rule is not registered in the PCA event. It appears that the midday recovery is attributed to the trapped particles that cause the essential part of the absorption on Sept 20. Another peculiarity of the midday recovery in this PCA event, as seen in Fig. 3, is that the midday recovery effect was not registered at any station in the southern polar cap. Perhaps again there is asymmetry in midday recovery appearance. But if during PCA (2) the asymmetry was connected with the sites situated in the center of the polar cap, during this PCA the asymmetry is related to the auroral zone station. The cause of the latest asymmetry should be carefully studied.

PCA (4)

During this PCA the midday recovery was not registered. This is consistent with the facts that after flares on the western side of the solar disk or behind it, midday recovery effect is not usually observed.

PCA (5)

Let us analyze the absorption variation in the Northern and Southern Hemispheres separately. There is no possibility to observe a midday recovery event in the Northern Hemisphere because of the small absorption values.

In the Southern Hemisphere at Molodezhnaya on November 23 near local noon a decrease of absorption is observed. That decrease looks like a midday recovery, however we do not consider this decrease to be connected with a midday recovery.

First of all, its duration is about 12 h; that is, 2-3 times longer than that of the usual midday recovery.

Second, this decrease is registered only at one station.

Third, the flare that is attributed to this PCA occurred on the western side of the solar disk and in such cases a midday recovery is not usually observed.

The PCA Latitudinal Structure

To determine the PCA latitudinal structure means to compare absorption values registered at the same moment in one and the same polar cap but at different geomagnetic latitudes.

To show by this comparison the dependence of absorption at such moments, we estimated (1) when auroral absorption was insignificant, (2) when the ionosphere above the stations being compared was in daylight.

PCA (1)

The comparatively large values of the auroral absorption do not allow us to find suitable moments for the analysis of the latitudinal structure of this PCA.

PCA (2)

For comparison of the absorption in the north cap we have chosen 04 UT of September 17. The absorption data at that moment are the following: A (Heiss Island) = 1.5 dB; A (Cape Zhelaniya) = 2.0 dB; A (Dixon Island) = 1.7 dB and A (Amderma) = 1.2 dB. Comparing these values we come to the conclusion that the latitudinal structure of the northern cap has the following character: maximum absorption is observed at the latitude ϕ = 70.3°N (Cape Zhelaniya) but at lower latitudes (in auroral zone) and at higher latitudes (in the center of the polar cap) the absorption is smaller.

In fact that in the auroral zone the absorption becomes smaller with the decrease of the latitude was confirmed several times.

In the center of the polar cap (ϕ>70°) the absorption decreases with the often observed fact that in the center of the polar cap absorption is independent of latitude. This does not agree with the often observed fact that in the center of the polar cap absorption is independent of the latitude.

PCA (3)

We have no opportunity to calculate the structure of this PCA, because there was great auroral absorption at the stations during this PCA.

PCA (4)

Let us compare the absorption at the stations in the Northern Hemisphere at 04 UT September 25. At that time the following magnitudes of absorption were registered: A (Heiss Island) = 1.3 dB; A (Cape Zhelaniya = 1.5 dB and A (Amderma) = 1.3 dB. It can be seen that the development in the latitudinal structure is the same as during PCA (2). At the stations of the Southern Hemisphere in the center of the polar cap (Mirny and Vostok) the absorption at the chosen time (02 UT September 25) was nearly equal (A = 1.5 dB); i.e., there was the plateau structure usually found at very high latitudes (ϕ>70°).

PCA (5)

Let us compare the absorption at the stations of the Southern Hemisphere (Vostok, Mirny and Molodezhnaya).

For the comparison we have chosen 02 UT September 25. The magnitudes of the absorption at all stations at the chosen moment are nearly equal (A = 3.0 dB). One can say that during this PCA event the plateau structure is observed at the stations in the center of the polar cap and reaches down to the latitude of Molodezhnaya station (ϕ = 67.6°S).

The ionosphere over the stations of the Northern Hemisphere was not illuminated and the magnitudes of the absorption were negligible.

PCA Asymmetry

PCA asymmetry is shown in such a way that the absorption is rather different at the stations situated at the conjugate geomagnetic latitudes in the center of the polar caps at the same moment. When the sign of the IMF is (+) then the absorption is more intense in the north polar cap and when the sign is (-) then the absorption is more intense in the southern cap [Shirochkov, 1979]. The most obvious times of the asymmetry effect are as follows: the first 10-12 h after the flare and the periods of absorption caused by trapped particles.

To reveal this effect we compare the absorption at the Heiss Island (northern cap) and Mirny (southern cap) stations. These stations are most suitable from the point of view of geomagnetic conjugacy and similarity of the sunlit conditions of the ionosphere over the stations.

PCA (1), PCA (2), PCA (3)

During these PCA events we did not discover a significant absorption difference at Heiss Island and Mirny that can be interpreted as the appearance of PCA asymmetry effect.

PCA (4)

To reveal the asymmetry effect in this PCA we have calculated ratio of the absorption at Heiss Island (A_x) to the absorption at Mirny station (A_m) for three times (September 24, 25 and 26 at 10 UT). The values of this ratio are the following: $A_x/A_m = 1.6$ (Sept 24); $A_x/A_m = 1.05$ (Sept 25) and $A_x/A_m = 1.1$ (Sept 26). The fact is that on September 24 the absorption on Heiss Island is 1.6 times higher than that at Mirny. We explain it as manifestation of the asymmetry effect. It can be proven by two arguments.

First, 10 UT Sept 24 is 2 h after the PCA onset; that is, this moment is within the period during which as a rule the effect of asymmetry is observed.

Second, the absorption is higher at Heiss Island (the north cap), i.e., at that polar cap where it should be higher because during this PCA the sign of the IMF was (+) [Mansurov, 1977].

PCA (5)

In this event the effect of the asymmetry cannot be observed, as the ionosphere over the north polar cap was in nighttime during the whole PCA, but over the south polar cap it was sunlit. This difference in illumination accounts for the absorption difference at the Heiss Island and Mirny.

REFERENCES

DRIATSKY, V.M. 1974 *Nature of Anomalous Absorption of Cosmic Radio Emission in Lower Ionosphere of High Latitudes*, L. Gidrometeoisdat (Leningrad, U.S.S.R.), 224 pp. (in Russian).

MANSOROV, S.M. 1977 *Monthly Data of Sector Polarity of Interplanetary Magnetic Field*, IZMIRAN, p. 4 (in Russian).

SCHIROCHKOV, A.V. 1977 North-South Asymmetry in Absorption Magnitude of PCA, *Geomagnetism and Aeronomia, 17*, 445-449 (in Russian).

ULYEV, V.A. 1977 Relation of Midday Recovery Effect Onset during PCA to Flare Longitude, *Trudy AANII, 350*, 84-88 (in Russian).

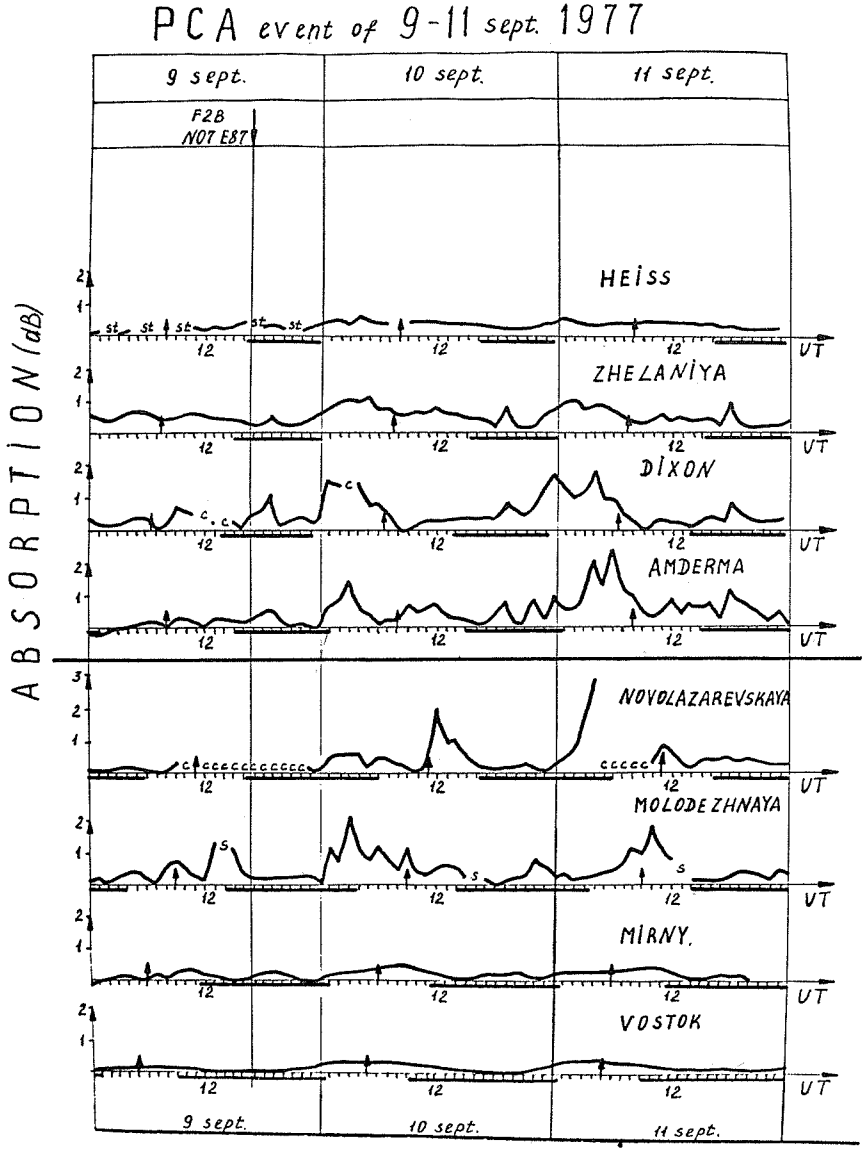

Fig. 1. PCA variations during September 9 - 11, 1977

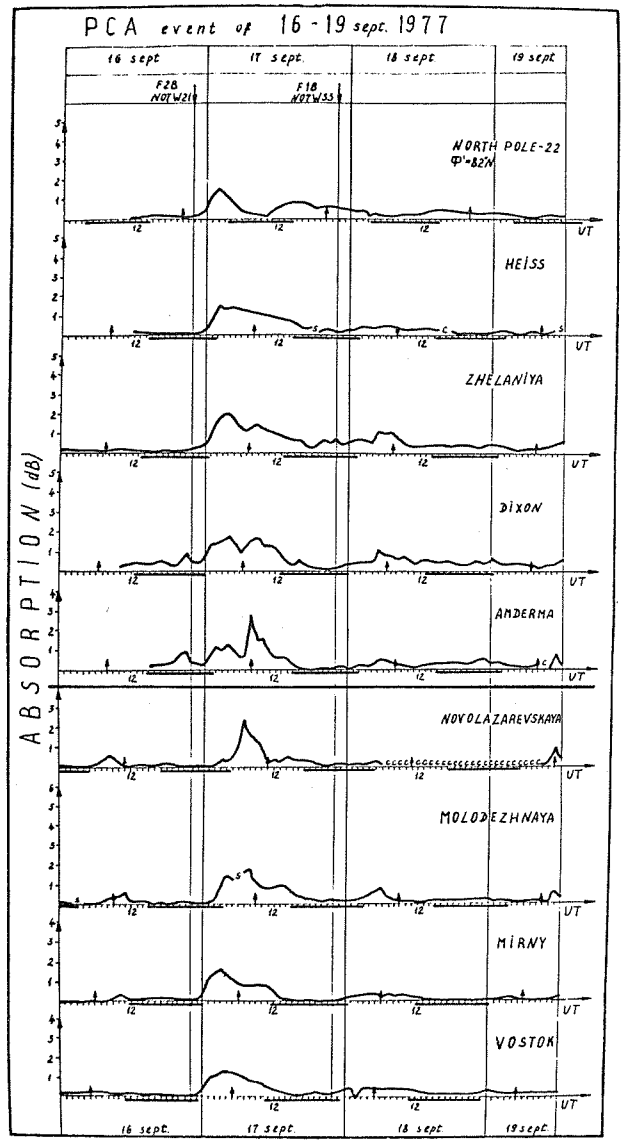

Fig. 2. PCA variations during September 16 - 19, 1977

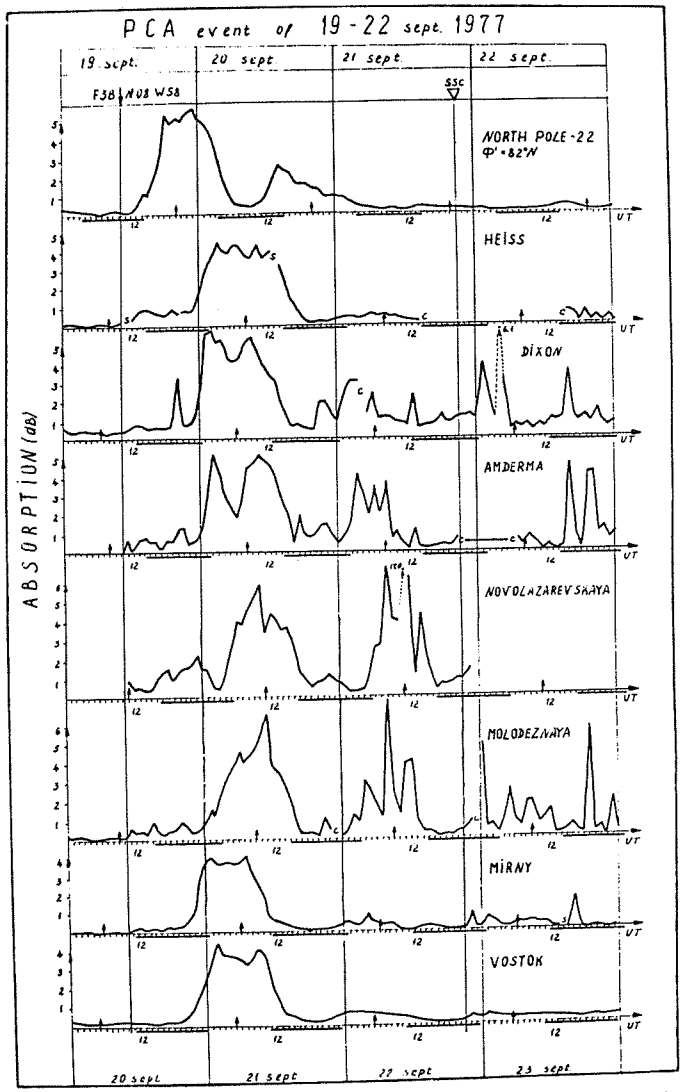

Fig. 3. PCA variations during September 19 - 22, 1977

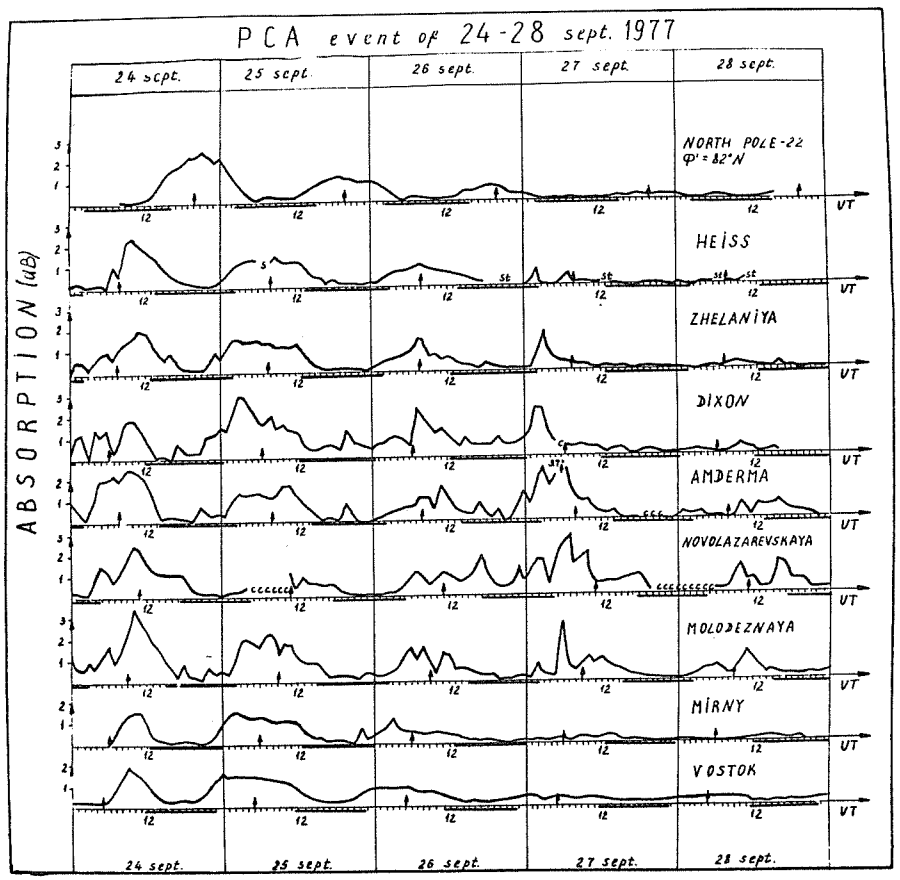

Fig. 4. PCA variations during September 24 - 28, 1977

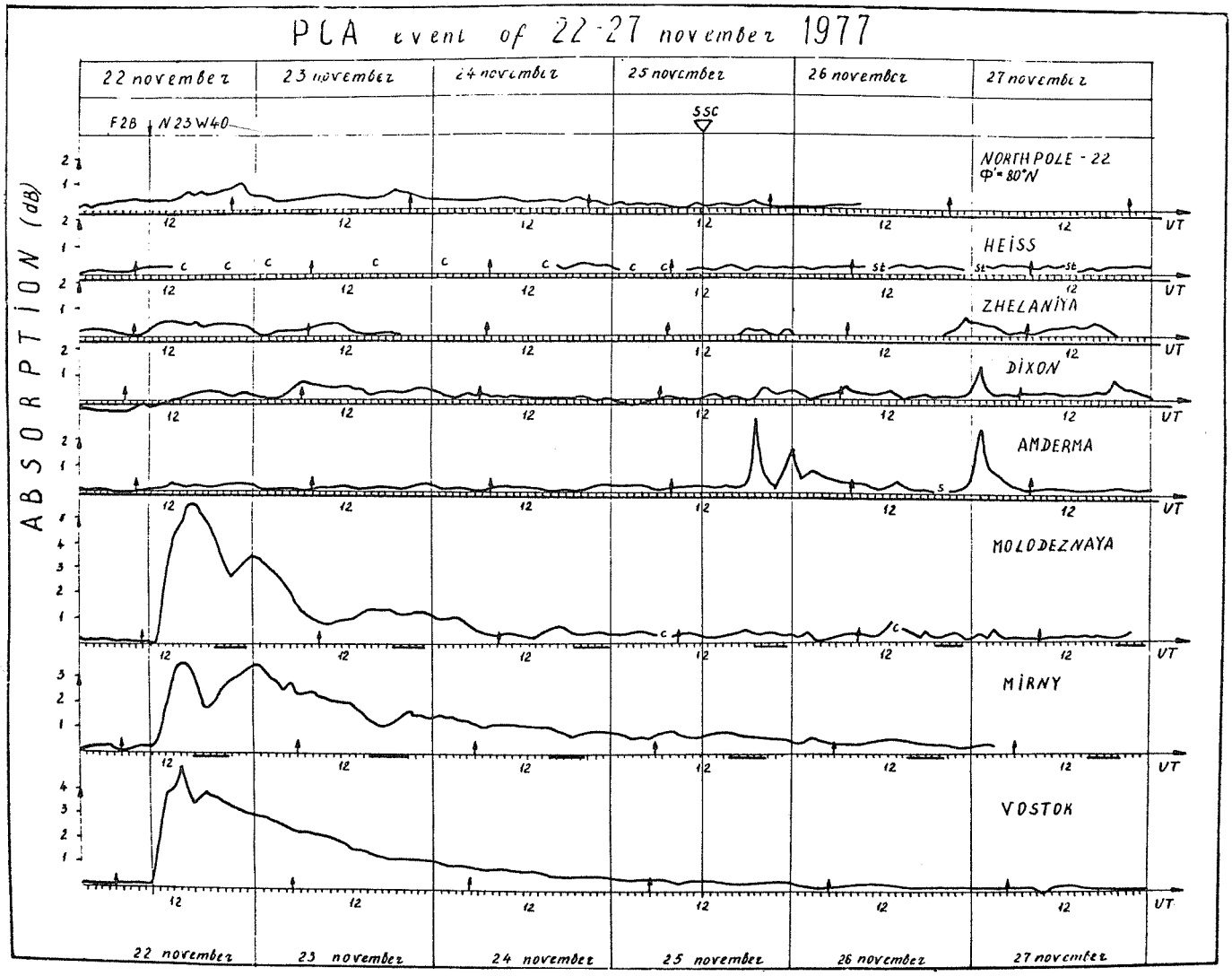

Fig. 5. PCA variations during November 22 - 27, 1977

Polar Riometer Absorption Data
September 5-28 and November 21-24, 1977

by

P. Stauning

Ionosphere Laboratory, Meteorological Institute
c/o Technical University, DK-2800 Lyngby, Denmark

ABSTRACT

The present paper contributes a summary of cosmic noise absorption data from the STIP periods: September 5-28 and November 21-24, 1977. The data have been obtained from a net of riometer observatories in Greenland, Iceland and North Norway. Riometer data are presented, and observations related to the occurrence of solar flares are discussed.

Introduction

The location of the riometer observatories, that have supplied the data presented below, are shown in Table 1. The observatories are all located within the northern polar cap. In addition to geographic and geomagnetic coordinates and 100 km L-values for each observatory the table gives receiving frequencies for the various riometers operated by the Ionosphere Laboratory. For each riometer the cosmic noise quiet day reference level has been derived as the upper envelope of a mass plot of the recordings through the actual month.

Table 1. Observatory locations and riometer receiving frequencies as of December 1977.

	Geographical		Geomagnetic		100km	Ionlab riometer	Station
Observatory	Latitude	Longitude	Latitude	Longitude	L-value	frequencies	operated by
Thule (Qanaq)	77.51°N	290.77°E	89.21°	356.40°	276	30	Danish Met.Inst.
Geopole	76.55°N	291.35°E	88.05°	02.39°	179	21 (30)	ETEE/AFSC
Godhavn	69.26°N	306.49°E	79.88°	32.59°	20.81	20,30	Danish Met.Inst.
Sdr.Strømfjord	67.02°N	309.28°E	77.44°	34.27°	14.47	31	GTO
Godthåb	64.19°N	308.27°E	74.81°	29.56°	10.98	21,30,40	GTO
Narssarssuaq	61.17°N	314.59°E	71.19°	36.76°	7.31	20,30,32,40	Danish Met.Inst.
St.Sirius Nord	81.60°N	343.30°E	80.69°	134.39°	38.85	30	Sirius Patrol
Danmarkshavn	76.77°N	341.37°E	79.43°	106.15°	20.92	32	GTO
Daneborg	74.30°N	339.18°E	78.19°	95.78°	16.25	21,30	Sirius Patrol
Kap Tobin	70.42°N	338.03°E	75.65°	81.63°	10.85	32	GTO
Angmagssalik	65.61°N	322.34°E	74.32°	52.63°	9.29	32	GTO
Tjörnes	66.20°N	342.90°E	71.2 °	79.5 °	6.7	30,40	NTNF/UiB
Torshavn	62.03°N	353.24°E	65.37°	84.77°	4.47	32	Danish Met.Inst
Ny-Alesund	78.92°N	11.92°E	75.40°	131.17°	16.64	21,30	NTNF/AO
Björnöya	74.51°N	19.18°E	71.08°	124.55°	9.62	30,40	VN/AO
Tromsö	69.70°N	19.00°E	67.14°	116.80°	6.33	30,40	AO

(ETEE/AFSC: VLF/ULF techn. Branch, HQ Rome Air Development Center, Hanscom AFB, Mass.; GTO: Greenland Technical Organization; NTNF: Royal Norwegian Council for Scientific and Industrial Research; UiB: Departm. of Physics, University in Bergen; AO: Auroral Observatory, University in Tromsö; VN: Met.Inst. for North Norway.)

Data presentation

The riometer data are presented in the form of diagrams with curves of absorption intensities versus UT time through a number of successive days for a selection of riometers. The curves have been arranged according to geomagnetic invariant latitude with the northernmost observatory (Thule) at the top. Diagrams with absorption intensities through 4 days are based on 5-minute averages of the data samples, while diagrams for the entire month are based on hourly values.

The riometer data have all been "normalized" to a reference frequency fo = 30 MHz through the relation: $A(fo) = A(f)\ (f/fo)^2$ where A(f) is the absorption (in dB) measured at the frequency f.

Some of the diagrams show equivalent absorption intensities (EOA) derived from IMP 7 and 8 measurements of high-energy proton fluxes. The differential flux intensities in the 4.0-12.5 MeV, 13.7-25.2 MeV, 20-40 MeV and 40-80 MeV channels shown in the reference have been converted to approximate 2π omnidirectional flux J(E>Eo) values. Using the theoretical expression derived by Potemra [1972], the equivalent 30 MHz daytime absorption A is given by: $A = m \cdot [J(E>Eo)]^{1/2}$. Using a threshold energy Eo = 7.0 MeV makes the coefficient m least sensitive to

proton spectral exponent γ. With A in dB and flux units as $(cm^2 \cdot sec)^{-1}$ the following conversion formula has been adopted here:

$$A = 0.083 \cdot [J(E>7.0\ MeV)]^{1/2}$$

The occurrence of H α solar flares is marked just above the upper frame of each diagram. The triangles are drawn to indicate the times of start, maximum intensity and end of the flares. The importance figure and the McMath-Hulbert plage region number is noted at each triangle. These auxiliary proton and flare data have been obtained from Solar-Geophysical Data 400 - Part I [1977] and 403 - Part II [1978].

Observations I. September 1977

The diagram in Figure 1 shows a summary of riometer absorption intensities through the month of September for a set of 11 different observatories. The riometers included in the diagram all have receiving frequencies at or close to 30 MHz, and the normalization, when required, is only a small correction of the original data. In Figure 2 the top field of the diagram shows the equivalent 30 MHz absorption (EOA) intensities derived from IMP 7 and 8 high energy proton fluxes. Below is shown riometer absorption intensities for the 5 northernmost observatories in the set.

It is evident from the data in Figure 1 and 2, that in September there are four rather distinct periods of enhanced absorption.

These are:

(i) September 7-15 This period beginning with the 4 flares of importance 1n on September 7, 9 and 10 in McMath region 14943 is characterized by weak and featureless but persistent high-energy proton fluxes. During most days of the period the IMP 7/8 equivalent absorption is 0.4-0.6 dB and so is the day-time polar absorption level. For the observatories closer to the auroral zone the period is characterized by an enhanced intensity of auroral substorm absorption activity during local night and morning hours. Directly related to solar flare activity, an event of sudden cosmic noise absorption (SCNA) and superimposed solar radio noise is seen in most of the original riometer recordings from 1630 to 1700 UT on September 9.

(ii) September 16-19 Following the flare 2n/14943 on September 16 with intensity maxima at appr. 2142 and 2300 UT the high energy proton flux increases rapidly. The IMP 7/8 equivalent absorption intensity shown in Figure 2 reaches a maximum level of 1.55 dB at about 04 UT in the morning of September 17. Later on the equivalent absorption decays exponentially with a time constant of about 24 hours. The 1n/14942 flare on September 18 is not seen to produce any discernible high energy porton flux. The riometer absorption diagrams in Figure 1 and 2 show the onset of a typical polar cap absorption (PCA) event of moderate intensity in the morning of September 17. The diagram in Figure 3 presents a more detailed plot of the absorption intensities from September 15 through 18 for the 11 riometers in the set. Most of the riometer observatories, considered here, are in darkness at the onset and also during the phase of maximum proton flux. At the most easterly observatory, Ny-Ålesund, the absorption reaches a maximum of 1.3 dB at 06 UT, while at the observatories in Greenland the absorption reaches maximum intensities of about 1.0 dB at 08-12 UT on September 17.

Through the September 16-19 period the level of auroral substorm absorption activity is rather low.

(iii) September 19-22 The flare 3b/14943 on the morning of September 19 lasting from about 10 to 12 UT with maximum phase at about 1040 UT is the most intense event of the month. At IMP 7 and 8 the high-energy proton fluxes increase sharply at about 12 UT and the equivalent absorption, shown in Figure 2, reaches a maximum intensity of 4.5 dB close to midnight on September 19.

The flare 2n/14943 at 03 to 09 UT on the morning of September 20 produces a contribution to the high-energy proton flux seen as a hump around noon on the decaying flux. After this time the equivalent absorption decays rather fast with an apparent time constant of about 15 hours.

In the original riometer charts a SCNA event with superimposed solar radio noise is seen at most observatories from 1030 to 1115 UT during flare maximum on September 19. As seen in the absorption diagrams in Figure 1 and 2, an intense PCA develops during the day. More detailed plots of polar absorption intensities from September 19 through 23 are shown in Figure 4 for all 11 observatories in the present set and in Figure 5 for the six northernmost stations. All observatories have local night at the time of maximum high-energy proton flux. At the most westerly observatory, Thule, the absorption reaches a maximum (day-time) level of 5.0 dB at 21 UT near maximum proton flux, but only 2 hours before local sunset.

Through the September 19-22 period, particularly after the SSC at 2044 UT on September 21, the auroral absorption activity is quite intense.

(iv) September 24-29 At about 07 UT on September 24 the high-energy proton flux increases sharply. There is one report (Culgoora) of a precedent flare 1n/14962 at about 0215 UT in the morning. This flare, however, seems too early and too small to be responsible for the proton event. It is possible, that the intense flux of high-energy protons is associated with another flare in the very active region 14943 now rotated to a longitude about 25° behind the western limb.

The high-energy proton fluxes at IMP 7 and 8 converted to equivalent absorption as shown in Figure 2 reach maximum intensity of 1.8 dB at 20 UT on September 24. The subsequent decay is rather slow having a time constant of about 36 hours.

The associated riometer PCA event is seen in Figure 1 and 2 and is shown more detailed in Figure 6 from September 24 through 27 for the set of 11 riometers. In addition to the very clear daily variation seen here, the PCA event shows the same general features as the high-energy proton flux. A quite steep increase, an extended period of maximum phase and a slow recovery. On September 24 the maximum absorption at Thule is about 2.2 dB.

During the September 24-29 period, the substorm absorption activity at auroral zone observatories is moderate or weak.

Observations II. November 1977

The diagram in Figure 7 shows the riometer absorption intensities for November 21 through 24 for a set of 10 different observatories. Following the solar flare of importance 2b in McMath region 15031 on November 22 lasting from 0945 to 1105 with maximum phase at 1007 UT, an intense PCA develops. At the southernmost observatory, Torshavn, a strong 30 MHz solar radio noise burst is seen in the recordings from 1003 to 1025. The polar cap absorption starts about 1050 UT and develops gradually during the day to reach a level of 5.5 dB at 16 UT in Sdr. Strømfjord and Godthåb. The northernmost observatories Thule and Ny-Ålesund have polar nights with the Sun 7.7° and 9.1°, respectively, below the horizon at local noon, and the absorption intensities remain at night level throughout the event. At Danmarkshavn the Sun is 7.0° below the horizon at noon, and the absorption increase produced by solar illumination of the radio wave absorbing region is just discernible. This implies, that the bulk absorption takes place below about 57 km, which is quite low even for a PCA.

For Godhavn, Kap Tobin and Ramfjord the Sun just rises to the horizon at local noon, while the remaining observatories have a normal (but short) day.

During the entire period the level of auroral absorption is very low indeed.

Acknowledgments

The various stations with riometer installations are operated by the Danish Meterological Institute, the Greenland Technical Organization, the Sirius Dog Sledge Patrol, the Universities in Tromsø and Bergen, the Royal Norwegian Council for Scientific and Industrial Research and the Meteorological Institute for North Norway. The support and assistance received from these organizations and from the many individuals responsible for the daily operation of the riometers is gratefully acknowledged.

The assistance received from B. Christensen, I. M. Duelund, S. Beauvais, I. Garms, O. B. Jensen and other members of the staff at the Ionosphere Laboratory is greatly appreciated.

References

POTEMRA, T. A. 1972 The Empirical Connection of Riometer Absorption to Solar Protons during PCA Events, *Radio Sci. 7*, 571-577.

SGD 1978 *Solar-Geophysical Data*, 403 Part II, U.S. Department of Commerce, (Boulder, Colorado, U.S.A. 80303).

SGD 1977 *Solar-Geophysical Data*, 400 Part I, U.S. Department of Commerce, (Boulder, Colorado, U.S.A. 80303).

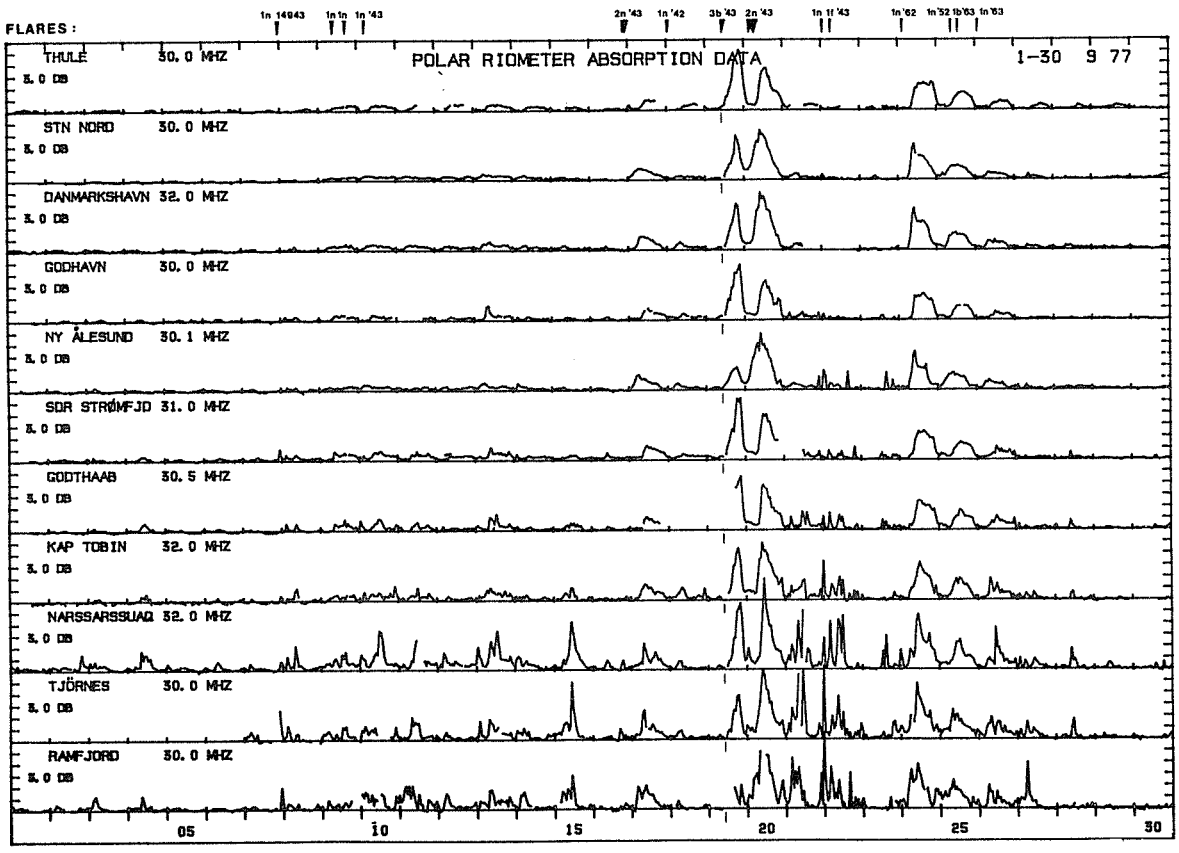

Figure 1. Riometer absorption intensities for September 1-30, 1977 at 11 polar cap and auroral zone observatories. The absorption values are normalized to 30 MHz.

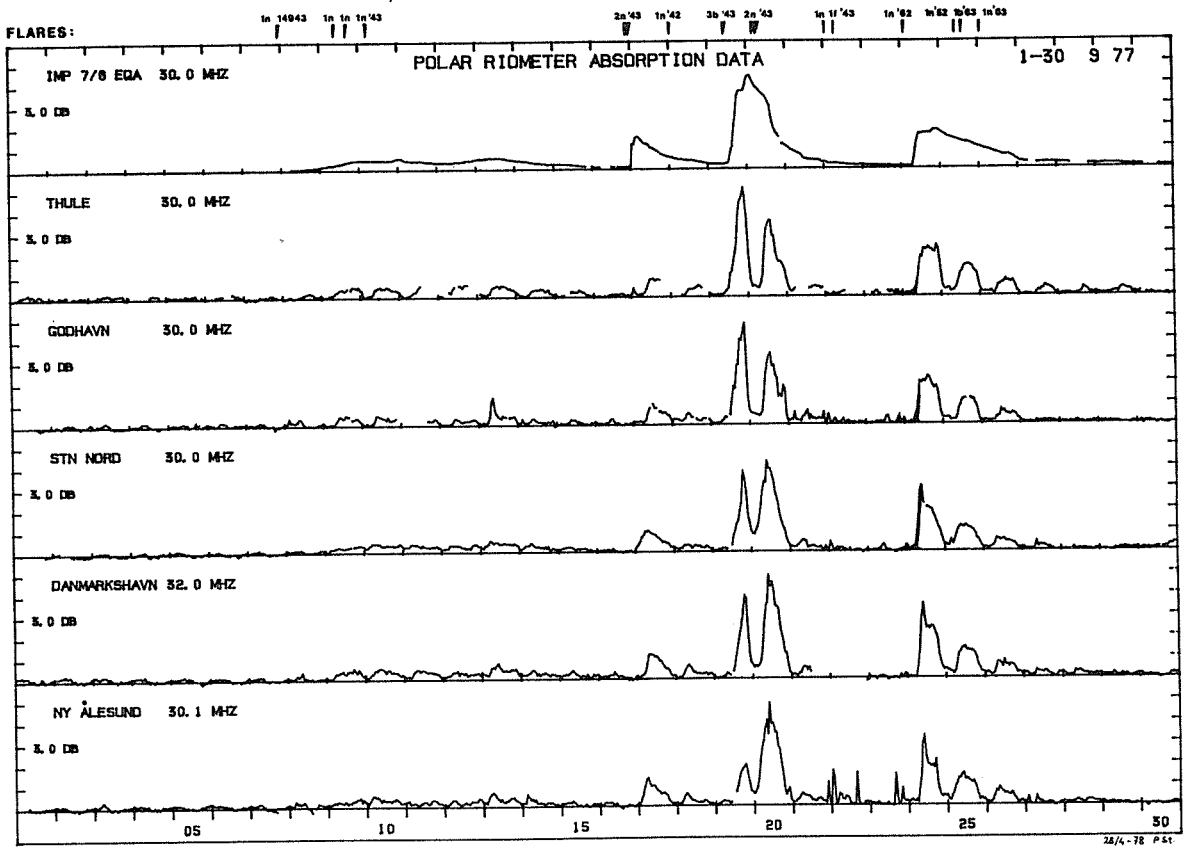

Figure 2. Equivalent absorption derived from IMP 7 and 8 high energy proton data and riometer absorption intensities at 5 polar observatories for September 1-30, 1977.

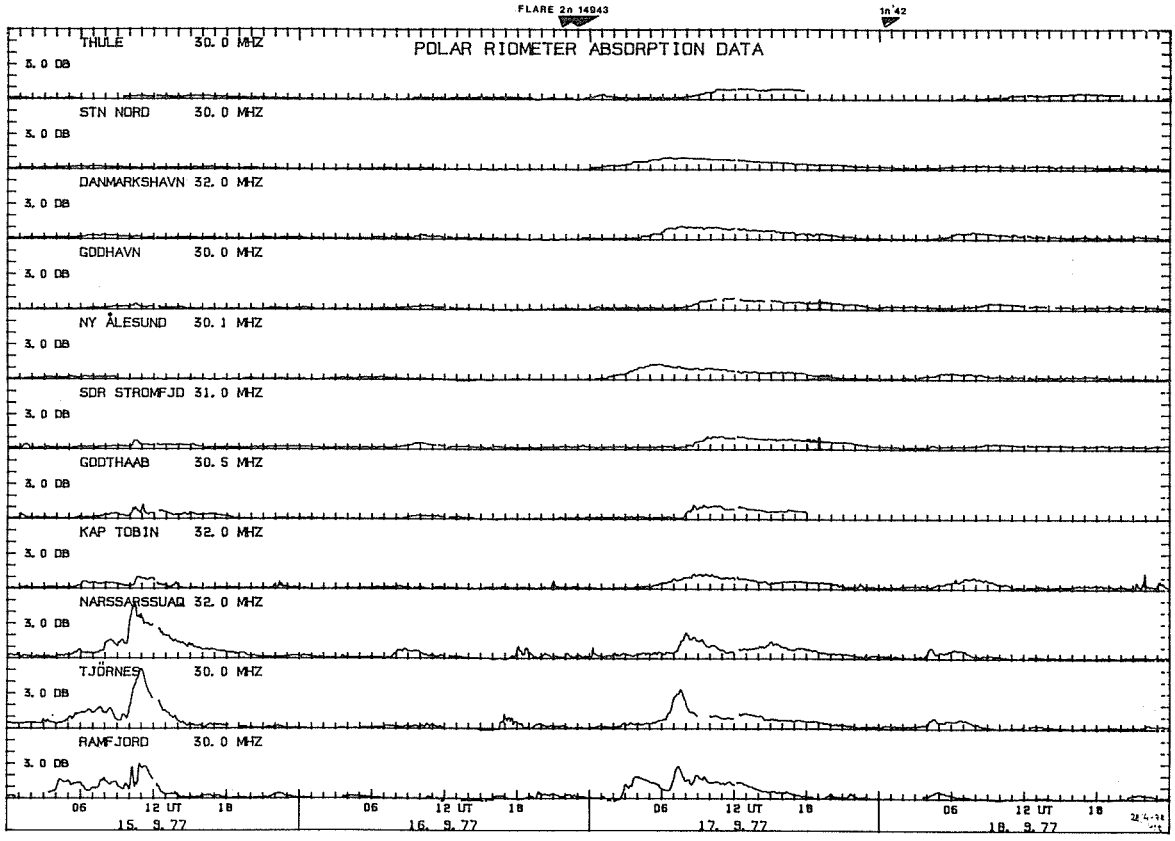

Figure 3. Riometer absorption intensities for September 15-18, 1977 at 11 polar and auroral observatories.

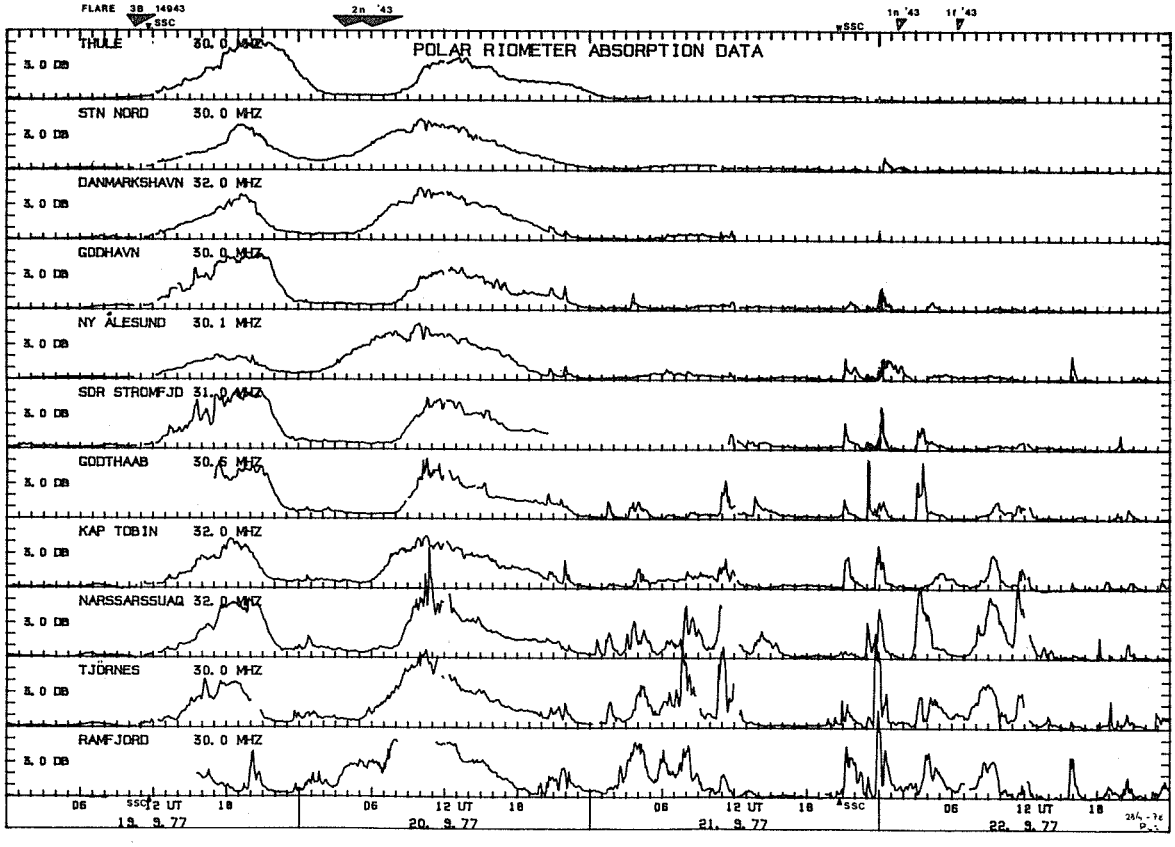

Figure 4. Riometer absorption intensities for September 19-22, 1977 at 11 polar and auroral observatories.

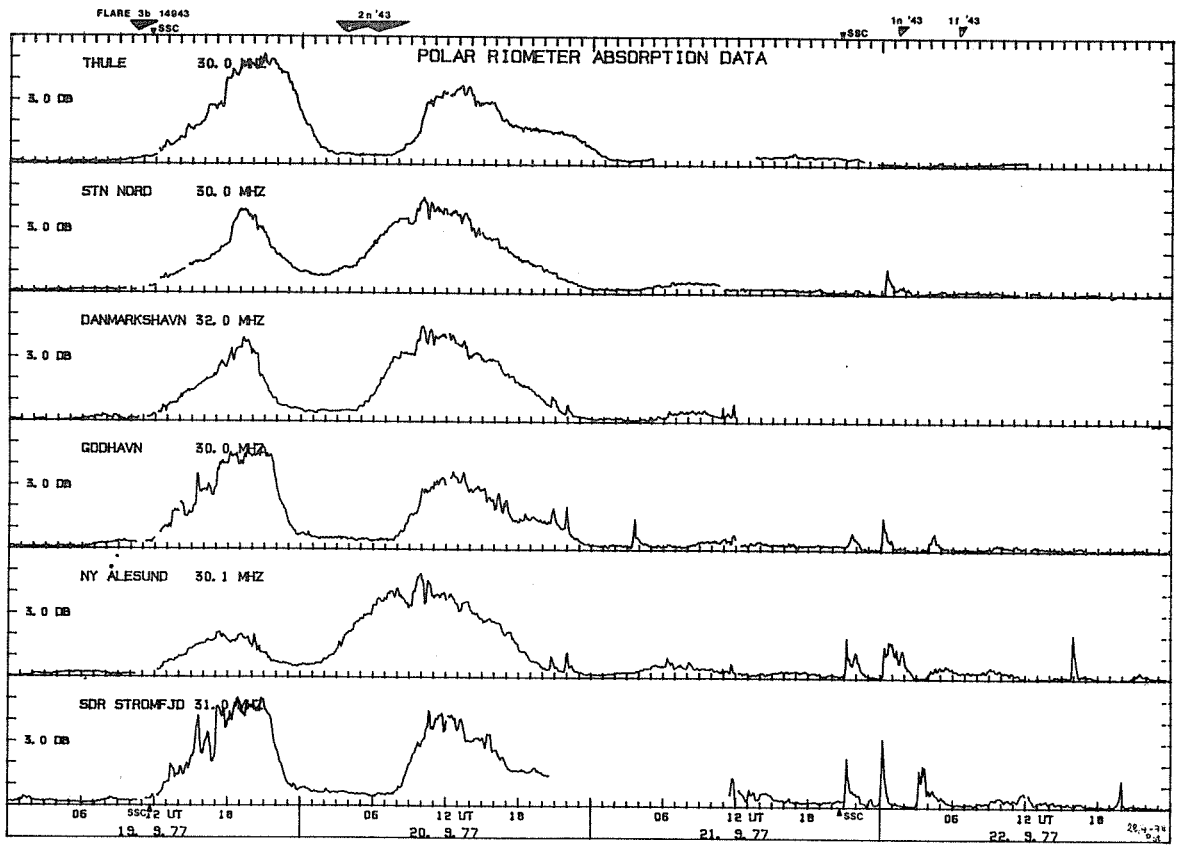

Figure 5. Riometer absorption intensities for September 19-22, 1977 at 6 polar observatories.

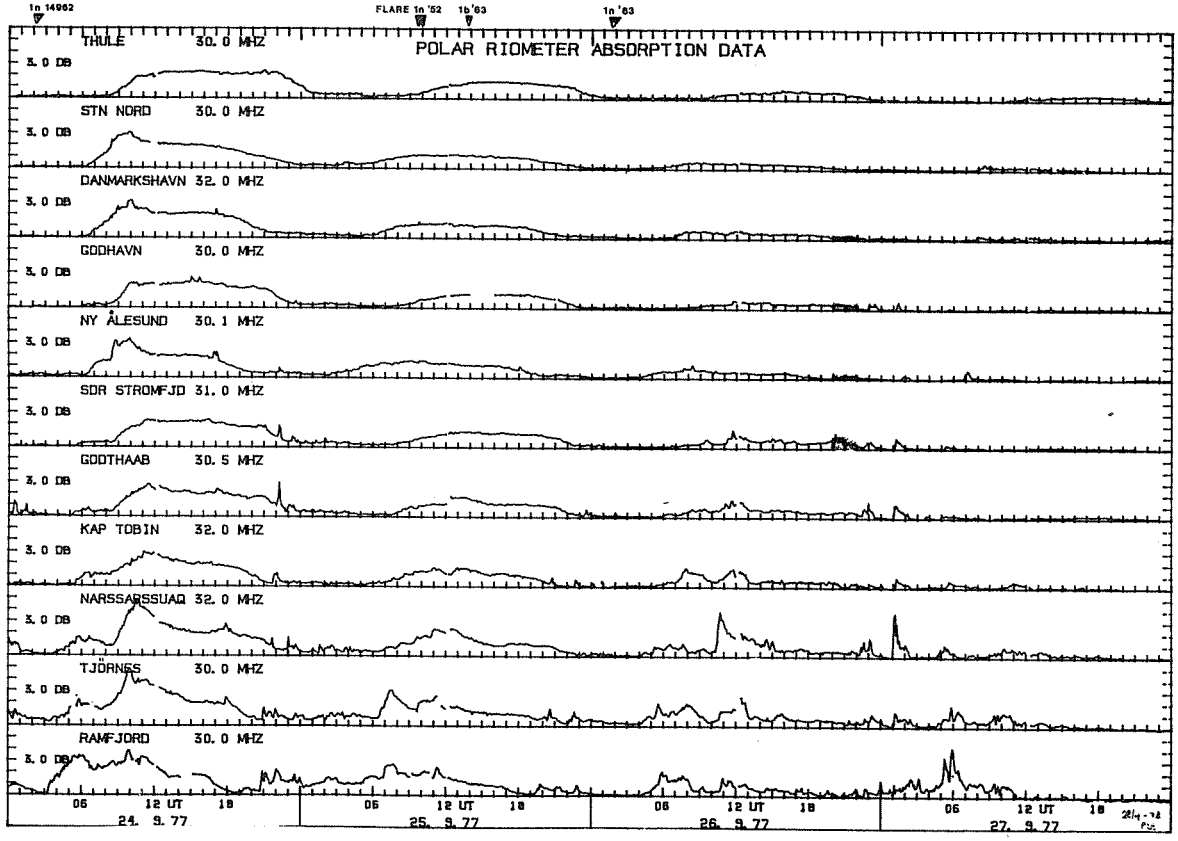

Figure 6. Riometer absorption intensities for September 24-27, 1977 at 11 polar and auroral observatories.

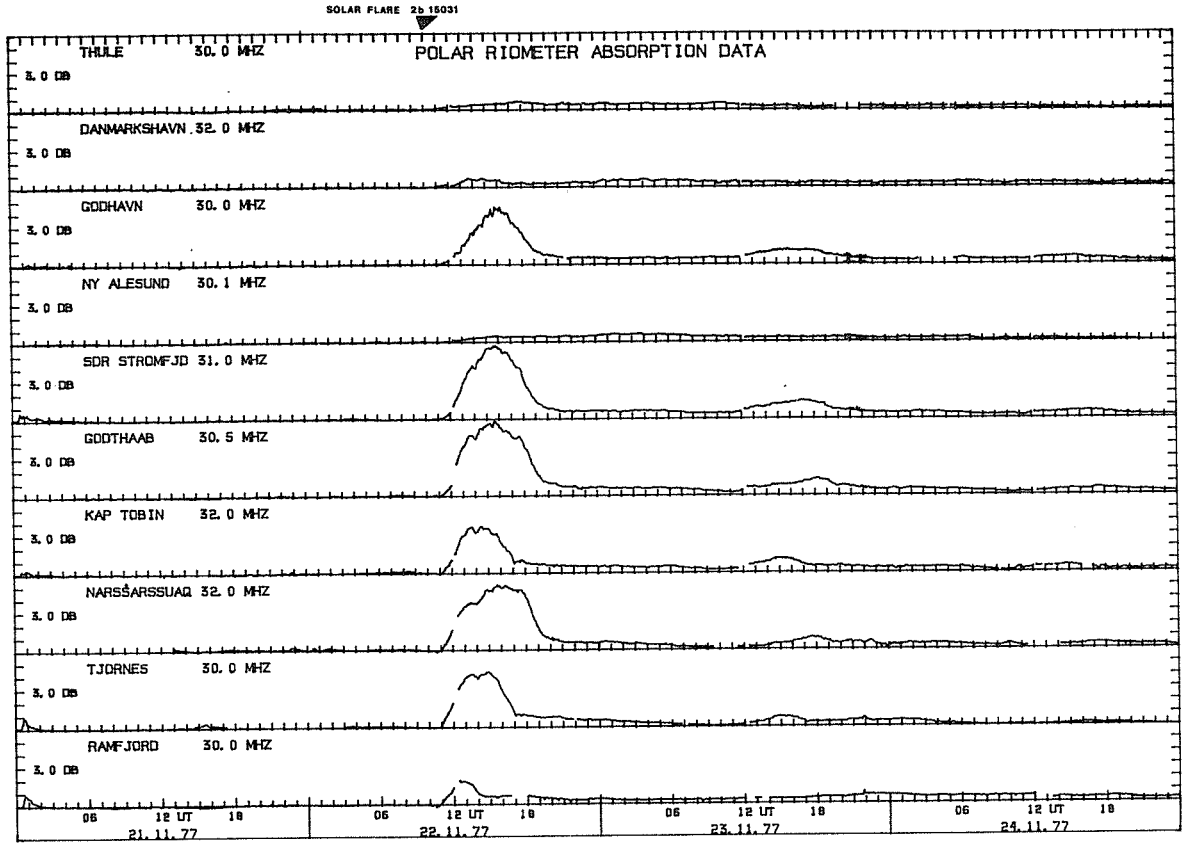

Figure 7. Riometer absorption intensities for November 21-24, 1977 at 10 polar and auroral observatories.

Scandinavian and Icelandic Riometer Records
September 7-24, 1977 and November 22, 1977

by

J.K. Hargreaves and J.M. Penman
Department of Environmental Sciences
University of Lancaster
Bailrigg, Lancaster, U.K.

Introduction

Data collected from five 30-MHz-wide beam riometers in Scandinavia and three similar installations in Iceland are presented as a written summary covering the first 12 days of the September period and November 22nd, and photographically for the remainder of the September period when the most intense activity was observed.

The written summary records, in general, only events with maximum absorption definitely exceeding 1 dB, although weaker events may be noted if the corresponding absorption at another station in the same group exceeds 1 dB. Absorption estimates are accurate to about 0.2 dB, and times are given to the nearest 10 min UT (for the beginning and end of events) or else to the nearest minute. The duration given refers to the main part of the event and not to extended periods of weak absorption preceding or following it. Where a particular station is not mentioned in connection with an event, the relevant data were not available.

The photographs were taken of the charts as received; dates and times (UT) are indicated. The scale is linear in intensity.

The riometer stations and their geographic coordinates are listed in Table 1 below.

TABLE 1. Riometer Stations

		Lat.	Long.	
Kiruna	(Ki)	67.53° N	20.15° E	Scandinavian Group
Skibotn	(Sk)	69.25° N	20.15° E	
Abisko	(Ab)	68.21° N	18.50° E	
Andøya	(An)	69.18° N	16.10° E	
Fauske	(Fau)	67.17° N	15.25° E	
Fagurhólsmýri	(Fag)	63.53° N	16.39° W	Icelandic Group
Siglufjördur	(Si)	66.09° N	18.55° W	
Leirvogur	(Le)	64.18° N	21.70° W	

Written Summary - Scandinavian Group (all times UT)

7.9.77	Ab :	2200-2330 Somewhat irregular feature containing a sharp edge at 2212. Peak 1.4 dB at 2224
	An :	Sharp onset at 2211 followed by an irregular feature with periodic structure. Peak 2 dB at 2249.
8.9.77	Ab :	Small sharp onset at 2055, peak 0.8 dB at 2056, followed by weak absorption.
	An :	Sharp onset at 2052, peak 1.4 dB at 2056, followed by variable absorption including a sharp 1.2 dB peak at 2132.
9.9.77		No events exceeding 1 dB observed at An or Fau.
10.9.77	An :	0000-0430 structured feature, fairly sharp peak 2.4 dB at 0230.
	Fau:	0000-0400 structured feature with 2 broad maxima, broad peak 1.5 dB at 0100.
	An :	0550-0740 smooth feature, peak 1.2 dB at 0617.
	Fau:	No corresponding feature.
	An :	1210-1500 practically smooth dip, preceded and followed by periods of weaker absorption. Broad peak 2 dB at 1338. At Ab, the corresponding feature has peak absorption 1.7 dB but accurate timing is impossible.
	Fau:	No corresponding feature.

10.9.77/11.9.77 An : Sharp edge at 2131 preceeding a period of very irregular absorption, level about 1 dB, which lasts until about 0400 and is followed by a series of smooth features lasting until about 1300. Sharp peak 1.4 dB at 2139, broad peak 1.8 dB at 0721.

Ab : (Accurate timing continues from 2230). From 2300 until 1300 the record shows a series of broad features, some with a little structure but nothing so irregular as An before 0400. Broad peak 1.7 dB at 0346.

11.9.77 An : 1700-2400. Three irregular dips of which the first has sharp structure near 1800. Sharp peak 1.9 dB at 1801.

Ab : These features are weakly represented, and without the sharp structure in the first. Sharp peak 0.9 dB at 2254.

12.9.77 Ab : 0400-0620. Smooth feature with two maxima. Peak 1.2 dB at 0456.

An : 0340-0630. Similar feature, broad dip with small scale structure. Peak 2.5 dB at 0511.

13.9.77 Ab : 0000-0330. Somewhat irregular depression of trace with structure in first hour. Broad peak 0.9 dB at 0152.

Fau: 2330-0330. As Ab. Broad peak 1.2 dB at 0151.

Ki : 2330-0330. As Ab. Broad peak 0.8 dB at 0055.

Ab : 0720-1340. Broad depression of trace, about 1 dB max., followed by about 2½ hours' structured absorption. Sharp peak 2.2 dB at 1229.

An : Similar to An, but structure less pronounced. Sharp peak 1.5 dB, but accurate timing is impossible.

Fau: 0720-1340. Similar to Ab, but absorption before 1230 is weaker and more irregular. Fairly sharp peak 1.3 dB at 1228.

Ki : 0720-1340. Similar to Ab. Sharp peak 2.2 dB at 1228.

Fau, An, Ab, Ki : 1930-2230 (approx.). Period of highly structured absorption with several edges. Feature has a precursor of maximum absorption 1.1 dB at 1801 (Fau), 1.3 dB at about 1730 (An), 0.5 dB at 1802 (Ab) and 0.9 dB at 1800 (Ki). Maximum absorption is 2.4 dB at 2018 and 2022 (Fau), 3.8 dB at about 2025 (An), and 2.8 dB at 2025 (Ab) and 2.6 dB at 2026 (Ki).

14.9.77 Ab : 0140-0320. Somewhat irregular feature. Peak 1.2 dB at 0224.

Ki : 0140-0320. As Ab. Peak 1.7 dB at 0308.

An : 0200-0350. As Ab. Peak 2.3 at about 0235.

Fau: 0200-0320. As Ab. Peak 1.3 dB at 0210.

All features preceded and followed by periods of weak absorption.

15.9.77 Ab : 0400-1400. Series of broad dips, the largest of which is between 0940 and 1400 and has peak absorption 2.5 dB at 1047.

An : 0340-1430. Similar to Ab, but largest dip (0930-1430) shows more structure. Peak 2.7 dB at about 1100.

Fau: 0400-0700. Dip with 2 maxima, 1.1 dB at 0429. 1000-1430. Almost smooth feature with fairly rapid onset (~ 30 min), rounded peak and gradual decline in absorption. Peak 5.6 dB at 1027.

Ki : 0400-1000. 3 broad depressions, each having max. absorption about 1 dB. 1000-1430, similar to Fau, but rather less smooth. Peak 4.0 dB at 1023.

16.9.77 Ab & Ki : 1620-1720. Small structured feature with 2 or 3 minature edges. Maximum absorption about 1.2 dB at 1647.

An : Feature shows little structure and is weak.

Fau: Feature hardly represented.

An : 1945-2000. Small structured disturbance, maximum absorption about 1.3 dB. Feature is hardly represented at Ab or Ki, and there is interference at Fau.

17.9.77 Ki : 0240-1700., Large, smooth, slowly varying feature. Max. absorption 3.2 dB at 0747.

Ab : Similar to Ki, but absorption very weak before 0640. Max. absorption 1.7 dB at 0756.

An : 0230-1900. Similar, but initial onset more rapid. Max. absorption 2.7 dB at about 0718.

Fau: Similar to Ab. Maximum absorption 2.4 dB at 0750.

18.9.77 No events exceeding 1 dB at Ki, Ab, An or Fau.

Written Summary - Icelandic Group (all times UT)

7.9.77 Le : 2100-0012. Relatively weak, irregular depression containing sharp onset at 2210, peak 3.9 dB at 2211.

Si : Sharp onset at 2210, peak 2.4 dB at 2211 after which absorption declines rather irregularly almost to zero by 2330.

Fag: Sharp onset at 2209, peak 1.6 dB at 2212, followed by rather irregular dip lasting until 2330.

8.9.77 Le : 0205-0215. Rounded peak surrounded by weak absorption. 1.7 dB at 0212.

Si : 0200-0420. Two somewhat irregular depressions, max. absorption <1 dB, no rounded peak.

Fag: 0130-0430. Rather similar to Si.

Le : 0750-0930. Smooth depression, maximum absorption 0.7 dB at 0814.

Si : 0750-1000. As Le, maximum absorption 1.3 at 0820.

Fag: Features hardly represented.

9.9.77 Fag: 1205-1410. Smooth feature. Maximum absorption 1.4 dB reached at 1231 followed by gradual decline. Weak depression after 1410.

Si : 1200-1610. Two broad depressions. 1.5 dB at 1306.

10.9.77 Fag: 0000-0500. Variable absorption with some structure. Fairly sharp peak, 1.6 dB at 0055.

Si : 0000-0530. As Fag, but more irregular. Broad peak, 1.5 dB at 0111.

11.9.77 Fag: Before midnight - 0700. Period of irregular absorption, general level 1.0 dB, sharp peak 1.6 dB at 0258.

Si : This disturbance hardly represented. Few minor features, non reaching 1 dB max.

Fag: 0700-0950. Feature with relatively rapid onset, followed by slow decline. Peak 1.7 dB at 0714.

Si : 0700-0940. A.most symmetrical dip. 1.4 dB at 0810.

Fag: 0950-1300. Feature wih two fairly sharp peaks. 1.9 dB at 1025.

Si : 0940-1320. Two broader maxima, 3.0 dB at 1024.

12.9.77 Si : Two small peaks, 1.4 dB at 2218 and 1.3 dB at 2305 lying in period of weak absorption.

Le : Trace depressed slightly, but sharp peaks are not represented.

Fag: Peaks not represented.

13.9.77 Le : 0040-0430. Feature whose maximum is fairly sharp peak, 2.0 dB at 0148.

Si : 0100-0320. Feature with two maxima followed by a sharp peak 1.1 dB at 0152.

Fag: 2210-0340. More extended feature whose limits are difficult to define. Peak is a blunt cusp, 2.0 dB at 0146.

13.9.77 cont.

Le : 0700-1130. Featureless depression, max. 2.1 dB at 0835.

Si : 0700-1120. As Le 1.6 dB at 0829.

Fag: 0720-1120. As Le. Max. 1.6 dB at 0755.

Le : 1130-1430. Broadly symmetrical feature. 3.3 dB at 1249.

Si : 1120-1430. As Le, but with more broad structure, 1.6 dB at 1221.

Fag: 1120-1430. As Le, but peak more pronounced 3.4 dB at 1221.

Le : 1940-2100. Feature with several sharp onsets. Max. absorption 3.3 dB at 2007. Extended periods of more or less steady absorption surround this feature.

Si : 1940-2100. As Le, but edges have different emphasis. Main edge at 2006 preceeds peak of 4.8 dB at 2007.

Fag: At Fag, the edges are degraded and there is less structure. The absorption assumes the form of a main feature between 1940 and 2100 surrounded by 'wings' extending back to 1730 and forward to 2230.

14.9.77 Le : 0010-0700. Trace depressed with broad sructure. Max. 1.7 dB at 0238.

Si : 0030-0700. As Le, but absorption weaker. Max. 1 dB at 0436.

Fag: 2350-0600. As Le. Max. 1.4 dB at 0255.

15.9.77 Le : 0920-1220. Broad dip, max. 5.1 dB at 1035, surrounded by 'wings' extending back to about midnight and forward to at least 1900.

Si : As Le. Main feature between 0920 and 1400, max. 4.6 dB at 1101, wings go back to 0430 and forward to about 1900.

Fag: Main feature between 0950 and 1040 is shorter. Max. 3.1 dB at 1013. Wings extend back to 0130 (and include a broad feature of ~1 dB max. between 0320 and 0630) and forward to about 1900.

16.9.77 Le : 1700-1900. Irregular, though symmetrical, dip followed by a sharp peak 1.9 dB at 1754.

Si : 1630-1900. As Le, but earlier and without sharp peak following. Center of dip about 1715 1.1 dB at 1656 and 1735.

Fag: Roughly comparable feature between 1840 and 2030, 0.7 dB at 2030.

17.9.77 Le : 0630-0810. Rounded feature, max. 3.7 dB at 0706, surrounded by weak absorption extending backward to 0230 and forward to 2300.

Si : 0600-0810. As Le. Max. 3.0 dB at 0728. Weak absorption extends backward to 0500 and forward to 2000.

Fg : 0600-0830. As Le. Max. 2.3 dB at 0720. Weak absorption back to midnight and forward to 2400 at least.

18.9.77 Le : 0400-0500. Symmetrical dip. Max. 1.2 dB at 0427.

Si : 0400-0500. As Le. Max. 0.5 dB at 0430, weak absorption follows.

Fg : Blunt cusp peaking at 0430 (1.1 dB). Absorption merges with previous feature and extends forward to 0630.

Scandinavian Group - Activity on November 22nd (all times UT)

Ki: 1055-1410 Smooth symmetrical depression reaching 1.1 dB at 1220 and followed by a long, weak tail declining gradually from 0.3 dB to zero about 1830. No other activity.

Sk: 1055-1410 As Ki, 1.7 dB at 1222. After 1410, absorption declines from 0.7 dB to zero by about 2000.

Scandinavian Group cont.

Ab:	1055-1420	As Ki, 1.4 dB at 1220. After 1420, absorption declines from 0.4 dB to zero by about 2000.
An:	1100-1420	As Ki, 1.6 dB at 1253. Absorption declines from 0.6 dB at 1420 presumably to zero, but record is incomplets.
Fau:	1100-1420	As Ki, 1.0 dB at 1257. Tail confused by interference.

Icelandic Group - Activity on November 22nd (all times UT)

Fag:	1100-1800	Smooth, somewhat symmetrical feature, 1.7 dB at 1539.
Si:		No data.
Le:	1100-1740	Smooth, slightly symmetrical feature, 3.2 dB at 1453.

Acknowledgements

We are grateful to the following people for their help with the riometer networks: Drs. A. Brekke and O. Harang (University of Tromsø), Dr. G. Gustafsson (Kiruna Geophysical Institute) and Dr. T. Saemundsson (University of Iceland), and also to Mr. O. Jónsson (Fagurhólsmýri), Mr. S. Kristinsson (Siglufjördur), Mr. S. Kristensen (Fauske) and staff at the Abisko Scientific Research Station and Andøya Rocket Range for their help at individual stations. The work was supported by the Science Research Council of Great Britain.

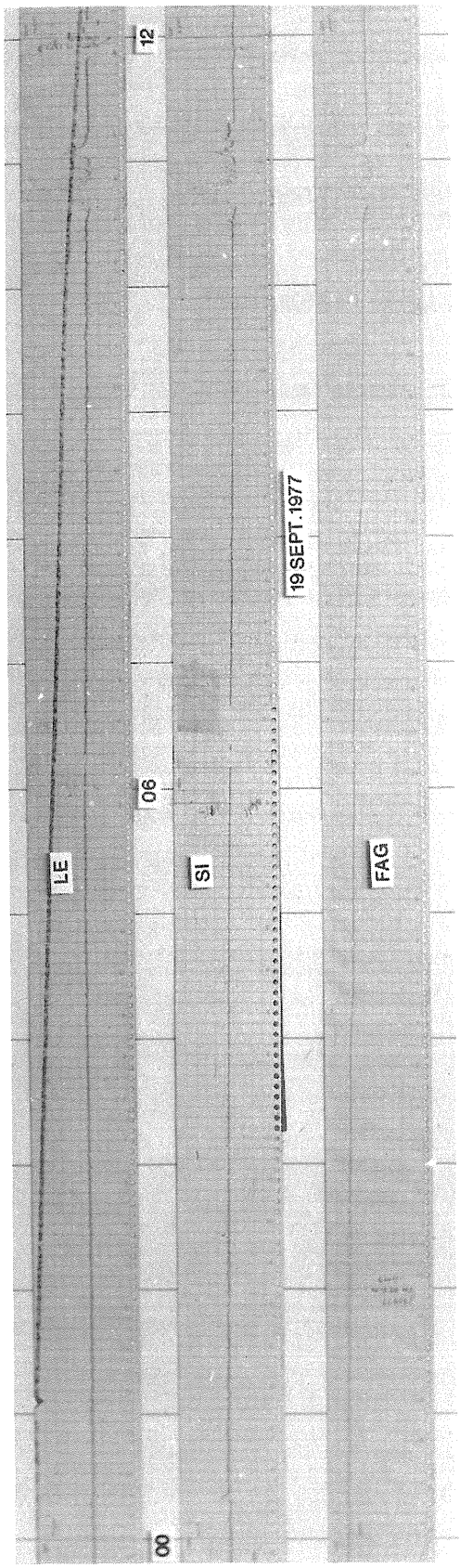
12
06
08
LE
SI
19 SEPT. 1977
FAG

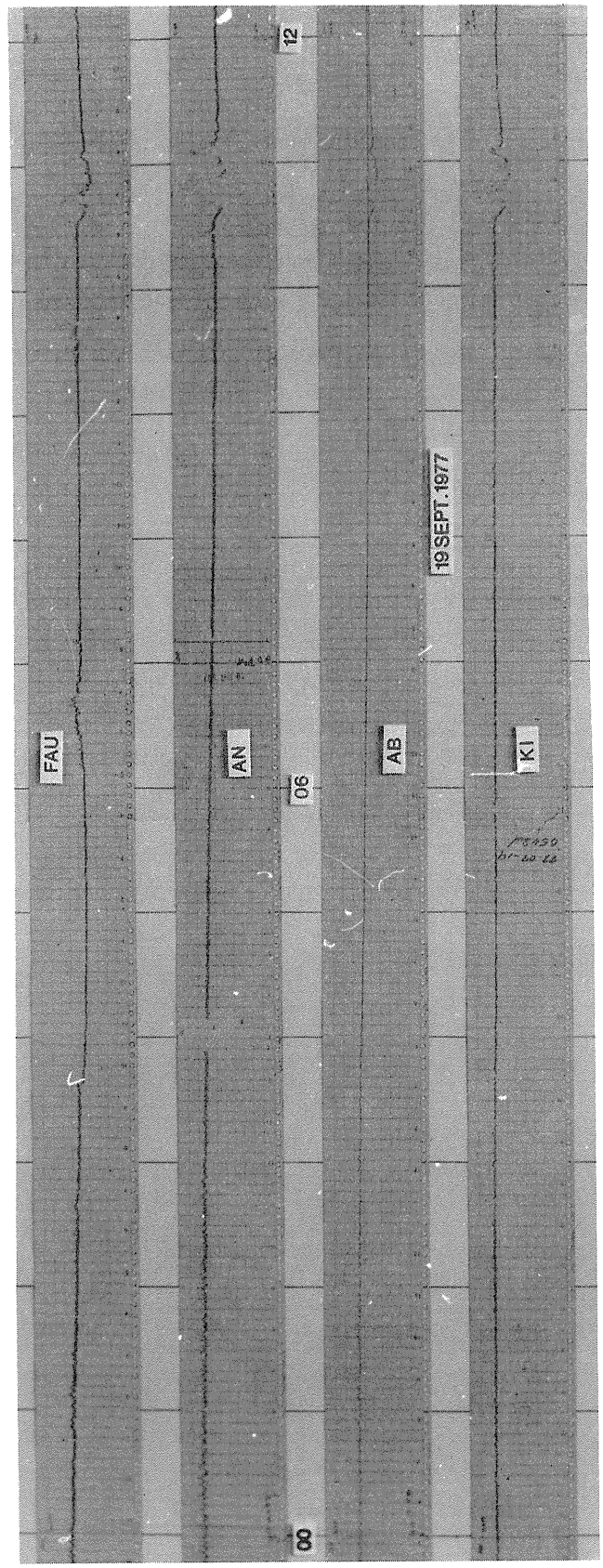
12
06
08
FAU
AN
AB
19 SEPT. 1977
KI

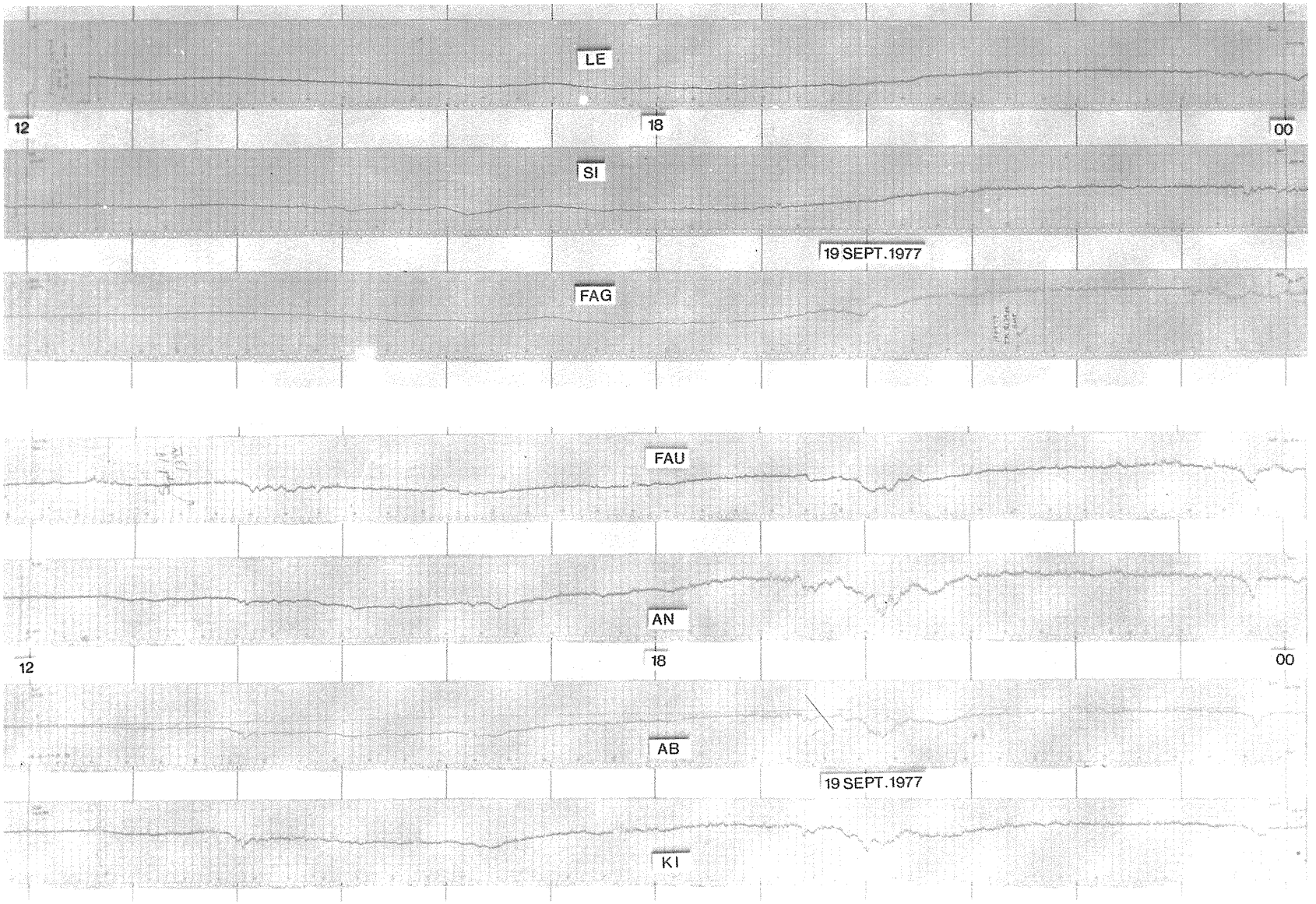
LE
12
18
00
SI
19 SEPT. 1977
FAG
FAU
AN
12
18
00
AB
19 SEPT. 1977
KI

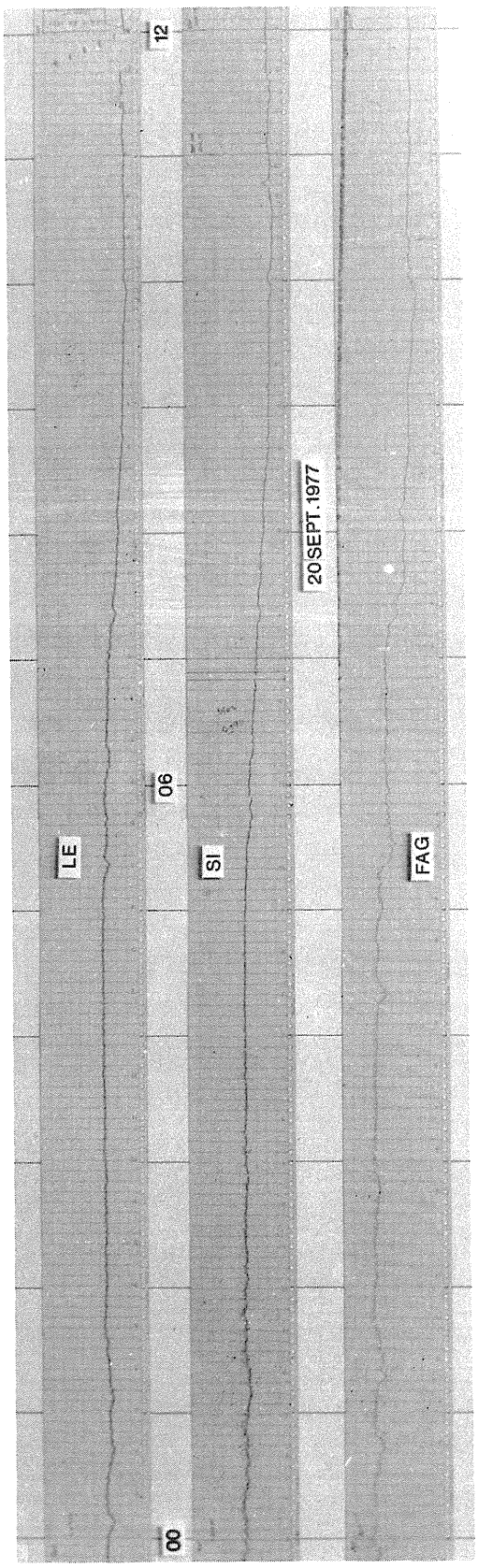
12
06
00
LE
SI
FAG
20 SEPT. 1977

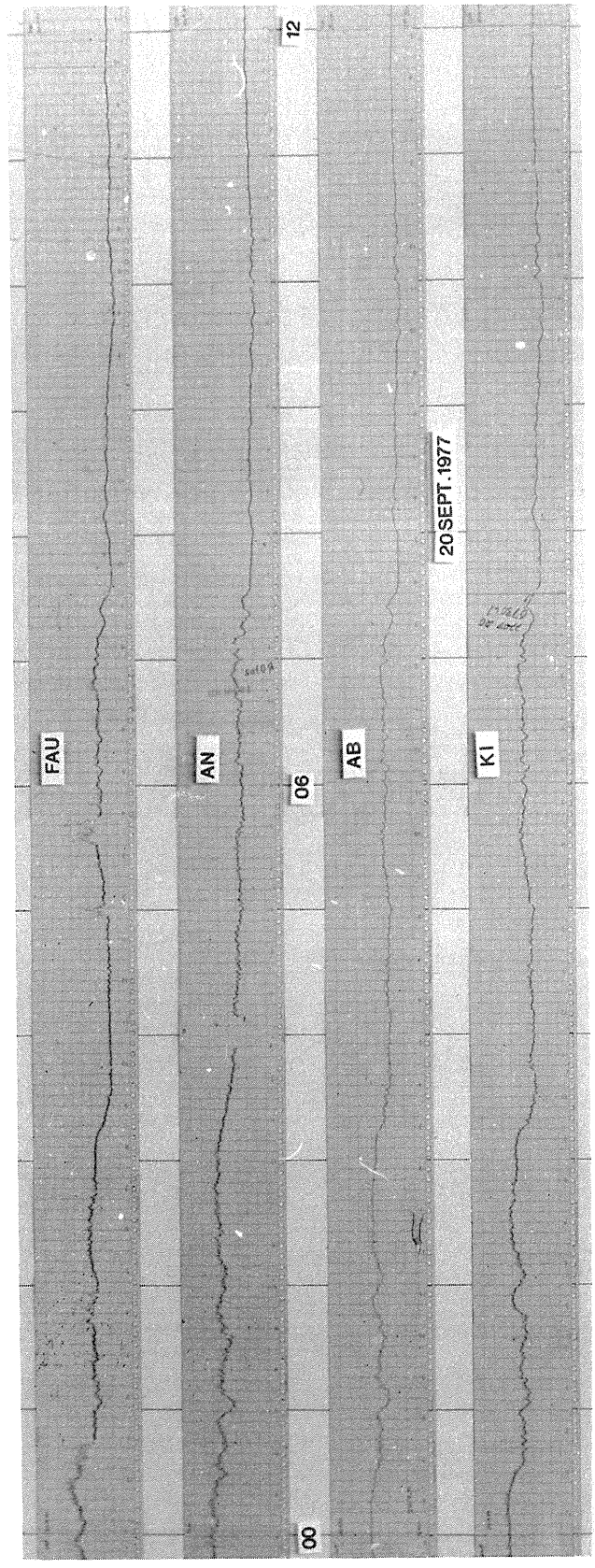
12
06
00
FAU
AN
AB
KI
20 SEPT. 1977

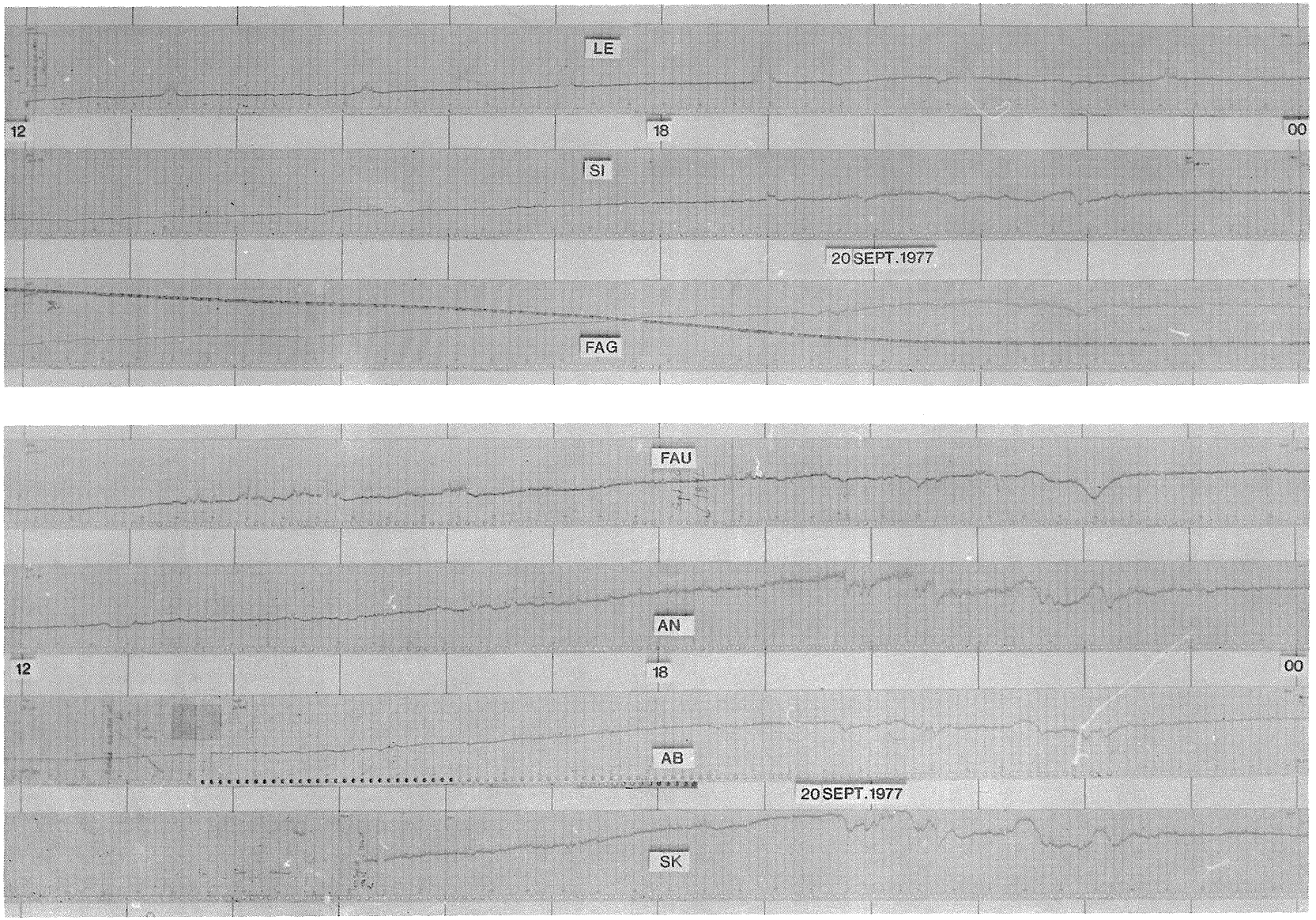
LE
12
18
00
SI
20 SEPT. 1977
FAG
FAU
AN
12
18
00
AB
20 SEPT. 1977
SK

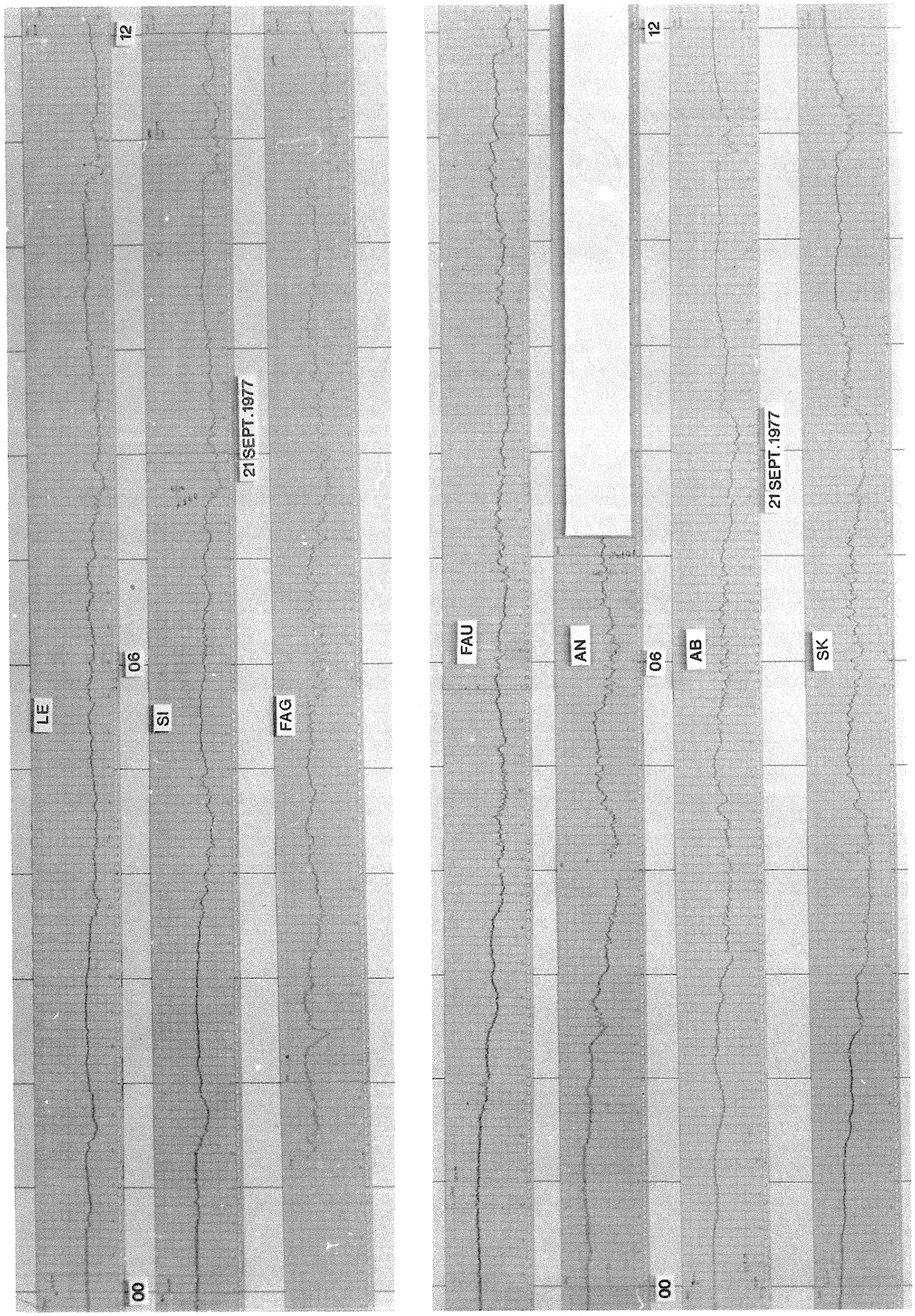
12
06
00
LE
SI
21 SEPT. 1977
FAG
12
06
00
FAU
AN
AB
21 SEPT. 1977
SK

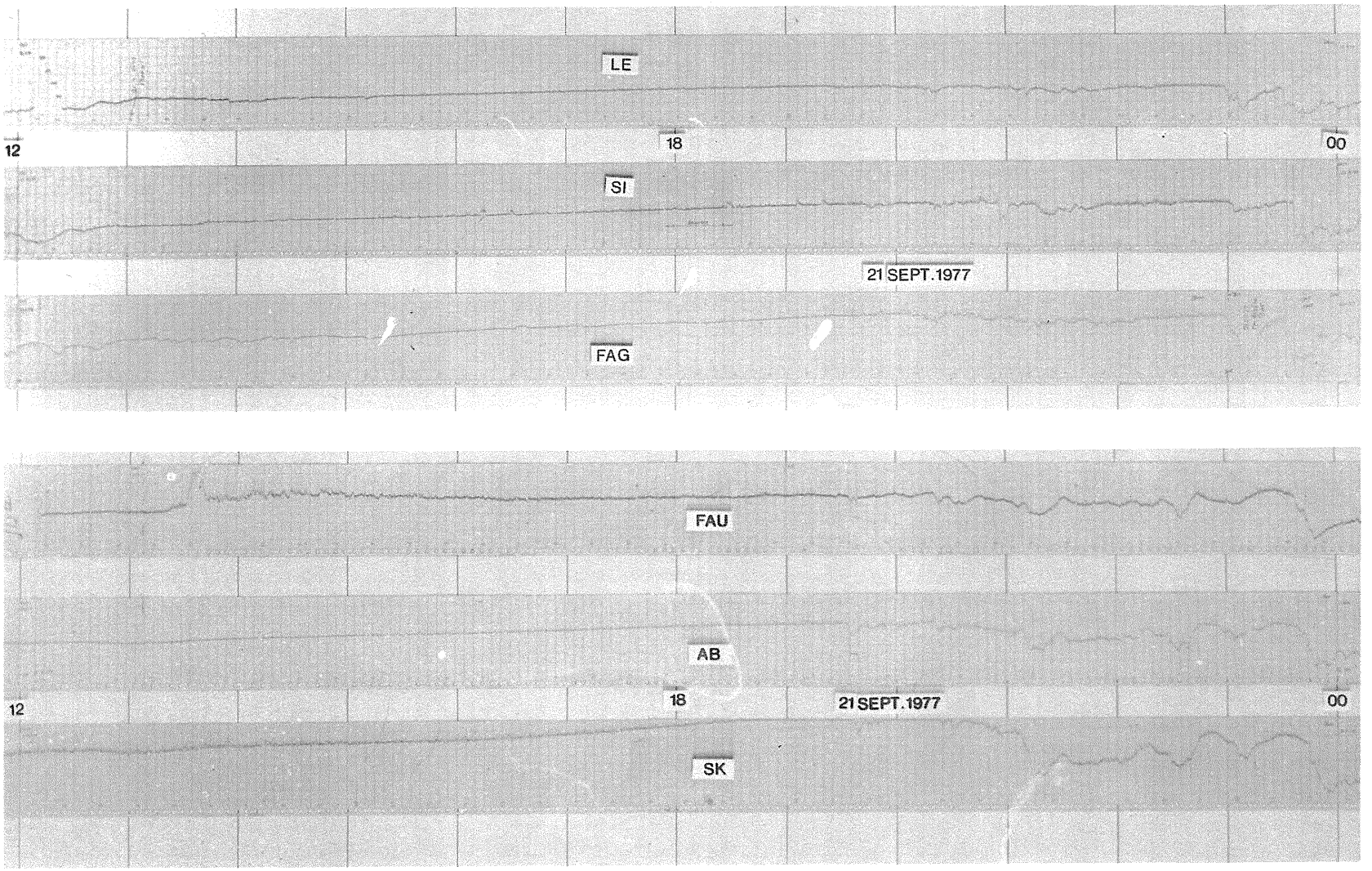
LE
12
18
00
SI
21 SEPT. 1977
FAG
FAU
AB
12
18
21 SEPT. 1977
00
SK

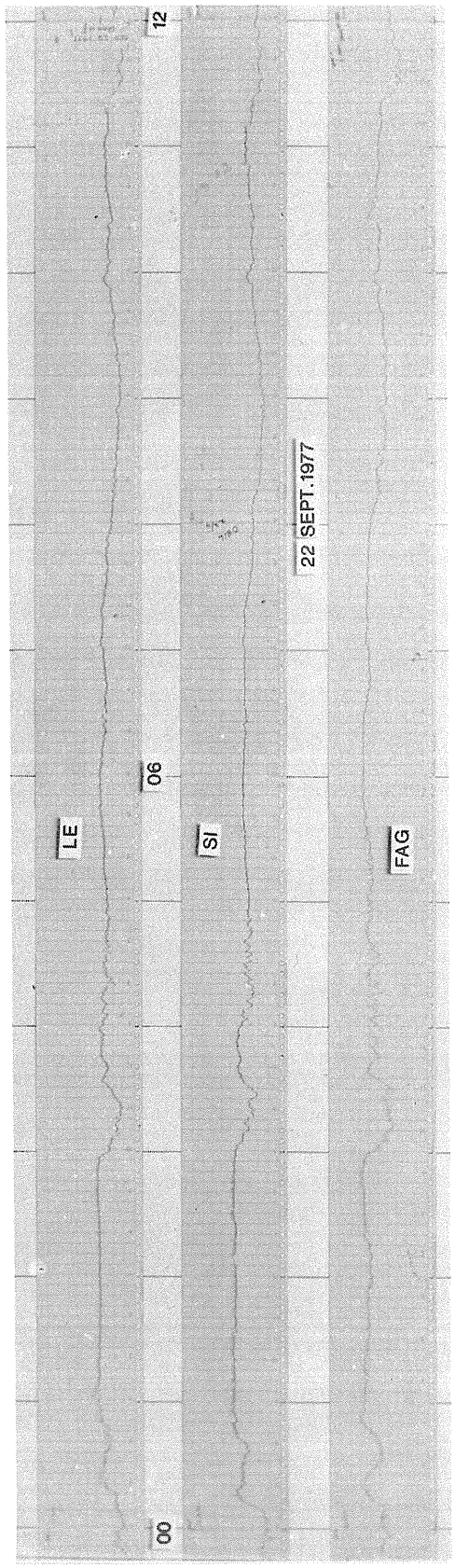
12
06
00
LE
SI
FAG
22 SEPT. 1977

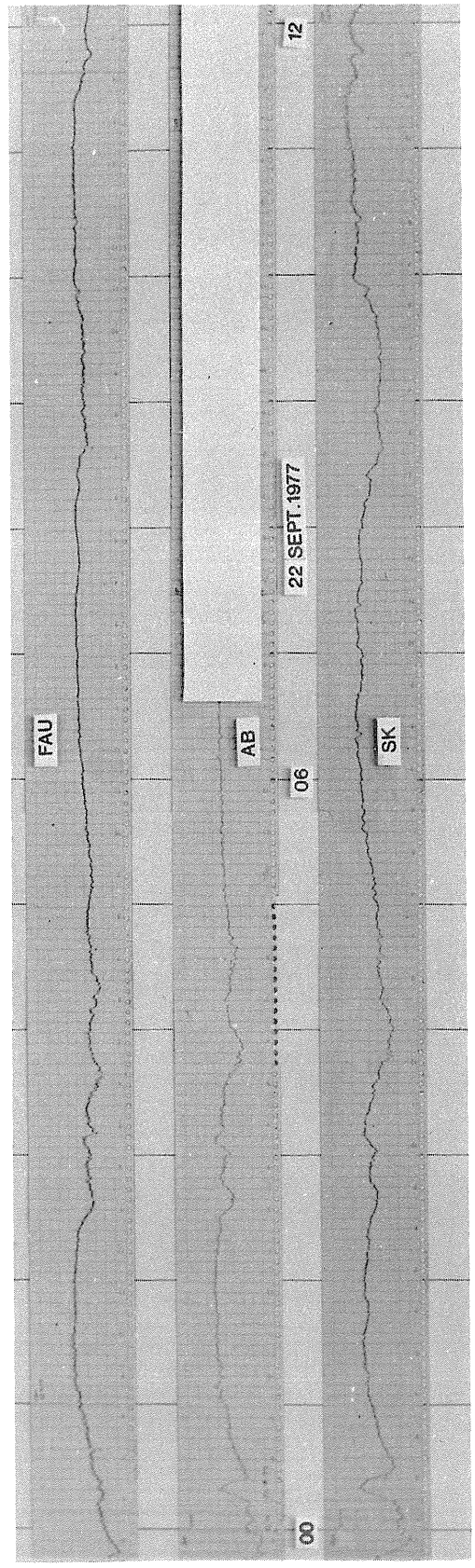
12
06
00
FAU
AB
SK
22 SEPT. 1977

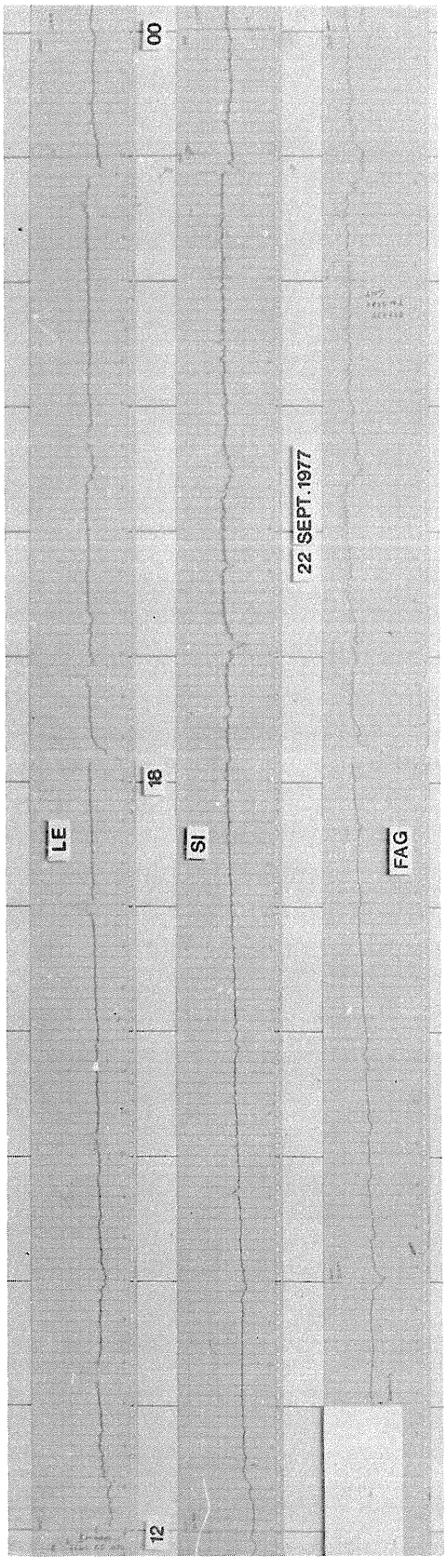
00
18
12
LE
SI
FAG
22 SEPT. 1977

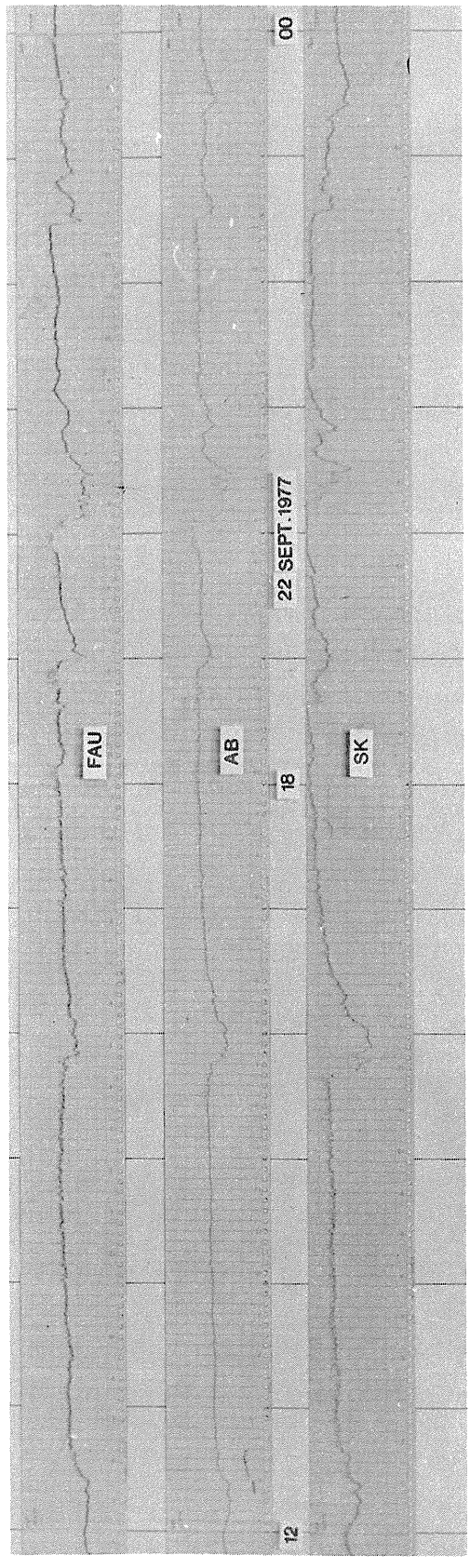
00
18
12
FAU
AB
SK
22 SEPT. 1977

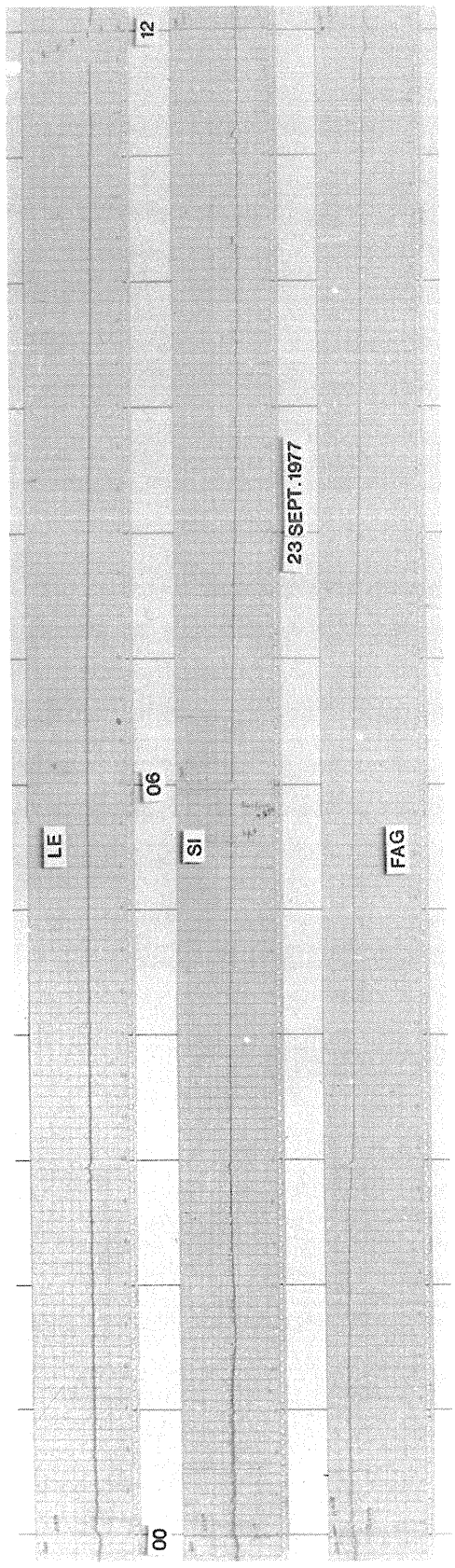
12
06
00
LE
SI
23 SEPT. 1977
FAG

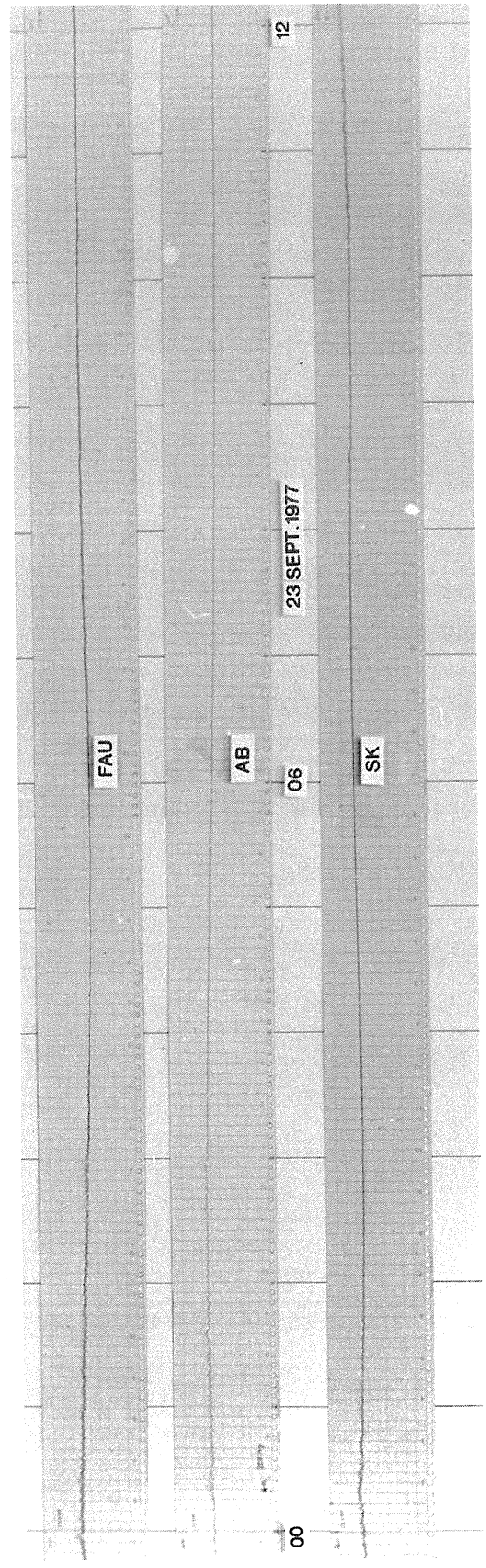
12
06
00
FAU
AB
23 SEPT. 1977
SK

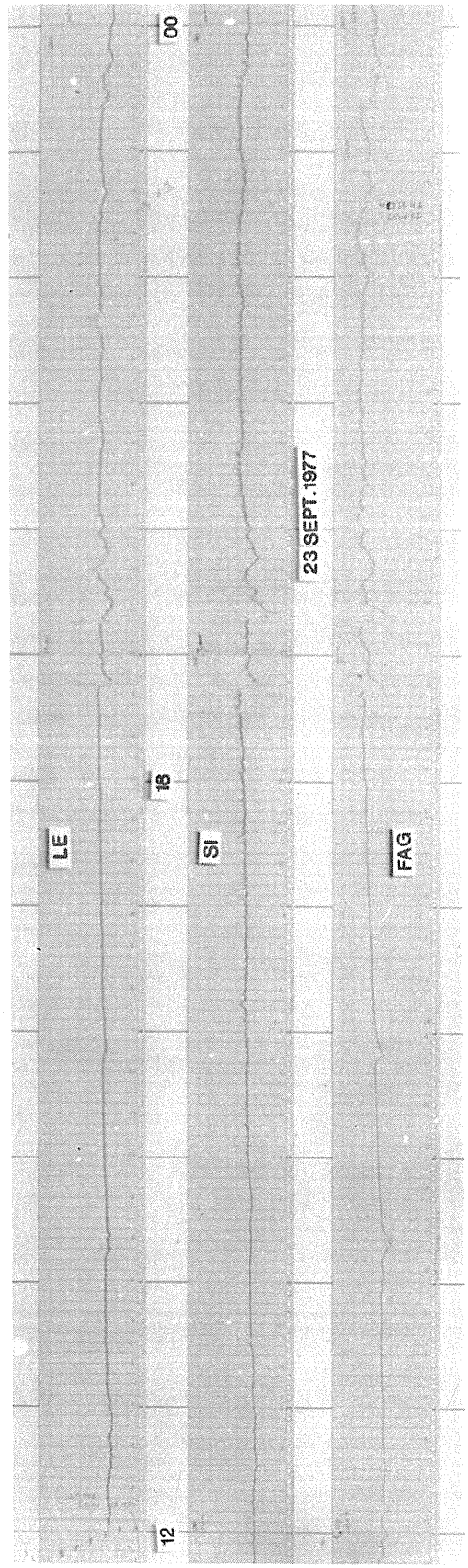
00
18
12
LE
SI
FAG
23 SEPT. 1977

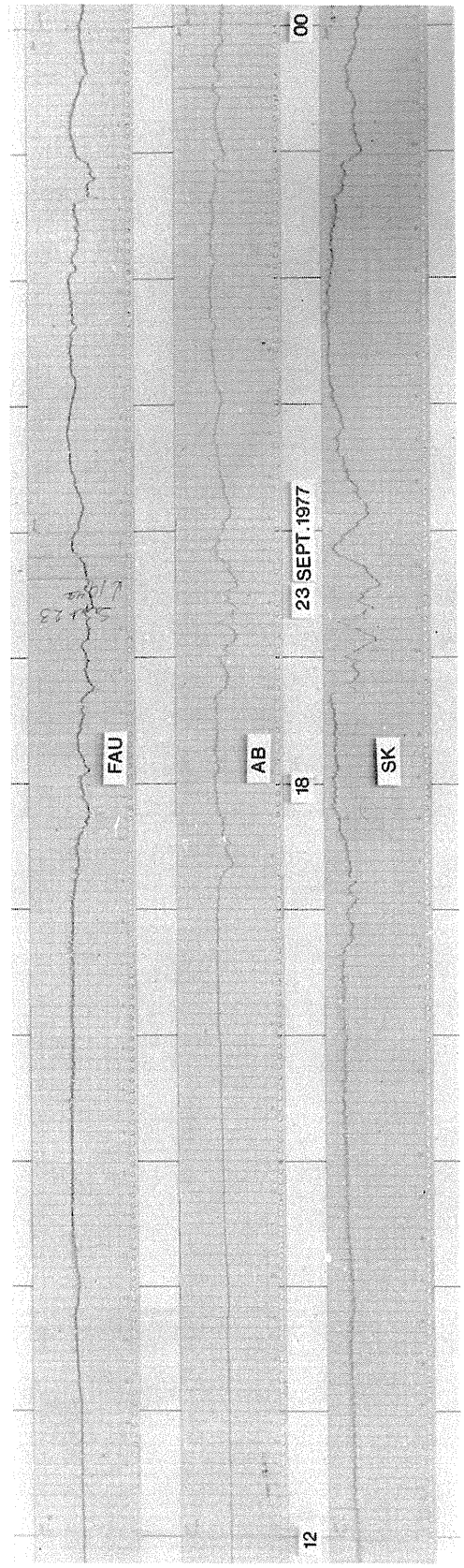
00
18
12
FAU
AB
SK
23 SEPT. 1977

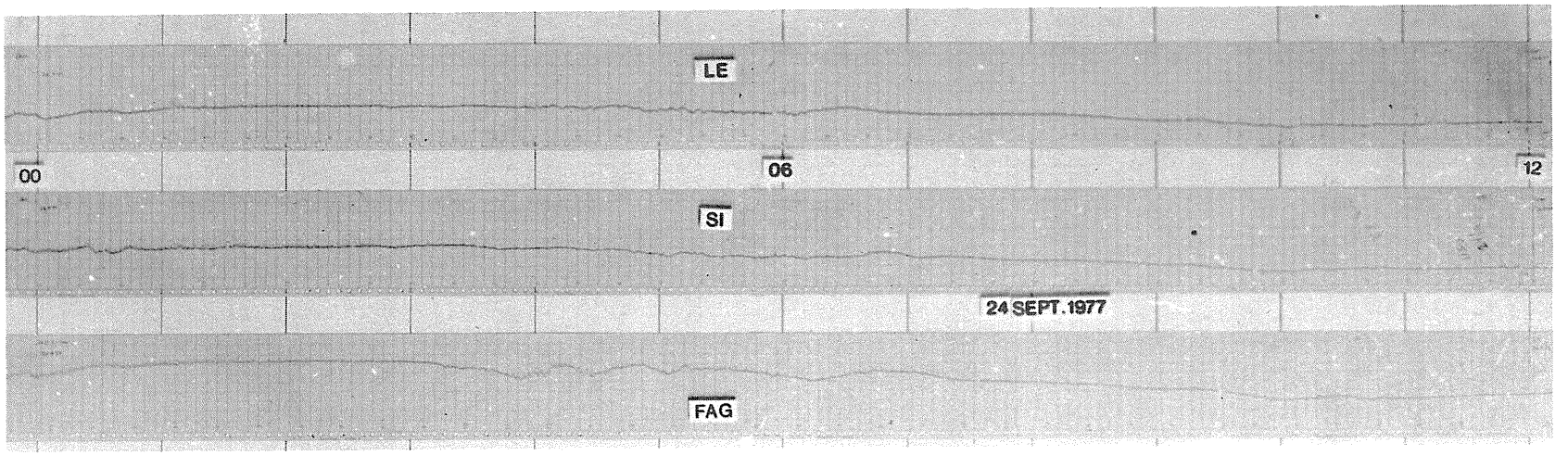
LE
00
06
12
SI
24 SEPT. 1977
FAG

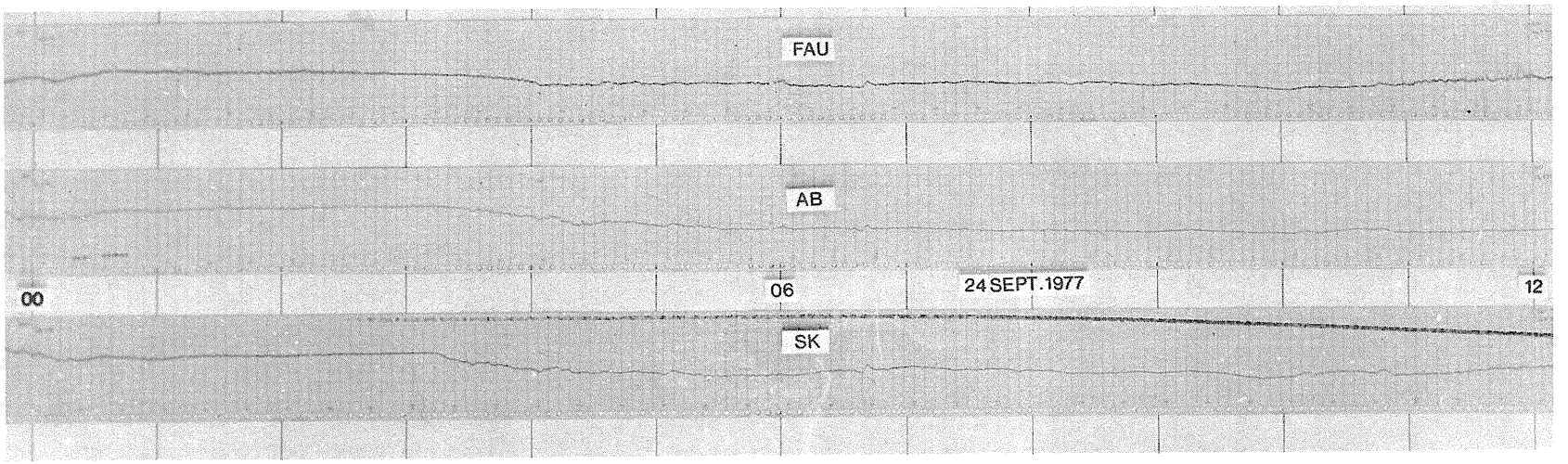
FAU
AB
00
06
24 SEPT. 1977
12
SK

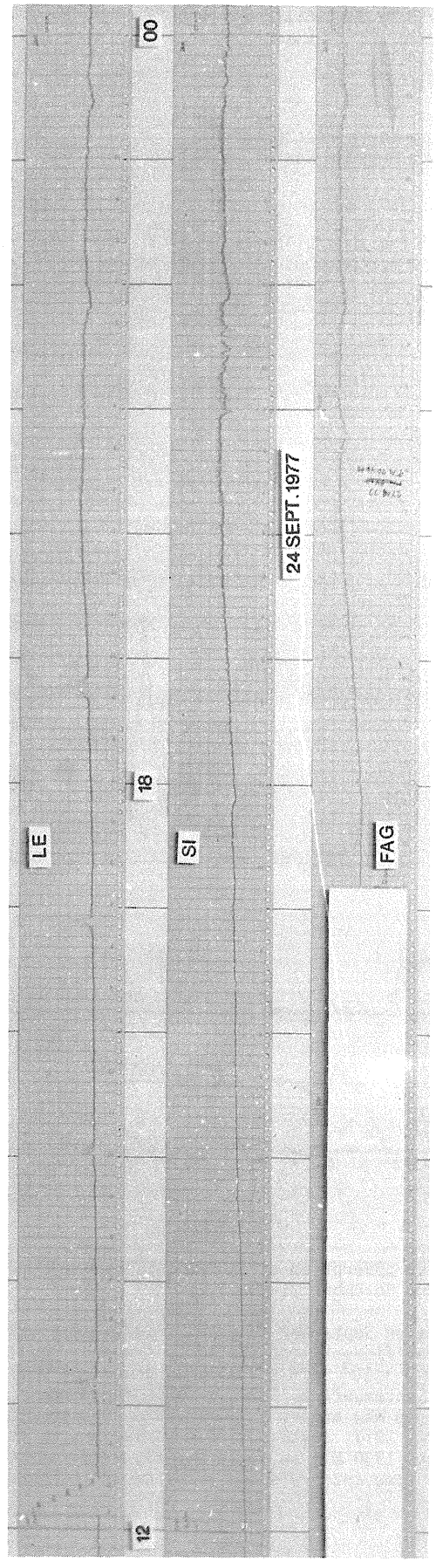
00
18
12
LE
SI
24 SEPT. 1977
FAG

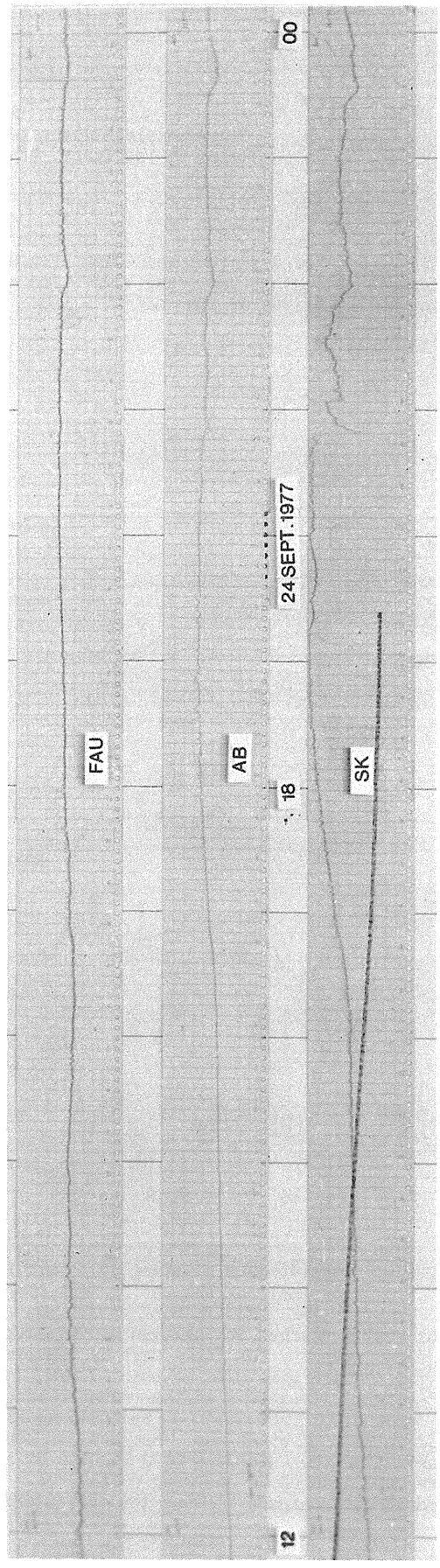
00
18
12
FAU
AB
24 SEPT. 1977
SK

Variations of Cosmic Radio Noise Absorption at Cape Schmidt in September and November 1977

by

A.I. Gusev
Cosmophysical Observatory of the North-West Complex
Research Institute, Cape Schmidt, Magadan Region, USSR

This paper presents 10-min values of cosmic radio noise absorption recorded at Cape Schmidt by 32-MHz (antenna toward zenith) and 40-MHz (antenna toward north geographic pole) riometers (Figure 1). Data are plotted against Universal Time. The arrows show the time of sunrise and sunset at ground level and at the height of 100 km.

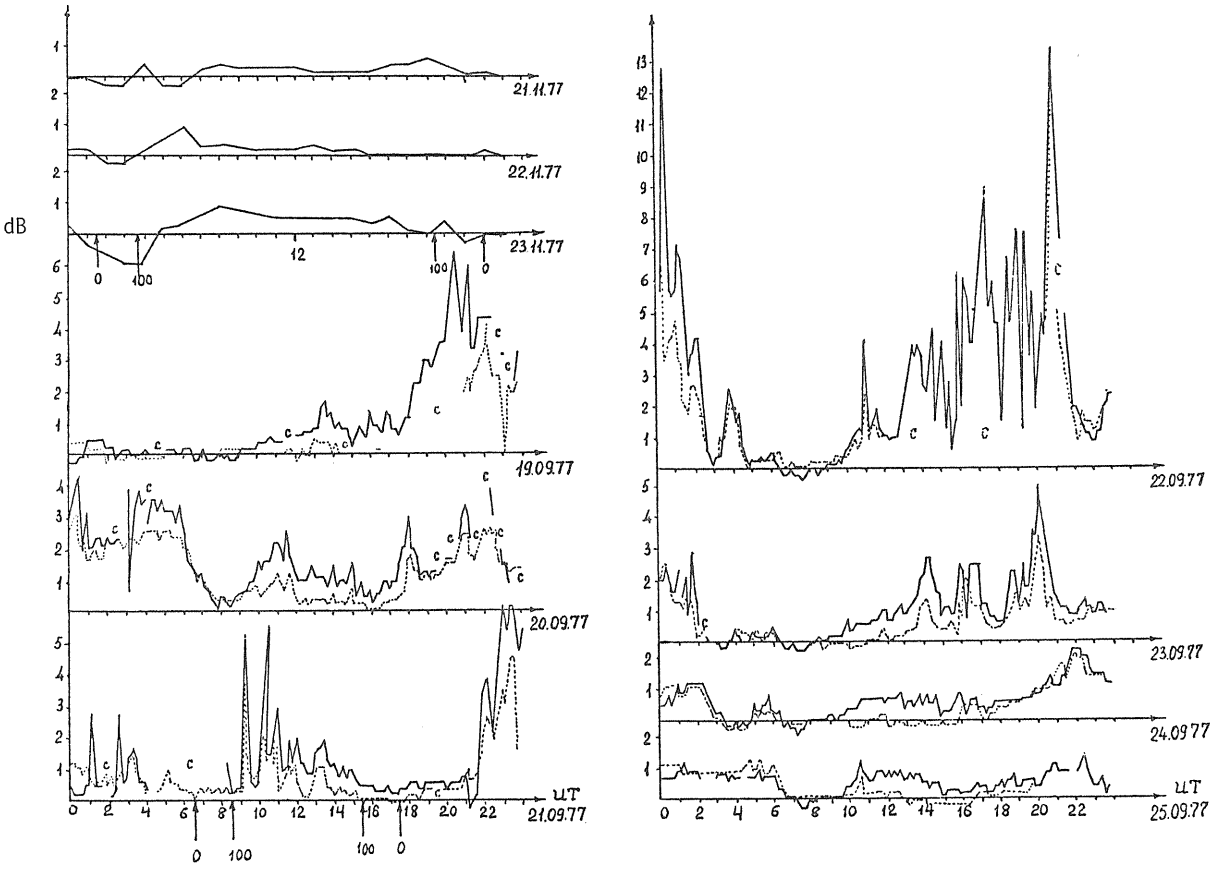

Fig. 1. Cape Schmidt 10-min values of cosmic radio noise absorption at 32 MHz (solid line) and 40 MHz (dashed line) for the period September 19-25 and November 21-23, 1977.

Absorption reaches its maximum during daytime hours on September 19 and 22, 1977. Evaluation of proton flux intensity for these days by the riometric coefficients introduced in Krymskii et al. [1977] yields for the energies greater than 15 Mev, I_{19} (>15) ~9 • 10^2 cm^{-2} s^{-1} $ster^{-1}$, and I_{22} (>15) ~4 • 10^3 cm^{-2} s^{-1} $ster^{-1}$. Analysis of the riometer records for September 21, 1977 reveals radio noise in the intervals 1915 to 1940 UT and 2345 to 2355 UT at 40 MHz and in the intervals 2100 to 2150 UT and 2230 to 2240 UT at 32 MHz. Besides, on September 22, 1977 quasi-periodic variations of absorption are observed in the intervals 0000 to 0400 UT and 1400 to 1930 UT; on September 23, 1977 these intervals are 0000 to 0100 UT and 2000 to 2100 UT. The wide time intervals may evidence the different physical mechanisms responsible for the variations.

The diagrams show that the November 22, 1977 event does not result in a noticeable increase of cosmic noise absorption, which may be connected with the low intensity of proton flux.

REFERENCES

KRYMSKII, G.F. A.I. GUSEV and YU.A. ROMASCHENKO 1977 On the Relation of Riometric Absorption with the Flux of Precipitating Particles and Atmospheric Parameters, *Relation of Physical Processes in the Earth's Ionosphere and Magnetosphere with the Parameters of Solar Wind*, Yakutsk, 3-26.

Absorption of Cosmic Radio Emission in Low Ionosphere from Tixie Bay Data for September 19-26, 1977

by

A.M. Novikov and V.I. Ipatiev
Institute of Cosmophysical Research and Aeronomy, Yakutsk Branch
Siberian Department of the USSR Academy of Sciences, Yakutsk, USSR

In the second half of March 1977 a series of solar flares was observed in the course of which energetic protons were generated. The greatest solar flare of importance 3B was on September 19 at 0955-1125 UT. The flare coordinates were N05W57. Solar protons were registered over Tixie Bay (71.6°N, 128.9°E) ten hours after the flare began.

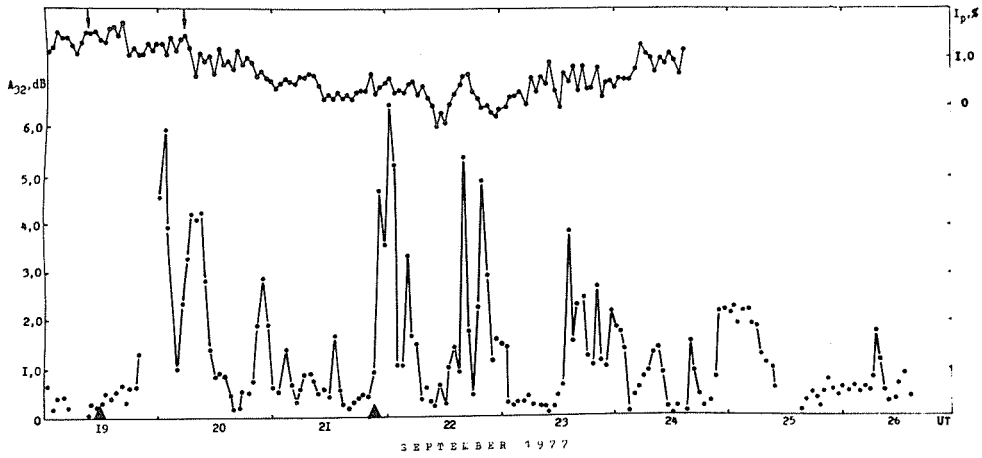

Fig. 1. Temporal variations of the cosmic radio emission absorption and of meson component intensity of cosmic rays on the Tixie Bay ionization chamber measurements from September 19-26, 1977. Arrows show beginning of the solar flares, triangles show beginning of geomagnetic substorms.

Figure 1 gives the temporal variations of the cosmic radio emission absorption level on the frequency 32 MHz following the September 19 flare. The flare was followed by a Forbush decrease of galactic cosmic ray flux. The Forbush decrease was registered by the meson ionization chamber located on the ground. This chamber did not register the flashes. This fact testifies that the solar protons of particles with energies 10^9 eV and more were not in the spectrum.

The temporal variations of the cosmic radio emission absorption on the frequency 32 MHz, registered from September 20-26, are characterized by two groups of intensive increases. The first group of increases with maximum amplitude 6.0 dB was probably caused by invasion of solar protons into the low ionosphere from the flare on September 19 and was observed at the end of September 19, 20 and 21. The second group of increases with maximum amplitude 6.5 dB was observed at the end of November 21, 23, 24 and 25. This group of the increases was probably caused by the solar flare of importance 1B on September 20 at 0605-0650 UT. The flare coordinates were N08W60.

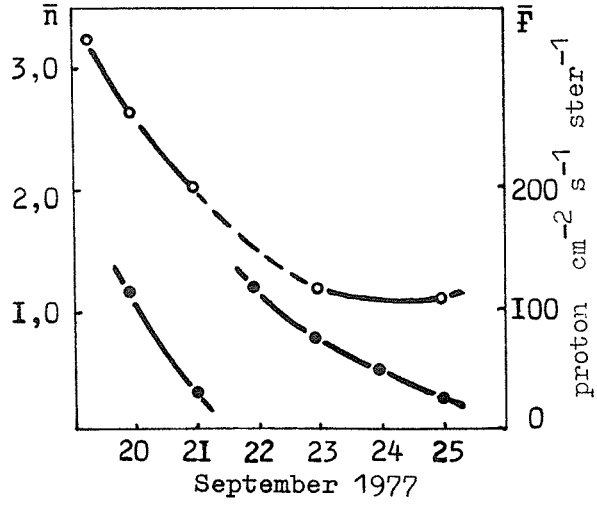

Fig. 2. Temporal variations of the proton flux F and of the frequency dependence coefficient $\bar{n}$ in September 1977 for observations at Tixie Bay. Time is 135 E.

During September 20-25 we analyzed the frequency dependence which connects the magnitude of the cosmic radio emmission absorption in the ionosphere with radiowave frequency according to V. M. Driatsky [1974] as follows: $\frac{A_{32}}{A_{40}} = \left(\frac{f_{32}}{f_{40}}\right)^{\eta}$ where A_{32} and A_{40} are absorption in decibels on the frequencies 32 and 40 MHz, η is the coefficient of the frequency dependence.

Calculations allowed one to establish the average coefficient $\bar{\eta}$, for a number of days during September 20-25. The results are presented in Figure 2 where the decrease of $\bar{\eta}$ with time is seen. This testifies that the absorbing layer is decreasing with time and, consequently, the spectrum is hardening with time. The temporal variations of the proton flux on September 20 and 21 differ from the proton variations on September 22-25.

The main absorption increase at the beginning of September 20 was observed at the time of the main phase of magnetic substorm, the amplitude of which was 1000 γ in the H-component at Tixie Bay. On the afternoon of September 20 a sharp absorption decrease was observed. Probably, one can consider this decrease as the standard one due to a change of the effective rigidity of the geomagnetic cutoff for particles which reach the polar cap edges in dependence upon the local time.

TABLE 1. September 20, 1977

Time UT	$\frac{A_{32}}{A_{40}}$	η	F
05	2.29	3.71	89.13
06	2.72	4.48	154.90
07	1.66	2.27	234.40
08	2.29	3.71	223.90
09	1.71	2.40	229.10
10	1.59	2.07	120.20
11	1.45	1.66	37.15
12	2.15	3.43	89.51
13	1.55	1.96	20.42
14	1.49	1.78	24.55

The absorption of the cosmic radio emission on September 20 from 0500 to 1100 UT was followed by considerable variation of the frequency dependence coefficient which indicates the distribution of solar protons in the spectrum in the process of their invasion into the ionosphere (see Table 1). Estimation of magnitude of the proton flux F was made on the basis of the expression $F=20\ A^{1.7}$ where A is the radio emission absorption on the frequency 32 MHz and is given as protons/cm^{-2} s^{-1} ster^{-1}.

REFERENCE

DRIATSKY, V.M. 1974 "Priroda Anomalnogo Pogloscheniya Kosmicheskogo Radioizlucheniya v Nizhnei Ionosfere Vysokikh Shirot," *Gidrometeoizdat*, Leningrad, *145*, 173.

Observations of Disturbances at Kola Peninsula Stations

by

B.E. Brunelli, G.A. Loginov, G.A. Petrova, and N.V. Shulgina
L.T. Afanasieva, G.F. Totunova, N.F. Fedorova
Polar Geophysical Institute
Academy of Sciences of the USSR
Apatity, Murmansk Region, USSR

Introduction

Some results of ground based observations carried out at stations of the Polar Geophysical Institute are presented here. Figure 1 shows H-component records at Loparskaya (L = 5.2) and intervals with registration of pulsations (Lovosero, L = 5.1). Variations of ionospheric absorption (Loparskaya) are given in Figure 2. Figure 3 gives f plots (Murmansk, L = 5.4) and Figure 4 the intensity of auroral emissions (Loparskaya).

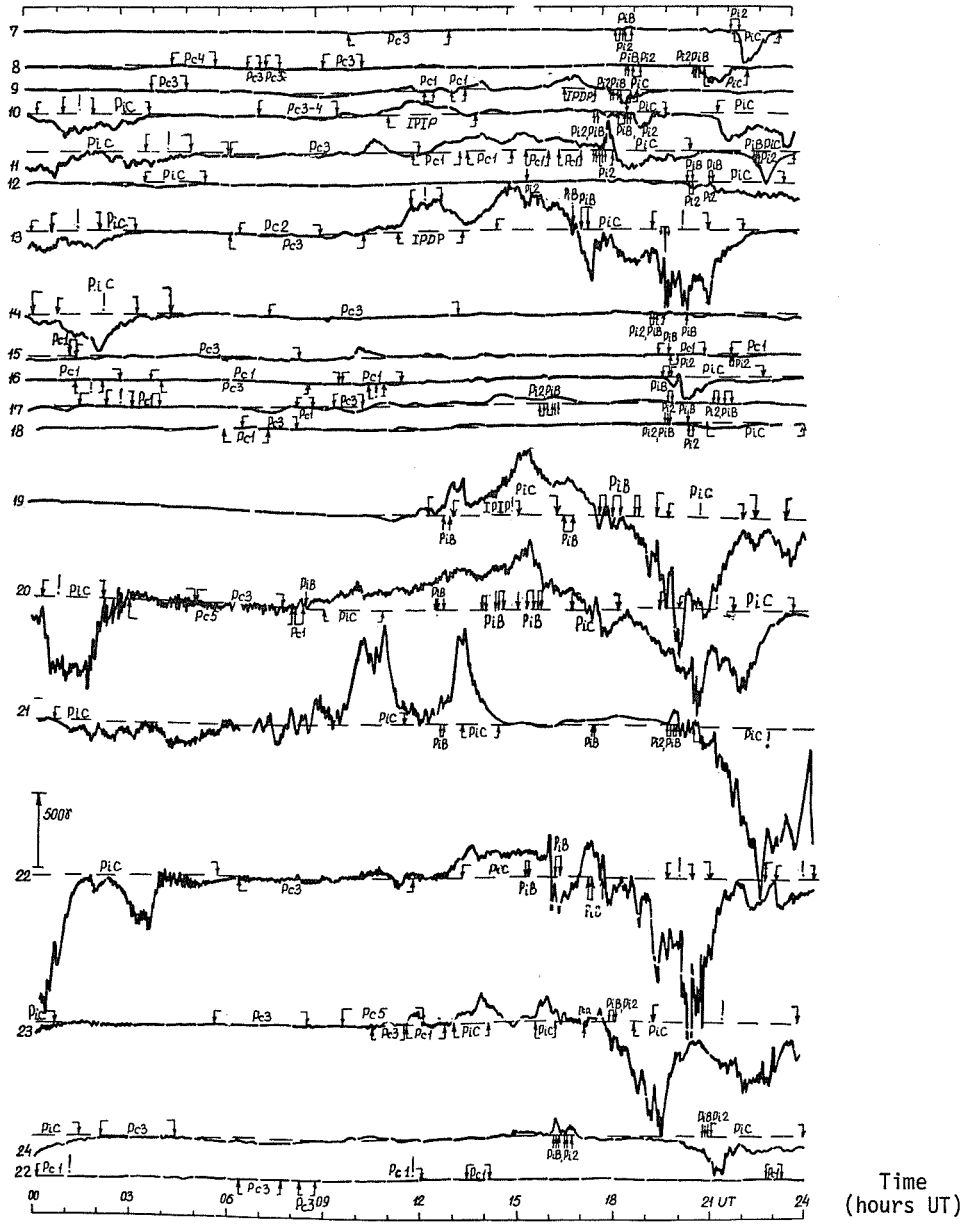

Fig. 1. H-component geomagnetic field records at Loparskaya (L = 5.2) and intervals with registrations of pulsations at Lovosero (L = 5.1).

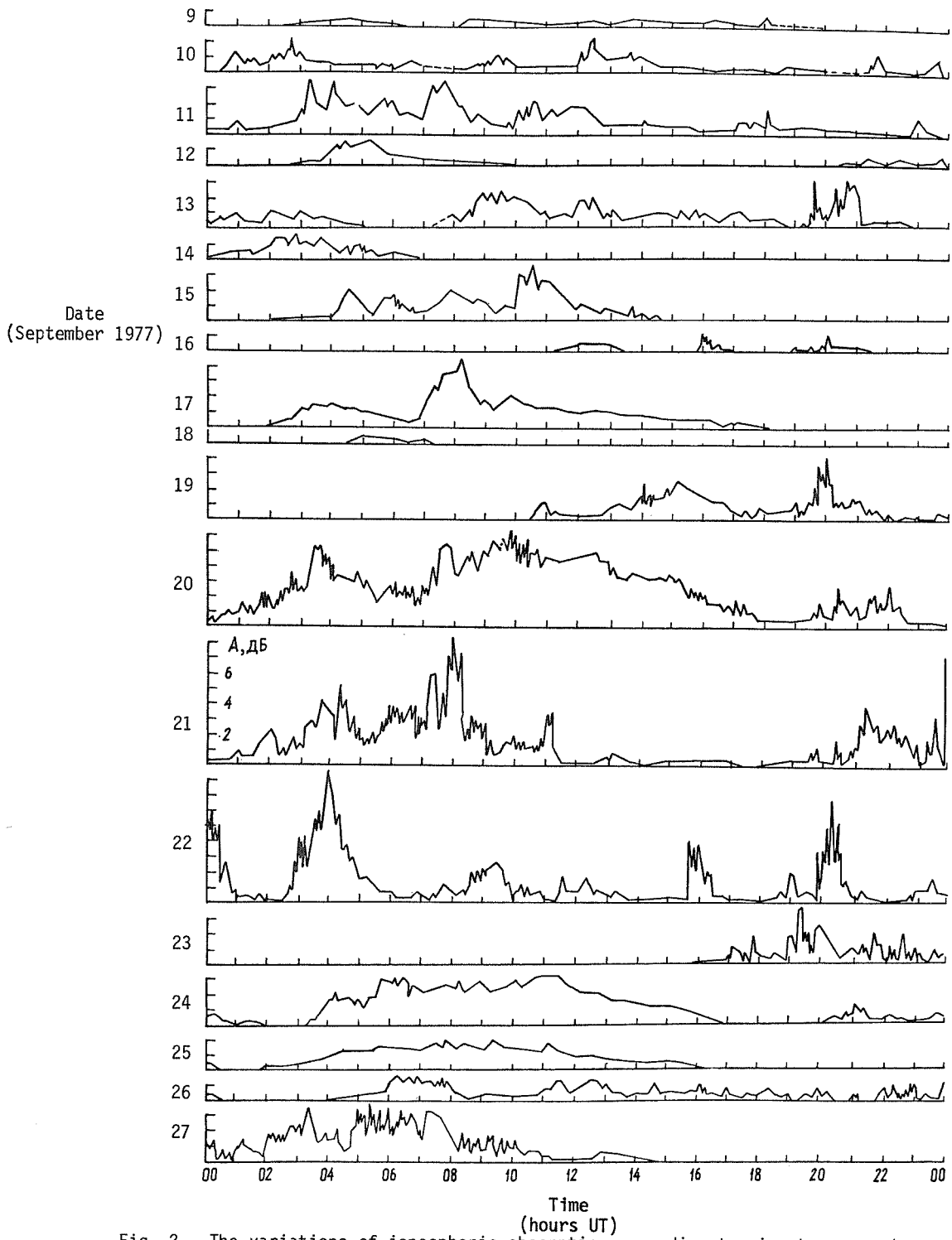

Fig. 2. The variations of ionospheric absorption according to riometer records (Loparskaya, 32 MHz).

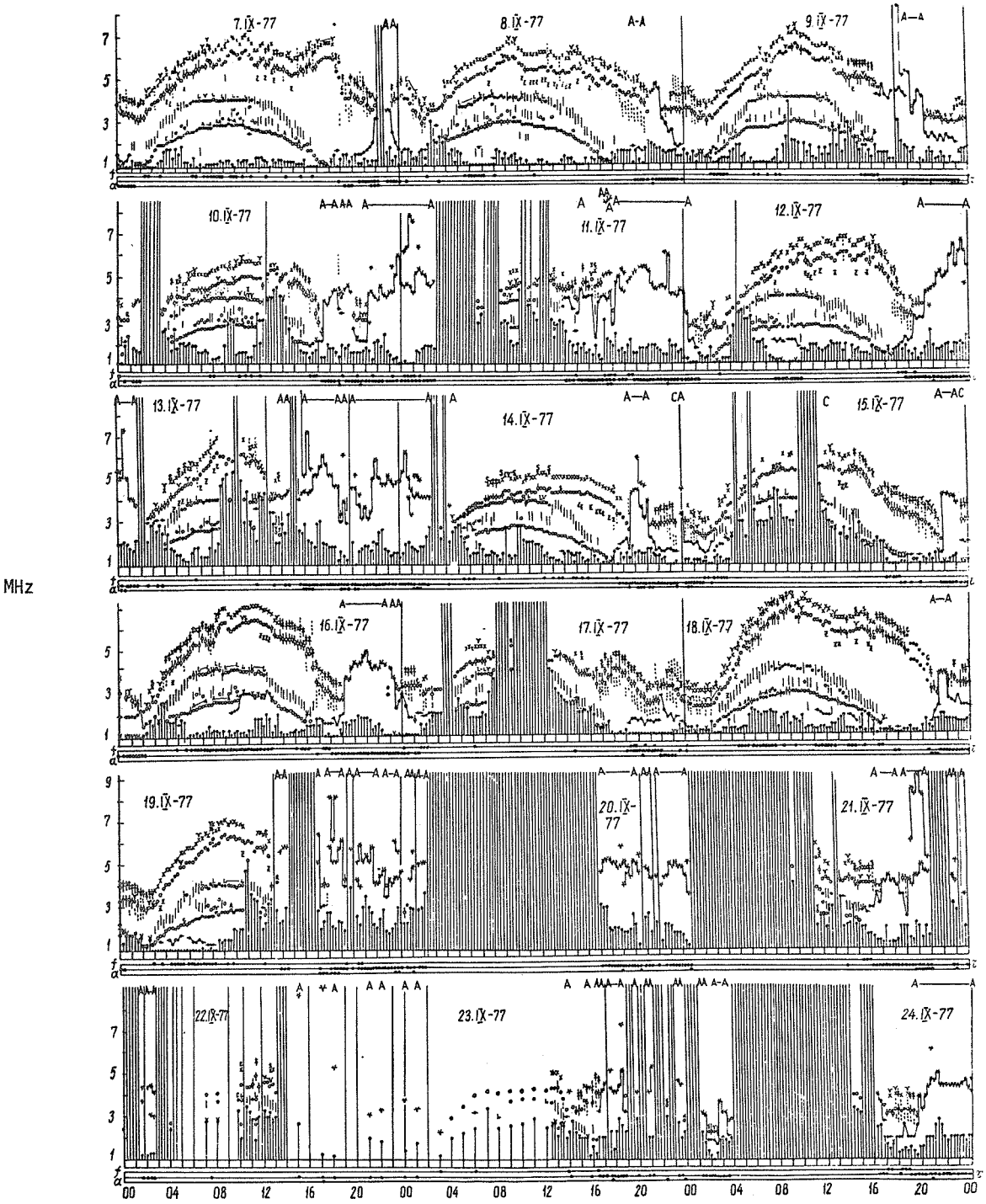

Fig. 3. f plots (Murmansk, L = 5.4).

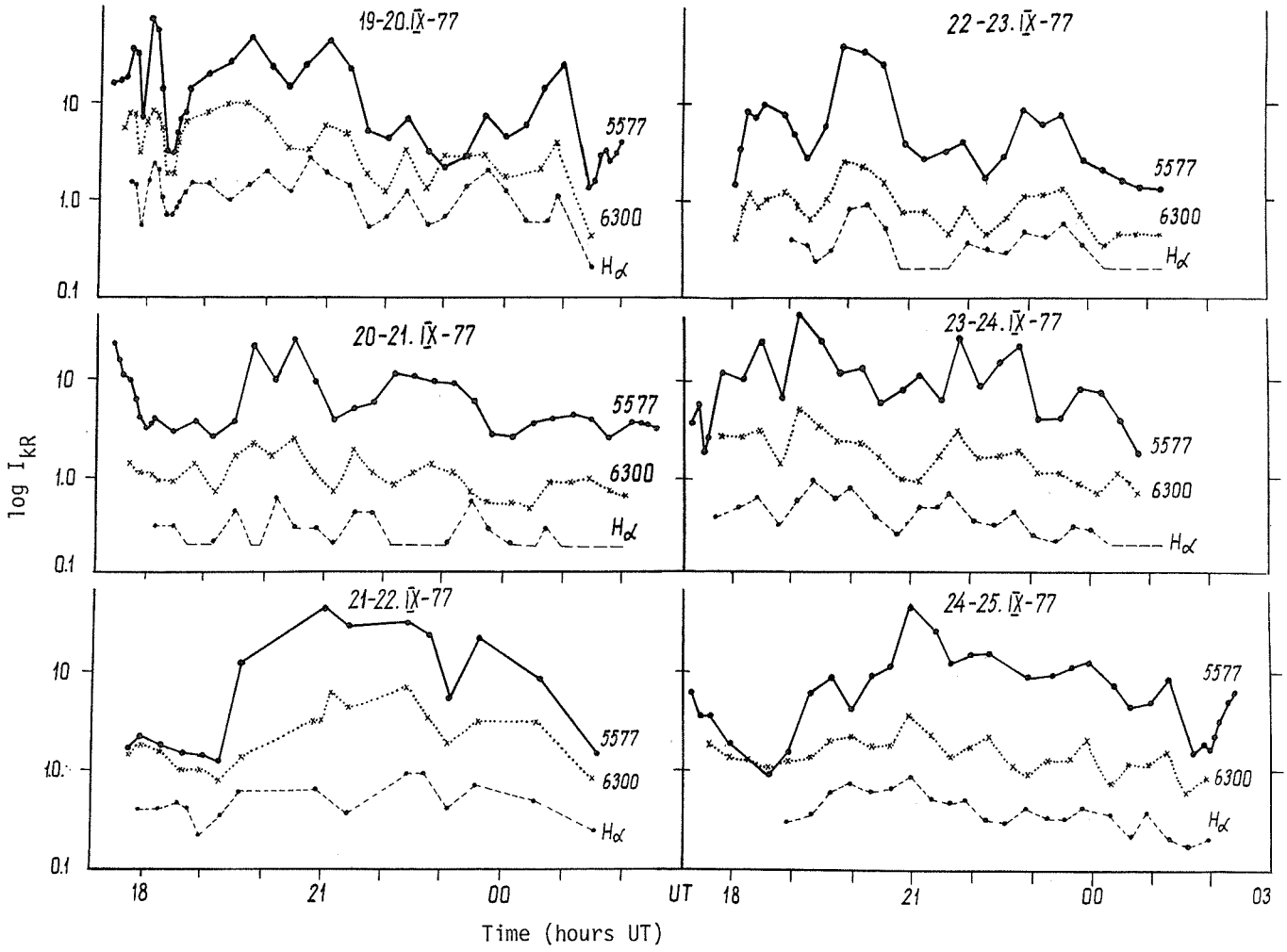

Fig. 4. The intensity of various auroral emissions (log I_{kR}).

As one can see from these data, some geophysical phenomena which appeared during the interval of September 7-24 are connected with proton precipitations. Characteristics of these phenomena are a smooth increase of absorption during daytime; from sunrise to sunset a relatively constant value or some decrease near noon; the existence of Pc-2, IPDP or IPIP pulsations; and the presence of hydrogen emission in aurora.

The first few days were weakly disturbed, but during daytime of September 9, 10, and 11 increased absorption, pulsations IPDP, Pi-2 + PiB during geomagnetic bays, and increasing of ionization in the F region which breaks the smooth variations of foF2 were observed. The changes of absorption were not as smooth as during common hydrogen events. Variations of absorption, perhaps connected with moderate hydrogen precipitation, were also observed on September 13 and 15. The short-time intensifications of absorption were superposed on the smooth daytime increases of the previous days. During the second half of September 13 the moderate magnetic storm began. The sequence of geophysical phenomena which arose on September 13 and 14 were typical for electron precipitation.

The day of September 16 was relatively quiet; only small increases of absorption were registered. At evening a substorm with typical pulsations and a dense sporadic layer appeared. A weak aurora with intensity about 2-3 kR in 5577 Å and 0,I - 0.15 kT in Hα-emission was observed northward from Loparskaya. The energy of the electron flux, according to our spectral observations, was about 1 erg/cm^{2}s. The substorm was followed by the increase of morning type absorption and, after sunrise, a new increase perhaps connected with the developing PCA-event. The variations of absorption as before are more complicated than usual for PCA. During the night of September 17-18 only a weak aurora ($I_{5577} \geq 1$ kR) was observed. During the following night, after a relatively quiet day, a weak aurora with slight Hα-emission was observed northward from Loparskaya.

On September 19 a moderate magnetic storm appeared. Its beginning coincided with unusually intense IPIP pulsations. At the dark time the bright aurora (I_{5577}~30 + 50 kR, I_H ~ 3.5 kR) was observed. The shape of Hα corresponds to 10-30 keV particle energy. The intensity of Hα-emission undergoes multiple changes simultaneously with the bursts of PiB pulsations.

During the whole day of September 20 the high level of absorption occurred. Its daytime increase is similar to that of a PCA-event, but the existence of PiB pulsations, especially intense between 1300 and 1700 UT, as well as short-time increases of absorption indicate the presence of precipitating electrons superimposed on the PCA-event. During the night the electron aurora was observed, the intensity of Hα-emission was weak, not more than 0.7 kR.

A magnetic storm was in progress during September 21. During the late morning hours and at noon two positive bays were recorded. The data of the chain of magnetic stations allowed us to construct the latitude-time distribution of H-component (Fig. 5). It is interesting to mark two sharp width reductions of the disturbed region (ionospheric current sheet) near 1010 UT.

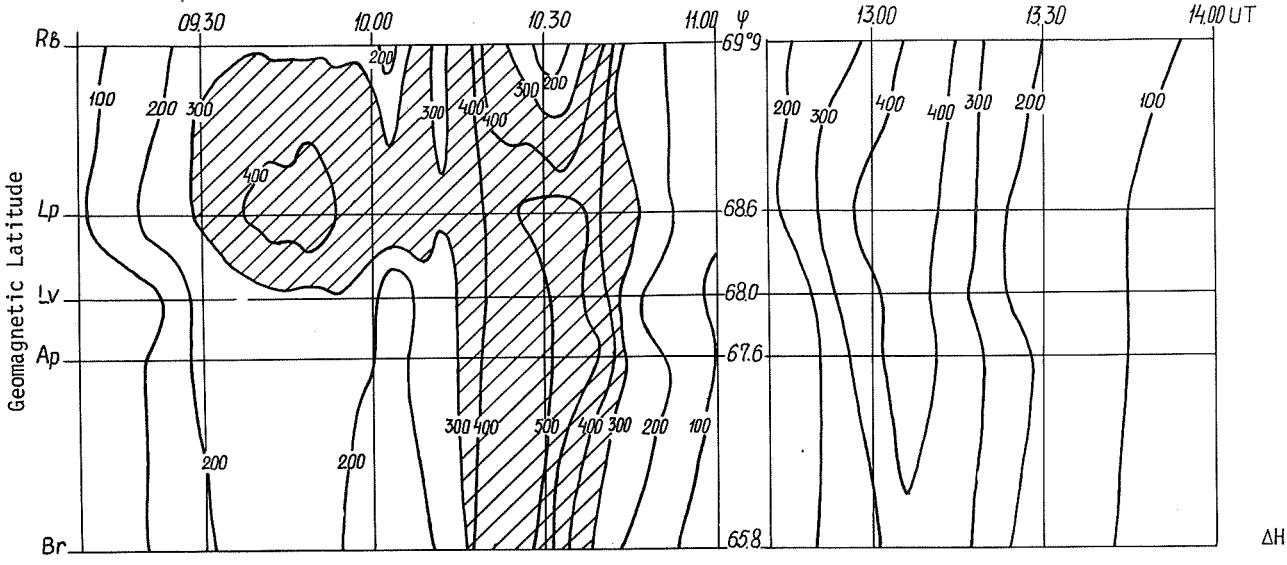

Fig. 5. The variation of latitude distribution of ΔH.

The two following days were highly disturbed, with decreasing foF2 values. On September 24 the intense PCA-event was recorded; the geomagnetic field was perfectly quiet. The smooth increase of fmin was registered by ionosonde also on September 25 and 26.

On November 22 activity was weak, without any exceptional geophysical phenomena. We can, however, mark the existence of long Pc-1 pulsations with unusually large amplitudes, up to 1 nT. One can note also the disturbances in the smooth variation of foF2 and some increase of absorption.

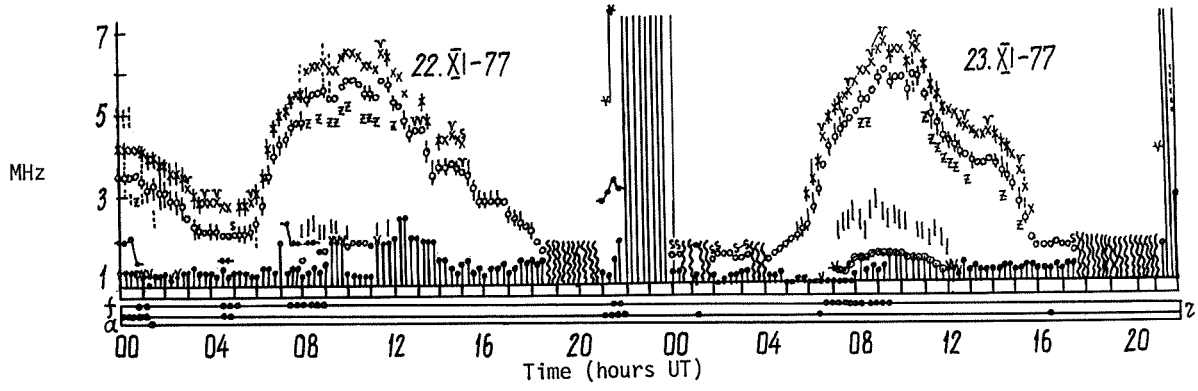

Fig. 6. f plots for November 22 and 23.

Acknowledgment

The authors wish to thank V.Ta.Gorelov for assistance.

Some Significant Ionospheric Disturbance Events During September 1977

by

Harald Derblom
Uppsala Ionospheric Observatory
S-755 90 Uppsala, Sweden

Introduction

Data collected at Uppsala Ionospheric Observatory (geographic coordinates N59.8 E17.6; geomagnetic coordinates N58.5 E105.9; L = 3.3) have been examined in search of significant events during the solar rotations No. 1968-1971 (Aug. 29 - Dec. 14). Only five events were found to be so distinct that they were easy to identify by a visual scan of the records. The times of these events are marked in Figure 1 by the letters A, B, C, D, and E. Four of them occurred in a concentrated period of 3 days, Sept. 19-22.

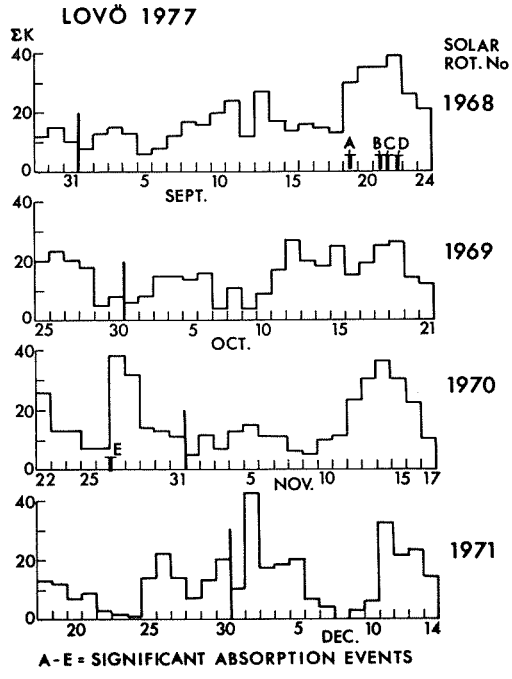

Fig. 1. Variation of the daily ΣK index at Lovö during September-December 1977. Significant absorption events are denoted A-E.

The impression is that the magnetospheric-ionospheric activity is generally higher during September (solar rotation No. 1968) than during the 3 subsequent months. This can be seen in the ΣK distribution presented in Figure 1 and by comparing the monthly sum of the K indices given in Table 1, from Lovö Observatory, which is situated about 70 km east of Uppsala.

Table 1. Variation of ΣK with month at Lovö

Month	ΣK
September	546
October	483
November	394
December	364

It is also apparent in Figure 1 that the activity maximum between Sept. 19-24, which is probably associated with McMath plage region 14943, recurs during the three following solar rotations. Since almost all of the activity obviously occurs during September, this period and the associated events A to D have been selected for a closer study.

September Ionospheric Observations

In Figure 2, ground observations of solar activity, some ionospheric parameters and geomagnetic indices are assembled for comparison. The solar data are from NOAA [*SGD* 1978a and b], the ionosonde data are from Uppsala, and the geomagnetic indices are from Lovö. The Lovö magnetic indices are also considered to be representative for Uppsala.

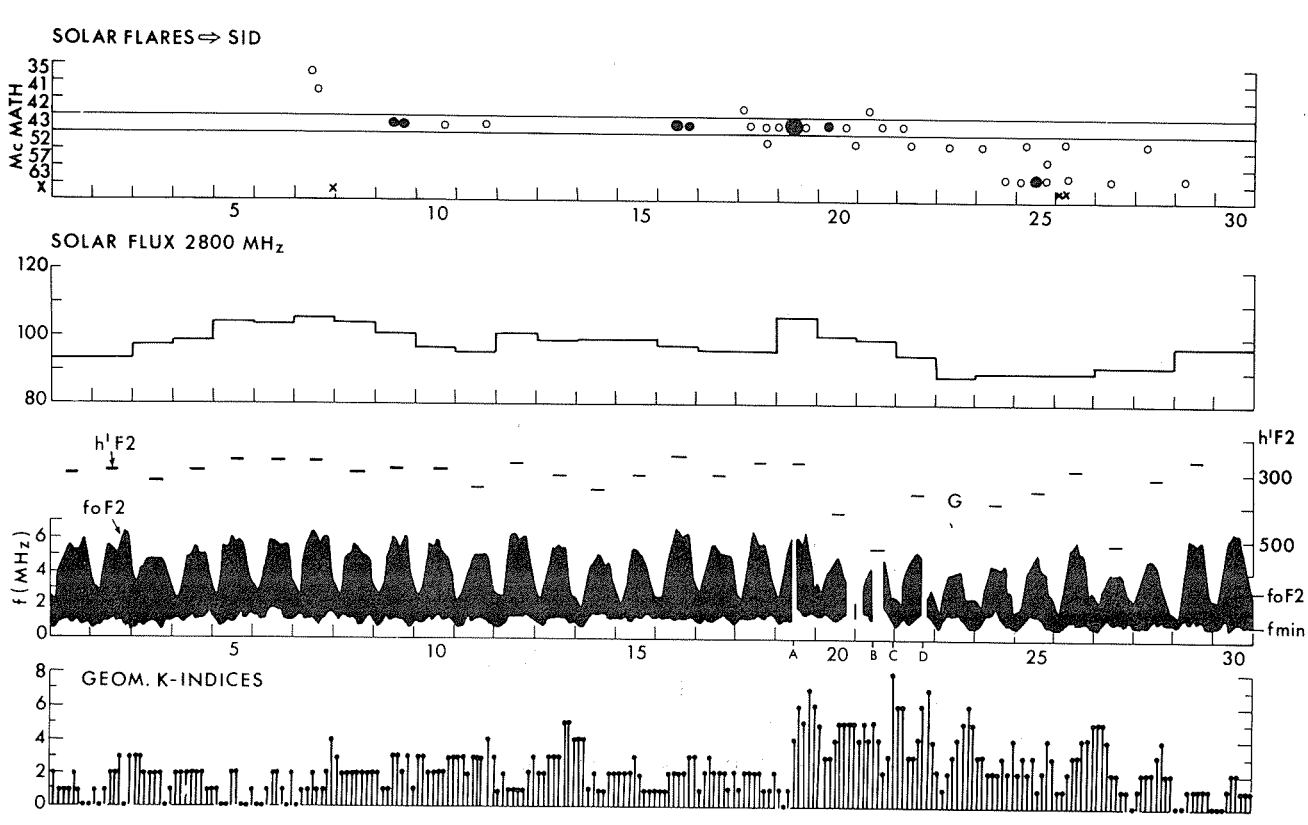

Fig. 2. Assembled solar and ionospheric data for September 1977.

In the upper part of Figure 2 the open and filled circles represent solar flares of different importances and X's denote X-ray events associated with different McMath regions. Region 14943 lies within the pair of horizontal lines. Only events leading to reported SIDs are indicated. An open circle denotes a flare of importance 1, a small dot indicates a flare of importance 2, and a large dot a flare of importance 3. It is obvious that the activity in McMath plage region 14943 is insufficient to explain the great number of disturbances seen in the ionosonde data. Furthermore, no very good correlation exists between the solar flux at 2800 MHz and the activity in the McMath region. Indeed, the solar flux increases in connection with the great flare of September 19 and subsequent activity, but a similarly large flux is found earlier in the month, centered around September 7, without any apparent connection to the McMath plage. However, when we compare the solar flux with the ionosonde data, we find some evidence for a positive correlation: the parameter foF2 is high when the solar flux is high and is low when the solar flux is low. For instance, the foF2 seems to follow the solar flux during the first broad maximum between Sept. 3 and 12, and there is a maximum in solar activity on Sept. 12 as well as a peak in foF2. Also during the period Sept. 19-26, it can be seen that foF2 is high when the solar flux is high and low when the solar flux is low. There are, of course, many exceptions too.

Some other interesting features are found in the ionosonde data shown in Figure 2. An increase in absorption, indicated by fmin, is observed to start Sept. 3 and remains at a high level almost to the end of the month. Comparably low values of fmin, as in the beginning of the month, are reached again only after Sept. 25, when the large disturbance that started Sept. 19 had ceased. An unusual fmin behavior is seen between Sept. 13 and 23. During this period there is no daily variation in the fmin, the absorption being high both day and night. Probably this enhancement of fmin is an indication of PCA, which does not show up in the magnetic activity represented by the K indices in the lowest panel of Figure 2. In fact, it has been reported in the IMS newsletter [1977a] that McMath region 14952 crossed the solar disk between Sept. 8 and 21 and caused enhanced solar proton fluxes on Sept. 9, 13, 16, 19-21, and 24. The largest flux was observed Sept. 19 at 2130 UT, when PCA was reported to reach 4.5 dB. In our data there is no marked enhancement of absorption at that time, which is presumably an indication that the PCA did not reach as far south as Uppsala. The usual daily variation is seen again after Sept. 22.

The noon fmin during the normal period is about 1 MHz, and it increases to 1.4 MHz during the high absorption period after Sept. 13. Assuming that the absorption is proportional to $1/f^2$, we estimate that the absorption is enhanced by a factor of two during this period.

The F2 data exhibit some characteristic features. One is found in the day-to-day variation of foF2. When a disturbance occurs there is a sudden drop in the foF2 and then a gradual increase for some days until a new, sudden decrease appears. Thus, the averaged daily values form a saw-tooth curve that is clearly seen, for instance, between Sept. 3-5, 14-16, 17-19, 23-26, and 27-30, and also on a smaller scale during other days. It seems that the F2 layer is in a continuous state of recovery but really never reaches a steady state.

Moreover, whenever the foF2 value decreases, the h'F2 increases. There is a direct and close correlation between these parameters. In Figure 2, averaged daily values of the virtual height (h'F2) are plotted with a reverse height scale just to enhance visually the close correlation. It is seen that the virtual height and foF2 follow each other in an amazing way and that the virtual height is a very sensitive indicator of disturbed conditions. To verify further the correlation between the F-layer plasma frequency and virtual height, the averaged daily foF2 and corresponding h'F2 values for the month of September are depicted in Figure 3. The correlation is obvious and scattering of the individual points is small.

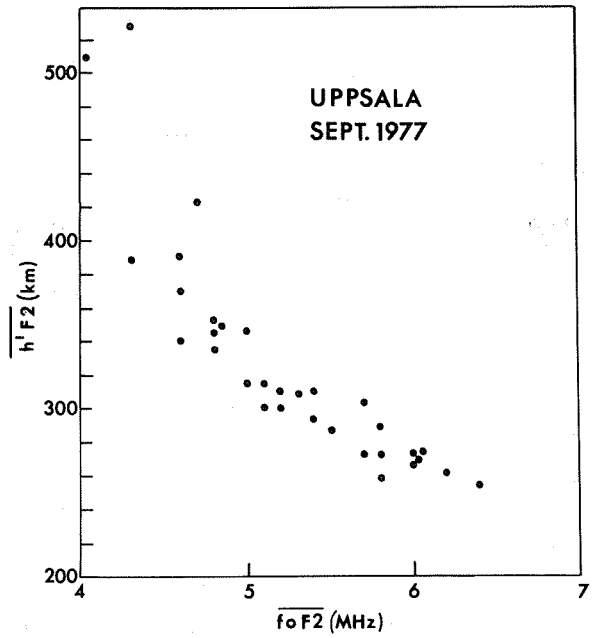

Fig. 3. Plot of the daily average virtual height versus the daily average plasma frequency for the F2 layer.

Of course, it is of interest to interpret what is causing the observed decrease of foF2 and increase of h'F2. An inspection of the parameters characterizing the ionosphere beneath the F layer shows that the increase in h'F is not caused to any significant extent by an increased time delay of the probing radio pulse in the D and E layers. For instance, only a few kilometers increase is found in the h'F1 when the h'F2 increases by 100 km. The correct interpretation seems to be that during a disturbance a real change in the plasma density profile takes place that leads to the observed effects. It is not clear if the driving force behind the redistribution of ions is a change in the ion chemistry or in the transport mechanism or a combination of both. In any case, it seems that whatever the mechanism, it is able to act fast, since we have noticed that a substantial increase in h'F2 (up to 1000 km) and corresponding decrease in foF2 may take place in 10-15 min.

The Selected Events A-D

Portions of the riometer and magnetometer records for the significant events selected are shown in Figure 4. The riometer operates on 27.6 MHz.

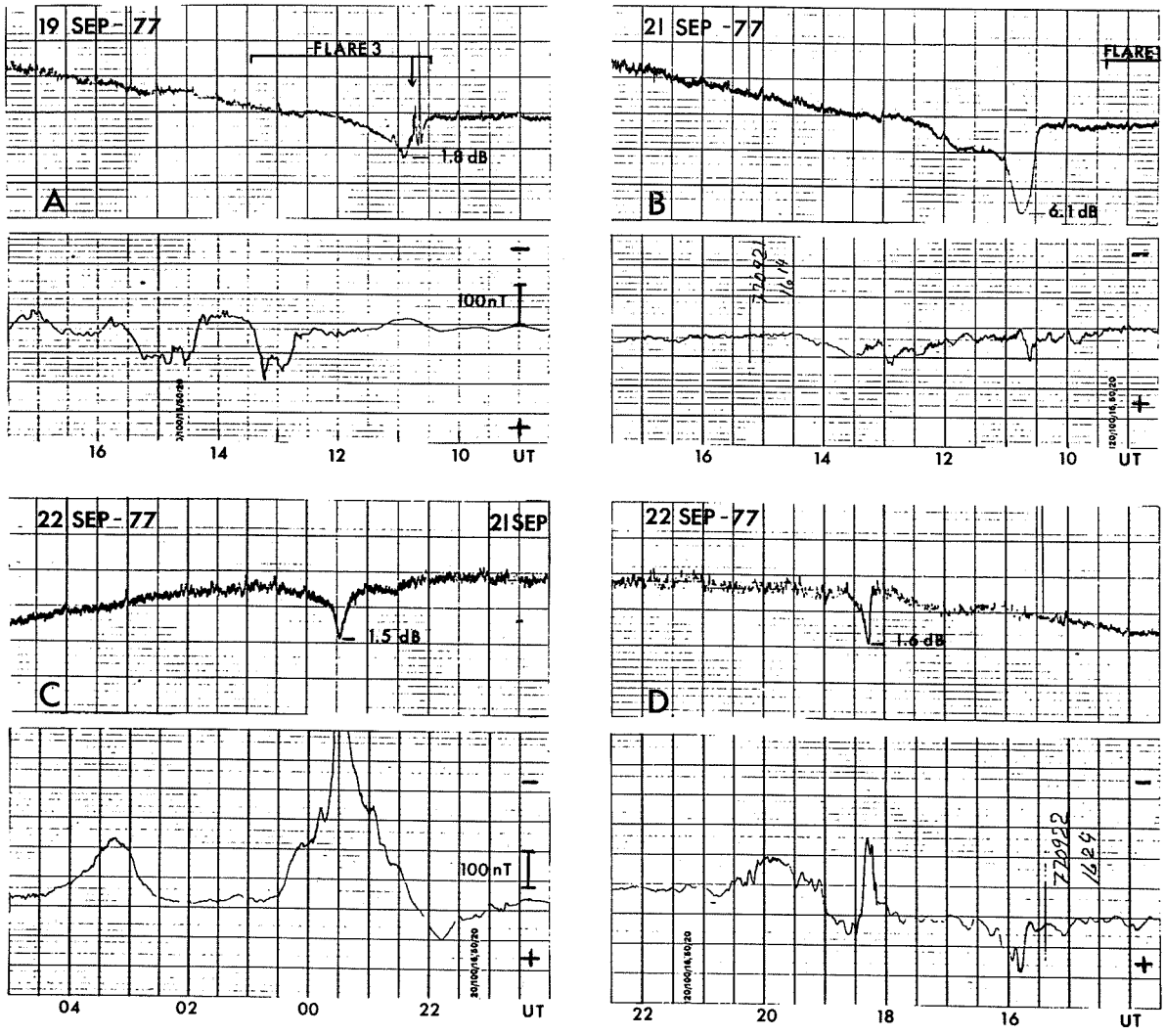

Fig. 4. Selected riometer absorption events observed at Uppsala and corresponding records of geomagnetic H intensity.

Day event of Sept. 19. According to data published in *SGD* [1978c], a 3b optical solar flare with an X2 X-ray maximum began at 1028 UT, maximized at 1045 UT, and ended at 1324 UT. In connection with that flare, indicated in Figure 2 to be in McMath region 14943, a riometer absorption event was recorded at Uppsala that began around 1025 UT, had a maximum absorption of 1.8 dB at 1054 UT, and ended around 1230 UT. No pronounced effect is seen simultaneously in the magnetic activity. It seems obvious that the absorption is caused by enhanced ionization low in the D region produced by solar X-rays. The ionospheric currents are not affected markedly. A blackout occurred in the ionosonde records at 1100 UT and a strongly enhanced fmin occurred between 1200 and 1300 UT. There exist reports of a large, highly energetic proton flux that starts during the flare and reaches its maximum by 2130 UT. No evidence for this is found in our data.

Day events of Sept. 21. This event is denoted by letter B in Figures 1 and 2. A blackout is seen on the ionosonde records at 1100 and 1200 UT followed by high fmin during the 4 following hours. Looking at the riometer record in Figure 4, one sees that a major riometer absorption begins at 1020 UT, shows a maximum absorption of 6.1 dB at 1043 UT, and ends around 1245 UT. The geomagnetic field is slightly disturbed that day but no trace of correlation with the absorption event is seen. We have no explanation for this event. It looks like a flare effect but, to our knowledge, no appropriate flare was reported. The events on Sept. 21 are of considerable interest, because on this day the solar and geomagnetic activity seems to be the highest since the GEOS satellite was launched. GEOS experimenters have reported in the IMS newsletters [1977b, 1978] that the vehicle was located on the dayside magnetosphere and observed at 1015 UT the magnetopause moving past its position toward Earth. Around 1100 UT, GEOS observed large variations in the magnetic field--ones in which the field almost went to zero. The inward push of the magnetosphere occurs some 5 min. before the onset of the absorption event seen at Uppsala. The violent variations in magnetic field seen by GEOS occur in the recovery phase of the absorption bay. No corresponding variations in the magnetic field are seen on the magnetometer records at Uppsala.

Night event of Sept. 21. Event C differs from the two preceding disturbances, since there is strong geomagnetic activity related to the absorption peak. The absorption starts around 2230 UT, has a very sharp maximum of 1.5 dB at 2326 UT, and ends around 0030 UT on Sept. 22. The pronounced negative bay in the magnetic H intensity corresponds exactly with the riometer absorption. We suggest that this event is due to precipitation of energetic electrons. This view is supported by ATS-6 observations of electron injection in the energy range of 20 keV around 2200 UT.

Evening event of Sept. 22. Event D is very sharp and has a remarkably short duration. The absorption begins at 1812 UT, has its maximum of 1.6 dB at 1815 UT, and ends around 1835 UT. It is accompanied by a simultaneous negative geomagnetic bay of the order of 200 nT. The ionosonde shows a blackout at 1700 UT but nothing unusual in the hourly records before and later. Examining the riometer record more carefully, we see that there is a broad absorption with maximum absorption of about 0.5 dB centered around 1700 UT but no related deviation in the H intensity. Tentatively, it is suggested that the absorption around 1700 UT is due to solar X-ray activity. A spike-type absorption event at 1815 UT may be caused by particles of very high energies having a limited effect on the E region and, hence, the geomagnetic activity, but a large effect on the absorbing D region.

Summary

Evidently the ionosphere is more disturbed during September 1977 than during the subsequent months of October, November, and December. An increase in absorption in the HF range by a factor of two is observed to begin September 3, lasting to September 26. Between September 13 and 26, the high daytime absorption also remains during the night.

The foF2 values show a sudden drop when a disturbance starts, followed by a gradual recovery over several days. This pattern is repeated several times. It seems that the F2 layer is in a continuous state of recovery but never reaches equilibrium.

The plasma frequency and virtual height of the F2 layer are closely coupled. Whenever foF2 decreases, the h'F2 increases. This is likely due to a major redistribution of plasma during an ionospheric storm.

Four significant absorption events are analyzed separately. The first day event, September 19, can be linked to a known flare. The second day event, September 21, has a similar pattern but no appropriate flare is reported. The third and fourth events, Sept. 21 and 22, respectively, seem to be caused by high energetic particle precipitation.

REFERENCES

SGD	1978a	*Solar-Geophysical Data,* 403 Part I, 8, March 1978, U.S. Department of Commerce (Boulder, Colorado, U.S.A. 80303).
SGD	1978b	*Solar-Geophysical Data,* 403 Part II, 8-19, March 1978, U.S. Department of Commerce (Boulder, Colorado, U.S.A. 80303).
SGD	1978c	*Solar-Geophysical Data,* 403 Part II, 14, March 1978, U.S. Department of Commerce (Boulder, Colorado, U.S.A. 80303).
IMS	1977a	*IMS Newsletter,* No. 77-10 (World Data Center A for Solar-Terrestrial Physics, Boulder, Colorado, U.S.A. 80303) p. 10.
IMS	1977b	*IMS Newsletter,* No. 77-10 (World Data Center A for Solar-Terrestrial Physics, Boulder, Colorado, U.S.A. 80303) p. 7.
IMS	1978	*IMS Newsletter,* No. 78-4 (World Data Center A for Solar-Terrestrial Physics, Boulder, Colorado, U.S.A. 80303) p. 6.

Ionospheric Behavior at Sanae, Antarctica, Grahamstown, South Africa, and Intermediate Points

by

J.A. Gledhill, R. Haggard and J.P.S. Rash
Department of Physics, Rhodes University
Grahamstown, South Africa

Introduction

This paper reports briefly on some unusual ionospheric events that were observed on September 19 and 24 and November 22, 1977, at Sanae (70°18'S, 02°21'W), at Grahamstown (33°17'S, 22°31'E), and on oblique ionograms taken between these two places.

September 19, 1977

SANAE: The hourly f plot (Fig. 1) shows high absorption near local noon (fmin rises to 4.7 MHz at 1100 UT), and from 1600 UT to midnight. The maximum value reached by fmin was 5.8 MHz at 1900 UT. The following day, September 20, showed blackout conditions until 2200 UT. The F layer also showed a very unusual enhancement coinciding with the latter absorption event, foF2 reaching a value of 9.25 MHz at 1700 UT. It is normally about 5 MHz at this time in September; the values for the preceding two days (September 17 and 18) were 5.5 and 5.4 MHz, respectively.

The high values of fbEs from 2000 UT onward are almost certainly due to particle precipitation, with a- and r- type Es being recorded.

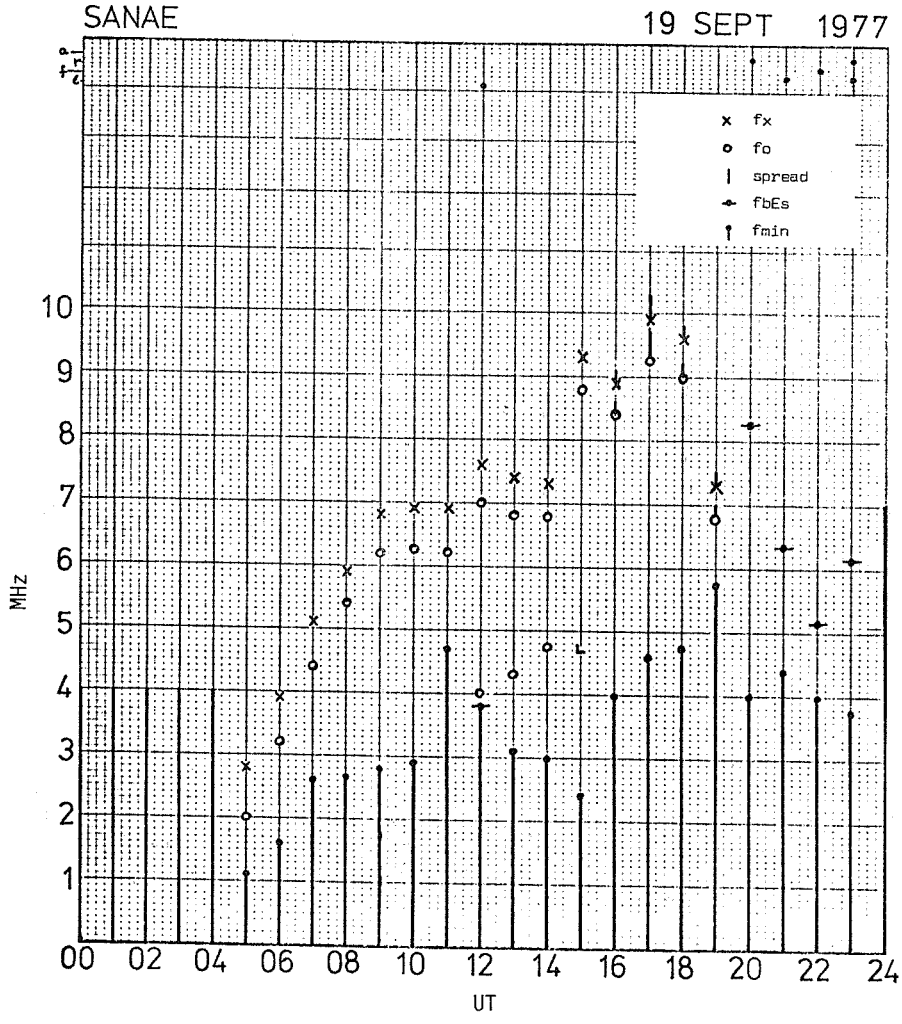

Fig. 1. f plot for Sanae, Antarctica September 19, 1977.

GRAHAMSTOWN: There is a blackout at 1300 LT (1100 UT) (Fig. 2) followed by a high value of fmin 4.0 MHz at 1200 UT. The behavior of the F region is normal until 1500 UT, when an enhancement, similar to that at Sanae, but smaller, occurs, lasting until 2100 UT. The maximum value of foF2, 6.9 MHz at 1700 UT, coincides exactly in time with that at Sanae.

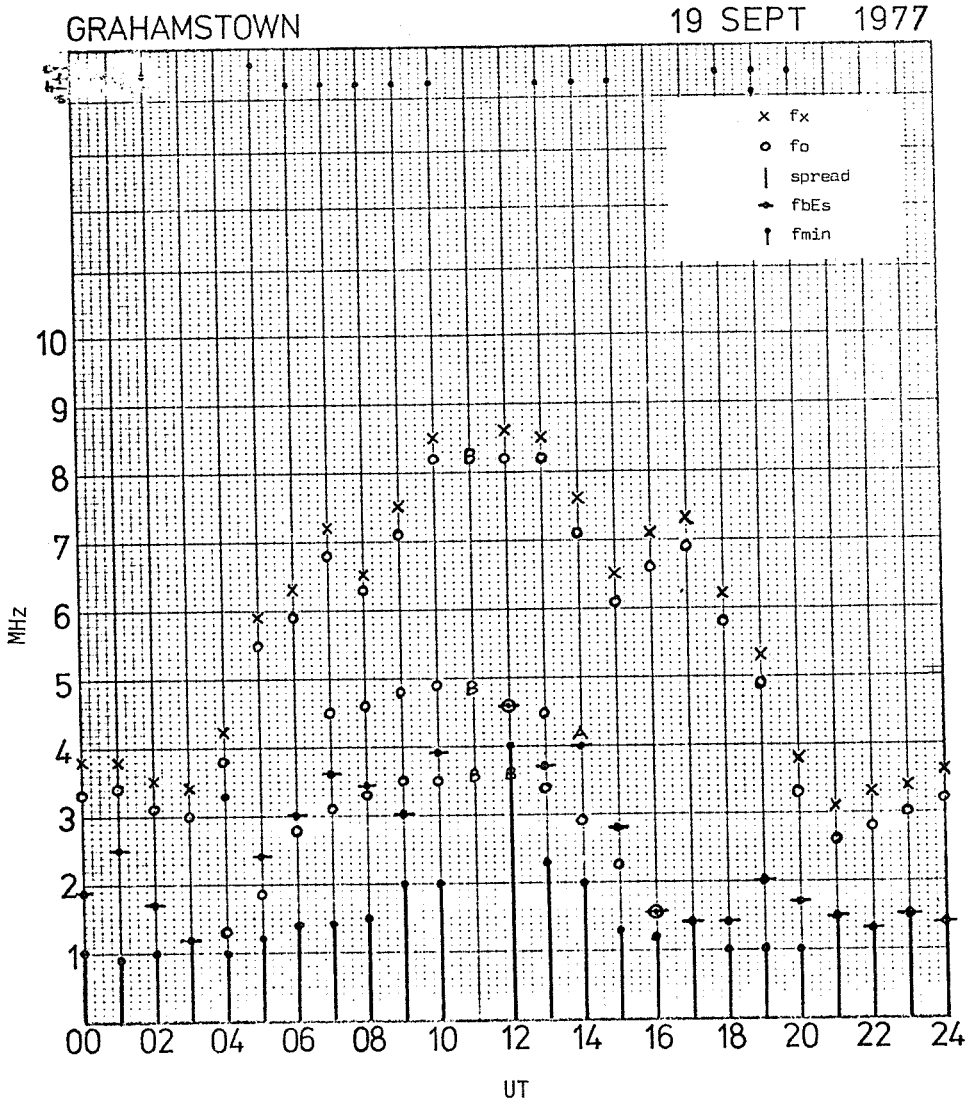

Fig. 2. f plot for Grahamstown, South Africa, September 19, 1977.

OBLIQUE INCIDENCE: Fig. 3 shows a plot of hourly values of the maximum observed frequency (MOF) propagated by each mode over the Sanae - Grahamstown path, a distance of 4470 km; one hop via the F layer is designated 1F, two hops 2F, etc. The 2F and 3F MOF's show considerable enhancement during the same period (approximately 1500 - 2000 UT); their values normally decrease rapidly during the afternoon hours. The 2F MOF value at 1800 UT is 21.5 MHz, compared with values of 9.2 MHz and 10.8 MHz, respectively, on the preceding 2 days.

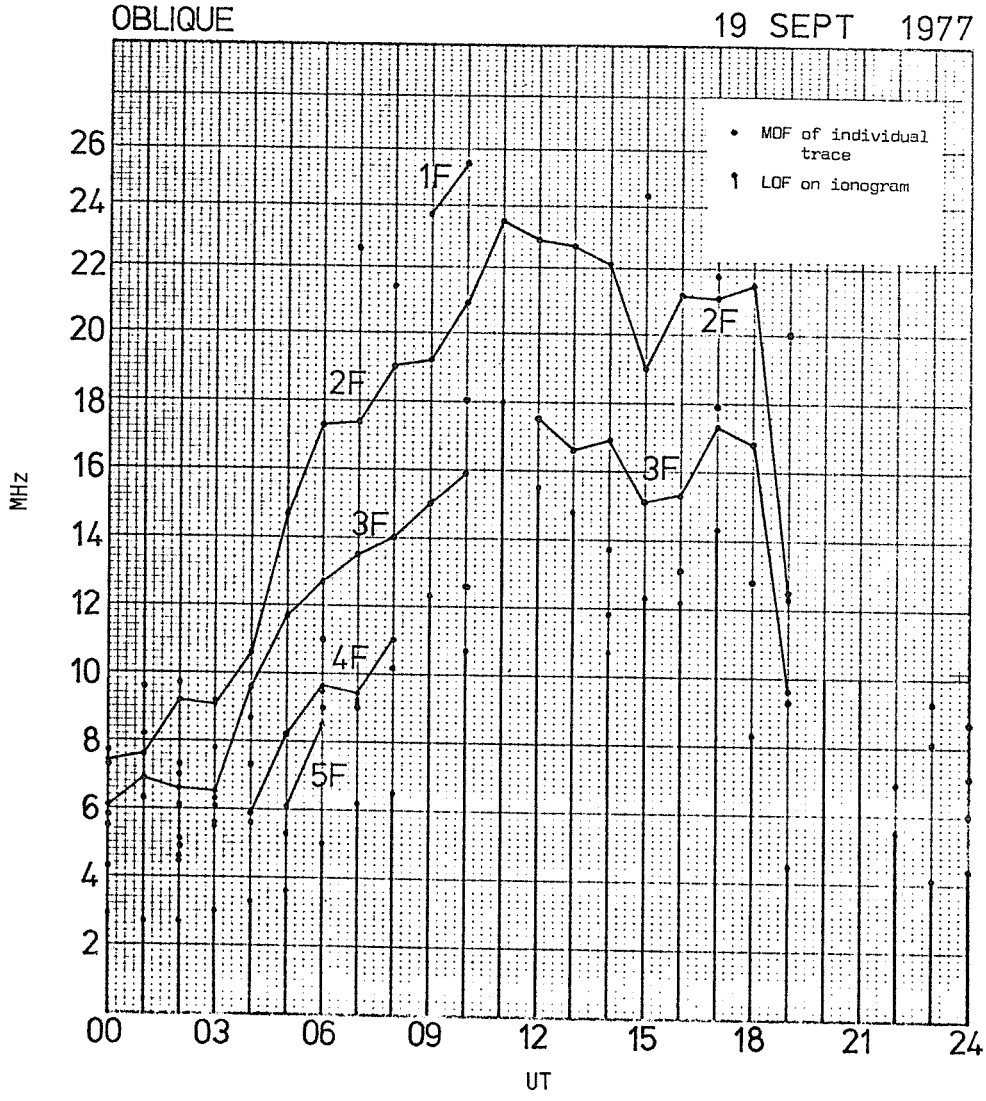

Fig. 3. Oblique f plot for Sanae - Grahamstown path (4470 km) September 19, 1977.

Our experience has shown that the ionosphere at the first reflection point of the 2F-mode transmission is generally the controlling factor in determining the behavior of the 2F MOF; this first reflection point is at about 62°S, 11°E. The presence of the enhancement between 1500 and 1900 UT is evidence of an enhancement of foF2 in this region. Similarly, the increase in the 3F MOF at the same times is evidence of an enhancement of foF2 at the first reflection point of the 3F mode, at about 64°S, 7°E. The maxima of both the MOF's coincide in time with those observed at Sanae and Grahamstown at 1700 UT. The lowest observed frequency (LOF) on the oblique ionogram also shows a maximum at this time, indicating increased absorption.

September 24, 1977

SANAE: The f plot (Fig. 4) shows a blackout between 0300 and 1200 UT. When ionization in the F region does become visible, it is considerably less intense that normal at midday. The high values of fmin (between 4 and 5 MHz) should also be noted.

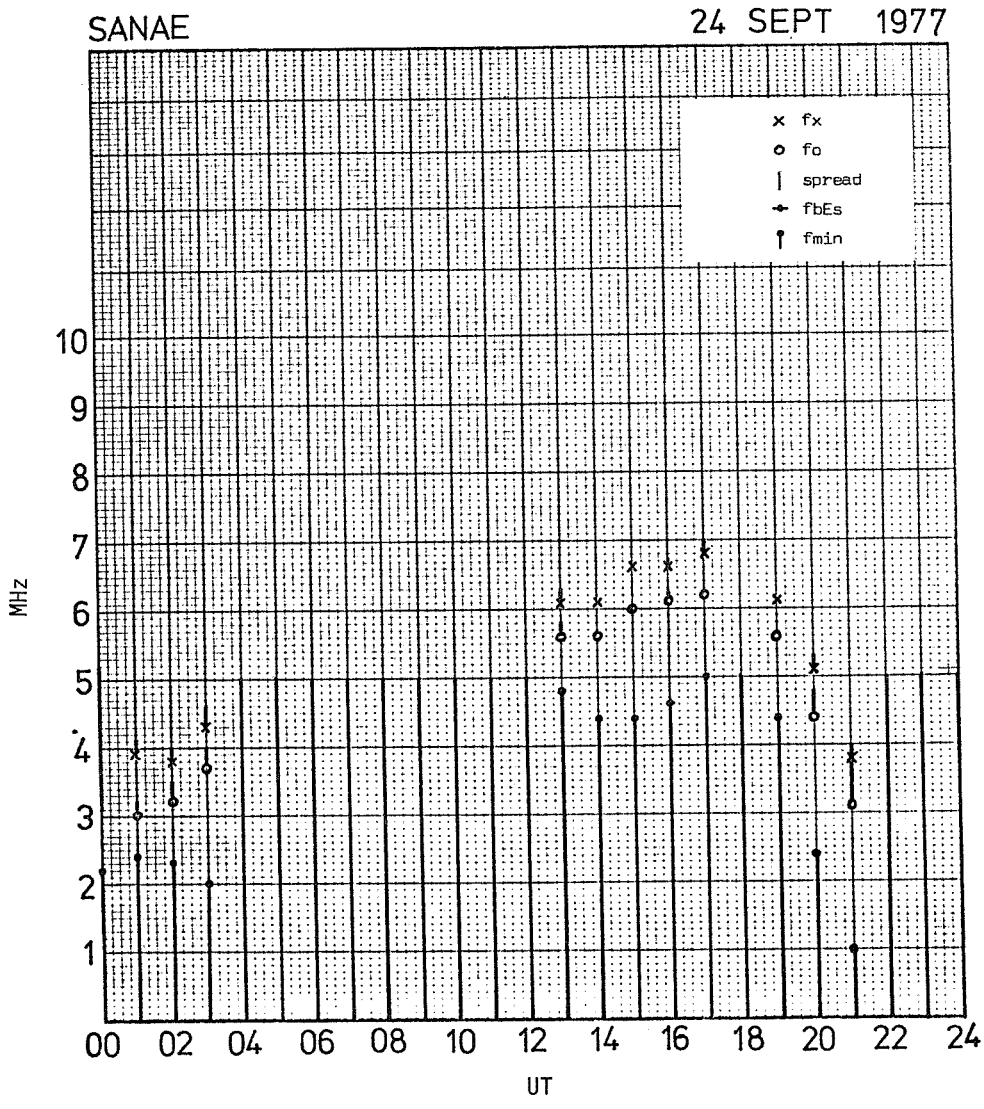

Fig. 4. f plot for Sanae September 24, 1977.

GRAHAMSTOWN: Conditions here were much more normal (Fig. 5) except for the increase of fmin, peaking at 3 MHz at 1100 UT. The median value for fmin for surrounding days is about 2 MHz. The 1200 UT (1400 LT) value of foF2 is appreciably depressed.

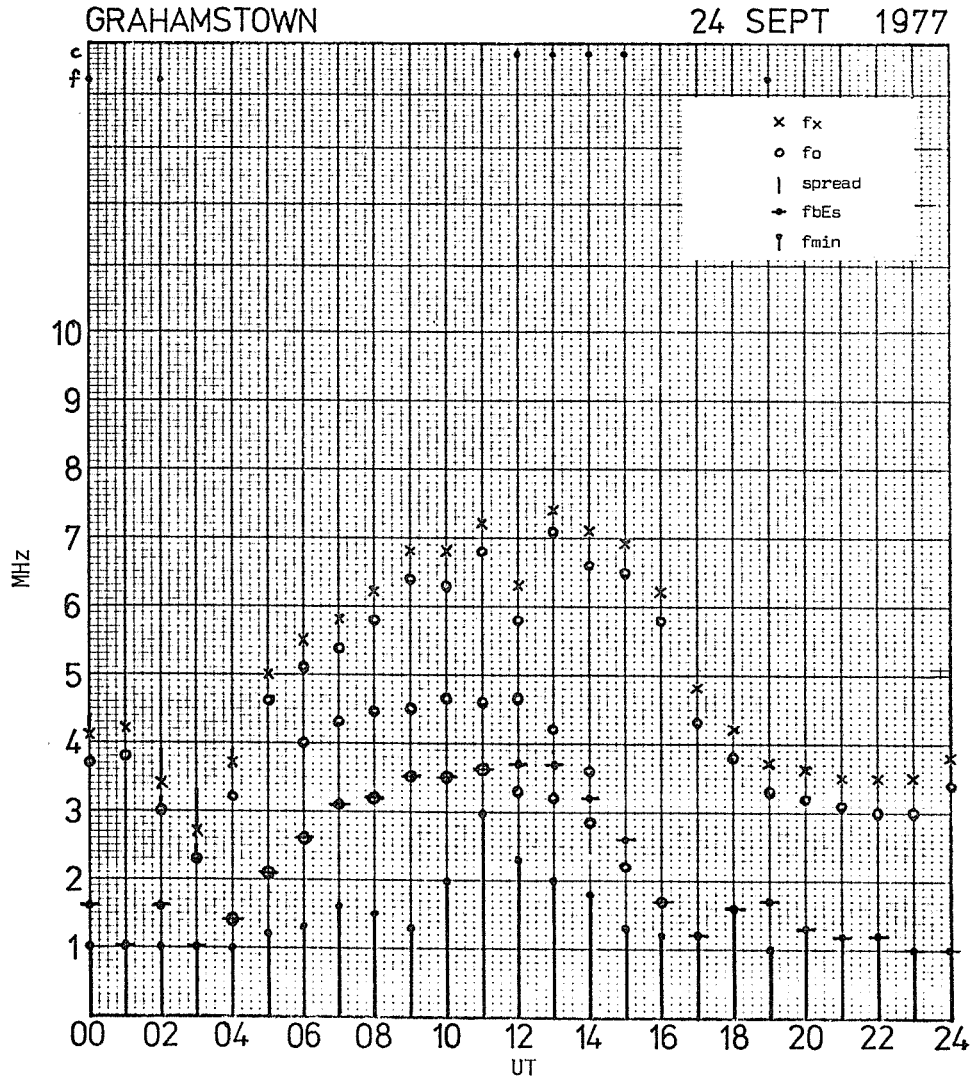

Fig. 5. f plot for Grahamstown September 24, 1977.

OBLIQUE INCIDENCE: The oblique f plot (Fig. 6) shows high absorption (high LOF) for most of the day. The 2F and 3F MOF's appear to be normal around the middle of the day. From 2200 UT, however, the LOF drops considerably, down to 2 MHz (the lower limit of the oblique frequency sweep) at 2400 UT.

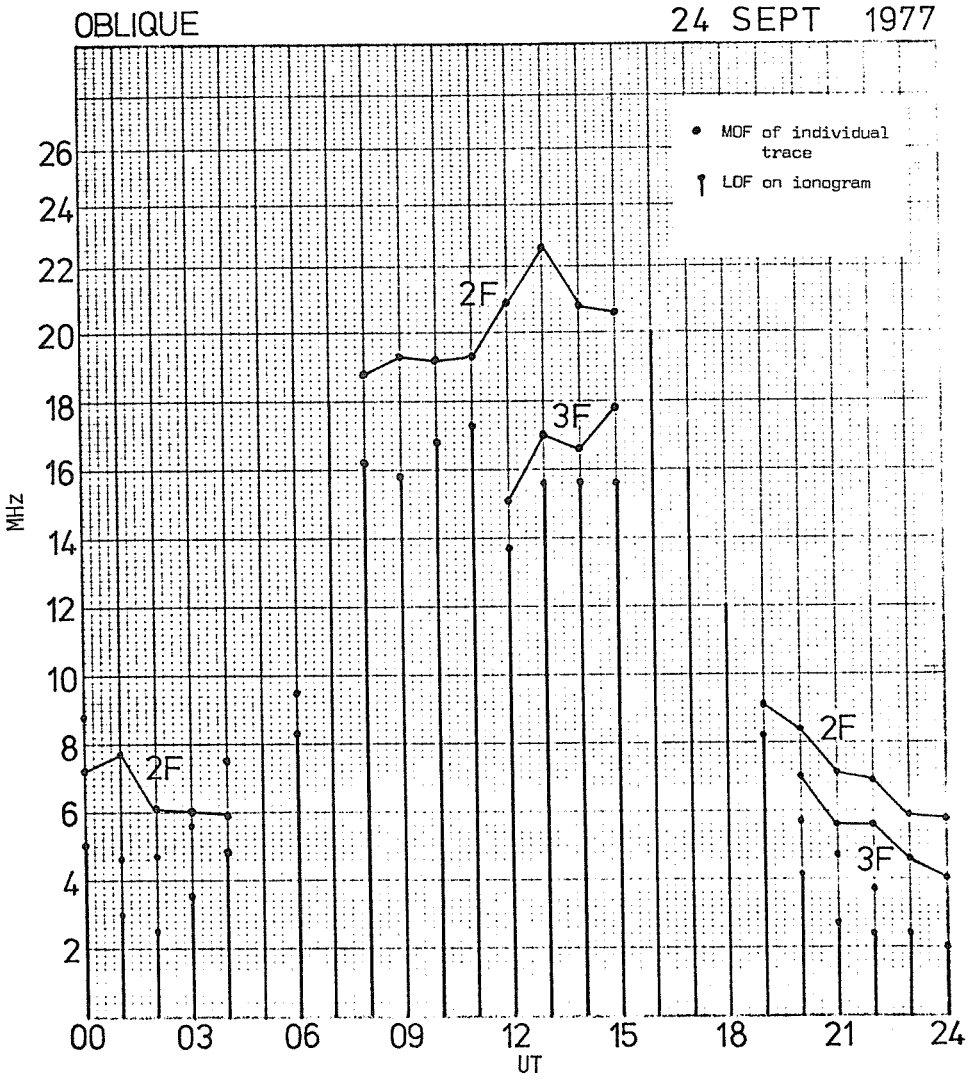

Fig. 6. Oblique f plot for Sanae-Grahamstown path September 24, 1977.

November 22, 1977

SANAE: The behavior of foF2 (Fig. 7) is almost a classic example of UT control, with an early morning maximum at 0600 UT and a corresponding minimum at 1800 UT, usually attributed to wind effects. Absorption, as shown by fmin, is unusually high, especially at 1100 UT.

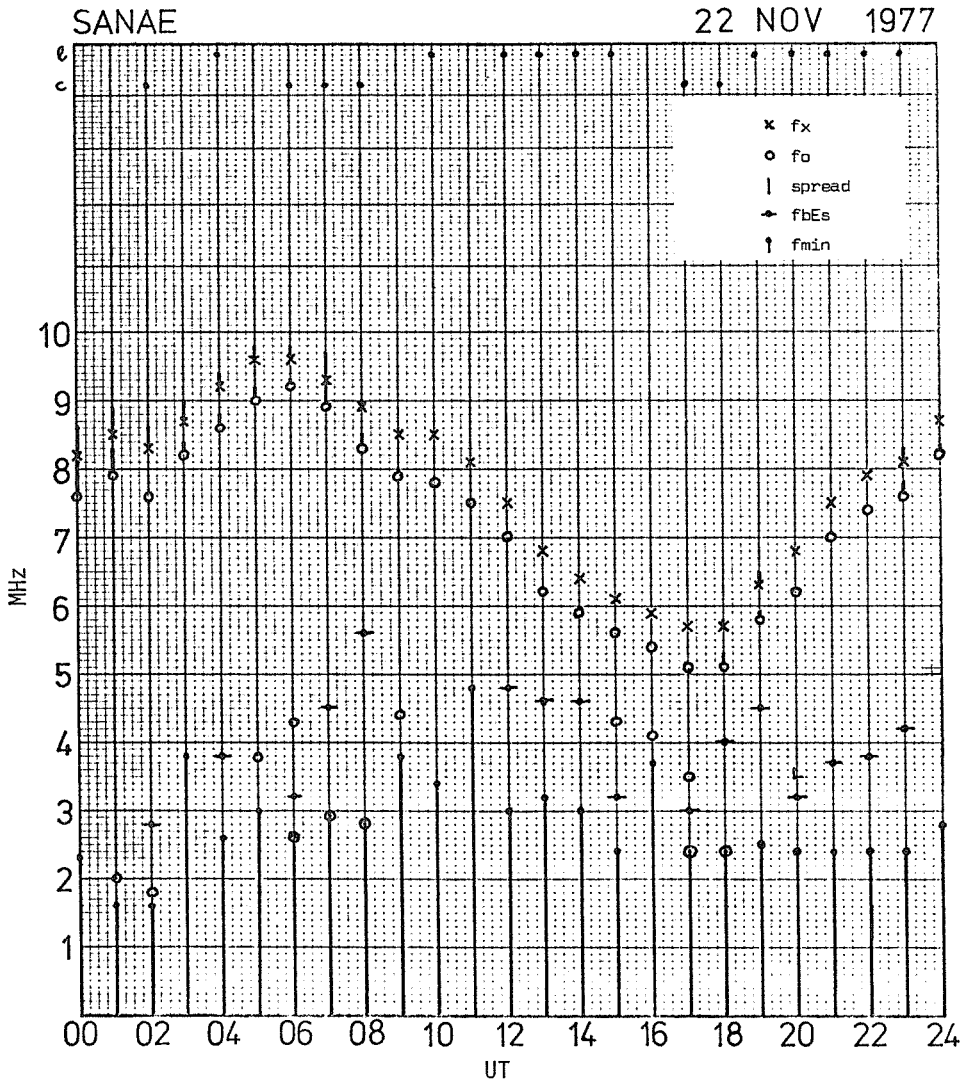

Fig. 7. f plot for Sanae November 22, 1977.

GRAHAMSTOWN: Here too (Fig. 8) the behavior is fairly normal for this time of year except for the sudden increase of absorption at 1100 UT, coinciding with that at Sanae.

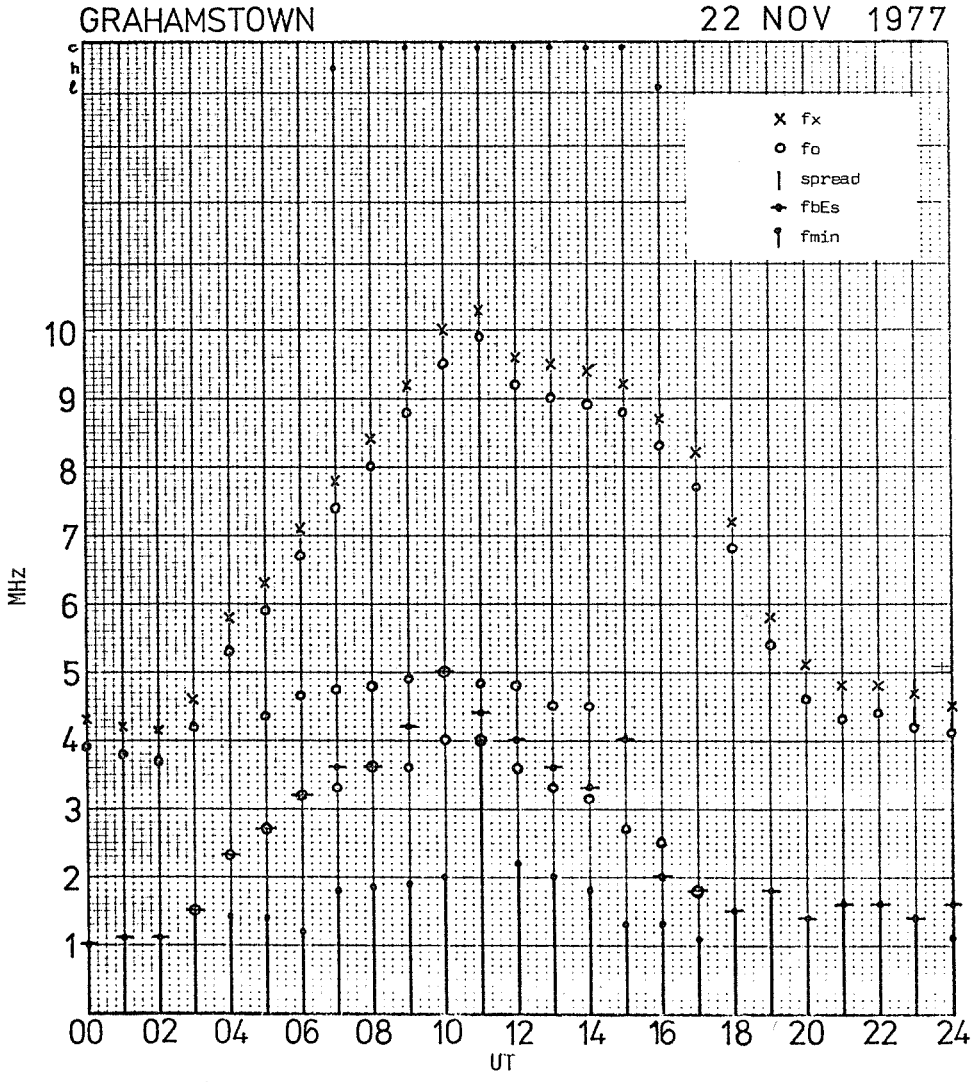

Fig. 8. f plot for Grahamstown November 22, 1977.

OBLIQUE INCIDENCE: Unfortunately, the transmitter and receiver were out of synchronization during this period so no oblique records are available.

DISCUSSION

Clearly the event of September 19 was quite different from those of September 24 and November 22 in its ionospheric effects. It appears that, during the former, ionization in the F2 region was greatly enhanced, with the vertical and oblique records all showing a peak at 1645 UT. The onset of the enhancement appears to have been at approximately 1415 UT at Sanae, 1435 UT on the 2F mode, 1450 UT on the 3F mode, and 1530 UT at Grahamstown (these are the times of the quarter-hourly records showing the first significant increase in foF2 (or MOF). These quarter-hourly values are not shown on the f plots (Figs. 1-3)). All the records also showed an initial peak in foF2 (or MOF); at Sanae this occurred at 1515 UT; on both the 2F and 3F oblique modes at 1535 UT; and at Grahamstown at 1545 UT. This would appear to indicate rapid propagation of the ionization enhancement over the Sanae - Grahamstown path.

We intend studying this event in more detail, in particular by the determination of electron density profiles, from both the vertical and oblique ionograms, at various times during the event.

The events of September 24 and November 22 appear to be more regular ionospheric absorption events, with high fmin accompanied by a depletion in F-region ionization at Sanae.

Quarter-hourly vertical-incidence data for Sanae and Grahamstown and oblique incidence data for the period September 7-24 are available, as well as vertical incidence data for November 22; monthly median data are in preparation. We thank Mr. G.P. Evans and Mrs. C. Opland for assistance in scaling the vertical ionograms.

September 1977 Events Observed at Buenos Aires Sounding Station

by

A.E. Giraldez and M.I. Lama
LIARA, Buenos Aires, Argentina

Introduction

Data from the period September 5-27 by 15-minute vertical sounding routine show perturbations at all ionospheric layers (D, E and F layers), due to solar and geomagnetic activity, as expected for a midlatitude station. Several cases of sudden fmin increase which were not correlated with available solar event data are reported.

Sporadic-E phenomena have been observed every day, and some peculiar Es events are reported.

The F layer shows a typical stormtime pattern, highly asymmetric in time and variable in frequency. The effects produced by the SC magnetic storm on Sept. 21 are clearly distinguished at F-layer height by the abnormal ionization maxima and spread-F echoes.

Detailed observations and comments are being made in separate paragraphs for each region.

D Region

The only parameter obtainable from ionograms which is related to D-region ionization is fmin. A close correlation between fmin and 2.8-GHz solar events [SGD 1977a] is observed for most cases of sudden fmin enhancements, as shown in Figure 1.

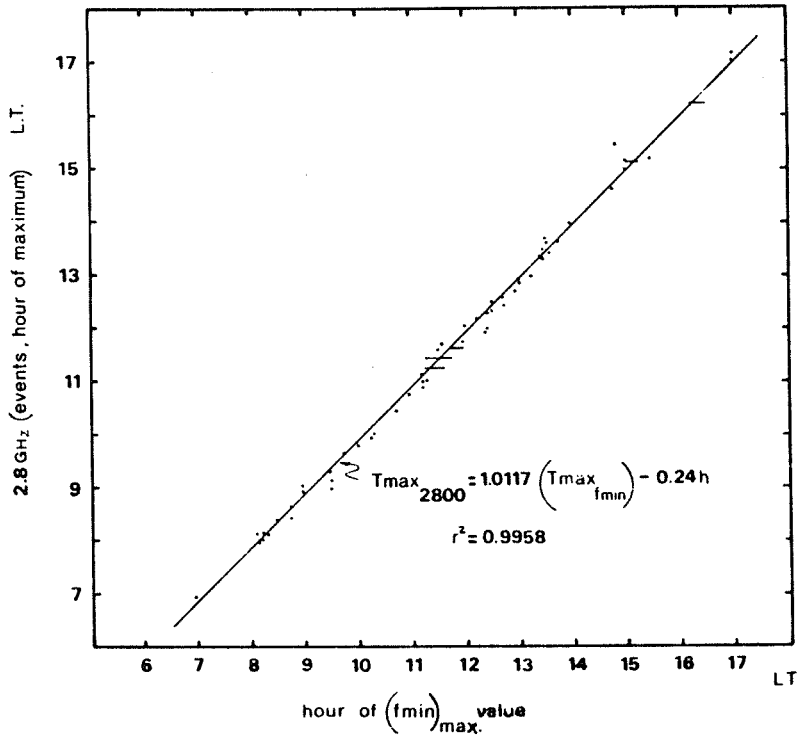

Fig. 1. Points and horizontal bars indicate simultaneous peaks of 2.8-GHz Solar Burst, and fmin values observed on ionograms. Oblique line is linear correlation curve. T_{max} = local time of maxima; r = correlation coefficient.

Also there are cases of sharp fmin increase not correlated with available 2.8-GHz flare data. These cases might correspond to 0-8Å flare events not observed at longer wavelengths [Deshpande et al., 1972; Donnelly, 1976]. Table 1 contains information on those cases not correlated with 10.7-cm wavelength events.

TABLE 1.

DAY	Hour of Occurrence (UT)	Percent Increase in fmin Value from Background
6	1630-1645	20 %
7	1500	30
8	1645	15
11	1500-1545	33
22	1530-1630	30
23	1500-1600	30
24	1315-1400	20
	1445	20
	1515-1530	30
	1700	30
26	1430	40
	1530	30
	1615-1700	40

One of the selected Solar Noise Bursts from SGD [1977a] occurred during daytime at this station. The simultaneous fmin evolution is shown in Figure 2 for comparison.

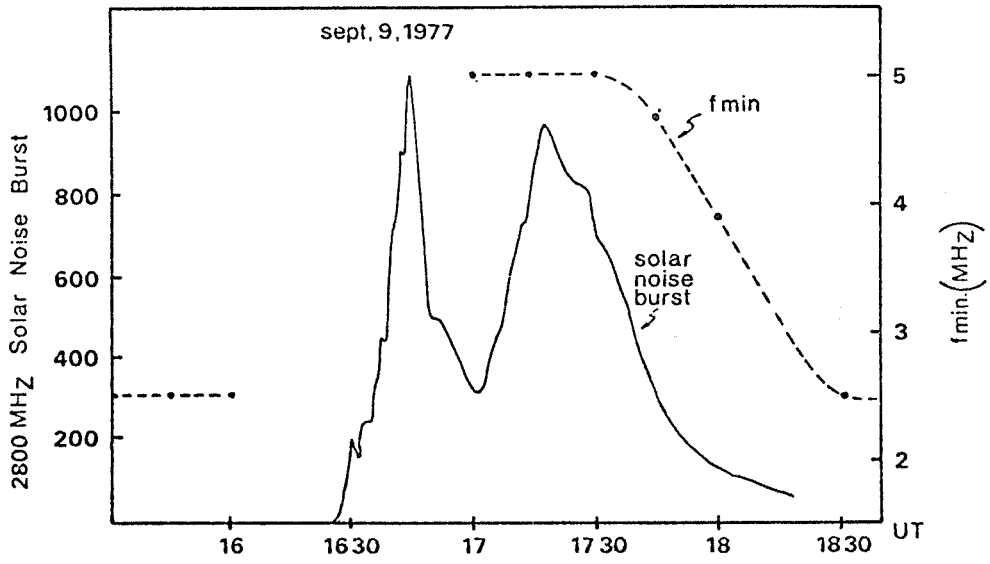

Fig. 2. Comparison between selected 2.8-GHz Solar Noise Burst from A.R.O. Ottawa (Canada) full line, and fmin values observed, dotted line.

E Region

The E Layer seems not to be seriously disturbed during this period, showing a quite regular pattern. Even so, departures from predicted values [Davies, 1965] of several kHz in foE are shown in Figure 3.

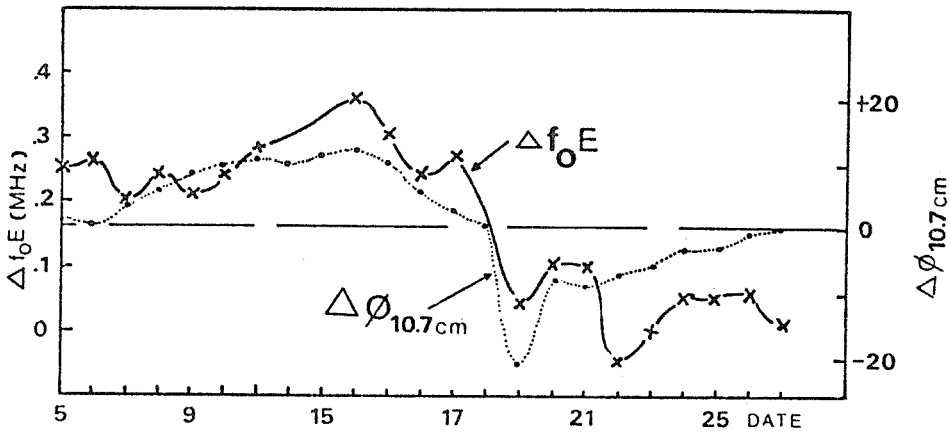

Fig. 3. Crosses indicate daily mean values of foE, $foE_{obs.}$-$foE_{predic.}$ Points indicate daily $\phi_{2.8\ GHz}$ values. The horizontal discontinuous line is the mean foE value for the period (foE=0.167 MHz).

The observed evolution is not directly correlated with simultaneous magnetic perturbations or radiation flux density. A small correlation between ΔfoE = $foE_{observed}$ -$foE_{predicted}$ and 10.7-cm flux [SGD, 1977b] is obtained by comparing ΔfoE with $\Delta\phi 10.7$, where:

$$\Delta\phi_{10.7}(n) = \phi_{10.7}(n) - \sum_{i=1}^{4}\phi(n-i)/4$$

n = day number

as shown in Fig. 3. This correlation indicates that the modification of E-layer electron density depends on the time history of the solar radiation flux rather than on the simultaneous flux level.

Sporadic-E Phenomena

This period is demonstrated to be a rather active one, as shown in Fig. 4. Es layers were present all days, with a relatively high population of Es events.

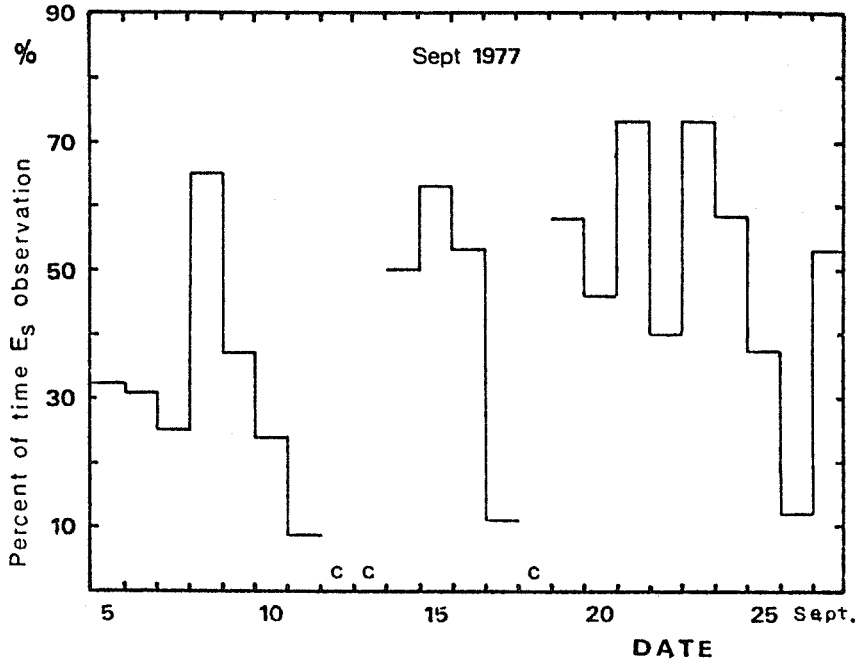

Fig. 4. Percent of time of day with observed Es layers of blanketing type, with blanketing frequency fbEs 2 MHz. Percent of time is taken based on 15-minute ionograms.

Outstanding Es events, with blanketing frequency at least 50% higher than that of normal E-layer frequency were observed. Those events persisted between 45 and 120 minutes before recovering their pre-event value without interruption of recorded echo.

The time elapsed between the maximum fbEs value reached and the recovery of the normal (pre-event) fbEs value varies between 30 and 60 minutes depending on the local time as shown in Figure 5 for each of the events shown. Virtual height (h'Es) ranges between 100 and 110 km for all of them.

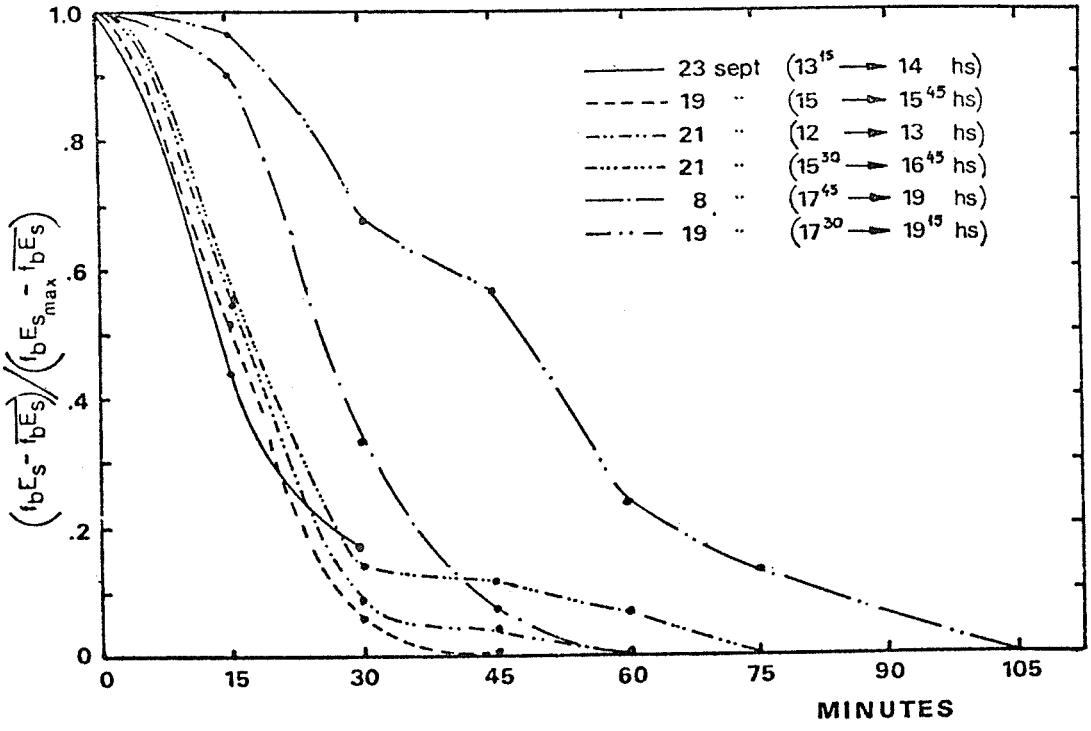

Fig. 5. Time development of outstanding Es blanketing events from the maximum frequency reached, down to the pre-event value. h'Es remains constant during all the events (between 100-110 km altitude).

F Region

F-region ionization shows a strong variability during the entire period, as expected for a magnetically disturbed period [Rishbeth, 1975]. Figure 6 shows a plot of the foF2 frequency for the period.

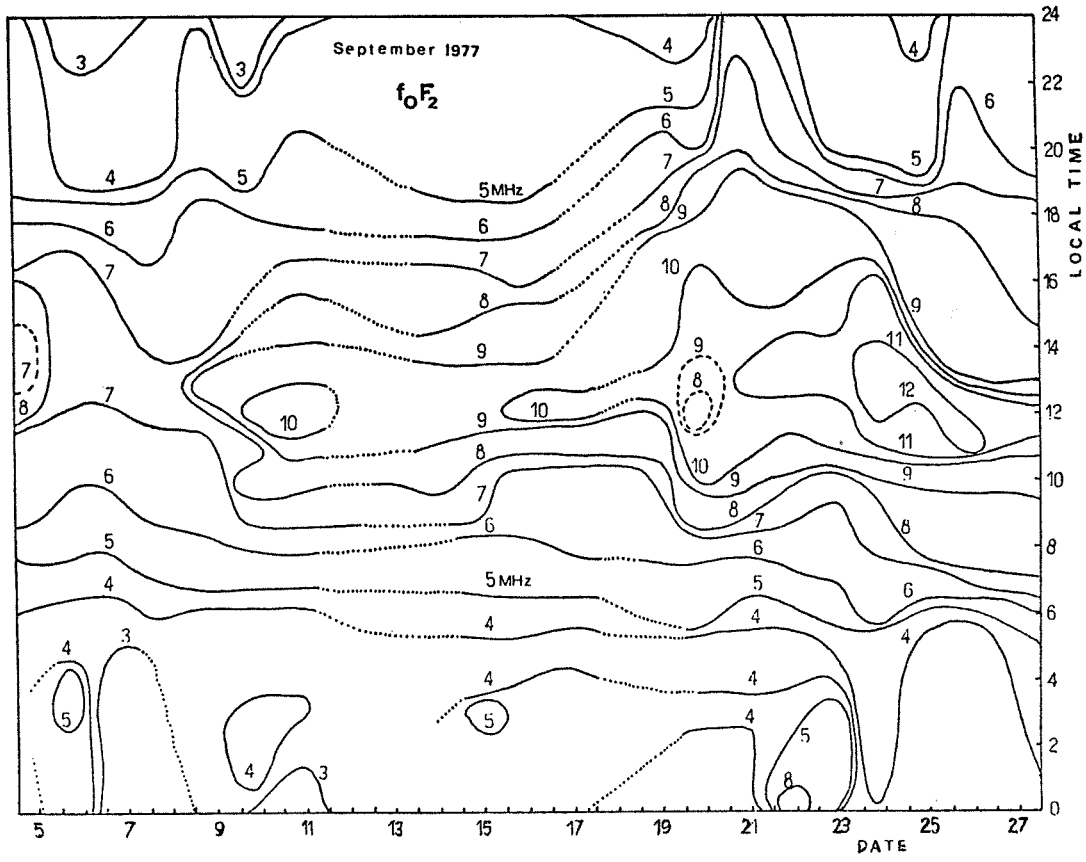

Fig. 6. Plot of foF2 values during the period under study. Dotted lines indicate missing data. Discontinuous lines are used to indicate abnormal frequency depression.

The last days of the period, which show an increase in foF2 maximum value are quite disturbed by the magnetic storm on September 21.

Nighttime ionization is also very irregular especially between Sept. 6-9 and Sept. 20-27 as observed.

A clear F-region perturbation is observed in Figure 7, where the effects produced by the SC magnetic storm on Sept. 21 are plotted.

Figure 7 also includes the SC on Sept. 19, which does not produce any effect as compared with the above mentioned magnetic storm on Sept. 21.

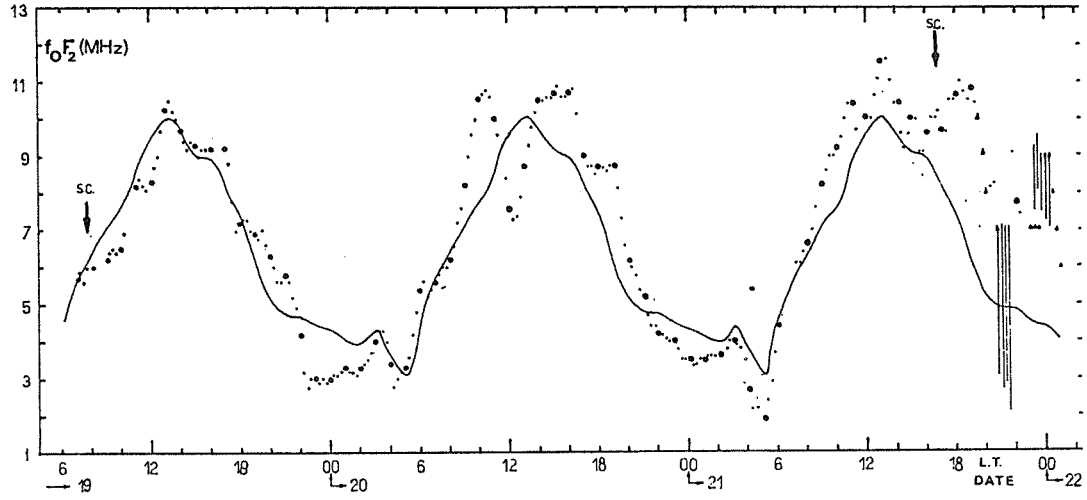

Fig. 7. foF2 plots for 3 days (points) and mean hourly values calculated for the month (full line). Downward arrows indicate hours of Sudden Commencement (SC) for magnetic storms. Vertical lines indicate spread-F values.

REFERENCES

DAVIES, K. 1965 Ionospheric Radio Propagation, *NBS Monograph 80*, 178-179.

DESHPANDE, S.D., SUBRAHAMANYAM, C.V. and MITRA, A.P. 1972 Ionospheric Effects of Solar Flares, I, II, III, *JATP, 34,* 211-267.

DONNELLY, R.F. 1976 Solar Flare X-rays and EUV Emission: A Terrestrial Viewpoint, *Proc. ISSTP,* Boulder, CO, *Vol. 1,* 178-192.

RISHBETH, H. 1975 F-Region Storm and Thermosphere Circulation, *JATP, 37,* 1055-1064.

SGD 1977a *Solar-Geophysical Data*, 398, Part 1, October, U.S. Department of Commerce (Boulder, Colorado, U.S.A. 80303).

SGD 1977b *Solar-Geophysical Data*, 399, Part 1, November, U.S. Department of Commerce (Boulder, Colorado, U.S.A. 80303).

Editor's Note

This reprint from the *Bulgarian Geophysical Journal, V,* No. 2, 10-17, 1979, was originally submitted for this UAG Report on May 8, 1978.

БЪЛГАРСКА АКАДЕМИЯ НА НАУКИТЕ • BULGARIAN ACADEMY OF SCIENCES

БЪЛГАРСКО ГЕОФИЗИЧНО СПИСАНИЕ, Т. V, № 2* BULGARIAN GEOPHYSICAL JOURNAL, VOL. V, No. 2

София · 1979 · Sofia

Ionospheric Behaviour at Mid-Latitudes during the Solar Events of September and November 1977

G. Nestorov

Geophysical Institute, Bulgarian Academy of Sciences, Sofia

M. Bossolasco, A. Caneva, A. Elena

Istituto Geofisico e Geodetico Universita di Genova, Genova

Introduction

Absorption and phase — height measurements on 15 paths at long, medium and short waves were made by the A3 — Method in the ionospheric observatories Sofia (42.6° N, 23.3° E) and Roburent (44.3° N, 7.9° E) during the period September 5-25 and November 22, 1977, as shown in Table 1. Simultaneously were realized vertical sounder routine measurements at the Sofia station. The ionosphere responded very actively to the solar phenomena.

A. Period September 5-25, 1977

1. Ionospheric Effects of Solar Flares

Table 2 gives an information for the basic parameters of the SID-effects at the main path No. 4 with highest representability [1].

As an illustration it is worth presenting the time courses of the field strength at the time of some strong flares. In Fig. 1-a are given the time courses of the field strength for several paths observed in Sofia at the time of solar flare 2b on the 9th of September 1977 with a maximum of SID-effect around 16 40 UT. On all paths (with the exception of No. 4) are reproduced the envelopes of the signal. The records show a total absorption of the signal around the SID-maximum, with the exception of path No. 4, where the signal is maximum because of the considerable increase of electron concentration gradient in the reflection region.

The records of paths No. 2, 9 and 10 are of special intersest, where the maximum of the SID-effects almost coincides with the sunset ($\chi=90°$) marked by the sign ☾. Evidently the solar X-radiation here is practically eliminated, but in spite of this the total absorption goes on for ten minutes longer for the

Table 1

No.	Path	Freq. f (kHZ)	Dist. d (km)	$f\cos i - f_l$(kHz)	Coord. of refl. point	
					N°	E°
1	Donebach-Roburent	151	580	45	47.0	08.7
2	Brasov-Sofia	155	370	75	42.7	23.4
3	Brasov-Roburent	155	1450	29	45.4	16.7
4	Allouis-Sofia	164	1720	25	45.5	13.2
5	Ankara-Sofia	182	850	35	41.4	28.0
6	Kiev-Sofia	209	1000	45	46.7	26.8
7	Monte Carlo-Roburent	218	75	200	44.0	07.5
8	Berromünster-Roburent	527	300	280	45.8	08.1
9	Pleven-Sofia	593	140	480	43.1	24.0
10	Pristina-Sofia	1412	170	1100	42.7	22.3
11	Nise-Roburent	1554	80	1500	44.0	07.5
12	Bern-Roburent	3985	280	2300	45.7	07.7
13	Tirana-Sofia	5055	310	2900	42.0	21.5
14	Wien-Sofia	6155	800	2800	45.7	19.9
15	Bern-Roburent	6165	280	5500	45.7	07.7
16	Ionospheric Station-Sofia	—	—	—	42.7	23.3

Table 2

Days 1977	Path No. 4			
	Start UT	Max UT	Dur min	Imp
9.9.	16 30	16 42	30	2+
10.9.	10 38	10 48	40	1+
17.9.	12 54	12 56	30	1−
19.9,	10 31	10 42	90	3
21.9.	08 15	08 20	30	1−
21.9.	10 55	11 02	50	1+
24.9.	09 43	10 35	220	3
25.9.	09 10	09 30	80	2−
25.9.	13 40	13 54	120	3
25.9.	17 00	17 30	50	2

path No. 2 and 20 minutes for path No. 9. This is the result of the ionospheric relaxation which is the measure for the effective recombination coefficient α_{eff} in the D-region. These cases may be utilized for the numerical estimation of α_{eff} [2].

In Fig. 1-b are represented the time courses of the field strength, observed in Roburent (Gorth-Western Italy). Here the maximum of SID's precede the sunset time by about an hour. On the path No. 11 can be seen the first SID as well with a maximum around 16 20 UT, and on the path No. 7 both SID's unite, because of the great signal absorption.

Evidently the total signal absorption on all paths, at that at a zenith angle of the sun $\chi=90°$, shows that the solar flare has been very strong; probably this refers to a solar proton flare of which the ionospheric aftereffects, the existence of Burst type IV and the data of the measurements of IMP 7 and 8 [3], witness. According to the method [4] the solar X-ray flux in the flaremaximum should be greater than 1.10^{-1} erg cm^{-2} s^{-1}.

Another strong proton flare took place on the 19th of September 1977 with a maximum of the SID effect around 10.40 UT. In Fig. 2 are represented only two original records of LW on paths No. 4 and 5. The abrupt increase of the field strength on path No. 4 after 10 30 UT is due to the fast increase of the electron

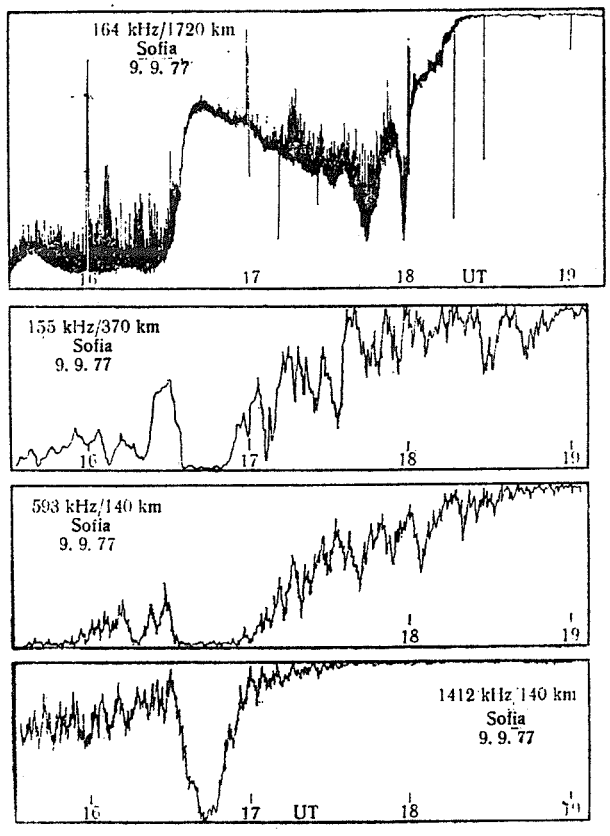

Fig. 1-a. SID-records at Sofia observatory, Sept. 9, 1977

concentration gradient in the reflection region; on the other hand, on path No. 5 can be seen very well the phase — height effect whereby can be calculated the lowering of the reflection height to the SID-maximum $\Delta h \approx 8.5$ km [5]. On all the rest of the paths there are also strong SID effects similar to those of the 9th of September 1977 but for the sake of brevity the records are not given.

The third important event noted in the letter of WDC-A (J. A. McKinnon) took place on September 24, 1977. It probably pertains to precipitation of the solar protons in the polar cap, an indication of which is the absorption $L=2.5$ dB registered by the riometer in Thule, as well as the data of SGD. The ionospheric effects of this event are represented in Fig. 3. Here for sake of brevity the records are represented only by three paths. On path NO. 4 can be seen a strong SID-effect with a maximum of about 10 35 UT. The increase of the ionizing radiation progresses very slowly (the initial phase lasts about an hour); path No. 1 gives the phase — height change: $\Delta h \approx 9.8$ km; at the same time a strong SSWF takes place on the path NO. 12 whose course can be seen in Fig. 3. Similar effects can

be observed on all the rest of the paths with the exception of these in which the daytime absorption is very high.

The picture of the SID-effect on the path No. 5 is unusual. During the 18-year period of observation SID of a similar course in September has not been registered.

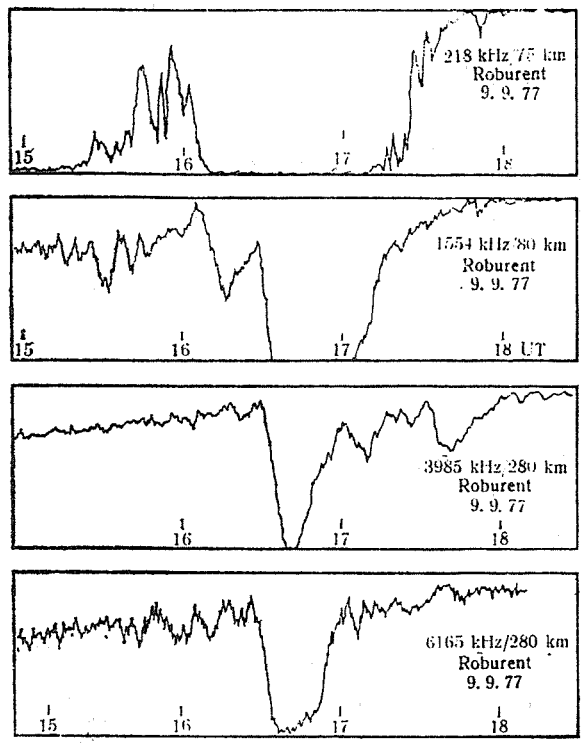

Fig. 1-b. SID-records at Roburent observatory, Sept. 9, 1977

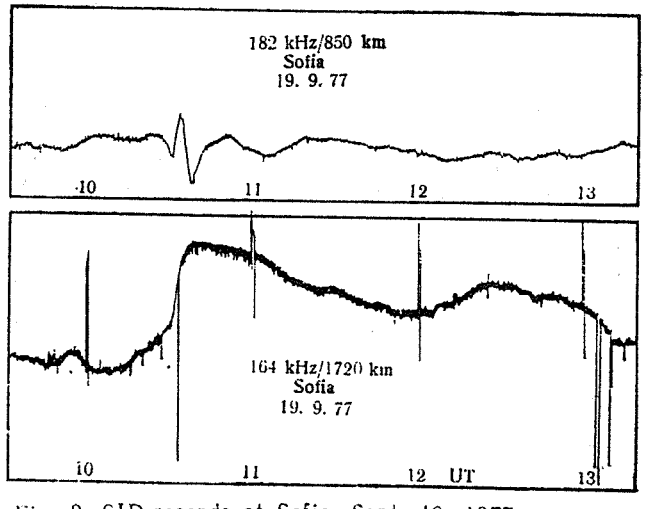

Fig. 2. SID-records at Sofia, Sept. 19, 1977

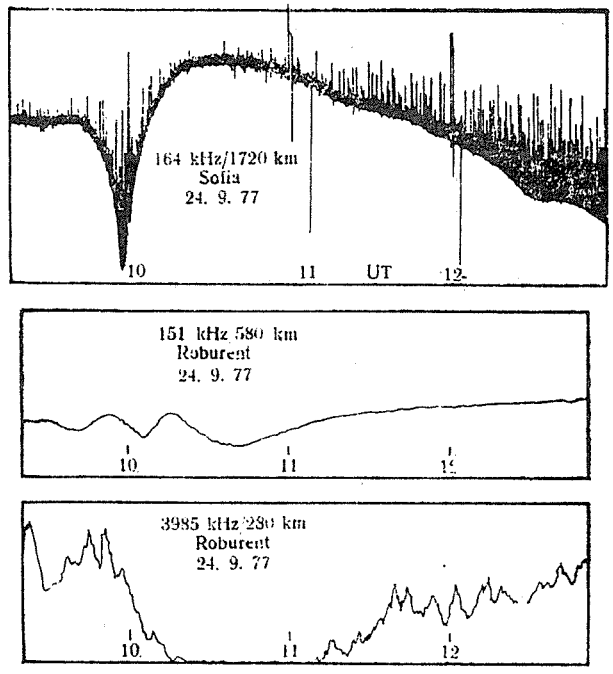

Fig. 3. SID-records at Sofia and Roburent, Sept. 24, 1977

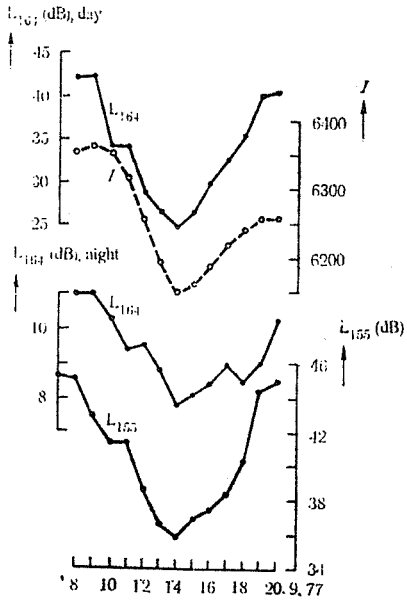

Fig. 4. Time history of ionospheric absorption and CR-flux, Sept. 8-20, 1977

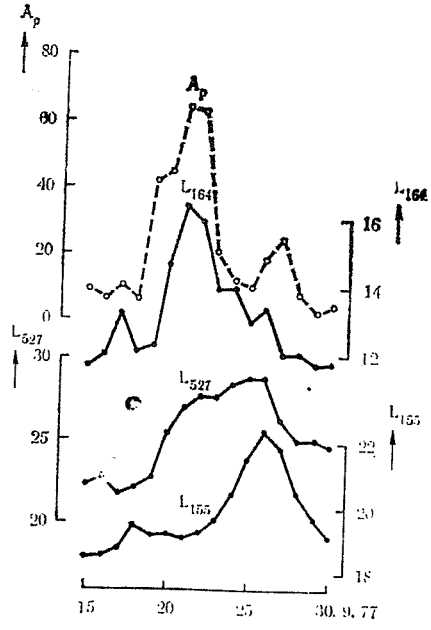

Fig. 5. Time history of A_p-index and ionospheric absorption, Sept. 15-30, 1977

The ionizing source has not an explosive character as usually happens in X-Ray Burst, and there is no data of such a X-Ray Burst.

Therefore, there is a possibility of strong ionization by energetic particles in the mesosphere.

2. Ionospheric Absorption and Vertical Sounding

As a result of the strong solar flare on September 9, 1977 accompanied by an injection of solar plasma in interplanetary space, after September 10, a Forbush decrease of the cosmic rays takes place. Parallel with that, path No. 4, as a good indicator of the modulation processes in the environmental plasma [6], [7] reacts significantly. In Fig. 4 the daytime absorption L_{164} on Sept. 14 drops by 17 dB below the level of the monthly median and is strongly correlated with the intensity of the cosmic rays I measured at the station of Kiel [8]. The correlation of I is high with the night absorption L_{164} as well. Path No. 3 reacts in a similar way, but on a lower scale — L_{155} (day). It is evident that here the absorption in the CR layer is strongly decreased which confirms the former results [9].

The solar proton flare on Sept. 9, 1977 leads to strong disturbances in the geomagnetic field in the period 19-23 Sept. 1977 (Fig.5). The night lower ionosphere reacts in a parallel way. In the same Figure can be seen the course of the nightly absorption on paths 2, 4 and 8. While path No. 4 reacts synchronously with A_p-index, for the paths 2 and 8 the reaction comes several days later — a proved fact by previous investigations [10].

An interesting result of the vertical sounding is the change of f_0F2 in the period 15-25 September 1977 which takes place almost parallel to the electron flux measured by IMP 7 and 8 in the same period (Fig. 6.).

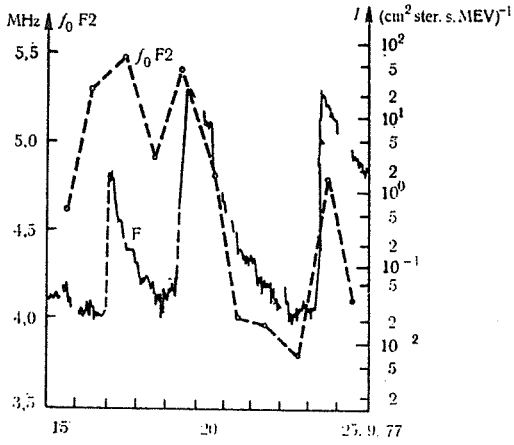

Fig. 6. Time history of critical frequency f_0F2 and electron flux F, Sept. 15-25, 1977

B. The Event on November 22, 1977

The solar cosmic ray burst on Nov. 22, 1977 is accompanied by a solar X-Ray Burst with a maximum of SID-effect around 10 12 UT. In Fig. 7 are reproduced LW-records on paths No. 4 and 6 and copies of the original records are given

for paths No. 7 and 12. From the phase-height record (path No. 6) is calculated the drop of the lower part of D-region with $\Delta h = 10.5$ km. On short and long waves by a steep incidence of the signal the absorption is total. On all the rest of the paths the absorption effects outside the SID interval cannot be ob-

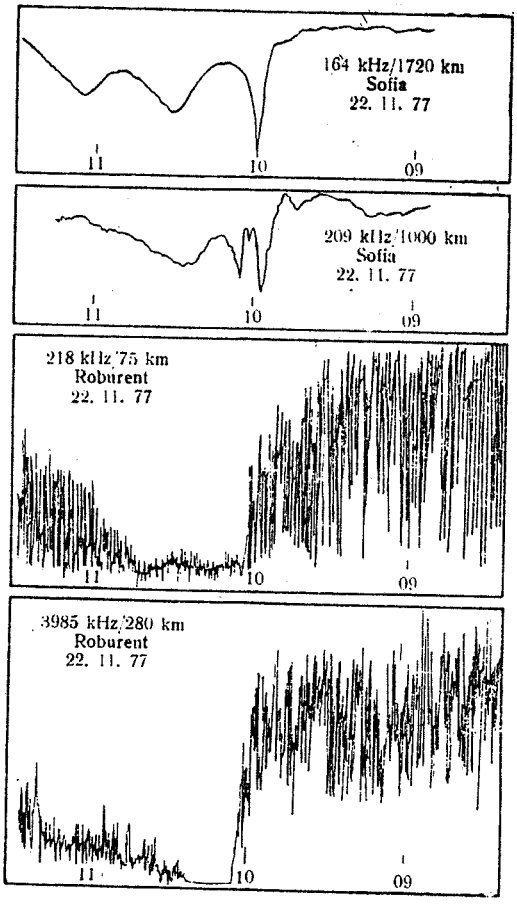

Fig. 7. SID-records at Sofia and Roburent, Nov. 22, 1977

served neither in the day nor at night. The data of vertical ionospheric sounding in the period ± 5 days around Nov. 22, 1977 are within the limits of the normal values.

Conclusion

The powerful solar proton flares from the period under consideration caused strong ionospheric disturbances. In the lighted side of the planet there sets in a total absorption of the radiowaves within the 150 kHz — 8 MHz range. The electron concentration gradient in the D-region increased 4 to 8 times, its lower boundary decreased by 8 to 12 km as a consequence of which the integral electron concentration under 100 km grew up to 10 times.

The flares were accompanied by powerful fluxes of solar plasma which after September 10 caused Forbush-decrease and modulation effects of the radiowaves with an equivalent frequency 25 kHz whose amplitude reached 17 dB.

The disturbances affected the high ionosphere too, the critical frequencies of the F2 layer in the course of 10 days followed the electron flux recorded by IMP 7 and 8.

Similar effects were obtained during the solar events of November 22, 1977 as well.

The analysed helio- and geophysical events show the advance of the ionosphere complex observation. The combined recordings of the ionospheric effects give a possibility to estimate the basic parameters of the lower ionosphere and to trace the reaction of the middle and high ionosphere at the precipitation of energetic particles in the high atmosphere.

References

1. Letfus, V., G. Nestorov. Representability of the SID-Effects Observed by Diferent Methods. — Bull. Astron. Inst. Czech., **24**, 191, 1973.
2. Nestorov, G. D-Region Relaxation after Sudden Cutoff of Ionization Source. — Compt. rend. Acad. bulg. Sci., **29**, 1976, 1433.
3. SGD, Solar Geoph. Data, Compreh. Rep. No. 403. 1978.
4. Nestorov, G. Contribution of Solar X-Radiation to Ionization of D-Region. — Compt. rend. Acad. bulg. Sci., **28**, 1975, 1609.
5. Nestorov, G., B. Fafradjieva. Zu den plötzlichen Feldstärkeanomalien im Langwellenbereich. — Compt. rend. Acad. bulg. Sci., **16**, 1963, 133.
6. Nestorov, G. Ionospheric Confirmation of the Modulation Processes in the Plasma around the Earth. — Compt. rend. Acad. bulg. Sci., **24**, 1971, 1317.
7. Nestorov, G. An Iono-Index about the Modulation Processes in Space Plasma. — Bulg. Geoph. J., **3**, 4, 1977, 35.
8. SGD, Solar Geoph. Data, Prompt Rep., **399**, 1978.
9. Nestorov, G. Signal Variation of LF Radio-Waves over the Sunspot Cycle. — J. Atm. Terr. Phys., **39**, 1977, 741.
10. Bossolasco, M., A. Caneva, A. Elena, G. Nestorov. Investigation on Ionospheric Absorption by Radiowave Propagation in North-Western Italy. — Part III, Rivista Italiana di Geofisica, **4**, 3/4, 1977, 135.

Received on April 25, 1979

Ionospheric Activity Observed at Japanese Stations in September 1977

by

R. Maeda, K. Yoshikawa, S. Taguchi and S. Hidome
Radio Research Laboratories
Koganei, Tokyo 184, Japan

Some ionospheric phenomena were detected as a disturbance effect of McMath plage region 14943 which passed the central meridian of the solar disk (CMP) on September 14, 1977. Solar flare events generated in the active region directly affected the ionosphere causing fmin increases (Sudden Ionospheric Disturbances) as shown in Table 1.

TABLE 1. Sudden fmin increases observed at Kokubunji in September 1977

Start		End		fmin increase
Day	UT	Day	UT	
7	2230	8	0700	3.7 MHz
16	2230	17	0500	2.2
18	0015	18	0430	2.4
20	0300	20	0730	3.5
26	0130	26	0245	2.3

After CMP, the ionospheric critical frequency foF2 showed positive deviations, and also foF2 decreased in amplitude (Ionospheric Storm) over Japan. Figure 1 shows the deviations of foF2 from its monthly median in September, for the observations at Wakkanai (35.3°N, 206.5°), Kokubunji (25.5°N, 205.8°), Okinawa (15.3°N, 196.0°) and Syowa (69.8°S, 78.2°). Above the Kokubunji data in Figure 1, sudden onsets of ionospheric disturbances and geomagnetic storms are denoted by arrows and triangles, respectively. The variations of foF2 recorded at Wakkanai and Kokubunji were similar with the deviations within ±3.0 MHz. The lower latitude station, Okinawa, showed a predominantly daily variation, and a moderate day-to-day variation was detected at the Antarctic station, Syowa, where many blackouts allowed only a little reliable data. Generally speaking, one part of the foF2 change is a daily variation and the other is a day-to-day variation. Their enhancements in the progress of an ionospheric storm are often recognized as a disturbance daily variation and a storm time variation.

A foF2 deviation of one MHz with the duration of one day is a reasonable criterion of the variation anomaly observed in Japan. Such a level jump in foF2 is found around the 14th through the 15th of September 1977. It was said, during the foF2 depression, that radio telecommunications over Japan were in unstable conditions because of the ionospheric disturbance effect. The decreases of foF2 were anomalous from the 19th to the 21st and from the 24th to the 26th. These events are the so-called summer type ionospheric storms which are frequently observed from April to September in Japan and cause propagation disturbances in the short wave circuits [Maeda, 1976].

Before the onset of the September 19 ionospheric storm, a solar proton event and a geomagnetic storm occurred following a severe solar flare. At Kakioka the geomagnetic storm had its beginning, main phase and ending at 1142 UT on the 19th, at 12.9h on the 19th, and at 15h on the 21st, respectively, with a range of 130Y. There was no evidence, however, of an obvious geomagnetic storm in association with the September 24 ionospheric storm. The above-mentioned ionospheric storms are shown in Figure 2, where the disturbed foF2 recorded at Kokubunji is represented by quarter-hourly values connected by solid lines, and the September and October monthly hourly medians are indicated by solid and dotted lines. It was obscure whether the September 21 geomagnetic storm with range of 82Y was associated with any ionospheric storm.

REFERENCE

MAEDA, R. 1976 "Ionospheric Storms," *Radio and Space Data, Nos. 2/3, Part 4*, 85-100, Radio Res. Labs., Japan.

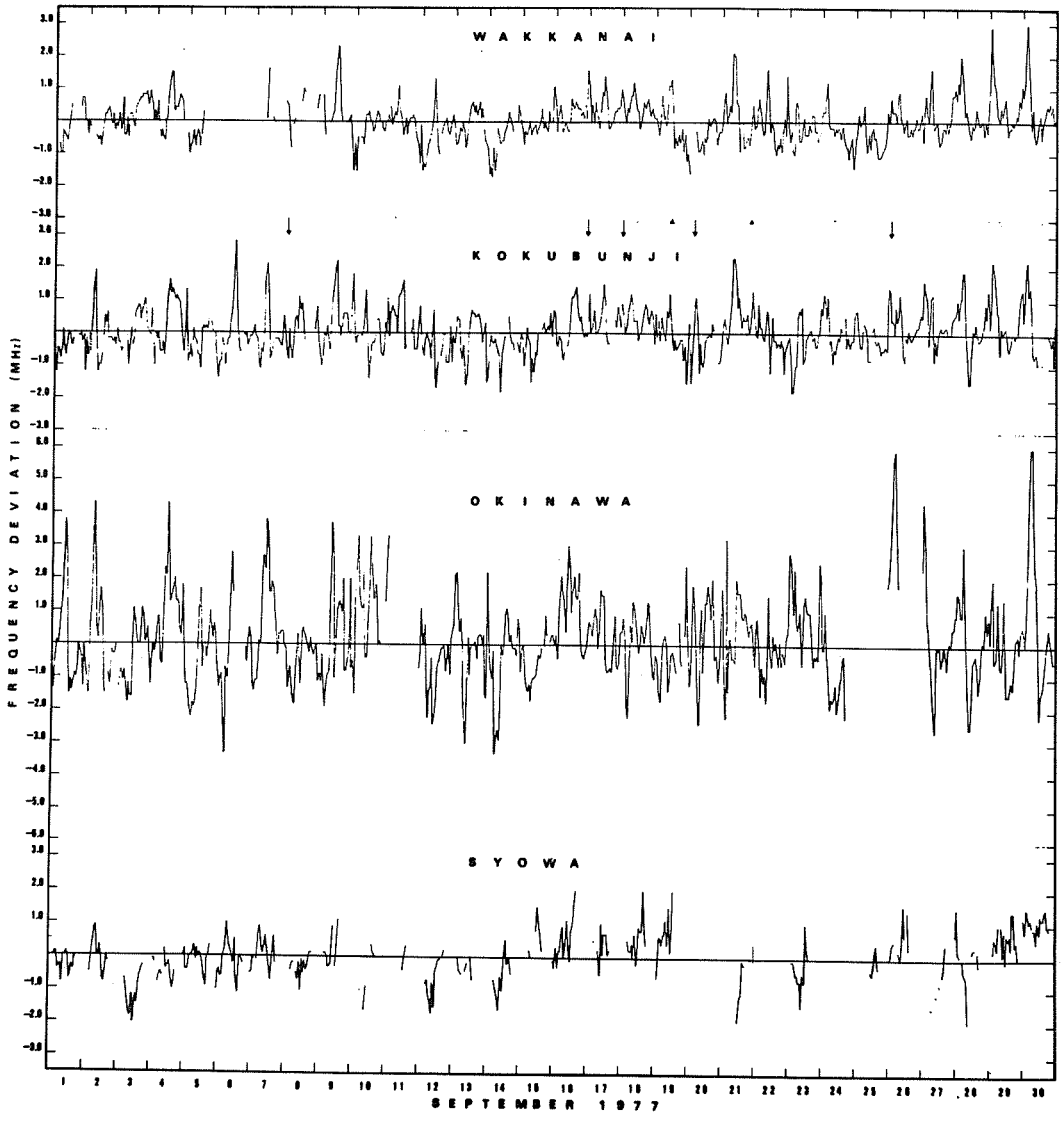

Fig. 1. The deviations of foF2 from monthly medians in September 1977, for the observations at Wakkanai (35.3°N, 206.5°), Kokubunji (25.5°N, 205.8°), Okinawa (15.3°N, 196.0°) and Syowa (69.8°S, 78.2°).

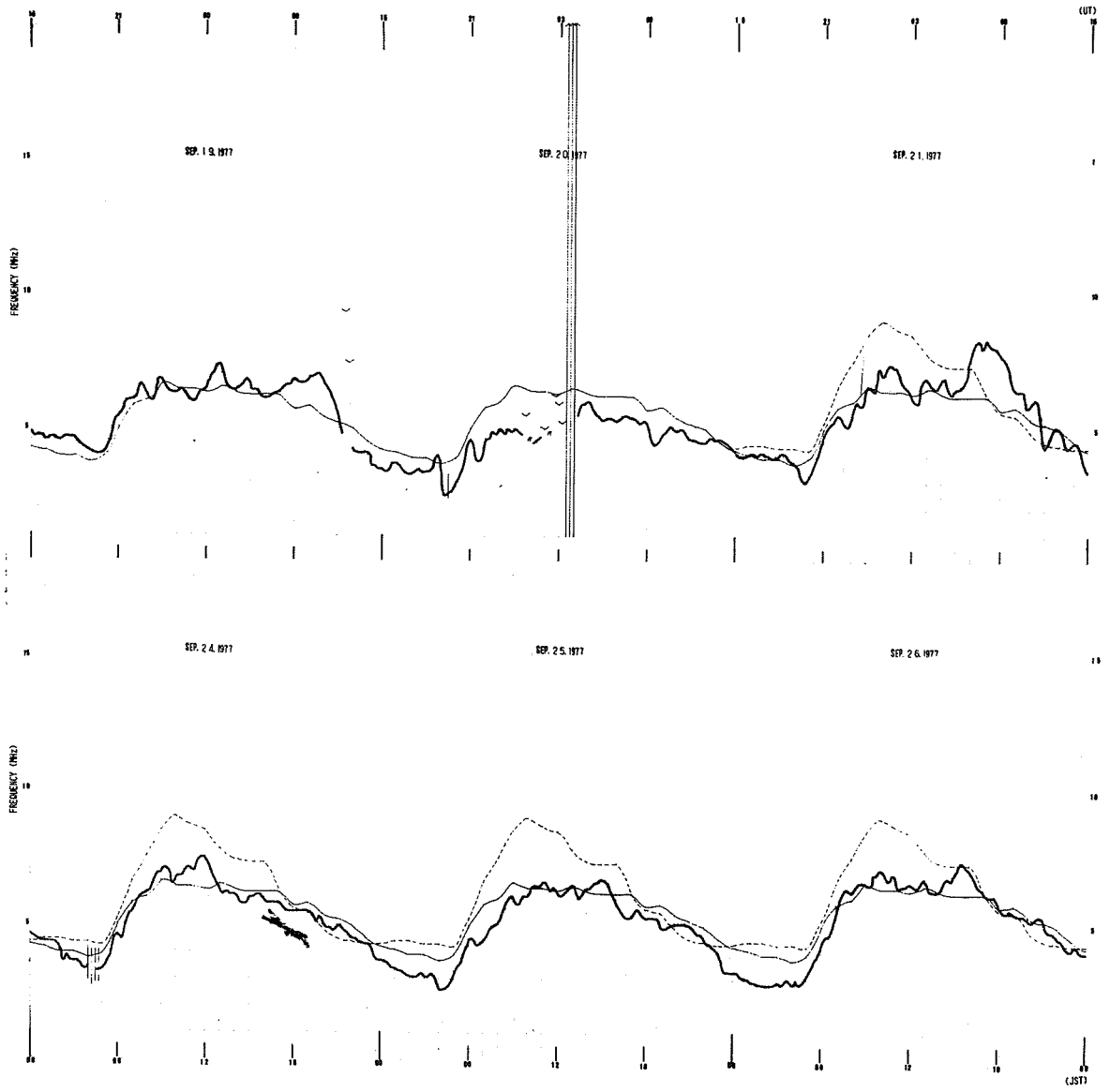

Fig. 2. The variations of foF2 observed at Kokubunji in the progress of the September 19 and 24 ionospheric storms, where fine solid and dotted lines indicate the monthly medians in September and October, respectively.

Proton Flare Effects on the Phase of VLF Radio Waves during Sept. 9-28 and Nov. 22-24, 1977

by

Takashi Kikuchi and Choshichi Ouchi
Inubo Radio Wave Observatory
Radio Research Laboratories
Tennodai 9912, Choshi, Chiba
Japan

Remarkable phase advances were observed on the VLF radio waves propagated through the upper part of the auroral zone ($\geq 65°$ in corrected geomagnetic latitude), corresponding to the invasion of solar protons (E_p > 10 Mev) into the polar cap ionosphere. The successive geomagnetic disturbances also caused phase advances on VLF signals propagated in the auroral zone and the nighttime subauroral region.

Phase measurements of VLF waves propagated over great distances have been made at Inubo Radio Wave Observatory (35°42'N, 140°52'E) by means of a cesium beam frequency standard. Three signals over the auroral zone path (ALDRA, GBR, N. DAKOTA) and one over subauroral region (NPG/NLK) were used for detection of the increase in the ionization in the lower ionosphere caused by energetic particles in association with high solar activity. The 13.6 kHz frequency of the Omega ALDRA (66°25'N, 13°8'E) and N. DAKOTA (46°22'N, 98°20'W) was received by a phase tracking receiver "TRACOR 599R" and GBR 16.0 kHz (52°22'N, 1°11'W) and NPG/NLK 18.6 kHz (48°12'N, 121°55'W) by the same type receivers "TRACOR 599K". Among the four signals, ALDRA and GBR, with their paths passing through the upper part of the auroral zone (65° ~ 68° in corrected geomagnetic latitude), were very sensitive to the solar protons invading into the polar cap ionosphere. The magnetic disturbances, on the other hand, caused appreciable phase advances on the signals over the auroral zone and the nighttime subauroral region.

Figure 1 shows phase variations during the period Sept. 6-30, 1977, along with the proton flux of energy range 20-40 Mev observed on the satellites Imp 7 and 8 and also the geomagnetic index K_p (Solar-Geophysical Data, NOAA). Each phase curve represents the deviation from a quiet-time diurnal variation on Sept. 5 which is referred to the straight dashed line. It is apparent that the remarkable phase advances observed on ALDRA and GBR correspond to the increase of the proton flux during the periods 9-15, 16-18, 19-20 and 24-27. The magnitude of the phase deviation is approximately proportional to the logarithm of the proton flux. The relationships between them are expressed empirically by

$$\Delta\phi = 60\ \mathrm{Log}(F) + 140$$

for ALDRA and

$$\Delta\phi = 60\ \mathrm{Log}(F) + 120$$

for GBR, where $\Delta\phi$ and F represent the phase advance in degrees and the proton flux in protons/(cm^2 ster sec Mev) respectively. The geomagnetic disturbances with Kp >3 occurred in relation to the proton flares and caused smaller effects on the auroral zone path, but short-term phase advances were observed on Sept. 13, 22 and 23 corresponding to high Kp indices. The magnetic effects are more distinct on GBR than on ALDRA, whereas the phase disturbances due to solar protons are larger on ALDRA than on GBR by about 20 degrees on the average. The subauroral zone signal NPG/NLK was significantly disturbed in the nighttime by the enhanced geomagnetic activity which started on Sept. 19. It should be noted that the geomagnetic effects on NPG/NLK appeared with a delay of a day from the onset of the geomagnetic disturbances, while the auroral zone signals responded almost simultaneously to the increase of solar protons and geomagnetic activity.

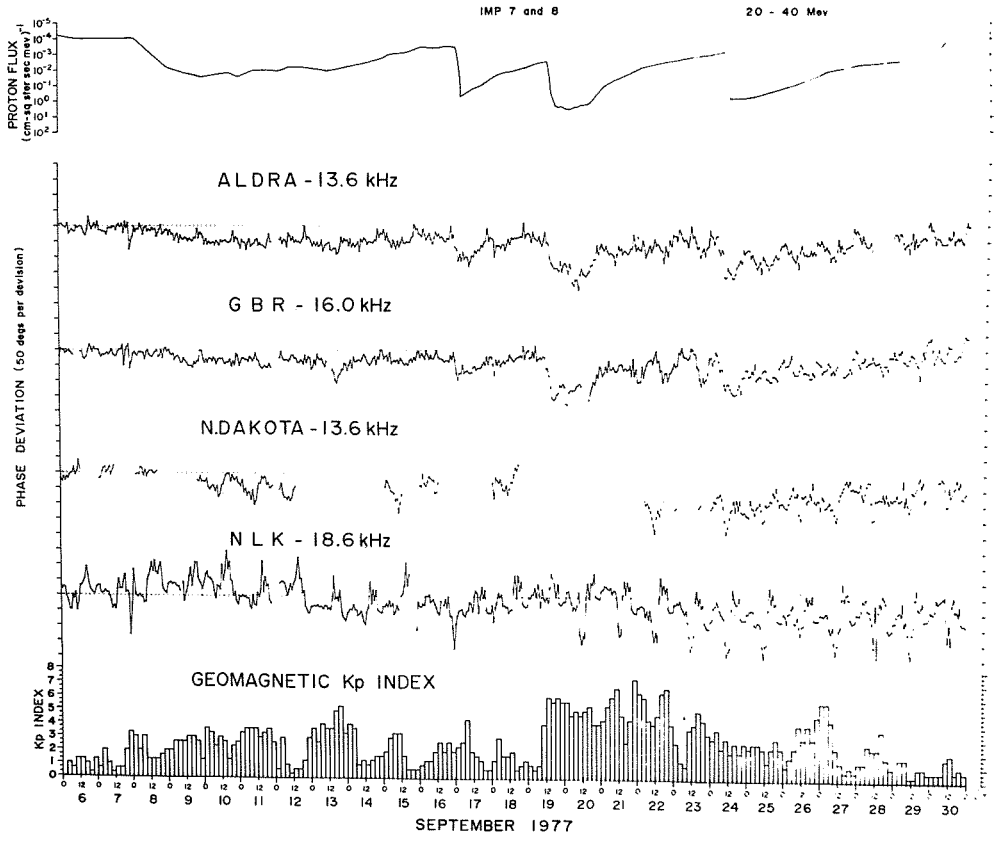

Fig. 1. Phase variations of VLF signals over auroral zone (ALDRA, GBR, N. DAKOTA) and over subauroral region (NPG/NLK), along with solar proton flux and geomagnetic activity index Kp. Each curve represents the deviation from a quiet-time diurnal phase variation on Sept. 5.

Figure 2 shows the phase deviations of three auroral zone path signals over the period Nov. 20 - Dec. 10. The reference diurnal phase variation used for deducing the phase deviation is an average diurnal variation over the whole period. Remarkable abrupt phase advances are seen on the signals ALDRA and GBR on Nov. 22, whereas no appreciable effects show on N. DAKOTA. All three signals are disturbed during the period Nov. 25-26 and Dec. 1-5 in correspondence to high geomagnetic activity. The N. DAKOTA signal, which travels over the lower part of the auroral zone ($\lesssim 62°$ in corrected geomagnetic latitude), seems to suffer more effects of geomagnetic disturbance than the signals over the upper part of the auroral zone. It is apparently seen that the solar proton effects appear on the signals with their path reaching the auroral region of $\gtrsim 65°$ in corrected geomagnetic latitude, which agrees with the range of PCA deduced by Hakura [1967] using the fmin data available in the polar cap region.

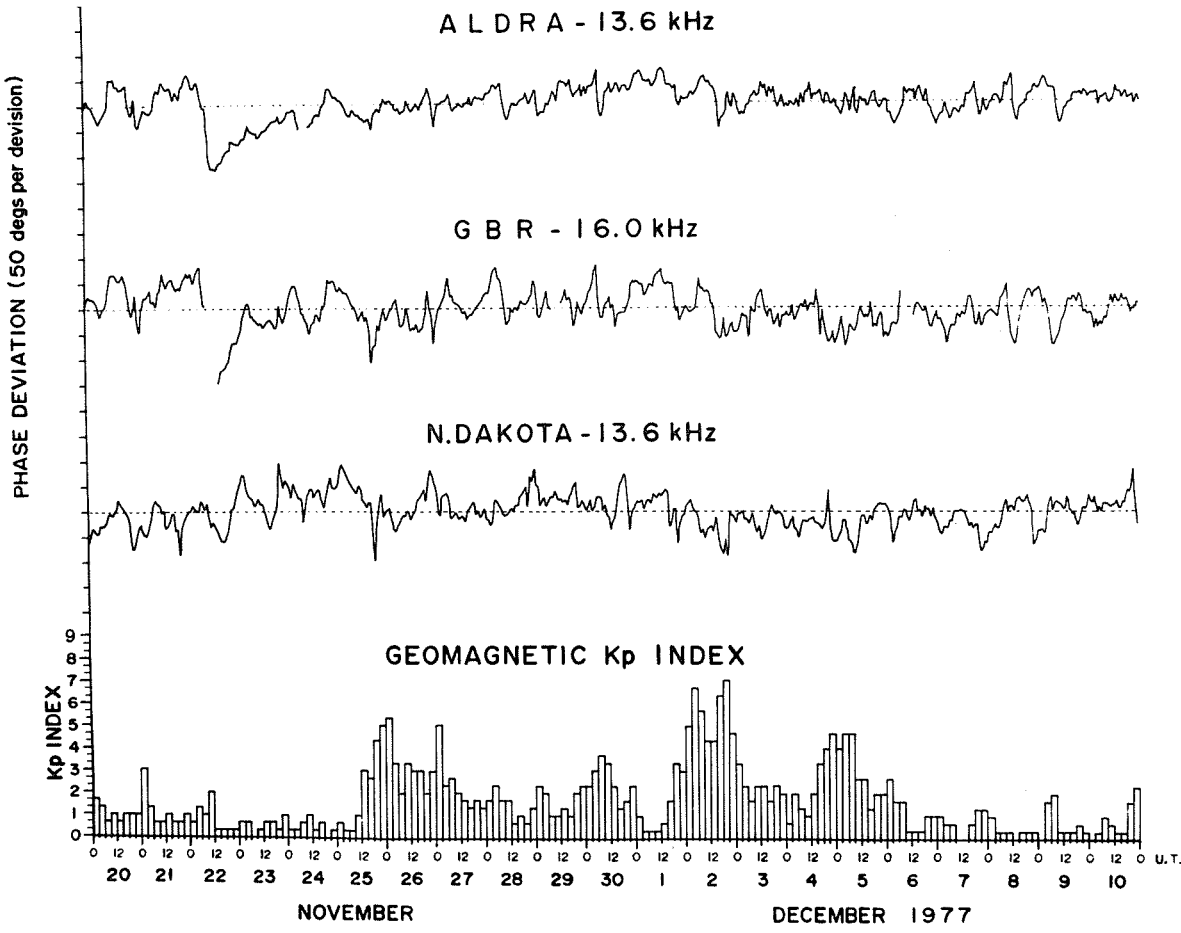

Fig. 2. Phase deviations of VLF signals over auroral zone from an average diurnal variation over Nov. 20 - Dec. 10.

REFERENCES

HAKURA, Y. 1967 Entry of Solar Cosmic Rays into the Polar Cap Atmosphere, *J. Geophys. Res.*, *72*, 1461.

SID's Detected by RRL/Japan During 7-24 September 1977

by

K. Marubashi, T. Ishii, C. Nemoto and C. Ouchi
Hiraiso Branch, Radio Research Laboratories
Nakaminato, Ibaraki 311-12, Japan

and

T. Kikuchi
Inubo Radio Wave Observatory, Radio Research Laboratories
9961 Tennodai, Choshi, Chiba 288, Japan

This report summarizes sudden ionospheric disturbances (SID) observed by the Radio Research Laboratories, Japan, by means of various radio techniques during 7-24 September 1977. The SID phenomena reported here are: (1) sudden phase anomalies (SPA) from the VLF observations at Inubo, (2) sudden enhancement of signals (SES) detected at Hiraiso by the observation of the amplitude of the Loran C pulse signals, (3) sudden increase in f_{min} (SIF) from the ionosonde data obtained at four ionospheric sounding stations, and (4) short wave fadeout (SWF) detected by the amplitude recording of HF radio signals at Hiraiso. Characteristics of the propagation circuits are shown in Table 1.

Figure 1 illustrates the time of maximum and the maximum deviation from the quiet level for each of detected SID phenomena. For SIF are shown the maximum f_{min} values themselves, and not deviation from the quiet level. During 7-22 September, 1977, McMath plage region 14943 was very active and most SID's in Figure 1 were associated with this region. The activity of McMath 14943 was rather low from 11 to 15 September and the occurrence frequency of SID's is well correlated with this activity change [Nozaki *et al.*, 1978].

Figure 2 shows the result of analysis on the quantitative relationship between SIF and SPA. The SPA's used in this analysis are indicated in Figure 1 by attaching letter A. The propagation circuits were wholly in the sunlit hemisphere with solar zenith angles less than 85° for these SPA phenomena. The maximum phase deviations were normalized to a fixed distance (10000 km), to a fixed wave frequency (20 kHz), and to a fixed solar zenith angle (0°). The dependence of phase deviation on the wave frequency and distance was taken from Muraoka *et al.* [1977] as

$$\Delta\phi = -360 \frac{d}{\lambda} \left(\frac{1}{2a} + \frac{\lambda^2}{16 z^3} \right) \Delta z$$

where d is the distance, λ is the wavelength, a is the radius of the earth, and z is the reflection height taken to be 70 km. The average value of $\sec \chi$ was calculated by taking the average of $\sec \chi$ values computed for 500 km intervals along the propagation path. Sato [1975] presented the empirical relationship among the solar X-ray in the 1-8 A band, F, f_{min}, and the solar zenith angle χ as

$$f_{min}\ (\mathrm{MHz}) = 10\ F^{1/4}\ \cos^{1/2} \chi$$

Thus, $f_{min}^4 \sec^2 \chi$ is considered to be the quantity proportional to the solar X-ray flux. In the figure, small dots indicate values from individual observations and open circles indicate the average value for each event. The dashed line presents a possible relationship between these two quantities.

REFERENCES

Muraoka, Y., H. Murata and T. Sato — 1977 — The Quantitative Relationship Between VLF Phase Deviations and 1-8 A Solar X-Ray Fluxes During Solar Flares, *J. Atmos. Terr. Phys., 39,* 787.

Nozaki, K., K. Marubashi, Y. Miyamoto and K. Ohbu — 1978 — Overview of Solar-Terrestrial Physics Phenomena Associated with McMath Region 14943 Based on Ursigram Data, *Solar Terrestrial Environmental Research in Japan, 2,* 61.

Sato, T. — 1975 — Sudden f_{min} Enhancements and Sudden Cosmic Noise Absorptions Associated with Solar X-Ray Flares, *J. Geomag. Geoelectr. 27,* 95.

Table 1. Characteristics of SID-monitoring circuits and stations

Type of SID	Transmission				Reception	Distance (km)
	Station	Geographic Coordinates	Frequency	Radiation Power (kW)		
SPA	RUGBY	55°22'N 001°11'W	16.0 kHz	40	INUBO 35°42'N 140°52'E	9550
	REUNION	20°58'S 055°17'E	13.6	10		10970
	NORTH WEST CAPE	21°49'S 114°10'E	22.3	1000		6990
	HAIKU	21°24'N 157°50'W	13.6	10		6100
	JIM CREEK	48°12'N 121°55'W	18.6	250		7620
SES	IWOJIMA	24°48'N 141°20'E	100 kHz	40000	HIRAISO	1290
SIF	WAKKANAI	45°24'N 141°41'E				
	AKITA	39°44'N 140°08'E				
	KOKUBUNJI	35°42'N 139°29'E				
	OKINAWA	26°19'N 127°47'E				
SWF	MOSCOW	55°45'N 037°16'E	6/8/11/16 MHz	20-30	HIRAISO 36°22'N 140°38'E	7490
	SHEPPARTON	36°20'S 145°25'E	15	100		8100
	KAUAI	22°00'N 159°46'W	15	10		5910
	FORT COLLINS	40°41'N 105°02'W	15	10		9150

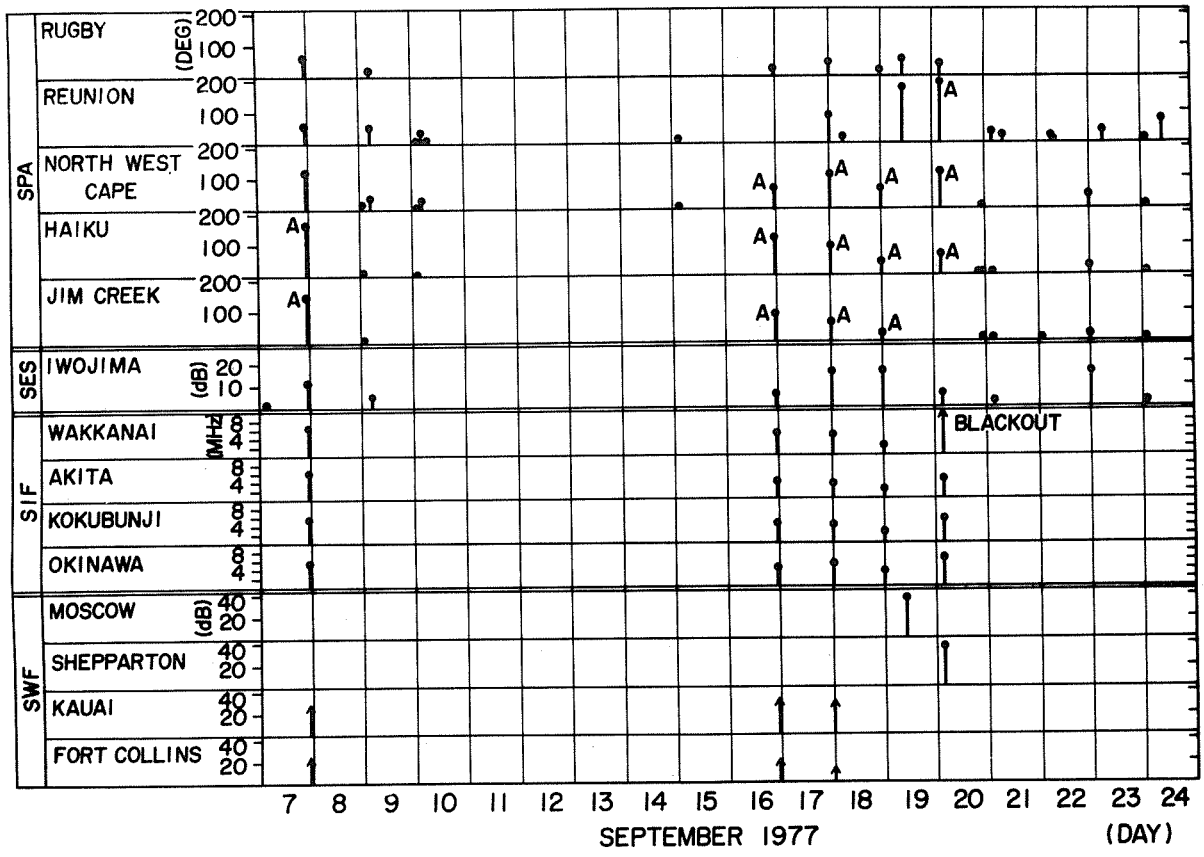

Fig. 1. SID's detected by Radio Research Laboratories, Japan, during 7-24 September, 1977. The maximum values of SID effects and the times of maximum are illustrated.

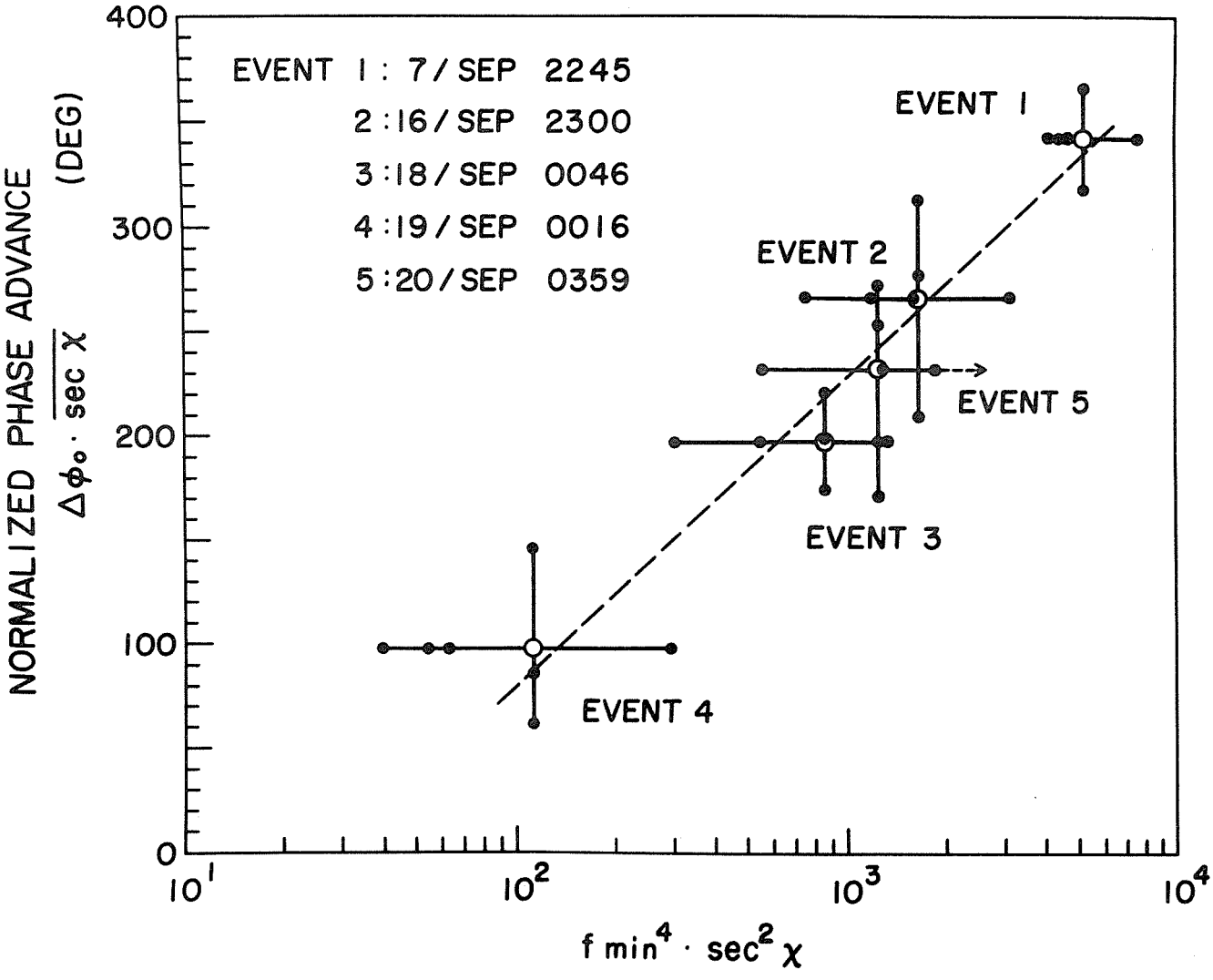

Fig. 2. Relationships between SIF and SPA obtained from selected five SID events.

Perturbation of the Ionosphere Above Paris During the Ground Level Event on 19 September 1977

by

G.C. Rumi
Instituto Elettrotecnico Nazionale "Galileo Ferraris",
Torino, Italy

Introduction

The data in Fig. 1 are the phase and amplitude of the signal on 16 kHz (GBR) and on 60 kHz (MSF), transmitted from Rugby, U.K., as received at the Instituto Elettrotecnico Nazionale (IEN) at Torino, Italy, and with ionospheric path midpoint above Paris, France. The geographical coordinates of the transmitter site are 52°22'N, 1°11'W, while those of the receiver site are 45°03'N, 7°40'E.

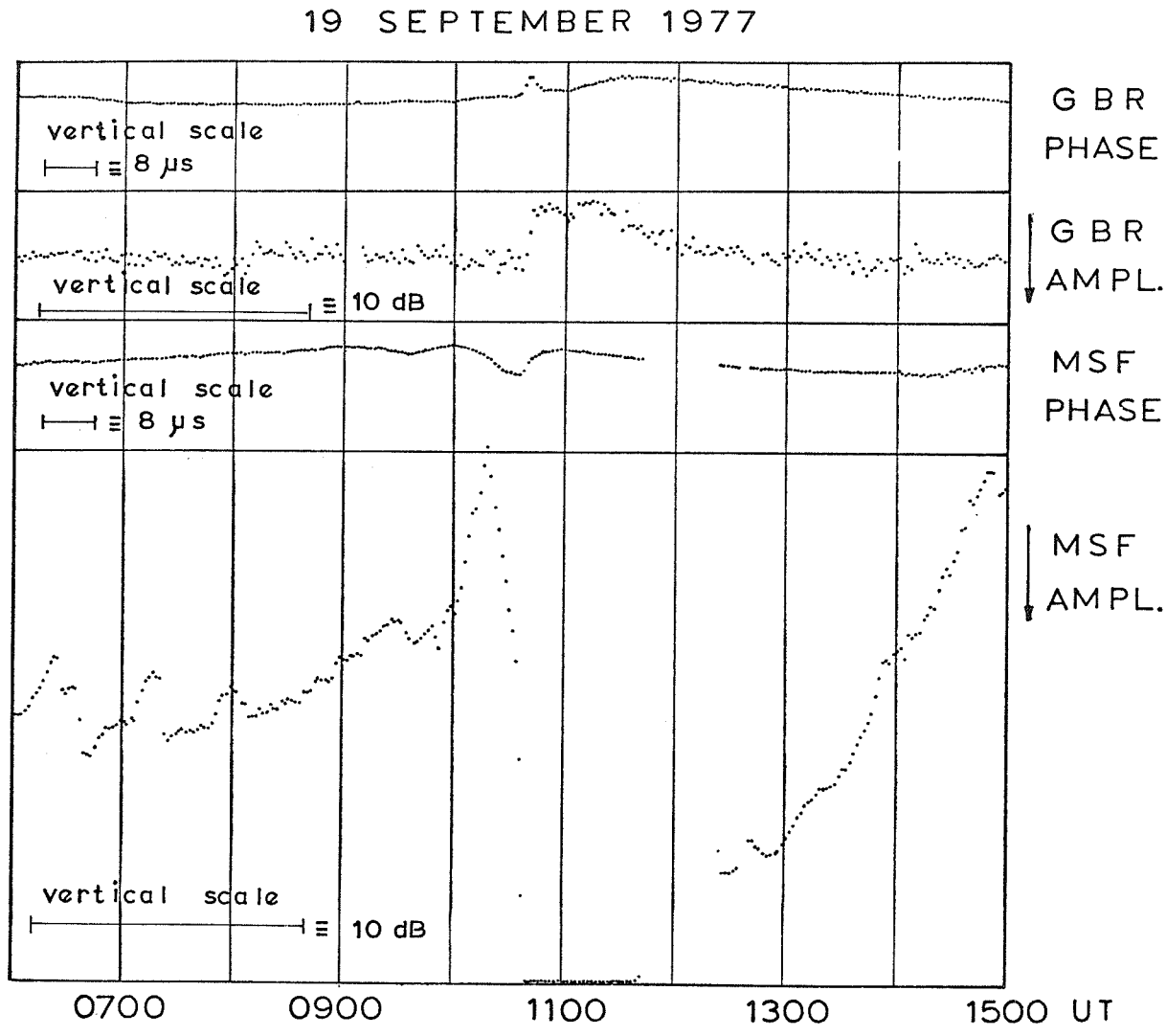

Fig. 1. Phase and amplitude of the signal on 16 kHz (GBR) and on 60 kHz (MSF) received at the IEN on September 19, 1977.

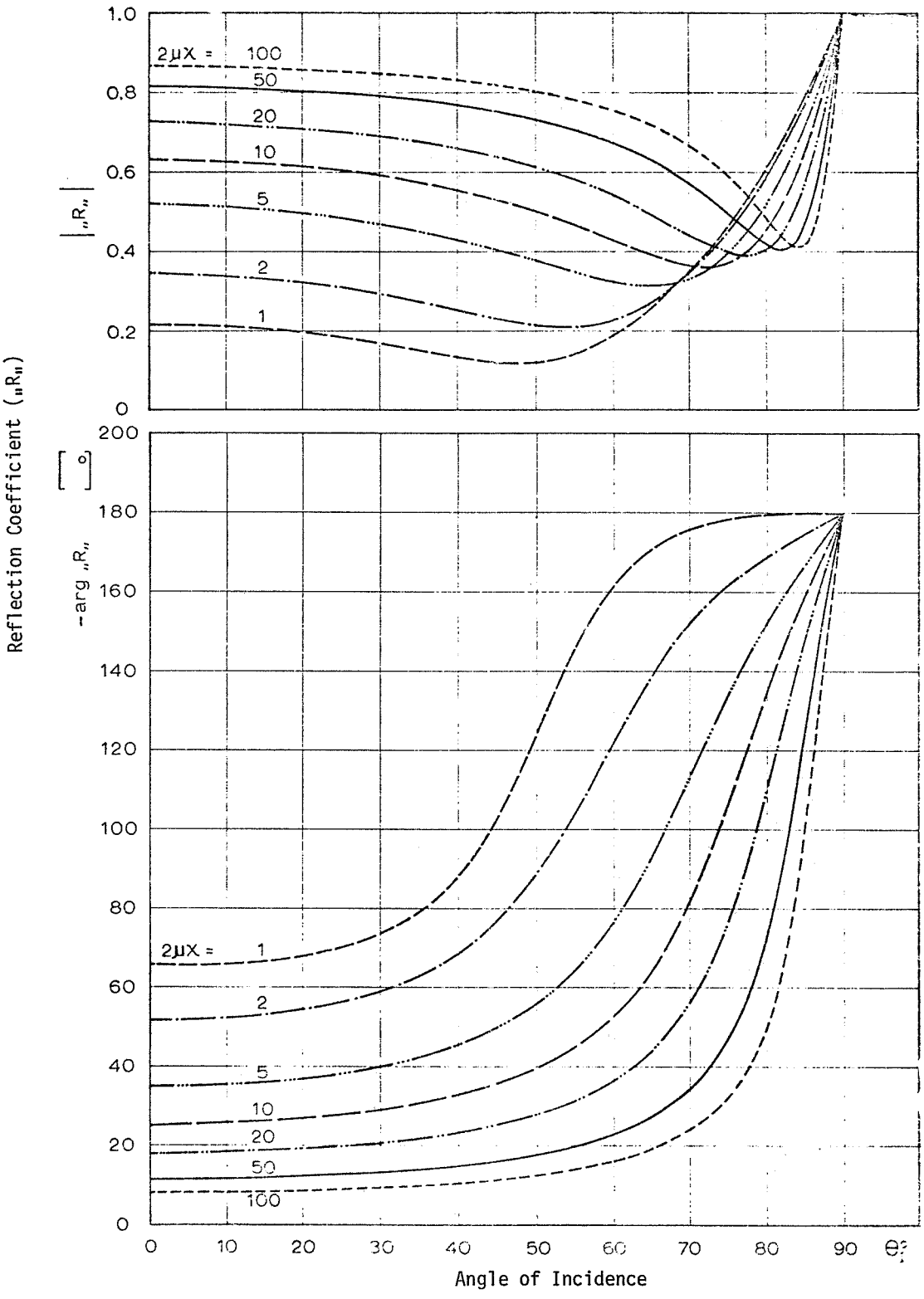

Fig. 2. The reflection coefficient - absolute value and argument - versus the angle of incidence, for several values of $2\mu\chi$. Case of specular reflection of parallel polarized waves, transverse magnetic field, and collision frequency much larger than the operating frequency.

The data of Fig. 1 are characterized by the following events:

1) a sudden phase advance for GBR at 1040 UT, followed by a superimposed phase delay which gradually dies off;
2) a sudden amplitude decrease for GBR at 1040 UT, which dies off simultaneously with the gradual disappearance of the related phase delay;
3) a gradual phase delay for MSF beginning at 1000 UT, followed at 1040 by a sudden phase advance, which disappears together with the perturbation on GBR;
4) an amplitude crevass for MSF between 1000 and 1040 UT, followed by a steady high signal level during the perturbation of GBR signals.

Notice that between 1150 and 1220 UT the data on MSF are missing.

Let us attempt an interpretation of these data according to a most simple scheme, i.e. let us suppose that the VLF and LF propagation between Rugby and Torino takes place via a one-hop ray, reflected midway on the ionosphere above Paris, and that the associated ground wave is diffracted away from the receiver site by the highest Alpine peaks. In terms of ray optics and of the diagrams of Fig. 2, which give amplitude and phase of the reflection coefficient for the specular case versus the angle of incidence, at several values of the parameter $2\mu\chi$ (the double product of the real and imaginary parts of the refractive index, pertinent to the reflecting layer), the following considerations can be formulated.

The Ground Level Event observed on September 19, 1977, by neutron monitors implies a strong increase of ionization at the reflection height of GBR and MSF. The phase changes after 1040 UT can be explained with a lowering of the reflection heights and hence an increase of the angle of incidence from 73° upward. In the case of GBR even a change in the value of the parameter $2\mu\chi$ is implied, with a final value larger than 1. Then a phase advance tied with the height lowering and the curve shift is counter-balanced by the increase in θ_I and its phase delay, in obeyance to the curves of Fig. 2. On the contrary, MSF should operate in the region such that $0.5<2\mu\chi<1$. The difference between the 2 frequencies is coherent with the fact that, near 60 km height, an increase of electron density from 10^8 to 10^9 electrons per meter cube does not produce a sensible change in μ and χ at 60 kHz, while it affects them at 16 kHz.

When dealing with the frequency bands under examination, even the amplitude is controlled mostly by the reflection coefficient. The 2 dB decrease of GBR at 1040 UT is explained with the decrease of $|{}_{\shortparallel}R_{\shortparallel}|$ coherent with the decrease of arg ${}_{\shortparallel}R_{\shortparallel}$ discussed above. On the other hand, the jump of 13 dB observed between 0830 UT and 1040 UT in the amplitude of MSF can be attributed to a change between a gradual reflection, which during the day should be accompanied by a $|{}_{\shortparallel}R_{\shortparallel}|$ of the order of 0.02, to specular reflection which according to Fig. 2 is accompanied by a $|{}_{\shortparallel}R_{\shortparallel}| \sim 0.5$ at θ_I 73°. The estimate of $|{}_{\shortparallel}R_{\shortparallel}| \sim 0.02$ is obtained by observing the variation of the amplitude of MSF between night and day that amounts to a decrease up to 16 dB and realizing that $|{}_{\shortparallel}R_{\shortparallel}|$ must be ≤ 1. The crevass recorded before 1040 UT finds a justification that has been discussed by Rumi [1972].

In conclusion, it appears that a very elementary scheme based on the trends illustrated in Fig. 2 suffices to explain the records of Fig. 1. A further comment is in order. A retardation of the phase on GBR of the kind observed at 1100 UT is quite unusual: even on the occasion of the strongest solar flares the records show only an advance. It can be inferred that during the GLE of September 19, 1977, the high energy tail of the ionizing radiation spectrum was exceptionally strong and that the ionization profile reached exceptionally deep strata in the atmosphere above Paris.

REFERENCES

RUMI, G.C. 1972 A new method for the determination of N(h) in the D-region, Il Nuovo Cimento, 10B, N. 1, 240.

Large-Scale Irregularities in Plasmasphere Obtained by Whistlers Observed September 24, 1977

by

T.M. Ralchovski
Geophysical Institute, B.A.S.
Moskovska 6, Sofia 1000, Bulgaria

An interesting result has been obtained by studying whistlers registered at Sofia Observatory, situated at N41.2 geomagnetic latitude. From observations over many years in our submidlatitude station, it has been established by Ralchovski [1977] that in a period of relatively low solar activity whistlers are registered only during (1) moderate geomagnetic disturbances for which Kp does not exceed 5 or (2) in the recovery phase of strong geomagnetic storms.

The data presented here refer to the second case above, which coincides with Retrospective Interval September 19-23, 1977, when a strong geomagnetic storm began with a sudden commencement. During the whole of September not a single whistler was detected except those registered during the recovery phase of the above-mentioned geomagnetic storm. The whistlers began on September 23 at 2150 UT and were observed until 0452 UT the next day.

We evaluated equatorial electron concentration (N_{eq}) by calculating nose frequencies (f_n) and their respective time delays (t_n) according to the Dowden-Allcock [1971] technique. We then determined the equatorial electron concentrations by using a diffusive equilibrium model for the distribution of plasma along the field lines (Angerami, 1966). We set parameters of the model to the following values: H^+=8%, He^+=2% and O^+=90% at a 700-km base level and T = 1600 K.

The results obtained for N_{eq} are shown in Figure 1 as a function of the location of the field ducts defined by the L-parameter. The solid line curve presents the mean value over 8 years of change in N_{eq} for the interval L=1.8 to 2. Note that some whistlers propagate along the same L surface but have nose frequency time delays. This implies the existence of regions on a given L surface with different contents of plasma [Carpenter, 1970].

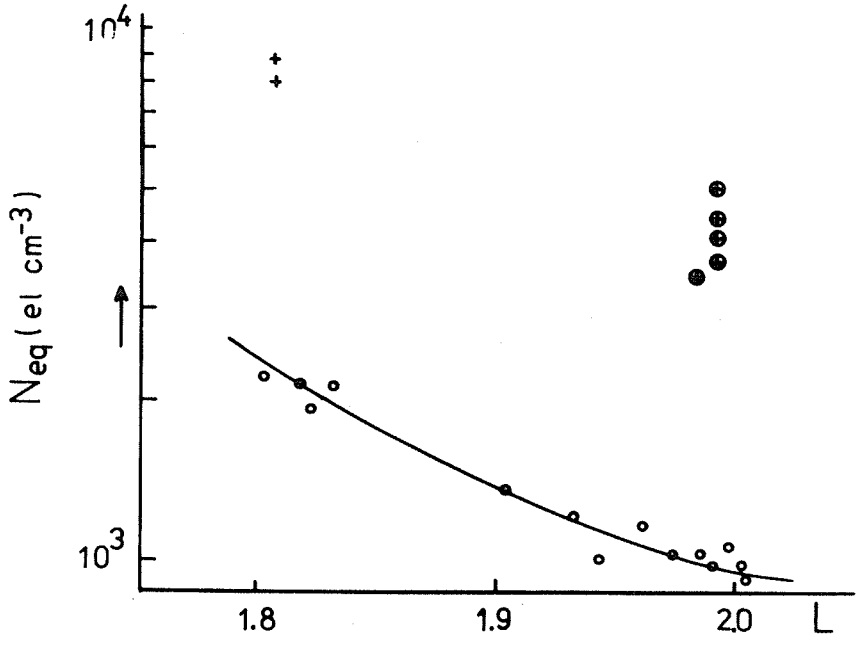

Fig. 1. N_{eq} as a function of L-shell.

The three types of symbols represent three different values of N_{eq}. The open circles grouped around the solid line curve establish concentrations that coincide with the normal annual mean values. On L surfaces near 1.8 and 2.0, considerably different values of the normal N_{eq} have been established: 8-9 x 10^3el/cm^3 and 3-5 x 10^3el/cm^3. Plus signs mark the higher values and plus signs enscribed in circles mark the lower values. Thus within the $\pm$15° longitudinal view of the observatory two regions with different levels of ionization exist. The anomalous concentration at L=1.8 is increased about three times. This order is almost retained for L=2.0.

The temporal distribution of the above observations is shown in Figure 2. The electron concentration is on the vertical axis and the time of observation on the horizontal. The same symbols are used as in Figure 1. It is obvious that the inhomogeneous density distribution at L=2.0 (L parameters are given in brackets under the symbols) at 2350 UT were registered at the beginning of the period. The second irregularity was registered 5 h later at a lower level, L=1.8. Whistlers dispersed from the normal electron concentrations, 1-2 x 10^3el/cm^3, for these high regions (marked with little circles) were observed during the whole interval 2350 - 0452 UT. The geomagnetic conditions represented by the hour value of the Dst-index is shown at the top of Figure 2. The horizontal component of the geomagnetic field is still negative but there is a tendency for its normalization.

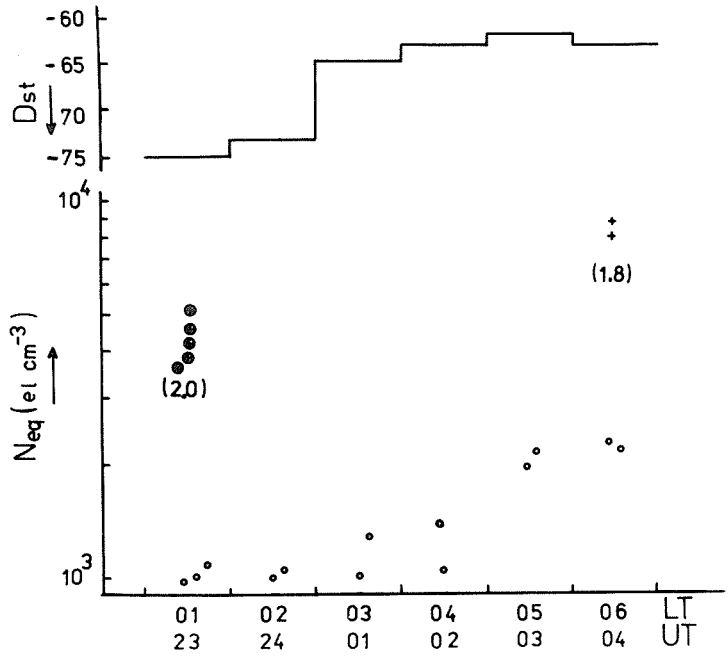

Fig. 2. N_{eq} variation by time of day. Dst also shown.

The above results can be interpreted as due to the large-scale irregularities in the plasmasphere which exert considerable effect on the whistlers propagating through them. As has already been shown, these structural anomalies are placed in a horizontal direction on an L surface but nothing can be said now about their relative situation because of lack of observations by other observatories in the neighborhood of Sofia. It can be assumed that the established structures represent a cloud with higher electron concentration than its surroundings which moves toward smaller L surfaces.

REFERENCES

RALCHOVSKI, T. 1977 Geomagnetic Dependence of the Cases of Whistler Appearance at Invariant Latitude 40°, *Bulg. Geophys. J., III*, 54.

DOWDEN, R. and G. ALLCOCK 1971 Determination of Nose Frequency of Non-nose Whistlers, *J. Atm. Terr. Phys., 33*, 1125.

ANGERAMI, J. 1966 Report SEL-66-017, Radio Science Lab, Stanford Univ., 1966

CARPENTER, D. 1970 Remarks on the Ground-based Whistler Method of Studying the Magnetospheric Thermal Plasma, *Ann. Geophys., 26*, 363.

Catalog of VLF Whistler Data

by

L. E. S. Amon
University of Otago
Box 56, Dunedin, New Zealand

The Physics Department, University of Otago, holds a VLF Whistler data set covering the period September 7-24, 1977. Table 1 lists the UT recording times at Dunedin for VLF Whistler observations. Many of these coincide with recordings taken at Campbell Island and with VLF recordings taken from ISIS 1 and ISIS 2. The recordings from Campbell Island are also held by us together with some of the recordings from the ISIS spacecraft.

Data are recorded on 2-channel, 4-track, ¼-inch magnetic tape at 3.75 in/sec giving a data bandwidth of 16 kHz. NASA-36 time code is recorded on the outside channel. Timing is generally kept to within ±5 msec of UTC with corrections known to within ±1 msec.

We are not equipped to copy or process large quantities of these data, but would endeavor to assist with data requests for specific intervals. Further, inquiries should be directed to the author of this note.

Table 1. VLF Whistler Recordings

Date	UT	Date	UT	Date	UT
Sept 7	1937 - 1951	Sept 14	0525 - 0920	Sept 18	0249 - 0303
Sept 8	2014 - 2058	Sept 14	0914 - 0928	Sept 18	0757 - 0811
Sept 8	2219 - 2234	Sept 14	1209 - 1555	Sept 18	1857 - 1911
Sept 9	1858 - 1912	Sept 14	1819 - 1833	Sept 19	1740 - 1754
Sept 9	2151 - 2206	Sept 14	2009 - 2023	Sept 20	1818 - 1832
Sept 10	1936 - 1950	Sept 15	0757 - 0807	Sept 20	2252 - 0011
Sept 10	2122 - 2137	Sept 15	1857 - 1911	Sept 21	0200 - 0210
Sept 11	2014 - 2028	Sept 16	0327 - 0341	Sept 21	0230 - 0236
Sept 11	2052 - 2108	Sept 16	0641 - 0655	Sept 21	0330 - 0454
Sept 12	0758 - 0812	Sept 16	0836 - 0850	Sept 21	0904 - 0935
Sept 12	1858 - 1912	Sept 16	1740 - 1754	Sept 21	0947 - 1001
Sept 13	0837 - 0851	Sept 16	1851 - 1905	Sept 21	2357 - 0152
Sept 13	1504 - 1518	Sept 17	0212 - 0226	Sept 22	0235 - 0245
Sept 13	1740 - 1754	Sept 17	0719 - 0733	Sept 22	0358 - 0540
Sept 13	1933 - 1947	Sept 17	1819 - 1833	Sept 22	1740 - 1754
Sept 14	0405 - 0419	Sept 17	2010 - 2024	Sept 23	1818 - 1832

All recordings taken at Dunedin, New Zealand. Recordings of 14 min duration normally coincide with an ISIS VLF recording.

The Total Electron Content as Observed in Sodankyla/North Finland and the Absorption Data from Finnish Riometer Chain for September 7-24, 1977 and November 22, 1977

by

A. Ranta
Geophysical Observatory Sodankylä Finland

and

A. Tauriainen
University of Oulu, Finland

Introduction

Since June 1975 the coherent signals transmitted by the NNSS satellites have been regularly received on 150 and 400 MHz. The number of the passes received per day is normally 6, but the capacity of the automated equipment allows 12 passes to be received. The combined receiving system detects and records the dispersive phase shift and radioholographic data. The former can be used to determine the total electron content (TEC) of the ionosphere and the latter to reconstruct the irregularities of the electron density causing scattering of the radiowave.

This report includes only the TEC data and the absorption data from the Finnish riometer chain observed on 27.6 MHz. The holographic data will not be treated in this connection because of lack of remarkable scatter process.

TEC Observations

During the period under consideration signals from only 4 NNSS satellites (30120, 30130, 30140, 30200) are registered. The receiving station is located at Pittiövaara (67.4°N, 26.4°E) near the Sodankylä Observatory. The transmitter frequencies 150 and 400 MHz are the 3rd and 8th harmonics of the 50 MHz frequency. After conversion to the same frequency the phase shift between the two signals can be measured. A brief description of the system is given by Hartman et al. [1973].

The phase shift data is interpreted manually and punched on cards. Finally, the calculations are carried out by a computer at the University of Oulu. The resulting TECs are plotted as a function of the geographic latitude as shown in the attached figures. In the figures are given the station (PITTIOEVAARA), satellite number (e.g. SAT. 30120), data and local time (LT). The local time is related to the universal time as follows:

$$UT = LT - 2$$

Two methods are used to evaluate the TECs. The crosses and the open squares distinguish the different methods. When the ionosphere is regular, the two methods give nearly the same results. In cases of strong gradient the results are different referring to unsatisfied assumptions of the evaluation methods. (See Figures 1-9.)

TEC Results

During the period from September 7 to 24, 65 passes were recorded and successfully evaluated. For November 22 only one recording is entered. The values of the TECs are normal for this season indicating strong gradients especially by night. The trough of TEC can also be found, e.g., in the recording on September 17 at LT 1.52 - 2.07.

There are four recordings on September 19 and six recordings on the 24th. However, at the time of GLE it is by no means exceptional as seen in the TEC recordings.

Data from Finnish Riometer Chain

Data from the Finnish riometer chain are given in Figures 11 - 16 from the time interval September 19-24, 1977. The geographic and geomagnetic coordinates and L-values of the stations are given in Table 1 and their locations are shown in Figure 10 with the ellipses giving the antenna patterns of riometers projected to the 100-km level in the ionosphere.

Table 1. Location of Finnish riometers (Coordinates as in IMS Bulletin 2).

	Geographic Coordinates	Geographic Coordinates	L-values
Kevo	69.8°N 27.0°E	65.6°N 123.8°E	6.0
Ivalo	68.6°N 27.5°E	64.5°N 122.9°E	5.5
Sodankylä	67.4°N 26.4°E	63.7°N 120.9°E	5.1
Rovaniemi	66.6°N 25.8°E	63.0°N 119.4°E	4.8
Oulu	65.1°N 25.5°E	61.7°N 118.0°E	4.3
Jyväskylä	62.4°N 25.7°E	59.2°N 116.0°E	3.7
Nurmijärvi	60.5°N 24.7°E	57.6°N 113.8°E	3.3

All riometers operate at 27.6 MHz using a three-element yagi antenna. In Figures 11 - 16 the quiet day levels are also given with the approximate scale of absorption in dB calculated at 0000 UT. On the right-hand side the record levels are marked so that the exact absorption values can be calculated.

Results

September 19, 1977

During the hours 0000-1000 UT no absorption can be seen at any station. At 1038 UT at every station a very intensive radio burst can be seen. After that absorption is seen at every station, the highest absorption in Kevo is about 4 dB. Beginning at 1940 UT auroral absorption is seen to the north of Jyväskylä.

September 20, 1977

Almost all day very strong absorption is seen to the north of Oulu. In the daytime there is PCA type absorption, in the evening auroral absorption is also seen.

September 21, 1977

During this day auroral-type absorption is seen both in the morning and evening. At 10 - 12 UT very strong absorption is seen at every station, even in Nurmijärvi the absorption is about 2 dB.

September 22, 1977

On September 22 different kinds of absorption can be seen. In the morning, strong auroral absorption is seen at every station located to the north of Oulu. At 1340 - 1410 UT very likely REP-type absorption is seen in Oulu. A sharp onset of auroral absorption is seen in Ivalo and Kevo at 1530 UT.

September 23, 1977

In the morning no absorption can be seen at any station. Auroral type absorption begins at about 1700 UT north of Oulu.

September 24, 1977

PCA type absorption is seen very clearly to the north of Oulu and also small absorption in Jyväskylä and Nurmijärvi. In the evening the auroral type absorption is seen in Ivalo and Kevo beginning at 2040 UT. At 0555 UT a strong radio noise burst can be seen at every station.

References

HARTMAN, G.K., G. SCHMIDT, and A. TAURIAINEN 1973 Total Electron Content of the Ionosphere over Lindau/Harz by Dispersive Doppler Effect, July 26 - August 12, 1972. WDC-A Report UAG-28, Part II, 511-524, NOAA, Boulder, CO 80303, USA.

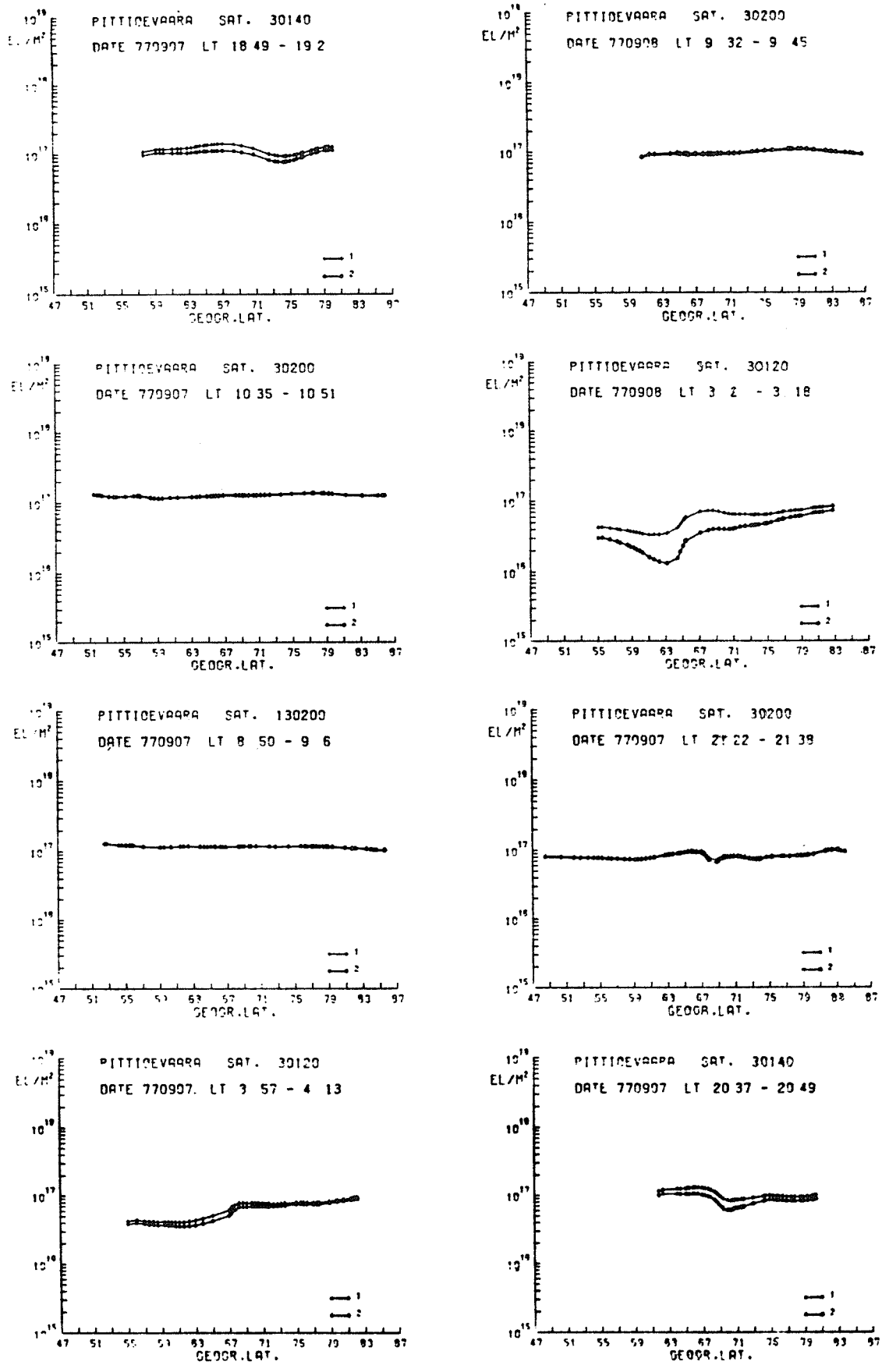

Fig. 1. Total electron content.

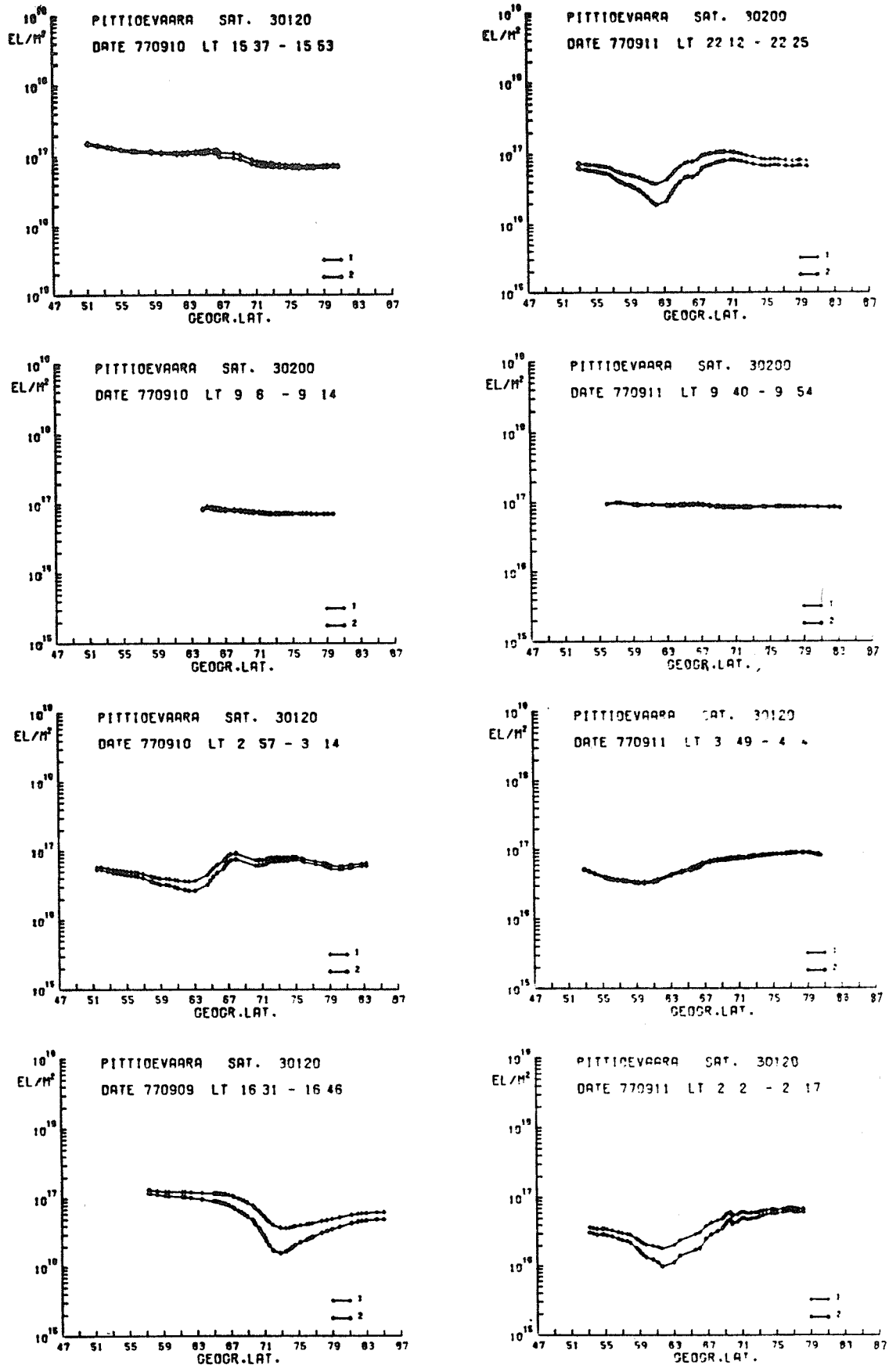

Fig. 2. Total electron content.

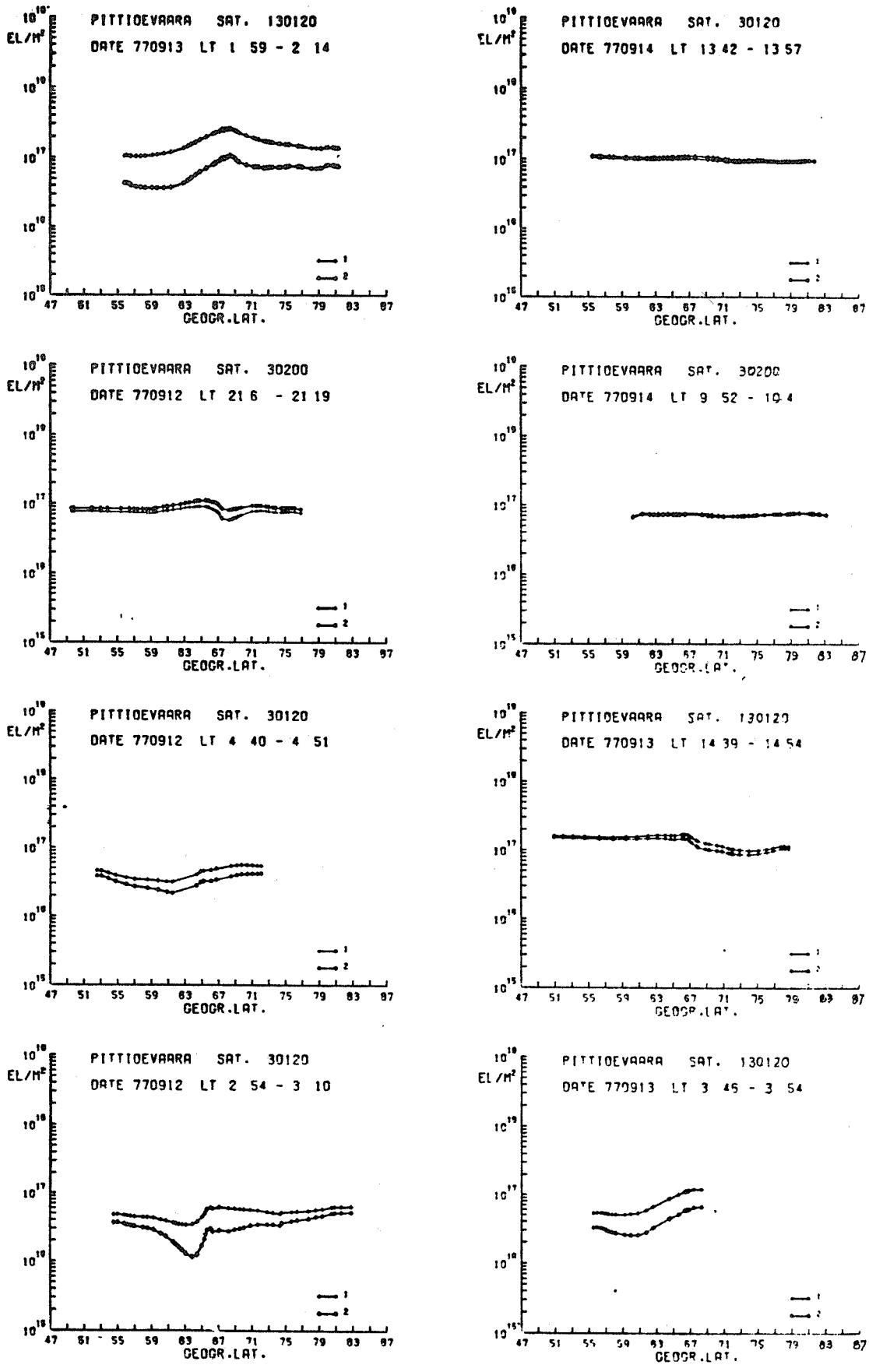

Fig. 3. Total electron content.

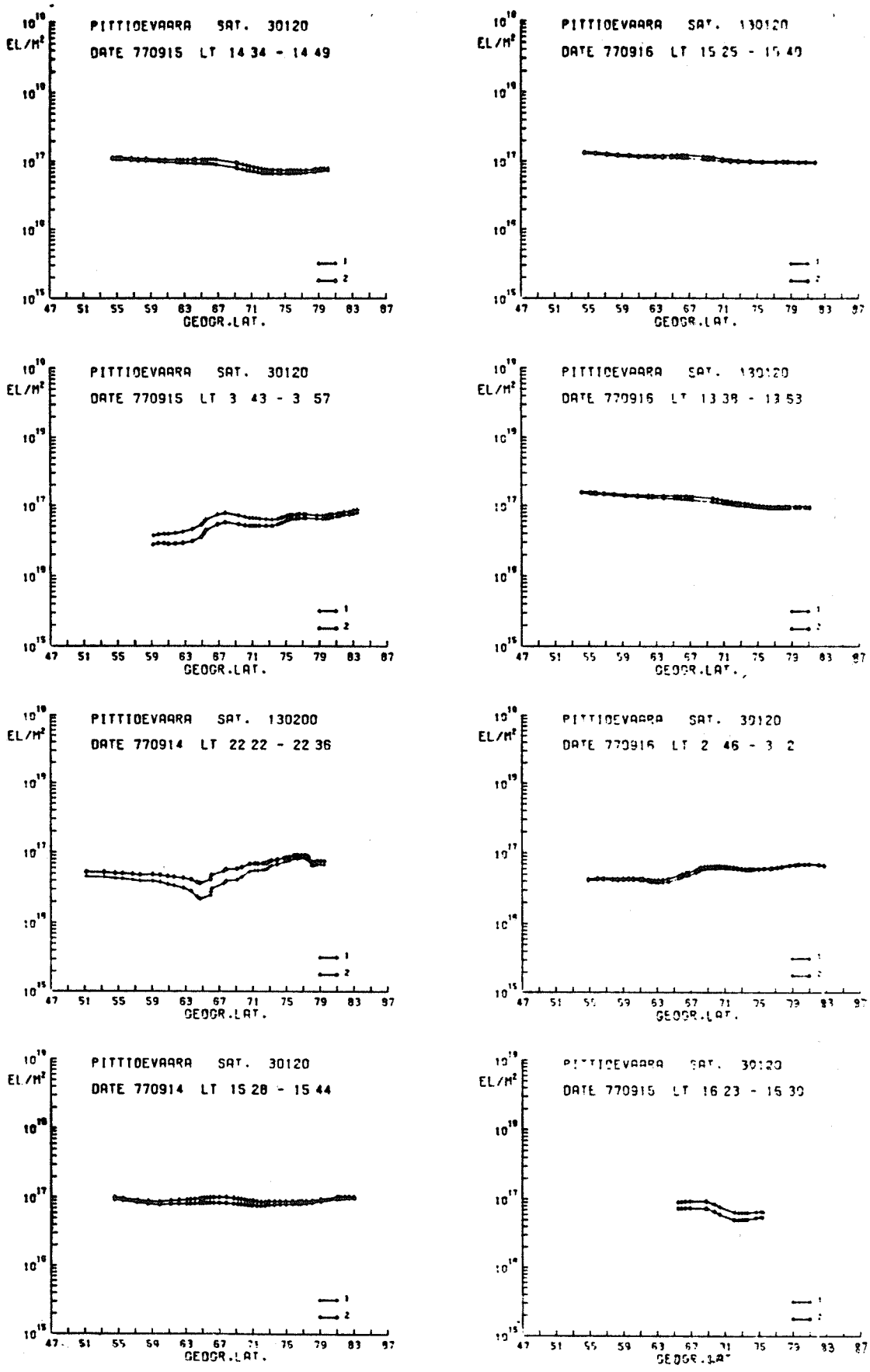

Fig. 4. Total electron content.

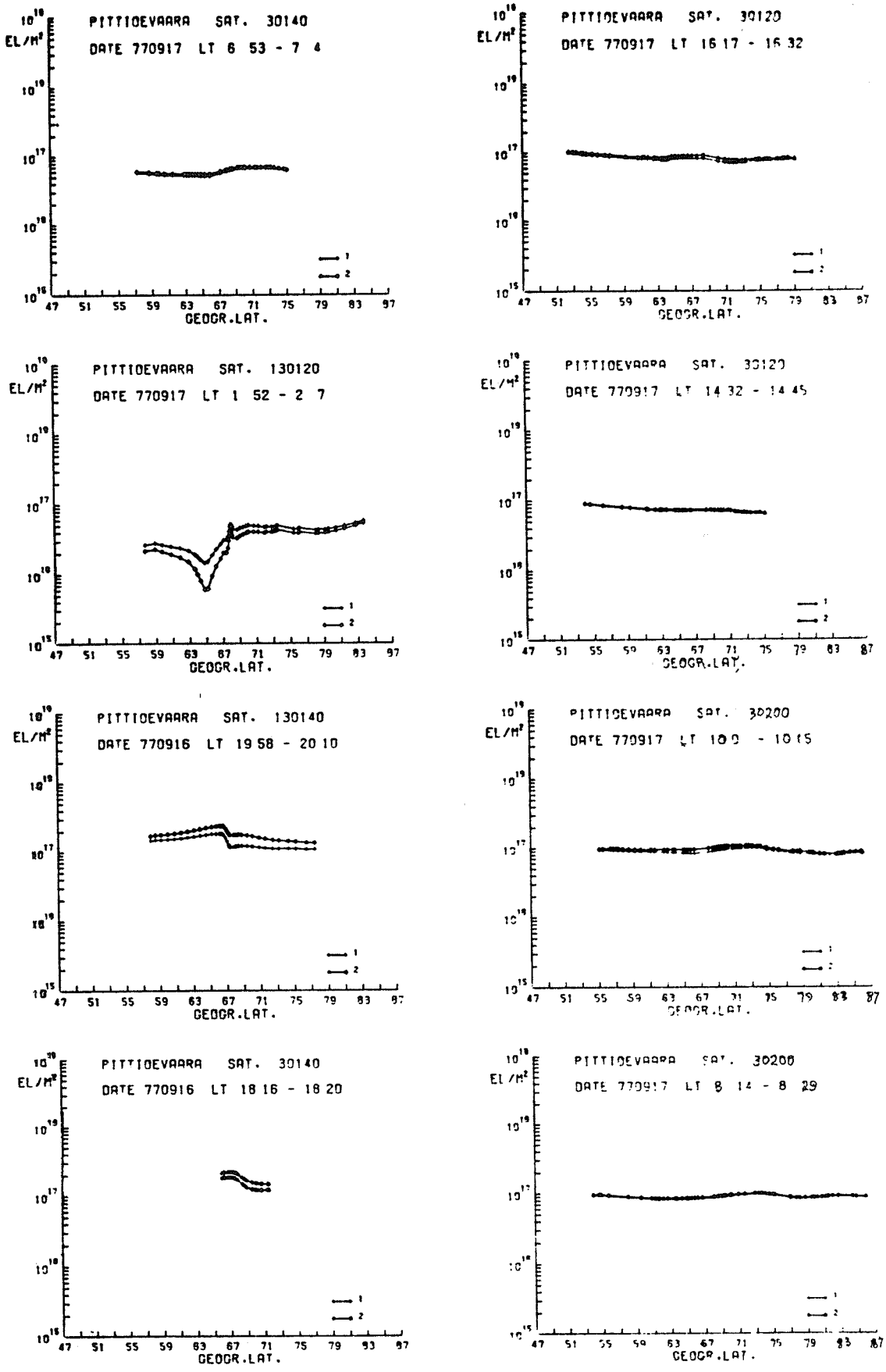

Fig. 5. Total electron content.

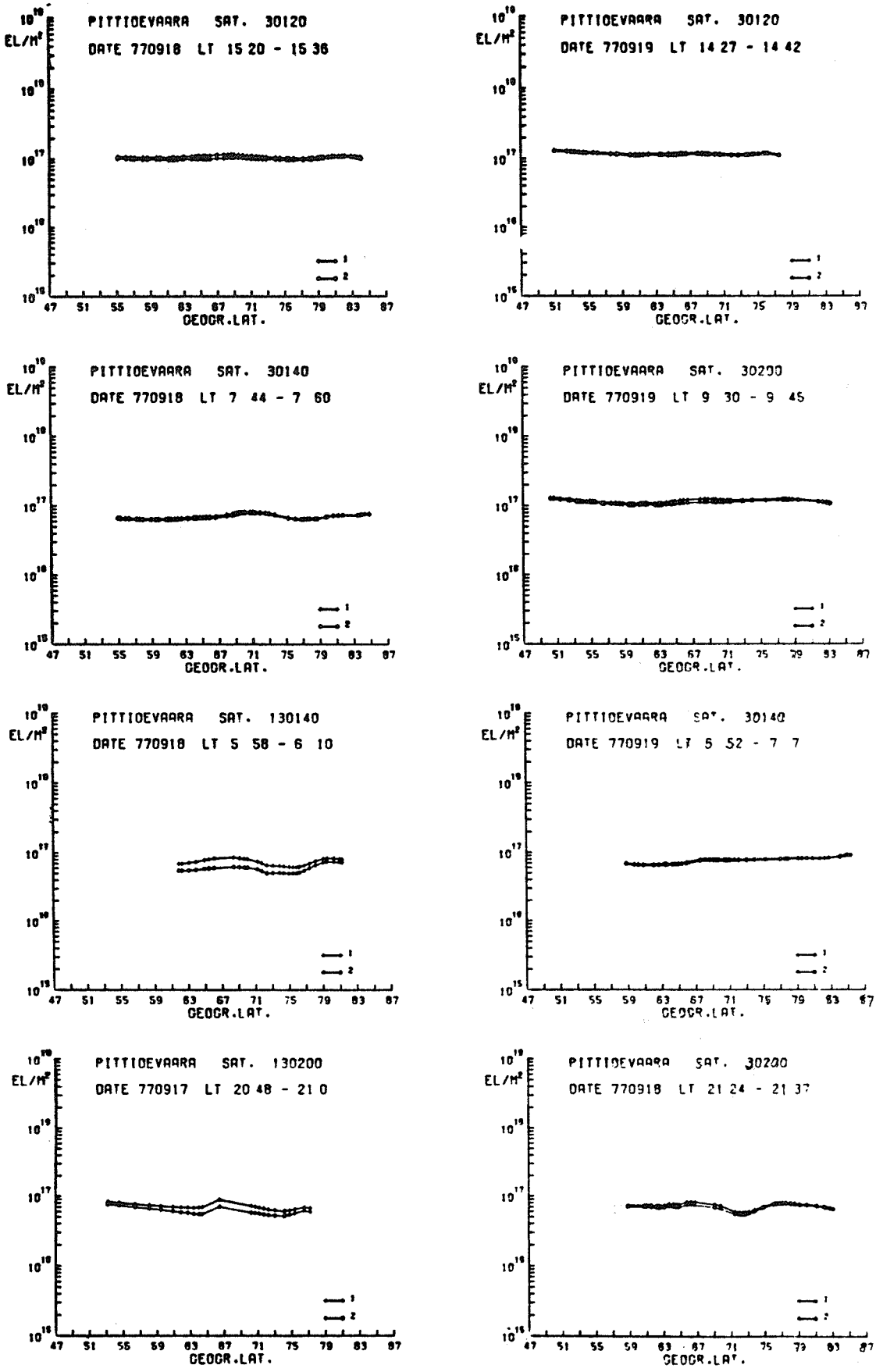

Fig. 6. Total electron content.

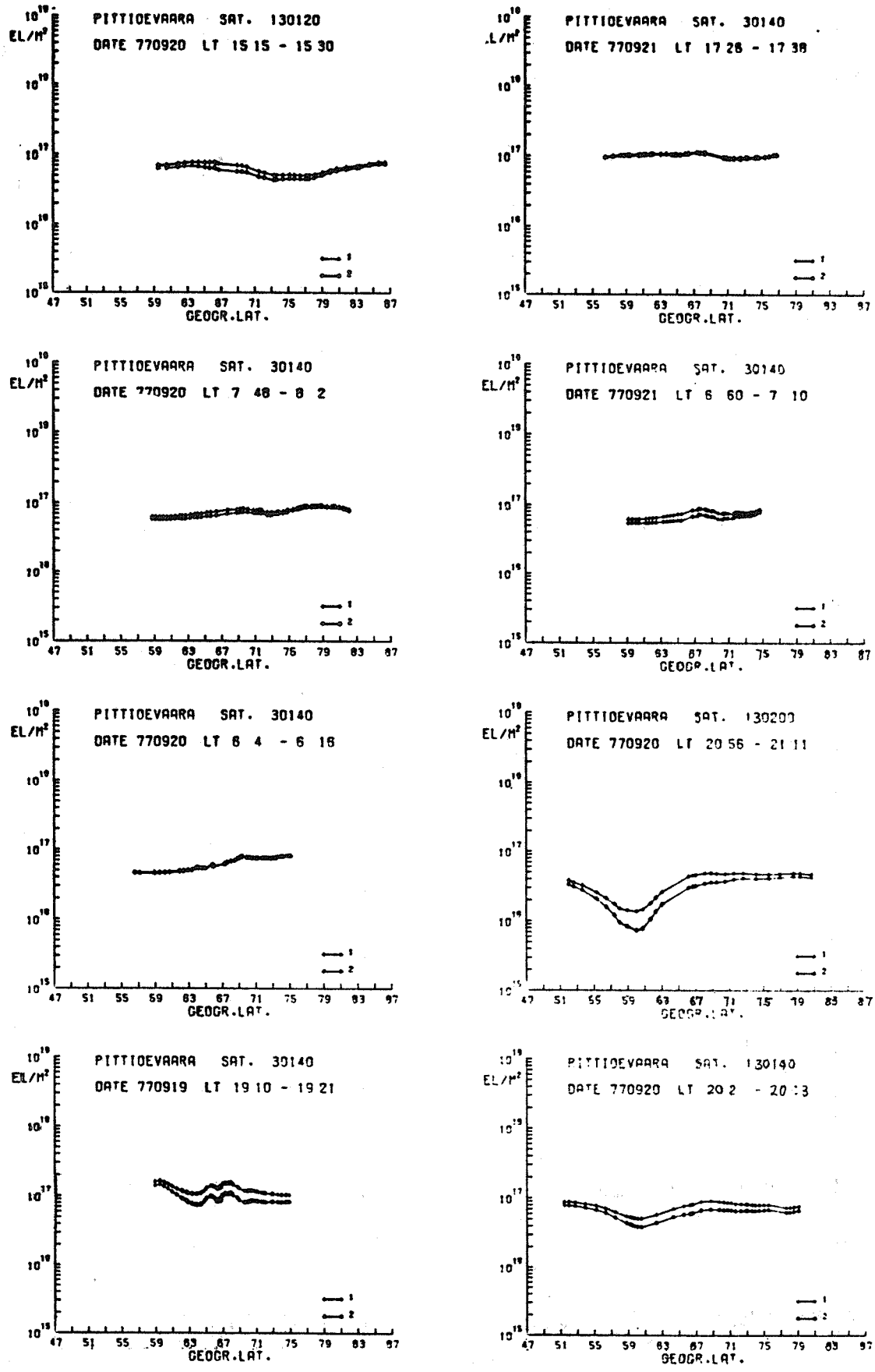

Fig. 7. Total electron content.

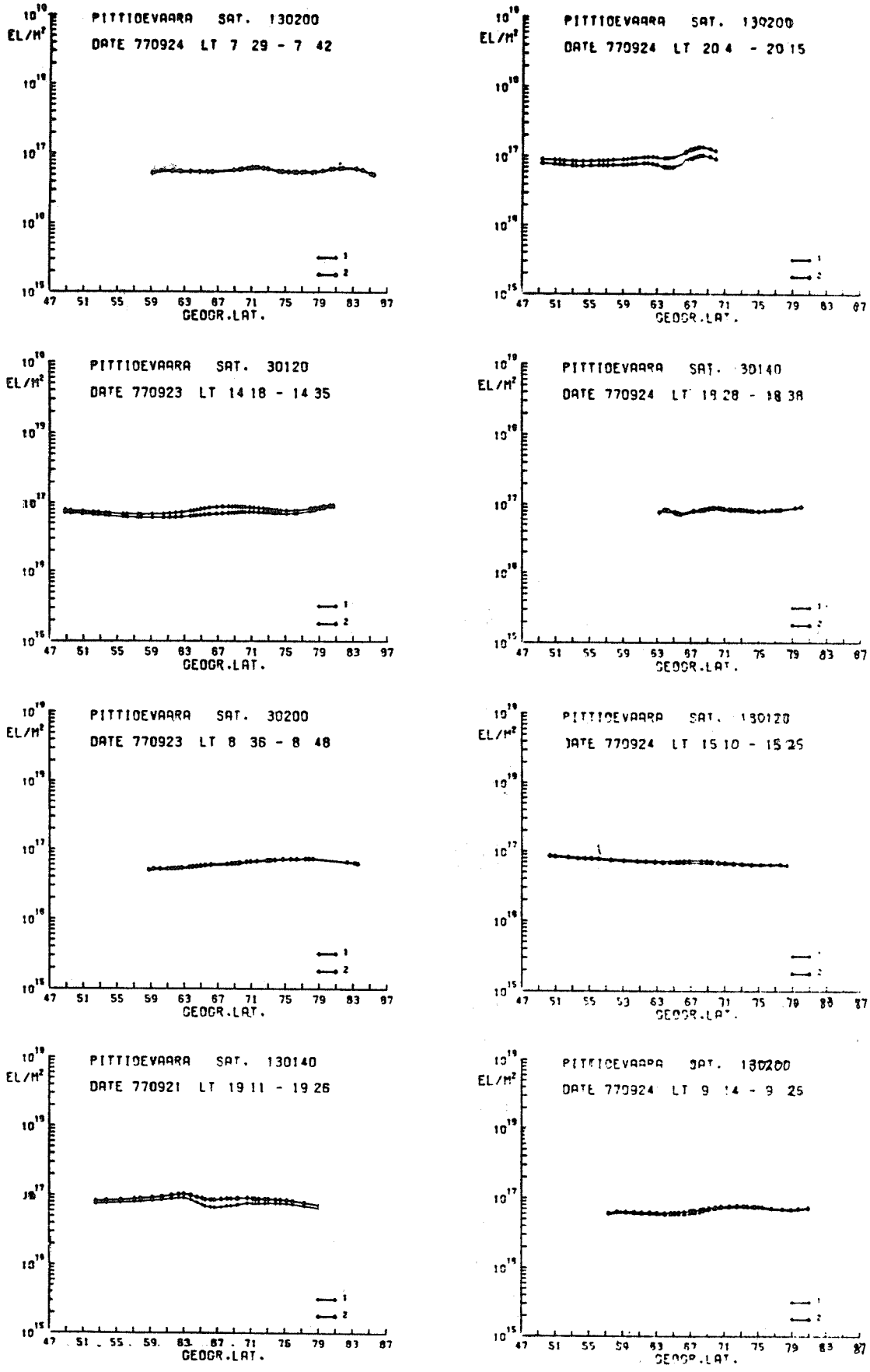

Fig. 8. Total electron content.

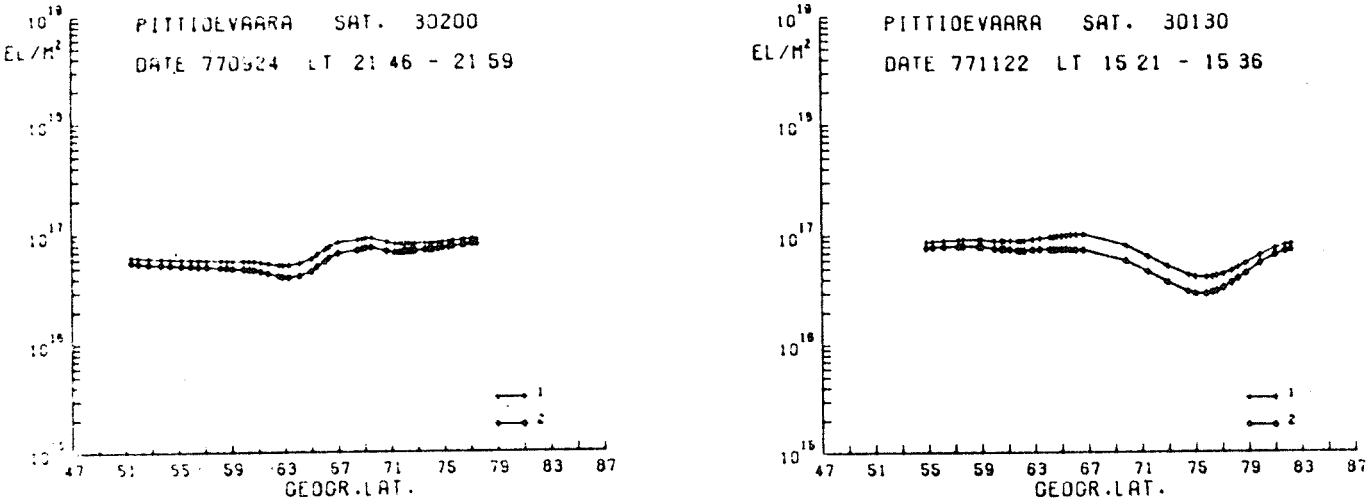

Fig. 9. Total electron content.

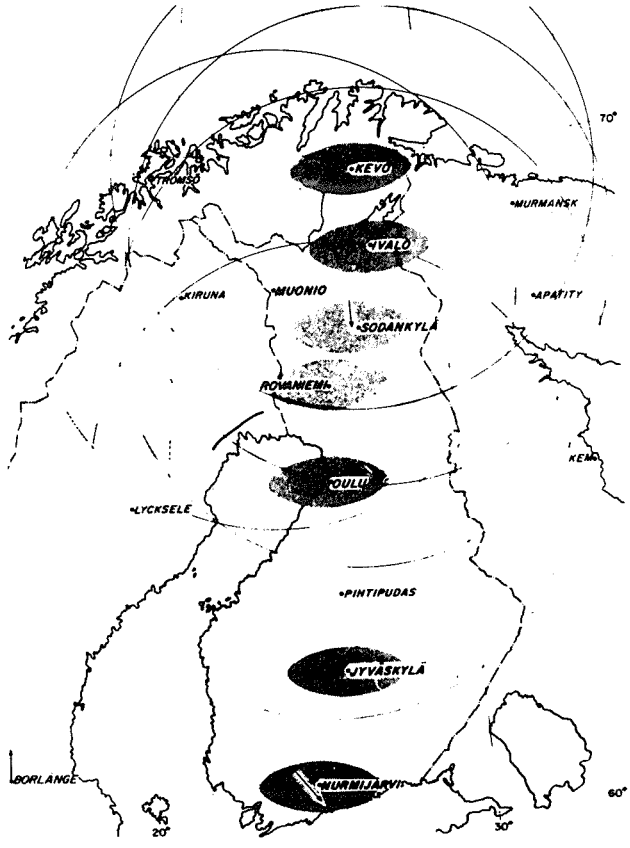

Fig. 10. The location of Finnish riometer chain giving also the antenna patterns of riometers projected to the 100-km level.

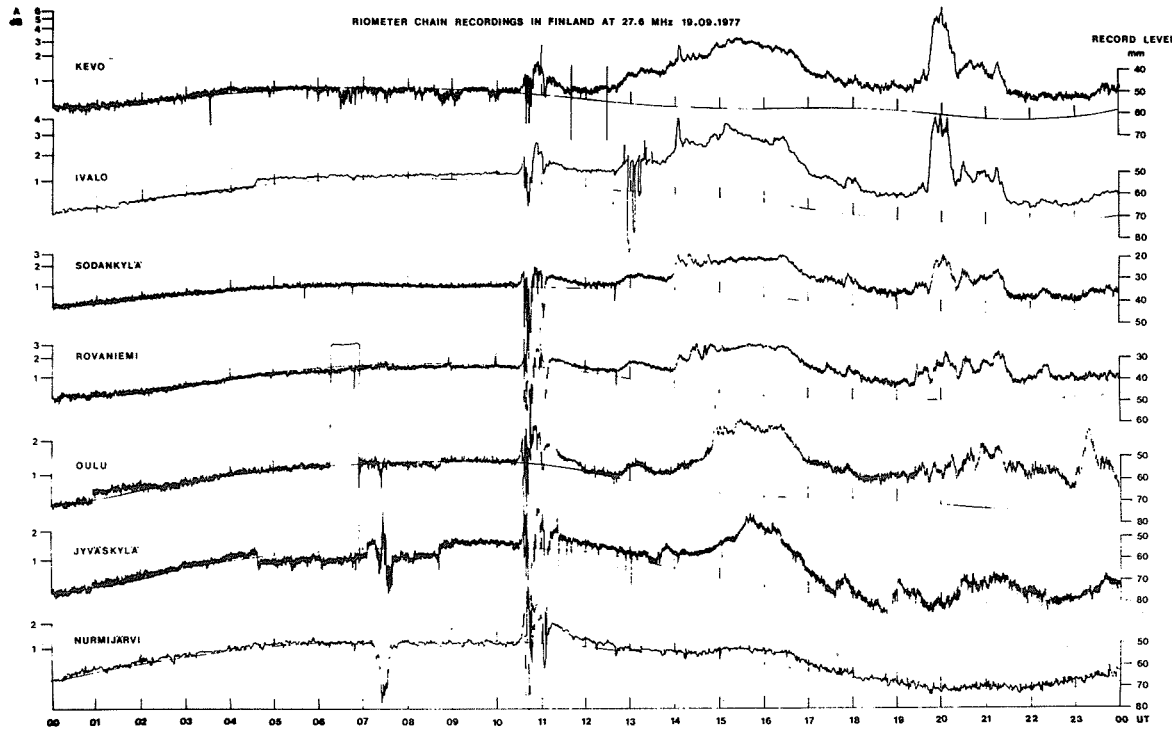

Fig. 11. The riometer recordings of the Finnish riometer chain September 19, 1977 including the quiet day level.

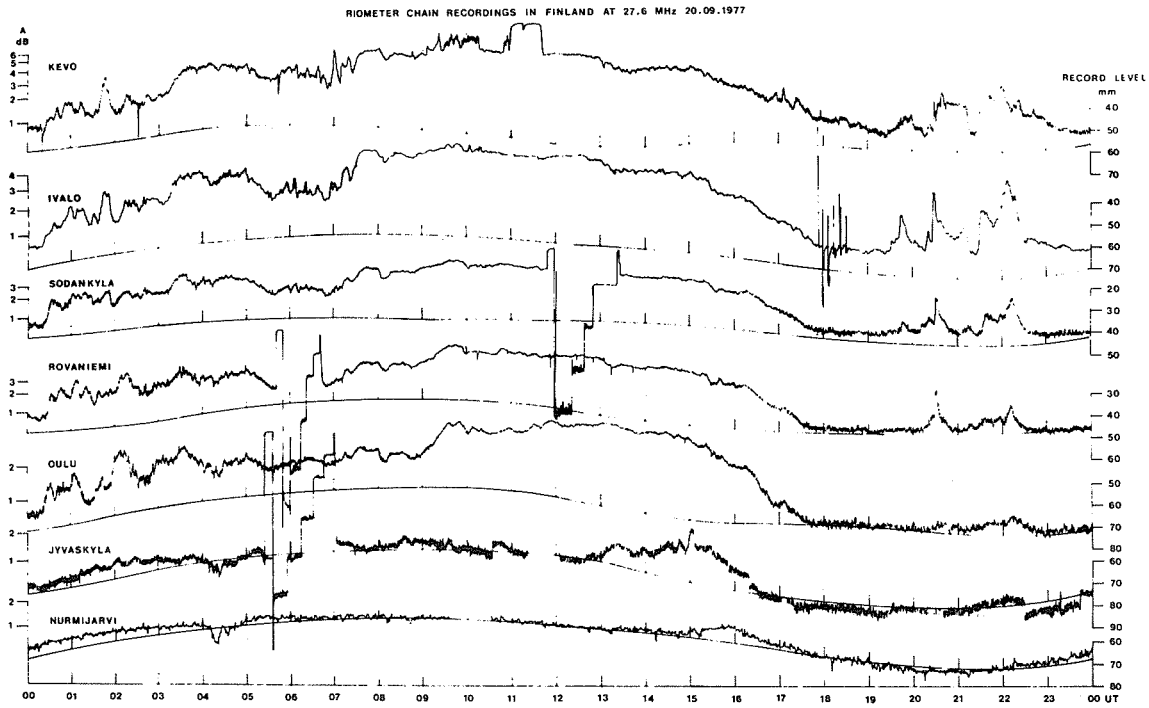

Fig. 12. The riometer recordings of the Finnish riometer chain September 20, 1977 including the quiet day level.

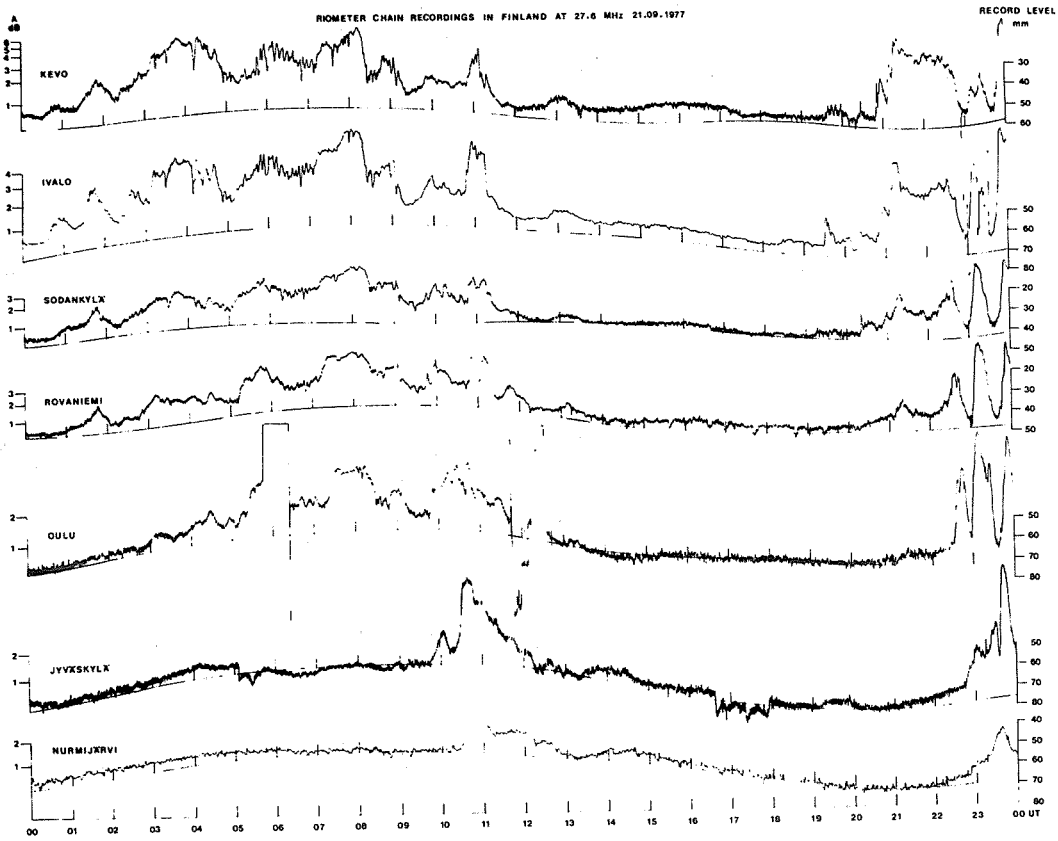

Fig. 13. The riometer recordings of the Finnish riometer chain September 21, 1977 including the quiet day level.

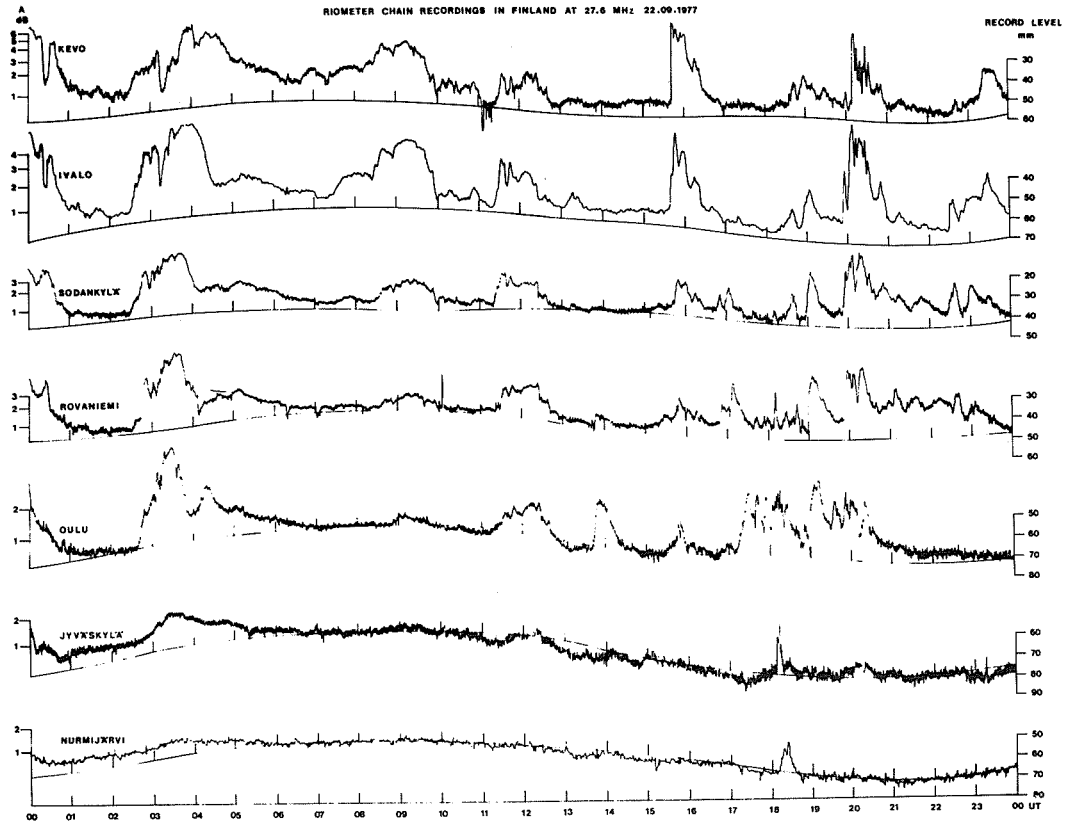

Fig. 14. The riometer recordings of the Finnish riometer chain September 22, 1977 including the quiet day level.

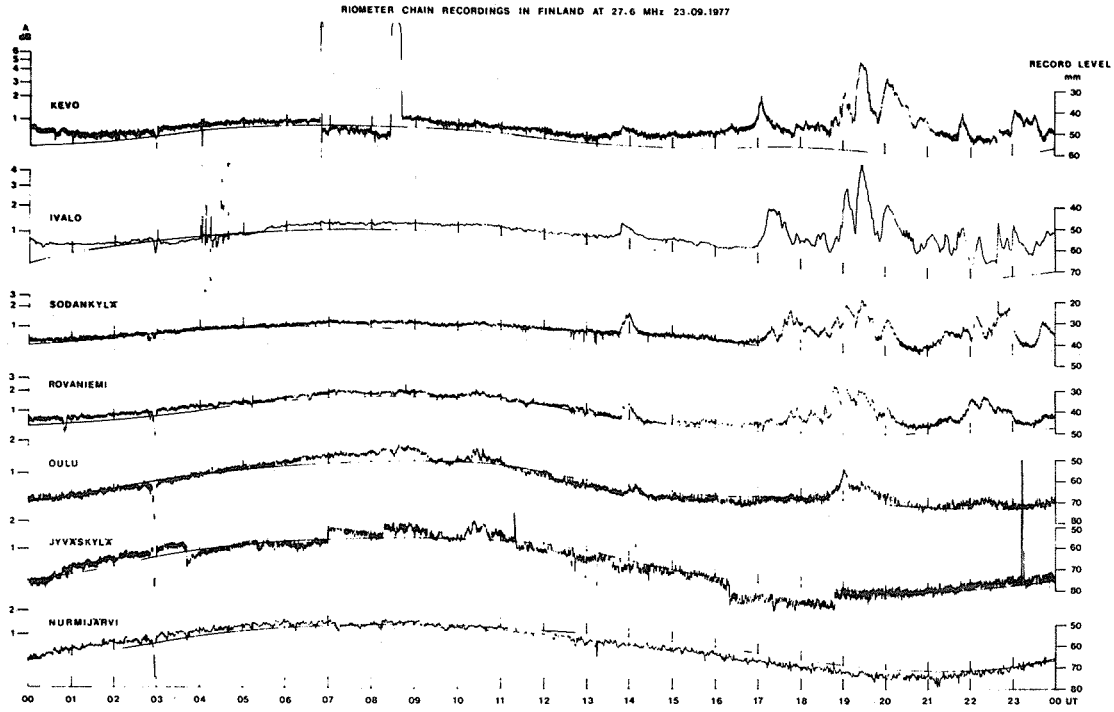

Fig. 15. The riometer recordings of the Finnish riometer chain September 23, 1977 including the quiet day level.

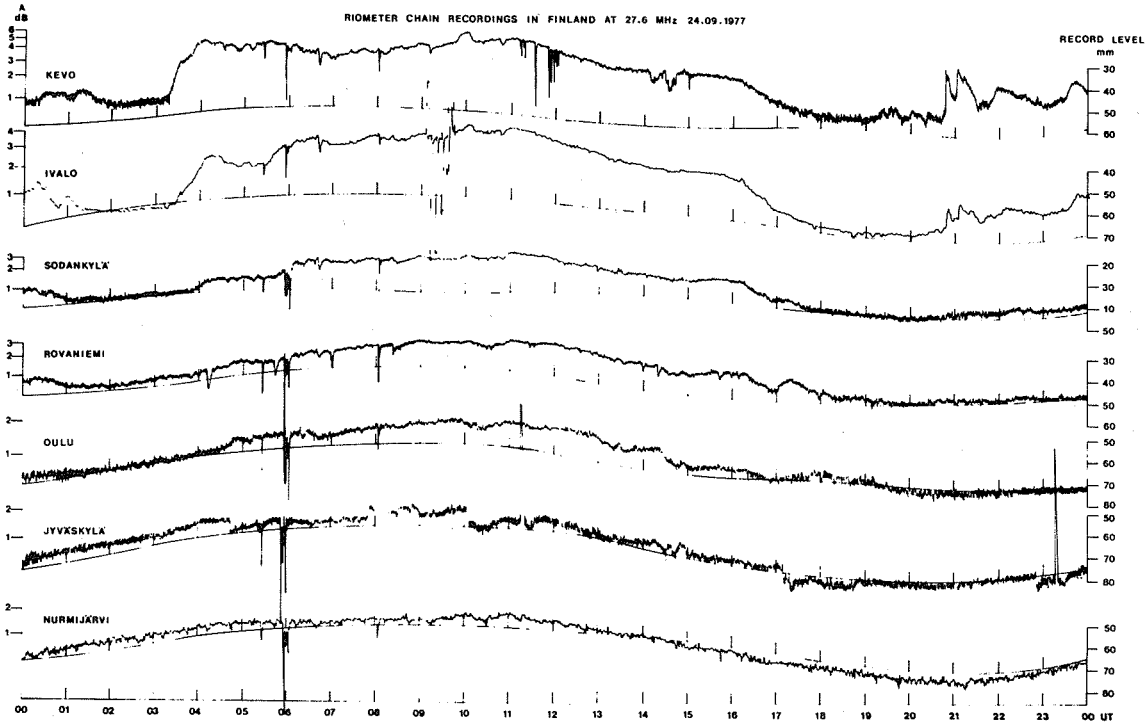

Fig. 16. The riometer recordings of the Finnish riometer chain September 24, 1977 including the quiet day level.

6. GEOMAGNETISM

Forecasts of Geomagnetic Activity during September 7-24, 1977

by

K. Marubashi, Y. Miyamoto and K. Nozaki
Hiraiso Branch, Radio Research Laboratories
Nakaminato, Ibaraki 311-12, Japan

The Hiraiso Branch of the Radio Research Laboratories conducts the daily forecast of geomagnetic activities as the Forecast Center of the Western Pacific Regional Warning Center under the program of the International Ursigram and World Days Service. This note shows how the forecasts were made at this Center during September 7-24, 1977, and how the forecasts agreed with the actual magnetic activity.

During September 7-24, 1977, McMath plage region 14943 was very active and most solar-geophysical activity was associated with this region. Figure 1 illustrates the solar-terrestrial physics phenomena having close relevance to the forecast of geomagnetic activity for the period. The data are mostly from the Ursigram-interchanged data source. This chart includes the following:

(a) Day-to-day variations in the area of the sunspot group, the number of spots in the group, and the Zurich sunspot class from Boulder; and the plage area from McMath-Hulbert. All of these are for McMath region 14943.

(b) The time of flare maximum and the flare importance for 72 reported flares in the period. The flares in McMath region 14943 and in its vicinity are indicated by solid lines, and those in other regions by dashed lines.

(c) The spectral features of selected major solar radio burst events. The selected events are those which exhibit radio emissions of wide frequency range and of longer duration. The thick line indicates the start time of radio burst, and the maximum flux values are plotted toward right in logarithmic scale.

(d) The radio flux of 3-cm wavelength and the flux ratio of 3-cm to 8-cm wavelength from the noise source in McMath region 14943 measured at Toyokawa.

(e) The start, maximum, and end times of PCA events and the maximum absorption measured by riometers at Russian Arctic stations. Proton events and electron events are indicated by letters P and E, respectively.

(f) Variations in the geomagnetic Kp index (solid line) and K index from Kakioka (dashed line), together with the time intervals for which coronal holes pass the central meridian of the solar disk within the latitude range -23° to 37°. The daily sums of Kp and K, and the times of SC's are also shown.

At the bottom of the Figure the days for which MAGALERT's were issued are indicated by shading. Normally, MAGALERT is issued for such a day in which the daily sum of Kp indices is expected to exceed 25 and/or the commencement of a magnetic storm is expected. The decision of daily forecast is made around 0100 UT. In general, the forecasts of geomagnetic activity are decided by taking into account evolutionary changes in the solar-terrestrial environment. It is seen in the Figure that the activity of McMath 14943 was rather low from September 11 to 15. This feature is clear in the number of flares, major radio bursts, and PCA's. Such tendencies can be seen also in the spot area and the radio flux of 3-cm wavelength.

The solar flare on September 7 was disregarded because it was too far east to cause a magnetic storm. The first interval of MAGALERT (September 11 to 13) was decided on September 9 by the consideration of recurrent activity. Little attention was paid to the flare on September 9 around 1600 UT, because MAGALERT had already been issued for the 11th through the 13th.

The issuance of MAGALERT from September 18 to 23 can be divided into the following 3 epochs:

(1) The flare of September 16 around 2200 UT was accompanied by very large bursts of meter waves, and Culgoora reported very strong Type II and Type IV emissions. Thus, a magnetic storm was expected to commence on September 18 or later. On the 18th MAGALERT was issued for the interval September 18-20.

(2) The storm did not commence until September 19, so we concluded that the period of disturbance would continue until September 21. Therefore, MAGALERT was extended to the 21st on September 20.

(3) On September 21, we expected magnetic storms to occur on September 21 or 22 judging from the solar flares on the 19th and 20th and the associated radio phenomena. Thus, MAGALERT from September 21 to 23 was issued.

In conclusion, geomagnetic storms of SC type occurred on September 12, 19 and 21 during the period concerned. As has been shown, the overall agreement between forecast and actual activity is quite satisfactory for this period. The MAGALERT for September 18 was the only false alert and we did not miss any magnetic disturbance in our forecast. However, we are not certain whether the reasoning for the forecast was correct or not. The September 12 and 19 events could be caused by either the coronal hole-related stream or the flare-associated stream. We must wait for more detailed data to conclude which is the main cause of the magnetic storm for these two events.

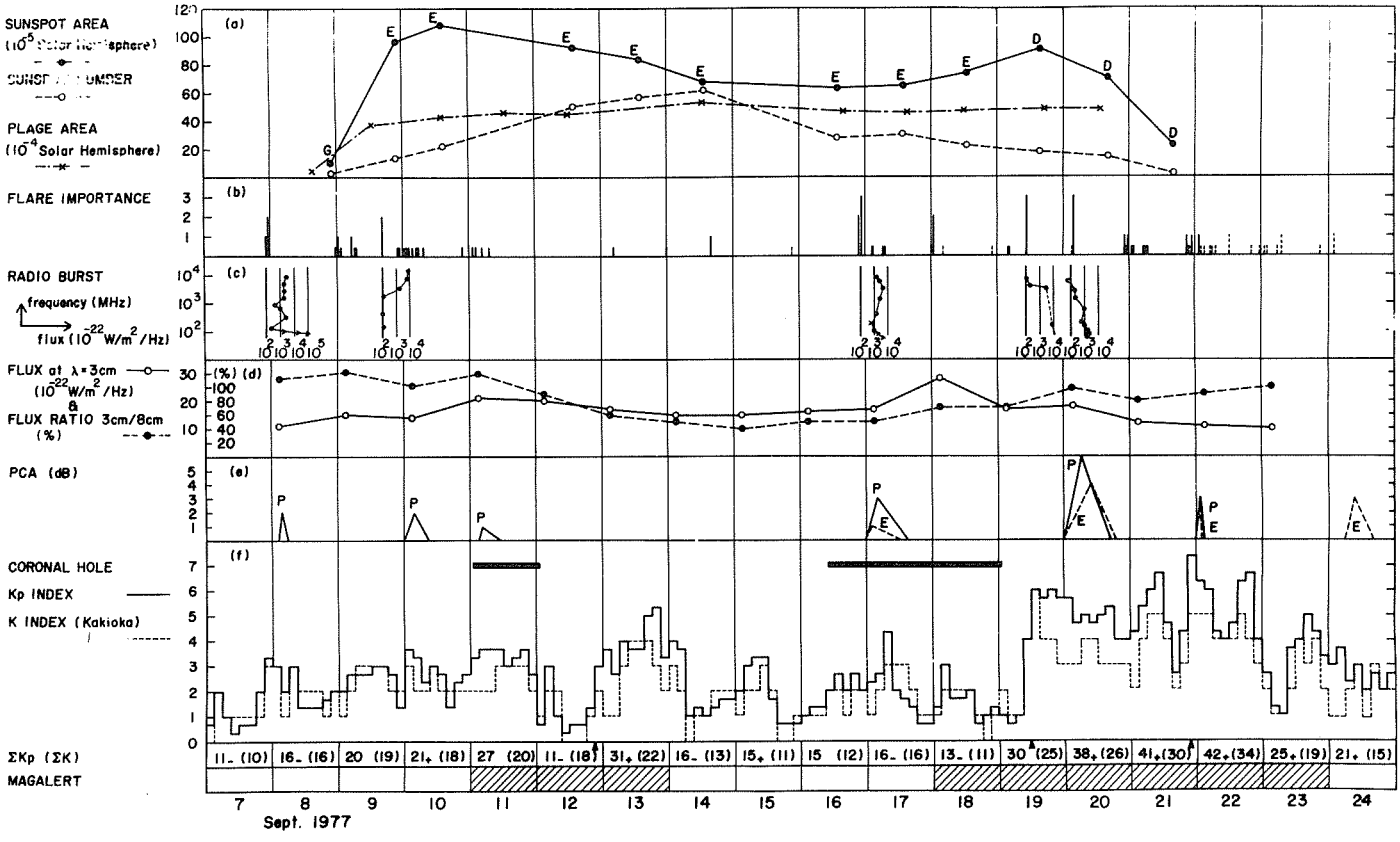

Fig. 1. Solar-terrestrial activity chart for the period from 7 to 24 September, 1977. The days for which magnetic disturbances were forecast are indicated by shading at the bottom of the figure.

Dst Index for September 7 - November 27, 1977

by

M. Sugiura and D.J. Poros
Electronics Branch, GSFC/NASA
Greenbelt, MD 20771

The Figure below presents the first Dst values by 27-day Carrington rotation for September 7 through November 27, 1977.

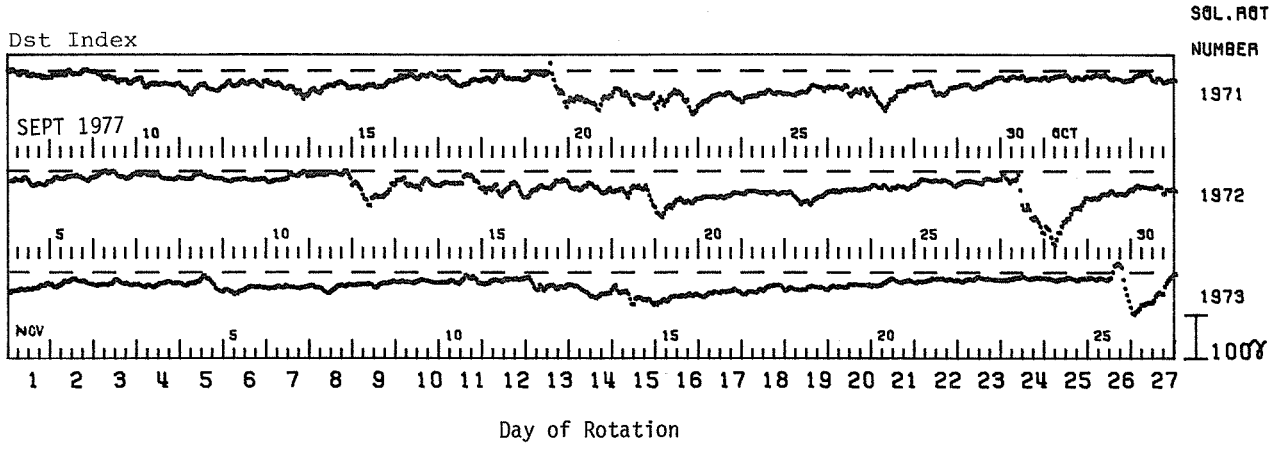

Geomagnetic Pulsations at Auroral Latitudes during September 21-22, 1977

by

O. Hillebrand, E. Steveling, J. Watermann, and U. Wedeken
Institut für Geophysik der Universität
Herzberger Landstrasse 180
3400 Göttingen, F.R.G.

Introduction

The Geophysical Institute of the University of Göttingen is participating in the IMS by operating a pulsation magnetometer chain on a meridional profile in Northern Scandinavia. In 1977 those six stations were active from September 10 to December 16. At the same time one of the induction coil magnetometers used in the research program "Geomagnetic and Magnetotelluric Soundings in the Area of the European Riftsystem" was tested at the midlatitude side Bramwald (BWD).

Instrumentation and Recording Sites

The sensors for the three components H, D and Z of the geomagnetic pulsations recorded in Scandanavia are Grenet-type induction variometers. The period range of the instruments extends from 2s to approximately 600s. In the period range around 20s the maximum resolution is 0.05 nT. The sensitivity decreases towards shorter and longer periods, e.g. at 100s the resolution is approximately 10 digital steps/nT and decreases linearly with the period. At BWD a triple coil induction magnetometer was used. The frequency response of this type of pulsation magnetometer differs slightly from that of the Grenet-type magnetometer. The recorded periods are between 6s and 600s with a linear decrease of sensitivity above 10s (approximately 200 digital steps/nT at 20s and 40 steps/nT at 100s respectively). So the records from both types of instruments are directly comparable for periods longer than 40s.

The three northern stations in Scandanavia have a digital recording system with 1 sample/s for each component, the other three IMS instruments are equipped with FM tape recorders. The station at BWD has a digital recording system too with a sampling rate of 2s. A time accuracy better than 0.1s at all stations can be assured. Table 1 shows some details of the stations.

Table 1. Pulsation Recording Sites in Northern and Central Europe 1977.

Station	Abbr.	Equipment *	Geographic Coordinates Lat. N	Long. E	L-value
SKARSVAAG	SKA	D1	71° 7'	25°50'	6.8
KUNES	KUN	D1	70°21'	26°31'	6.4
KEVO	KEV	D1	69°45'	27° 2'	6.1
IVALO	IVA	FM	68°36'	27°28'	5.5
MARTTI	MAR	FM	67°28'	28°17'	5.1
KUUSAMO	KUU	FM	65°55'	29° 3'	4.6
BRAMWALD	BWD	D2	51°31'	9°19'	2.3

*Types of equipment:
D1 - Grenet-type magnetometer, 7-track digital tape recorder
FM - Grenet-type magnetometer, FM tape recorder
D2 - induction coil magnetometer, digital cassette recorder

Observation of Geomagnetic Storm Pulsations on September 21-22

A short example of data will be given in this report. On September 21-22, 1977, the geomagnetic activity was rather high (Kp values between 3- and 7+), and storm associated geomagnetic pulsations were observed by our auroral and midlatitude stations.

A summary plot of the pulsation activity at KEV, 1800-0600 September 21-22, 1977, is given in Figure 1. Six intervals, each containing two hours of data of the three components H, D and Z, are plotted one below the other. The ssc at 2044 UT is mainly visible in the H-component. After this at about 2050 UT the major activity starts. The first interval of strong pi2 pulsations lasts until 2250 UT. Then the activity is less for about one hour, and at 2347 UT the pi2 pulsations show a new onset with maximum amplitudes of more than 60 nT. After a relatively quiet period between 0100 and 0200 UT (the automatic calibration occurs at 0130 - 0134 UT) regularly shaped large amplitude pc4 pulsations can be observed. It is remarkable that in the main phases the D component shows larger amplitudes than the H component. After 0300 UT the periods of the pulsations shift into the pc5-range and the whole activity decreases slowly.

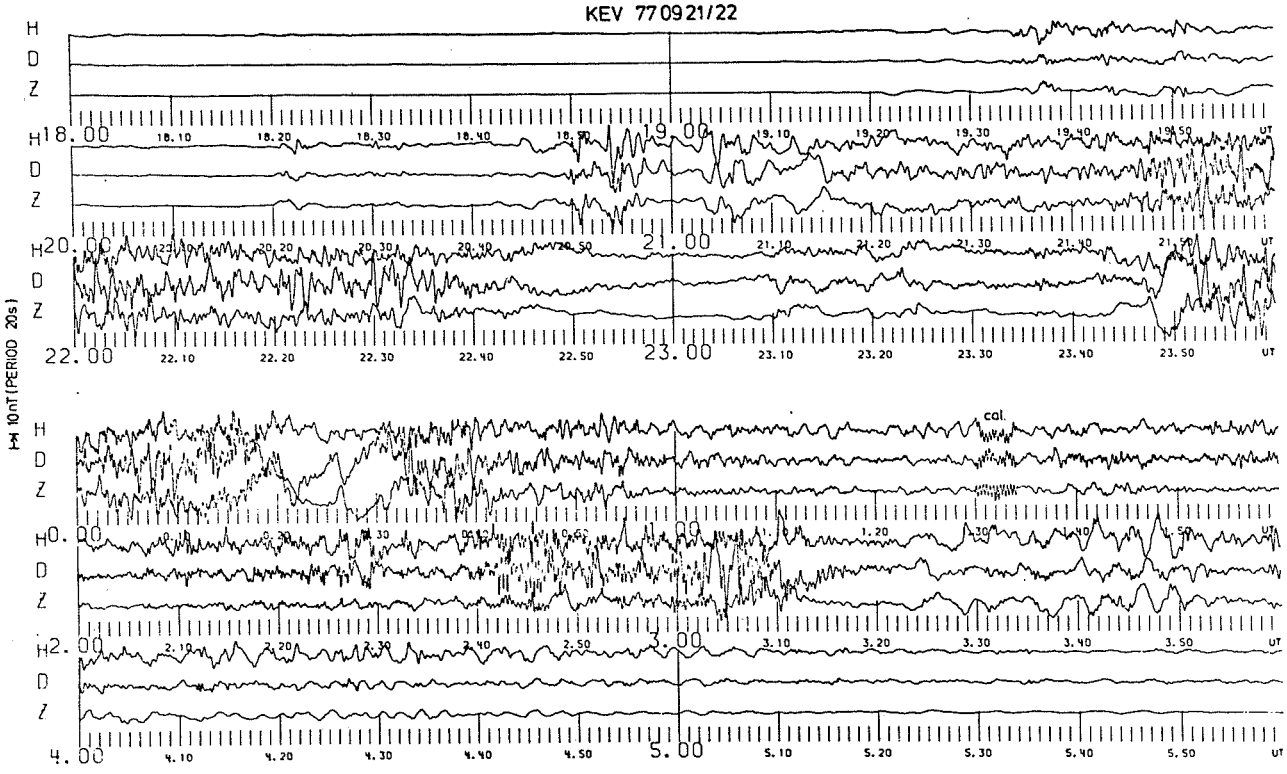

Fig. 1. Geomagnetic pulsations recorded at KEV, 1800 - 0600 UT September 21-22, 1977 (Kp=4+7+6+6o).

A selected time interval showing two examples of pi2 pulsations at all seven stations is plotted in Figure 2. Because of the larger scale factor the pulsations of this time interval can be seen more distinctly than in Figure 1. The first pi2 effect around 2021 UT is an example where the phase of the H component of the midlatitude station is nearly opposite (notice the difference in scale factors between BWD and the other stations). Maximum amplitudes of H and D are found at IVA and MAR. The D component of the first pi2 effect does not show very characteristic features. At SKA the Z component is larger than the horizontal components and opposite to H because of the shore effect.

The second pi2 effect is associated with the ssc at 2044 UT. The H-component traces at the northern stations are similar (note the later beginning and the shorter period at BWD).

Data Availability

Data from the three northern stations SKA, KUN, KEV are available in copies from the compressed digital working tapes. The data from the FM stations IVA, MAR, KUU are not yet completaly digitized, but they are available, on special request only. Copies from the data files of the station BWD are available too. All data can be requested at the author's address.

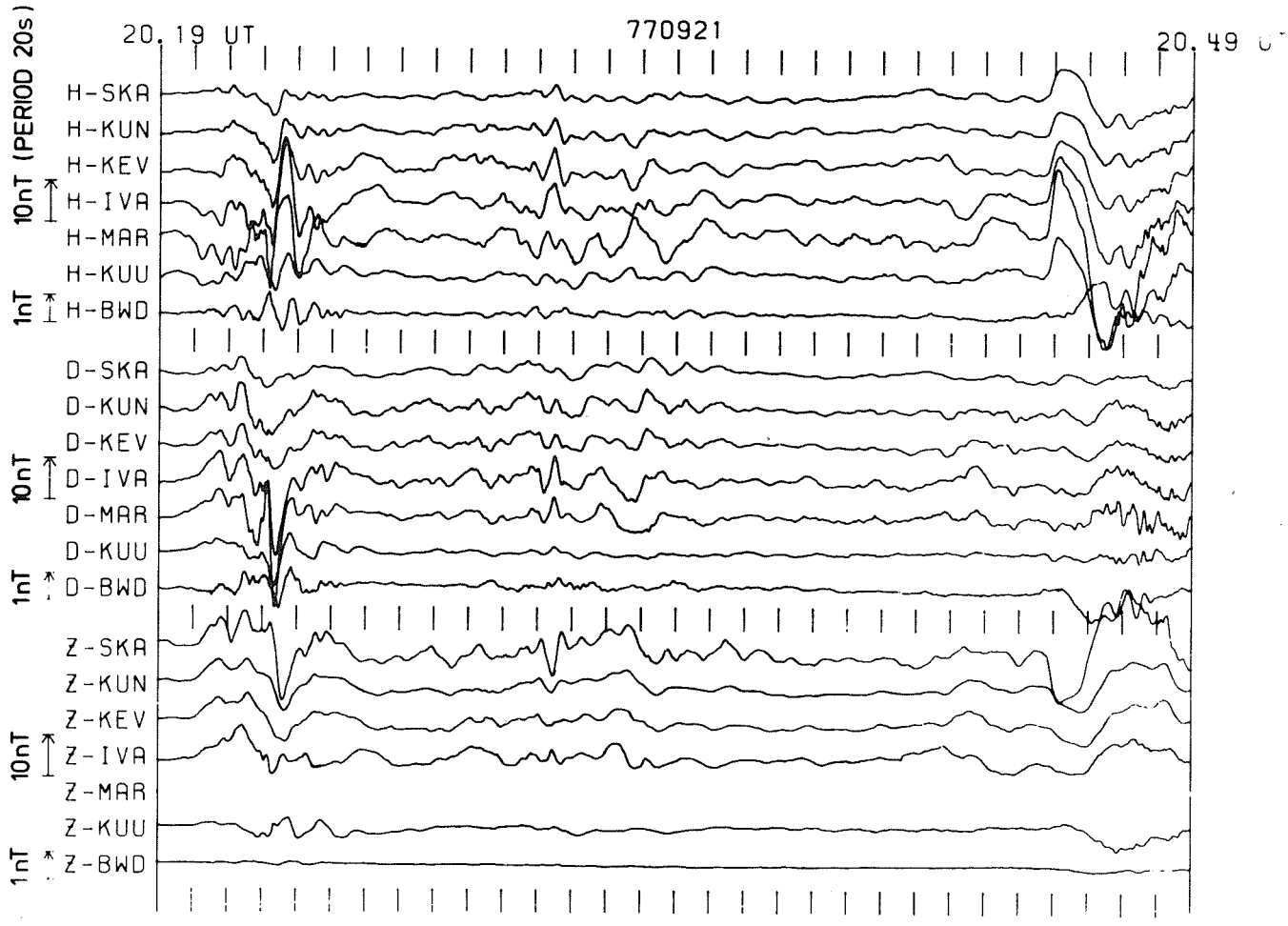

Fig. 2. Recording of all seven stations for the time interval 2019 - 2049 UT September 21, 1977. There were no Z-MAR data at this time.

Geomagnetic Pulsation Data of the Nagycenk Observatory for September 1977

by

L. Holló and J. Verö
Geodetic and Geophysical Research Institute of the
Hungarian Academy of Sciences, Sopron

Introduction

A catalog of geomagnetic pulsation data and daily pulsation indices has been prepared at the Nagycenk Geomagnetic Observatory since 1966. The daily pulsation indices are regularly published in the Observatory Reports. A detailed description of the processing of the pulsation data has also been published (see References). Here only a short summary of the main points is given.

September 1977 Pulsation Catalog

The Nagycenk Observatory is situated at geographic coordinates ϕ = 47° 38' (lat.), λ = 16° 43' (long.) and geomagnetic coordinates Φ = 47.2°(lat.), Λ = 98.3°(long.), in Western Hungary. Earth-current records have been continuously made since 1957, rapid run earth-current records since 1966. The basic interval for the pulsation catalog is 30 min. A characteristic section of each 30-min record is selected for determining the pulsation activity and amplitude in each of 12 bands. These bands are the following (the names of the bands are identical with those of the daily pulsation indices discussed below):

P1	1 - 5 sec	P7	30 - 40 sec
P2	5 - 10 sec	P8	40 - 60 sec
P3	10 - 15 sec	P9	60 - 90 sec
P4	15 - 20 sec	P10	90 - 120 sec
P5	20 - 25 sec	P11	120 - 300 sec
P6	25 - 30 sec	P12	300 - 600 sec

Tables 1 - 18 contain the data of the pulsation catalog for September 7 - 24, 1977. Here UT refers to the beginning of each 30-min interval. The abbreviations used for the various kinds of pulsations are the following:

O,	sinusoidal oscillations with periods changing by less than 10%
Q,	sinusoidal oscillations with periods changing by 10-50%
W,	sinusoidal oscillations with periods changing by more than 50%
pt,	pi-type events
T,	irregular pulsations
TH,	two-component irregular pulsations; the longer period is longer than 2 min
TD,	two-component irregular pulsations; the longer period is shorter than 2 min

The numbers under the band/period column headings indicate which bands were active and represent amplitudes in arbitrary units of 0.2 mV/km.

Daily Pulsation Indices

The activity indices are computed from the daily sum of the number of 30-min intervals with activity in the corresponding band; O- and Q-type pulsations double weight. In a basic interval, the frequency of occurrence of each index between 1 and 5 was statistically the same, owing to the 6 mm/min chart speed. The shorter period bands were seldom active, their corresponding activity indices are less reliable, and often equal 1.

Figure 1 shows the bands active in all 30-min intervals for the period September 7 - 24, 1977. The vertical axis corresponds to all periods between P1 and P12. Figure 2 represents the daily activity indices for the days studied. The average amplitudes of these data are shown in Figure 3 where the amplitude values are arbitrarily expressed in mV/km.

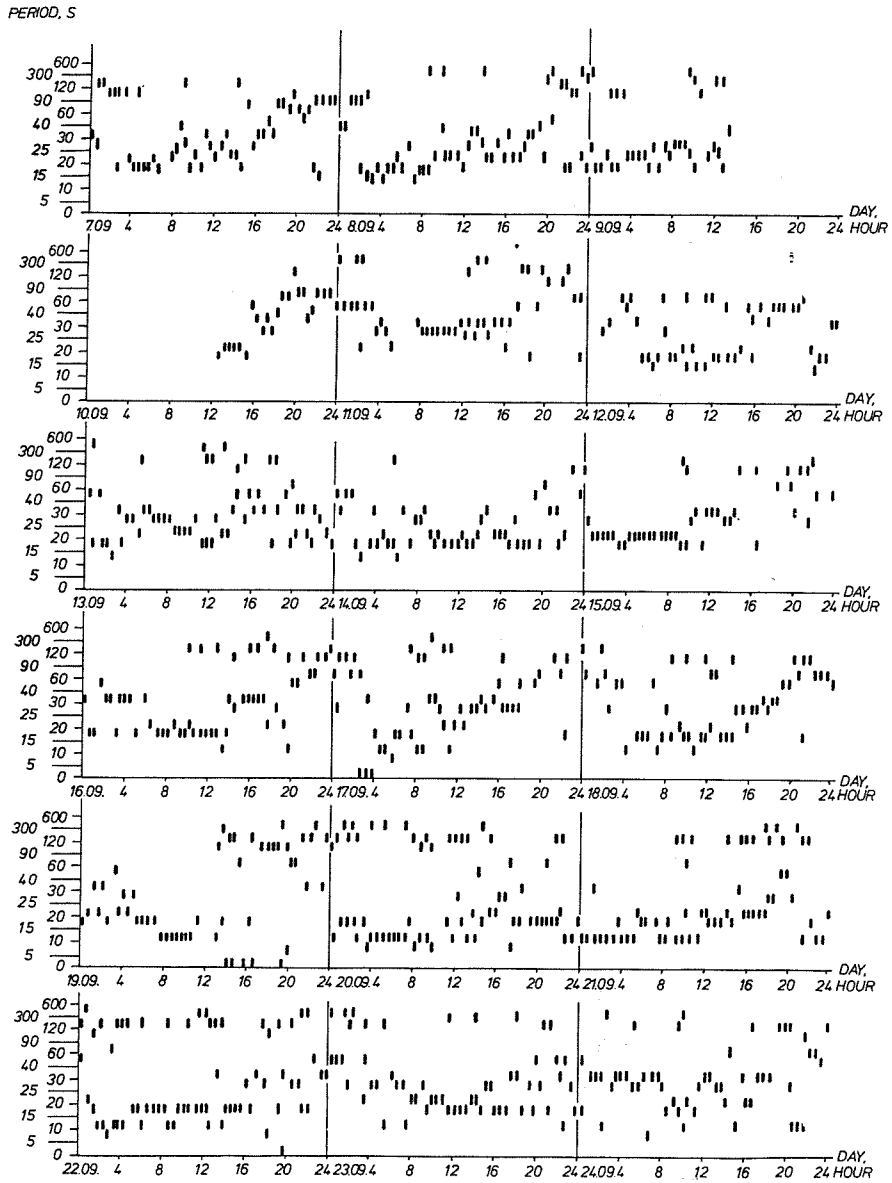

Fig. 1. Active bands of geomagnetic pulsations recorded at Nagycenk Observatory during the period September 7-24, 1977. Each vertical tic mark denotes activity measured within a 30-min interval. The units along the y axis measure the pulsation periods in seconds.

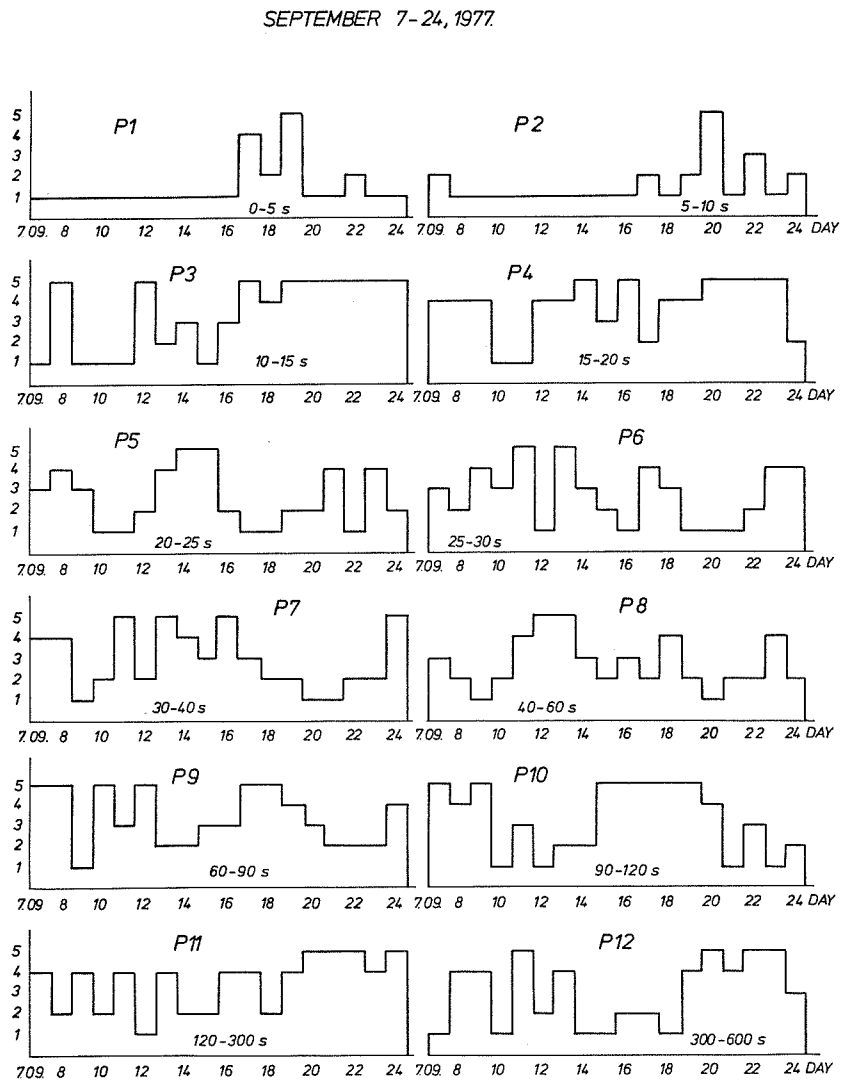

Fig. 2. Daily activity indices for each of the 12 pulsation bands during the September 7-24, 1977, period. Activity indices are computed from the daily occurrence frequency (in 30-min intervals) of each kind of geomagnetic pulsation.

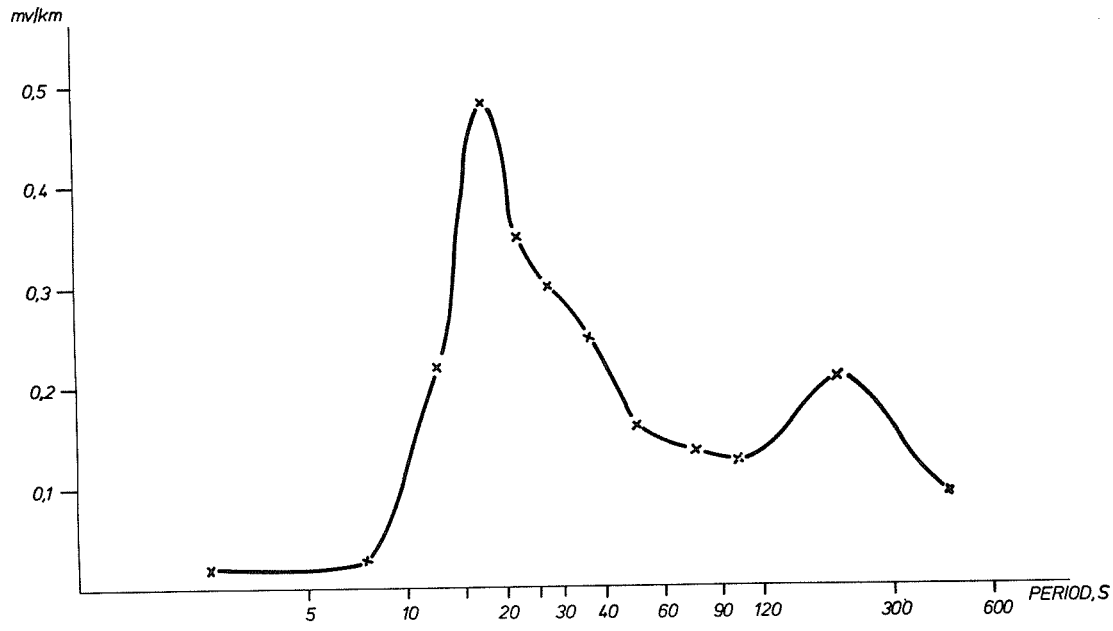

Fig. 3. Average pulsation amplitude as a function of pulsation period during the September 7-24, 1977, interval. Average amplitudes are expressed in mV/km, the periods in sec.

Figure 4 suggests a connection exists between the data of the pulsation catalog (active bands similar to Figure 1) and the scalar value of the interplanetary magnetic field (right-hand vertical scale). The interplanetary field is represented by the curve. Similar connections exist in a rather high percentage of all available data. Pulsation amplitudes are strongly influenced by the energy of the solar wind velocity, by the direction of the interplanetary magnetic field and by magnetospheric processes. Although these connections are likely to exist between geomagnetic pulsations with periods of 10 - 120 (300?) sec, the shortest and longest period pulsations have different properties.

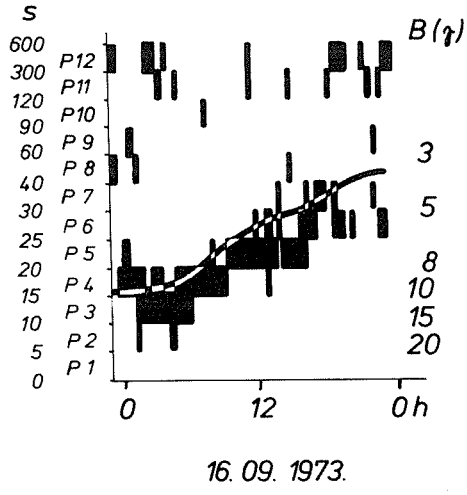

Fig. 4. Relationship between the geomagnetic pulsation period in sec and the scalar value of the interplanetary magnetic field in gammas on September 16, 1977. The solid curve traces the diurnal magnitude variation of the interplanetary magnetic field.

More detailed data, or data from other intervals can be sent on request.

References

HOLLÓ, L., M. TÁTRALLYAY and J. VERŐ 1972 Experimental Results with the Characterization of Geomagnetic Micropulsations, Part I. Acta Geodaetica, Geophysica, et Montanistica Hungaricae, 7, 155 (in Hungarian).

MILETITS, J. CZ. L. HOLLÓ M. TÁTRALLYAY and J. VERŐ 1978 Experimental Results with the Characterization of Geomagnetic Micropulsations, Part VI, Acta Geodaetica, Geophysica et Montanistica Hungaricae, 13, 231 (in Hungarian).

Table 1

SEPTEMBER 7, 1977.

UT	Type	BAND P1	P2	P3	P4	P5	P6	P7	P8	P9	P10	P11	P12
		PERIOD,S 0-5	5-10	10-15	15-20	20-25	25-30	30-40	40-60	60-90	90-120	120-300	300-600
0000	T							2					
0030	TH						1					6	
0100	T											2	
0130	T										2		
0200	T										3		
0230	pt				1						6		
0300	T										3		
0330	TH					1						4	
0400	T				1								
0430	TD				1						5		
0500	T				2								
0530	T				2								
0600	T					7							
0630	T				1								
0700	-												
0730	W					7							
0800	T						2						
0830	T								2				
0900	TH						1					3	
0930	T				1								
1000	Q					8							
1030	Q				3								
1100	T							5					
1130	W						6						
1200	Q					5							
1230	Q						4						
1300	T							3					
1330	T					1							
1400	TH					1						3	
1430	T				1								
1500	T									4			
1530	T						2						
1600	T							2					
1630	T							1					
1700	T								1				
1730	T							1					
1800	pt									17			
1830	pt									20			
1900	T								2				
1930	T										2		
2000	T									1			
2030	T								2				
2100	T									4			
2130	T				1								
2200	pt		1/2							13			
2230	pt									31			
2300	T									7			
2330	T									2			

Table 2

SEPTEMBER 8, 1977.

UT	Type	BAND P1	P2	P3	P4	P5	P6	P7	P8	P9	P10	P11	P12
		PERIOD,S 0-5	5-10	10-15	15-20	20-25	25-30	30-40	40-60	60-90	90-120	120-300	300-600
0000	T							1					
0030	T							1					
0100	T									2			
0130	T									2			
0200	pt				1					8			
0230	TH			1/2							3		
0300	T			1/2									
0330	T				1								
0400	T			1/2									
0430	T				1								
0500	W				2								
0530	T					1							
0600	T				1								
0630	T						1						
0700	T			1									
0730	T				2								
0800	T				1								
0830	TH				1								6
0900	W					2							
0930	TH							3					14
1000	O					5							
1030	Q					10							
1100	O												
1130	O				7								
1200	Q						8						
1230	T							5					
1300	W							6					
1330	TH						1						11
1400	T					1							
1430	T					2							
1500	T						2						
1530	T					2							
1600	T							1					
1630	T				1/2								
1700	T					1							
1730	T						3						
1800	T							1					
1830	T							4					
1900	T								3				
1930	TH					1/2						5	
2000	T												9
2030	pt								37				
2100	pt										30		
2130	TH				1						4		
2200	pt				2					16			
2230	T									3			
2300	TH					1							7
2330	TH				1							5	

Table 3

SEPTEMBER 9, 1977.

UT	Type	BAND P1	P2	P3	P4	P5	P6	P7	P8	P9	P10	P11	P12
		PERIOD,S 0-5	5-10	10-15	15-20	20-25	25-30	30-40	40-60	60-90	90-120	120-300	300-600
0000	TH						1						16
0030	T				1/2								
0100	T				2								
0130	T					1							
0200	pt				1						8		
0230	pt				2						6		
0300	T										4		
0330	T					3							
0400	W					4							
0430	W					3							
0500	W					2							
0530	Q				2								
0600	T						2						
0630	T				1								
0700	W						6						
0730	Q					7							
0800	Q						6						
0830	Q						14						
0900	Q						14						
0930	TH					1							8
1000	TH				1							5	
1030	T										11		
1100	W					3							
1130	TH						2					8	
1200	T					2							
1230	TH				1							5	
1300	T							2					
1330													
1400													
1430													
1500													
1530													
1600													
1630					n o	r e c o r d							
1700													
1730													
1800													
1830													
1900													
1930													
2000													
2030													
2100													
2130													
2200													
2230													
2300													
2330													

Table 4

SEPTEMBER 10, 1977.

UT	Type	BAND P1	P2	P3	P4	P5	P6	P7	P8	P9	P10	P11	P12
		PERIOD,S 0-5	5-10	10-15	15-20	20-25	25-30	30-40	40-60	60-90	90-120	120-300	300-600
0000													
0030													
0100													
0130													
0200													
0230													
0300													
0330					n o	r e c o r d							
0400													
0430													
0500													
0530													
0600													
0630													
0700													
0730													
0800													
0830													
0900													
0930													
1000													
1030													
1100													
1130													
1200													
1230	E				1								
1300	Q						4						
1330	T						7						
1400	T						14						
1430	T						2						
1500	T					2							
1530	T								3				
1600	T							2					
1630	T					1							
1700	T							2					
1730	T						4						
1800	T								2				
1830	T									9			
1900	T									3			
1930	T											2	
2000	T									1			
2030	T									1			
2100	T							1					
2130	pt								16				
2200	T									4			
2230	T									1			
2300	T									2			
2330	T								1				

Table 5

SEPTEMBER 11, 1977.

UT	Type	BAND P1	P2	P3	P4	P5	P6	P7	P8	P9	P10	P11	P12
		PERIOD,S 0-5	5-10	10-15	15-20	20-25	25-30	30-40	40-60	60-90	90-120	120-300	300-600
0000	T												5
0030	T								1				
0100	T								1				
0130	TH								2				19
0200	TH					2							7
0230	T								5				
0300	TW								4				
0330	T						1						
0400	T							9					
0430	TW						5						
0500	T					8							
0530													
0600													
0630													
0700													
0730	Q							14					
0800	Q						13						
0830	Q						6						
0900	WH						6						16
0930	O						13						
1000	O						23						
1030	Q						11						
1100	Q						13						
1130	Q						1						
1200	Q						9	10					
1230	TH							3				5	
1300	TH						2						8
1330	T							3					
1400	QH							8					15
1430	W						3						
1500	T							5					
1530	T							2					
1600	T					2							
1630	Q							4					
1700	T								2				
1730	T											5	
1800	T											2	
1830	T				1/2								
1900	T								1				
1930	T											3	
2000	T										2		
2030	-												
2100	-												
2130	T										1		
2200	T											5	
2230	pt									28			
2300	TD				1					4			
2330	-												

Table 6

SEPTEMBER 12, 1977.

UT	Type	BAND P1	P2	P3	P4	P5	P6	P7	P8	P9	P10	P11	P12
		PERIOD,S 0-5	5-10	10-15	15-20	20-25	25-30	30-40	40-60	60-90	90-120	120-300	300-600
0000	-												
0030	-												
0100	-												
0130	T						1						
0200	T							1					
0230	T												
0300	pt									7			
0330	T								4				
0400	T									5			
0430	T							2					
0500	T				1								
0530	T				1								
0600	T			1/2									
0630	T				1/2								
0700	T						1						
0730	T									1			
0800	T				1/2								
0830	T				1/2								
0900	T					1							
0930	TD			1/2						3			
1000	T					1							
1030	T			1/2									
1100	TD			1/2						1			
1130	T									2			
1200	T				1								
1230	T				1								
1300	T								3				
1330	T				2								
1400	T				2								
1430	W					2							
1500	pt								15				
1530	T				1								
1600	T							1					
1630	T								2				
1700	T						1						
1730	T								1				
1800	T								2				
1830	T								2				
1900	T												4
1930	T								1				
2000	pt								23				
2030	T									3			
2100	T					2							
2130	T			1									
2200	T				2								
2230	T				1								
2300	TH							1					
2330	T							2					

Table 7

SEPTEMBER 13, 1977.

UT	Type	BAND P1	P2	P3	P4	P5	P6	P7	P8	P9	P10	P11	P12
		0-5	5-10	10-15	15-20	20-25	25-30	30-40	40-60	60-90	90-120	120-300	300-600
0000	T								3				
0030	TH				2								7
0100	T								2				
0130	T				2								
0200	T				1								
0230	T			1									
0300	T							1					
0330	T				1								
0400	W						3						
0430	W						4						
0500	Q					6							
0530	QH							8				13	
0600	Q							6					
0630	Q						8						
0700	Q						11						
0730	Q						8						
0800	Q						8						
0830	Q					14							
0900	Q					12							
0930	Q					14							
1000	Q					8							
1030	Q						10						
1100	QH				5								16
1130	TH				2							9	
1200	TH				2							14	
1230	T						5						
1300	TH					2							10
1330	Q					5							
1400	W							3					
1430	TH								5		10		
1500	TH						2					15	
1530	T								8				
1600	T							2					
1630	T								5				
1700	T							1					
1730	T											8	
1800	TH				1							6	
1830	T							1					
1900	T								4				
1930	TD				1					14			
2000	pt					2			32				
2030	T								4				
2100	T					1							
2130	T				1								
2200	T								1				
2230	T							1					
2300	T					1							
2330	T				1								

Table 8

SEPTEMBER 14, 1977.

UT	Type	BAND P1	P2	P3	P4	P5	P6	P7	P8	P9	P10	P11	P12
					Period, s								
		0-5	5-10	10-15	15-20	20-25	25-30	30-40	40-60	60-90	90-120	120-300	300-600
0000	pt								7				
0030	T							2					
0100	T								2				
0130	T								2				
0200	T				2								
0230	T			1									
0300	T				1								
0330	T							3					
0400	T				3								
0430	T					3							
0500	T				2								
0530	TH				1								3
0600	T			1									
0630	W							4					
0700	O				4								
0730	O						14						
0800	O						14						
0830	Q							8					
0900	O					13							
0930	Q				8								
1000	Q					10							
1030	O				11								
1100	O				8								
1130	Q				12								
1200	Q					9							
1230	W				2								
1300	Q				7								
1330	Q					7							
1400	Q						8						
1430	W							6					
1500	Q					8							
1530	Q					7							
1600	Q					5							
1630	T				1								
1700	W						4						
1730	T				1								
1800	T				1								
1830	T				1								
1900	T								5				
1930	T				1								
2000	T									2			
2030	T							1					
2100	T							1					
2130	T				1/2								
2200	T					1							
2230	pt										8		
2300	T								3				
2330	pt										5		

Table 9

SEPTEMBER 15, 1977.

UT	Type	BAND P1	P2	P3	P4	P5	P6	P7	P8	P9	P10	P11	P12
		PERIOD,S 0-5	5-10	10-15	15-20	20-25	25-30	30-40	40-60	60-90	90-120	120-300	300-600
0000	T						2						
0030	T T					1							
0100	T T					1							
0130	T W					3							
0200	Q W					2							
0230	Q W					2							
0300	Q W				2								
0330	Q W				2								
0400	Q O					2							
0430	O O					2							
0500	O O					2							
0530	O O					2							
0600	Q O					2							
0630	Q O					1							
0700	O O					1							
0730	Q Q					1							
0800	Q W					2							
0830	W					2							
0900	TH				1							4	
0930	TD				2						7		
1000	T W						1						
1030	T W							6					
1100	T T				1								
1130	T T							2					
1200	T T							3					
1230	T T							2					
1300	T T						2						
1330	T T						2						
1400	T T							2					
1430	T -										2		
1500	T -												
1530	T -												
1600	T -										2		
1630	T -				1/2								
1700	T -												
1730	T -												
1800	T -												
1830	T									1			
1900	pt										10		
1930	T T									3			
2000	T T							1					
2030	T T										3		
2100	TD					2					7		
2130	T T											4	
2200	T -								2				
2230	T -												
2300	T -												
2330	T								1				

Table 10

SEPTEMBER 16, 1977.

UT	Type	BAND P1	P2	P3	P4	P5	P6	P7	P8	P9	P10	P11	P12
		PERIOD,S 0-5	5-10	10-15	15-20	20-25	25-30	30-40	40-60	60-90	90-120	120-300	300-600
0000	T							1					
0030	T T				1								
0100	T T				1								
0130	T T								2				
0200	T T							1					
0230	T T							2					
0300	T T				1								
0330	T T							2					
0400	T Q							6					
0430	Q Q							10					
0500	Q				2								
0530													
0600	T							7					
0630	T W					4							
0700	Q				5								
0730	Q O				3								
0800	Q O				7								
0830	Q O					7							
0900	O T				4								
0930	T				2								
1000	TH					2						10	
1030	W				3								
1100	TH				2								
1130	T T				2							13	
1200	T T				3								
1230	TH				1								
1300	T T			6								6	
1330	T T				2								
1400	T T							1					
1430	TD						2				7		
1500	T T							4					
1530	TH							2				30	
1600	T T							3					
1630	TH							5				15	
1700	T T							3					
1730	TH					1							10
1800	T T						1					3	
1830	T T												
1900	T T					1							
1930	TD			1							6		
2000	T T								5				
2030	T T								3				
2100	T T										5		
2130	T T									2			
2200	T T									1			
2230	T T										2		
2300	T T										2		
2330	T											2	

Table 11

SEPTEMBER 17, 1977.

UT	Type	BAND P1	P2	P3	P4	P5	P6	P7	P8	P9	P10	P11	P12
		PERIOD,S 0-5	5-10	10-15	15-20	20-25	25-30	30-40	40-60	60-90	90-120	120-300	300-600
0000	T									2			
0030	TH						1				3		
0100											3		
0130										2			
0200											5		
0230	TH	1/2								4			
0300	TD	1/2						1					
0330		1/2											
0400					1								
0430				1									
0500				1									
0530			1/2										
0600					2								
0630					2								
0700							3						
0730	TH				1							5	
0800	TH			1							3		
0830	TH			1							5		
0900	Q							8					
0930	TH							4					11
1000							3						
1030	TH					1						8	
1100	TH			1/2								5	
1130						3							
1200							3						
1230						3							
1300							6						
1330							8						
1400								6					
1430							3						
1500								2					
1530									4				
1600	TH						2				5		
1630							2						
1700							1						
1730							1						
1800									1				
1830													
1900									1				
1930										2			
2000													
2030													
2100	pt										10		
2130	pt									8			
2200	TH										3		
2230													
2300													
2330	T											1	

Table 12

SEPTEMBER 18, 1977.

UT	Type	BAND P1	P2	P3	P4	P5	P6	P7	P8	P9	P10	P11	P12
		0-5	5-10	10-15	15-20	20-25	25-30	30-40	40-60	60-90	90-120	120-300	300-600
0000	T									1			
0030													
0100									2				
0130												6	
0200										3			
0230							1						
0300									2				
0330	TD								2				
0400	T			1									
0430													
0500					1								
0530					1								
0600					1								
0630									5				
0700	W			1/2									
0730					2								
0800	TD						3				21		
0830	W				1								
0900	T					1							
0930	T				2								
1000	TH				2						10		
1030	T			1									
1100	T				1								
1130	TD				1						5		
1200	TD					1				4			
1230	T									3			
1300	T				1								
1330	T				3								
1400	TD				1						10		
1430	T						5						
1500	T						4						
1530	T					1							
1600	T						1						
1630	T						1						
1700	T							1					
1730	T						1						
1800	T							1					
1830	T							1					
1900	T								1				
1930	pt								19				
2000	T										7		
2030	pt									13			
2100	TD										10		
2130	T				2						3		
2200	T									7			
2230	T									3			
2300	pt									10			
2330	T								2				

Table 13

SEPTEMBER 19, 1977.

UT	Type	BAND P1 0-5	P2 5-10	P3 10-15	P4 15-20	P5 20-25	P6 25-30	P7 30-40	P8 40-60	P9 60-90	P10 90-120	P11 120-300	P12 300-600
0000	T				1								
0030	T					1							
0100	T							1					
0130	T					1							
0200	T							1					
0230	T				1								
0300	T								2				
0330	T					1							
0400	T						1						
0430	T					1							
0500	T						1						
0530	T				1								
0600	T				1								
0630	T				1								
0700	T				1								
0730	T			1/2									
0800	T			1									
0830	T			1									
0900	T			1									
0930	T			1									
1000	T			1									
1030	T			1									
1100	T				2								
1130	T												
1200	T												
1230	T												
1300	TD			1							15		
1330	TH				7								23
1400	TH	1/2										21	
1430	TH	1/2										23	
1500	T								15				
1530	T	1/2											
1600	W				5								
1630	TH	1/2										16	
1700	T										7		
1730	T										6		
1800	T										3		
1830	T										4		
1900	TH	1/2											20
1930	T										11		
2000	TH		1/2						6				
2030	T								3				
2100	T											15	
2130	T							2					
2200	T											6	
2230	T												16
2300	T							2					
2330	T											14	

Table 14

SEPTEMBER 20, 1977.

UT	Type.	BAND P1 0-5	P2 5-10	P3 10-15	P4 15-20	P5 20-25	P6 25-30	P7 30-40	P8 40-60	P9 60-90	P10 90-120	P11 120-300	P12 300-600
0000	T										3		
0030	TH			1								15	
0100	TH				2								12
0130	QH				3							10	
0200	TH				3								36
0230	TH			5								14	
0300	T				2								
0330	Q		6										
0400	WH			8									23
0430	O			13									
0500	TH			6									25
0530	O			26									
0600	O			25									
0630	Q			13									
0700	QH			10									20
0730	Q				2								
0800	TH		1/2									7	
0830	TH			1							9		
0900	TH											15	
0930	TH		1/2								10		
1000	-												
1030	-												
1100	TH				1							10	
1130	TH			1								13	
1200	T						1						
1230	TH				2							6	
1300	TH			1/2								13	
1330	T					1							
1400	TH			1						3			
1430	TH				1								13
1500	TH					1						6	
1530	T					1							
1600	T						8						
1630	W						3						
1700	TH		1								5		
1730	T				1								
1800	T				2								
1830	T							4					
1900	T				2								
1930	T				1								
2000	T				1								
2030	TB				3					11			
2100	T				1								
2130	TH				1							4	
2200	TH					2						10	
2230	T			2									
2300	T			1/2									
2330	T				1								

Table 15

SEPTEMBER 21, 1977.

UT	Type	BAND P1 0-5	P2 5-10	P3 10-15	P4 15-20	P5 20-25	P6 25-30	P7 30-40	P8 40-60	P9 60-90	P10 90-120	P11 120-300	P12 300-600
0000	T			2									
0030	W			2									
0100	T							14					
0130	Q			2									
0200	Q			2									
0230	Q			1									
0300	Q			7									
0330	O				16								
0400	O			10									
0430	O			16									
0500	W			10									
0530	W					11							
0600	Q				18								
0630	Q				21								
0700	T				11								
0730	Q			9									
0800	T			7									
0830	T				6								
0900	TH			2								21	
0930	TH			4								25	
1000	TH					4				11			
1030	TH			3								25	
1100	Q			9									
1130	T					16							
1200	Q					47							
1230	Q				17								
1300	Q				4								
1330	T				7								
1400	TH					2						11	
1430	T				2								
1500	TH							4				11	
1530	TH					2						9	
1600	TH					2						6	
1630	Q					9							
1700	T					7							
1730	TH					3							8
1800	TH						1					4	
1830	TH						1						5
1900	TH								10			33	
1930	T								9				
2000	T						6						
2030	I												90
2100	T											16	
2130	TH			1								6	
2200	T				3								
2230	T			3									
2300	T			2									
2330	T					7							

Table 16

SEPTEMBER 22, 1977.

UT	Type	BAND P1 0-5	P2 5-10	P3 10-15	P4 15-20	P5 20-25	P6 25-30	P7 30-40	P8 40-60	P9 60-90	P10 90-120	P11 120-300	P12 300-600
0000	TH								4			14	
0030	TH					1							17
0100	TH				1						2		
0130	T			2									
0200	TH			2								12	
0230	T		3										
0300	T									6			
0330	TH			3								7	
0400	TH			1								11	
0430	TH			2								16	
0500	T				3								
0530	T				3								
0600	TH			4								10	
0630	W				10								
0700	O				10								
0730	T				9								
0800	Q				13								
0830	TH			4								12	
0900	Q			12									
0930	O				25								
1000	O				21								
1030	TH				5							27	
1100	O				18								
1130	TH				2								7
1200	TH				3								27
1230	TH			1								12	
1300	TH							3				18	
1330	TH			1								13	
1400	TH				3							12	
1430	T				2								
1500	T				2								
1530	T				2								
1600	T						3						
1630	T				2								
1700	T							1					
1730	T											18	
1800	T						2						
1830	TH		1								9		
1900	TH				2							20	
1930	pt	1/2						14					
2000	TH						2					10	
2030	T						3						
2100	T												13
2130	TH				1								8
2200	T				1								
2230	pt								9				
2300	T							1					
2330	T							1					

Table 17

SEPTEMBER 23, 1977.

UT	Type	BAND P1	P2	P3	P4	P5	P6	P7	P8	P9	P10	P11	P12
		PERIODS 0-5	5-10	10-15	15-20	20-25	25-30	30-40	40-60	60-90	90-120	120-300	300-600
0000	TH								1				11
0030	T								1				
0100	T								2				
0130	TH						1						30
0200	T											9	
0230	T												8
0300	T					1							
0330	TH								1			9	
0400	T						1						
0430	T						1						
0500	TH			1/2								3	
0530	-												
0600	O						7						
0630	Q					4							
0700	W						3						
0730	Q			1									
0800	T					5							
0830	T					2							
0900	T						2						
0930	T				2								
1000	Q					12							
1030	O					20							
1100	O					28							
1130	TH				14								23
1200	O				18								
1230	Q				25								
1300	Q				13								
1330	O					17							
1400	TH					2							10
1430	T				5								
1500	T						2						
1530	T						15						
1600	T				1								
1630	T				2								
1700	T				1								
1730	T						2						
1800	TH						2						16
1830	T				3								
1900	T						4						
1930	T				1								
2000	T									1			
2030	TH						2					10	
2100	TH				1/2							3	
2130	T								1				
2200	T							1					
2230	TD		1						8				
2300	T					1							
2330	T				1								

Table 18

SEPTEMBER 24, 1977.

UT	Type	BAND P1	P2	P3	P4	P5	P6	P7	P8	P9	P10	P11	P12
		PERIOD,S 0-5	5-10	10-15	15-20	20-25	25-30	30-40	40-60	60-90	90-120	120-300	300-600
0000	T								1				
0030	T				1								
0100	T							1					
0130	T							1					
0200	T							1					
0230	TH			1/2									5
0300	T						4						
0330	T							4					
0400	T							1					
0430	T							3					
0500	T						2					7	
0530	T						2						
0600	T							5					
0630	T		1/2										
0700	T							4					
0730	T							1					
0800	W						2						
0830	TD				1					2			
0900	T						2						
0930	TH				1							7	
1000	TH			1									9
1030	T					2							
1100	T				2								
1130	Q						3						
1200	W							3					
1230	Q							4					
1300	T						7						
1330	Q						6						
1400	Q					4							
1430	T											19	
1500	T			1									
1530	T							6					
1600	Q					6							
1630	TH					1						10	
1700	W							3					
1730	T							2					
1800	T						1						
1830	T							1					
1900	T											2	
1930	T											2	
2000	TH					1						3	
2030	T			1									
2100	TH			1							3		
2130	TD			1						2			
2200	T									2			
2230	T								1				
2300	T								1				
2330	T											4	

Pulsations Observed at Choutuppal (India) During September 7-24, 1977 and November 1977

by

Y.S. Sarma
National Geophysical Research Institute
Hyderabad-7, India

Pulsations in the frequency range 0.0016 to 3.0 Hz, observed during September 7-24, 1977 at the Choutuppal Observatory near Hyderabad (Geomagnetic Latitude: N7.5°), are presented in the following Figure.

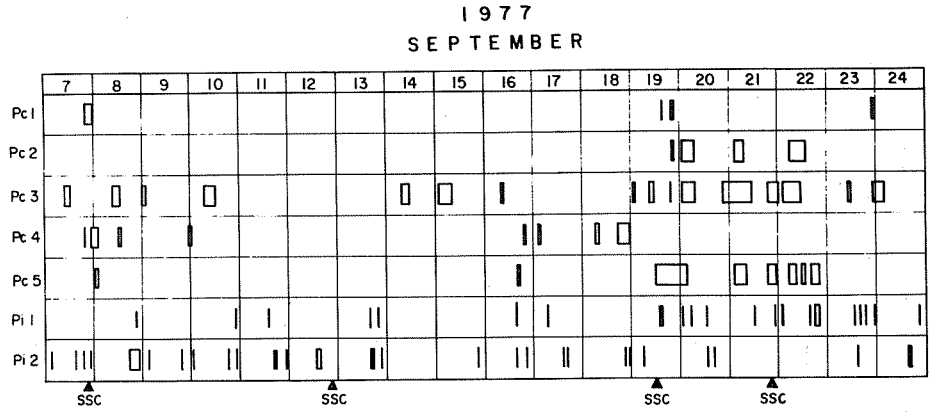

PULSATION ACTIVITY OBSERVED DURING SEPTEMBER 7-24, 1977

The main features of the pulsation activity during this period are:

i. Pc 1 and 4 activity are low.
ii. Pc 2 and 5 are seen only during the period September 19-22, 1977 following the magnetic storm of September 19, 1977 (ssc at 1140 UT) and September 21, 1977 (ssc at 2045 UT).
iii. An increase in Pc 3 and Pi 1 activity is seen during the September 19-22, 1977 period.
iv. Pi 2 activity decreased during this period in comparison to its activity in the precding days.

No unusually significant events were seen during November 1977.

Abnormal Pc3 Activity in the Telluric Pulsations at Nagarampalem (India) on September 11, 1977

by

M. Srirama Rao and K. Sitaramam
Department of Physics, Andhra University
Waltair, India

It is reported in this short communication that Pc3 pulsations at Nagarampalem (N17°45' E83°20') showed abnormal behavior on Sept. 22, 1977 from about 1500-1800 LT, viz., abnormal increases in amplitude and percentage duration of occurrence and decrease in period. The data during this period have been compared with those of other days in this month.

Nagarampalem is a coastal station where the coastal normal is oriented at about 60° with respect to north. The component of the telluric field along the E-W direction is generally observed to be about double that along the N-S direction [Rao and Sitaramam, 1978]. Hence, only the E-W component is considered in the present investigation.

Abnormal Pc3 pulsations observed around 1600 LT on Sept. 22, 1977 are shown in Fig. 1(a). A typical record taken on Sept. 29, 1977 around the same local time is shown in Fig. 1(b) to show the normal Pc3 pulsations on a quiet day. The amplitude of Pc3 pulsations observed during the period 1515-1645 LT on Sept. 22, 1977 increased to about 3 mv/km. The amplitude variation for the interval 1430-1745 LT is shown in Fig. 2, which clearly indicates the abnormal rise in amplitude. The corresponding amplitudes around the same local time on Sept. 23 and 24 have also been plotted in Fig. 2 for comparison. The values are considerably lower on these days, with those on Sept. 23 slightly higher.

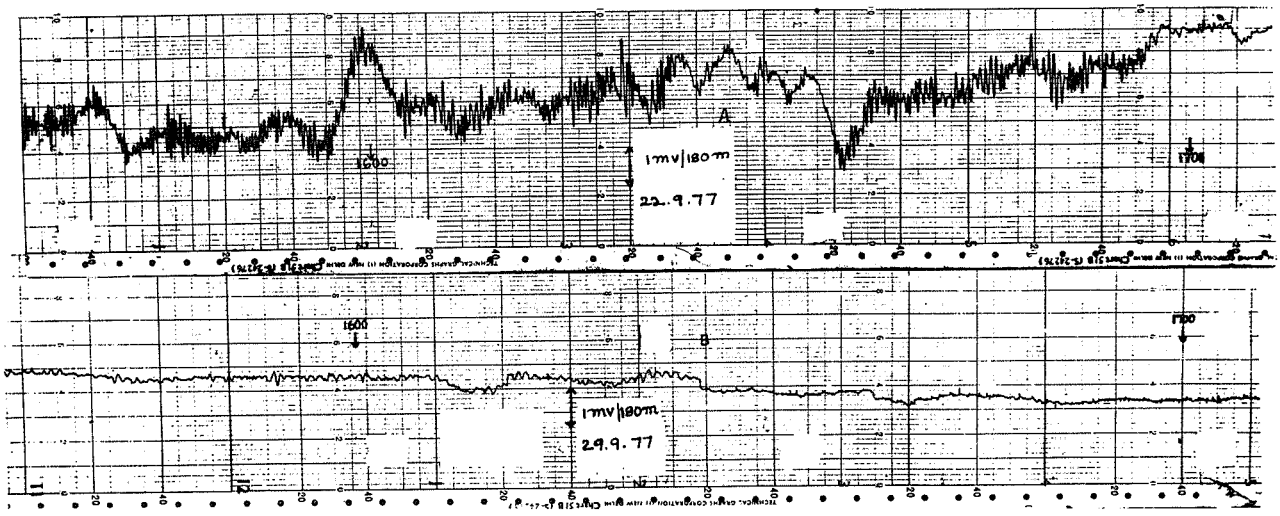

Fig. 1. Records of Pc3 pulsations A on September 22, 1977
B on September 29, 1977

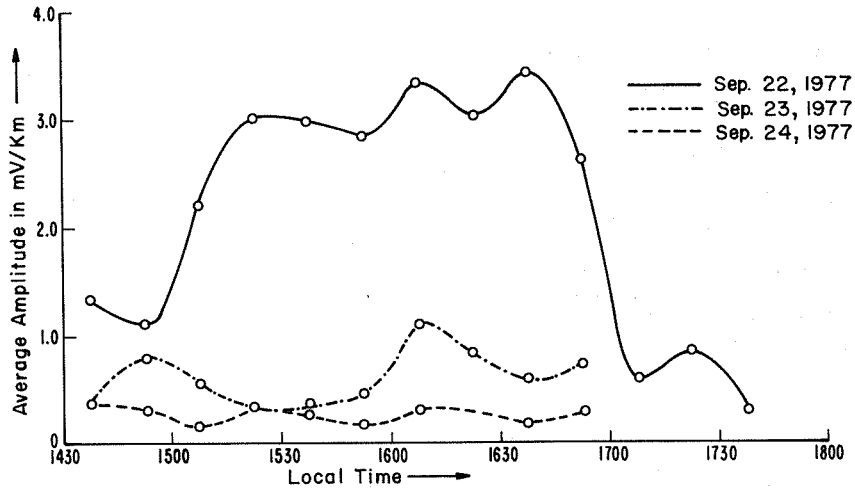

Fig. 2. Amplitude variation of Pc3 pulsations for the interval 1430-1745 LT on September 22, 23 and 24, 1977

The average amplitudes during the period 1600-1700 LT have been plotted in Fig. 3(a) for all the days from Sept. 6 to Sept. 30, 1977 for which data are available. It can be seen from this the amplitude on Sept. 22 is about 3 mv/km, whereas on all other days it is below 1 mv/km. The observed average periods of Pc3 pulsations during 1600-1700 LT on these days are presented in Fig. 3(b). It can be seen that the period is below 20 sec on Sept. 22, and above 20 sec on all other days. The percentage durations of occurrence of Pc3 pulsations during 1600-1700 LT are presented in Fig. 3(c). It can be seen that the percentage duration is abnormally high on Sept. 22 being around 85 percent, and less than 80 percent on the other days.

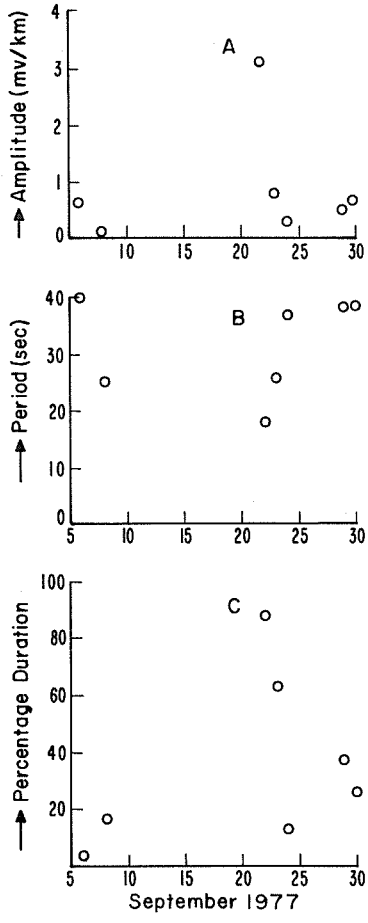

Fig. 3. Day-to-day variation of amplitude, period and percentage duration for the interval 1600-1700.

The change in period and percentage duration can be interpreted as due to the increase in solar wind velocity. From the observed $T_{pc} \simeq 18$ sec and Sept. 22, 1977 for the period 1600-1700 LT the average solar wind velocity should be around 679 $\pm$ 29 km/sec according to Troitskaya's [1967] formula.

The solar wind velocity around the same time on a typical quiet day, viz., Sept. 29, 1977 is around 508 $\pm$ 44 km/sec. The observation that there are no Pc4 pulsations in this time interval on Sept. 22 is consistent with the results of the satellite studies [Troitskaya, Bolshakovam, Shchepetnov, 1967] that no Pc4 pulsations are observed for solar wind velocities greater than about 550 km/sec.

It is reported [Bolshakova, 1966] that Pc3 pulsations are caused by the quasi-stationary emission from the active regions of the Sun. Thus the Pc3 amplitude variation may correspond to the variation of the intensity level of this radiation. Hence, the increase in the Pc3 amplitude may be due to an increase in solar flux density.

Conclusions

Abnormal Pc3 pulsations are observed at Nagarampalem during the solar flare event on Sept. 22, 1977. The E-W amplitude has been found to rise to 3 mv/km, the normal amplitude being less than 1 mv/km. The period has decreased to below 20 sec, the normal values being above 20 sec. The percentage duration of occurrence has been found to be above 80 percent, the normal values being below 80 percent.

Acknowledgments

One of the authors (K.S.) is thankful to the Council of Scientific and Industrial Research for providing him a Junior Research Fellowship.

References

BOLSHAKOVA, O.V. 1966 Stable geomagnetic micropulsations and solar corpuscular streams, Journal of Geomagnetism and Aeronomy, 6, 849-851.

SRIRAMA, Rao, M. and SITARAMAM, K. 1978 Coastal effect on telluric pulsations at Nagarampalem, National Academy Science Letters., 1, 70-72.

TROITSKAYA, V.A. 1967 Micro pulsations and the state of the magnetosphere, Solar-Terrestrial Physics (Eds. J.W. King and W.S. Newman), p. 213-274.

TROITSKAYA, V.A. O.V. BOLSHAKOVA and R.V. SHCHEPETNOV 1967 On the possibility of introduction of the solar wind index W_{SW} with applications of properties of micropulsations of the electromagnetic field of the Earth, IUGG Assembly, Zurich, 1967.

Magnetic Activity in the Canadian Sector September 19-23, 1977

by

E.I. Loomer, J.C. Gupta, J.K. Walker and H.L. Lam
Division of Geomagnetism
Earth Physics Branch
Energy, Mines and Resources Canada
1 Observatory Crescent
Ottawa, Canada

ABSTRACT

An analysis has been made of the most significant magnetic events recorded at Canadian stations following the solar flares September 16-19, 1977. Sudden storm commencements, pulsations, polar substorms and longer period bays are described for the interval September 19-23. Magnetic perturbations for the more outstanding events have been measured and tabulated, and the location and intensity of equivalent systems have been determined. Eastward and westward electrojets were observed to occur simultaneously in the day sector. The most intense westward electrojet (1300kA and 19° latitudinal extent) was found for the substorm beginning 0940 UT, September 21.

INTRODUCTION

Prior to the relatively strong magnetic activity observed September 19-23, 1977 the following solar flares were reported by Solar-Geophysical Data (Prompt Report No. 398, Part I).

DATE	START TIME UT	LOCATION	MCMATH PLAGE REGION	IMPORTANCE
Sept 17	2140	N 07 W 21	14942	2B
18	0019	N 07 W 33	14942	1B
19	0955	N 05 W 57	14943	3B
19	1028	N 08 W 58	14943	3B

In the Space Environment Laboratory, Boulder summary for this period, it is stated that the magnetosphere responded to 2 flares, the second of which occurred on September 19 (class 3B).

Table 1 lists Kp for the days September 19-23 inclusive and the most intense Dst value in each of the 3-hour Universal Time intervals for these days. Although Kp had returned to a quieter level by September 23, Dst remained strongly negative until the end of the month.

Table 1

Kp VALUES SEPT. 19 - 23

(The largest Dst value in each 3-hour U T interval is shown in brackets)

Three - Hour Universal Time Intervals

Date 1977	1	2	3	4	5	6	7	8	ΣKp
Sept. 19	1o (-17)	1- (-11)	1o (-14)	4o (-11)	6o (-24)	6- -(55)	6o (-76)	6- (-87)	30o
20	6- (-73)	5- (-69)	5o (-74)	5- (-78)	5o (-92)	5+ (-94)	4o (-67)	4o (-62)	38+
21	4+ (-45)	5+ (-59)	6o (-67)	7- (-81)	5- (-64)	3- (-67)	4+ (-66)	7+ (-91)	41+
22	6+ (-75)	6o (-83)	4+ (-60)	4o (-56)	5- (-70)	6+ (-87)	7- (-103)	4o (-95)	42+
23	3- (-79)	1+ (-74)	1o (-61)	4- (-58)	4o (-58)	5o (-60)	4+ (-69)	3+ (-75)	25+

Reversals were observed in the direction of the inferred interplanetary magnetic field (IMF), given in the monthly listing from IZMIRAN, on all days between September 18 and September 23. The IZMIRAN list for September was based on the examination of mean hourly values in the vertical (Z) component from Resolute and Thule in the arctic and Vostok in the antarctic. Two of the sector changes may be seen on the Resolute Bay records: near 1820 UT on September 19 (positive to negative) and between 19 and 21 UT on September 21 (negative to positive). The sector was positive on the days preceding and following the interval under study.

Magnetic activity following these flares is studied from the magnetograms of the stations listed in Table 2. Records were analog plots of one-minute AMOS data except at Mould Bay, where the standard-run Ruska photographic magnetograms were used. All magnetic storm perturbations were measured from the quiet night-time level (03-05 UT) of September 19. In some of the analyses use has also been made of the College, Alaska (CMO) and Tromso, Norway (TRO) magnetograms reproduced in the preliminary monthly reports issued by these observatories.

Table 2

STATIONS	COORDINATES					
	GEOGRAPHIC				GEOMAGNETIC	
	N Lat.		W Long.		N Lat.	E Long.
	°	'	°	'	° '	° '
Resolute Bay (RES)	74	42	94	54	83.1	287.7
Mould Bay (MBC)	76	12	119	24	79.1	255.4
*Pelly Bay (PEB)	68	32	89	31	78.6	329.4
Cambridge Bay (CBB)	69	06	105	00	76.7	294.0
Baker Lake (BLC)	64	20	96	02	73.9	314.8
*Eskimo Point (EKP)	61	06	94	04	71.1	321.8
Yellowknife (YKC)	62	28	114	28	69.1	292.7
Fort Churchill(FCC)	58	48	94	06	68.8	322.5
*Fort Severn(FSV)	55	59	87	14	66.8	333.0
Great Whale River (GWC)	55	18	77	45	66.8	347.2
*Thompson (TMP)	55	43	97	53	65.4	319.3
*Island Lake (ISL)	53	53	94	41	64.0	324.4
Meanook (MEA)	54	37	113	20	61.8	301.0
Whiteshell (WHS)	49	48	95	15	59.9	325.3
St. John's (STJ)	47	36	52	41	58.7	21.4
Ottawa (OTT)	45	24	75	33	57.0	351.5
Victoria (VIC)	48	31	123	25	54.3	292.7

*Churchill Line (IMS) of Variation Stations recording H,D,Z. All other stations record X,Y,Z.

Equivalent line currents were calculated, using data for observatories and the IMS stations TMP and ISL, from the magnetic perturbation vectors for a height of 112 km (equivalent to one degree of latitude), according to a method developed by P.H. Serson [Loomer and Jansen van Beek, 1971]. It was arbitrarily assumed that 25 percent of the observed magnetic effect could be attributed to induction within the Earth. To give some estimate of the position of the equivalent currents relative to the station, both the horizontal and vertical components of the perturbation vectors were used in the calculation. In a few cases, for stations near the center of the current circulation, when relatively large Z effects were associated with small perturbations in the horizontal components, the current intensity and distance from the station were obviously unrealistic and have been either omitted from the current vector plots or arbitrarily recalculated for a reduced Z perturbation. In the latter case, current vectors are represented as dashed arrows. It is not well-established that the currents which give rise to polar magnetic substorms are three-dimensional and flow along field lines as well as in the ionosphere [Akasofu, 1977]. Equivalent current vectors have been used solely to provide a concise visual representation of magnetic disturbance. It is not intended to imply that magnetic disturbance is a result of two-dimensional current flow in the ionosphere. The current vector plots are discussed in the section Discussion of Current Systems.

In addition, the equivalent current intensity was determined along the Churchill meridian using all available H (X) data from the IMS Churchill line of variation stations and from the observatories RES, BLC and FCC. The current intensity is calculated from a system of narrow east-west current elements which are assumed to be at a height of 110 km and at intervals of 0.8° (90 km). An image current system, which is mirrored at a depth of 200 km, is assumed to simulate the induced currents. A 7% correction is also made for the end effect of type 1 field-aligned currents [Bostrom, 1964] on the horizontal component. The model current system is determined by iterating the ionospheric and induced current systems until their horizontal magnetic field component (H) is within a few nanoteslas of the observed horizontal magnetic perturbation. The maximum intensity location and direction of the electrojets for selected events are tabulated in Table 3. The current intensity is also integrated for each of the eastward and westward electrojets flowing across the meridional section and the total values listed in Table 3.

Table 3

ELECTROJETS

DAY Sept. 1977	TIME UT	MAX. INTENSITY A/m	DIRECTION*	LATITUDINAL* EXTENT* °	TOTAL kA
19	1950	.33	E	61-70	260
		.33	W	71-PC	350
	2025	.93	E	60-67	450
		.87	W	67-PC	750
	2135	.33	E	61-70	250
		.68	W	72-PC	320
20	2115	.51	E	61-72	340
		.33	W	72-PC	250
	2145	.54	E	61-69	250
		.29	W	69-PC	250
	2215	.39	E	61-70	170
		.11	W	70-PC	100
21	1015	3.0	W	60-68	1300
	1020	2.2	W	60-70	1300
	1038	1.3	W	61-80	1200
	2205	.40	E	61-67	220
		.49	W	68-PC	450
	2310	.79	E	60-65	350
		.70	W	65-PC	560
	2320	.62	E	60-65	260
		.41	W	65-PC	520
22	0245	.49	W	64-70	180
	0256	.78	E	60-64	310
		2.4	W	64-70	830
	0325	1.8	W	61-77	1000
	0825	.85	W	60-67	340
	1047	.94	W	63-72	350
		.18	E	72-PC	200
	1335	1.0	W	62-68	470
	1502	.76	W	64-75	470
	1911	.61	E	60-65	200
		.42	W	65-76	300
	2015	1.1	E	60-65	370
		.57	W	65-76	570
	2023	1.0	E	60-65	330
		.78	W	70-PC	600
	2028	.82	E	60-66	470
		.35	W	66-PC	800
	2030	.83	E	60-67	420
		.35	W	67-PC	720
	2033	.63	E	60-67	350
		.64	W	67-PC	620
	2050	.64	E	61-68	230
		.35	W	72-PC	260

*E= Eastward W = Westward PC = Polar cap

SEQUENCE OF EVENTS

September 19 (Day 262)

The storm on September 19 began gradually between 11 and 12 UT at all Canadian stations (see Figs. 1a and 2a). The SC reported by many other observatories at 1143 UT is not seen on the Canadian records. A distinctive feature of the early phase of this storm is the long period X bay which begins about 1240 UT and lasts until 1800 UT, and follows an enhancement of X during the preceding hour at the auroral and lower latitude Canadian stations. This enhancement was maximum near 1210 UT (90 nT at YKC and 50 nT at FCC above the quiet night-time level). The bay is negative south of YKC and positive at stations to the north. Three well-defined substorms are superimposed, with maximum intensity in X at FCC: -405 nT at 1256 UT; -485 nT at 1430 UT; and -375 nT at 1715 UT.

Also from 1200 to 1800 UT, at FCC and to the north, a long positive Z bay is observed, with maximum intensity at YKC at 1440 UT (+610 nT). At GWC and to the south the Z bay is negative with maximum negative perturbation at MEA at 1445 UT (-300 nT). These observations suggest that the disturbance in the Canadian sector was most intense around 1440 UT near the YKC meridian. The westward electrojet associated with these substorms flows south of FCC and YKC with return currents in the polar cap and to the south of the auroral zone.

This moderate substorm activity was followed at all sites except RES by a long-period X transition bay beginning about 1700 UT and lasting until 0100 UT on September 20. The initial cycle of this bay was positive in X everywhere. It was strongly indented at Baker Lake between 1750 UT and 1905 UT when X decreased by 450 nT and at 1830 UT was only 100 nT above the quiet night-time level. Perturbations in X(H), Y(D) and Z from the quiet midnight level of September 19 were measured at selected times and are listed in Table 4. Equivalent current vectors were drawn for these times.

Table 4

Perturbations on Sept. 19, 1977 Measured from the Quiet Midnight Level

	X (H) nT							Y (D) nT							Z nT						
Station/ U T	1750	1830	1905	1950	2025	2050	2135	1750	1830	1905	1950	2025	2050	2135	1750	1830	1905	1950	2025	2050	2135
RES	-191	- 84	-108	-370	-436	-335	-108	+ 6	73	159	110	73	85	104	-122	-293	-201	-134	- 37	+ 12	+195
MBC	-134	- 13	- 38	-268	-383	-320	-179	+ 99	+125	+202	176	167	129	-197	- 12	-169	-121	- 58	+ 33	95	+315
CBB	- 57	+290	105	-260	-414	-330	-377	+ 80	170	256	174	74	77	-196	-236	-226	-206	- 70	+ 80	95	230
BLC	+515	+100	400	-210	-430	-340	-335	- 45	+ 20	+380	145	15	50	-135	-135	+155	- 55	-165	+ 5	+ 5	-150
YKC	+ 72	- 30	+ 20	-130	-390	-420	+ 70	+ 20	5	5	124	- 20	- 56	+ 24	+160	0	116	116	-214	-270	- 64
FCC	+ 20	60	120	140	-410	-300	+100	- 70	0	+180	220	-100	0	+ 20	+ 60	16	140	- 64	-160	-160	-184
GWC	+ 25	70	260	345	- 92	+ 28	250	- 88	- 26	+ 64	105	- 78	- 40	+ 40	+ 77	57	77	-203	-293	-353	-150
YHP	+100	100	100	160	200	160	200	0	60	140	220	150	260	120	70	80	140	160	-440	-400	+ 10
(CMO)					(-403)																
ISL	+ 40	60	100	180	400	420	200	- 30	+ 30	100	150	150	245	70	+ 50	70	90	140	-270	-410	0
MEA	- 10	- 20	- 50	- 90	- 35	+ 25	15	- 55	- 15	- 10	+ 25	+ 35	+ 25	- 40	+ 10	+ 15	30	45	120	140	75
WHS	- 40	- 35	- 30	- 15	+120	230	30	- 65	- 30	- 10	0	- 5	+ 40	- 35	0	+ 10	35	70	160	180	100
STJ	- 60	- 35	+ 15	+ 70	+ 90	+ 70	- 40	- 30	- 30	- 45	- 45	+ 5	- 35	- 25	+ 20	+ 30	+ 75	145	180	150	90
OTT	- 60	- 35	0	+ 30	70	150	- 30	- 60	- 40	- 30	- 30	- 50	- 70	- 60	+ 10	15	40	80	180	210	105
VIC	- 16	- 36	- 56	-100	-116	-100	- 60	- 20	0	- 6	- 16	- 56	- 80	- 86	- 32	- 32	- 28	- 32	- 32	- 28	- 12

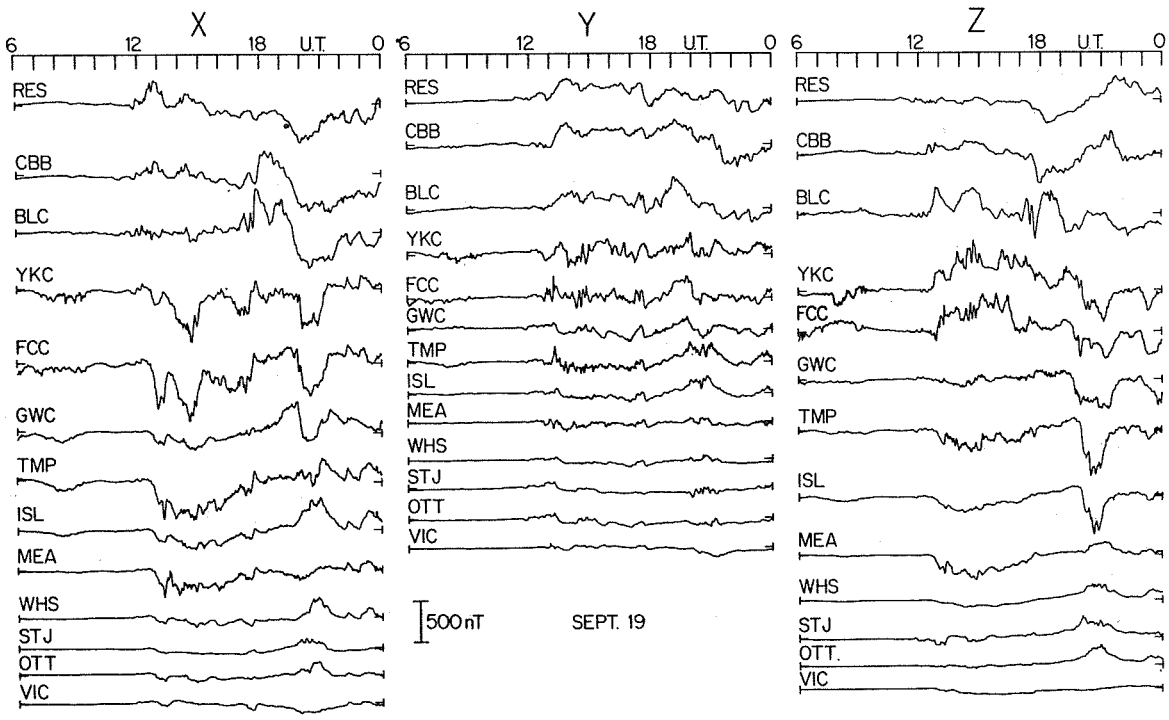

Fig. 1 (a). Magnetograms plotted from 1-minute digital data.

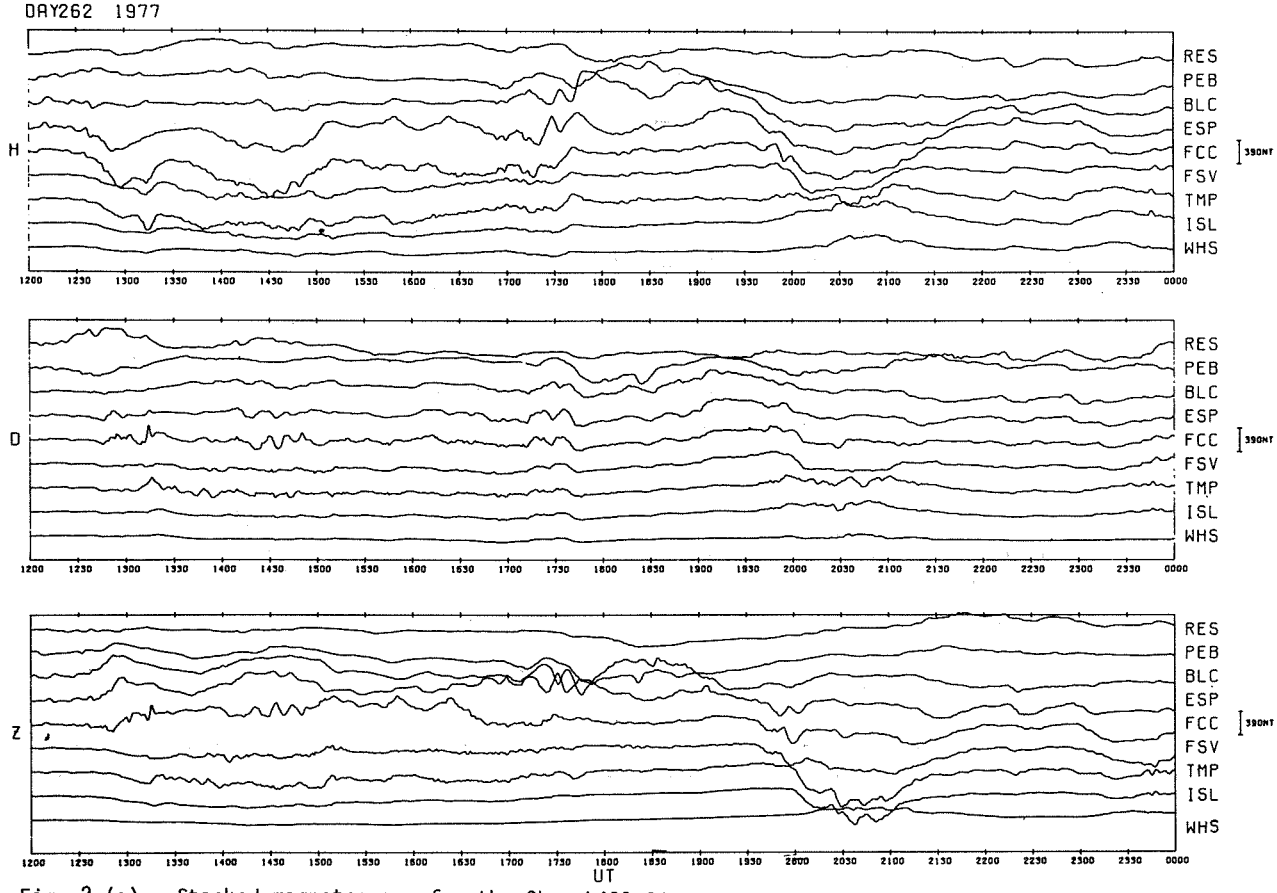

Fig. 2 (a). Stacked magnetograms for the Churchill line of stations plotted from 1-minute digital data.

September 20 (Day 263)

A sudden impulse was observed around 0008 UT on September 20. This impulse was most intense in the polar cap, with maximum amplitudes at MBC (192 nT) and at CBB (180 nT) but the signature is clearly present at most Canadian sites. (Figs. 1b and 2b).

About an hour later a negative X bay began at 0120 UT at OTT and STJ and probably a little later elsewhere to the north and west (e.g. 0130 UT at GWC). A sharp positive spike in X is seen at 0143 UT at OTT, lasting until 0153 UT, and peaking at 0148 UT. Also at OTT a sharp negative bay is observed in Z with a small reverse impulse at 0143 UT. At this time, there was a sharp positive rise in X at GWC to the north, followed by a negative bay with a pulsational beginning at 0152 UT. This feature is also seen in the Z records at TMP and ISL to the northwest. These magnetic effects imply a rapid movement of the electrojet north of OTT at 0143 UT. The electrojet passes north of GWC at 0205 UT. Effects of the surge are seen also in X on the WHS record.

Several smaller substorms followed during the next few hours. The largest, at 0335 UT had maximum intensity at GWC (400 nT below the quiet level). Transitional bays are clearly seen in the Y component at stations to the south of GWC. At MEA an eastward electrojet is evident in X as long positive bay from about 0010 to 0620 UT, on which are superimposed several distinct substorms in the interval 01 to 04 UT. Evidence for an eastward electrojet is seen also at College (CMO) and WHS and probably at ISL and TMP as well.

In the midnight sector, at MEA and WHS, polar substorms began abruptly at 0650 UT with maximum at MEA at 0710 UT (-740 nT in X). These persisted at WHS until about 1130 UT and for a considerably longer period at MEA. To the north substorm activity began somewhat later: shortly after 0800 UT at YKC, TMP and ISL, and about 0900 UT at GWC, FCC, CBB and BLC. Multiple substorms are evident at all stations. Maximum intensity was observed at YKC at 1256 UT (-850 nT in X).

About 0900 UT large positive Z bays began at BLC and CBB, and a large negative Z bay at GWC. These bays persisted for approximately 6 hours. Both positive and negative variations in Z of approximately the same amplitude were observed at YKC. These effects would result from westward electrojets flowing between FCC and GWC, and approximately overhead on the average at YKC.

At the end of this period of substorm activity, large amplitude (1110 nT in Z and Y) variations with 10 to 15 min periods are seen at TMP between 1400 and 1500 UT (the time of maximum occurrence of Pc5 pulsations). Elsewhere the largest amplitudes were at FCC (700 nT), ISL (300 nT) and YCK (180 nT). Periods were between 10 and 15 min at all sites. Along the Churchill meridian the maximum D-peak occurred around 1415 UT when the Z component made the transition from negative to positive. The H (X) variations for the same time interval are significantly smaller in magnitude. These are the characteristics of azimuthal propagating magnetic structures as pointed out recently by Rostoker and Kawasaki [1978].

The next interesting feature was the event observed at all stations the Canadian sector between 2010 and 2240 UT. Perturbations for selected times are given in Table 5. Equivalent current vectors are drawn for the times listed in the table.

A well-defined transitional bay is seen in Y at MBC, with Y east maximum at 2114 UT and Y west maximum at 2216 UT. The Y demarcation line, measured at the time the Y variation passes through the quiet level of the field, was observed at MBC at about 2155 UT. This is close to the time of maximum substorm activity at Tromso (2151 UT). These observations suggest that the storm center in the night sector of the auroral oval crossed the meridian through MBC and the invariant pole near this time.

September 21 (Day 264)

Following a quiet interval lasting about 4 hours a very long (12 hr) negative bay began about 0200 UT in X at auroral and sub-auroral stations, on which substorms and pulsational activity were superimposed (Figs. 1c and 2c). Within the polar cap a positive X bay was observed during these hours. At lower latitudes (e.g. OTT and STJ) there were probably four well-developed substorms in the night sector, but within the auroral zone (e.g. GWC) up to 10 substorms could be distinguished over the following nine hours, superimposed on the long-period negative X bay.

Two Pi2's, beginning at 0120 UT and 0205 UT were clearly seen at TMP, MEA, ISL and WHS. The period for both Pi's was very close to 120 sec, and amplitudes ranged from 8 to 44 nT, being maximum at TMP and MEA. The second Pi2 was especially well-defined. Indications of these Pi2's were too vague to permit measurement at the other locations. At 0120 UT there is evidence of small substorm activity at GWC and perhaps at FCC and at 0205 UT substorms begin at FCC, GWC, TMP and ISL. These observations confirm previous findings reported by Saito [1969]. Subsequent substorms were observed to be most intense at TMP and MEA.

A substorm began at MEA at 0445 UT and lasted about 60 min. It reached maximum intensity in X (-940 nT below the quiet level) at TMP with an electrojet flowing westward north of OTT and between GWC and MEA and passing nearly overhead at TMP and ISL. Return currents to the north and south of the main current flow were evident in the polar cap records and at Victoria (Table 6).

Table 5

Perturbations on Sept. 20, 1977 Measured from the Quiet Midnight Level

	X (H) nT				Y (D) nT				Z nT			
Station/ UT	2015	2115	2145	2215	2015	2115	2145	2215	2015	2115	2145	2215
RES	- 55	-280	-250	-100	+ 20	0	- 40	- 80	-110	- 90	- 40	- 26
MBC	- 49	-230	-217	-102	+116	+216	+ 75	-167	- 60	- 36	- 18	-109
CBB	+ 93	-170	-187	+ 10	+130	+104	+ 24	- 10	-120	- 73	- 73	- 93
BLC	+160	-125	-130	- 30	+150	+ 90	+ 10	+ 45	- 50	-205	-180	- 80
YKC	+ 50	+ 40	+ 90	+ 30	+ 20	+115	+164	+ 56	+ 70	+ 6	- 90	+ 60
FCC	+120	+245	+ 90	+100	+ 60	+135	+ 75	+ 60	+ 65	-135	-245	- 30
GWC	+125	+200	+200	+165	+ 14	+ 20	+ 12	+ 50	+ 70	+ 15	-120	- 15
TMP	+ 60	+200	+170	+ 50	+ 30	+100	+100	+ 40	+ 60	+ 40	+ 20	+ 50
CMO)												
ISL	+140	+260	+260	+140	+120	+165	+180	+140	+170	+180	+150	+160
MEA	- 15	+ 25	+ 30	- 25	- 20	+ 15	+ 40	0	+ 45	+ 80	+100	+ 65
WHS	- 15	+ 45	+ 45	- 15	- 15	0	+ 15	0	+ 45	+ 90	+ 90	+ 60
STJ	- 20	+ 10	- 10	- 20	0	+ 22	+ 33	+ 52	+ 40	+ 45	+ 40	+ 20
OTT	- 26	+ 5	- 15	- 45	- 10	+ 15	0	+ 13	+ 35	+ 65	+ 65	+ 50
VIC	- 60	- 56	- 72	- 72	- 36	- 36	- 26	- 32	+ 6	+ 8	+ 8	+ 12

Table 6

Perturbations on Sept. 21, 1977 Measured from the Quiet Midnight Level

	X (H) nT		Y (D) nT		Z nT	
Station/ UT	0515	0715	0515	0715	0515	0715
RES	+240	+220	- 40	+ 30	+ 60	+110
MBC	+192	+186	-150	+ 80	+110	+ 33
CBB	+140	+132	-100	- 56	+360	+126
BLC	40	+ 10		- 46	+300	+430
YKC	-530	-1200	-440	-676	-120	+246
FCC	-540	-480	-760	-410	+ 40	+596
GWC	-340	-652	+ 20	- 56	+110	+526
TMP	-940	-860	-240	-580	+360	+180
ISL	-880	-1260	-320	-200	- 70	+200
MEA	-640	-380	-240	-170	-400	-410
WHS	-590	-332	-280	- 50	-400	-480
STJ	-120	-132	+ 37	- 2	-122	-154
OTT	-230	-190	- 50	- 89	-235	-246
VIC	+ 15	- 36	+ 85	+ 84	- 30	- 42

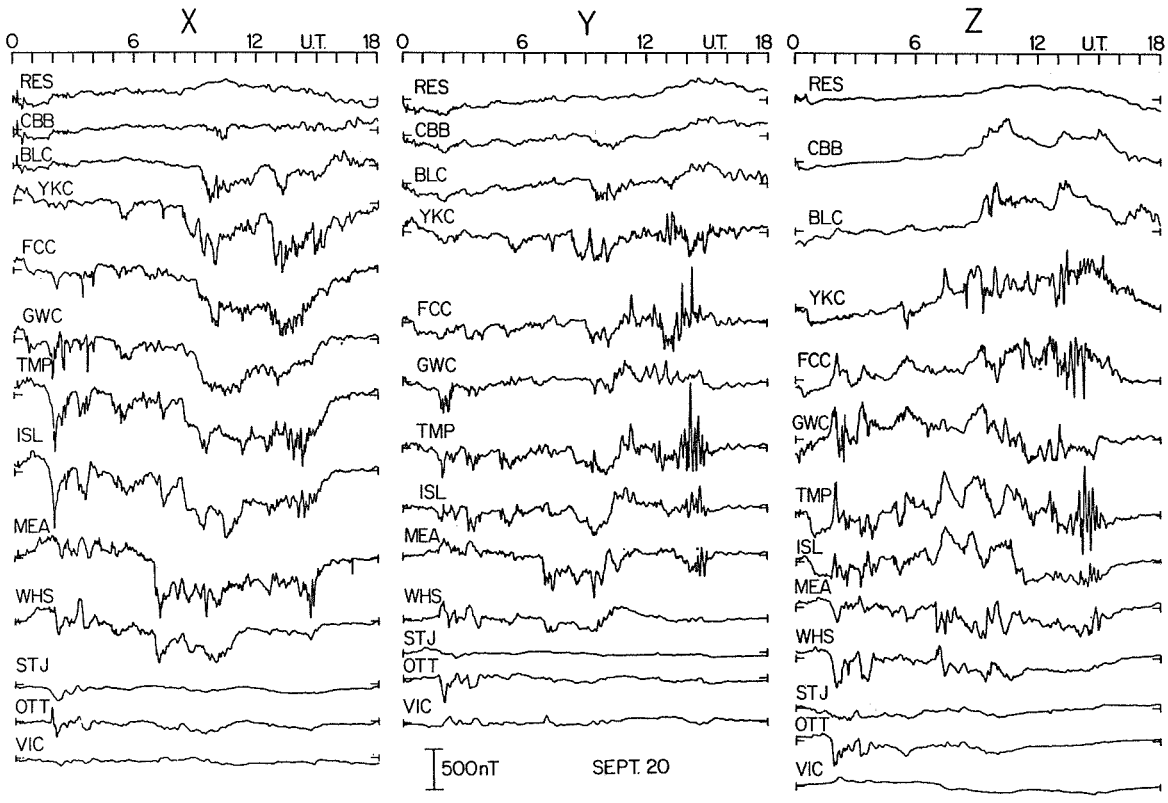

Fig. 1 (b). Magnetograms plotted from 1-minute digital data.

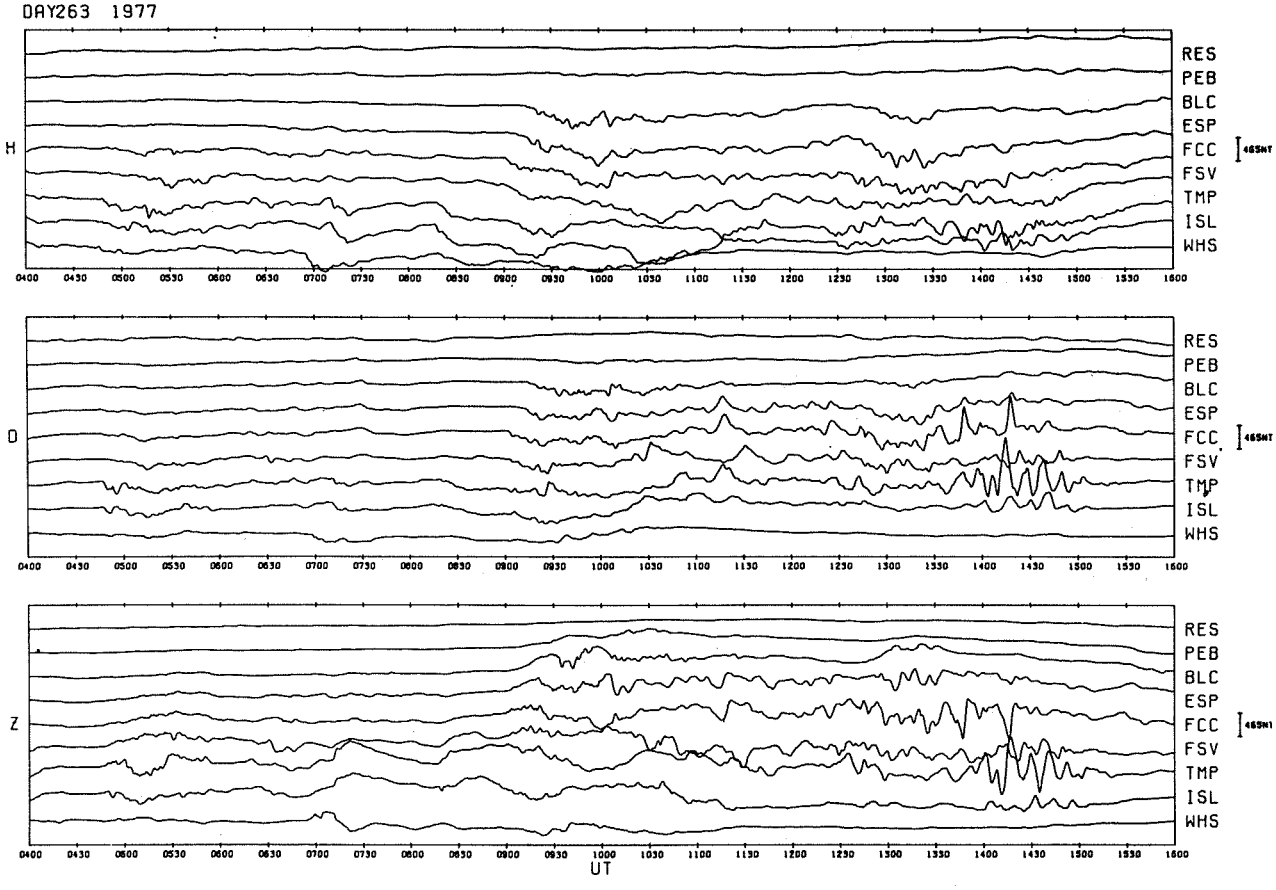

Fig. 2 (b). Stacked magnetograms for the Churchill line of stations plotted from 1-minute digital data.

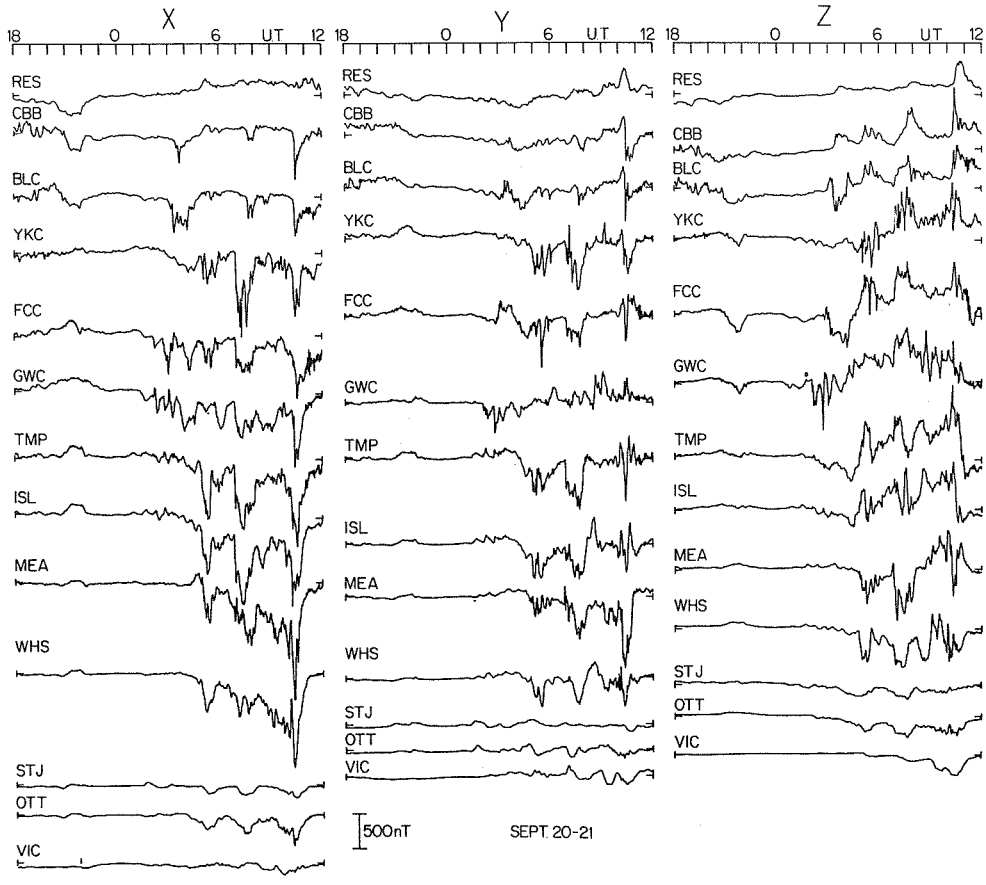

Fig. 1 (c). Magnetograms plotted from 1-minute digital data.

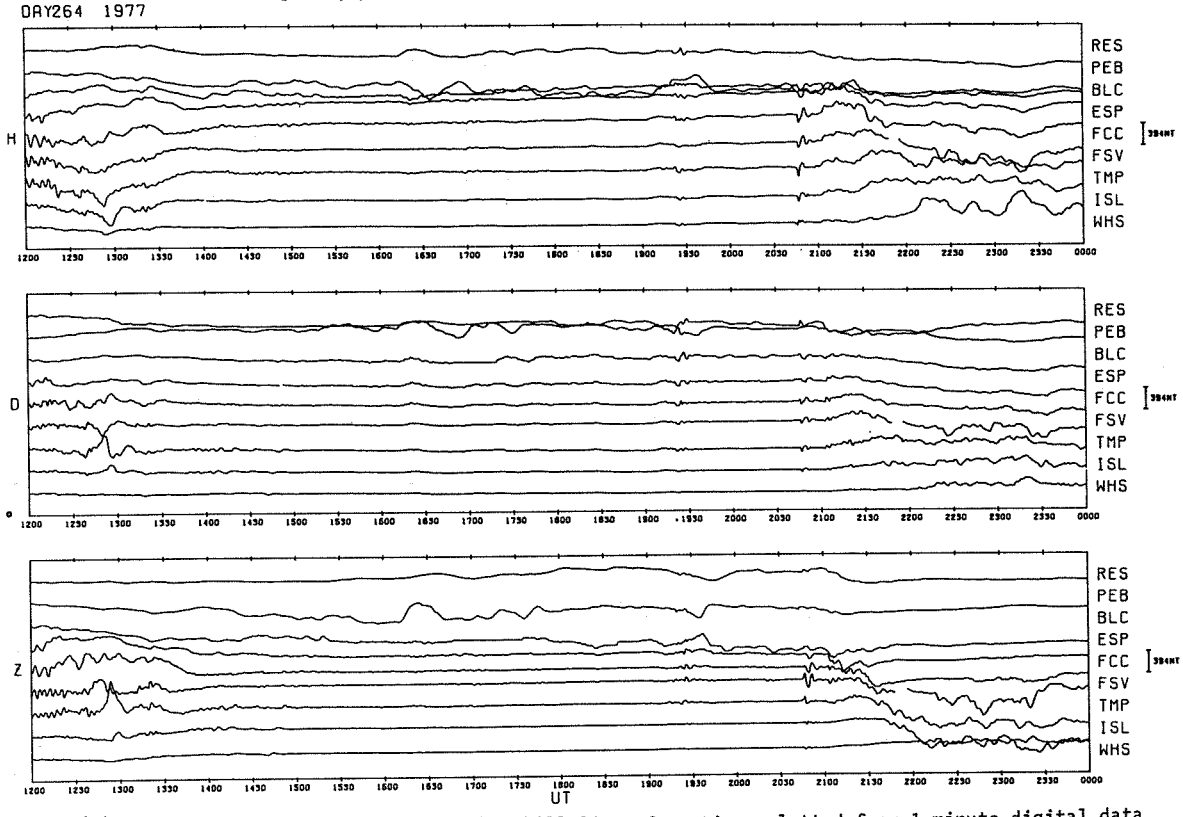

Fig. 2 (c). Stacked magnetograms for the Churchill line of stations plotted from 1-minute digital data.

A second complex substorm began at 0650 UT and lasted about 75 min with maximum intensity at 0715 UT at ISL (-1260 nT in X) and YKC (-1200 nT in X) (Table 6). The most intense substorm in this series of storms began at 0940 UT (Table 7) at FCC and reached maximum intensity at 1015 UT at MEA (-1760 nT in X).

Table 7

Perturbations on Sept. 21, 1977 Measured from the Quiet Midnight Level

	X (H) nT				Y (D) nT				Z nT			
Station/ UT	1015	1020	1038	1253	1015	1020	1038	1253	1015	1020	1038	1253
RES	+ 170	+ 150	+180	+ 70	+340	+380	+160	+190	+150	+150	+460	+100
MBC	+ 230	+ 185	-447	+ 79	+356	+482	-685	+170	+206	+259	+545	+105
CBB	+ 72	0	-276	+ 84	+108	+244	-316	+120	+206	+400	+276	+140
BLC	- 20	- 80	-380	+120	+294	+214	-204	+134	+180	+360	+600	+300
YKC	- 290	- 630	-760	0	- 66	-516	-756	+ 24	+696	+256	+576	+226
FCC	- 303	- 460	-720	-340	+220	+160	+220	+190	+416	+526	+496	+250
GWC	- 412	- 320	-780	-242	+ 42	+ 80	+ 40	+ 72	+316	+596	- 24	+ 26
TMP	-1100	-1120	-700	-600	0	-220	+160	+ 80	+820	+900	+680	+460
CMO)			(-832)				(0)				(+652)	
ISL	-1060	- 940	-860	-460	-140	-240	+340	+110	+560	+660	+120	-190
MEA	-1760	-1700	-660	+560	-886	-970	-604	+ 36	+350	-390	+190	-100
WHS	-1300	-1360	-610	-152	-200	-350	0	+ 20	-420	-120	-300	-100
STJ	- 170	- 175	-125	- 95	+ 5	- 5	- 85	+ 35	+ 84	- 67	- 39	- 68
OTT	- 470	- 380	-185	-100	- 54	- 89	- 9	+ 20	-251	-221	-220	- 37
VIC	- 120	- 100	- 52	- 96	- 96	- 92	- 92	+ 4	-292	-132	-132	- 72

Current vectors were calculated for 0715 UT, 1020 UT and 1038 UT.

Considerable pulsational (Pc5) activity was superimposed on the last substorm, which began about 12 UT at MEA. Pulsations persisted at all sites except RES and CBB until at least SC reported at 2044 UT, and probably until about 0100 UT September 22. These pulsations were particularly well-defined at YKC, and at FCC and TMP, where they began about 1045 UT. The amplitude and period of the largest cycle in three consecutive one-hour intervals are given in Table 8. In these three one-hour intervals the location of the largest Pc5 amplitude changed from FCC (380 nT; 1100-1200 UT) to TMP (244 nT; 1200-1300 UT) to MEA (113 nT; 1300-1400 UT). This indicates that the region of instability in which the hydromagnetic activity was generated was near the dawn meridian (6 LT at FCC) and that, with the rotation of the auroral oval, stations to the west of FCC recorded the largest Pc5 amplitude in progressivly later hours, as would be expected. It was noted that the amplitude of these Pc5'c increased towards the auroral zone, decreasing at higher latitudes. It is evident in Table 8 that measured periods vary considerably (180 sec to 360 sec). Much of this variability could result from the fact that measurements for most sites were made on plots of 1-min digital data. The waxing and waving amplitude profile of Pc5's during the entire interval suggest that the activity resulted from a beating effect of at least 2 Pc5 waves. The maximum effect was observed for a large impulsive event beginning 1909 UT. The event, clearly seen at all Canadian sites, is identified as a PC5. The $H=(X^2 + Y^2)$ amplitudes of the largest Pc5 cycle are given in the last column of Table 9. Clearly the amplitude increases in intensity with latitude and is maximum in the cusp region. In general the more westerly stations recorded the larger amplitudes.

The impulsive event of 1909 UT was followed by a SC at 2044 UT. The SC had maximum amplitude at TMP (295 nT in H). The amplitudes, as seen in Table 9, rose steeply from the latitude of VIC (30 nT) to TMP, and decreased rapidly to RES in the polar cap (125 nT).

Following the SC at 2044 UT negative bays (2120 UT September 21 to 0130 UT September 22) were observed at GWC and FCC, and well-defined positive bays to the south at ISL, MEA, WHS, STJ and OTT. Both the positive and negative bays were heavily loaded with substorm activity. Current vectors were plotted for selected times during this period. Perturbation measurements are listed in Table 10.

Table 8

Pc 5 event Sept. 21, 1977

Amplitude and period of largest and most sinusoidal cycle in X component in three consecutive one-hour intervals

Station	11-12 UT		12-13 UT		13-14 UT	
	AMP (nT)	PERIOD (Sec)	AMP (nT)	PERIOD (Sec)	AMP (nT)	PERIOD (Sec)
RES	54	180	30	396	30	180
MBC	42	270	45	270	25	196
CBB	30	216	20	360	-	-
BLC	120	270	30	270	-	-
YKC	105	198	20	300	-	-
FCC	380	270	220	360	55	180
GWC	92	306	80	288	90	180
TMP	150	252	244	270	100	198
ISL	80	288	110	216	110	216
MEA	95	360	102	180	113	180
WHS	36	270	20	180	32	180
STJ	12	180	5	270	5	216
OTT	40	252	10	252	9	126
VIC	4	306	6	270	9	216

Table 9

Amplitudes (maximum to minimum) of Pc 5 beginning at 0909 UT and of the Sudden Commencement at 2044 UT on September 21.

Station	Amplitude nT	
	Pc5	SC
RES	150	125
MBC	227	180
CBB	206	183
BLC	165	169
YKC	222	272
FCC	114	277
GWC	92	214
TMP	134	295
ISL	65	246
MEA	86	257
WHS	41	91
STJ	16	43
OTT	38	58
VIC	36	33

Table 10

Perturbations on Sept. 21,1977 Measured from the Quiet Midnight Level

	X (H) nT			Y (D) nT			Z nT		
Station/UT	2205	2310	2320	2205	2310	2320	2205	2310	2320
RES	-260	-120	-100	-120	-260	-200	0	- 10	0
MBC	-294	-179	-147	- 30	-145	-120	- 32	- 86	- 86
CBB	-230	-170	-137	- 46	-186	-166	- 53	- 70	- 73
BLG	-300	-280	-260	- 48	-200	-194	-160	-140	-120
KC	- 15	+100	- 10	+ 40	+ 95	+ 45	-185	-410	-305
RCC	-105	-280	-230	- 45	-150	-210	-215	-230	-240
GWC	-120	-332	-500	-158	+180	+140	-133	-565	-525
TMP	+120	+ 80	+ 40	+160	+160	+ 80	-240	-480	-440
ISL	+200	+320	+240	+100	+160	+ 80	-400	-480	-400
MEA	+100	+190	+480	+ 55	+155	+155	+ 85	+170	- 10
WHS	+205	+350	+290	+ 40	+120	+205	+ 90	+140	+190
STJ	- 10	+138	+ 20	+ 75	+135	- 33	- 32	- 82	- 85
OTT	+120	+100	+ 10	≈ 10	+270	+120	+220	+230	+ 10
VIC	- 56	- 60	- 46	≈ 16	+ 6	0	+ 12	+ 84	+ 88

September 22 (Day 265)

Localized Pc5 activity was observed (Figs. 1d & 1e, 2d & 2e) to start 0005 UT, September 22, at MEA and WHS and at YKC, FCC and GWC with the largest amplitude (226 nT) occurring at MEA. The period of this event at MEA was 270 sec over the initial 4 cycles. A second well-defined group of Pc5's is seen at TMP and ISL between 0100 and 0200 UT. Maximum amplitude was 140 nT at TMP; periods were about 360 sec.

Polar substorm activity began 0230 UT and reached maximum intensity 0325 UT at BLC (-X: 1010 nT). Three measurements were made, (Table 11) and current vector plots were drawn for 0245, 0256 and 0325 UT which were the times of maximum intensity (-X) at GWC, FCC and BLC, respectively.

Beginning about 0700 UT and lasting until about 1800 UT a series of negative X bays is observed in the midnight sector. Measurements were made at 0825, 1047, 1335 and 1502 UT, the times of maximum (-X) intensity at MEA, where the bay sequence is most clearly seen (Table 12): current vector plots were drawn for 0825, 1047, and 1502 UT.

Finally, the magnetic activity between 1600 and 2100 UT was studied and current vectors were drawn for selected times. Perturbation measurements are listed in Tables 13 (a) and 13 (b). As is seen on the magnetograms (Fig. 1e and 2e) magnetic activity for the period under study ended abruptly about 2030 UT at the lower latitude Canadian stations. Relatively weak bay activity persisted at the more northerly sites for several hours but by 0300 UT September 23 quiet conditions (Kp=1+) were re-established at all Canadian stations.

Table 11

Perturbations on Sept. 22, 1977 Measured from the Quiet Midnight Level

Station / UT	X (H) nT 0245	0256	0325	Y (D) nT 0245	0256	0325	Z nT 0245	0256	0325
RES	30	50	60	-180	-180	-210	30	30	110
MBC	- 13	- 13	- 13	-162	-162	-197	- 50	- 44	- 14
CBB	- 7	- 27	-107	-166	-190	-230	- 10	7	232
BLG	20	-40	-1010	-155	-185	-305	120	130	310
YKC	- 40	-105	-550	-116	-150	130	-120	- 94	-144
FCC	-150	-990	-395	-190	40	-430	75	195	-295
GWC	-785	-657	-902	-108	-378	-158	-338	-313	-213
TMP	-200	-390	-230	-120	20	-120	- 60	- 60	-380
(CMO)									
ISL	- 80	60	-200	- 30	240	- 40	-130	-310	-290
MEA	120	150	- 50	45	125	235	70	10	0
WHS	0	130	- 36	46	171	96	66	110	-107
STJ	- 35	- 25	- 50	40	25	25	-139	-139	-100
OTT	5	30	- 15	184	184	- 23	- 21	- 51	- 84
VIC	- 56	- 96	-112	- 52	- 32	80	40	40	68

Table 12

Perturbations on Sept. 22, 1977 Measured from Quiet Midnight Level

Station	X (H) nT UT 0825	1047	1335	1502	Y (D) nT UT 0825	1047	1335	1502	Z nT UT 0825	1047	1335	1502
RES	+110	+104	+ 80	+ 84	+100	+100	+180	+244	+110	+ 60	+120	+110
MBC	+134	+128	+ 77	+154	+ 78	+ 0	+107	+260	+192	+ 91	+142	+252
CBB	+ 53	+ 88	+ 48	+ 15	+ 44	+ 60	+110	+174	+227	+132	+217	+290
BLG	0	+ 60	- 70	-100	+ 64	+ 44	+ 94	+184	+220	+296	+360	+360
KC	-560	- 70	-310	-270	-546	+ 26	+ 45	- 76	+566	+196	+416	+476
RCC	-100	-225	-505	-460	+ 10	+ 90	+ 55	+ 30	+285	+220	+425	+285
GWC	-202	-242		-130	+ 62	+112		+102	+282	- 83		- 28
TMP	-380	-390	-400	-380	-300	130	-120	- 80	+290	+120	+ 40	- 70
ISL	-300	-220	-260	-180	- 55	+ 80	+ 80	+ 60	+260	-180	-100	- 85
MEA	-545	-340	-370	-605	-320	+ 40	+ 90	+105	-150	- 95	-220	-300
WHS	-396	-70	-190	-180	-130	+ 46	+ 70	+ 57	-170	- 87	- 39	- 26
STJ	- 62	- 25	-115	-135	- 23	+ 8	+ 45	+ 5	- 24	- 38	- 5	+ 14
OTT	-145	- 20	-110	-122	- 30	+ 38	+ 2	+ 14	- 66	- 32	+ 11	+ 13
VIC	+ 4	- 52	- 72	- 76	- 96	+ 34	+ 32	+ 50	- 42	- 16	- 66	- 76

Table 13 (A)

Perturbations on Sept. 22, 1977 Measured from the Quiet Midnight Level

	X (H) nT				Y (D) nT				Z nT			
Station / UT	1815	1911	2015	2023	1815	1911	2015	2023	1815	1911	2015	2023
RES	-100	-180	-200	-160	+220	+180	+190	+170	+ 94	+ 90	+110	+130
MBC	0	-124	-109	-105	+189	+176	+129	+ 34	+238	+150	+164	+160
CBB	-107	-130	-235	-325	+254	+194	+244	+ 40	+227	+177	+227	+380
BLG	-165	-220	-370	-440	+235	+190	+110	+ 35	+100	+ 60	+ 30	+120
YKC	-190	-290	-695	-480	+114	+124	- 30	- 86	+300	+270	- 94	-285
FCC	-250	-240	-330	- 40	+170	+140	+ 15	- 60	+100	- 70	-115	-200
GWC	0	-110	- 62	-112	+152	+ 32	- 36	- 18	-193	-273	-303	-295
TMP	- 10	- 60	+ 5	+ 70	+170	+150	+120	+140	- 80	-190	-280	-410
(CMO)	-608	-532	-335	-152	+257	0	+103	+ 51	+118	+ 34	- 84	-152
ISL	+180	+260	+360	+360	+260	+300	+260	+210	+ 30	- 50	-200	-140
MEA	-110	- 70	+ 50	+100	0	+ 45	+ 45	+ 45	+ 50	+ 60	+ 15	+ 80
WHS	0	+120	+205	+240	+ 50	+ 60	+ 10	+ 55	+110	+160	+120	+110
STJ	+ 85	+ 65	+ 25	+ 25	- 50	-125	- 55	+ 10	+170	+215	+220	+120
OTT	+ 10	+ 70	+ 85	+150	+ 30	0	- 60	- 55	+105	+175	+190	+190
VIC	-152	-152	-116	-116	- 56	- 80	- 76	- 76	- 48	- 48	+ 10	+ 10

Table 13 (B)

Perturbations on Sept. 22, 1977 Measured from the Quiet Midnight Level

	X (H) nT				Y (D) nT				Z nT			
Station / UT	2028	2030	2033	2050	2028	2030	2033	2050	2028	2030	2033	2050
RES	-240	-250	-260	-130	+165	+170	+165	+ 20	+160	+190	+210	+220
MBC	-128	-128	-153	-166	+ 32	+ 22	+ 35	- 68	+176	+183	+202	+221
CBB	-525	-495	-465	-265	+ 40	+ 44	+ 40	-115	+370	+327	+340	+105
BLG	-495	-480	-440	-190	- 25	- 40	- 30	- 70	+ 50	+ 10	0	- 30
YKC	-270	-260	-110	0	- 16	+ 34	+125	- 46	-345	-445	-374	+ 46
FCC	-340	-240	-140	+ 50	- 50	- 60	- 50	+ 20	-400	-365	-365	- 90
GWC	-137	- 5	+160	+ 96	- 28	- 98	- 10	0	-430	-513	-318	- 50
TMP	+320	+280	+270	+ 80	+180	+160	+140	+ 60	-430	-360	-300	- 45
(CMO)	0	- 15	+ 46	+ 30	0	- 10	- 41	- 21	-169	-219	-253	- 84
ISL	+460	+440	+360	+200	+240	+220	+215	+180	-135	-135	- 20	+100
MEA	+150	+160	+ 70	+ 30	+ 50	+ 85	+ 30	- 55	+110	+130	+110	+ 50
WHS	+340	+320	+180	-213	+ 45	+ 40	+ 20	0	+160	+140	+100	+ 65
STJ	+200	+115	+ 40	- 50	+105	0	- 25	+ 5	+175	- 20	- 15	0
OTT	+155	+145	+ 70	- 50	- 50	+ 10	+ 80	- 10	+285	+230	+125	+ 40
VIC	- 92	- 76	- 96	- 92	- 70	- 70	- 70	- 70	+ 20	+ 20	+ 20	+ 30

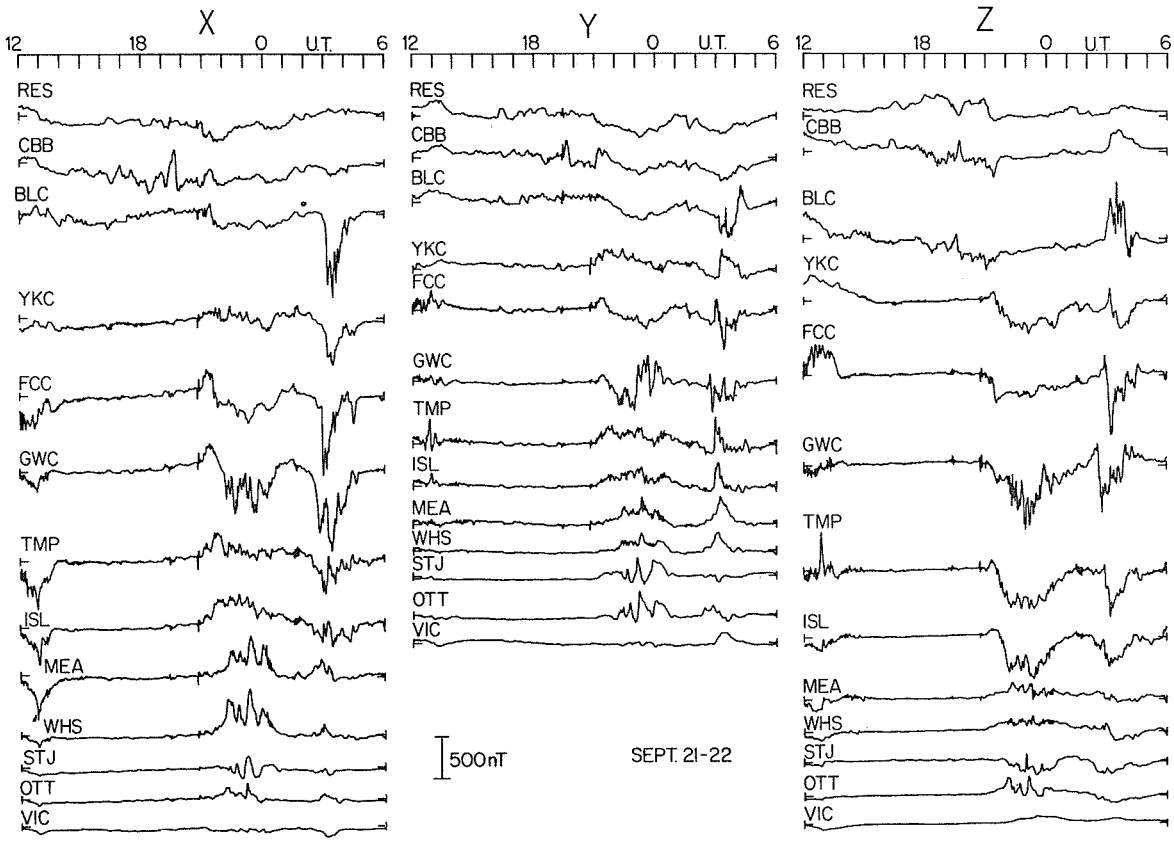

Fig. 1 (d). Magnetograms plotted from 1-minute digital data.

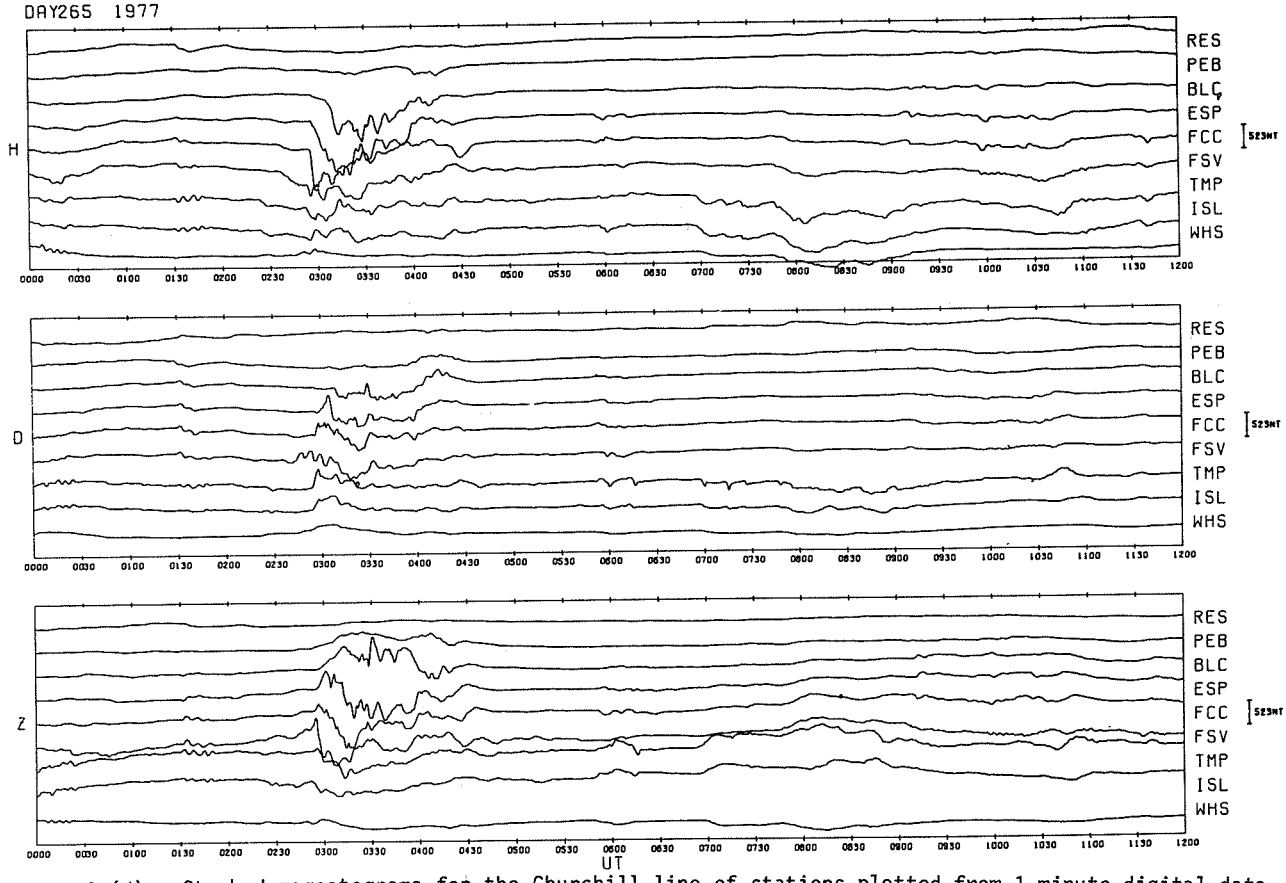

Fig. 2 (d). Stacked magnetograms for the Churchill line of stations plotted from 1-minute digital data.

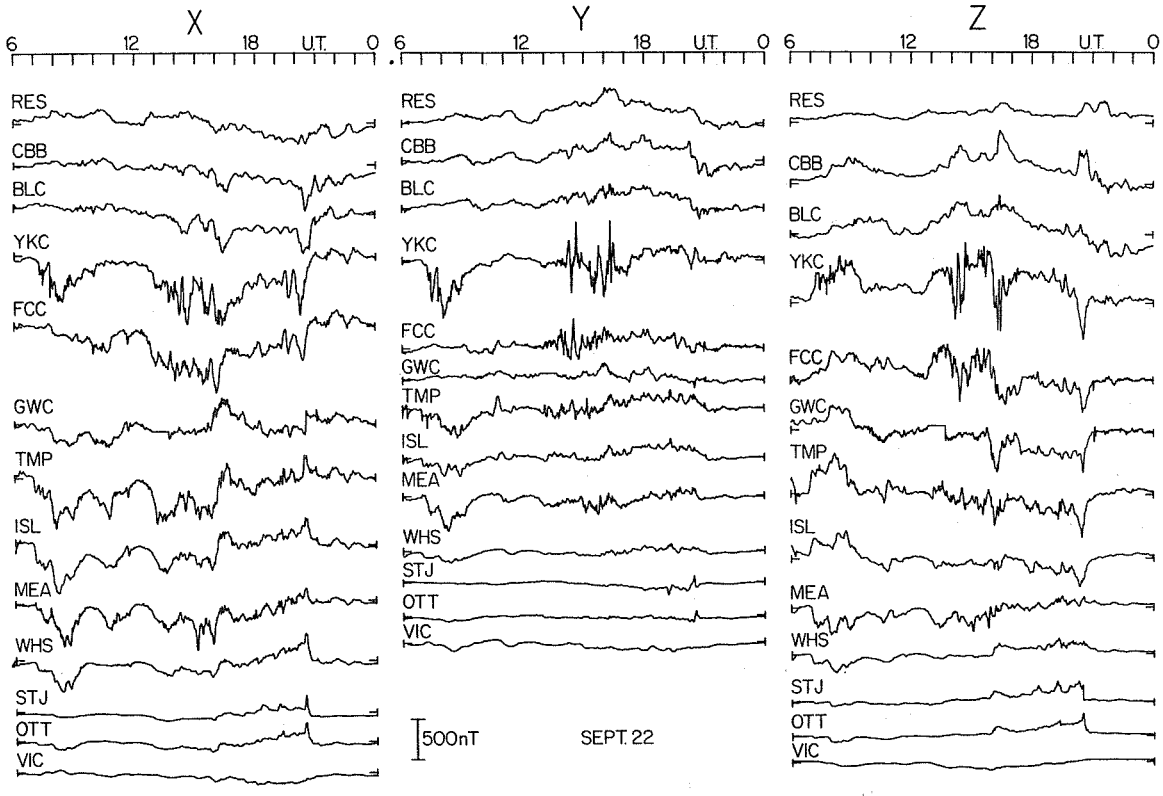

Fig. 1 (e). Magnetograms plotted from 1-minute digital data.

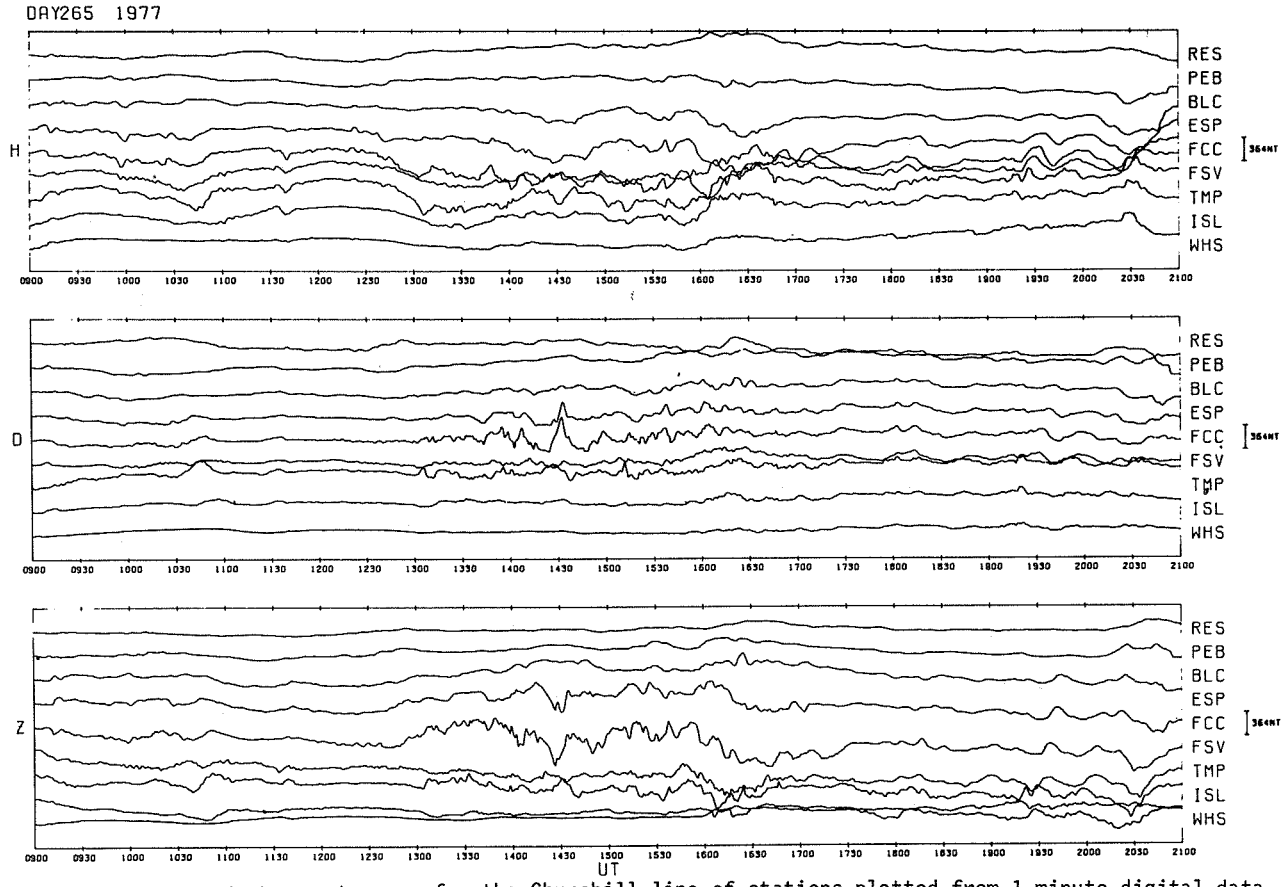

Fig. 2 (e). Stacked magnetograms for the Churchill line of stations plotted from 1-minute digital data.

DISCUSSION OF CURRENT SYSTEMS

The records of the Alert neutron monitor show a large reduction in the level of cosmic ray intensity from September 10 to September 24 following the solar flares that occurred September 7 and 9, 1977. During the recovery phase of this Forbush decrease the solar flare of September 19 occurred (Importance 3B) reducing the level of the cosmic ray intensity well below that seen on preceding days. Such decreases result from the fact that galactic particles may be prevented from entering the magnetosphere when it is compressed by the enhanced solar wind.

The SC reported by IAGA at 1143 UT on September 19 followed the solar flares on September 16 and 17 (see Introduction) by about 61 and 37 hours, respectively. However, this SC was not seen on the standard magnetograms at any Canadian station. According to the Rapid Variations Report from Toledo observatory in Spain the SC was of the type having an initial reverse impulse, known as SC*. As pointed out by Matsushita [1962] from a study of IGY data, the occurrence of SC* is strongly local-time dependent and would not normally be observed before 0700 or 0800 LT at midlatitude stations. At the most easterly Canadian station the LT of this SC was 0812. At Huancayo, which reported the SC as class A (0641 LT) a strong day-time enhancement of SC is expected and has been noted by several authors.

An enhancement of X at auroral and sub-auroral stations (Fig. 1a, 2a) followed the SC and persisted until the commencement of the long-period negative bay which began at 1240 UT. This enhancement is the signature of the compression of the magnetosphere in the initial phase of the storm (Dst was 16 nT at 1200-1300 UT).

Long period bays (6 hours or more) heavily indented with magnetic activity were observed throughout the storm period September 19-23. In the generally accepted model (Fig. 3), such loaded bays [Crooker and McPherron, 1972; Fukushima and Kamide, 1973; Gupta, 1978] occur when the ring current in the equatorial plane flowing along field lines, short-circuits in the auroral oval ionosphere, where an eastward current is established in the afternoon-evening sector and a westward current in the midnight-morning sector. Short negative bays superimposed on the long-period negative X bay in the night sector, the so-called polar substorms, result from the merging of field lines in the tail.

Shortly before 1800 UT September 19 long-period positive bays were observed at Canadian stations indicating westward current flow in the day-side auroral oval. These bays persisted for at least 6 hours, shortly after which substorm activity began at GWC. This is in good agreement with the time predicted by the model for westward current in the midnight-morning sector (Fig. 3).

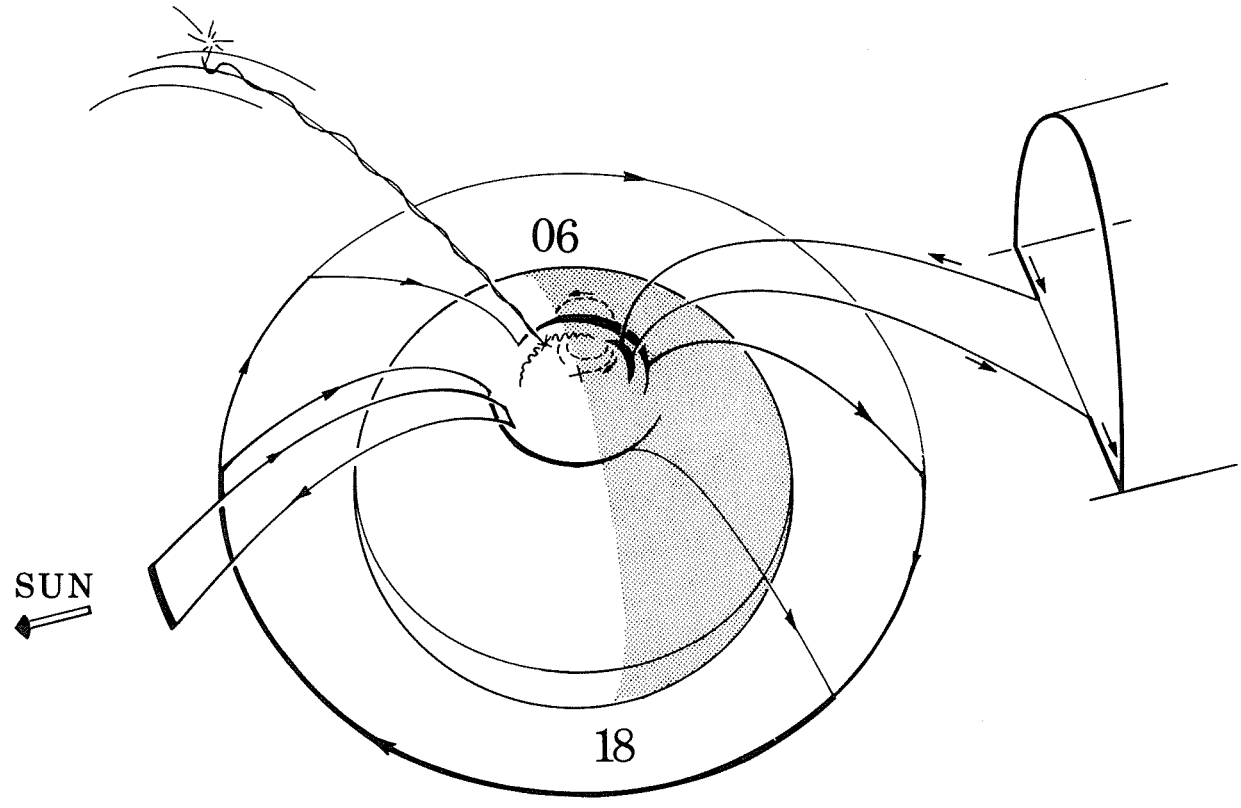

Fig. 3. Schematic representation of the model magnetosphere [Gupta, 1978].

A map showing the stations used in this analysis is given in Fig. 4.

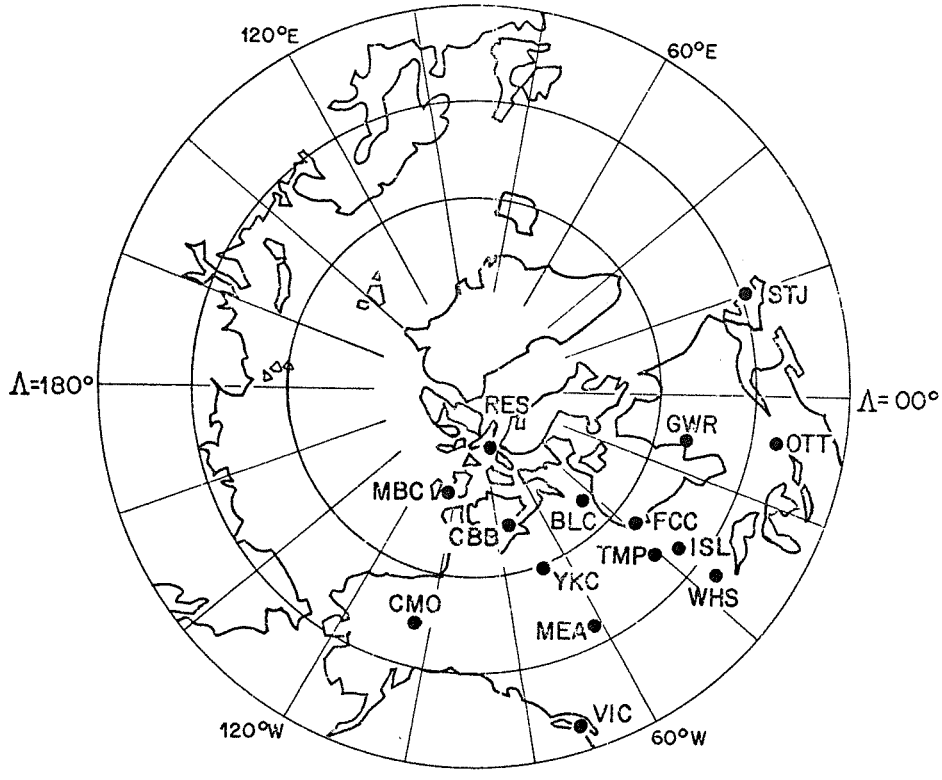

Fig. 4. Map in geomagnetic coordinates of the stations used for the analysis.

Equivalent line current vectors drawn for selected times in the interval 1950 to 2135 UT September 19 are shown in Fig. 5 (a). A counter-clockwise current circulation was observed at 1750 UT (not illustrated) with current flowing to the south-west in the polar cap and eastward between YKC and BLC. This counter-clockwise flow was still present at 1950 UT. Across the Churchill meridian the eastward electrojet was dominant from 1730 to 1950 UT. It extended in (geomagnetic) latitude from 61° to 71°, with maximum intensity .33A/m at 69°. A westward convection electrojet extends from 71° to the polar cap. The total magnitude of the eastward electrojet is 260kA and that of the westward electrojet is 350kA. (Table 3). These postnoon cleft region electrojets are larger, more intense and further south than those determined by Walker et al. [1978] for quiet conditions. At 2025 UT a strong westward flow is observed north of GWC and YKC and between FCC and BLC, as stations north of TMP come under the influence of the main westward electrojet. This is evident from Fig. 1a, 2a where a strong negative indentation is observed in X at all sites north of TMP between 1945 and 2130 UT. This indentation was most intense at BLC at 2025 UT (-430 nT in X), when the westward electrojet observed across the Churchill meridian was maximum (750 kA) and centered at 69° (Table 3). At Tromso a negative H bay was in progress at this time, with maximum intensity at 2008 UT (-1200 nT in H). At Canadian stations south of TMP a strong positive bay was recorded during this interval with maximum at ISL at 2050 UT (420 nT). The current vectors calculated for stations south and east of TMP suggest the existence of an eastward electrojet at this time. An eastward electrojet was observed across the Churchill line between 60° and 67° latitude at 2025 with intensity .93 A/m.

By 2135 UT only BLC, CBB (and MBC) remain under the influence of the main westward electrojet. An eastward current flows along the 65° geomagnetic parallel south of YKC, FCC and GWC (see also Table 3). Current vectors at MEA and OTT are directed approximately poleward, and probably indicate field-aligned currents in the vicinity of these stations. Current flow in the polar cap as seen at RES is approximately sunward and may be associated with the substorm activity still evident at Tromso at this time.

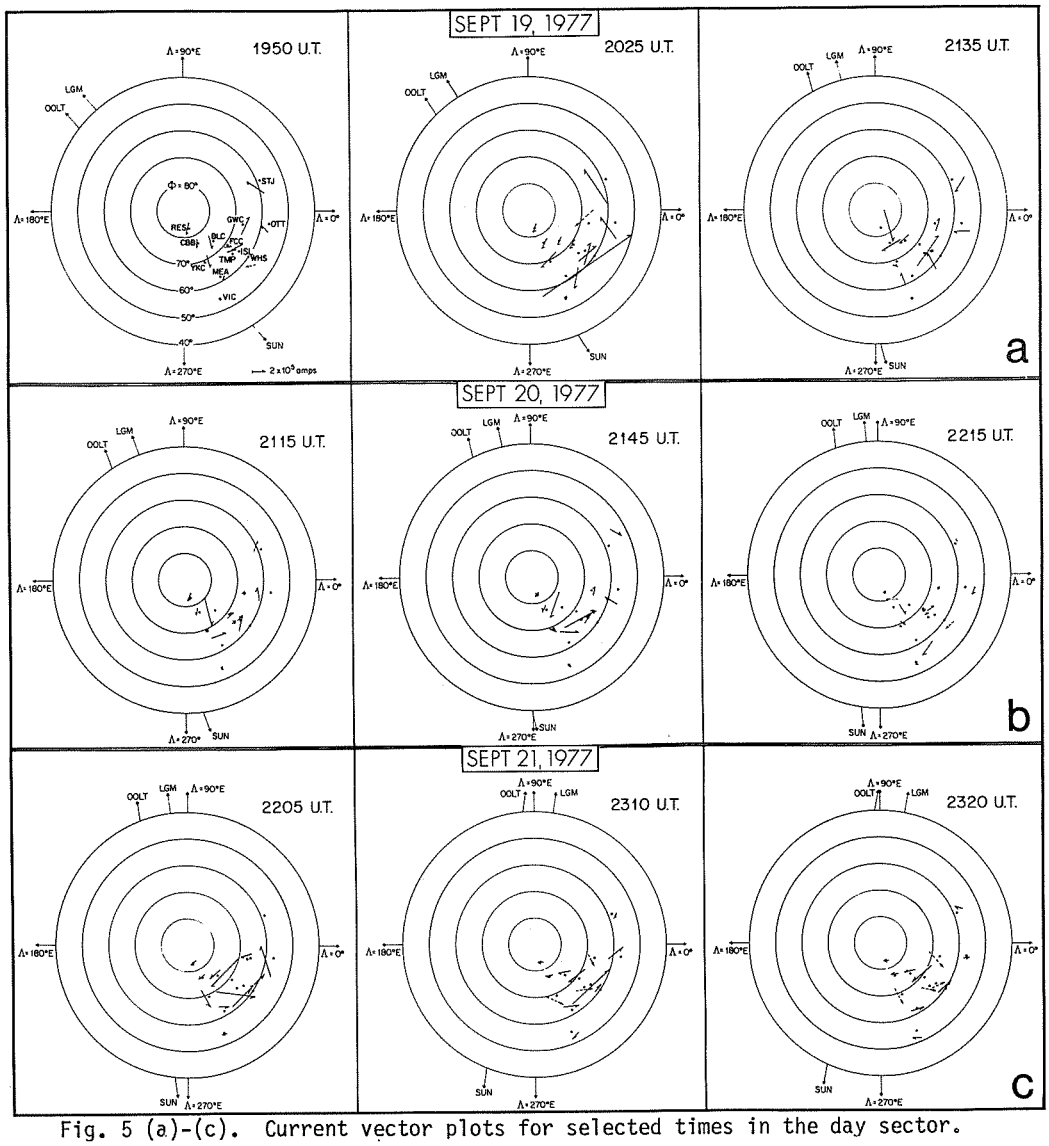

Fig. 5 (a)-(c). Current vector plots for selected times in the day sector.

On September 20 at 2015 UT near the beginning of the event observed in the Canadian sector, there is evidence for an eastward electrojet flowing between ISL and BLC, and between YKC and CBB. It is likely that stations in the polar cap and to the south of ISL are in current systems associated with this eastward electrojet. An hour later, at 2115 UT (Fig. 5 (b)) the current vectors suggest the extension into the dayside auroral oval of the westward electrojet evident at Tromso in the night sector where a large negative H bay is observed with minimum at 2151 UT (1025 nT). The current vectors are consistent with the two-dimensional equivalent current system, with current from the main westward electrojet flowing to the south of the vicinity of BLC and CBB. The situation is similar at 2145 UT (see also Table 3), but movement to the west is apparent. At this time both eastward and westward electrojets were observed across the Churchill line. Near the end of the disturbance at 2215 UT it is likely that an independent eastward electrojet has reestablished itself, following the termination of the substorm activity, and current flow is similar to that observed at 2015 UT.

The next period of magnetic activity in the day-sector occurred September 21 following the large SC recorded at 2044 UT (Table 9). The SC at 2044 UT occurred before the recovery of the magnetospheric storm of September 19. The strong westward electrojet in the midnight sector which is inferred from activity at Tromso extended into the Canadian sector where large negative bays are seen between 2120 UT September 21 and 0130 UT September 22 at the auroral stations GWC and FCC and westward electrojets were observed across the Churchill line. The magnetic activity on these bays is consistent with the model of merging field lines in the tail producing substorms in the night sector. This merging apparently occurred frequently at intervals of a few minutes (10-20 min). The positive bays and superimposed substorm activity observed at the lower latitude stations during these hours, and the large currents to the north of the auroral oval are probably attributable to return currents from the westward electrojet, as the lower latitude and polar ionosphere are likely to be sufficiently conducting to sustain such currents during day hours. Information concerning the electric fields which exist at this times is not known.

Plots of current vectors at 2205 UT Fig. 5 (c) showed a tight counter-clockwise cell centered near ISL. In the polar cap, westward flowing currents were observed, and are probably return currents of the westward electrojet flowing in the midnight sector (at Tromso H was minimum at 2212 (-1000 nT) and at 2401 UT (-1260 nT). Current vector plots for 2310 and 2320 UT were very similar with GWC and probably FCC under the influence of the main westward electrojet flowing north of these stations, and with eastward currents to the south between WHS and TMP, and south of MEA. At 2310 UT acros the Churchill line an eastward electrojet of 350 kA was observed between latitudes 60° and 65° with a westward electrojet to the north of 560 kA. By 0100 UT September 22 the eastward electrojet had expanded poleward to the vicinity of ESK.

The last period of day-time activity investigated was 1600 to 2100 UT on September 22. Current vector plots are shown in Fig. 5 (d) for selected times in this period. During this interval long-period positive bays in X were observed at stations south of TMP with negative bays to the north.

At 1815 UT there is a suggestion of two cells in the Canadian-Alaskan sector: a clockwise cell with westward current passing south of YKC and CMO, possibly part of the northern return current system from the westward electrojet which is still active in the midnight sector; and, as shown by the current vectors at FCC and at lower latitude stations to the east of MEA, a counter-clockwise current system also. About an hour later, at 1911 UT (not shown) the situation remained essentially unchanged, except that the current vectors at GWC and MEA suggest the movement to the west of the counter-clockwise system. At 2015 (not shown) and 2023 UT the westward electrojet in the night sector extended into the day sector, as evident from the negative X bays at CBB, BLC, YKC and FCC (Fig. 1d & e, 2d & e). Westward flow is south of BLC and north of YKC and CMO. At these times, the strong eastward current north of MEA and between ISL and WHS is consistent with return currents flowing to lower latitudes for the main westward electrojet.

The long-period X bays terminated very suddenly at 2030 UT. Between 2028 and 2033 UT X increased at GWC by 277 nT and decreased at WHS and STJ by 160 nT. At 2030 UT the magnetogram from Tromso showed maximum deflection of the negative H bay there (-868 nT). In the interval 028 to 2033 UT the current vector at GWC rotated out of the westward flow north of GWC at 2028 UT, when the station was influenced by the main electrojet, to an eastward flow south of the station when GWC came strongly under the influence of the eastward current now flowing between GWC and OTT. Essentially the current vector pattern is similar, but at 2033 UT a contraction in the westward extension of the main electrojet is indicated by the rotation to the southwest of the westward current vector of YKC.

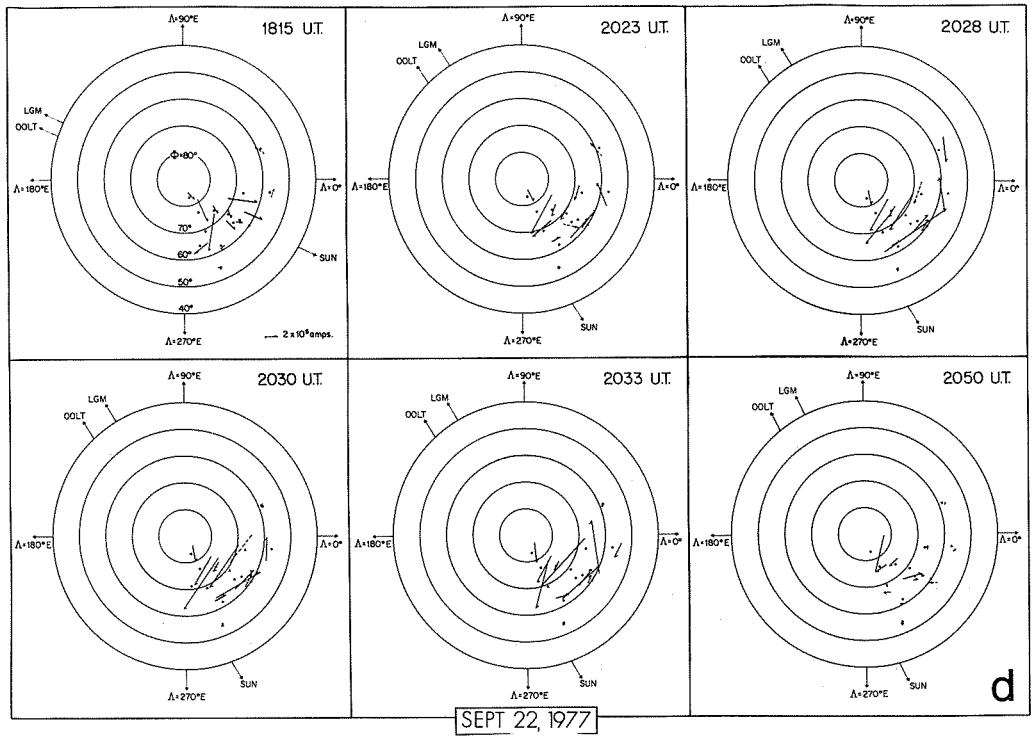

Fig. 5 (d). Current vector plots for selected times in the day sector.

Both eastward and westward electrojets were evident across the Churchill line at 1911 UT and persisted until about 2100 UT (Table 3).

At 2050 UT, following termination of this period of magnetic activity, the normal westward current flow is reestablished at STJ, OTT, WHS and VIC. A westward current is observed north of BLC and an eastward current flows between FCC and WHS and south of GWC (see Fig. 5 (d) and Table 3).

Current vector plots were also drawn for selected times during substorms which were observed in the night sector on September 21 and September 22. These plots are shown in Figs. 6 (a), (b) and (c).

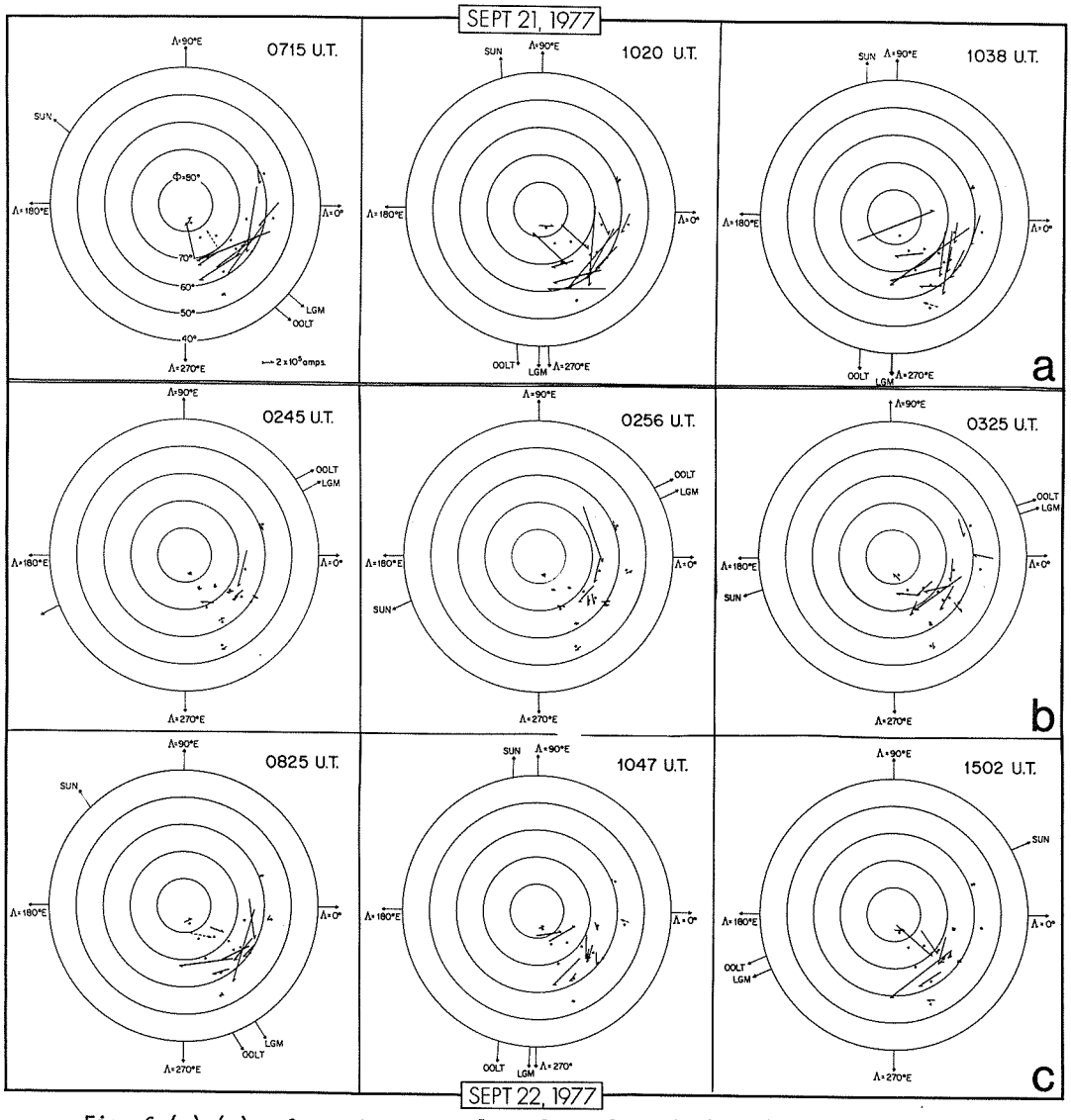

Fig. 6 (a)-(c). Current vector plots for selected times in the night sector.

In the series of complex polar substorms on September 21 (Fig. 1c & d, 2c & d) the electrojet for the sustorm beginning 0445 UT at MEA flowed westward north of OTT and between GWC and MEA, passing nearly overhead at TMP and ISL (see Sequence of Events: September 21). The analysis of data from the Churchill line indicates a movement of the westward electrojet south of TMP by 0500 UT, with the equatorward edge probably south of WHS. The electrojet for the next storm, with maximum intensity at 0715 UT at ISL, flowed between GWC and MEA and south of TMP and ISL (Fig. 5 (a)). This suggests that the auroral oval rotated westward with time and expanded to the south following the previous substorm.

At 1015 UT (Fig. 1c & d, 2c & d) sharp impulsive negative X bays began at MBC, CBB and BLC in the polar cap, bringing these stations out of the return current system and under the influence of the main westward electrojet. Maximum intensity at MBC was at 1038 UT (447 nT below the quiet level in X); however, the amplitude of the negative X bay, which was superimposed on a preexisting long period (0400-1400 UT) positive bay, was 790 nT.

The current vector plot (Fig. 6 (a)) at 1015 UT shows a westward electrojet (1300 kA) flowing between OTT and GWC and north of VIC. MBC, RES and BLC were in the polar cap current system associated with this electrojet. At 1020 UT the situation was essentially the same, except that a movement of the electrojet system to the west may be inferred from the vector plot. Westward current flow across the Churchill line was 1300 kA at 1015 UT, with the westward electrojet extending from south of WHS to about 68°. This was the maximum current flow observed in the interval under study.

Current vectors at 1039 UT show strong intensification of the storm system at the northern edge of the auroral oval with westward current flowing south of MBC, CBB and BLC as well as south of YKC, MEA and TMP. This suggest an expansion of the auroral oval by 10 to 15 degrees in the midnight sector. The westward electrojet observed across the Churchill line at this time extended from 61° to 80°.

On September 22 current vectors for 0245 UT (Fig. 6 (b)) clearly show an intense electrojet north of GWC passing between TMP and FCC but apparently of limited extent. Equivalent current flow in the polar cap is between BLC and CBB and between MBC and RES. An eastward current flowing north of CMO (not shown) and MEA and a westward flow south of VIC suggest the possibility of a second equivalent current cell. The current pattern is very similar at 0256 UT, except that ISL is now under an eastward current (see also Table 3).

At 0325 UT CMO, MEA and VIC are clearly in the current system south of the auroral oval associated with the westward electojet. At this time the electrojet has moved considerably north and west with maximum intensity at BLC (-1010 nT in X). A westward electrojet was observed across the Churchill line at this time with intensity 1.8 A/m extending from 61° TO 77° latitude.

At 0825 UT a well defined westward electrojet is evident across Canada, south of GWC and flowing between ISL and WHS and between YKC and MEA in the west. The intensity (-X) of the substorm was maximum at YKC (560 nT) and MEA (545 nT).

Later, at 1047 UT (Fig. 6 (c) and Table 3) a westward electrojet was observed north of GWC and flowing between TMP and ISL and to the north of MEA. FCC, previously in the polar cap current system, is now under the influence of the main electrojet.

About two hours later, another substorm is evident at all auroral stations, with maximum intensity at CMO (-670 nT in X) at 1335 UT (not shown). The westward electrojet is located between FCC and ISL, YKC and MEA (and south of CMO). The intensity of the substorm is relatively high to the east in the dawn sector (-505 nT at FCC in X). Maximum intensity across the Churchill line at this time was 1.0 A/m.

A complex negative bay began about 1430 UT at MEA where maximum (-X) intensity was 610 nT at 1502 UT. The maximum intensity for this event at CMO in the midnight-morning sector was -1051 nT in X, with westward current flowing approximately over the station. The next storm (not shown) in the Canada-Alaska sector had maximum intensity at CMO at 1530 UT (-1350 nT in X). X at FCC and YKC was -690 nT and -700 nT respectively at this time. Westward current flow was to the north of CMO. The complex negative bay which followed at YKC reached maximum there near 1620 UT (830 nT in -X).

CONCLUSIONS

Investigations carried out using magnetogram data from Canadian stations for September 19-22, 1977 revealed a variety of magnetic activity following the solar flares observed September 17 and 19. The direction of the inferred interplanetary magnetic field in this interval was variable.

The analysis clearly demonstrated the existence of eastward and westward electrojets in the auroral oval. The equivalent currents seen to the north and south of the auroral oval may be mainly due to magnetic fields of field-aligned currents, as postulated by more recent models of magnetospheric currents. Occasionally movement with time of the westward electrojet could be inferred from the observations. Maximum current flow across the Churchill line of variation stations, as calculated from current density modelling, was 1300 kA at 1015, 1020 UT, September 21, and westward near geomagnetic latitude 61°. This is in good agreement with the equivalent line current vectors (1300 kA average for TMP and ISL at 1015 UT and 1500 kA at 1020 UT). Maximum width of the westward electrojet across the Churchill line was 19° at 1038 UT.

At times (Fig. 5 (d)) eastward and westward currents have been observed simultaneously in the day sector. There are two possible explanations for this. The conductivity south of the auroral oval in the day sector may be sufficiently high to sustain eastward return currents from an extended westward electrojet originating in the night sector. On the other hand, there may be an independent eastward electrojet in the day sector (resulting from the short-circuiting of the ring current) which exists simultaneously with the main westward electrojet.

The absence on the Canadian records of the SC* on September 19, 1143 UT was expected because of its time of occurrence [Matsushita, 1962].

The long-period positive and negative bays with superimposed substorms and pulsations were consistent with the model previously discussed by Gupta [1978].

In summary, the large solar activity associated with the McMath plage region 14943 did not appear to cause any exceptional magnetic activity in the Canadian sector.

Acknowledgments

The assistance in programing given by Mr. J. Morris, Computer Science Centre, Energy, Mines and Resources Canada is very much appreciated. We also gratefully acknowledge the assistance given by Messrs. Gerrit Jansen van Beek and F.C. Plet in handling the observatory and IMS variation station data.

We are grateful for the facilities and assistance provided by the Ontario Ministry of Transport and Communications at Ft. Severn, the National Research Council at Thompson, the Department of Transport at Eskimo Point and the Atmospheric Environment Service at Island Lake.

REFERENCES

AKASOFU, S.-I. 1977 Physics of Magnetospheric Substorms, Astrophysics and Space Science Library, p. 47, D. Reidel Publishing Co., Dordrecht-Holland/Boston, USA.

BOSTROM, R. 1964 A model of the auroral electrojet, J. Geophys. Res., 69, 498.

CROOKER, N.W. and R.L. MCPHERRON 1972 On the Distinction Between the Auroral Electrojet and Partial Ring Current System, J. Geophys. Res., 77, 6886-6889.

FUKUSHIMA, N. and Y. KAMIDE 1973 Partial Ring Current Models for Worldwide Geomagnetic Disturbances, Rev. Geophys. Space Sci., 11, 795-853.

GUPTA, J.C. 1978 Geomagnetic Bays and Pc5 Pulsation Substorms at High Latitudes, J. Atmos. Terr. Phys. 40, 169-181.

LOOMER, E.I. and G. JANSEN VAN BEEK 1971 Magnetic Substorms, December 5, 1968. Pub. Earth Phys. Br., 41, No. 10, 183-198.

MATSUSHITA, S. 1962 On Geomagnetic Sudden Commencements, Sudden Impulses and Storm Durations, J. Geophys. Res., 67, 3753-3777.

ROSTOKER, G. and K. KAWASAKI 1978 East-west asymetries in auroral zone current distributions during magnetic substorms, Final Report EMR Contract No. OSU77--00020 from Institute of Earth and Planetary Physics, University of Alberta.

SAITO, T. 1969 Geomagnetic Pulsations, Planet. Space. Sci., 10, 319-412.

WALKER, J.K., P.W. DALY, M.B. PONGRATZ, H.C. STENBAEK-NELSEN and J.W. WHITTEKER 1978 Cleft currents determined from magnetic and electric fields, J. Geophys. Res., 83, 5604-5616.

Magnetic Storms Recorded at the 145° Geomagnetic Meridian Observatories during September 19-24, 1977 and November 1977

by

L.N. Ivanova, B.A. Undzenkov, V.A. Shapiro, B.L. Shirman
Institute of Geophysics, Urals Scientific Center USSR Acad. of Sciences
Pervomaiskaya Str. 91
Sverdlovsk, 620219, USSR

Figure 1 shows the geomagnetic storm records in H component at Nyda and Ugut stations in September 1977.

Another magnetic storm with the sudden commencement was observed by the net of stations along the geomagnetic meridian 145° during the period November 25-26, 1977 (Fig. 2). Probably this storm was the result of the November 22 solar flare.

Fig. 3 shows the rapid run H, D and Z component magnetic records of the geomagnetic storm sudden commencement at the Arty observatory on November 25, 1977.

The locations of the stations are listed in Table 1.

Table 1. Geographical coordinates of the stations on the geomagnetic meridian 145°

Station	N Lat.	E Long.
Nyda	66.6°	73.0°
Numto	63.5°	71.1°
Ugut	60.5°	74.0°
Arty	56.4°	58.6°
Karaganda	49.8°	73.1°
Alma-Ata	43.3°	76.9°

Geomagnetic data of Alma-Ata and Karaganda stations were contributed by Dr. M.P. Rudina.

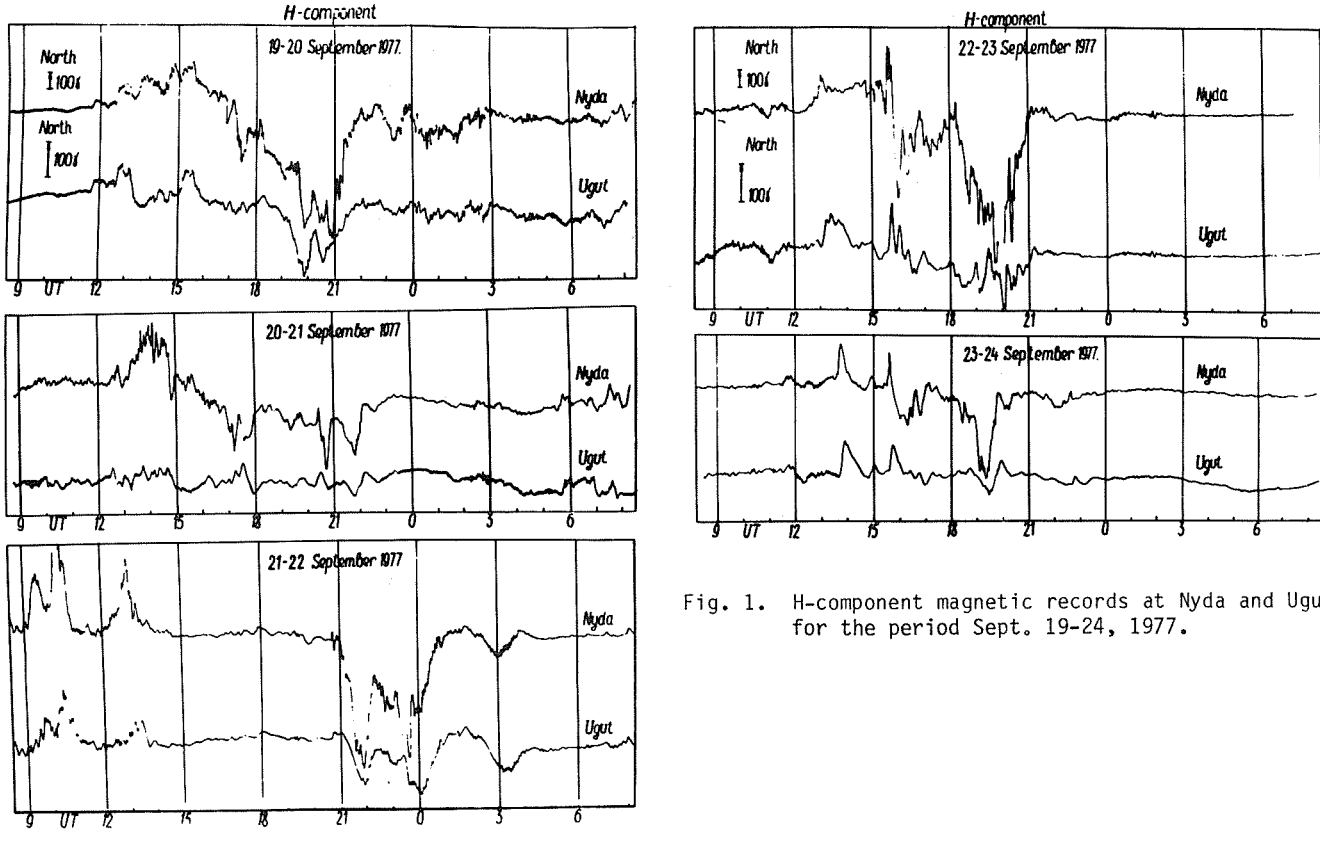

Fig. 1. H-component magnetic records at Nyda and Ugut for the period Sept. 19-24, 1977.

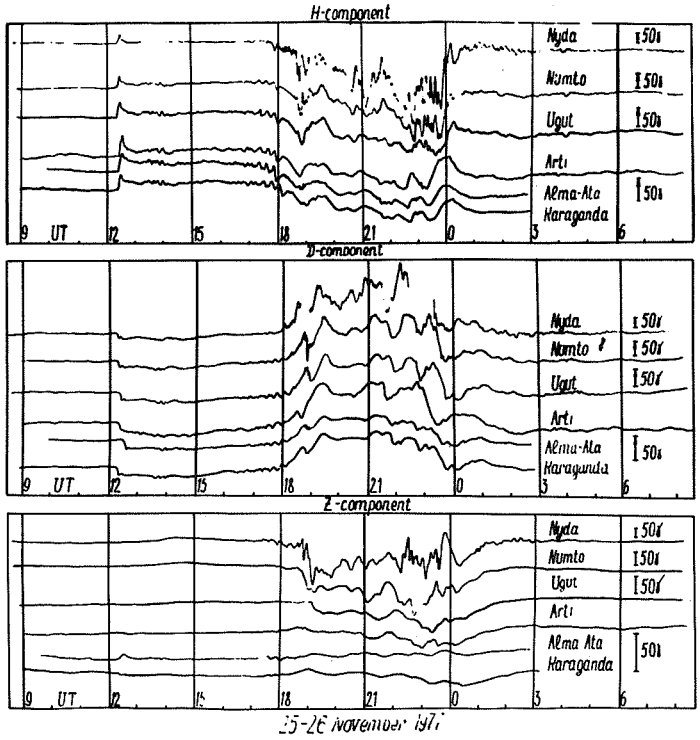

Fig. 3. Geomagnetic storm sudden commencement at the Arty observatory for November 25-26, 1977.

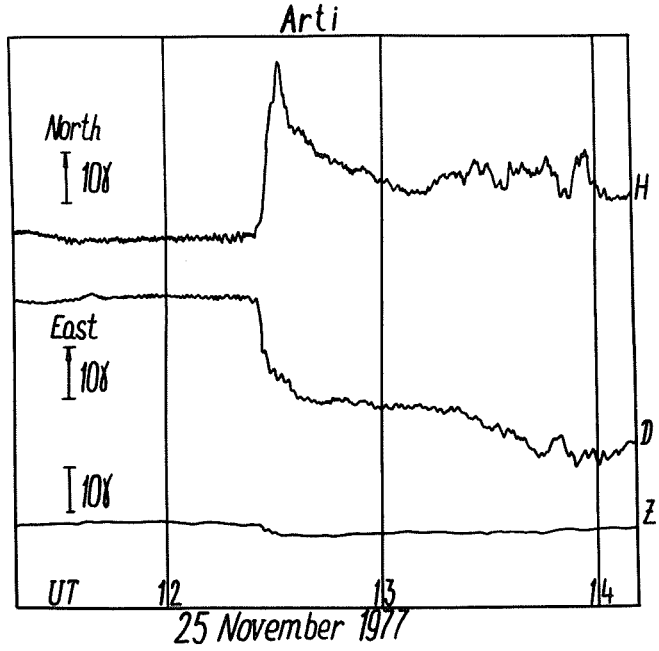

Fig. 2. Geomagnetic storm H, D, Z records at Nyda, Numto, Ugut, Arty, Alma-Ata and Karaganda for the period November 25-26, 1977.

Magnetic Activity in Iceland during September 1977

by

G.R. Moody and A.N. Hunter
Department of Environmental Science
University of Lancaster, Bailrigg
Lancaster, Lancashire, England

The Lancaster Array

Lancaster University has been operating an array of six Dominion Observatory EDA Fluxgate magnetometers in Iceland as part of the UK contribution to the International Magnetospheric Study. Figure 1 shows the positions of the six stations while Table 1 contains their geographic coordinates.

Data recorded digitally on cassettes at a sampling rate of 10 seconds have been processed onto master tapes at Lancaster and are available for five of the six stations during this period. Analog chart records are available for the sixth station Hveravellir where cassette recording failed.

Figure 1. The Lancaster Magnetometer Array.

TABLE 1

Station Name	Abbreviation	Geographic Coordinates N. Lat. deg.	min.	W. Long deg.	min.
Siglufjordur	SIG	66	09	18	55
Fagurholsmyri	FAG	63	53	16	39
Hveravellir	HVE	64	52	19	35
Reykjaskoli	REY	65	16	21	04
Isafjordur	ISA	66	05	23	06
Thorshofn	POR	66	12	15	17

Magnetic Activity September 7-18

At high latitudes the magnetic field is rarely quiet for long periods. Magnetic disturbances can be observed at most times and the magnetograms for September 7-18 seem typical. It is unusual for the magnetic field to be nonactive in the hours before and after local midnight. From September 7-18 magnetic storms of varying intensity occur around midnight every day, except for during the nights of September 15/16 and 18/19. By comparison the nights exhibiting the greatest degree of magnetic disturbance are those of September 10/11, 12/13 and 13/14.

Figures 2a, b and c show the magnetograms for the five stations processed from digital records for the early hours of September 14. This appears to be a fairly typical magnetic storm and, as such, may be worth examining in more detail.

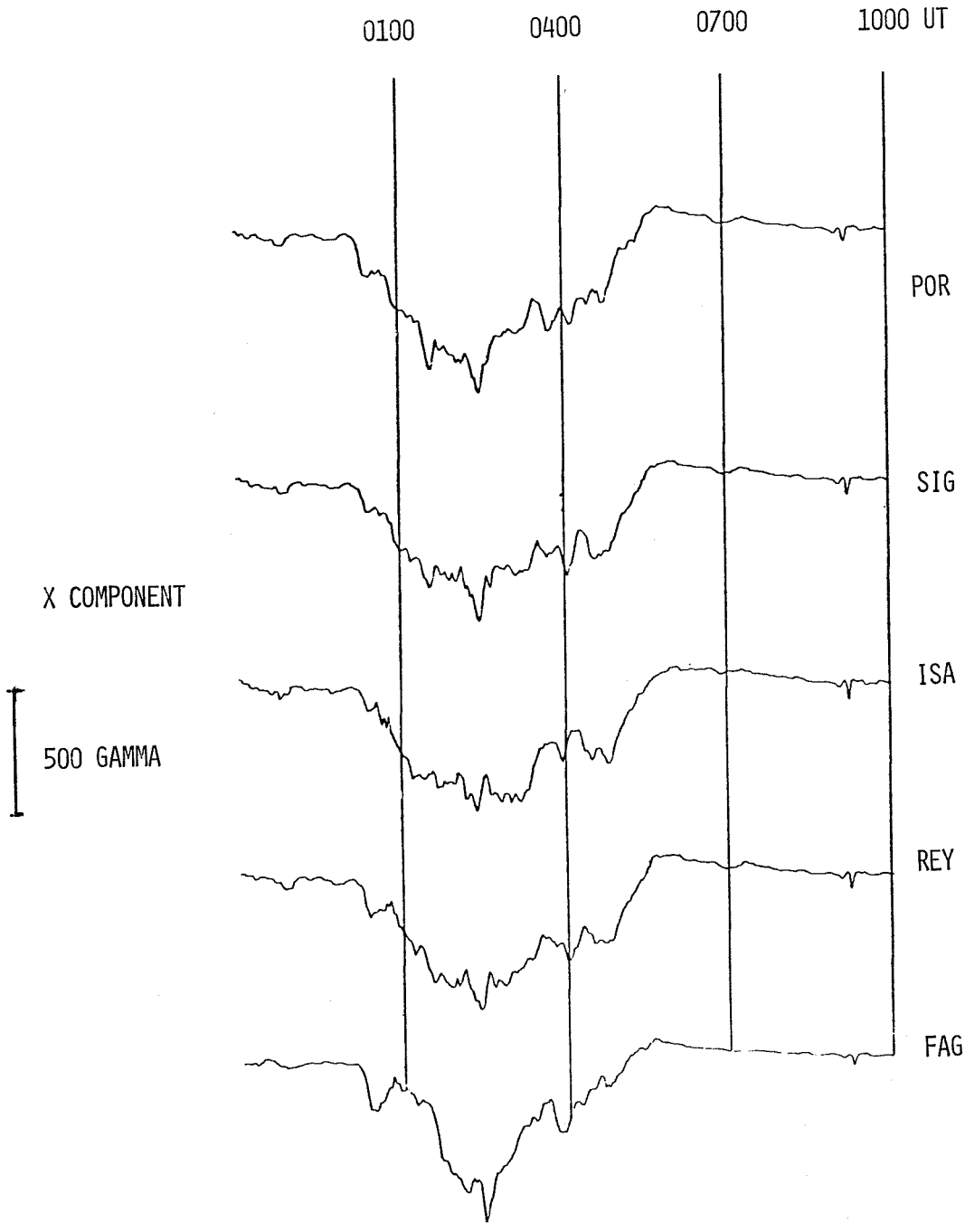

Figure 2a. - The North-South component of the magnetic field, 14th September 1977.

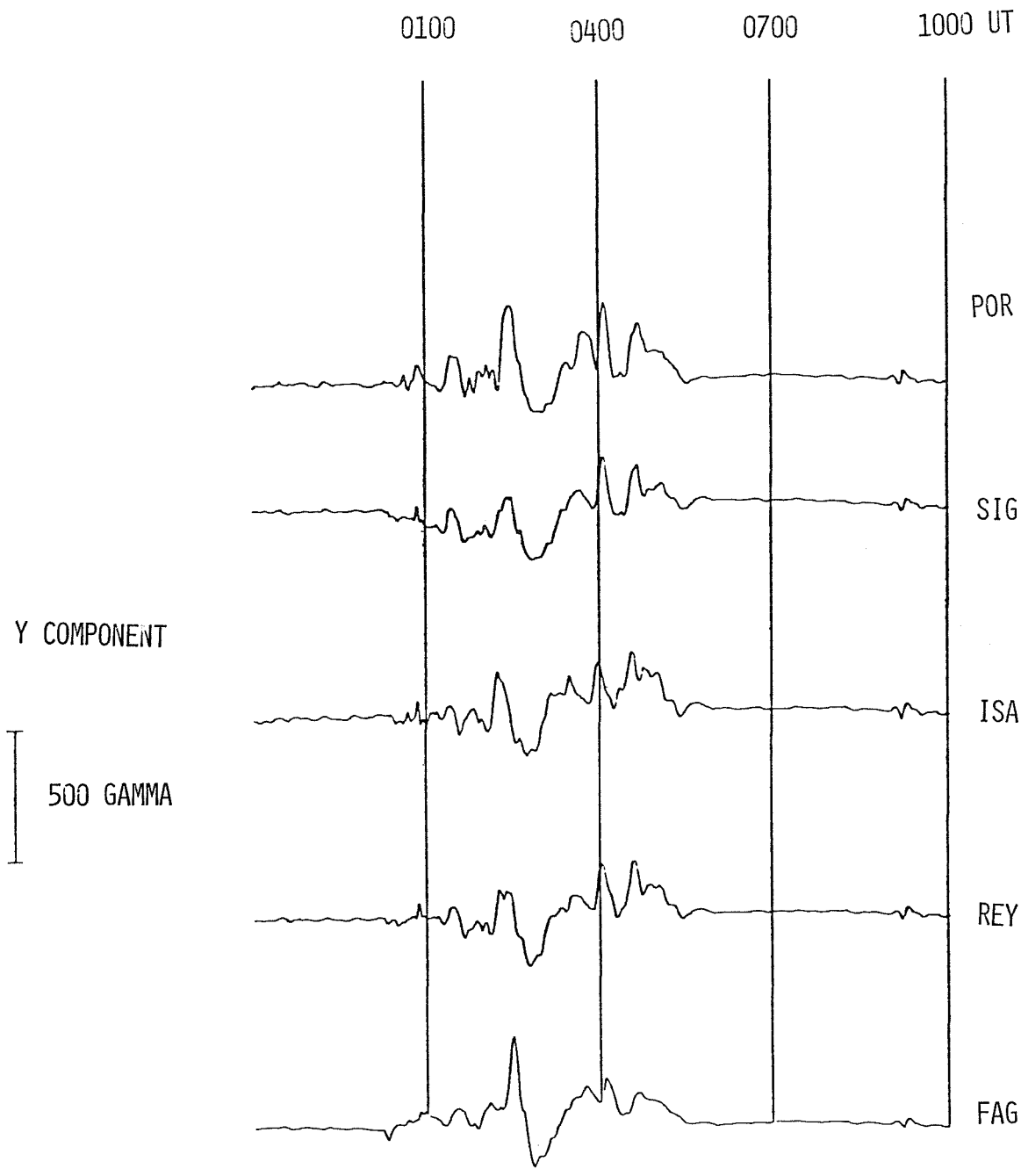

Figure 2b. The East-West component of the magnetic field, 14th September 1977.

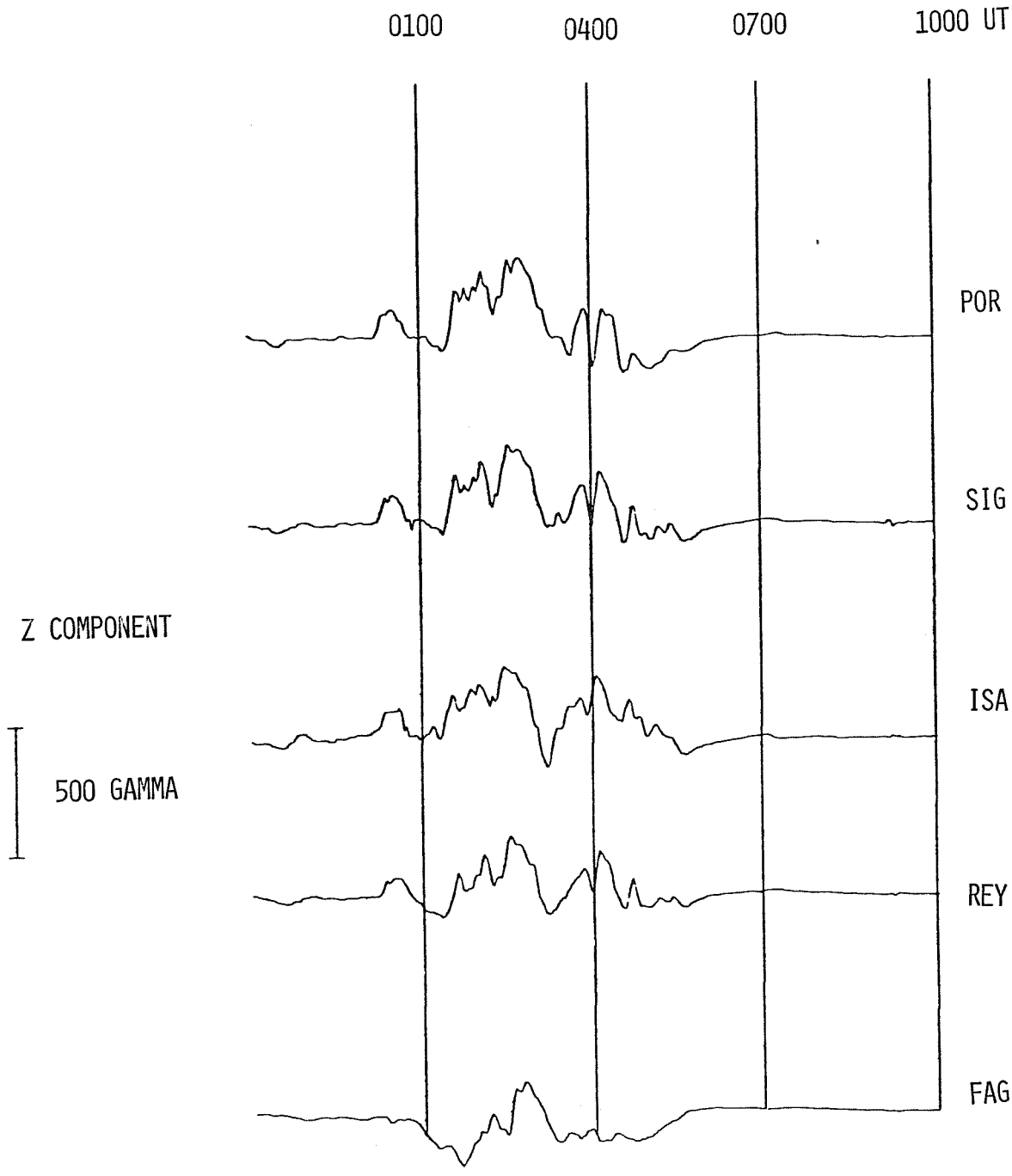

Figure 2c. The vertical component of the magnetic field, 14th September 1977.

The magnetic field has been moderately disturbed during the late afternoon of September 13 but had returned to a quiet state for several hours before the onset at 0013 UT. The effect of the storm is clearly seen in a reduction in the X component at all stations together with a simultaneous increase in the Z component. This indicates an enhanced westward electrojet flowing to the north of Iceland. The north-south component of the magnetic field continues to decrease until 0226 UT when the recovery phase of the storm begins.

The traces show great similarity between stations, especially in the X and Y components. The horizontal magnetic field at FAG appears to be modified slightly by its more southerly position. The difference between the vertical component at FAG and the other stations is probably due to a combination of its increased distance from the electrojet and its different inductive response to the source field. This is suggested by early results from induction studies carried out using data from this array.

The Magnetic Storms of September 19-24

Figure 3 shows the magnetograms from station SIG for September 19 to 24. During this period the magnetic field is almost continuously disturbed. Particularly strong events occur at 0427 UT and at 2400 UT on September 21. The latter of these can be examined in more detail in Figures 4a, b and c.

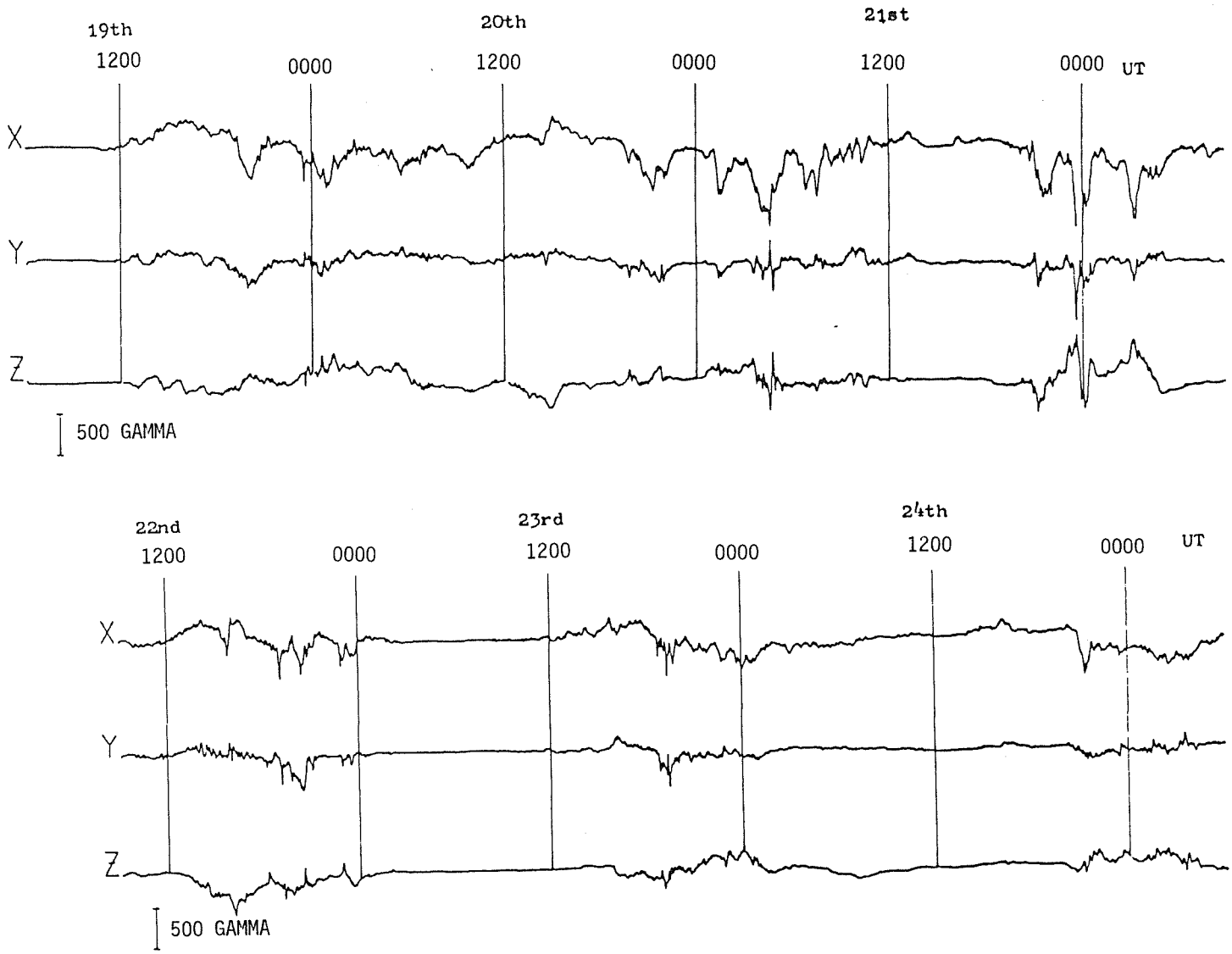

Figure 3. Station SIG magnetograms 19th-24th September 1977.

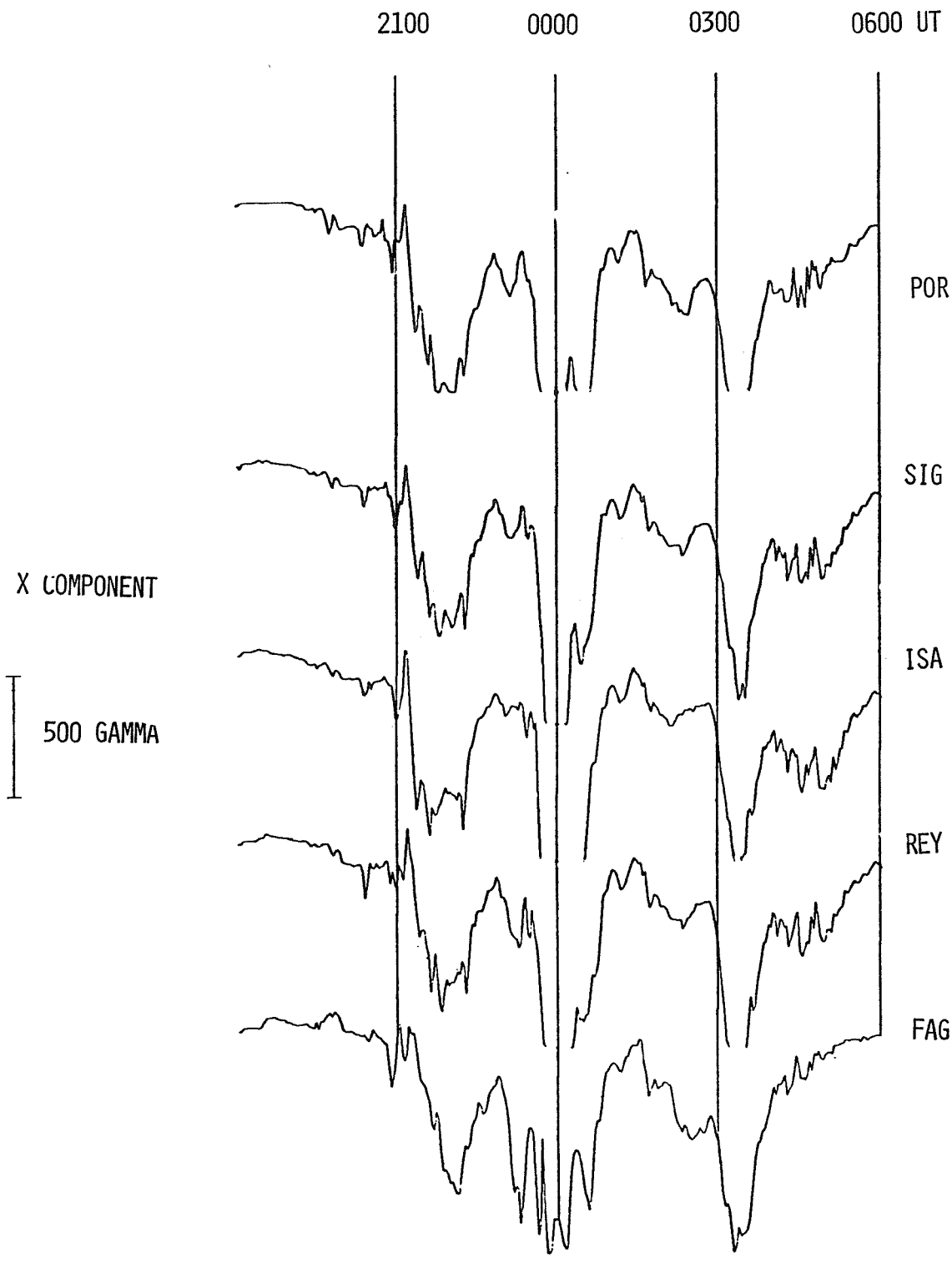

Figure 4a. The North-South component of the magnetic field, 21st/22nd September 1977.

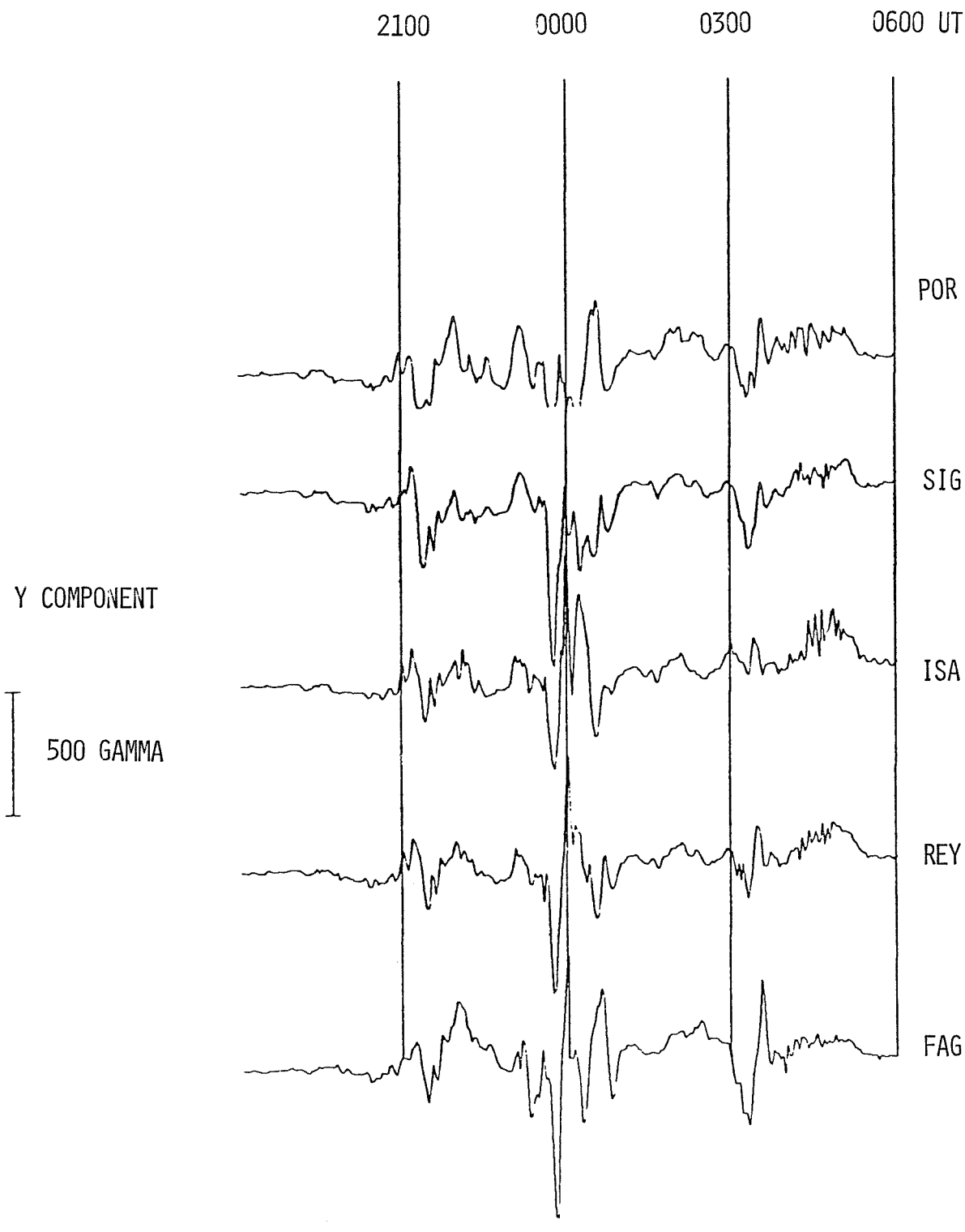

Figure 4b. The East-West component of the magnetic field, 21st/22nd September 1977.

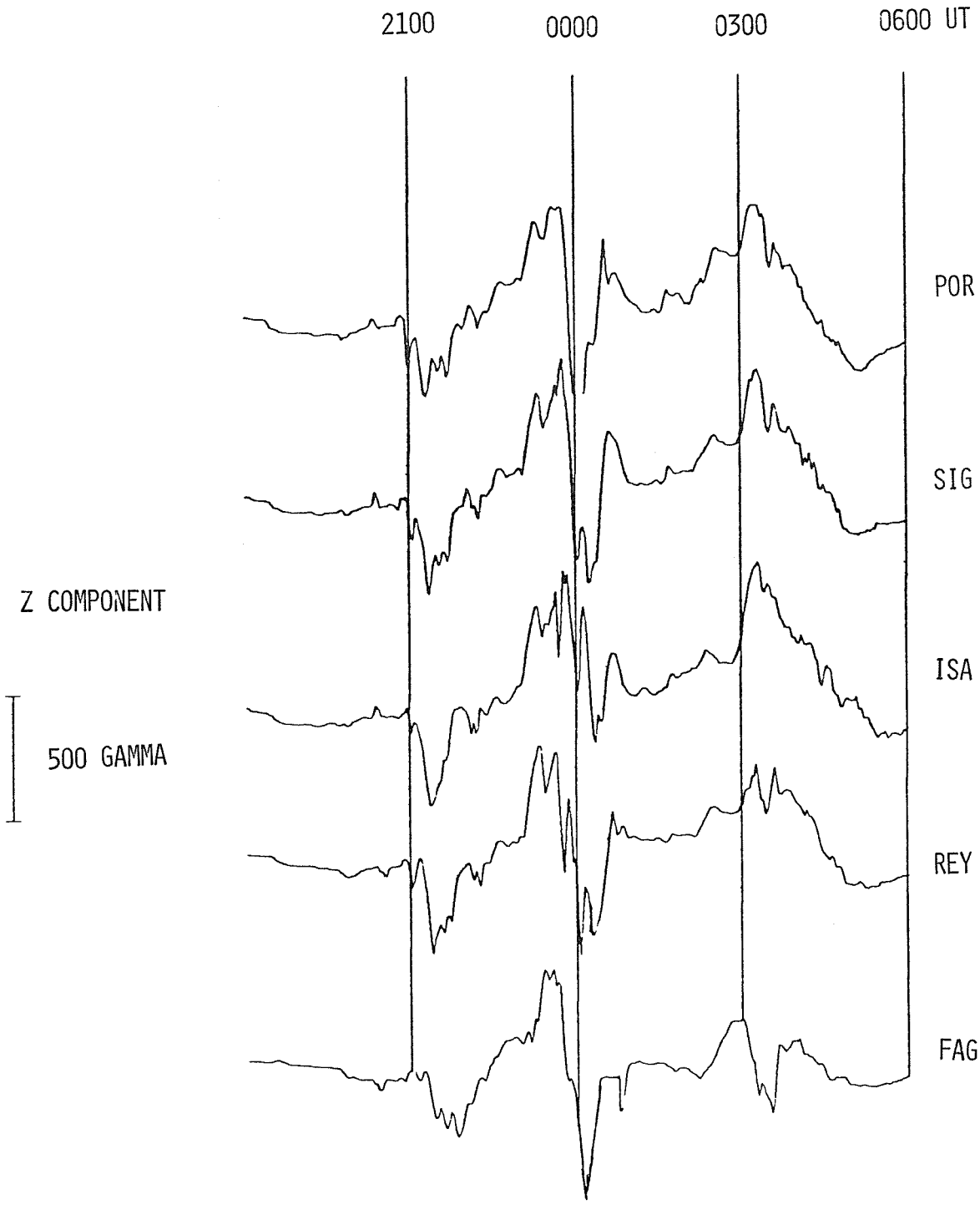

Figure 4c. The vertical component of the magnetic field, 21st/22nd September 1977.

In comparison with the storm of September 14 the magnetic response here is considerably more complicated. It is not possible to identify a single bay in the X component but rather a series of three bays centered at 2152 UT, 0000 UT and 0309 UT. The gaps in Figure 4 show that the minimum of several of these events is out of the range of the recording equipment. The east-west component is similarly complicated but again three separate events can be recognized each exhibiting a signature, stronger but essentially similar in form, to that shown in Figure 2b. This disturbance can therefore be thought of as a summation of the geomagnetic responses of three storms each one of greater magnitude but shorter duration than that of September 14.

The times when the storms were directly overhead in Iceland can be obtained more accurately from the east-west component. This component should be negative when the central meridian lies to the west and zero when directly overhead, assuming that the recording station is to the south of the electrojet (otherwise vice versa) [Pytte et al., 1976]. Thus from Figure 4b it can be seen that the central meridian of each storm was overhead at station REY at 2123 UT, 2354 UT and 0309 UT. For each case a maximum and a minimum can be picked out which are smoothly connected together. Further it should be noted that for storms two and three the sequence is minimum-zero-maximum whereas for storm one the sequence is maximum-zero-minimum; this can be identified consistently in each of the five traces and for each of the three storms.

The vertical component of the magnetic field again exhibits the effects of three separate storms despite being complicated by the local inductive response at each station. However the direction in which the vertical component is deflected appears to change between the first and last storms. This would indicate that the electrojet had jumped northward over Iceland during this period. This suggestion is supported by a close inspection of the Y component of the field where as we noted earlier the usual negative to positive deflection as exhibited during the second and third storms is reversed during the first.

REFERENCES

PYTTE, T., R.L. McPHERRON and S. KOKUBUN — 1976 — The Ground Signatures of the Expansion Phase During Multiple Onset Substorms, Planet. Space Sci., 24, 1115-1132.

On ULF Geomagnetic Variations Observed at Garchy (France) Between 7 and 24 September 1977

by

M. Six and J. Roquet
Institut de Physique du Globe de Paris

For the period September 7-24, 1977, we have normal "La Cour" and "Mascart" magnetograms from the Chambon-la-Foret (48 01'N and 02 16'E), rapid run and geomagnetic ULF recordings (5 to 1/300 Hz) from the Garchy observatory (47 18'N and 03 06'E) on magnetic tape and also on paper chart. The magnetic components H, D, Z, and the telluric components EW and NS are noted and the time accuracy is 50 ms.

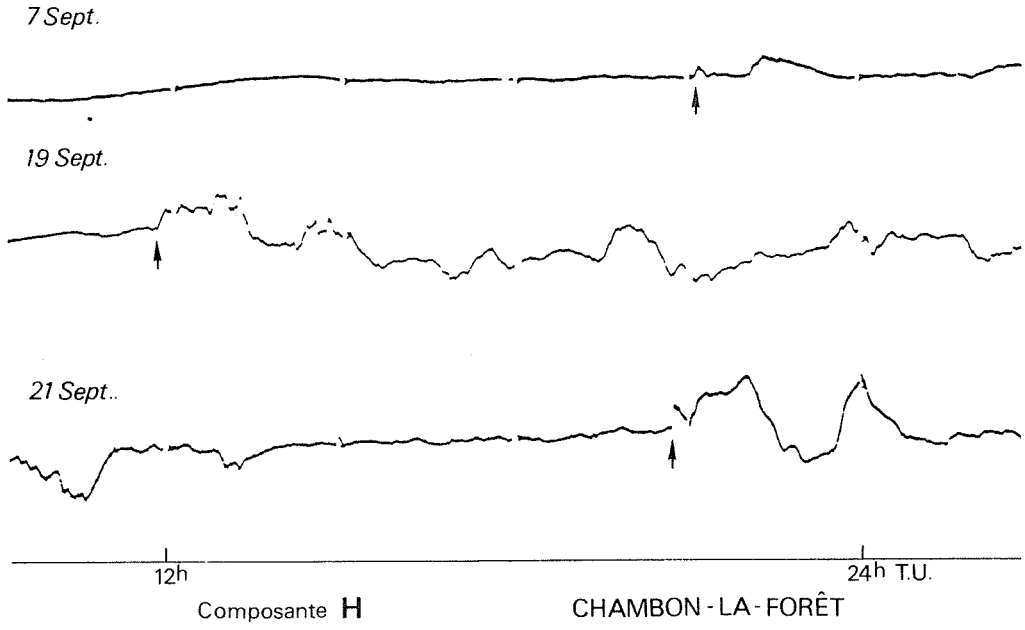

Fig. 1 "Mascart" H component at 10 mm/hour at Chambon-la-Forêt September 7, 19 and 21, 1977.

On Figure 1 have been assembled the Mascart-type recordings of the H component for September 7, 19 and 21. The original sensitivity for this component is 8.7 nT/mm, for a chart speed of 10 mm/h, and the direction of increase is toward the top of the page. We note the following:

September 7: The event classified as an "sfe" at Huancayo, beginning at 2110 UT and ending at 2120 UT (IAGA Bulletin), corresponds to a magnetic perturbation at Chambon-la-Forêt that looks like an sfe or a small bay, beginning at about 2113 UT ending near 2128 UT. The maximum deviation in H is 12 nT.

September 19: A small magnetic storm exists for most of the day at Chambon-la-Forêt. The record does not clearly define the exact time or amplitude of the SC as illustrated by the schematic representation of the H variation given in Figure 2. The commencement appears to be at "c", but it might also be an $SC(H)^{+-+}$-type with a commencement at "a". It is necessary to compare the exact shape of this SC registered on magnetograms from various latitudes and longitudes to be able to decide if this event is of the $SC(H)^{+}$-type (cd) or of the $SC(H)^{+-+}$-type (abcd).

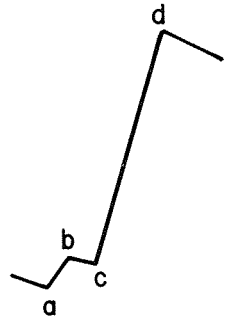

Fig. 2 Schematic representation of the H variation.

The amplitudes of this event recorded on the "La Cour" magnetograms are:

$\Delta H(ab) \cong +5nT \quad \Delta H(bc) \cong -2nT \quad \Delta H(cd) = +28nT \quad \Delta H(ad) = +31nT$

"a" is difficult to precisely define on the ULF recordings because it occurred during a weak general activity (pc 3). However, our estimate for "a" is 1141:40 UT and "c" occurred about 4 to 5 min later.

September 21: There is a small magnetic storm at Chambon-la-Forêt this day. From the ULF records the time of the commencement (SC) is 2045:30 UT ±2s in the H component (Figure 3). In D the SC cannot be determined as there is an inverse variation that had started about 1 min earlier. From our normal run records this extra movement does not seem to be connected with the SC but is a part of the weak magnetic activity already present.

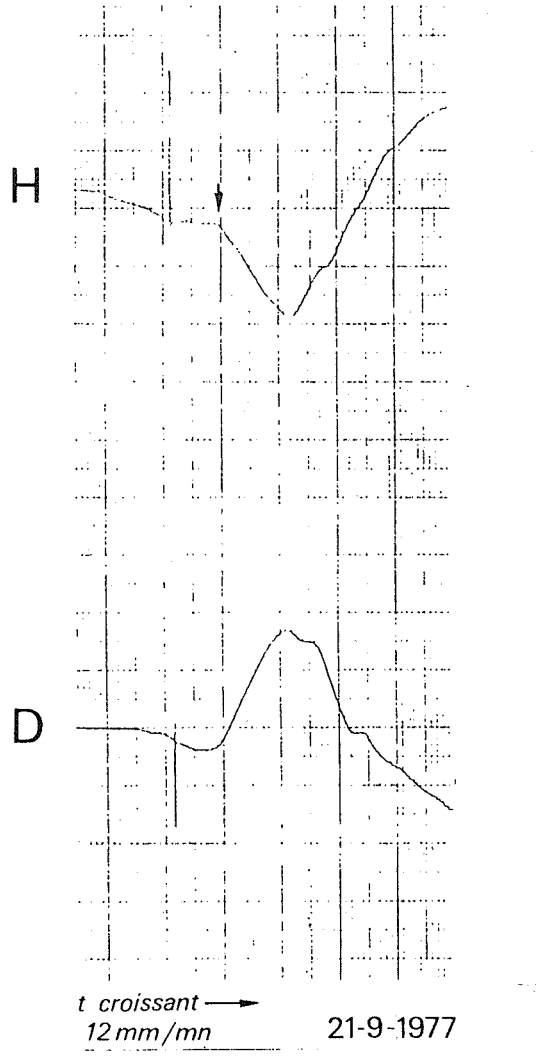

Fig. 3 Time of SC on September 21, 1977 from ULF record at Chambon-la-Forêt.

The amplitude of the SC is found to be + 33 nT in the H component, about -18 nT in D, accounting for the reverse movement we have mentioned above.

The ULF variations show the following:

Pc 1 activity

1) A series of emissions was recorded between September 15 at 2000 UT and September 16 at 0800 UT with a maximum intensity at 2330 UT, period of 1.5s and amplitude of 35 pT.

2) A series of emissions occurred between September 16 at 2030 UT and September 17 at 0400 UT with the maximum intensity at 0230 UT, period of 1.5s and amplitude of 200 pT.

3) A short emission was seen on September 24 at 2030 UT with a period of 2.1s and an amplitude of 25 pT. This event preceeds a series on September 25 between 0330 UT and 1500 UT with the maximum intensity at 0530 UT, period of 0.9s and amplitude of 125 pT.

Pc 3 activity: September 12, 17, 18 and 24 were especially quiet with sporadic pc 3's of small amplitude. But pc 3 of quality A, large amplitude, were recorded on the days following the two storms:

1) On the 20th, between 0348 UT and 0727 UT, with periods from 15 to 20s, and an amplitude up to 3.6 nT

2) On the 22nd, between 0614 UT and 1124 UT, with periods from 18 to 25s (dominant period was 20s) and an amplitude up to 8 nT

Pc 4 activity: No pc 4 activity of significant amplitude was recorded between September 7 and 24, 1977.

Pi 2 activity: Many pulsation trains were observed as usual with a great variety of periods. We have also observed some pi 1 activity of very short period associated with trains of pi 2, most notably on September 11 between 1750 UT and 1830 UT and on September 22 between 1800 UT and 1910 UT.

Pamatai Geomagnetic Observatory Data During the September 19-22, 1977 Event

by

H. G. Barsczus
Observatoire de Géophysique Pamatai
Centre ORSTOM
B.P. 529, Papeete/Tahiti, French Polynesia

Introduction

The Geomagnetic Observatory of Pamatai is located on the island of Tahiti, which lies in the Windward group of the Society Islands, and has geographic and geomagnetic coordinates as follows: (S17.57 E210.42) and (S15.35 E282.77). Standard geomagnetic data were obtained during the whole period under consideration from two sets of La Cour variometers (recording speed: 15 mm/hour; scale values; H = 2.09 and 2.52 nT/mm; D = 0.47 and 0.48 '/mm; Z = 1.90 and 3.00 nT/mm) as well as from micropulsation sensors (quick run recording speed = 6 mm/min and ultraquick run recording speed 60 = mm/min).

The Data

Standard microfilms of magnetograms are available through WDC-A for Solar-Terrestrial Physics or from the observatory. For copies of selected quick run records please send your enquiries to the observatory, because even though the quick run records show a large amount of interesting phenomena, they are not processed on a routine basis.

Table 1 presents K indices for the month of September 1977, Table 2 storm data, and Table 3 special events for the same period. Figures 1a and b show the onsets of magnetic storms from activity in McMath Region 14943 as recorded with the quick run system.

Table 1. Pamatai - September 1977 K Indices

Date (UT Day)	Three-Hour Indices K 1 2 3 4	5 6 7 8	Sum	Date (UT Day)	Three-Hour Indices K 1 2 3 4	5 6 7 8	Sum
01	0 0 1 1	1 1 0 0	04	16	1 1 1 1	1 1 1 1	08
02	1 1 0 1	2 2 2 2	11	17	0 1 3 1	1 1 1 0	08
03	2 3 1 1	1 1 1 0	10	18	1 1 1 1	1 0 0 1	06
04	1 1 2 2	0 1 1 1	09	19	1 1 1 3	4 3 4 3	20
05	1 0 0 1	0 0 1 0	03	20	4 4 4 3	3 3 2 3	26
06	0 0 1 1	1 0 0 1	04	21	2 4 5 5	2 2 3 6	29
07	0 1 1 1	0 0 1 2	06	22	4 4 4 4	2 3 4 2	27
08	2 2 3 1	1 1 1 2	13	23	1 1 1 2	3 3 2 1	14
09	1 1 1 2	3 1 2 1	12	24	1 2 2 2	1 1 0 1	10
10	0 1 1 4	3 0 0 0	09	25	1 1 2 2	1 0 2 1	10
11	2 2 2 3	2 1 2 1	15	26	0 1 3 3	2 3 2 4	18
12	1 1 1 0	0 0 0 2	05	27	2 3 4 3	1 0 1 1	15
13	1 1 2 4	3 2 2 1	16	28	1 1 2 3	1 1 1 0	10
14	2 1 0 0	0 1 1 0	05	29	0 0 1 0	0 0 1 1	03
15	1 2 3 3	1 0 1 0	11	30	0 1 0 2	2 0 0 0	05

Note: At Pamatai K=9 has a lower limit of 350 nT.

Table 2. Pamatai - Magnetic Storm Data from Normal Magnetogram

Date (1977)	Start (UT)	Type	SC Amplitudes D(')	H nT	Z nT	Maximum 3-Hour Index K Day (3-Hour Period)	K	Ranges D(')	H nT	Z nT	UT End Day	Hour
Sept. 19	1140	SC	- ?	+ 19	- 4	21 (3,4)	5	2.8	74	25		
21	2044	SC	?	+ 20	- 7	21 (8)	6	1.0	108	10	24	12

Table 3. Pamatai - Special Events from Normal Magnetogram

Date (1977)	Start (UT)	Type	End (UT)	Amplitudes D(')	H nT	Z nT	Remarks
Sept. 07	2110	SFE	2122	+0.1	+ 8	- 1	
08	2123	SFE ?	2132	?	- 3	+ ?	crochet
12	2112	SI		?	+12	?	D, Z calibration
14	0916?	SGE ?		?	+ 1	- 1	? very weak
26	2316	SI		-0.6	-19	+ 3 ?	

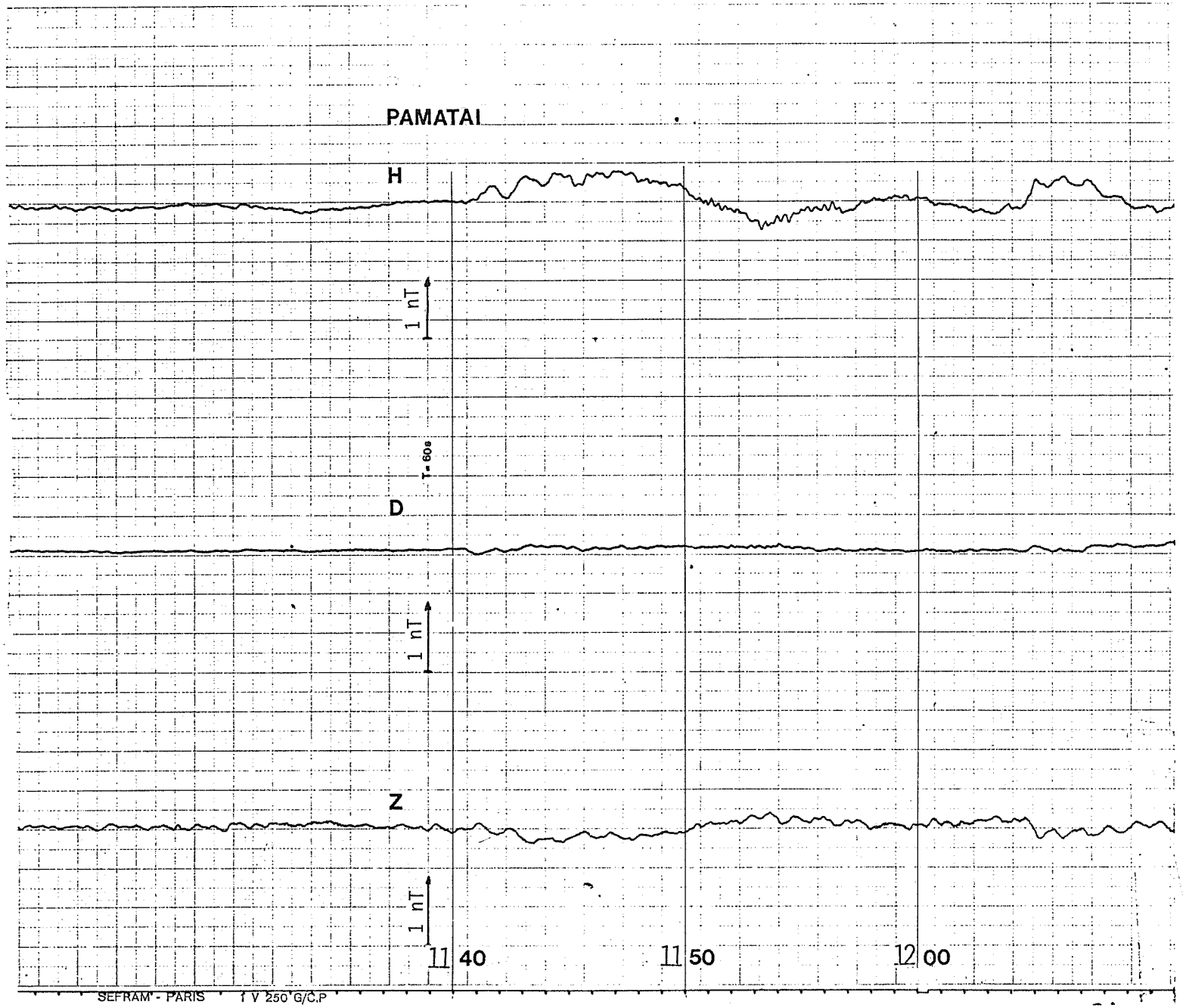

Fig. 1a. Portion of rapid run record (6mm/min) taken at Pamatai Geomagnetic Observatory on September 19, 1977. Heavy vertical lines mark 1140, 1150 and 1200 UT, and the storm begins about 1140 UT.

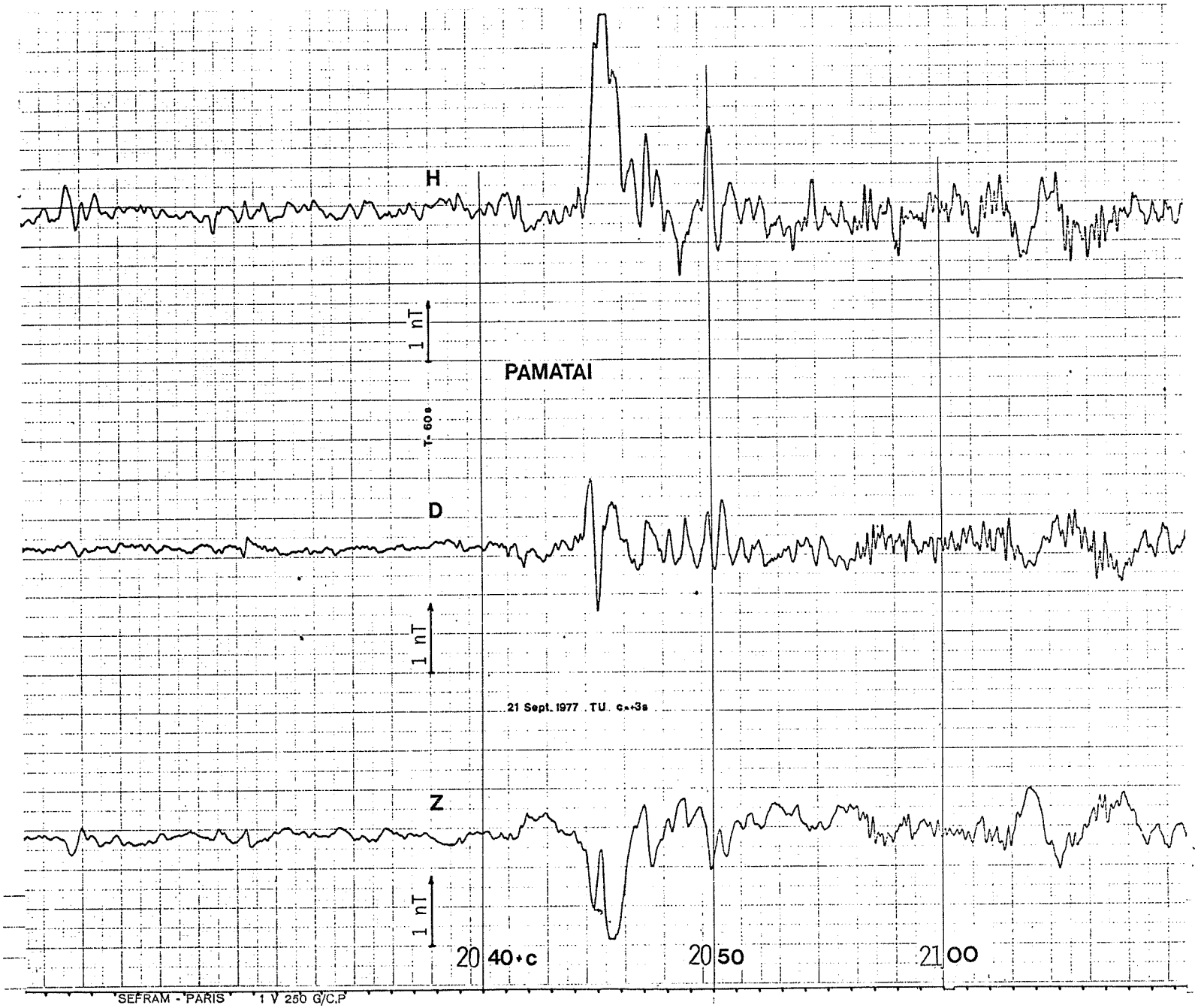

Fig. 1b. Portion of rapid run record (6mm/min) taken at Pamatai Geomagnetic Observatory on September 21, 1977. Heavy vertical lines mark 2040, 2050 and 2100 UT. The storm begins about 2044 UT.

Low Latitude and Equatorial Geomagnetic Field Variations during September 1977

by

G.K. Rangarajan
Indian Institute of Geomagnetism
Colaba, Bombay 400 005
India

The Indian Institute of Geomagnetism has under continuous operation, a network of 5 magnetic stations close to E75 and one near E92 longitude. A new magnetic observatory at Gulmarg, near the focus of Sq was commissioned on September 7, 1977; coinciding with the beginning of the special interval. Coordinates of these magnetic stations are listed in Table 1. The period September 7-24, 1977 did not include any of the five internationally quiet days of the month while all the five internationally disturbed days were confined to this period. Four consecutive days, September 19-22, had Ap values of more than 40. The lowest value of Ap was 6. The equatorial Dst was moderately negative between September 19-23 with largest value of -103 nT on Sept 22. While Ap, Dst and 3 hourly Kp showed large variations, the solar parameters Rz and flux at 2800 MHz did not exhibit large scale changes (see Solar-Geophysical Data, Prompt Report No. 399, Pt. I, November 1977).

Table 1. Station Coordinates

Station	Code	Geographic		Dipole		Type of variometer
		Latitude	Longitude	Latitude	Longitude	
Gulmarg	GLM	N 34°03'	E 74°24'	N 24.5°	147.2°	La Cour
Jaipur	JPR	N 26 55	E 75 48	N 17.3	147.4	Izmiran IV
Shillong	SHL	N 25 34	E 91 53	N 14.6	162.4	La Cour
Ujjain	UJN	N 23 11	E 75 47	N 13.4	147.0	Izmiran IV
Alibag	ALB	N 18 38	E 72 52	N 9.5	143.6	Izmiran II
Annamalainagar	ANR	N 11 22	E 79 41	N 1.4	149.4	Askania
Trivandrum	TRV	N 8 29	E 76.57	S 1.2	146.4	Izmiran II

During the interval, three distinct magnetic disturbances with sudden commencement were recorded at the Indian magnetic observatories. Statistics for the three storms are listed in Table 2. Reproductions of H-component magnetograms for two of the disturbances are given in Fig. 1 and Fig. 2. It is interesting to note that while at the two equatorial stations, TRV and ANR, the storm ranges in H for the three disturbances are nearly the same in magnitude (with slightly larger values for the storm commencing on September 19), the ranges are significantly different at other low latitude stations. In the Z and D variations, there appears to be no such distinction. For all the storms, the minimum field value in H was observed at local night hours and hence no equatorial enhancement was seen. The maximum field values were, however, near local noon for storms of September 12, and 21 and between 1700-1800 LT for that of September 19. The difference in storm ranges between low and equatorial latitudes suggests that the equatorial electrojet strength was significantly different on these occasions.

The rise-time of SSC was the least (only 3 min) for the September 21 storm and largest (about 9 min) for the preceding SSC of September 19. The rise-time for the September 12 SSC was about 6 min. The characteristics of the three SSCs are also different. The SSC shows a clean sharp rise in H on September 21, it is rather slow on September 19, and depicts a sequence of step-function-like rises on September 12. H-traces for these three SSCs as also that of two SIs during the disturbances, from the fluxgate magnetometer coupled to a continuous recorder (speed 100 mm/h) and a bandpass filter-unit with upper and lower cut-offs at 30 and 1100 sec, operational at Alibag, are shown in Fig. 3.

Following the SSC on September 12 there was no appreciable change in the magnetic field at low latitudes and even the (Sq + Jet) current signature was clearly evident at the equatorial stations. The main phase decrease commenced only after a lapse of more than 12 h. It was marked by significant bay events. The entire storm duration was characterized by 'low' noise.

In contrast, the September 19 storm had an initial phase of very short duration and the main phase decrease was quite rapid. After a significant minimum in the H component at 1650 UT, just 5 h after the SSC, a partial recovery was in progress. This was marked with moderate agitation of the field. However, before the completion of the recovery phase, further decrease of the field but with reduced 'noisy' component was seen. A second minimum of the field was registered at 1515 UT followed by positive bay events. After an interval of several hours during which field change was nominal, further decrease leading to another minimum at 1033 UT on September 21 set in.

Table 2. Details of Geomagnetic storms recorded at Indian Magnetic Stations.

Date 1977	Time UT Begin h m	End d h	Parameter		TRV	ANR	ALB	UJN	SHL	JPR	GLM
Sept. 12	21 13	14 11	SSC Amp.	D	-	-0.7	-0.4	-0.4	-0.4	-0.6	-0.6
				H	16	19	15	19	14	17	18
				Z	18	11	-4	-4	2	-3	-
			Range	D	4	5	6	7	7	8	9
				H	183	143	84	77	68	70	71
				Z	61	77	50	42	19	43	31
Sept. 19	11 38	21 15	SSC Amp.	D	-	-0.8	-0.3	-0.1	-0.4	-0.2	-0.2
				H	24	30	24	32	25	27	25
				Z	29	21	-4	-7	2	-5	-
			Range	D	5	5	7	8	7	9	9
				H	194	176	160	182	160	172	172
				Z	115	77	49	50	33	50	62
Sept. 21	20 43	24 04	SSC Amp.	D	-	-1.1	-0.7	-0.6	-0.4	-1.1	-0.9
				H	23	25	20	26	18	22	25
				Z	27	14	-6	-6	4	-7	-3
			Range	D	5	5	7	7	6	8	9
				H	168	138	101	124	93	104	119
				Z	100	88	45	37	31	40	32

Before the field associated with the September 19 disturbance could regain the pre-storm level, the third SSC was recorded at 2043 UT on September 21. This magnetic disturbance was also characterized by prolonged initial phase and absence of a marked main phase. A positive bay of large amplitude was recorded on September 22 at all the Indian stations between 1530 and 1645 UT. Even though a distinct main phase decrease was absent, fluctuations in the field level continued almost until the end of September 23.

In Table 3 are listed the details of several bay events recorded during this interval. While variation in Z (with larger amplitudes) during the course of a bay was usually prominent at Trivandrum and noticeable at Annamalainagar (with less amplitude compared to H) they are absent on the low-latitude magnetograms. Maximum change in H during the bay events appears to be recorded at Gulmarg and Ujjain and the lowest values at Alibag. H records for a typical bay of the Indian stations during disturbance is shown in Fig. 4.

Table 3. Details of Significant positive bays recorded at Indian magnetic stations.

Date 1977	Time UT Begin	Max	Amplitude* (in nT) TRV H	TRV D	ANR H	ANR D	ALB H	UJN H	SHL H	JPR H	GLM H
Sept. 11	1751	1212	22	24	28	16	23	29	28	26	-
Sept. 13	1600	1706	47	46	54	28	52	64	54	60	66
Sept. 21	1651	1736	43	32	47	20	44	52	47	49	55
	2021	2045	31	34	34	18	33	39	34	35	38
Sept. 22	1524	1601	58	73	69	41	61	78	69	69	78
	1939	2016	39	40	43	18	42	49	43	45	51
Sept. 23	1339	1403	31	40	40	26	33	44	40	39	45
	1533	1558	31	34	37	20	33	41	37	37	41

*Amplitude calculated as the range (Maximum-Beginning)

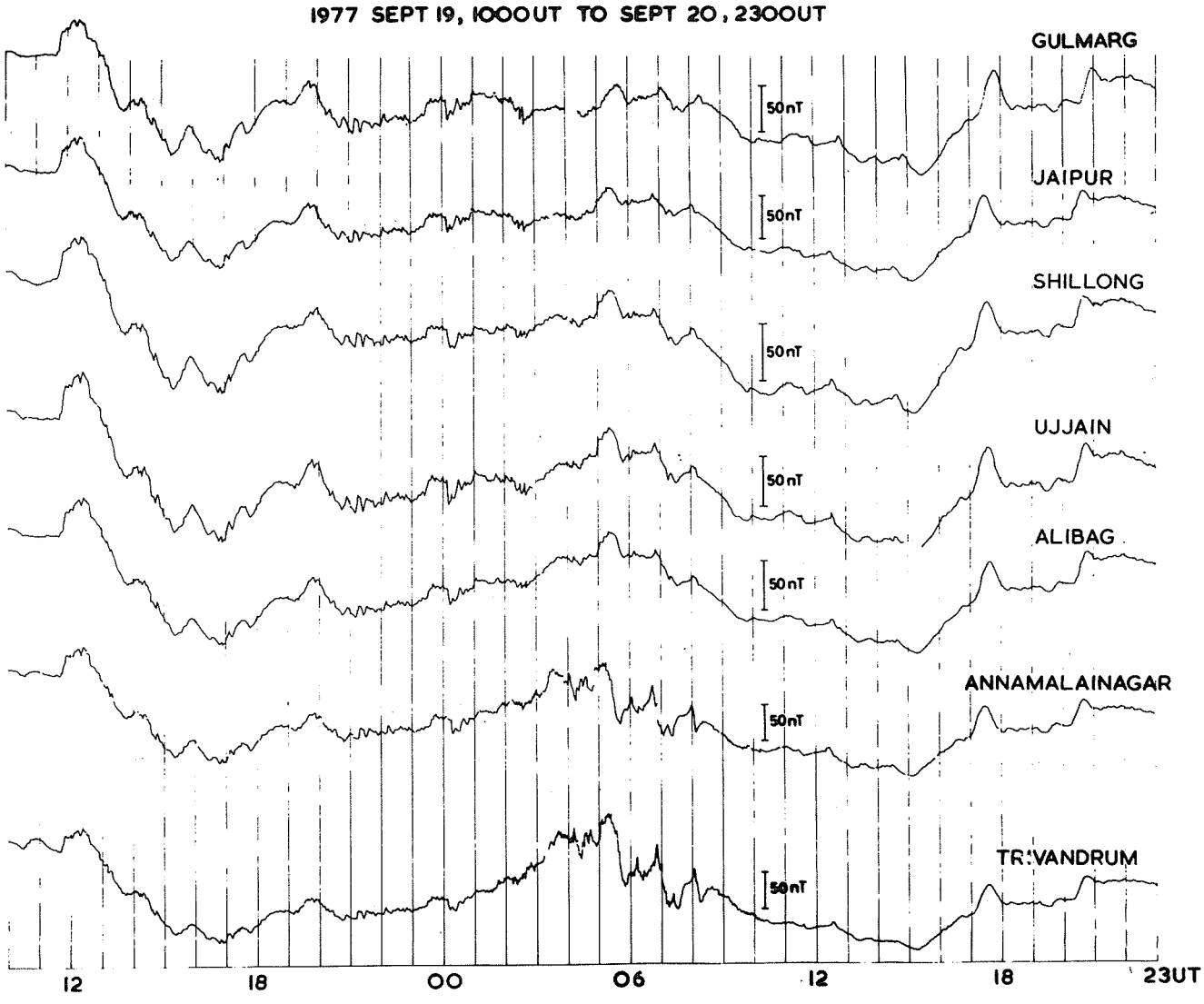

Fig. 1: H-component at Indian chain of geomagnetic observatories, Sept. 19 - 20, 1977

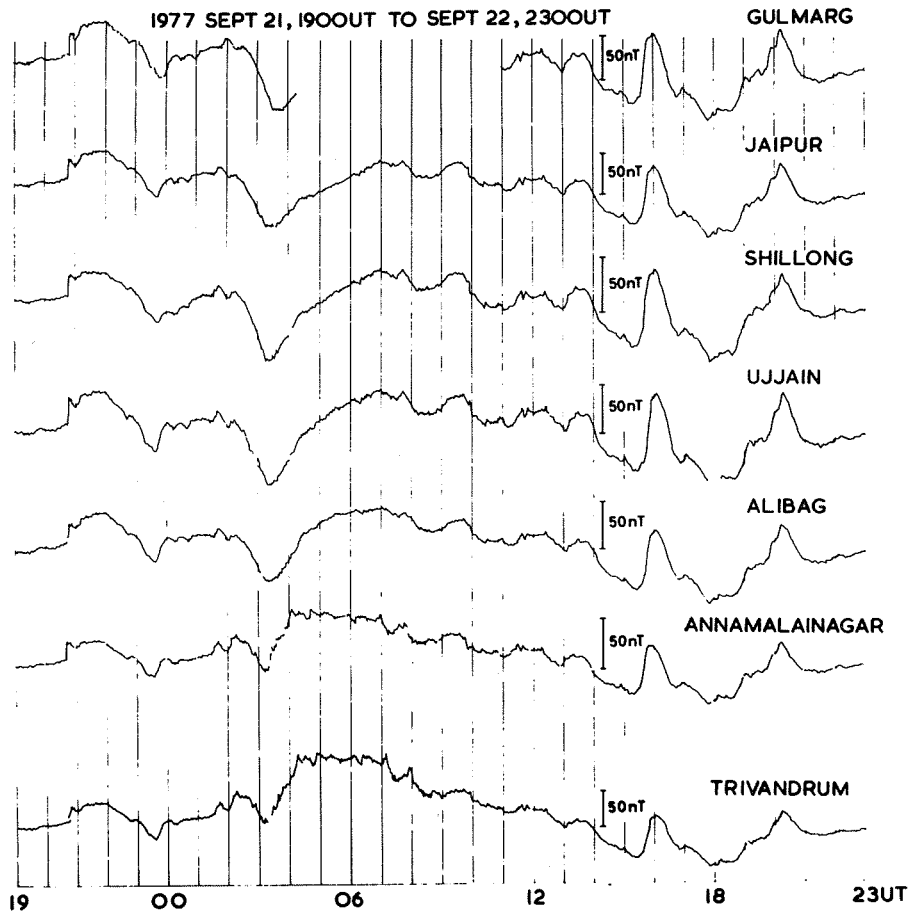

Fig. 2: H-component at Indian chain of geomagnetic observatories Sept. 21 - 22, 1977

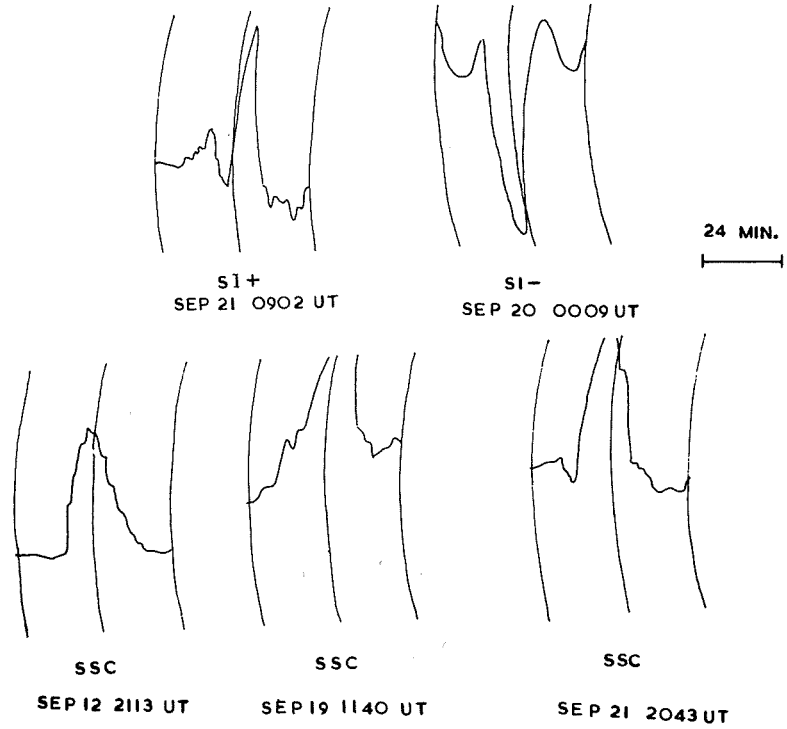

Fig. 3: Sudden commencements at Alibag, Sept. 12, 19, 20 and 21, 1977

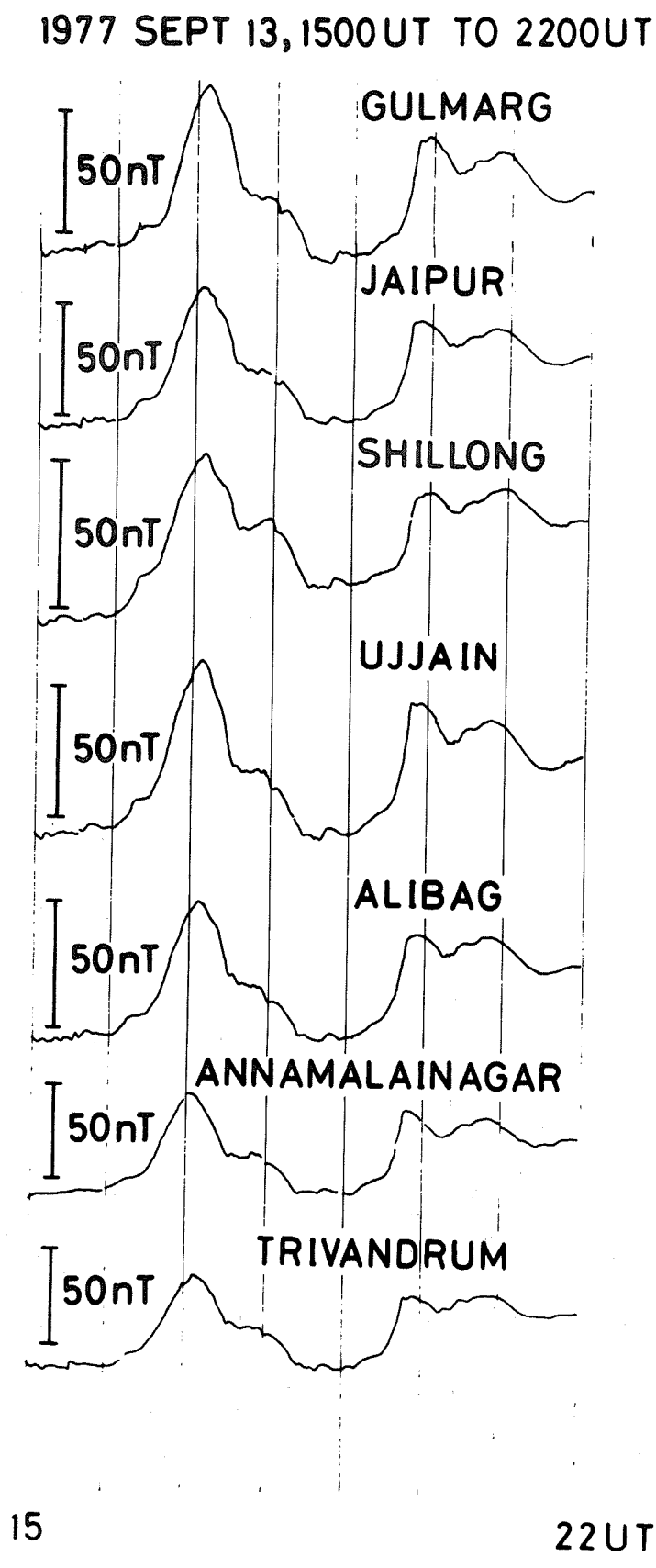

Fig. 4: Typical bay on H-component at Indian chain of geomagnetic observatories, Sept. 13, 1977

Ground Observations of Geomagnetic Activity at Equatorial Observatory, Etaiyapuram (INDIA) during September 7-24, 1977 and November 1977

by

T.S. Sastry
National Geophysical Research Institute
Hyderabad - 500007, India

Introduction

This station, established under Indo-Soviet collaboration, is in the close vicinity (Geomag. Lat: 0.6°) of Dip Equator in India and has been in continuous operation since mid-October 1975. The equipment is of the induction type, recording magnetic field variations photographically at two speeds of recording viz., 30mm/min. and 90mm/nr. to cover the period range of all the classes of pulsations excluding that of Pc 6 (which are seen only on rare occasions). The station, in addition, is supplemented with the conventional LaCour magnetic setup to record longer period variations in the three components H, D & Z of the Earth's magnetic field.

Observational data

The data on magnetic storms recorded at this station are given in Table 1. and the pulsation activity observed is depicted in the accompanying Figure 1. In this Figure 1 the pulsation activity on each day is represented in the form of bands for Pc3, Pc4, Pc5, Pi1 and Pi2 in that vertical order, for

Table 1

Commencement				SC Amplitude			Range of Main Phase			End	
Date	UT h	m	Type	H(α)	D(')	Z(α)	H(α)	D(')	Z(α)	UT d	h
Sep. 12	21	12	SC	14	+0.1	--	185	2	--	13	22
Sep. 19	11	39	SC	19	0.1	--	190	2	--	21	15
Sep. 21	20	43	SC	17	0.2	--	167	3	--	22	23

the duration over which the activity exists in each class of pulsations. The activity is qualified 'Moderate', 'Good' and 'Very good' to describe the intensity of activity depending on the amplitudes of pulsations as well as their defined nature.

It may be seen from the above table that the storms that occurred during this period are only of moderate intensity in respect to storm range, as well as the intensity of disturbance during different phases of the storm. It is also seen from a general scrutiny of the LaCour records and Figure 1 on pulsation activity that there is a higher level of magnetic activity during the second half of this interval when the McMath plage region 14943 is on the western limb of the solar disk.

The only storm before the CMP of this plage region viz., that of September 12 is of lesser intensity with no marked disturbance during the course of the storm; the pulsation activity is also generally low. In contrast, the storms of September 19 and 21 exhibit considerable pulsation activity with larger amplitude Pc5 and Pc3 pulsations occurring concurrently. The SC at 1139 UT on September 19 is preceded by a bay-like event on the magnetogram occurring around 1020 UT corresponding to which there appears a damped type event with a period of 600 sec. It is also seen from the pulsation records that the initial impulse in the case of SC on September 19 is 90 sec period with simultaneous triggering of longer period (500-600 sec) Pc5 pulsations which continue (with comparatively less periods) into the night hours. In the case of the SC at 2043 UT on September 21 the initial impulse is of damped type with period of 240 sec, followed by Pc5 pulsations of longer period, and intense activity of short-period (15-20 sec) Pc3 pulsations lasting until 0100 UT (0630 LT).

Among the two GLEs in the cosmic ray neutron monitor events reported for Alert on September 19 and 24 magnetic activity is seen only in the case of former while in case of later event the magnetic activity both in long-period variations and in pulsations is comparatively low.

No significant event was observed in geomagnetic activity at the time of November 22 GLE.

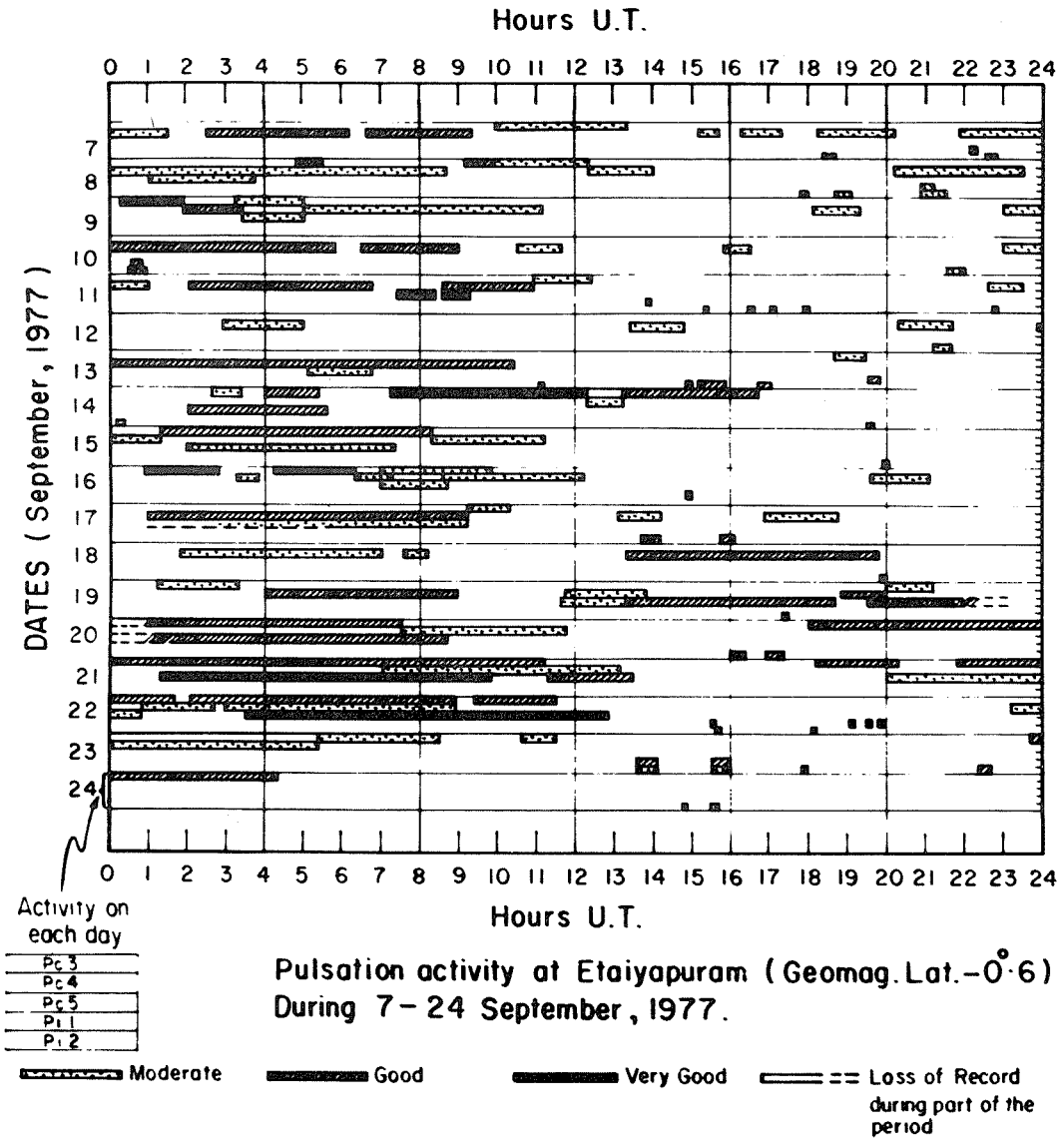

Pulsation activity at Etaiyapuram (Geomag. Lat. $-0^{\circ}\cdot6$)
During 7 – 24 September, 1977.

Geomagnetic Observations at Hyderabad for the September and November 1977 Events

by

B.J. Srivastava
National Geophysical Research Institute
Hyderabad-500007, India

Introduction

The purpose of this note is to examine and discuss the geomagnetic activity recorded at Hyderabad for the solar and cosmic ray events observed in September 1977 associated with McMath plage region 14943 and on November 22, 1977, around 1300 UT associated with McMath plage region 15031. The Hyderabad Magnetic Observatory (Geomag. Coords. 7.6 N and 149.2 E) of NGRI is recognized as an international low-latitude key station by IAGA. It is located outside the influence of the equatorial electrojet and the records are free from oceanic induction effects, the station being sufficiently inland.

The Data

The reduced data for the magnetic storms recorded at Hyderabad in September 1977 are given in Table 1, the K and C indices of geomagnetic activity in Table 2, and the rapid magnetic variations (SFEs, SIs and bays) in Table 3. The K and C indices for November 22 through 24, 1977, are also included in Table 2 to show the magnetic conditions following the solar and cosmic ray event of November 22 (2B solar flare 0945-1105 UT, reported by Haute Provence).

TABLE 1. Magnetic Storms Recorded at Hyderabad in September 1977

DATE	COMMENCEMENT			SC AMPLITUDES			MAXIMUM 3-HOUR K INDEX			RANGES			UT END	
1977	Day	UT	Type	D(')	H(nT)	Z(nT)	Day	(3-hour period)	K	D(')	H(nT)	Z(nT)	Day	Hour
September	02	12 30	..				02 03	(5,6) (1,2)	3	5	46	19	03	17
	07	21 10	SC	-0.2	+6	-1	08 09	(1,2) (4,5,7)	3	7	83	35	09	21
	12	21 13	SC	-0.3	+16	-1	13	(6,7)	5	6	103	43	14	06
	19	11 40	SC	-0.1	+27	-1	19	(5)	7	7	188	32	21	15
	21	20 43	SC	-0.5	+18	-2	22	(6,7)	6	6	122	28	23	23
	26	07 32	SC	0	+6	0	26	(6,8)	4	6	103	41	27	14

Discussion

Of the six magnetic storms recorded in September 1977 (Table 1), two were of moderate intensity (September 19 and 21), H-ranges being less than 200 nT, and the rest of only slight intensity. Geomagnetically, the most active period was from September 19 through the end of September 23. These storms show oscillations of about an hour duration and pulsations with periods of 5-10 min (Fig. 1). The different phases of the storms are not well defined.

TABLE 2. K and C Indices of Geomagnetic Activity at Hyderabad
September 1977/November 1977

Scale values of variometers in nT/mm D 3.5, H 4.5, Z 4.0
Range for K9=300nT

September 1977

UT Day	K - Indices		Sum	C
1	1121	2111	10	0
2	1111	3322	14	1
3	3322	1101	13	1
4	1122	1111	10	0
5	1111	1011	7	0
6	0111	1112	8	0
7	1211	0122	10	1
8	3132	2112	15	1
9	2223	3231	18	1
10	3113	3133	18	1
11	2223	3232	19	1
12	1110	0013	7	1
13	2124	4553	26	1
14	2211	1221	12	0
15	1331	1111	11	0
16	1212	2232	15	1
17	1221	1311	12	0
18	2221	1111	11	0
19	1114	7654	29	1
20	3443	4653	32	1
21	3446	4245	32	1
22	4533	4662	33	1
23	2112	4544	23	1
24	1111	1213	11	0
25	2112	1132	13	0
26	1223	3424	21	1
27	4323	1111	16	1
28	1122	3421	16	1
29	0111	1111	7	0
30	1112	2211	11	0

November 1977

22	1111	1111	8	0
23	1111	1111	8	0
24	1011	1201	7	0

TABLE 3. Rapid Events (SFEs, SIs and Bays) Recorded at Hyderabad in September 1977

Date	UT of Beginning	UT of Ending	Amplitudes D	H	Z	Type
SFEs 1977 September 19	1030	1115	-0.6	0	-3	
SIs 1977 September 02	1716	1722	+0.3	-13	+1	
03	0503	0509	-0.2	+14	-2	
20	0008	0011	+0.8	-18	+1	
26	2315	2320	+0.5	-23	+1	
Bays 1977 September 07	1835	1910	-0.1	+5	0	bp
11	1751	1900	-0.6	+23	+2	bsp
13	1630	1740	-0.9	+41	+3	b
20	1700	1810	-0.8	+38	+3	b
22	1535	1650	-0.9	+17	+4	bsp
23	1335	1440	-0.5	+32	+2	bp
23	1525	1700	-0.6	+39	+3	b
28	1510	1615	-0.7	+21	+2	bp

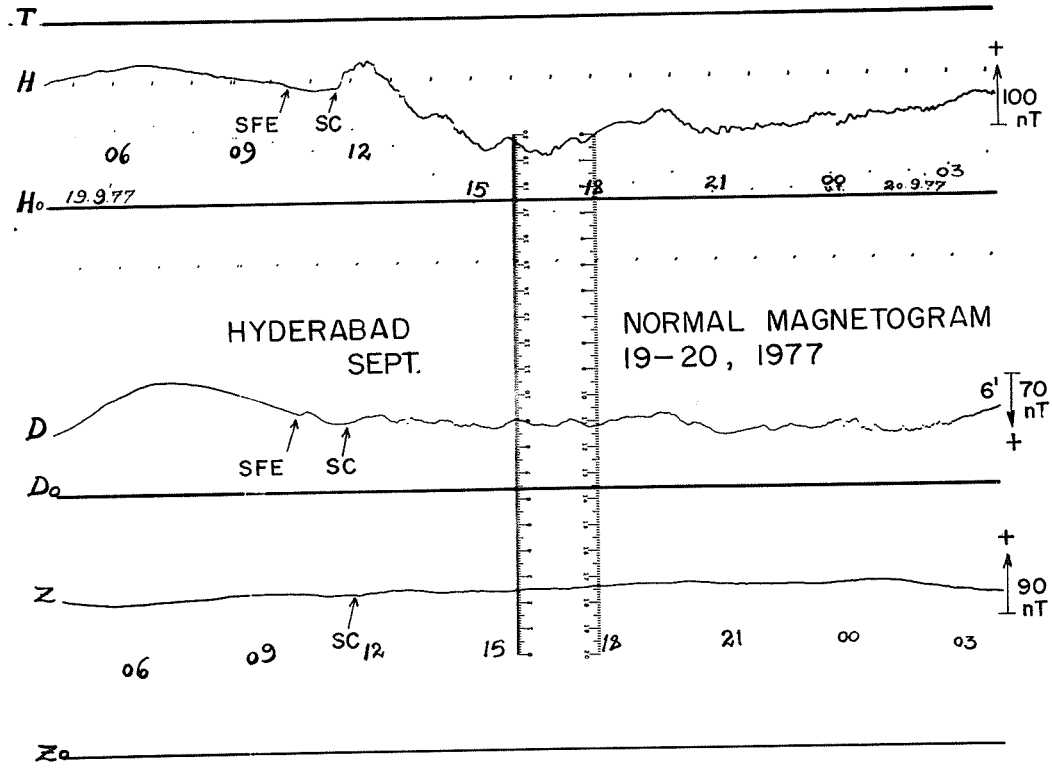

Fig. 1. Standard magnetogram (H, D and Z components) recorded at Hyderabad on September 19-20, 1977, showing the SFE and the SC-storm of moderate intensity.

For the H_α solar flares reported for September 1977, just one solar flare effect (geomagnetic crochet) was clearly observed at Hyderabad and occurred on Septemer 19 at 1030 UT (Fig. 1) following the flare of importance 3B reported by the Ramey Observatory. This was followed by an SC-storm on September 21. The solar flare and cosmic ray event of September 24 was followed by an SC-storm on September 26 (Table 1).

Another interesting geomagnetic phenomenon observed was that of the recurrent bays recorded on the nights of September 22 and 23 when three consecutive bays were recorded between 1300 and 2100 UT. These bays also resembled the three bays recorded on September 13 between 1300 and 2100 UT.. Such events could be generated night after night due to the injection of charged particles into the auroral zone atmosphere from the same active source in the trapped region of the magneto-tail.[Chapman and Bartels, 1940; Srivastava and Habiba Abbas, 1975].

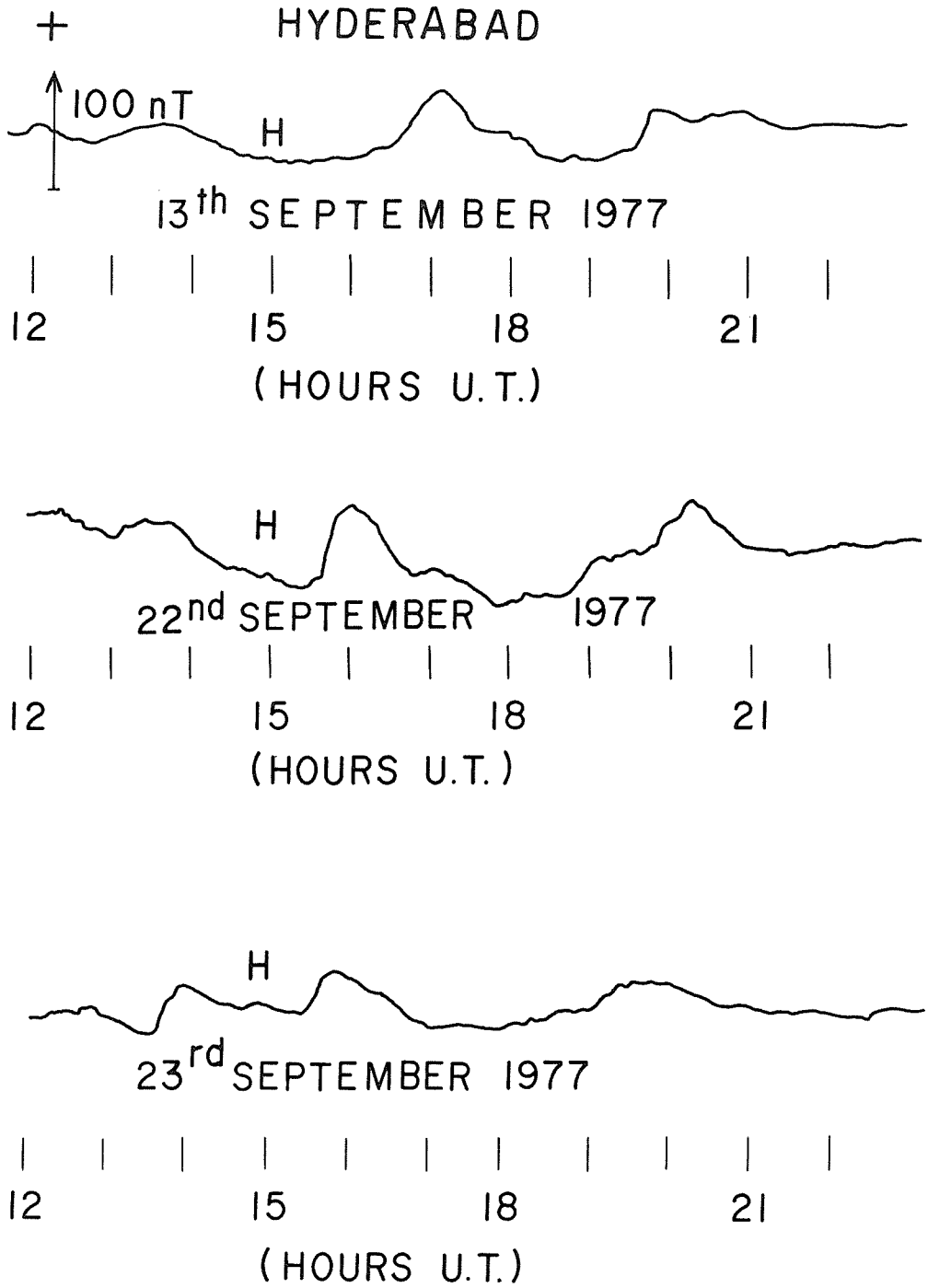

Fig. 2. H-records of the recurrent geomagnetic bays taken at Hyderabad on September 13, 22 and 23, 1977, during night hours.

The solar flare (2B) and cosmic ray event of November 22, 1977 (0945-1300 UT) produced no geomagnetic effect observed at Hyderabad on November 22, 23 or 24. All three days were quiet ones. An SC-storm of moderate intensity did occur on November 25 at 1224 UT, with a range of 123 nT in H.

Acknowledgments

I am grateful to the Director, National Geophysical Research Institute, Hyderabad, for permission to publish this note. I am also indebted to my colleagues at the Hyderabad Geomagnetic Observatory for assistance in compiling the data.

REFERENCES

CHAPMAN, S. and J. BARTELS 1940 *Geomagnetism, Vol. 1*, Clarendon Press, Oxford, p.341.

SRIVASTAVA, B.J. and HABIBA ABBAS 1975 Characteristics of magnetic bays at Hyderabad, *Proc. Symp. Equat. Geomag. Phen.*, May 1975, Bombay, 153-160.

High-Time-Resolution Study of the September 21, 1977, Sudden Commencement Using AFGL Magnetometer Data

by

P.F. Fougere
Air Force Geophysics Laboratory
Hanscom AFB, MA 01731

Introduction

In this paper the data of Knecht, Hutchinson, and Tsacoyeanes from the Air Force Geophysics Laboratory (AFGL) magnetometer network are used to study the sudden commencement of Sept. 21, 1977. The network consists of seven stations producing digital information that is returned to a central collection point at AFGL in Bedford, Mass. There are five northern stations at about 55° corrected geomagnetic latitude (CGL), and they are roughly equally spaced across the country. From west to east they are in the States of Washington (WA), South Dakota (SD), Wisconsin (WI), Michigan (MI), and Massachusetts (MA). There are also two southern stations at about 40° CGL, in California (CA) and Florida (FL), but the CA station had not been completed by September 1977. The WI station was inoperative on September 21.

Each station has identical instrumentation: a fluxgate magnetometer measuring the X, Y, and Z components once each second and a coil system measuring $\dot{X}$, $\dot{Y}$, and $\dot{Z}$ five times each second ($\dot{X} = dX/dt$). The Z component points down vertically; X lies along a magnetic meridian pointing north; and Y is orthogonal to X and Z, measuring essentially the D element.

Results

Figure 1 shows an ssc on Sept. 21, 1977, at about 2040 UT. Five stations are superposed. In the X component (bottom panel) there is a sudden decrease followed by a much larger sudden increase. The Y component shows a small increase followed by a large decrease. On this time scale, the X and Y components show nearly simultaneous deflections.

Figure 2 zooms in on the same event in a slightly different format. Each panel shows a different station as indicated by the character code on the right side. The X component is plotted as a dotted line. Each point is a 1-s observation. Also shown is the $\dot{X}$ component as a solid line (actually, 5 points/s are plotted). By concentrating attention on the northern stations WA, SD, MI, and MA, it is evident that the disturbance depicted is traveling across the country from west to east in the sequence WA, SD, MI, and MA. The numbers along the left-hand axis and following the word "nanotesla" represent the scale factors for X and $\dot{X}$, respectively. Thus, the distance between tick marks is 23 nT and 258 units. At WA the ΔX between the minimum and maximum is over 50 nT. Notice, too, that X takes on an extreme value whenever $\dot{X}$ passes through zero. This verifies that the zero for $\dot{X}$ has been chosen correctly. Note that the disturbance is sharpest at WA and flattens and attenuates as it moves east.

Figure 3 shows Y and $\dot{Y}$ in an identical format for the same event. In this case, the disturbance in Y is smaller than that in X, and the figure has scale factors of 12 nT for Y and 211 units for $\dot{Y}$. Here again the disturbance is traveling from west to east and flattening and decaying as it goes, in agreement with the corresponding results for X.

This particular ssc was produced by a very large solar flare of class 3b at N08 W57 that began about 1026 UT on Sept. 19, 1977, within McMath plage region 14943 (L = 197). The associated ssc began at 2045 UT on Sept. 21, 1977, after a delay of approximately 58.32 h. Thus, the flare-associated shock wave traveled with an average speed of (1.5×10^8 km/58.32 x 3600 s) or 714 km/s.

Figure 4 shows the location of the stations in a plot looking down on the ecliptic plane over the North Pole. Noon is at the top and 1800 UT is on the left. It is the dusk side. If the disturbance sweeps across the Earth from the Sun, we might expect the stations to respond in the order of their distance from the subsolar point, that is, in the sequence WA, SD, FL, MI, and MA. The easterly direction of motion reflects exactly what was observed.

Acknowledgments

Construction and operation of the AFGL magnetometer network has been under the direction of David J. Knecht, Charles W. Tsacoyeanes, and Robert O. Hutchinson. Their cooperation is gratefully acknowledged.

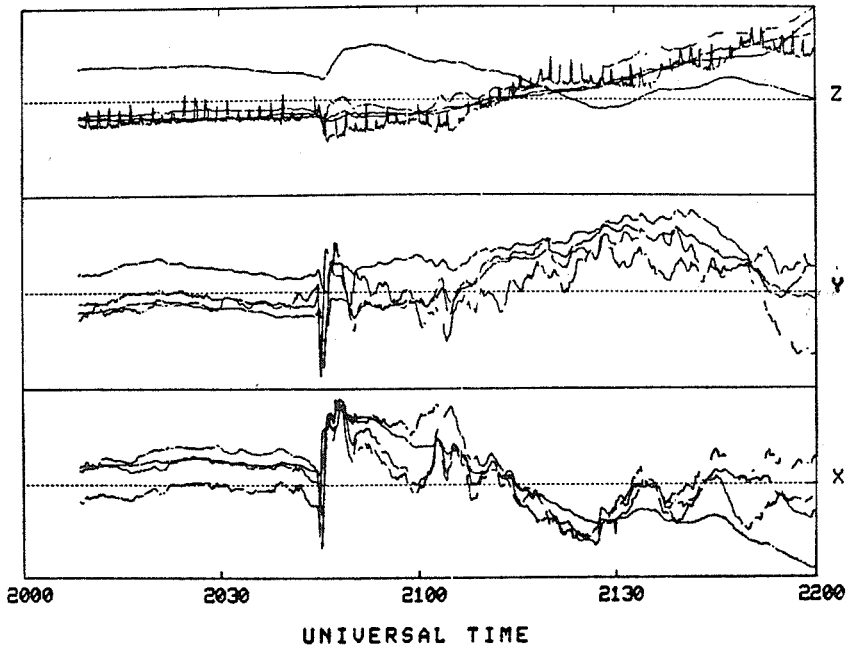

Fig. 1. The ssc of Sept. 21, 1977, as observed by AFGL magnetometers located in Washington, South Dakota, Florida, Michigan, and Massachusetts.

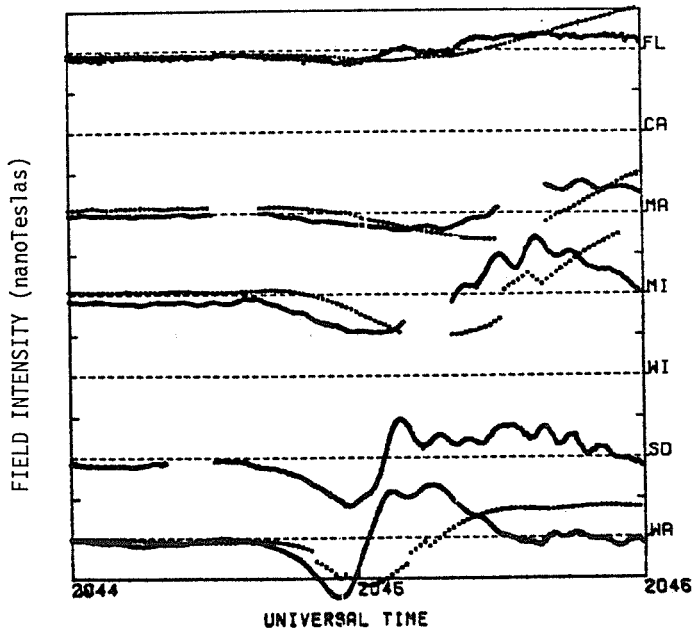

Fig. 2. The X (dotted lines) and $\dot{X}$ (solid lines) components at a greater time resolution than that given in Figure 1 for each of the five operating stations during the ssc of Sept. 21, 1977. See text for key to 2-letter station codes. The distance between tick marks is 23 nT and 258 units for X and $\dot{X}$, respectively.

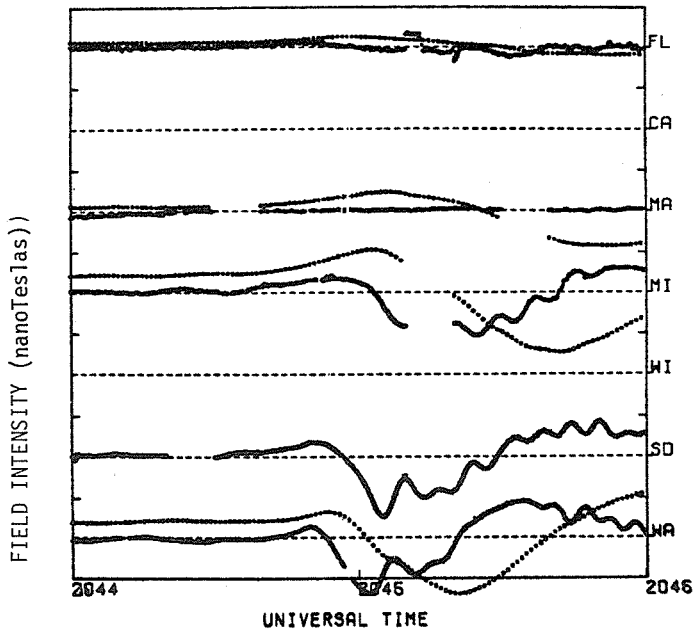

Fig. 3. The Y (dotted lines) and $\hat{Y}$ (solid lines) components at a greater time resolution than that given in Figure 1 for each of the five operating stations during the ssc of Sept. 21, 1977. See text for key to 2-letter station codes. The distance between tick marks is 12 nT and 211 units for Y and $\hat{Y}$, respectively.

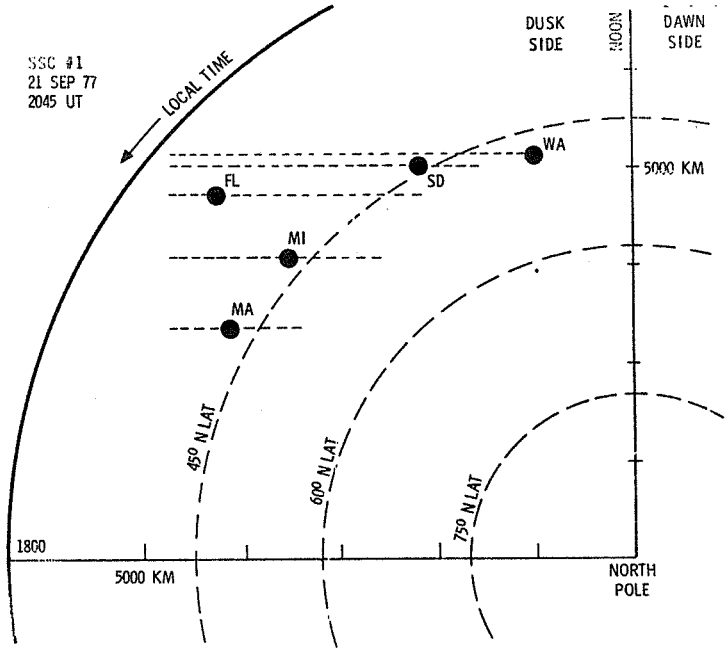

Fig. 4. Locations of operating magnetometer stations in the AFGL network. View is from the north geographic pole. For the local times shown, a disturbance sweeping over Earth would be detected initially by the station in the State of Washington, then by the South Dakota site, and finally by the instrument in Massachusetts.

Responses of Tropospheric Circulation Patterns to Solar Events of 7-24 September 1977, and 22 November 1977

by

Roger H. Olson
Aspen Institute
Boulder, Colorado 80302

Introduction

We have found, in solar cycles 18, 19, and 20 that large and active solar calcium plages affect the Northern Hemispheric circulation in the Earth's troposphere (500 millibars) in at least two ways. First, as the plage crosses central meridian, the vorticity area index (VA1) rises to values 10-15 percent above background for a few days centered on CMP date. The VA1 is a measure of the magnitude of cyclonic activity integrated over the Northern Hemisphere. Second, with the onset of geomagnetic activity, which normally follows CMP by a few days, there is a marked minimum in VA1, centered perhaps 4-5 days after CMP. These results have been described in a paper which has been submitted for publication [Olson et al., 1978]. It was also found that the plages whose CMP dates were accompanied by maxima in Ottawa 10.7 cm radio flux were most effective in producing weather changes. The two events described in the present paper each had at least a slight maximum in Ottawa flux at about CMP date of the appropriate plage. However, the geomagnetic responses were weak.

Procedure

As of the date of preparing this report (24 April 1978), the computation of the VA1 for the appropriate dates had not been completed. However, Woodbridge [Woodbridge et al., 1959] found that a good estimate of the strength of cyclonic activity could be obtained by simply measuring the length of contour lines on a constant pressure map. If the flow is zonal, the contours tend to be short. If the flow is more meridional, the cyclones (and anticyclones) are more pronounced and the contours are longer. In the present study, we used Northern Hemisphere maps at 500 mbs. Measurements were made of all contours which could be traced continuously around the hemisphere. Generally the southernmost such contour was at about 30° N and the northernmost at about 70° N. It was possible to measure 9 such contours for the September case and 11 for the November case. The lengths of the 9 or 11 contours were measured and summed each day, and that is the parameter plotted in Figures 1 and 2. We also plot, for each case, the Ottawa 10.7 cm solar radio flux each day. We plot the data from 10 days before to 15 days after the CMP date of the appropriate calcium plage. The map set used for this analysis contained a few gaps; hence there are some missing days in the contour data. The McMath region plage numbers were 14943 and 15031.

Results

Both cases show some interesting results which are consistent with what we have found in our comparison of VA1 with plage dates. In the 4-5 day period just prior to CMP day, the contour lengths increase by 20-25 percent, analogous to the increase in VA1 previously mentioned. However, the minimum in VA1 following CMP does not seem to be reflected in these data. Perhaps this is a result of the fact that geomagnetic activity was not well developed in these two cases. Note that in the November case the contour length and the Ottawa flux are both rising rapidly towards the end of the period of study. Thus, we can tentatively conclude from this study that the relationships between solar activity and weather previously discovered will probably continue to be found in cycle 21.

REFERENCES

OLSON, R.H., W.O. ROBERTS, H.D. PRINCE and E.R. HEDEMAN — 1978 — Solar Plages and Vorticity of the Earth's Atmosphere, *Nature*, 141.

WOODBRIDGE, D., N.J. MAC DONALD and T. POHRTE — 1959 — Geomagnetic Disturbances and Atmospheric Circulation, *JGR, 64,* 333.

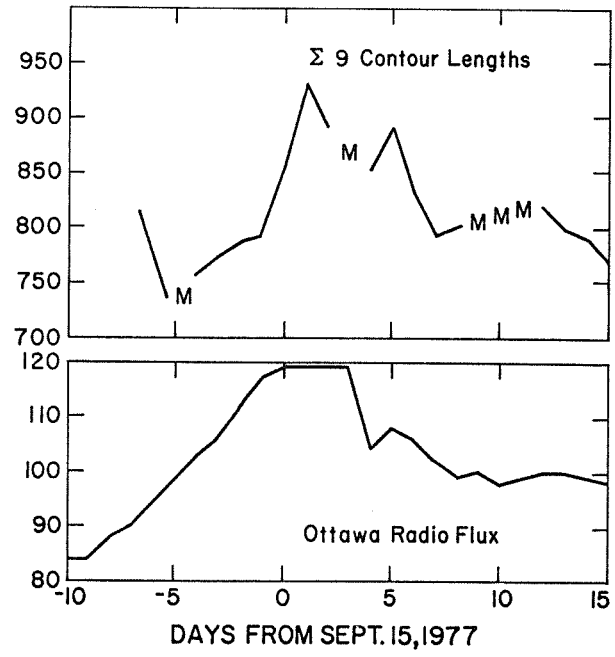

Fig. 1. Top curve shows the daily value of the summed lengths of the contour lines on a 500-mb chart that could be traced continuously around the Northern Hemisphere. Units are centimeters measured on a map with a scale of approximately 1:32,000,000. Bottom curve shows the daily radio flux (10.7 cm) as measured at Ottawa. Both curves are shown with 0- date equal to 15 September 1977.

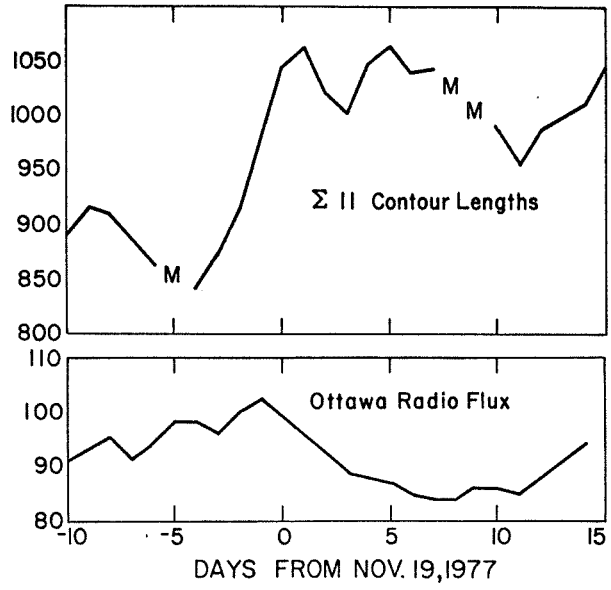

Fig. 2. Same as Figure 1, with 0-date equal to 19 November 1977.

1. SOLAR REGION OF NOVEMBER 22, 1977

Extracted from "The Rise, Decline and Possible Relationship between Two Proton Flare Producing Regions including Details of the Activity Patterns of their known Antecedent and Descendent Plages", Proceedings of the STIP Symposium in Australia on Solar Radio Astronomy, Interplanetary Scintillations and Co-ordination with Spacecraft, November 1979 (In press).

by

Susan McKenna-Lawlor
Physics Department, St. Patrick's College
Maynooth, County Kildare, Ireland

In order to summarize the waxings and wanings of activity within transiting plages rotation by rotation, an "activity profile" was prepared for each transit described which shows, in tabular form, the day-by-day evoluation, as monitored in calcium light, of the plage concerned, as well as information concerning variations in the field strength, area, spot count and magnetic classification of its underlying spot group. The frequency, with respect to class, of any observed flares is also given and the numbers of SIDs, X-ray bursts and single frequency and dynamic radio events attending the flares mentioned are listed.

For convenience, those anomalous locations within the solar atmosphere in which the proton flares of November 1977 and April-May 1978 developed will hereafter be referred to as Active Regions I and II.

Sources and kinds of solar data analyzed

The experimental data used were taken primarily from the monthly publication "Solar-Geophysical Data" compiled by the National Geophysical and Solar-Terrestrial Data Center, Boulder, Co, U.S.A. Errata or revisions to primary data sets which appear in these Bulletins from time-to-time are incorporated without comment into the material presented.

Flare data were taken from the SGD "Comprehensive Reports". Flare importance is generally deemed to be that assigned in the associated summary "Group Reports" but, in individual cases where no importance rating was originally ascribed, a suggested importance, based on such flare parameters as were available, is here supplied with an added question mark to indicate special uncertainty.

Data concerning calcium plage regions were taken directly from the daily SGD reports of the McMath Hulbert and Catania Observatories. Sunspot data used includes the Mt. Wilson and NOAA (Boulder, Ramey, Manila) SGD reports. Original drawings of the individual groups made at Mt. Wilson (and supplied by WDC-A) were also consulted and used where necessary to correct the SGD classification listings.

Information concerning the X-ray variability of individual solar regions was taken from SGD "quick-look" OSO-8 maps. These displays, some of which are reproduced in Fig. 1, were constructed from coverage obtained during a representative thirty minute period (neither the quietest nor the most active).

Satellite data concerning X-ray bursts and worldwide reports of SIDs were taken from composite SGD lists. Suggestions contained in these compilations as to the possible association of individual events with flares are altered without comment in the text when updated information renders this necessary. Similar corrective treatment is accorded to SGD lists of 'flare-related' radio bursts recorded at fixed and swept frequencies.

Data concerning solar proton events were taken from SGD "provisional lists".

Developmental history of Active region I

Active region I was first identified during Carrington Rotation 1661, when it was designated McMath Plage 15031. Only adjacent Plage 15033 had previously crossed the solar disk, i.e. once as Plage 15015, of Fig. 1, and this latter feature was already in an advanced state of decline and showed no special activity during the November transit. Structures 15028, 15034, 15036, 15037 and 15040 had, on the other hand, all emerged since the previous rotation so that Plage 15031, which first came over the east limb on November 12, 1977, was born at a previously "quiet" location during a period characterized by ambient rising flux.

Plage 15031

OSO-6 observations indicate that Plage 15031 constituted a weak X-ray source up until November 18, by which time it displayed a moderate intensity enhancement. After an ensuing decline it became "highly variable" on November 22 (the day of the proton flare), returning to a steady condition by the succeeding day, compare maps (e) and (f) of Fig. 1. These events were complimented by a rising level of sub-flaring in the plage previous to November 22, an effect apparent, cf. Table 1, despite significant gaps in the flare patrol record over the days concerned. This waxing solar activity culminated on November 22 in the production, at 0945 UT, of an Importance 2B flare accompanied by an importance 2-SID of Widespread Index 5 and broadband single as well as swept frequency radiation. An X-ray burst was also associatively recorded. These related occurrences were climaxed, in less than an hour, by the onset of a ground level particle event.

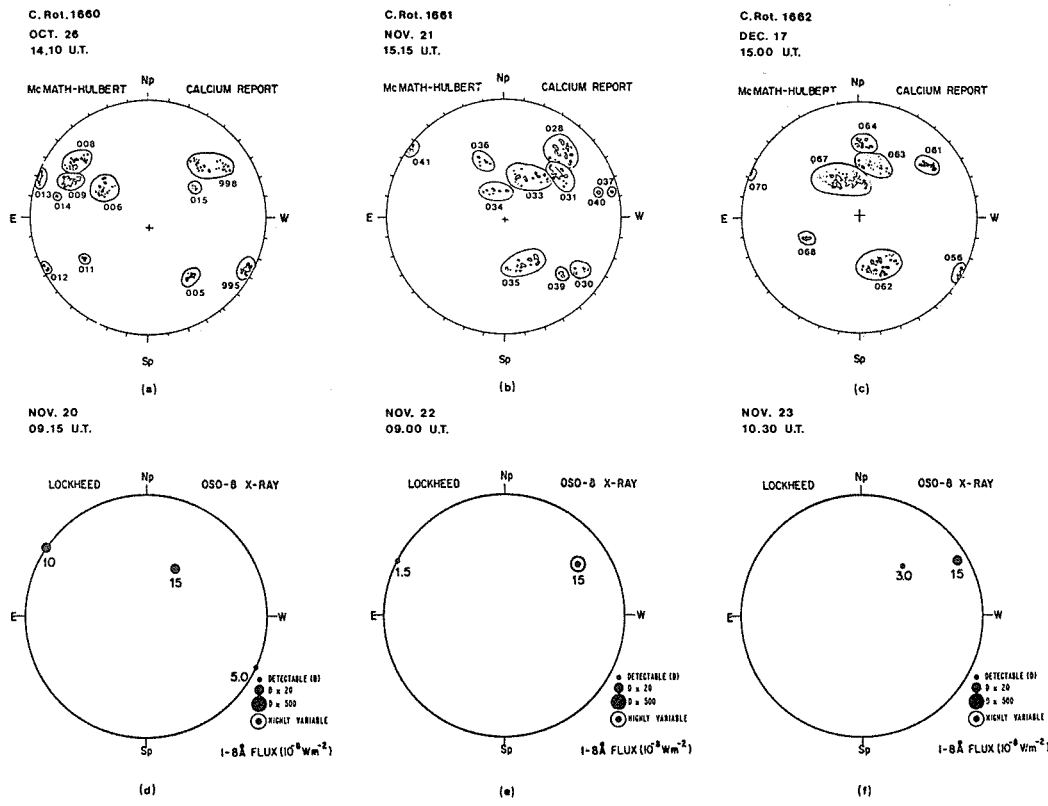

Fig. 1. Top: Calcium plage reports of the McMath Hulbert Observatory showing the same general region of the solar atmosphere during Carrington rotations 1660, 1661 and 1662. Plage 15031 (cf. 1b), which returned to the disk as Plage 15063 in December, was associated on November 22, 1977 with the occurrence of an important proton event. Bottom: OSO-8 X-ray maps taken before, on the day of and following the proton event. The relative-intensity of a region is here indicated by dots of different sizes where "detectable", (D), nominally corresponds to 5X times the background value. The three dot sizes employed represent D-20D, 20D-500D and >500D. If the source varied by more than an order of magnitude over a time period of <2h, a "highly variable" indicator, consisting of a dot surrounded by a circle, is used rather than a 'typical' intensity.

It is noted that three of the flares occurring on November 22 prior to the Importance 2B event, were associated with the generation of minor centimeter burst radiation (cf Table 2). The closest recorded event to the major flare was additionally associated with the production of an Importance 1-SPA of Widespread Index 1. The first flare to be associated with an ionospheric disturbance previous to this was an Importance sf event at 1132 UT on November 20. (accompanied by an Importance 1-SEA of Widespread Index 1). After the major flare of November 22 no further activity other than an Importance sf event on November 24 was reported in region 15031 prior to its limb transit.

Examination of the original Mt. Wilson drawings reveals that, by 1645 UT on November 17, a B(D) configuration was present in the underlying spot group, compare Figs. 2a and 2b.

The next available record, made at 1610 UT on November 20, shows that, by this time, the following spots had become dominant. No magnetic observations were made on the day of the major flare. Thereafter, the spot group was seen to be in rapid decline, reaching class af by November 24. A report from Boulder indicates that the largest spot in the group had an asymmetric or complex penumbra on the day before the major flare and a rudimentary penumbra on the succeeding day, cf. Table 1.

Plage 15063

On its next disk transit, when it was renamed McMath Plage 15063, the region which had previously supported the proton flare was so substantially reduced in area and brightness as to be of negligible significance, cf. Table 2.

No observed flaring occurred during the course of its transit and the Mt. Wilson observers reported no spots in the underlying magnetic field.

Table 1.

1 DEVELOPMENTAL HISTORY AND ACTIVITY PROFILE OF McMATH PLAGE 15031

McMATH PLAGE NO.	DATA 1977	E (1) NOV. 12	13	14	15	16	17	18	19	20	21	22	23	24			W (1) NOV.
15031	PLAGE AREA *	200	400		200	600	1200		1800		1500			1800			
	INTENSITY	1.0	1.0		2.0	3.0	3.5		3.5		3.0			3.5			
	MT. W. CLASS				(B)	(BP)	B(D)	(B)		BF(D)	(BF)		(BF)	(AF)			
MT.WILSON NUMBER	FIELD STRENGTH				3	4	5	4		5	4		4	2			
19894	AREA*				10	10	110	440	420	230	180		120				
	SPOT COUNT				2	1	15	21	0	16	4		9				
	NOAA CLASS				AXX	AXX	CRI	DAC	XX	DAI	DAC		DRI				
H ALPHA ACTIVITY	REPT. FLARES				1(sn)		2(sn)	3(sf)	3(sf)	4(sf)	4(sf)	2(sn)		1(sf)			
										1(sn)		1(1f)					
												1(2b)					
X-RAY ACTIVITY	NO. OF SIDs									1		2					
	NO. X-RAY BTS.						1					1					
SF BST. ACTIVITY	NO. OF cm BTS.											3					
	NO. cm-dm BTS.																
	NO. cm-m BTS.											1					
DYNAMIC RADIO	NO. TYPE II																
EVENTS	NO. TYPE IV											1					

Table 2.

3 DEVELOPMENTAL HISTORY AND ACTIVITY PROFILE OF McMATH PLAGE 15063

McMATH PLAGE NO.	DATA 1977	E (1) DEC. 10	11	12	13	14	15	16	17	18								W (1) DEC.
15063	PLAGE AREA *	300	600					700	700	900								
	INTENSITY	1.0	1.0					1.5	1.5	1.0								
	MT. W. CLASS																	
MT.WILSON NUMBER	FIELD STRENGTH																	
-----	AREA*																	
	SPOT COUNT																	
	NOAA CLASS																	
X-RAY ACTIVITY	NO. OF SIDs																	
	NO. X-RAY BTS.																	
SF BST. ACTIVITY	NO. OF cm BTS.																	
	NO. cm-dm BTS.																	
	NO. cm-m BTS.																	
DYNAMIC RADIO	NO. TYPE II																	
EVENTS	NO. TYPE IV																	

*Areas are measured in millionths of the Solar Hemisphere.

Note: Tables 1 and 2 give the evolution, as monitored in calcium light, of those plages in which the proton flares of November 1977 developed. The sources of these data, together with complimentary information concerning plage-related magnetic features, flare activity, SIDs, X-ray bursts, and single frequency and dynamic radio events, are described in section 2. The conventions of presentation adopted are generally similar to those contained in SGD (Supplement) No. 390, February 1977. The number of flares identified within a particular plage having an importance class within the range sf to 4b is indicated according to the scheme number of flares identified (reported flare importance). In cases where no importance rating was assigned in the source material to a particular flare, a suggested importance, based on such parameters as are available, is assigned by the author and the event listed according to the scheme 1? (suggested flare importance).

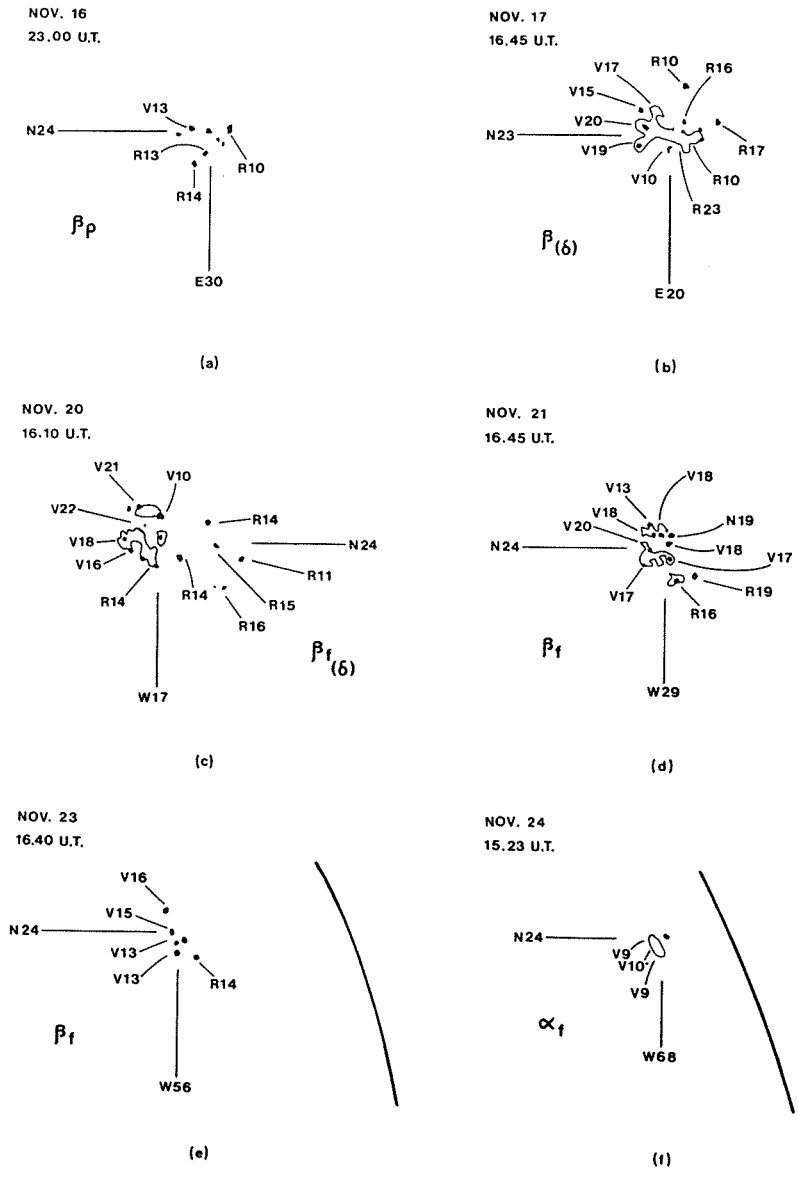

Fig. 2. Reproduction of drawings of spot group Mt. Wilson 19894, originally made at the Mt. Wilson Observatory during Carrington rotation 1661. North-top, west-right.

Possible common relationship of the active regions to a long lived sub-photospheric source of magnetic flux.

The history of the rise and decline of Plage 15031 forms part of a larger study made by the author of the waxings and wanings of all active regions within a zone of the northern Solar Hemisphere extending between heliographic longitudes L25° and L85°, over the periods of their visibility from Earth during Carrington Rotations 1659-1672 (that is within the bridging interval of a terrestrial year from September 1977 to September 1978).

Against this background, which involved the study of 30 independent plages, some 8 of which executed >3 traversals of the solar disk, it was noted that the ability of a particular plage to survive depended directly on the level of complexity of its underlying magnetic field. Within the atmospheric zone considered, strong fields surfaced only with a narrow band extending roughly from mean latitudes N16-N26. To the north and south of this domain, the fields that emerged were markedly weaker with no

recorded births to the north of (mean) N39 and to the south of (mean) N13. Since the level of flaring observed within a particular plage was itself a close function of the level of complexity of the underlying magnetic field, the locations at which energetically important flares were triggered showed the same latitude dependency as that exhibited by long lived plages and complex magnetic fields.

Those plage sequences producing the various proton flares considered (and many other energetically significant events as monitored by their electromagnetic accompaniments), were further spatially associated with a persistent, although somewhat intermittently yielding "well-spring" of magnetic flux, situated between heliographic longitudes L52-L79*. Specifically, Mt. Wilson Group 19984, underlying 'November' Plage 15031, was reported on emergence** to be located at (mean) latitude N23 and (mean) heliographic longitude L61.

Mt. Wilson Groups 20018 and 20019, underlying that western part of Plage 15266 associated with the production of the April-May proton flares, were, on the other hand, reported on emergence to extend between (mean) latitudes N19-N25 and (mean) heliographic longitudes L71-L79. A temporally and spatially related group which developed at (mean) latitude N25 and (mean) heliographic longitude L52 was specially associated with energetic flaring showing a different morphology to that of the homologous proton events but present in the eastern part of the same plage.

These spatial relationships suggest that, while their component plage structures and precise positions were different, the important proton flares of November 22, 1977 and April-May 1978 may have constituted responses to instabilities associated with the presence beneath the photosphere of an anomalous region capable of causing the episodic emergence over an extended time period of strong magnetic flux within the confines of a solar zone lying roughly between latitudes N16-26 and (mean) heliographic longitudes L52-L79.

Compare this finding with the assertion by Svestka [1965] that "proton flare activity regions are not randomly distributed on the solar disk but tend to occur in complexes of activity which stay on the solar surface for many months and even years". See also Dodson and Hedeman [1968] and a general discussion of related work by Svestka [1976].

Acknowledgments

My best thanks are due to E. Ruth Hedeman of the McMath Hulbert Observatory for valuable discussions and for the gift of on- and off-band McMath H-alpha spectroheliograms of the proton flares of April 28 - May 1, 1978.

References

DODSON, H.W. and E.R. HEDEMAN — 1968 — "Some patterns in the development of centres of solar activity, 1961-1966", Proc. IAU Symp, No. 35, Ed. K.O. Kiepenheuer, D. Reidel Publ. Co., Dordrecht-Holland, p. 56.

McKENNA-LAWLOR, S.M.P. — 1980 — "Short-term prediction of the potential of an active region to produce recurrent proton flares", Solar-Terrestrial Predictions Proc. Vol. III, Ed. R.F. Donnelly, p. 8-12.

SVESTKA, Z. — 1968 — "Loop prominence systems and proton-flare active regions", Proc. IAU Symp. No. 35, Ed. K.O. Kiepenheuer, D. Reidel Publ. Co., Dordrecht-Holland, p. 287.

SVESTKA, Z. — 1976 — "Solar Flares" Geophysics and Astrophysics Monograms, Vol. 8, D. Reidel Publ. Co. Dordrecht-Holland.

SMART, D.F., M.A. SHEA, J.E. HUMBLE and P.J. TRANSKANEN — 1979 — "A model of the 7 May 1978 cosmic ray event", AFGL-SP 5-18, Air Force Geophysics Laboratory, Bedford, Mass., U.S.A.

*Another "well-spring" of flux, associated with the production, in other plage sequences, of energetically significant flares between September 1977 and September 1978, were located, within the same latitude limits, between heliographic longitudes L29 and L32.

**A systematic change with time of solar longitudes in a direction opposite to that of solar rotation was exhibited by all of the plages studied.

Morphological Structure and Energy Content of Flare of November 22, 1977 in Hα and Ca-K Lines and Associated Geomagnetic and SEA events.

by
E. Soyturk and A. Özguc
Kandilli Observatory, Istanbul, Turkey

Introduction

The MONSEE Steering Committee noted that the biggest GLE since 1960 occurred on November 22, 1977 (about 1300 UT). It is believed that the geophysical, ionospheric and ground level events (GLE) stemmed primarily from a solar flare that had a complex filamentary structure and two sudden disappearances occurred in one hour.

We describe the structure of McMath plage region 15031, solar events, isomaps, energy content of flare, SEA and geomagnetic perturbations on November 22, 1977.

During its first passage, this active center was located near N 26, and at approximate Carrington longitude 61°. According to the sunspot observations of Kandilli this plage comprised a C type, 16-member bipolar sunspot group on this day. The largest and most important flare (2b) started at 0948 UT, reached maximum at 1012 UT and had almost ended at 1112 UT (duration is 84 min.). We observed some perturbations on SEA records and also on the H and D components of geomagnetic records.

Chromosphere (Hα and Ca-K):

The observations were made with Halle Hα (0.5 Å) and Ca-K (0.6 Å) filters. Wing observations were made by Zeiss 0.25 Å Hα filter. The sun image diameters are about 15 mm and 20 mm, respectively. The isomaps were obtained with a Joyce isodensitracer.

Evolution of Flare:

The active center comprised five bright zones and four filaments. Two filaments were lying northward, named "North Filament 1 and 2" (NF1 and NF2), other two filaments, were lying eastward, named as "East Filament 1 and 2" (EF1 and EF2) (see Fig. 1a row 1, column 1 and 4). Referring to the chromospheric density as 0.00D, the contour which marks the plage's boundary, defines an average area of 550 millionths of hemisphere in Hα and 1500 millionths of hemisphere in Ca-K. This indicated that the plage is rather old. The zone numbered 1 was located at the north of the plage, the zone 2 was located between the spot region (SR) and NF2 and the zones 3,4 and 5 were alined to the south of EF1 and EF2. The active center represents a complex filamentary structure. It seems that EF2 is passing under EF1 and is taking a position parallel to EF1.

0853 UT: Before the flare, the region 3 was the brightest part of the plage (o.3D), second brightest part was region 2 (0.24D). Both EF1 and EF2 had about 75000-km length, and 6000 km width. And they had the density that normal quiescent filaments have (see Fig. 1a row 1).

0900 UT: During the observation we obtained a series of photographs, each completed in 30 sec. and taken every 0.25 Å step, between the wings of Hα ± 1 Å. First mass motion was observed at 0900 UT (see Fig. 2 row 1), material flowed from EF2 to the small spot group and was detected from off-band filtergrams which recorded at Hα + 1 Å . The filament EF1 wholly moved upward and was partly detectable up to Hα - 1 Å. The end of NF2 which terminates at SR is also detectable in the same frame.

0938 UT: Though, no flare occurred in the plage region, the EF1 filament lost its whole matter and density and disappeared (sudden disappearance 1). Thus EF2 appeared clearly (Fig. 1a row 1).

0948 UT: The flare commenced in region 2 at 0948 UT. This region placed at the crossing point of "V" shaped filament which is composed of NF1 and NF2. This point was outside of SR.

0951 UT: The flare developed in region 1, presented two parallel arms in region 2, and improved by following the west side of NF and EF channels. EF2 presented very diffuse traces. The flare developed along both sides of NF2 and also appeared in regions 1 and 3.

0954 UT: The flare developed in region 1 and presented two parallel arms in region 2 and improved by following the west side of NF and EF channels - EF2 was very diffuse.

1001 UT: The flare represented a rosette structure around a dark feature in region 1. In region 2 when the first arm slid to the SR, the second one came nearer to it and they closely surrounded the EF2 channel. The flare represented two parallel arms in region 3. Regions 4 and 5 had some slight brightenings along both sides of the channel of EF2. EF2 presented a dark but undefined structure. We suggest that these closed parallel arms have an important role in particle accelerations.

1004 UT: The flare continued in regions 1 and 2 with the same structure. The arms of the flare were crossed by a dark loop which ended at the biggest sunspot. When the local undisturbed chromospheric density is 0.00D two kernels which emerged in the region 2, had 1.08D. In the same region, a weak arm developed and surrounded the west of NF2. From the isomaps, at this phase, it is clearly evident that both filament's channels were saved between regions 2 and 3. The kernel in region 3 was as dense as the kernel of region 2 and was developing northward along NF1. EF2 has completely disappeared (sudden disappearance 2). Some brightenings which may be the cause of impact emerged at both sides of EF2.

1012 UT: The rosette structure disappeared in region 1. A dark arc which surrounded the region 2, crossed region 1 and ended at the biggest sunspot. The arms disappeared in region 2 but two kernels still continued by

1.08D. Region 3 developed northward and eastward along the channels of NF and EF, respectively. The flare diminished in region 4 and the two surges which emerged from the SR, terminated in region 5. At this end a lambda-shaped weak brightening surrounded the surges. This was the maximum phase of the flare and had an amorphous structure, i.e., there was no arm structure. Supposing the 0.18D contour is marking the flare boundary (mean quiet plage density), the flare area is 410 millionths of hemisphere at the maximum phase and the density of the brightest point of the flare (in region 3) is equal to 1.2D.

1016 UT: The flare maintained the same structure as it had at 1012 UT. Maximum brightness was 0.84D in region 3.

1022 UT: The surge which started at 1012 UT along the EF channel was nearly parallel to the surface of the Sun and it possibly created the impact brightenings in region 5. The east point of this surge was detectable up to Hα-1 Å and the other end was detectable at Hα+1 Å at its source in the SR. In the both wings the surge followed the same trajectory (Fig. 2 row 2).

1029 UT: The arms in regions 1 and 2 faded out, and the flare also faded out gradually from NF channel outward in region 3. In region 4 there was no brightness -- even that of the plage disappeared. The lambda-shape persisted in the region 5.

1043 UT: The arms in regions 1, 2 and 3 continued. Some weak brightenings were going on in region 5.

1055 UT: The material flowed toward the biggest spot by means of three streams which are detectable in Hα+1 Å. Another material group is flowing into the south end of the SR as a helical motion which is detectable in Hα+1 Å. Three helical knots are outlined clearly. The distance between these two knots is 25 seconds of arc (see Fig. 2 row 2 column 3).

1100 UT: The flare is almost gone. Only regions 2, 3 and 5 had weak brightenings.

1126 UT: Nearly the same appearance was maintained as it had at 1055 UT in the red wing of Hα (see Fig. 2 row 2 column 4). The biggest spot had two streams and another small stream emerged from the south end of SR.

1130 UT: The flare has completely ended. If we compare the last filtergram with the first one (0853 UT), we can detect great changes in the morphological structure of the plage.

Ca-K Isomaps:

Both the compact structure of the plage and the seeing conditions did not permit observation of the structure in detail in the Ca-K line. It seems that the flare has its maximum brightness at about 1016 UT in Ca-K line. The brightest point in region 3 is matched in both the Hα and Ca-K lines. Contrary to the Hα case, the plage maintains its morphology in Ca-K line.

Energy Content of Flare:

The isomaps obtained from Hα and Ca-K filtergrams show some different phases of the flare development. The flare energy graphs are illustrated in Fig. 3 a and b. These are corrected with respect to the central density. The total and the mean plage energy levels are given in Fig. 4. It is understood from the graphs that the flare started at 0940 UT and reached its maximum at 1012 UT and ended at 1112 UT.

The flare energies are:

$$3.3 \times 10^{28} \text{ ergs in H}\alpha$$

$$6.4 \times 10^{28} \text{ ergs in Ca-K}$$

These values are calculated from where the energy exceeded the mean plage energy level of Fig. 4, which is taken as a reference value.

SEA and Geomagnetic Events:

Fig. 5 shows the records of the H and D components of the geomagnetic field and 27-KHz tracings which were observed at Kandilli (ISK).

27-KHz records demonstrate four important perturbations as follows:

Begin UT	End UT	Type	Duration
0820	1020	3	120 m
1135	1205	2	30 m
1325	1335	1	10 m
1340	1430	4	50 m

The first perturbation of H component started at 0945 UT and became a typical flare effect (SFE) at 1058 UT. It reached its maximum at 1008 UT and faded out at 1038 UT. It ended at about 1108 UT.

When we compute the cross-correlation between the flare energy curve (Fig. 4) and the record of H component of geomagnetic field it gives r = 0.87 in the interval of 0930 - 1130 UT. When we do the same calculations with flare energy and the 27-kHz tracing for the same time interval it gives r = 0.72.

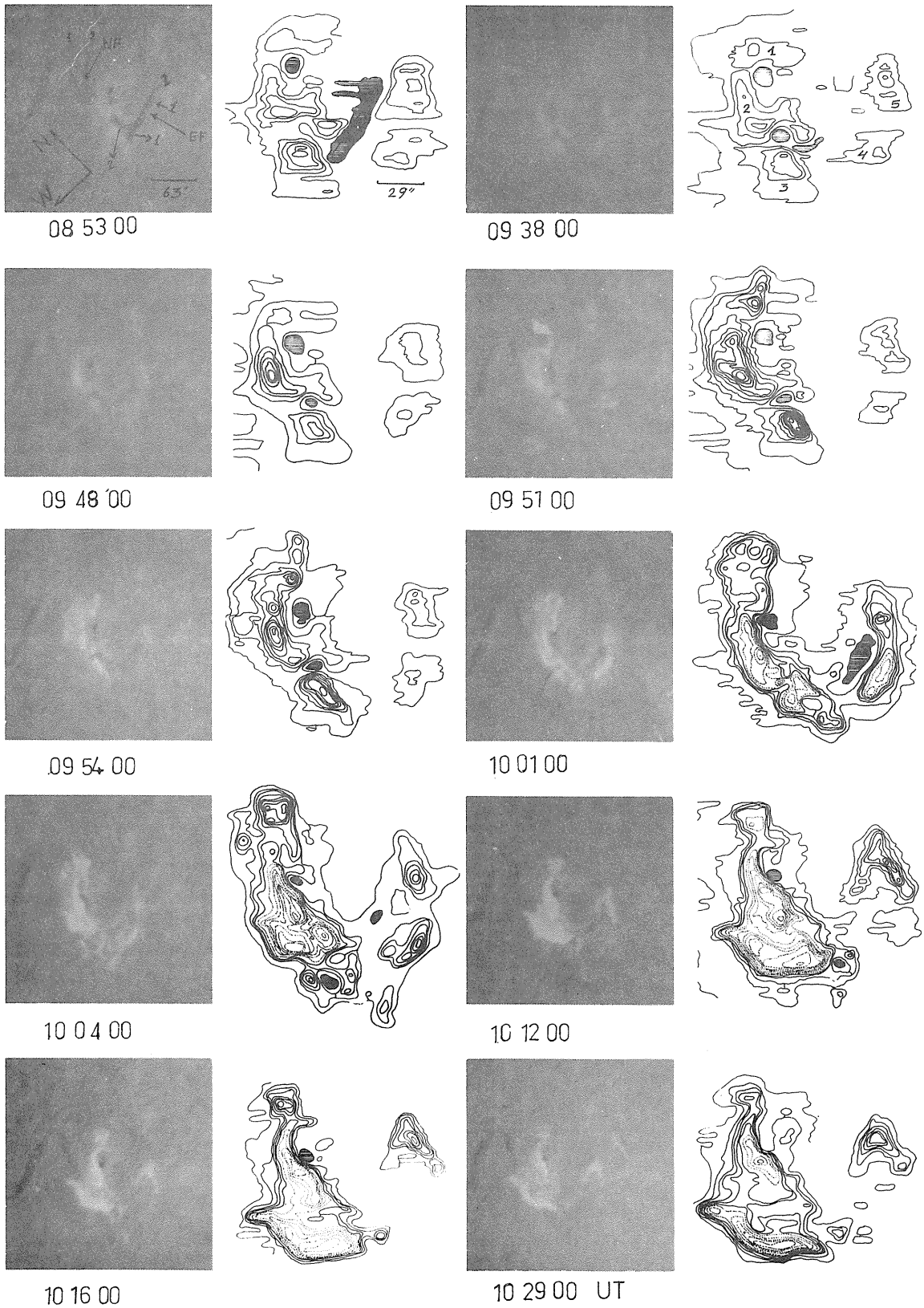

Fig. 1a The first column shows the Hα filtergrams, the second column shows the Hα isomaps obtained from the same filtergrams. Open contours correspond to the undisturbed chromospheric density. Every closed contour step is equal to a 0.12D difference.

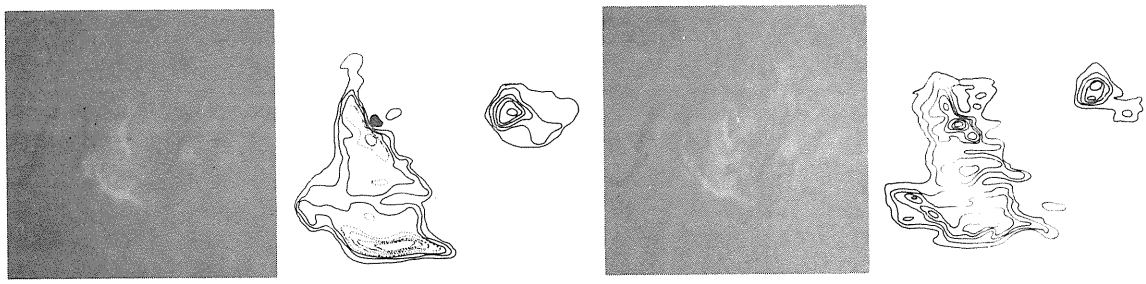

← FIG. 1a

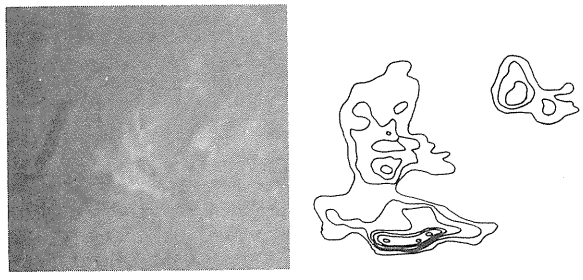

FIG. 1b ↓

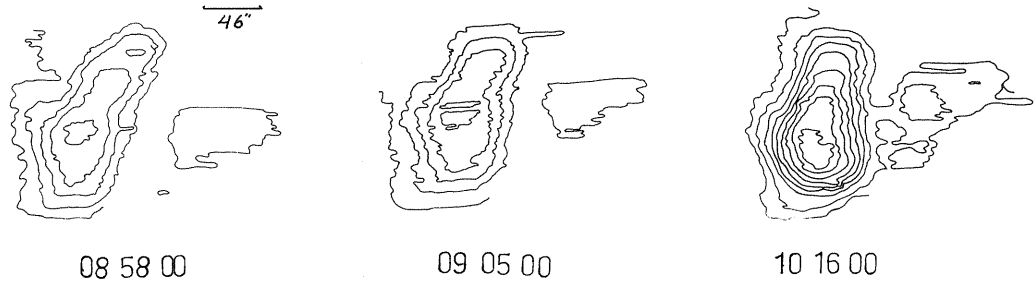

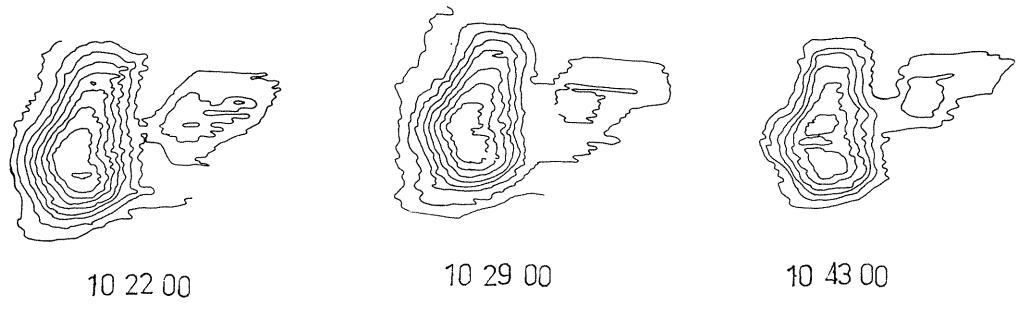

Fig. 1b Isomaps obtained from the Ca-K filtergrams.

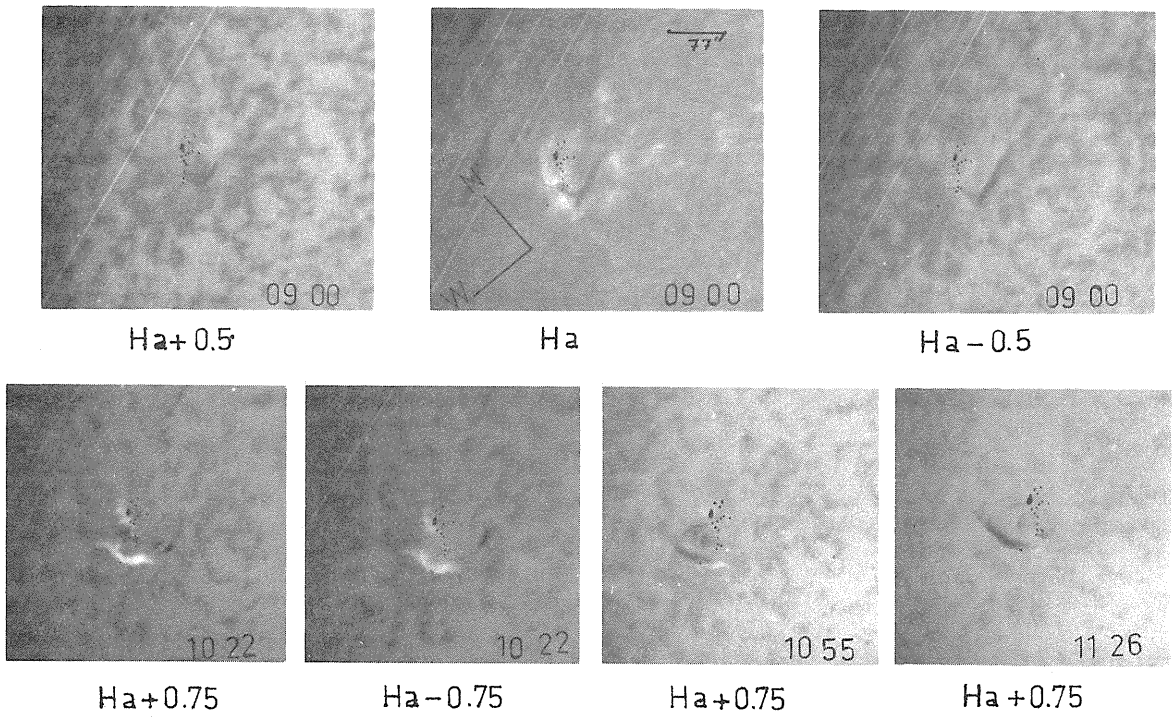

Fig. 2 These filtergrams show the wings of Hα. Each one shows the most representative phases of mass motions.

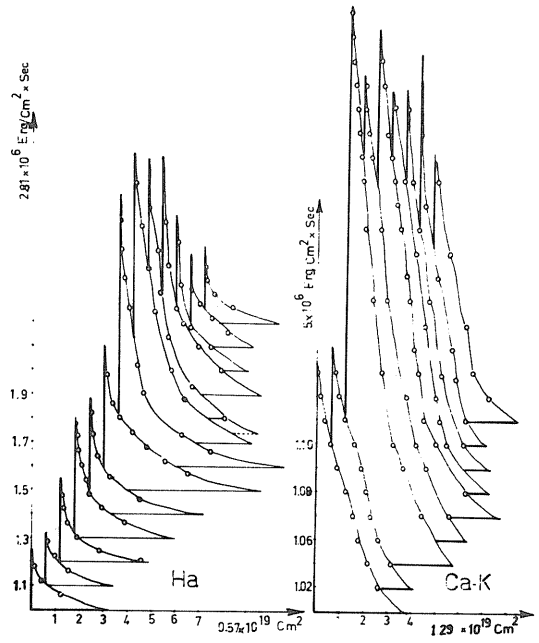

Fig. 3 The graphs show the flash energies in Hα and Ca-K lines. The abscissa shows the area in terms of cm^2 and the ordinate indicates the density steps. Every graph, however, has its own axis but in presentation they are demonstrated, perspectively. The graphs are not on a time scale but are arranged successively. Effects of the limb darkening, changes in atmospheric conditions and foreshortening are corrected.

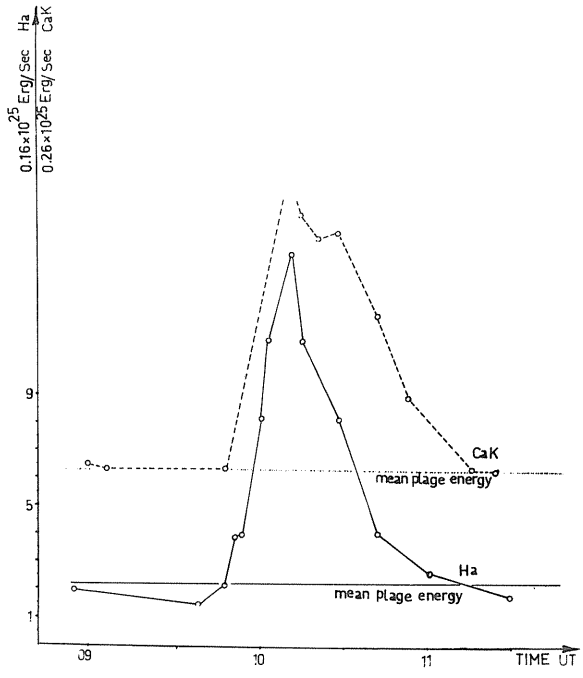

Fig. 4 Total energies for the plage and the flare in Hα and in Ca-K lines. The abscissa shows the time and the ordinate shows the energies in terms of ergs/second. The horizontal dashed and full lines show the mean energies of plage in Hα and in Ca-K lines.

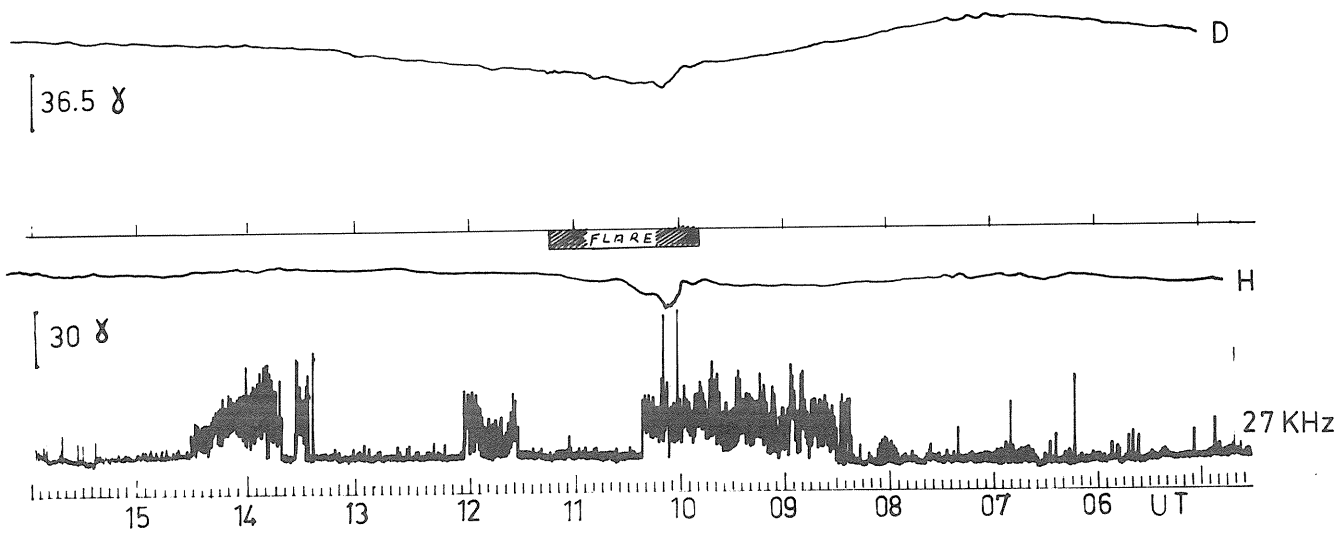

Fig. 5 Geomagnetic variations in H and D components and 27-kHz tracings.

2. SOLAR RADIO EVENTS

The Fine Structure of the Complex Type II - IV Radio Burst on November 22, 1977

by

L. M. Bakunin, G. P. Chernov,
A. A. Gnezdilov and O. S. Korolev
Solar Radio Laboratory, IZMIRAN, Moscow, USSR

The complex radio burst on November 22, 1977 was observed at Solar Radio Laboratory IZMIRAN at fixed frequencies 3000 and 202 MHz (Figure 1) and with two radio-spectrographs: one in the range 102 - 173 MHz [Korolev, 1975] and another covering 180 - 230 MHz [Markeev and Chernov, 1971]. The burst lasted approximately from 1000 to 1045 UT and was coincident in time with the maximum phase of the proton flare of importance 2b that occurred at N23 W40 in bipolar McMath Region 15031 [*SGD*, 1977].

The burst began almost simultaneously at 3000 and 202 MHz; however, it was more powerful at centimeter-wavelengths. At 3000 MHz the burst had one powerful maximum with small variations in flux, but some short-lived maxima were observed at 202 MHz during the beginning of the event and some smaller ones during the whole event. The principal peculiarity of this event was the presence of diverse fine structure during the whole burst.

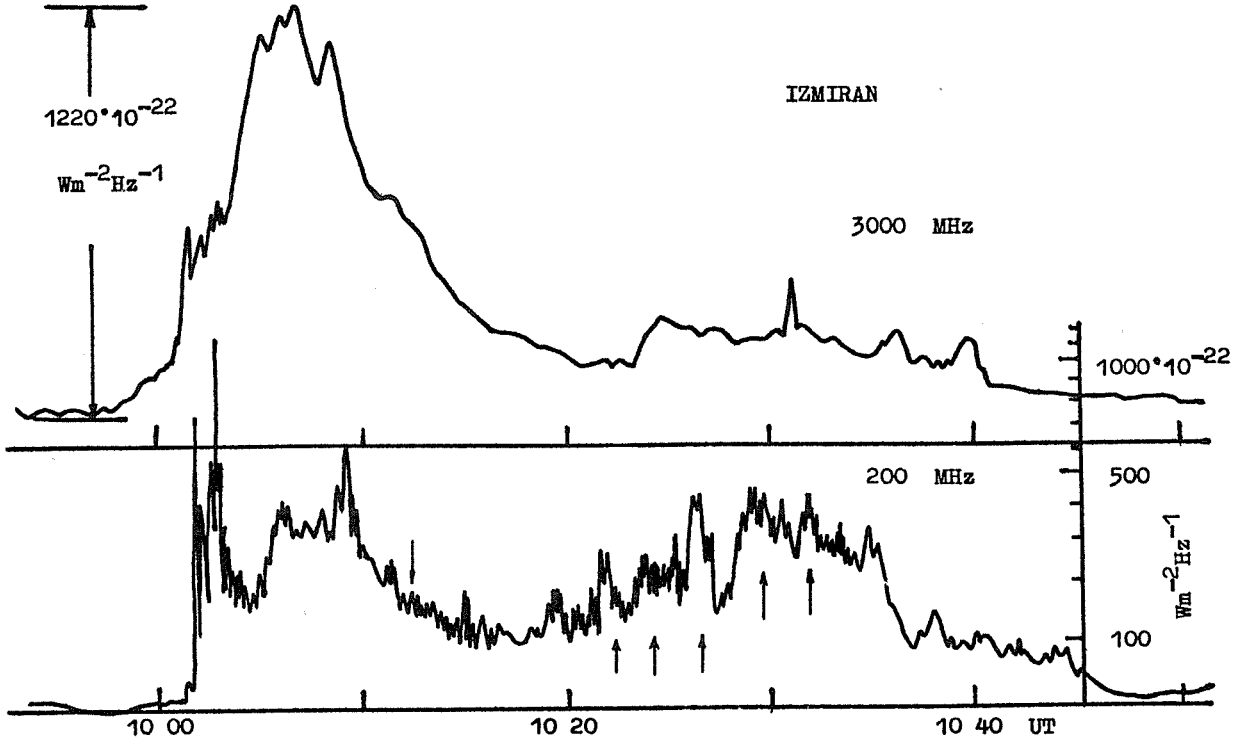

Fig. 1. Single frequency flux records of the outburst on November 22, 1977 at 202 and 3000 MHz. The upward pointing arrows show the minute variations of flux density at 202 MHz; the arrow at 1012.5 UT indicates the moment of the fiber burst.

The Pulsations With Time Scale of Seconds

In the metric range the event represents a Type IV burst with a sharp onset at 1001.8 UT. A general view of the spectrum in the range 102 - 173 MHz is shown in Figure 2, where one can see that the continuum contains several interruptions. Narrow frequency bandwidth pulsations with a time scale of 0.5 - 2 sec are evident at the very beginning of the first powerful phase of the burst (Figure 2c) and are characteristic features of such an event. These pulsations occupy the frequency range between about 10 and 20 MHz. Sometimes they show a reverse frequency drift, forming random groups that do not embrace the whole frequency range of the spectrograph. The series of seven pulsations during the 6 sec between 1002.3 and 1002.4 UT is the most outstanding group at the low-frequency edge of the spectrum; they exhibit practically no frequency drift.

The Fragments of the Type II Burst

The band of radiation consisting of patchy shapes and drift toward low frequencies at the rate $df/dt \approx 0.9$ MHz/sec began at 1002.5 UT and at frequencies below 120 MHz. It represents possibly a branch of the Type II burst. The estimation from the frequency drift of the speed of the agent gives the value ~ 900 km/sec, which corresponds to the speed of a shock wave. Thus, the emissions of Type II and IV bursts are possibly superposed on the spectrum. The series of reverse-drift bursts in the interval 1005 -1006 UT (Figure 2d) form the additional corroboration, because they look like fragments of "herringbone" structure in the emission of Type II bursts.

The Spike-Brightenings

In the interval between 1008 and 1010 UT there is a new increase of intensification of the continuum of the Type IV burst (Figure 3a). Here pulsating bursts with a time scale of about 0.2 to 0.3 sec are observed in different parts of the range of the spectrograph between 120 and 150 MHz, and occur side by side with the broadband 5-second enhancement. Precisely the same pulsating bursts were described as spike-brightenings by Bakunin et al. [1977] and Bakunin and Chernov [1978]. The fragment of spectrum with high resolution in the range 180 - 230 MHz for the same temporal interval is given in Figure 3b. It is seen that the continuum emission and the elements of the fine structure nearly reach 215 MHz. It is seen, too, that here the spike-brightenings have an infinitely great frequency drift.

A new series of spike-brightenings appears in the range 130 - 215 MHz at 1011 - 1012 UT (Figures 4a and 4b). Although the durations of the spike-brightenings are smaller than 0.1 - 0.2 sec, they have a visible positive drift $df/dt \approx 50$ - 100 MHz/sec and are accompanied by strong noise storm type activity at their low frequency edge.

On the other hand, between 1015 and 1016 UT bursts of the spike-brightening type developed into 1-second pulsations (Figures 4d and 4e) with no appreciable frequency drift. In the course of the event not only did the intensity of these pulsations strengthen, but their duration increased too--up to 5 - 10 sec (Figure 5).

The Minute Fluctuations

In the event on November 22, 1977 one can select another component--the fluctuations of the radio emission with a time scale of about several minutes (minute fluctuations). These fluctuations at fixed frequency 202 MHz were registered as variations of an enhanced continuum and displayed typical periods between 2 - 3 min and amplitudes of 100-250 $10^{-22}Wm^{-2}Hz^{-1}$ (20 - 50% of background). It is seen from Figure 1 that the fluctuations began about 1014 UT, which was after the maximum phase of the event, and continued until 1045 UT. The deep modulation and great flux variations of these fluctuations allowed their maxima to register on the 102 - 173 MHz and 180 - 230 MHz radio spectrographs. These fluctuations are seen in the dynamic spectra as a succession of isolated events from 125 MHz to the boundary frequency of the high resolution spectrograph (230 MHz). In Figure 5 arrows mark the most characteristic fluctuations--ones with 1- to 2-minute duration and an emission bandwidth equal to or greater than 80 MHz. It is possible that the whole series of events drifted to higher frequencies, because after 1032 UT the fluctuations that had been observed at the fixed frequency of 202 MHz and on the spectrum in 180 - 230 MHz range almost disappeared in the range 102 - 173 MHz.

The quasi-periodic minute variations reached maximum intensity on both the spectrum and the 202 MHz fixed frequency trace in the time interval 1026 - 1032 UT. The brightest element was observed at 1026.5 UT on the spectrum at frequencies from 130 MHz to 215 MHz (Figures 5a, b, and c), while its flux density at 202 MHz reached $420 \times 10^{-22}Wm^{-2}Hz^{-1}$ (Figure 1). Moreover, quasi-diffuse formations (Figure 5b and c) as well as fluctuations with some structure (Figure 5d and e) occurred on the spectrum. One can see that almost all the minute fluctuations have fine structure in the form of 1-second pulsations.

The fluctuations described here look like the minute quasi-regular variations of the flux density of the meter radio emission in the event of August 4, 1972 [Aurass et al., 1976]. The fluctuations in August 1972 as well as in November 1977 appeared after the end of the maximum phase of the whole event and were observed in a finite band of frequencies.

The Fiber Bursts

The fiber bursts with intermediate frequency drift were observed at 1012.5 UT (Figure 4c), 1016.5 UT (Figure 4d) and 1019 - 1020 UT (Figure 3c). The frequency drift of the first burst is 1.5 MHz/sec at a frequency of ~ 200 MHz, the second one drifts about 0.8 MHz/sec at a frequency of 155 MHz, and the third about 0.6 MHz/sec at 155 MHz. Only the second burst had noticeable absorption on its low frequency edge. Some fiber bursts also have precursors in the form of several points in the emission and absorption. The fiber burst between 1019 and 1020 UT (Figure 3c) is accompanied by two groups of point bursts at the high frequency edge of the spectrograph. These point bursts have a frequency band of ~ 1 MHz and a duration of ~ 0.2 - 0.3 sec.

It is noticed that the bandwidth of absorption at 1016.5 UT (Figure 4d) is of the order of 2 MHz and that the fiber burst's bandwidth of emission is $\approx 1 - 1.5$ MHz. The generating mechanism of the fiber burst is based on the coalescence of Langmuir waves and whistlers [Kuijpers, 1975]. An estimation of the whistler frequency $\omega_W \approx 0.4\ \omega_{He}$, where ω_{He} equals the electron cyclotron frequency, is given by the difference between the frequencies at which maximum emission and absorption occur. In Figure 4d this difference equals $\sim$ 1.5 MHz [see Chernov, 1976] and yields a magnetic field strength of $\sim 1.3 \times 10^{-4}$T.

According to Chernov [1976], the line widths in emission (Δf_{emis}) and absorption (Δf_{abs}) are approximately equal and in turn are equal to $[\Delta f + \vec{L} \cdot \text{grad}\ (f_{pe})]$ where Δf equals the frequency band radiating from one plasma level in the solar corona, $\vec{L}$ equals the linear scale of the whistler wave packets, and f_{pe} equals the plasma frequency. In the stationary sources of Type IV bursts, which usually give the stripes in emission and absorption, the electron beams have a velocity dispersion ($\Delta V/V$) equal to about 0.1. Thus, the value of Δf cannot be small; it must be of the order of 1 MHz to agree with the observed electron beam velocity dispersion. On the other hand, the value of the term $[\vec{L} \cdot \text{grad}\ (f_{pe})]$ must be very small, namely, about 0.1 to 0.2 MHz, corresponding to whistler wave packet scales $\vec{L}$ between 1 and 2×10^7cm.

Conclusion

The event in question contains almost all the elements of fine structure typical of the Type IV burst associated with proton flares. According to Chernov [1976], more than 80% of the bursts with fine structure in emission and absorption associate with proton flares. The present event is not an exception.

Note the explanation of spike-brightenings in the background of the Type IV continuum: a nonlinear interaction of plasma waves with whistlers [Bakunin and Chernov, 1978]. In this case, a different mechanism for spike-brightenings is postulated because the whistler wave packets have large scales when compared with the approximately 10^{10} cm size of the magnetic trapping region even though the energy density in these packets is small. Later, when the energy density increases, the wave packets become modulated and broken and can drift for a long time with the group veolocity. It is then that the fiber burst appears. In the burst on November 22, 1977 this same succession of events was observed. First the spike-brightenings appeared, then longer pulsations and fiber bursts followed.

REFERENCES

AURASS, H., A. BÖMME and A. KRÜGER 1976 Investigation of Quasi-Periodic Modulation of Spectral Type IV Burst Components at a Time Scale of a Few Minutes, *Phys. Solariterr., No. 2,* 71-92, Potsdam.

BAKUNIN, L. M., I. M. CHERTOK and G. P. CHERNOV 1977 The Fine Structure of Meter Radio Emission Associated with McMath Action Region 14143, *Collected Data Reports for STIP Interval II, 20 March - 5 May 1976,* (*Report UAG-61,* WDC-A for Solar-Terrestrial Physics, Boulder, Colorado, U.S.A. 80303), 106-113.

BAKUNIN, L. M. and G. P. CHERNOV Solar Spike-Brightening Bursts, *Solar Phys.* (in press).

CHERNOV, G. P. 1976 On Microstructure in Meter Bursts Type IV Continual Emission. Continual Emission Modulation by Whistler Wave Packets, *Astron. Zhournal, 53,* 1027. (In Russian)

KOROLEV, O. S. 1975 The Spectrographical Observation of the Sun's Radio Emission at IZMIRAN in the Range of 93 - 186 MHz, *Astron. Zhournal, 52,* 1247. (In Russian)

KUIJPERS, J. 1975 Collective Wave-Particle Interactions in Solar Type IV Radio Bursts, *Thesis,* Utrecht.

MARKEEV, A. K. and G. P. CHERNOV 1971 Observations of Solar Radio Bursts with High Spectral Resolution, *Soviet Astron., 14,* 835. (translation)

SGD 1977 *Solar Geophysical Data,* 400 Part I, 10, December 1977, U.S. Department of Commerce, (Boulder, Colorado, U.S.A. 80303).

SGD 1978 *Solar Geophysical Data,* 401 Part I, January 1978, U.S. Department of Commerce, (Boulder, Colorado, U.S.A. 80303).

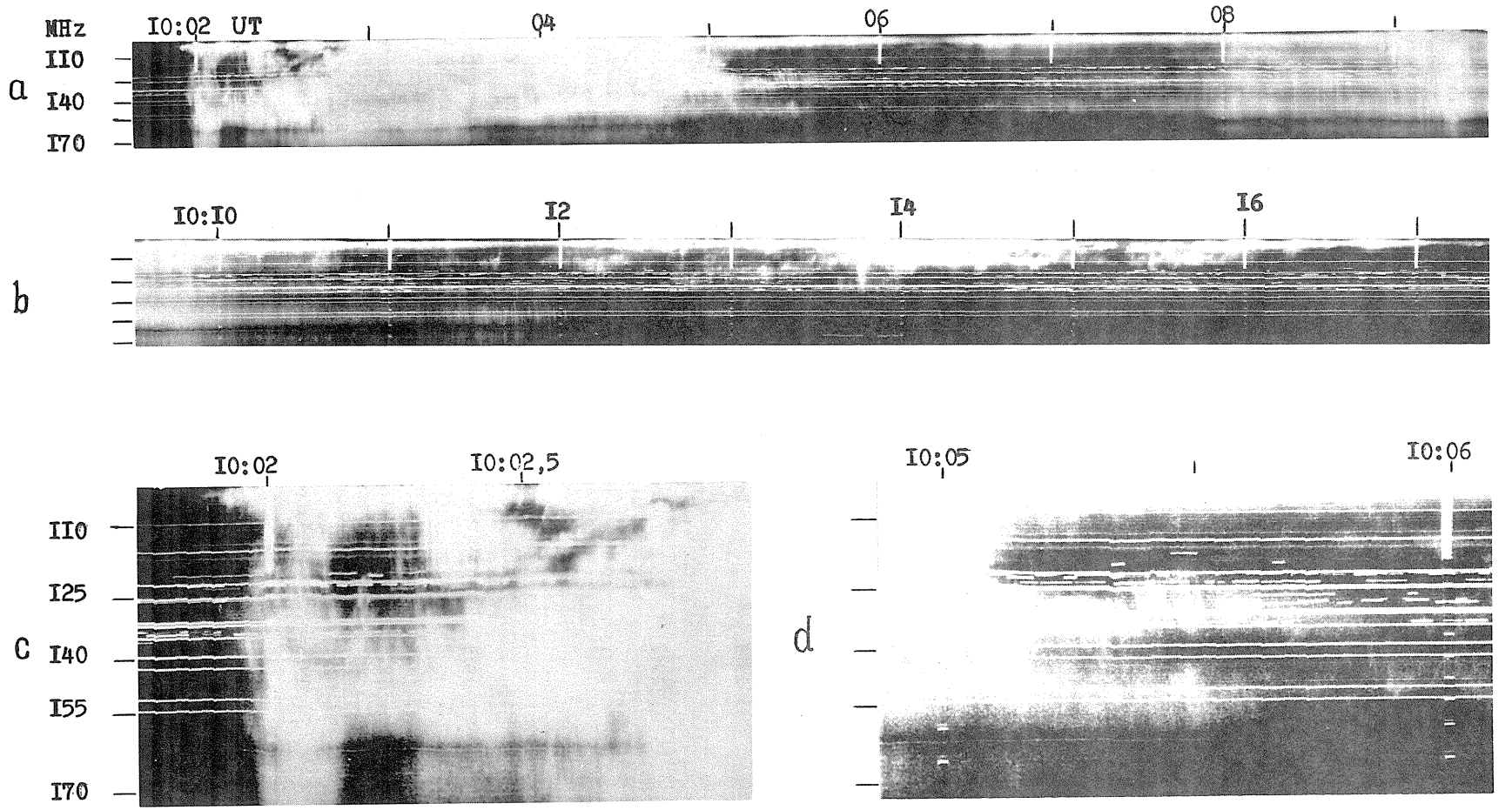

Fig. 2. Dynamic spectra of the outburst on November 22, 1977. (a) and (b) show the maximum phase of the event on the 102 - 173 MHz spectrograph; (c) shows an enlargement of the onset of the outburst with 1-second pulsations visible; and (d) shows an enlargement of the "herringbone" structure.

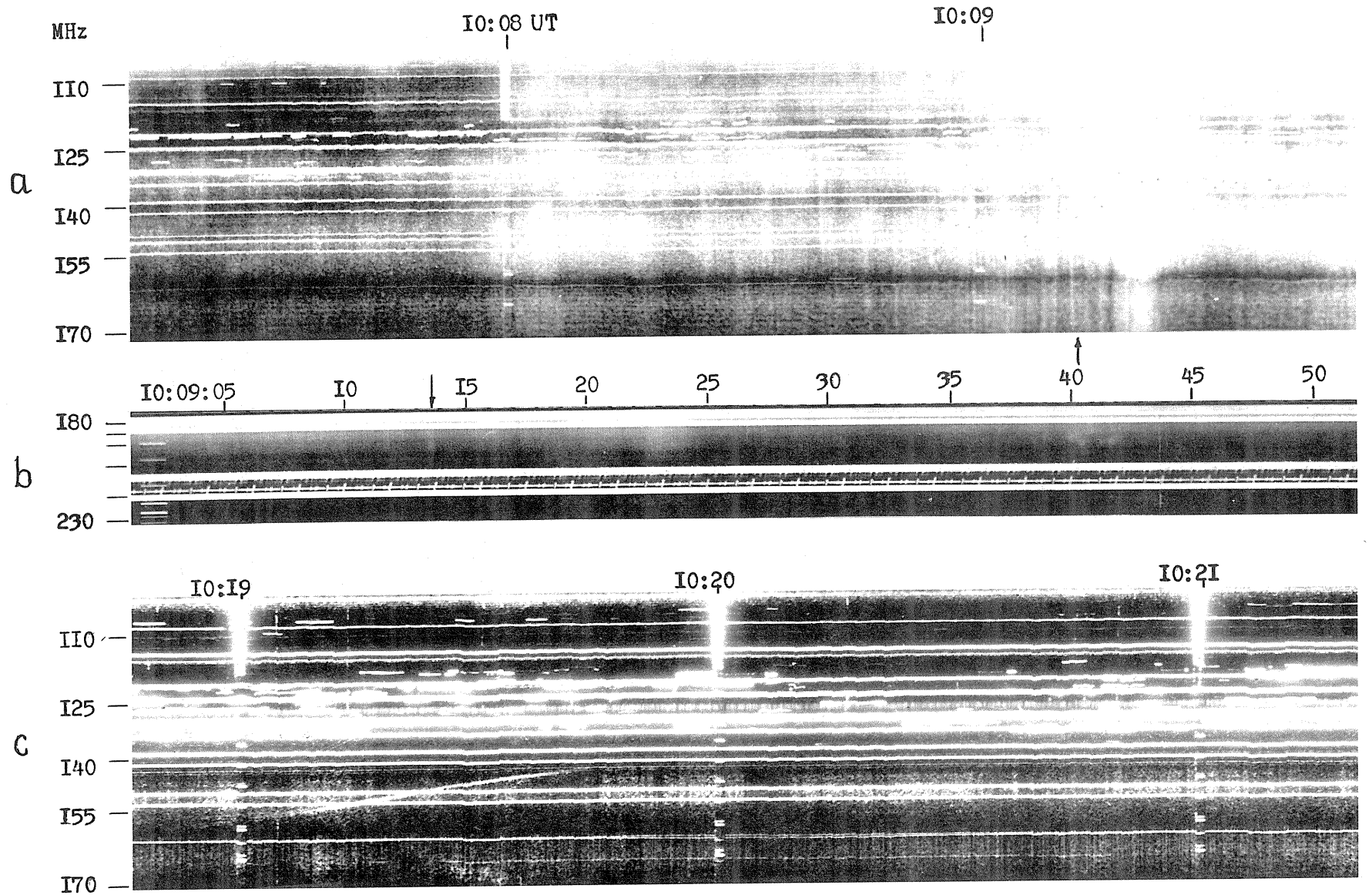

Fig. 3. (a) shows the enhancement of the continuum that contains spike-brightenings with a time scale of 0.2 - 0.3 sec; (b) shows with high resolution the HF boundary of the spike-brightenings marked by the arrow; and (c) shows the fiber burst from 1019.1 to 1019.7 UT on November 22, 1977.

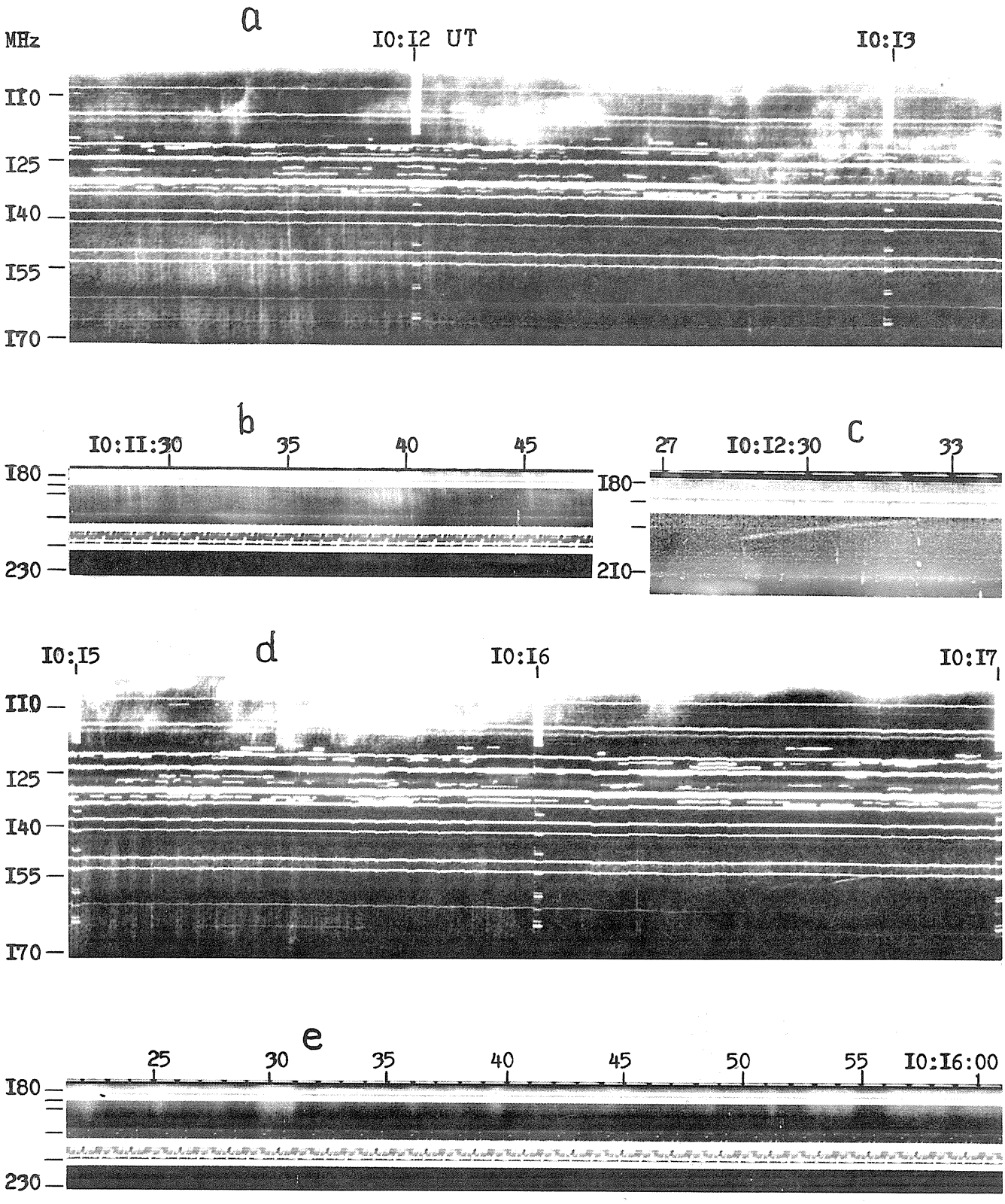

Fig. 4. (a) and (b) show the spike-brightenings with time scale of 0.15 - 0.2 sec in the range 135 - 212 MHz and with frequency drifts between 50 and 100 MHz/sec; (c) shows the fiber burst; (d) shows the fiber burst and point precursors in emission and absorption (1016.5 - 1016.7 UT) and 1-second pulsations; and (e) shows the HF boundary of the 1-second pulsations for November 22, 1977.

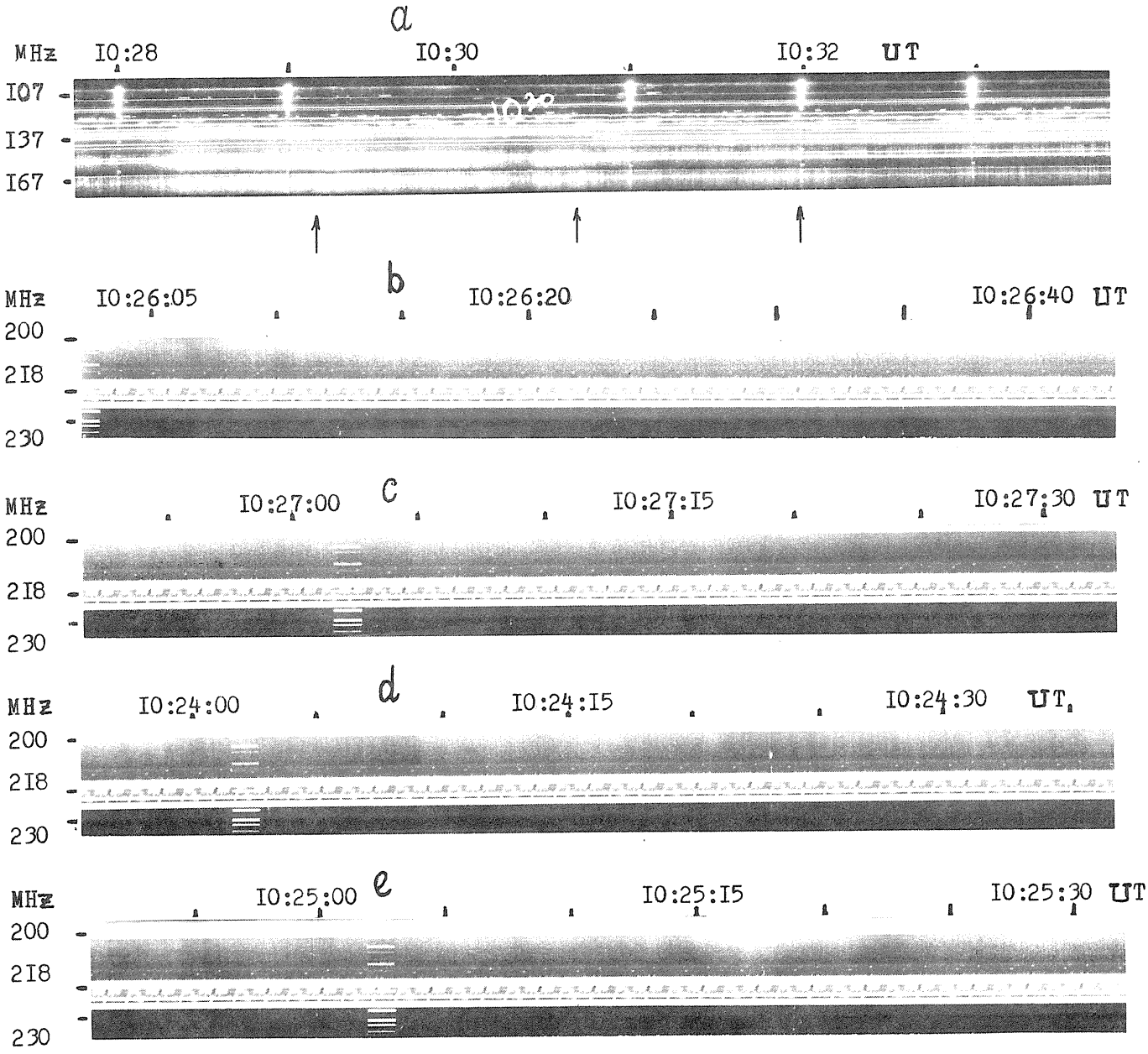

Fig. 5. Examples of the minute fluctuations marked by arrows in Figure 1. (a) shows the range 102 - 173 MHz; (b) and (c) show minute fluctuations at high resolution without fine structure in the range 180 - 230 MHz; and (d) and (e) show minute fluctuations with fine structure on a time scale of several seconds for November 22, 1977.

The Type IV Burst of November 22, 1977

by

H.W. Urbarz
Astronomical Institute of Tubingen University
Weissenau Station, 7980 Rasthalde, Ravensburg, G.F.R.

ABSTRACT

A short description is given of the dynamic spectrum of the Type IV burst of November 22, 1977, taken at Weissenau.

The event is associated with a large importance 2b flare at N24W40 as shown in the Comprehensive Report of SGD [1978]. After inspecting the film copies shown in Figures 1a-c, I can make statements:

(1) There is either no evidence of an associated Type II event or it is masked by the high fluxes that caused full saturation of the film between 1002 and 1025 UT.

(2) The dm flux rises some minutes before the m-wave continuum starts and within 0.5 min. in the 160 to 37 MHz band.

(3) The feature in channel 1 from 1002.3 to 1003.4 UT needs further investigation and comparison with other spectra.

(4) The 180 and 300 MHz band shows some Type III activity from 1002 to 1005 UT and the continuum there lasts only from 1004 to 1011.3 UT.

(5) There exists some reverse drift activity in channels 3 and 4, starting at 1020 UT. Since it is narrow banded and classified as Type III/RS, it may be interpreted as a release of weakly relativistic electrons from the coronal Type IV source.

(6) At 1025 UT there exists some reverse slope activity and pulsations in channel 1. Pulsations extend at 1027 UT to channels 2 and 3 and last to 1045 UT.

(7) It should be noted that channel 5 is saturated all the time because of an instrumental effect.

An impressive feature is the sudden onset of the m-wave component--an onset delayed by a few minutes with respect to the dm-cm component. It is a feature observed almost regularly during broad band Type IV bursts. One might speculate what is the leading process: the injection, the trap formation, or the magnetic reorientation of magnetoplasma structure at coronal heights, which cuts off the Type IV radiation. The decay should also give rise to a burst of high energy electrons from the radio burst source that adds up to the initial cloud of accellerated particles. Since it is an isolated event, associated events delayed by some days are worth investigating.

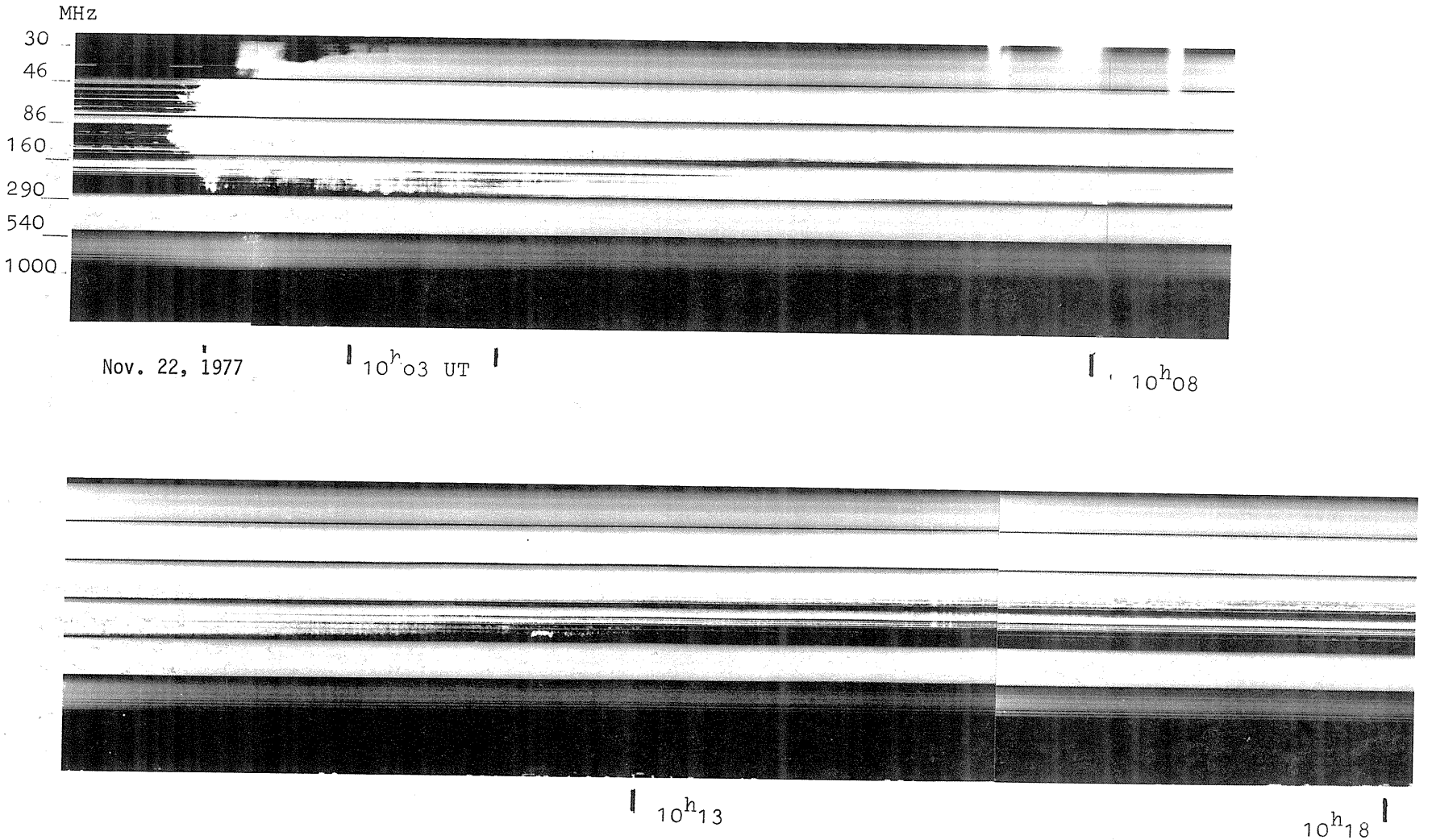

Fig. 1a. Dynamic spectra, Weissenau, November 22, 1977 (channel 5 is always saturated due to an instrumental effect).

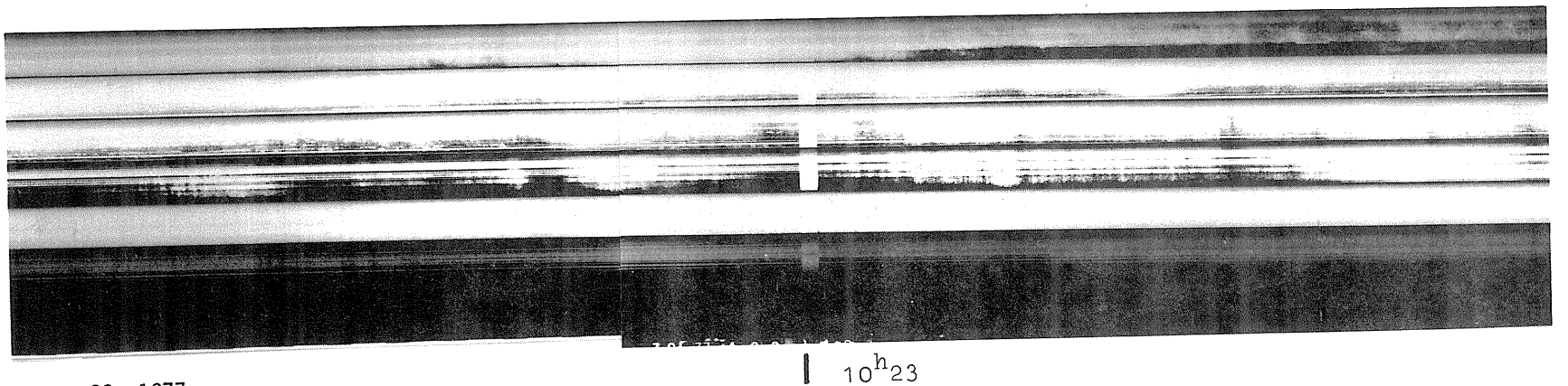

Nov. 22, 1977

10^h18

10^h23

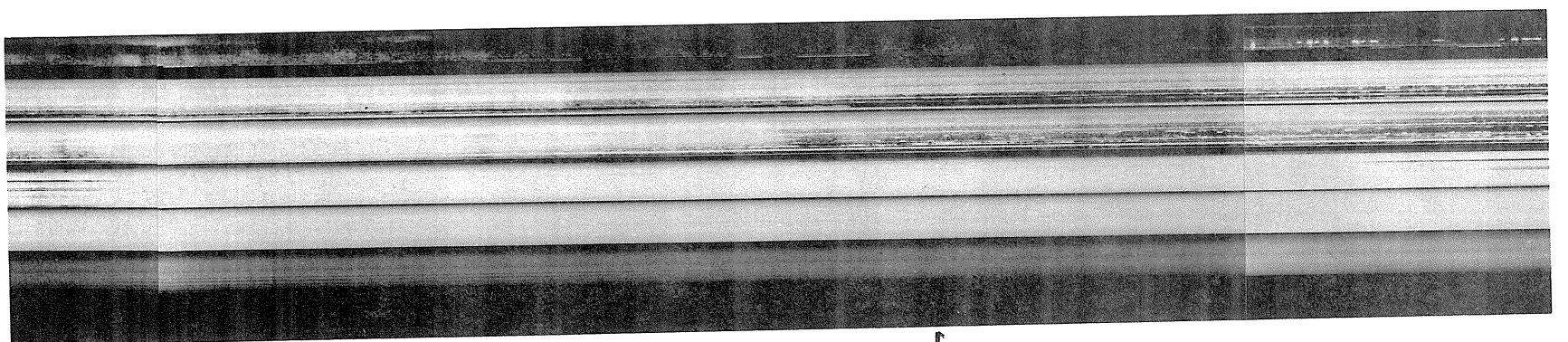

10^h28

10^h33

Fig. 1b. Continuation of Fig. 1a.

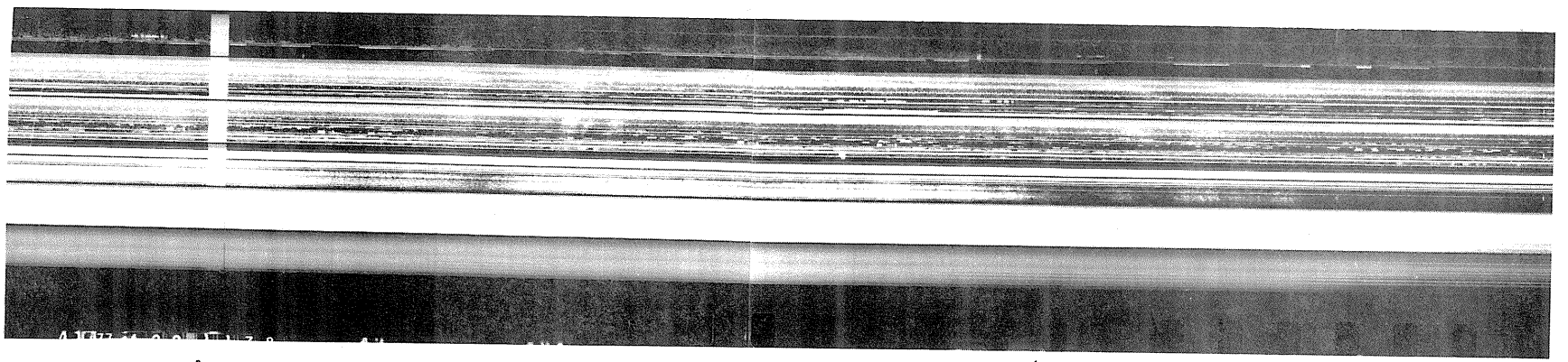

Nov. 22, 1977

Fig. 1c. Continuation of Fig. 1b.

The 120-800 MHz Radio Spectrum of the November 22, 1977 Outburst

by

A.O. Benz and H.K. Asper
Radio Astronomy Group, Microwave Laboratory
ETH, Zurich, Switzerland

Introduction

The Zurich Radio Astronomy Group marked the period from September until November 1977 for instrumental development of the analog as well as the digital radio spectrographs. For this reason little of the solar activity in this interval was recorded. None of the major events and only 22 of the Type III groups were digitally registered and those without polarization. The film recording (analog) instrument took data on the Sept. 9th (1629 to sometime after 1738 UT) and Nov. 22nd (1001 to 1102 UT) events, and it is these two radio bursts that are presented here.

Instrumentation

The Dürnten analog spectrograph [Tarnstrom, 1973] was tuned to sweep the 120-180 MHz range 4 times per second. Threshold sensitivity for film blackening was typically 50 s.f.u. (10^{-22} W/m^2 Hz sec) and saturation occurred at about 200 s.f.u. during this period; however, the gain of the receiver was rather uneven in frequency and produced a banded structure. Low gain bands were 200, 280, 330, 390, 460, 600, 640, and 720 MHz. The rest of the instrument worked satisfactorily.

Description of the Data

The September 9, 1977, event. A weak continuum at decimetric wavelengths suddenly started at 1629.8 UT, showing a tendency to drift from 500 MHz toward lower frequencies between 1631 and 1636 UT (possibly a weak Type II event). The level remained enhanced until sunset at Dürnten (1738 UT). A secondary brightening with maximum at 300 MHz occurred at 1720 UT. The whole event was weak and unimpressive.

The November 22, 1977, event. The radio data of this event are shown in Figures 1a, b, and c. Intensity is shown as bright areas in the frequency-time plane. Narrow band dark and bright horizontal lines are caused by TV or other terrestrial communication transmitters. Camera motion was uneven and produced straight vertical fluctuations of film brightness. Bright vertical lines are time marks of 1 min and the time correction is +1 sec. In the meter and decimeter wavelengths the activity showed three major parts:

The first part (Figure 1a) starts with a group of Type III bursts at 1001.8 UT, which was possibly accompanied by a Type V burst at 100 MHz from 1002.3-1005.5 UT. *Simultaneously* with the start of the Type III bursts a continuum commences with maximum at about 700 MHz. At 1003.4 and 1004.4 UT two drifting bands start at 400 and 700 MHz, respectively. They seem to represent a Type II burst because they continue to lower frequencies, but reports published in *Solar-Geophysical Data* [1978] do not confirm this.

The second part (Figure 1b) with maximum at 1035.5 UT does not drift and is clearly a Type IV event. It starts with seven aperiodic and unequal patches centered on 250 MHz. Contrary to the first part, the major event at 1023.4 UT has a very spiky high frequency boundary. This is especially prominent at 1029.2 UT, where possibly "sudden reductions" occur. Reverse-drift fiber bursts can be seen on the original image from 1043 to 1044 UT above 500 MHz, the frequency of maximum intensity.

The third part (Figure 1c) is much shorter in duration and has five maxima with different spectra. The event has a smooth appearance, but shows considerable fine structure of the fiber type. Again their drift is reversed above the frequency of maximum intensity (e.g. 1059.8-1101.5 UT). It is interesting to note that below the maximum the drift of the fibers is normal. This is also the case in the period 1051.3-1052.0 UT. *These observations represent the first report of a change in the drift of fiber bursts at about the frequency of the spectral maximum.*

The recent modifications of the Dürnten instrument probably make it the most sensitive broadband analog spectrograph operating at decimeter wavelengths. Whether this behavior of fiber bursts is typical or not needs to be investigated in future recordings, especially with the better resolution of the digital instrument. If we assume Kuijpers's [1975] interpretation of this fine structure to be correct, then this observation would show that whistlers are generated at one preferred location, which is close to or identical to the level of maximum Langmuir wave energy density.

Acknowledgment

The ETH radio spectrographs are in part financed by the Swiss National Science Foundation.

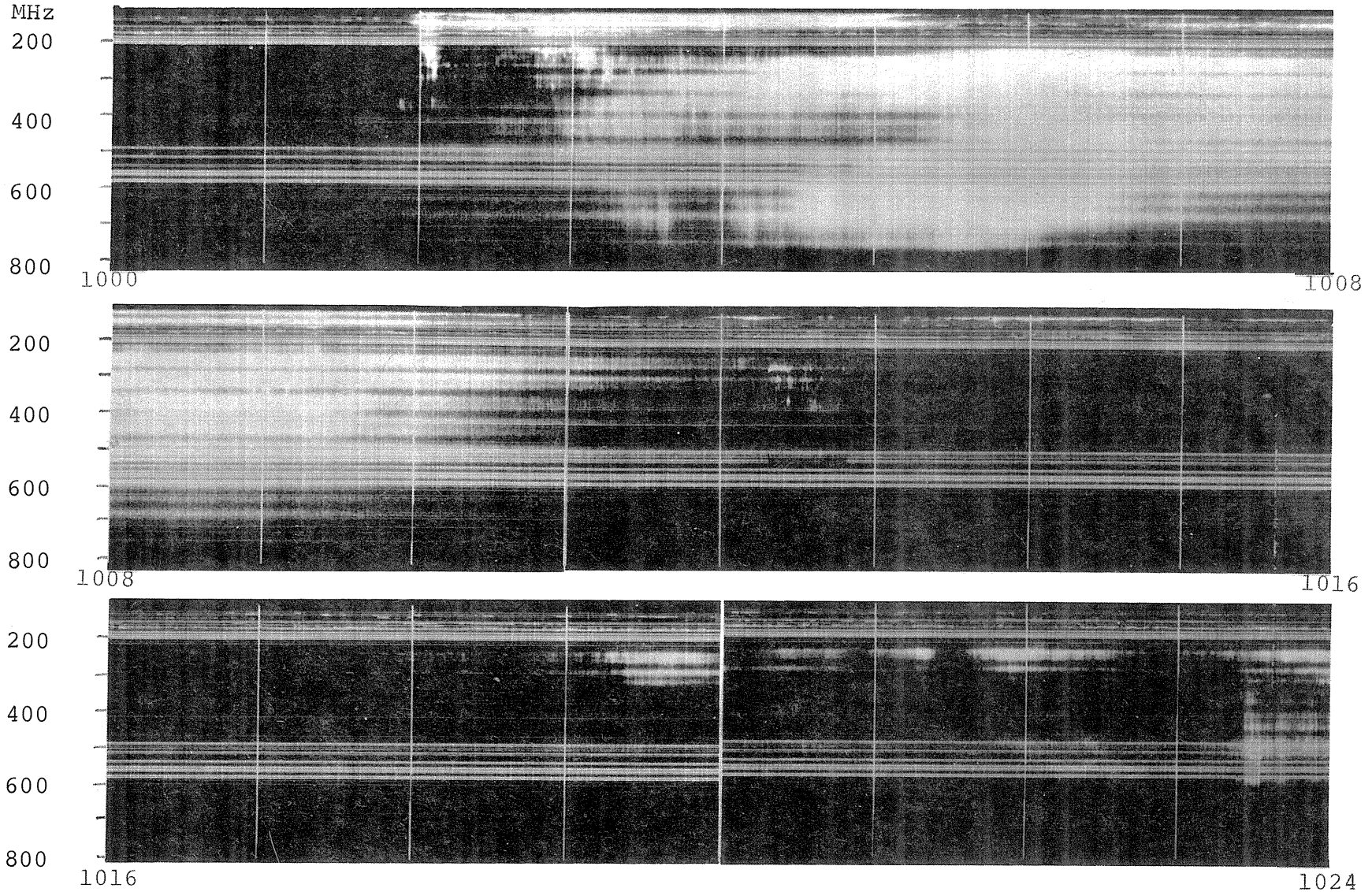

Fig. 1a. Solar radio spectral record of the Dürnten analog spectrograph taken on November 22, 1977. A group of Type III bursts begins at 1001.8 UT. Two drifting bands--one starting at 1003.5 UT and 400 MHz and the other at 1004.4 UT and 700 MHZ--seem to represent a Type II event, but they remain unconfirmed by reports in *Solar-Geophysical Data*.

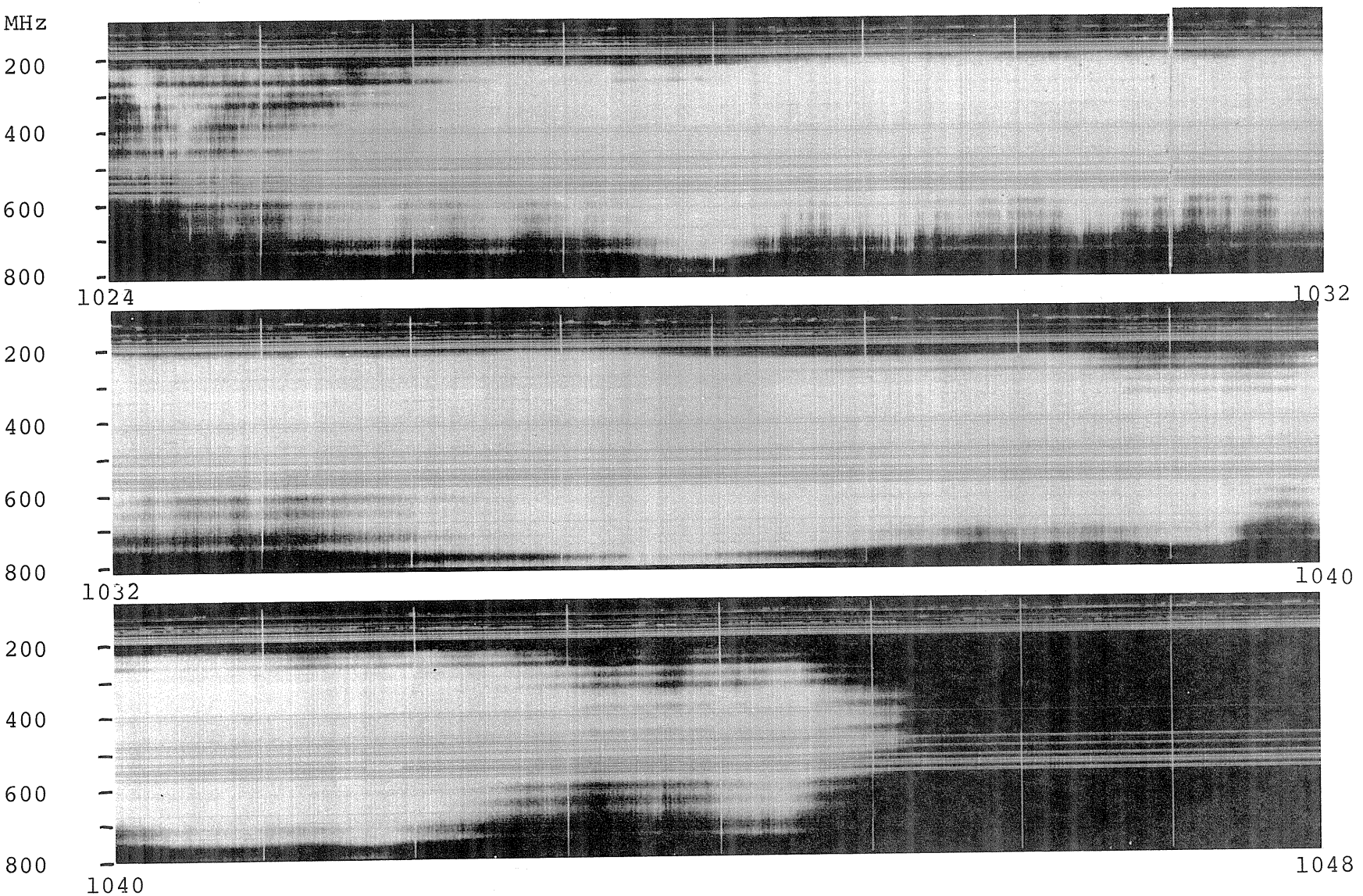

Fig. 1b. A continuation of the November 22, 1977, burst shown in Figure 1a. A clear Type IV event begins at 1023.4 UT, displaying a very spiky high frequency boundary.

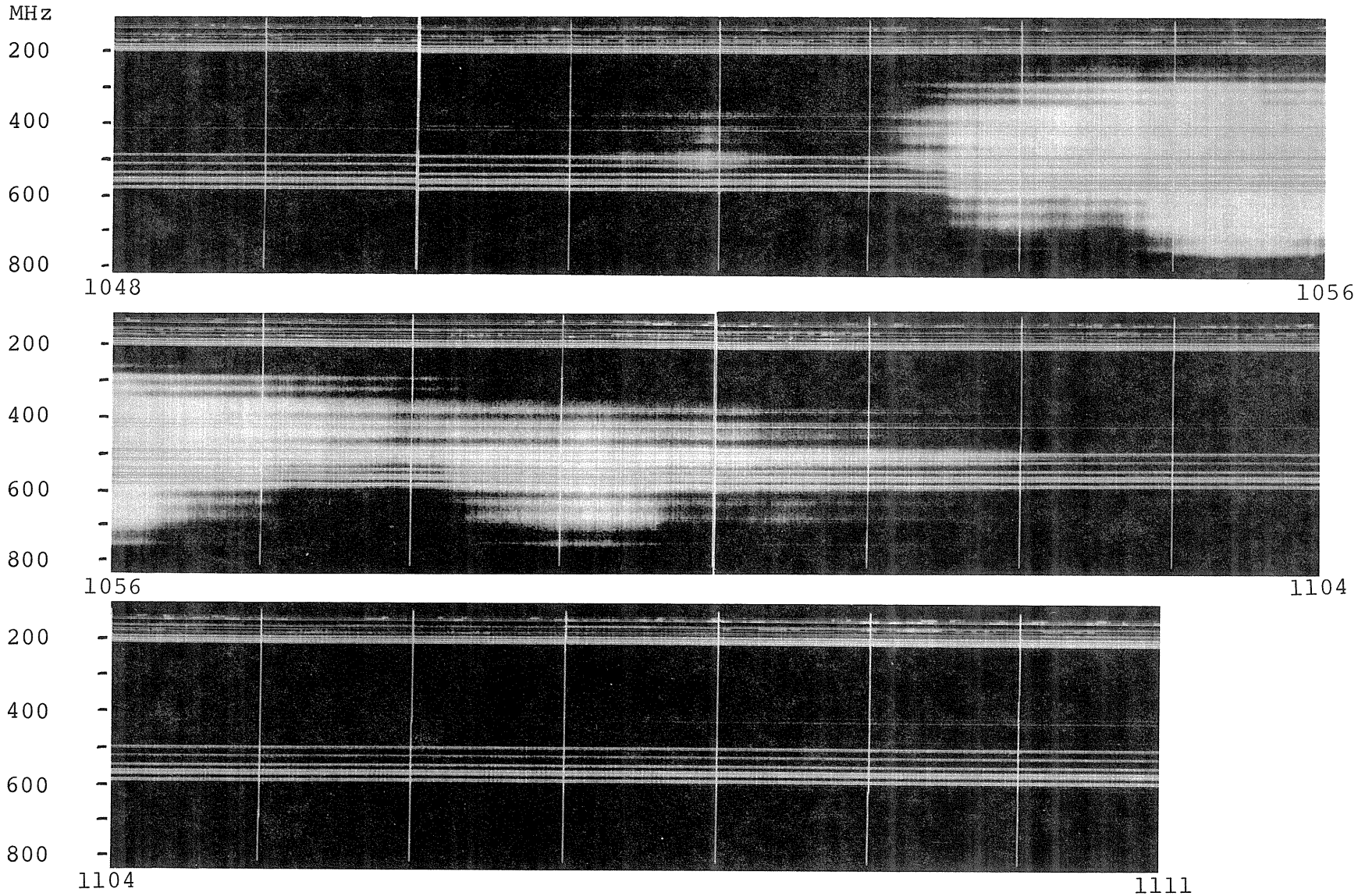

Fig. 1c. A continuation of the November 22, 1977, burst shown in Figure 1b. The event contains considerable fine structure of the fiber burst type. Each fiber burst drifts in reverse above its frequency of maximum intensity and in the normal sense below it.

REFERENCES

KUIJPERS, J. 1975 Generation of Intermediate Drift Bursts in Solar Type IV Radio Continua Through Coupling of Whistlers and Langmuir Waves, *Solar Physics, 44,* 173-193.

TARNSTROM, G.L. 1973 Preliminary Results of the Zurich Radio-Spectrograph, *Astron. Mitteil.* Eidg. Sternwarte Zürich, Nr. 317.

SGD 1978 *Solar-Geophysical Data*, 401 Part I, 104, U.S. Department of Commerce, Boulder, Colorado, U.S.A. 80303.

3. SPACE OBSERVATIONS

Solar Cosmic Rays on November 22, 1977 According to Neutron Component Data

by

A.V. Belov, Ya.L. Blokh, L.I. Dorman, E.A. Eroshenko,
R.T. Gushchina, O.I. Inozemtseva, and N.S. Kaminer
Institute for Terrestrial Magnetism and Radiowave Propagation (IZMIRAN)
Academy of Sciences of the USSR
P.O. Akademgorodok, Moscow Region 142092, USSR

The ground level event (GLE) of November 22, 1977 has been the largest increase of solar cosmic rays on the Earth in solar cycle 21, and at least one of the largest increases since the worldwide network of neutron supermonitor stations began operating. Presented below are the results of preliminary analysis of the neutron component data obtained from the Soviet network of cosmic ray stations, Kiel (Federal Republic of Germany), Lomnicky Stit (Czechoslovakia), and the Soviet station Mirny (Antarctica). The cosmic ray stations whose data are used in the present report are listed in Table 1. Here, A_m expresses the maximum amplitude in percent relative to the 0900-1000 UT value and Δt is the interval of neutron component detection.

Table 1. List of stations and their data that are used in this paper.

Station	Cutoff Rigidity		Geographic Coordinates		Elevation	Commencement Time	Maximum of Increase	A_m (%)	Δt minutes
	Rc_1* (GV)	R_{c_2}** (GV)	Lat,	Long,	h (m)				
1. Mirny	0.04	-	66.92S	93.00E	30	1015±2.5	1055±2.5	20.1	5
2. Tixie Bay	0.53	0.50	71.60N	128.90E	0	1018±2.5	1115±2.5	11.3	5
3. Apatity	0.65	0.65	67.55N	33.33E	182	1022±7.5	1100±7.5	13.9	15
4. Yakutsk	1.70	1.64	62.02N	129.72E	105	1018±7.5	1100±7.5	12.7	15
5. Magadan	2.10	-	60.10N	151.00E	0	1020±7.5	1045±7.5	12.9	15
6. Kiel	2.29	2.25	54.30N	10.10E	54	-	-	4.4	60
7. Sverdlovsk	2.30	2.22	56.73N	61.07E	290	1017±7.5	1045±7.5	8.0	15
8. Moscow	2.46	2.41	55.47N	37.32E	200	1013±2.5	1055±2.5	8.3	5
9. Novosibirsk	2.85	-	54.80N	83.00E	0	1015±2.5	1050±2.5	7.4	5
10. Kiev	3.62	3.51	50.72N	30.30E	120	1018±2.5	1045±2.5	4.4	5
11. Irkutsk	3.66	3.55	52.47N	104.03E	433	1021±2.5	1035±2.5	4.8	5
12. Lomnicky Stit	4.00	3.87	49.20N	20.22E	2632	-	1040±2.5	4.3	5
13. Alma-Ata	6.69	6.64	43.25N	76.92E	806	1018±2.5	1035±2.5	1.0	5
14. Tashkent	6.90	-	41.33N	69.62E	565	-	-	0.3	60
15. Tbilisi	6.91	6.71	41.72N	44.80E	510	-	-	0.4	60

*Calculated by Shea [1972].
**Calculated by Dorman et al. [1972].

The entire set of data was reduced to the same barometric pressure of 985 mb on the basis of the two-component scheme of Kaminer [1967]. The corrected intensity increases at the various stations (in percent of the average value for 0900-1000 UT on November 22) are shown in Figure 1.

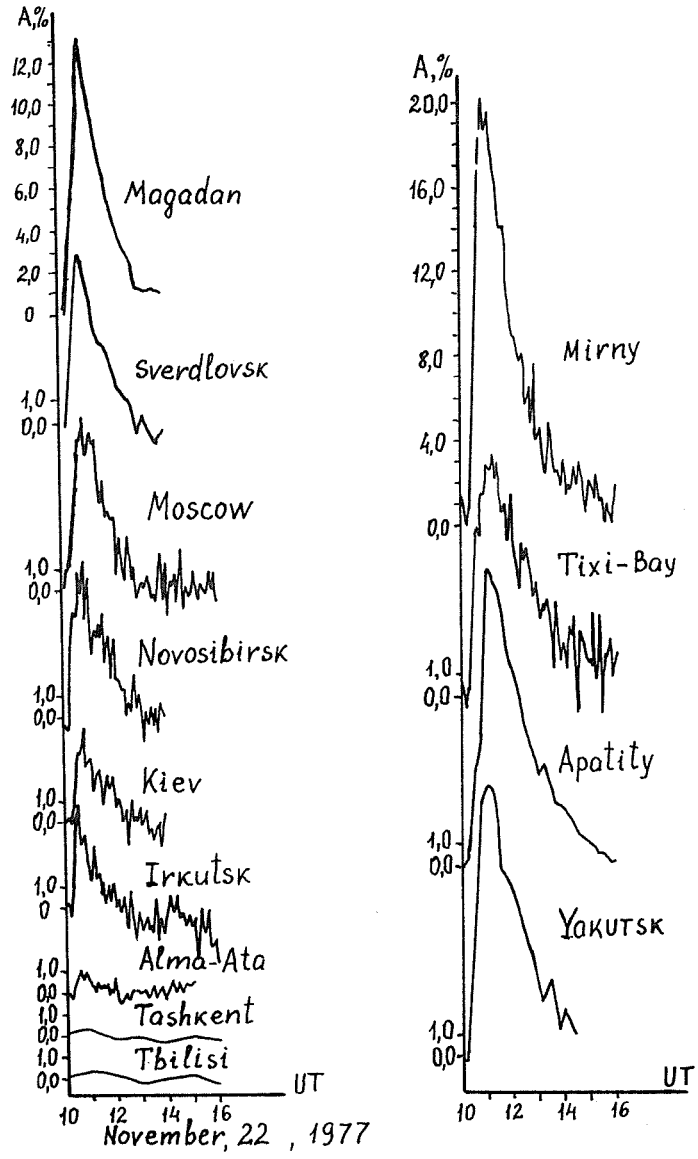

Fig. 1. Time dependence of the amplitude of the GLE (in percent of the average intensity for 0900-1000 UT on November 22, 1977) for various stations.

Since the GLE was large and covered a fairly wide range of cutoff rigidities (up to R_c = 6-7 GV), it proved possible to obtain the solar particle spectrum near the Earth by analyzing the latitude distribution of the effect. The stations located near sea level were selected from the list in Table 1. The values calculated by the method of Dorman et al. [1972] for the variation spectrum $\Delta D/D \propto R^{-4}$ were taken (ΔD= differential energy spectrum) on the basis of preliminary estimates of the spectrum, as effective cutoff rigidities. The expected increase was calculated using the formula

$$\frac{\Delta I}{I} = \frac{\int_{R_c}^{\infty} m(R)\,\Delta D\,(R)\,dR}{\int_{R_c}^{\infty} W\,(R)\,dR} \qquad (1)$$

The solar cosmic ray spectrum was set in the form $\Delta D(R)=aR^{-\alpha}$. Use was made of the integral generation multiplicity m(R) obtained as by Quenby and Webber [1959] on the basis of the data for the flare of February 23, 1956. The coupling coefficients for 1968 [Bednazhevsky, 1973], the year in which the latitude dependence of neutron component was similar to that in 1977, were also used.

Figure 2 shows the calculated curves for two forms of the spectrum, $\Delta D(R) \propto R^{-5}$ and $\Delta D(R) \propto R^{-6}$, and for two moments of time, 1100-1200 UT and 1300-1400 UT. The Figure also presents experimental data. The dependence of the amplitude increase on cutoff rigidity for 1100-1200 UT corresponds to the exponent of differential rigidity spectrum α=5.5±0.5. Probably, the spectrum becomes flatter with decreasing rigidity. At 1300-1400 UT the exponent α for 1-2 GV is again near 5.5, whereas the spectrum for rigidities R > 2 GV is steeper (α=7-8). Thus, the rate of the high-rigidity particle ejection from the Sun's vicinity is higher.

It can be seen from Table 1 and Figure 1 that the time dependence of the intensity is characteristic of increases from western flares. We can see the rapid arrival of the particles at the Earth, the rapid rise, and rapid fall of the intensity. It may be asserted that a noticeable bulk of the solar particles was already stored near the Earth at 1020 UT. To specify the time, t_i, of the increase commencement, we extrapolated the dependence of integral effect in the intensity at some stations [Santochi et al., 1960]. The material available to us has proven to be insufficient to reveal any relationship of t_i to cutoff rigidity or the coordinates of the stations. By averaging the integral effect over all the stations with a 5-min interval of monitoring, we have obtained $\bar{t}_i=(1015\pm2)$ UT as the most probable time of the increase commencement on the Earth. Therefore, we have every reason to assume that the 1-5 GeV particle generation began prior to the occurrence of Hα-line intensity maximum.

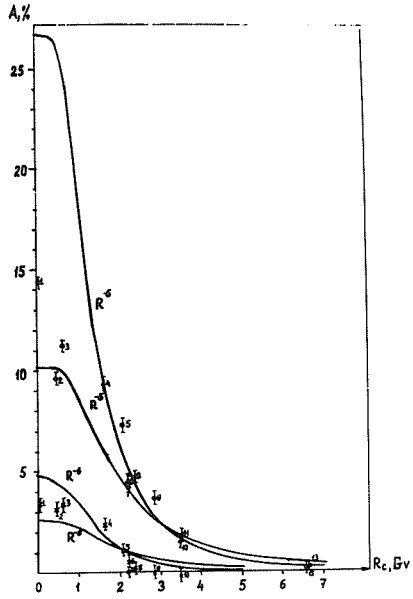

Fig. 2. Latitude dependence of the increase. The experimental data for 1100-1200 UT and 1300-1400 UT are marked with dots (.) and crosses (x) respectively. The numerals are the station numbers listed in Table 1. The solid curves present the results of calculations on the basis of formula (1) for two forms of the spectrum for those hours.

Figure 3 shows the times, t_i, of the increase commencement and the times, t_m, of the intensity maxima at various stations. Duration of the intensity increase phase is 40-50 min for the stations with low cutoff rigidities and about 20 min for the medium-latitude stations. Thus, 15-20 min probably may be considered the upper limit of duration of high-energy particle generation in the given flare.

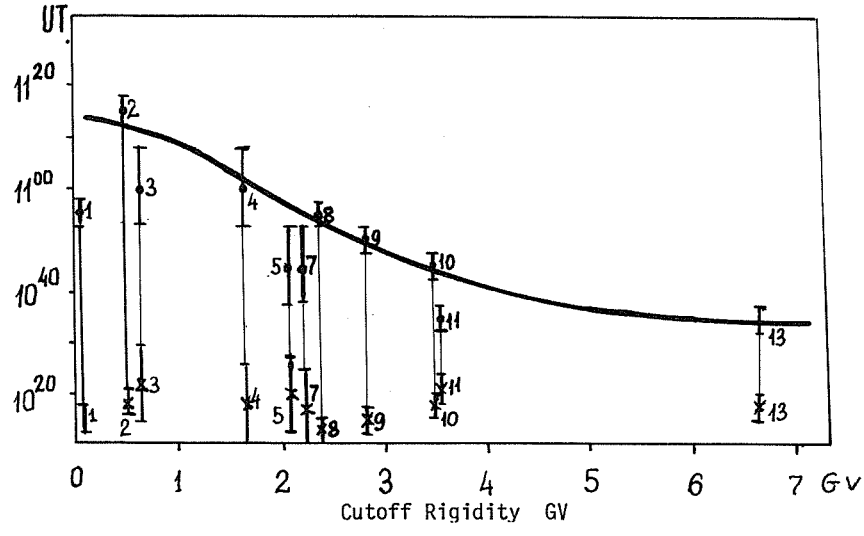

Fig. 3. The increase from onset time t_i indicated by x, to the effective maximum time t_m, indicated by ., according to the data from various stations. The solid curve shows the calculated dependence of t_m on cutoff rigidity.

The knowledge of $\Delta D(R)$ permits the use of the data on t_m to estimate the energy dependence of the parameters characterizing the solar particle propagation in interplanetary space. Let the time for the particles with rigidity R to reach their intensity maximum near the Earth be $\tau(R)$. Then the maximum at a station with rigidity R_c will be reached within time

$$\tau_c = \frac{\int_{R_c}^{\infty} \tau(R)\, m\,(R)\, \Delta D\,(R)\, dR}{\int_{R_c}^{\infty} m\,(R)\, \Delta D\,(R)\, dR} \qquad (2)$$

after the time of the maximum particle generation in the flare. By comparing τ_c so obtained with the data from various stations, we have found the best agreement for

$$\tau(R) = \tau_0 (R/3)^{-\beta}$$

(the solid curve in Figure 3), where $\tau_0 = 45 \pm 5$ min and $\beta = 0.5 \pm 0.2$. In terms of the three-dimensional isotropic diffusion [Dorman and Miroshnichenko, 1968] this fact would mean that the diffusion coefficient for solar particles is

$$H(R)=(2\pm1)10^{22}\ (R/3)^{0.5\pm0.2}\ \text{cm}^2/\text{s}$$ in the 2 to 6 GV rigidity range.

The time dependence during intensity decrease was examined by considering two laws of the decrease, namely e^{-t/t_0} and $t^{-\mu}$. The results of correlation analysis are summarized in Table 2. The decrease is in rather good agreement with the exponential law. At the same time, the decrease is close to the law $t^{-3/2}$ corresponding to three-dimensional isotropic diffusion. The increase in the decrease rate in time is probably indicative of an increase of the diffusion coefficient when moving away from the Sun.

Table 2. The Results of Correlation Analysis

Station	UT	e^{-t/t_0}		μ	$t^{-\mu}$
		t_0 minutes	correlation coefficient		correlation coefficient
Mirny	1100-1300	82±4	0.96±0.01	1.3±0.1	0.95±0.01
	1300-1500	112±12	0.67±0.07	2.1±0.5	0.67±0.07
	1100-1500	88±4	0.94±0.01	1.8±0.1	0.94±0.01
Kiev + Irkutsk	1045-1210	58±6	0.87±0.04	1.4±0.2	0.87±0.04

The deviation of the experimental points from the expected curves in Figures 2 and 3 is mainly due to anisotropy of the solar particle intensity. To estimate the value of the anisotropy and to determine the anisotropic phase duration, we found the amplitude differences at stations with similar R_c. It may be concluded already on the basis of our experimental data (only the data for the longitude interval from 10°E to 151°E were available to us) that the degree of the anisotropy reached at least 40%. It will be noted that the anisotropic phase of the flare lasted until approximately 1230 UT.

For the 13th hour when the increase became almost isotropic, we made an attempt to determine the effective absorption path λ_s, of solar cosmic rays in the Earth's atmosphere [Kaminer, 1967]. At that a time the effect was sufficiently large for high latitudes only, so we used the data from Mirny, Apatity, and Tixie Bay. Correction for the difference in cutoff rigidities and for the diurnal variation determined on subsequent days and hours of November 22, which were free of the flare particle effect, was inserted when comparing the barometric effects at the various stations. It has been found λ_s=95 g/cm^2 and ranges between 120 and 80 g/cm^2 for one standard deviation to either side.

Figure 4 presents the intensity increases for neutrons of various multiplicities, K. The effect can be clearly seen for $K \lesssim 3$, whereas for greater K the increase is comparable with statistical error. The intensity increase for $K \lesssim 3$ in the given flare is so significant that, if the solar particle spectrum is known, the data for the given flare can be used to find the coupling coefficients of "multiple" neutrons in the low-rigidity range where the conventional determination of the coupling coefficients is difficult to obtain because of the latitude effect.

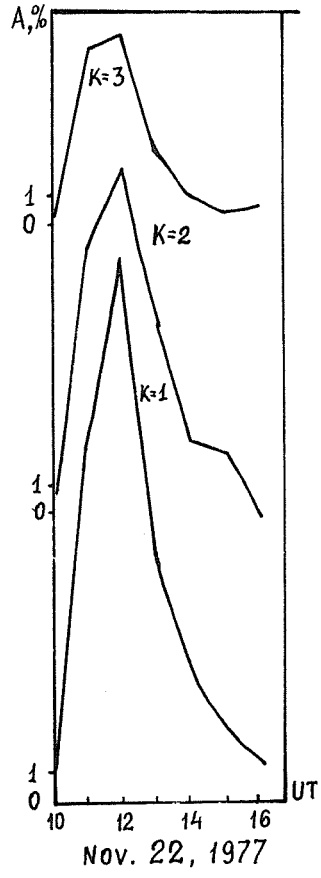

Fig. 4. Time dependence of intensity increase in neutrons of various multiplicities at Mirny.

References

BEDNAZHEVSKY, V.M. 1973 Studies of Cosmic Rays onboard Research Ship "Academik Kurchativ", Theses, Institute of Nuclear Physics, Moscow State University.

DORMAN, L.I., R.T. GUSHCHINA, M.A. SHEA and D.F. SMART 1972 Effective Cosmic Ray Cut-off Rigidities, Nauka, Moscow.

DORMAN, L.I. and 1968 Solar Cosmic Rays, Nauka, Moscow.

KAMINER, N.S. 1967 Allowance for the Barometric Effect of the Neutron Component During Cosmic-Ray Bursts, Geomagn. i Aeron., 7, No. 5, 656.

QUENBY, J.J. W.R. WEBBER 1959 Cosmic Ray Cut-Off Rigidities and the Earth Magnetic Field, Phil. Mag., 4, 654.

SANTOCHI, O.R., J.R. MANZANO and J.R. ROEDERER 1960 Cosmic Ray Increase on May 4, 1960, Nuovo Cimento 17, 119-121.

SHEA, M.A. 1972 Ground-Based Cosmic Ray Instrumentation Catalog, Air Force Cambridge Research Laboratories, Bedford, Massachusetts, USA.

X-Radiation from the November 22, 1977, Flare as Measured Aboard the Prognoz 6 Satellite

by

B. Valníček, F. Fárník and L. Křivský
Astronomical Observatory, Czechoslovak Academy of Sciences
Ondřejov, Czechoslovakia

O. Likin and N. Pisarenko
Space Research Institute
Academy of Sciences of the USSR, Moscow

The X-Ray Profile

We succeeded in tracking the course of the November 22, 1977, flare in x-rays with our x-photometer on board the Prognoz 6 satellite. Prognoz 6 has an apogee of 200,000 km (62.7 Earth radii). With two counters the photometer makes measurements in 6 energy windows, the upper and lower bounds of which are shown in Table 1. [Valníček et al., 1978].

Table 1. Characteristics of X-Ray Photometer Aboard Prognoz 6.

Detector	Passband (keV)	Channel ID	Response Time	Dynamic Range (cts/s)
Proportional Counter (Be window)	2.2 - 7	X6	10s	$10-10^4$
Scintillator NaI (Te)	6 - 10	X1	10	$10-10^4$
	10 - 19	X2	40	$10-10^4$
	19 - 39	X3	40	$1-10^3$
	39 - 58	X4	40	$1-10^3$
	58 - 98	X5	10	$1-10^3$

The course of the November 22, 1977, event approximately followed the outline given below (see Figure 1).

0947 UT Hint of an increase on channels X1 and X6.
0949 Sudden increase in x-emission began on X1, X2, X3 and X6.
0951 First emission peak; X1, X2 and X3 channels reached their first maximum, which lasted until 0959 UT.
1000 Another increase began on channels X1, X2, X3, X4 and X6.
1001 X1 and X6 channels saturated.
1003 Saturation of channel X3; X3, X4 and X5 increased.
1004 First maximum of X5.
1006 Second maximum of X5.
1008 Emission ended in X4 and X5.
1023 Signal in X5 indicated arrival of first particles.
1040 Signal in X4 indicated particle arrival.

After 1040 UT signal levels varied insignificantly with the exception of the X6 channel: it continued declining while the other hard components remained relatively constant.

Particle Acceleration

The x-ray record corresponded to the radio emission profile registered at Tremsdorf station [HHI, 1977]. At 1,470 and 3,000 MHz the emission began at 0946.5 UT. SIDs began at 0948 UT [SGD, 1978]. During this phase of the event, the plasma was apparently thermalized. The onset of the emission on the high energy channels corresponded, in all probability, to the particle acceleration phase in the active region. In this particular case this phase lasted for 5 min, ending at 1008 UT. It is interesting that the fine structure of the X4 and X5 channels showed a double maximum; the first one at 1004 UT, however, was more prominent. Since the NaI scintillator registers particles as well, the signal increase in the X5 channel after 1023 UT probably corresponds to the rise in cosmic ray intensity registered at Lomnicky Stit between 1020 and 1025 UT [Dubinský et al., 1981].

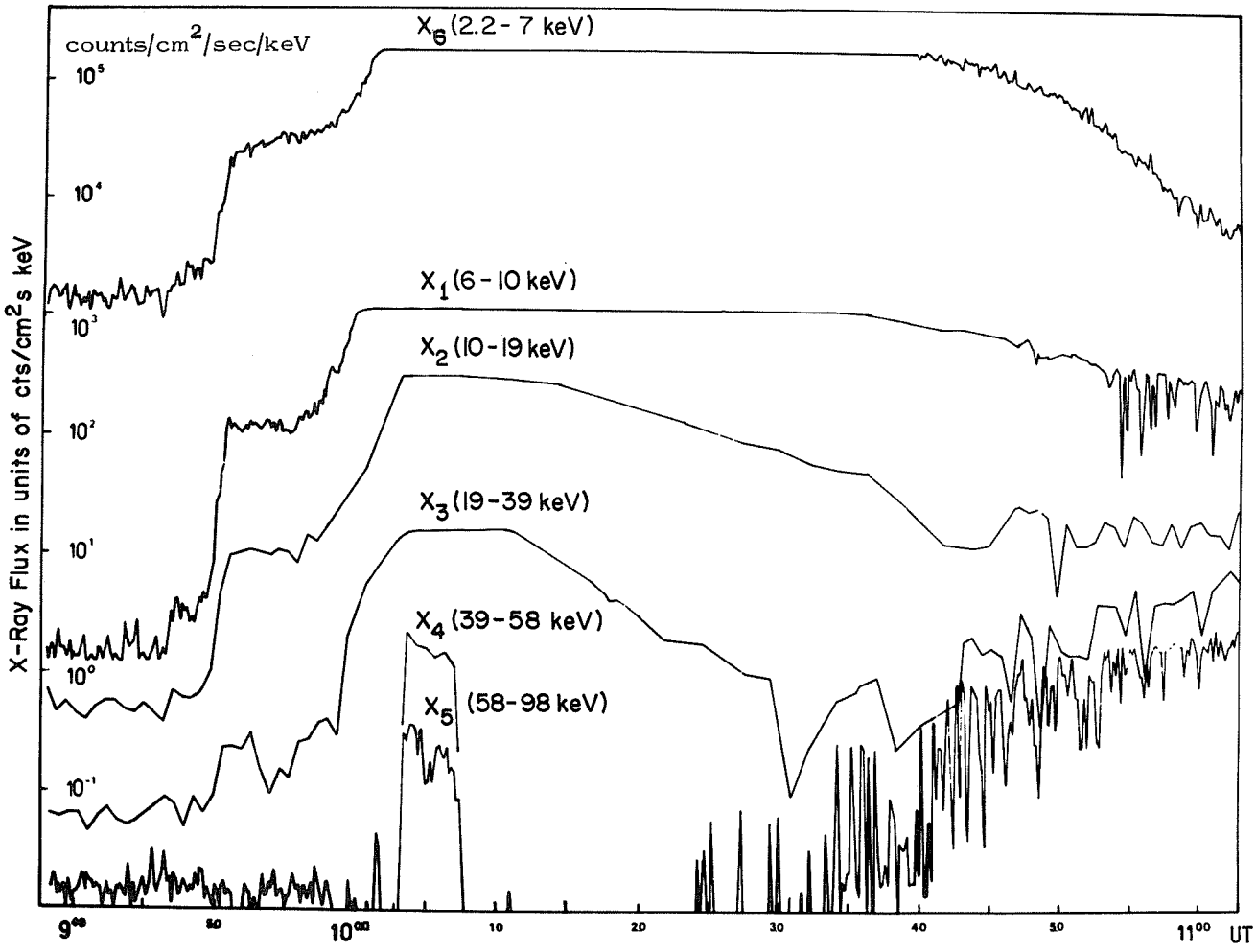

Fig. 1. X-ray profile of the November 22, 1977, 2b flare as recorded by the Prognoz 6 x-ray photometer. Increases in the X4 and X5 channels near 1005 UT indicate the flare's particle acceleration phase. The onset of a ground level event recorded at Lomnický Štít corresponds to the X5 signal increase that appears in the figure at 1023 UT.

After accounting for the finite speed of light, we get 0955 UT as the start time of the particle emission, which means that the fastest particles reached Earth in 28 min--a speed of about 90,000 km/s or 0.3c. When we compared the measurements of this flare with the proton flare of August 7, 1972, we found a similar train of events, a hard x-emission with several maxima, and an arrival of particles recorded by an apparatus similar to ours [Alberhene, et al., 1977].

REFERENCES

ALBERHENE, F., J. VEDVENNE, P. CAMBOU, M. KUDRYAVCEV, O. LIKIN, A. MELIORANSKY, N. NAZAROVA, V. PANKOV, N. PISARENKO D. SAVENKO, R. TALON and V. SHAMOLIN — 1977 — Problemy solnetschnoj aktivnosti i kosmicheskaya sistema "Prognoz," Moscow, 1977, p. 30.

DUBINSKÝ, J., J. ILENČÍK, J. STEHLÍK and L. KRIVSKÝ — 1981 — Increase of Solar Cosmic Rays on Nov. 22, 1977, and Determination of the Ejection Phase, in this issue.

HHI 1977 *Heinrich Hertz Institut Solar Data, 28,* 92.

SGD 1978 *Solar-Geophysical Data*, 401 Part I, 101, January 1978 (U.S. Department of Commerce, Boulder, Colorado, USA 80303).

VALNÍČEK, B., F. FÁRNÍK, B. KOMAREK, O. LIKIN and N. PISARENKO 1979 Long-term Measurements of Solar X-rays Onboard the Satellites Prognoz 5 and Prognoz 6, *Bull. Astron. Inst. Czech., 30, no.3,* 171-173.

Fluxes and Spectra of Solar Energetic Particles during November 22, 1977 by "Prognoz-6" Data

by

E.A. Devitcheva, O.R. Grigoryan, V.G. Kurt, Yu.I. Logachev,
V.F. Shesterikov, and V.G. Stolpovsky

Institute of Nuclear Physics, Moscow State University
Moscow 117234, USSR

Introduction

This report presents some data on the solar electron and proton fluxes measured by an instrument on the Prognoz-6 satellite following the Western Hemisphere at N15W40 importance 2b-3b solar flare of November 22, 1977. Prognoz-6 satellite was launched on September 23, 1977, in a highly eccentric orbit with an apogee about $32R_E$ and 65° inclination to the equatorial plane. During the first two days of the discussed event Prognoz-6 was in the interplanetary medium outside of the Earth's magnetosphere.

The detectors used on board Prognoz-6 were a set of G-M, semiconductor scintillation counters, covering a wide range of electron, proton and alpha particle fluxes in the energy range from 10 keV to 100 MeV with time resolution from 10s to 300s.

The Nuclear Physics Institute instrument on Prognoz-6 has been reported in the article Kurt et al. [1981] of this issue, p.

Particle Observations

The solar flare of November 22, 1977, was of great importance and was followed by X-ray and radio bursts. This event was accompanied by particle accelerations up to relativistic energies. Proton flux enhancement from this flare for E_p>100 MeV was 10^2 $cm^{-2}s^{-1}$. The high-energy particle enhancement from the flare was also clearly observed at sea level.

Figure 1 shows five-minute averages of the counting rates of G-M counters with different shielding (aperture ≈3.8 cm^2sr). The energies of protons and electrons penetrating the shielding is given on the figure. It can be seen from the figure that the curves are of diffusive form with the times of maxima corresponding to the proton energy. The sharp increase at the onset phase for Ep>30 MeV and Ep>15 MeV can be explained by the electrons and bremsstrahlung-produced contamination.

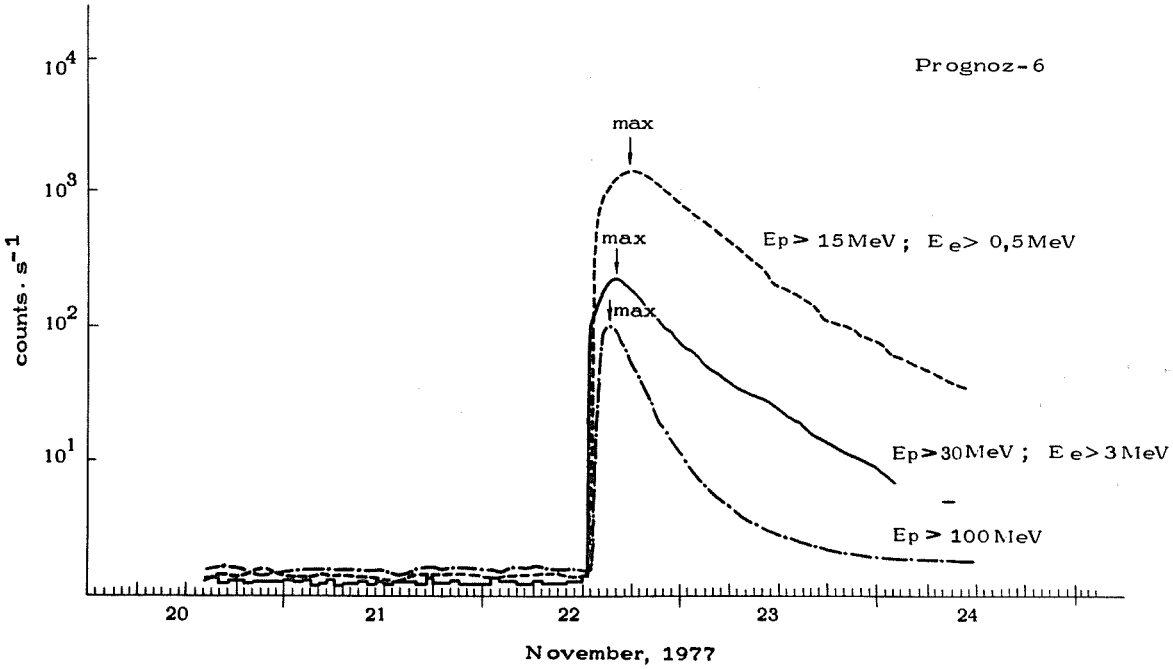

Fig. 1. High-energy proton and electron flux enhancements observed on Prognoz-6 following solar flare of November 22, 1977.

In Figure 2 Prognoz-6 half-hourly average counting rates are plotted: 1) protons Ep~1.4-5.8 MeV(p) (semiconductor detector with aperture G≈7x10^{-2}cm^{2}sr); 2) electrons, Ee>30 keV(e1) (detector with backward electron scattering effect from a surface with a high atomic number Geff≈0.1cm^{2}sr); 3) electrons Ee~10-30 keV(e2) (proportional counter, G≈10^{-2}cm^{2}sr). Also in this figure is shown the counting rate of electrons with Ee 0.3-1.3 Mev obtained with the help of experiment Gemaux S2 [Pissarenko et al., 1978].

The enhancement value of these counting rates covers 3 decades and curve form is also diffusive.

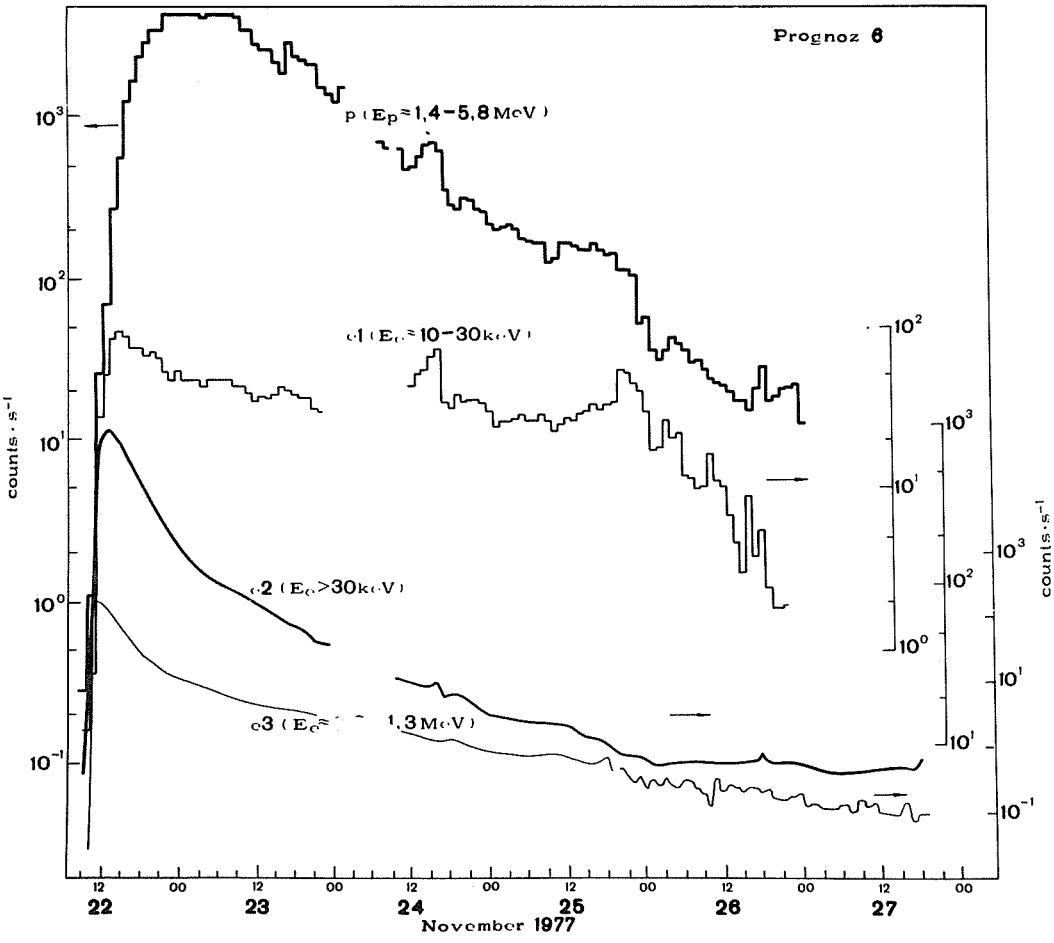

Fig. 2. Prognoz-6 half-hourly average counting rates November 22-27, 1977 for protons and electrons (curves P e^1, a^2). Curve e^3 is the counting rate from experiment Gemaux S2.

Figure 3 presents the proton counting rates for Ep>100 keV(Po) (proportional counter, G≈10^{-2}cm^{2}sr); Ep 0.12 - 0.22 MeV(p2); Ep 0.22 - 0.39 MeV(p3) (two energy channels of open semiconductor detector, G≈6x10^{-2}cm^{2}sr) and Ep 7-20 MeV(p6) (wide angle semiconductor telescope, G≈4.0 cm^{2}sr).

From this figure it can be seen that the amplitude of effect is 10^3 and form of the curve for Ep 7-20 MeV is diffusive. The time variations of proton fluxes with Ep<1 MeV and electron fluxes with Ee 30 keV (Fig. 2) near the Earth are more complicated.

The analysis of the time variations of the low-energy particle fluxes in this event is presented in the article Kurt et al. [1978].

The onset times on the November 22 event can be seen in Figure 4. To draw this figure we used data with a time resolution of ≈150-300s. From this figure you can see that relativistic particles appeared near 1 AU not earlier than 1016 UT on November 22. Also from this figure the arrival time of the particles differs with the different particle energies.

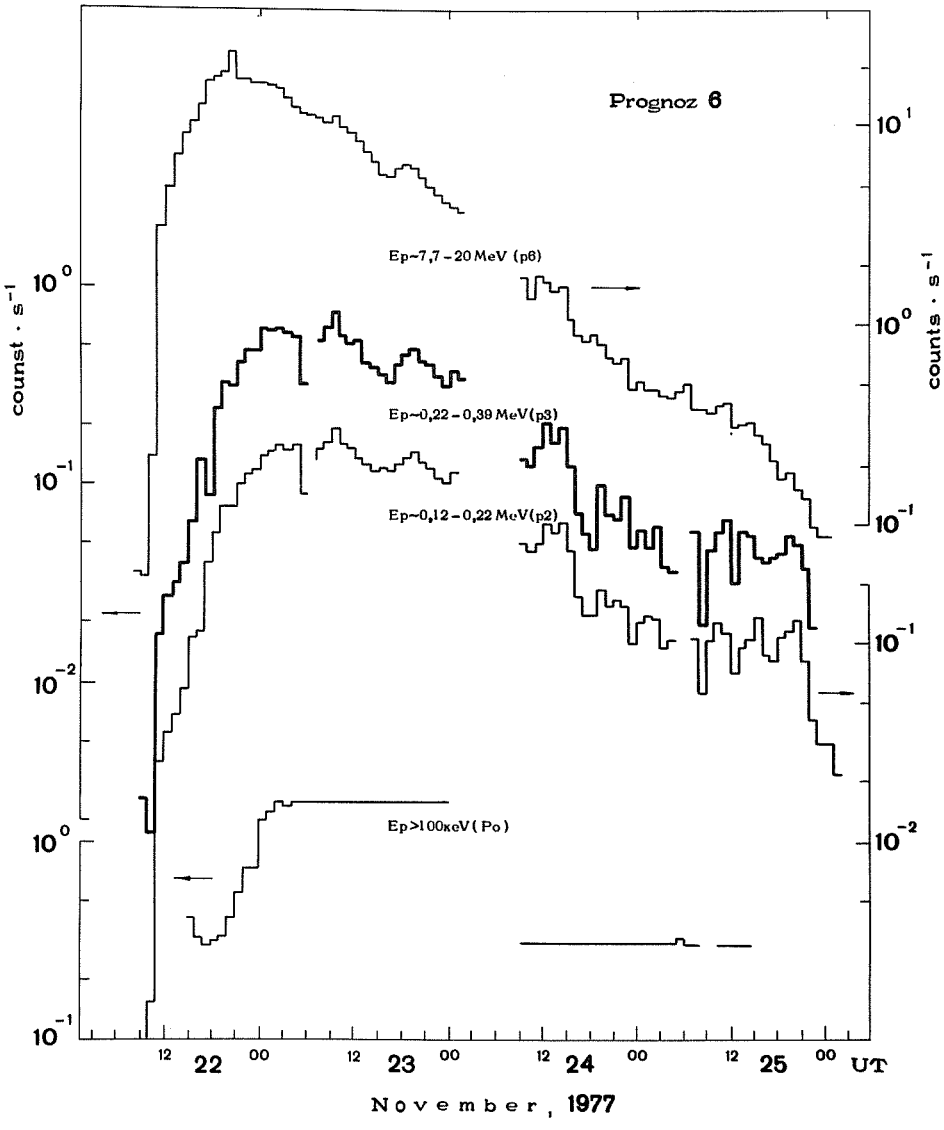

Fig. 3. Prognoz-6 low energy proton counting rates November 22-25, 1977.

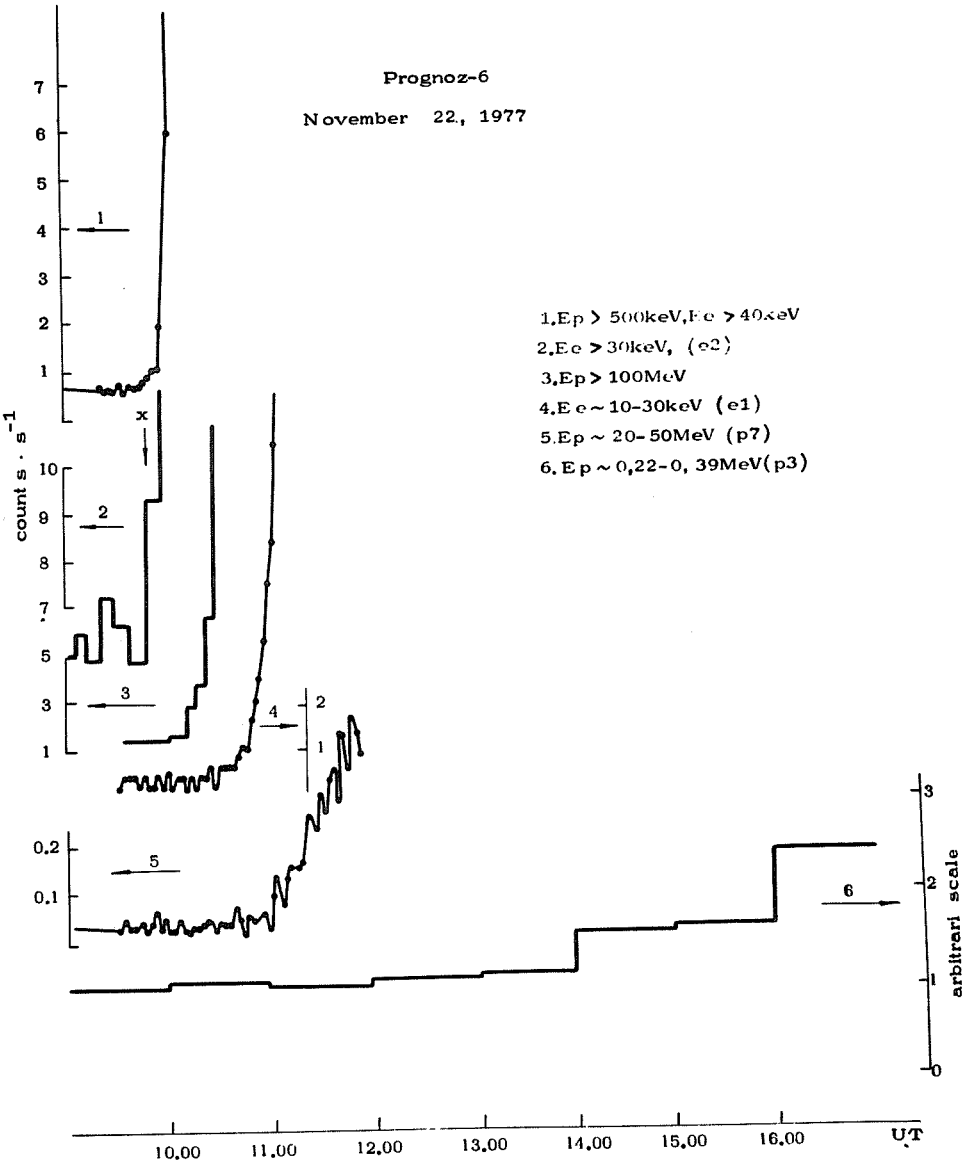

Fig. 4. Onset time for arrival of particles of different energies observed by Prognoz-6 on November 22, 1977.

The electron and proton energy spectra presented in Figure 5 have been constructed from the peak intensities of different energies. These spectra were obtained by the following procedure: first the integral detectors' data were used to estimate the spectral indexes; then this estimate was used for comparison with particle fluxes measured by differential detectors; next we calculated differental spectral index γ, effective energetic intervals $\Delta E_{eff.}$ for every channel of our detectors. It is not difficult to show that in the case of power spectrum $\Delta E_{eff.} \approx E_{d/\gamma-1}$, where E_d is the given discriminator level of detector.

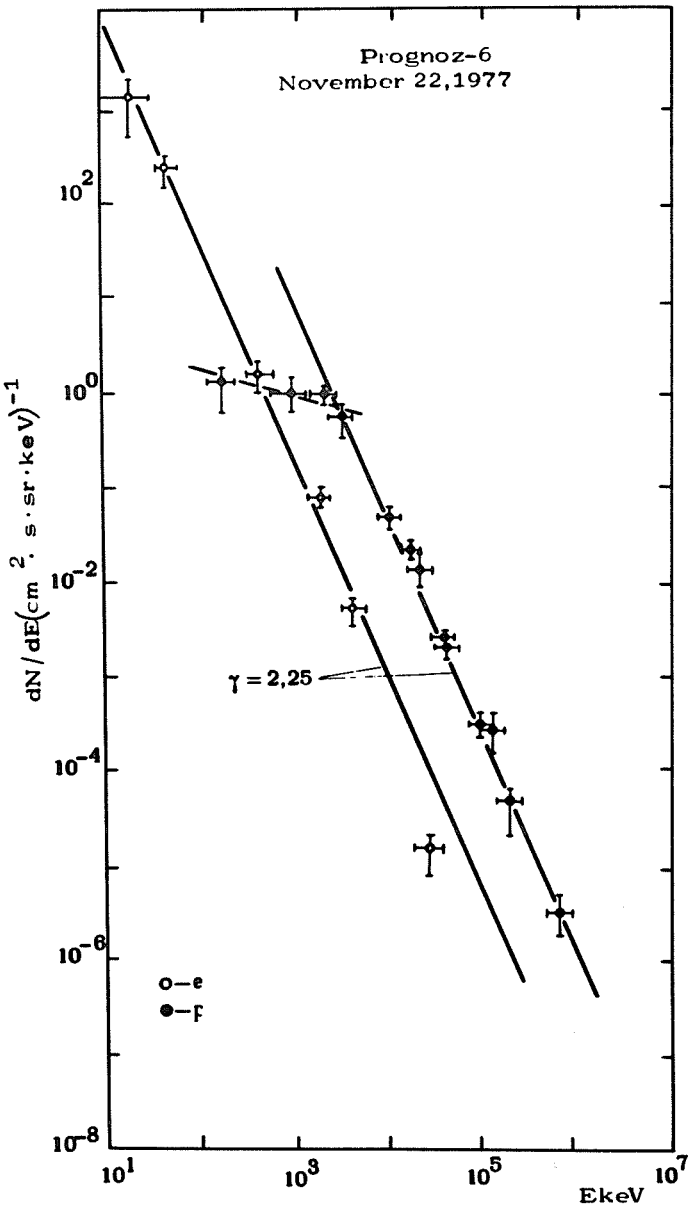

Fig. 5. Energy spectra of protons and electrons during November 22, 1977, event.

The spectra on Figure 5 were constructed from data obtained by the experiment of Nuclear Physics Institute and experiment Gemaux [Kurt et al., 1978]. The electron spectrum has a power law $dJ/dE \alpha E^{-\gamma}$ with $\gamma \approx 2.25$ at energies $E_e > 10$ keV; the proton spectrum has the same form at energy $E_p \geq 1$ MeV. At lower energies the proton spectrum has a smaller index γ.

REFERENCES

KURT, V.G., et al.	1981	in this issue
KURT, V.G., et al.	1978	Presented on XXI COSPAR Meeting, Innsbruck, Austria, May 29-June 10, 1978, article II, 2.5.
PISSARENKO, N.F., et al.	1981	in this issue

4. COSMIC RAYS

Energy Spectrum of Solar Particles on November 22, 1977

by

G.V. Skripin, V.A. Filippov, and A.N. Prikhod'ko
Institute of Cosmophysical Research and Aeronomy, Yakutsk Branch
Siberian Department of the USSR Academy of Sciences, Yakutsk, USSR

The solar cosmic ray flare from neutron monitor data is analyzed. Energy spectrum $D(\varepsilon)=\varepsilon^{-\gamma}$ softens with time and has $\gamma = 2$ at the flare beginning, $\gamma = 4$ at the period of maximum intensity and $\gamma = 5$ at the flare end. Propagation region of solar particles reaches the distance $r_i = 1.7$ AU.

Data from neutron monitors at the stations Yakutsk, Oktyomtsy (55 km south of Yakutsk), Tixie Bay, Magadan, Novosibirsk, Irkutsk and data of muon telescopes on the ground and at depths 7 and 60 m w.e. in Yakutsk are given in Fig. 1 for November 27, 1977.

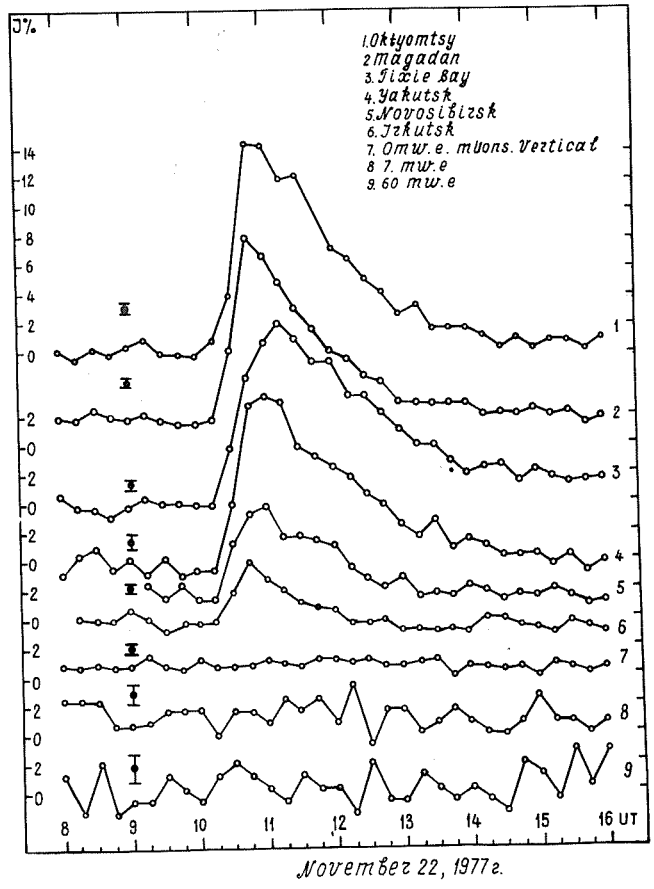

Fig. 1. (1-6) Data of the Oktyomtsy, Magadan, Tixie Bay, Yakutsk, Novosibirsk, Irkutsk neutron monitors and data of muon telescopes on the Earth's surface (Z_0) and at depths 7 and 60 m w.e. (Z_7; Z_{60}) in Yakutsk on Nov. 22, 1977.

Amplitudes (in %) of increase of solar prticles which began at 1015 UT and finished at 1300 UT on Nov. 22, 1977 for different UT intervals are given in Table 1.

From Fig. 1 and Table 1 it is seen that the increase amplitude is almost the same at initial moment of the flare from 1015 to 1030 UT at the stations Tixie Bay, Magadan, Oktyomtsy and Yakutsk. In this period the intensity increased up to 4%, the same increase was observed at the station Apatity. This fact shows that from the very beginning of the flare the solar particles had an isotropic distribution. At this time a comparatively large increase was observed by the middle-latitude stations Novosibirsk and Irkutsk.

Table 1

		Time Interval UT			
		1015-1030	1030-1100	1100-1200	1200-1300
1.	Oktyomtsky	4.04±0.29	14.44±0.21	10.41±0.16	3.11±0.16
2.	Tixie Bay	3.92±0.29	10.03±0.20	10.95±0.15	4.90±0.15
3.	Yakutsk	3.99±0.50	11.19±0.38	8.21±0.27	2.80±0.27
4.	Magadan	4.72±0.30	11.89±0.21	6.95±0.51	1.77±0.15
5.	Moscow	2.92±0.32	6.84±0.32	4.68±0.16	1.06±0.16
6.	Novosibirsk	3.34±0.29	5.64±0.21	3.34±0.15	0.69±0.15
7.	Irkutsk	1.87±0.27	3.47±0.19	1.21±0.13	0.17±0.13

For the next half an hour (1030-1100 UT) the largest increase of 14.5% was registered by the Oktyomtsy neutron monitor. Some time later the flare maximum was at Tixie Bay. Beginning with 1100 UT the increased amplitude started to diminish. And it was the slowest at Tixie Bay where the effect finished at 1500 UT but at Irkutsk and Novosibirsk the increase was over at 1300 UT.

During the whole flare the muon telescopes did not register any increase and this can be explained by the absence of solar particles with energy more than 5 GeV. As mentioned above behavior of the increase effect given earlier Prikhodko et al. [1978] testifies to difference of the energy spectrum of solar particles at different flare periods.

In Table 2 are presented stations, threshold rigidities R_c [Buhmann et al., 1974], average counting rate N_1 an hour before the flare reduced to 1000 millibar pressure level, conditional thickness of additional absorber above the monitor h_1 and the relative counting rate N_i/N_o.

Table 2

	Stations	R_c GeV	N_1, hour^{-1}	h_1, g/cm^2	N_i/N_o
1.	Oktyomtsy 12NM-64	1.75	412000	4	1
2.	Tixie Bay 18 NM-64	0.49	470000	43	0.76
3.	Yakutsk 6NM-64	1.65	140000	60	0.68
4.	Novosibirsk 18 NM-64	2.80	478000	42	0.77
5.	Moscow 12NM-64	2.37	402000	10	0.97
6.	Irkutsk 18NM-64	3.61	567000	46	0.74
7.	Magadan 18NM-64	2.08	436000	52	0.70

The conditional thickness of the additional absorber above the apparatus was determined from the ratio: $h_i = \frac{1}{\beta} \ln(N_i/N_o)$ where $\beta = -0.007$/mb is a neutron component barometric coefficient, N_i is a counting rate before the flare registered by 6NM at the i-th station, N_o is the same counting rate at the Oktyomtsy station.

From the Table 2 it is seen that h_i changes considerably at different stations. That is why, according to Webber and Quenby [1959] coupling coefficients must be different. From Webber and Quenby [1959] the coupling coefficients for observation level h_1 = 1000 g/cm^2 and h_2 = 680 g/cm^2 are known. Extrapolating them one can find the coupling coefficients for all stations using:

$$W_i(\varepsilon) = W_1(\varepsilon) e^{\frac{1}{\mu}(h_1 - h_i)} \quad \text{where } \mu = \frac{1}{h_1 - h_2} \ln\left[\frac{W_2(\varepsilon)}{W_1(\varepsilon)}\right];$$

$W_1(\varepsilon)$ and $W_2(\varepsilon)$ are coupling coefficients for levels 1000 g/cm^2 and 680 g/cm^2 respectively.

Normalized coupling coefficients for 3 stations: Oktyomtsy, Yakutsk and Tixie Bay are shown in Fig. 2. According to Table 2 for the Moscow station (h_1 <10 g/cm^2) one can use the coupling coefficients of the Oktyomtsky (Okt) station. The Tixie Bay coefficients will be suitable for Novosibirsk and Irkutsk, the Yakutsk ones - for Magadan as h_1 is almost the same. The energy spectrum of solar cosmic rays is presented in the form $D(\varepsilon) = A\varepsilon^{-\gamma}$. From the high energy side it is cut off at 5 GeV as the flare was not observed by meson telescopes on the Earth's surface. In Fig. 3 expected amplitudes of the increase effect for every i-th station A_i^o/A_{Okt}^o determined relative to the increase on the Oktyomtsy A NM A_{Okr} are given by solid curves as follows:

$$\frac{A_i}{A_{Okt}} = \frac{\int_{\varepsilon_1}^{5\text{GeV}} W_i(\varepsilon) \cdot \varepsilon^{-\gamma} d\varepsilon}{\int_{\varepsilon_1}^{5\text{GeV}} W_{Okt}(\varepsilon) \cdot \varepsilon^{-\gamma} d\varepsilon}$$

where $\varepsilon_1=R_c$ is for the station having the geomagnetic rigidity threshold $R_c > 2$ GeV and $\varepsilon_1 = 2$ GeV for the stations having the rigidity threshold $R_c < 2$ GeV. From the low energy side the spectrum is limited to 2 GeV as the NM coupling coefficients on the Earth's surface are not sensitive to energies <2 GeV.

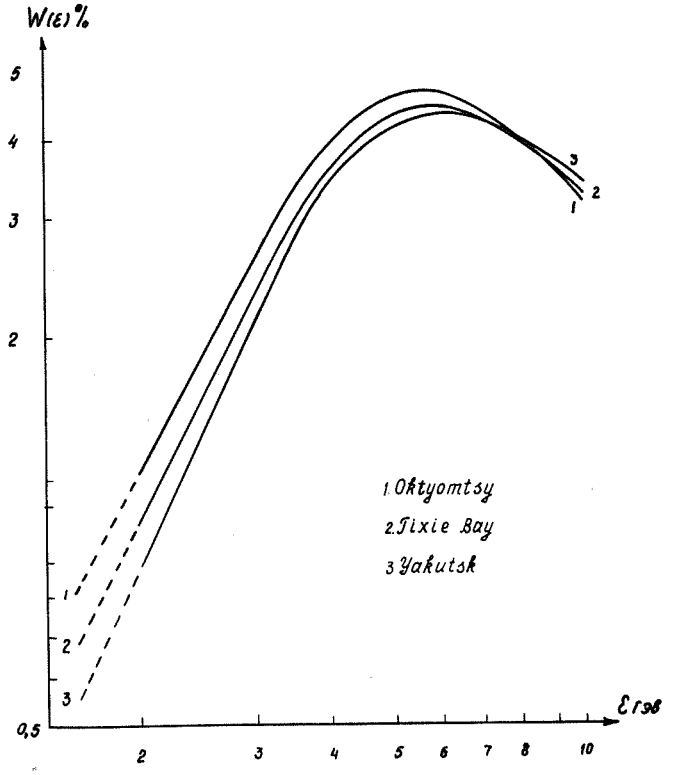

Fig. 2. Coupling coefficients W (ε) for the Oktyomtsy, Tixie Bay, Yakutsk stations.

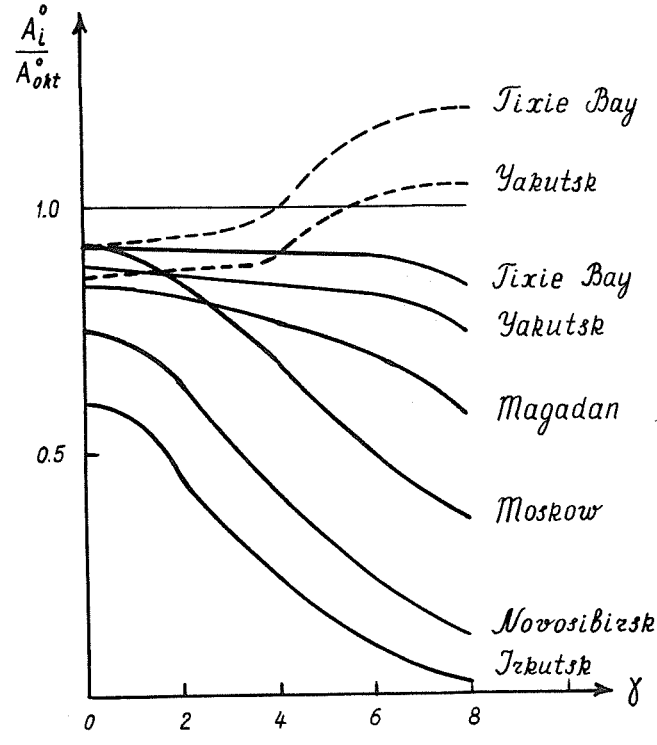

Fig. 3. Expected relative amplitudes of the increase in dependence upon γ. Solid lines show W (ε)=0 at $\varepsilon_1 \leq 2$ GeV. Dashed ones show at $\varepsilon_1 \leq 1.6$ GeV.

However, it is known from Dorman [1957] and Filippov and Chirkov [1976] that at the period of some flares can be less than 2 GeV. That is why, in Fig. 3 the expected amplitudes at $\varepsilon_1 = 1.6$ GeV for the Yakutsk and Tixie Bay stations are shown by dashed lines. From Fig. 3 it is seen that the increase effect of solar cosmic rays in Tixie Bay and in Yakutsk can be larger than in Oktyomtsy when the index γ is larger than 6.

Let us compare the flare expected amplitudes given in Fig. 3 with experimental ones in Table 1 at different periods of the flare using the criterion χ^2 determined by expression:

$$\chi^2 = \sum \frac{\left(A_i^e/A_{Okt}^e - A_i^o/A_{Okt}^o\right)^2}{A_i^o/A_{Okt}^o}$$

In Fig. 4 the dependence of criterion χ^2 upon the index for the different flare periods is presented. The minimum corresponds to the most probable value of the index γ. It is seen that at the flare initial period (1015-1030 UT) the energy spectrum is the hardest (γ<2). The softest spectrum of the form $D(\varepsilon) \approx \varepsilon^{-5}$ was observed at the end of the flare (1200-1300 UT). At the period of the largest increase of the flare (1030-1200 UT) the spectrum is described in the form: $D(\varepsilon)=\varepsilon^{-4\pm0.5}$. Thus, during the flare the gradual softening of the energy spectrum takes place.

Apparently, the observed increase is caused by solar particles accelerated in the flare of importance 2B with coordinates N23 W40. From [Solar-Geophysical Data] it is known that it began at 0945 UT, reached maximum at 1007 UT and ended at 1105 UT on November 22, 1977.

The model [Burlaga, 1967] of solar particle passage for the increase period of the cosmic ray intensity predicts its dependence upon the time in the form:

$$J(t)=K_i \exp(-2.5\ t_m/t)t^{-5/2}$$

where J(t) is the intensity increase, K=CONST, tm is time of the maximum intensity which is counted from injection moment of particles, t_0. For t_0 we took the moment 1005 UT which occurred 10-15 min before the beginning of the cosmic ray intensity increase.

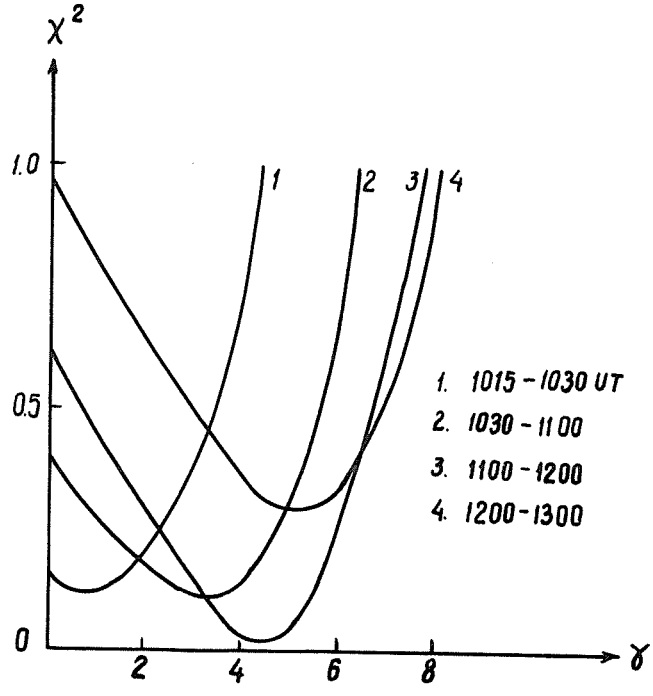

Fig. 4. Criterion χ^2 in dependence upon γ.

To find out the unknown K and t_m we'll make up the equation system using data of 15 min of cosmic ray intensity readings at the stations Tixie Bay, Yakutsk and Oktyomtsy $Z(t)=Y+\frac{1}{t}X$

Or it can be in the vector form as follows: $\overline{Z} = M\overline{U}$

Solving this system we have: $\overline{U}=(M^TM)^{-1}M^T\overline{Z}$

$X=-5/2t_m$, $Z(t)=\ln [J(t)t^{5/2}]$

$Y=\ln K_1$, $\overline{U}=\left|\begin{matrix}y\\x\end{matrix}\right|$; M; M^T and $(M^TM)^{-1}$

are right-angled, transformed and reciprocal matrices, respectively, of dimension 2 x 9.

It is found that t_m = 56 min., K = $3.7 \cdot 10^6$. Following from [Burlaga, 1967] t_m is a linear function $\theta_0^2 \cdot \theta_0$- is the effective angular distance between the Earth and the flare. Hence, θ_0= 36°.

For the flare decrease phase the intensity dependence upon the time is presented in [Burlaga, 1967] as follows: $J(t)=K_2\exp(-t/t_D)$ where K_2=CONST, t_D is time of the solar particle decay.

The equation system solved as above gives t_D=88 ± 13 min. According to [Burlaga, 1967] the boundary position of solar particle absorption is found as follows:

$$r_1 = \left(\frac{\pi^2 \cdot t_D}{10t_m - 6.5 \cdot 60 \cdot \theta_0^2}\right)^{1/2}$$

Substituting here the derived values t_D, t_m, θ^2 we have r_1= 1.7 AU.

References

BUHMANN, R.W., J.D. ROEDERER, M.A. SHEA and D.F. SMART — 1974 — World Data Center A for Solar-Terrestrial Physics Report UAG-38, Boulder, CO.

BURLAGA, L.F. — 1967 — J. Geophys. Res., 72, 4449.

DORMAN, L.I. — 1957 — "Variatsii kosmicheskikh luchei". Gostekhizdat, 492 s.

FILIPPOV, A.T. and N.P. CHIRKOV — 1976 — Ob uskorenii relativistskikh chastits v mezhplanetnoi srede". Yakutsk, 32 s.

PRIKHODKI, A.N., G.V. SKRIPIN, A.A. UPOLNIKOV and A.I. KUZMIN — 1978 — "Vspyashka kosmicheskikh luchei 22 noyabra 1977 goda". Bulletin NTI.

SGD — 1977 — Solar-Geophysical Data, No. 400, Part 1, Dec. 1977.

WEBBER, W.R. and J.J. QUENBY — 1959 — Philos. Mag., 4, 41, 654.

Solar Cosmic Ray Flare on November 22, 1977

by

A.T. Filippov, V.A. Filippov, N.P. Chirkov and V.I. Ipatiev
Institute of Cosmophysical Research and Aeronomy, Yakutsk Branch
Siberian Department of the USSR Academy of Sciences, Yakutsk, USSR

A.V. Sergeev and V.P. Karpov
Siberian Institute of Terrestrial Magnetism, Ionosphere and Radio Wave Propagation
Siberian Department of the USSR Academy of Sciences, Irkutsk, USSR

V.L. Borisov
Institute of Geology and Geophysics
Siberian Department of the USSR Academy of Sciences, Novosibirsk, USSR

V.K. Korotkov
Northeast Complex Research Institute
Far East Scientific Center of the USSR Academy of Sciences, Magadan, USSR

ABSTRACT

The cosmic ray flare on November 22, 1977, with energy E>1 GeV is investigated from data of the Siberian network of neutron monitor stations. It is shown that propagation of particles in the interplanetary medium during this flare is well described by an anisotropic diffusion model for solar cosmic rays. When flare longitude and time of particle injection are used with this model, it gives good agreement with observations.

The cosmic ray flare with energy E>1 GeV that occurred on November 22, 1977, was observed by ground stations. Energy characteristics, geographic coordinates of cosmic ray stations, event amplitude, A, between 1045 and 1100 UT, and the hourly statistical accuracy, σ, are given in Table 1.

Table 1. Soviet Network of Neutron Monitor Stations

Station	Cutoff Rigidity (GeV/c)	Geographic Lat. (degrees)	Geographic Long. (degrees)	A (%)	σ (%)
1. Apatity	0.65	67.55	33.33	14.0	0.17
2. Tixie Bay	0.52	71.60	128.90	9.4	0.14
3. Yakutsk	1.86	62.02	129.72	12.0	0.18
4. Magadan	2.16	60.10	151.0	11.0	0.14
5. Moscow	2.46	55.47	37.32	7.5	0.17
6. Novosibirsk	2.85	54.80	83.00	6.0	0.15
7. Irkutsk	3.74	52.47	104.03	2.35	0.18

The ground level unit amplitude is measured as a percentage of the pre-flare level, i.e., as a fraction of the average of the 15- or 5-min data between 0900 and 1000 UT. As is seen from Table 1 and Figure 1, the Apatity station neutron monitor registered the greatest amplitude increase in cosmic ray intensity--a rise of about 14% above the pre-flare level. According to 5-min data from the Siberian station network (Tixie Bay, Irkutsk and Novosibirsk), the cosmic ray increase began sometime between 1015 and 1020 UT. It is seen from Figure 1, that this cosmic ray event rapidly increased to maximum and then slowly decayed to the pre-flare level. It is also seen that the amplitude diminished with increasing geomagnetic cutoff rigidity.

Because the profile characteristics mentioned above all implied that this event was of solar origin, we applied models of solar cosmic ray propagation in the interplanetary medium to this flare to determine its coordinates and E>1 GeV particle diffusion coefficient. Figure 2 shows the results of the anisotropic diffusion model [Burlaga, 1967] in determining the initial moment of particle injection on the Sun and the flare longitude. Because one of us (A.T. Filippov) has applied this model to flares before [Filippov, 1975], we give only the main results obtained, namely, the time of particle injection on the Sun t_0 = 0955 ± 5 min UT and the flare longitude $\Theta_f \sim 30° \pm 5$ W. Figure 2 also presents the anisotropic diffusion model results of Krymsky [1966]: the initial time of particle injection and the diffusion co-

efficient. This model yields a value of 1000 UT for t_0. Thus, the onset times derived from the two models practically coincide. Furthermore, from Figure 3 it is seen that the parameter $\alpha = 1$, so that the diffusion coefficient $D = 1.1 \times 10^{22} cm^2 s^{-1}$.

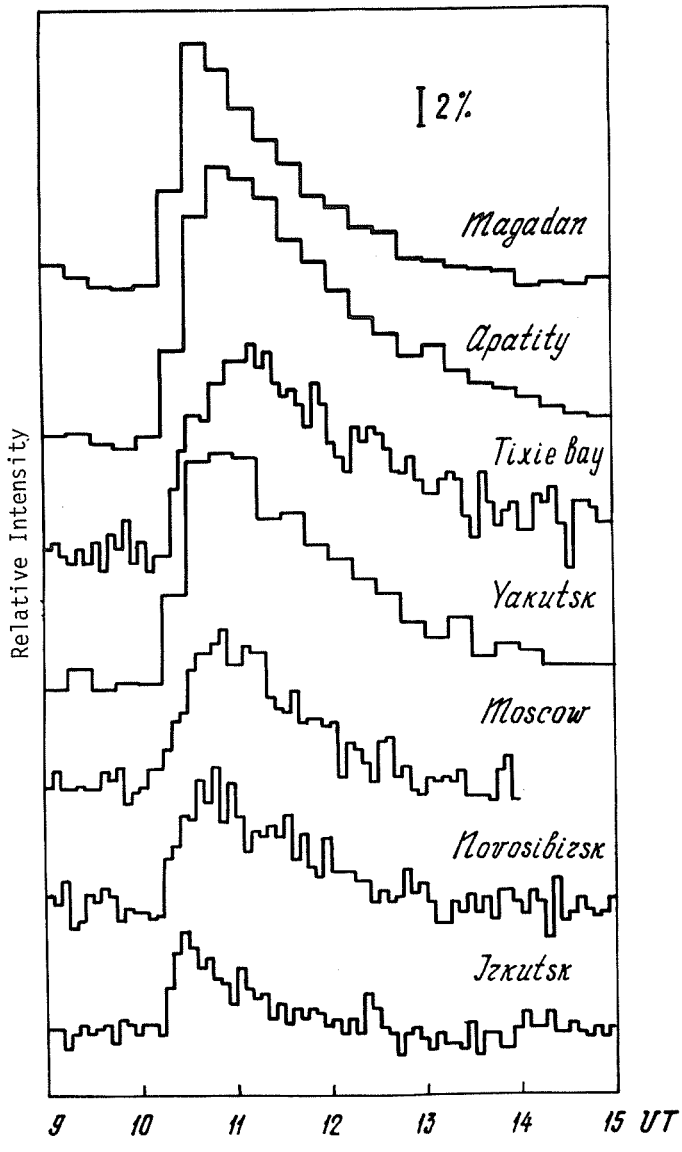

Fig. 1. Temporal dependence of cosmic ray variations on November 22, 1977, as observed by the Soviet network of neutron monitor stations. The counting rate is expressed as a percent of the level recorded between 0900 and 1000 UT.

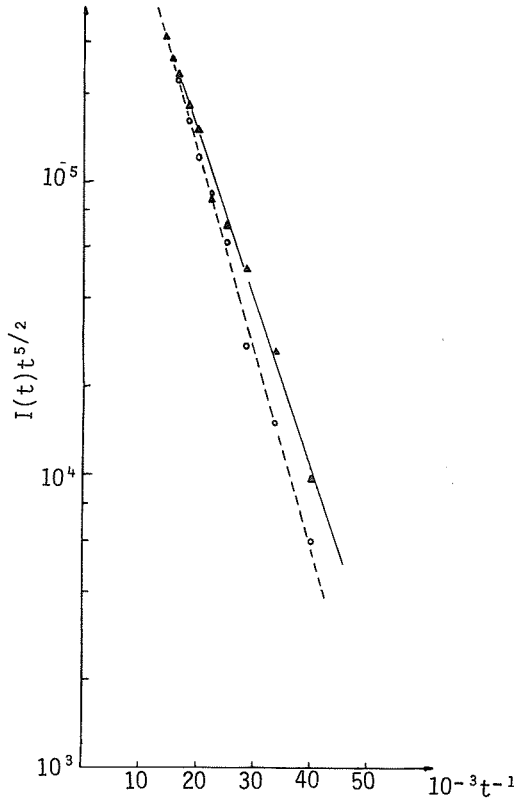

Fig. 2. The dashed line represents the theoretical intensity-versus-time profile for the Burlaga [1967] diffusion model; the solid line denotes Krymsky's [1966] diffusion model solution. Data from the Moscow neutron monitor (open circles) follow the dashed line more closely than they do the solid line. On the other hand, the Tixie Bay data fall much closer to the solid line profile than to the dashed one.

Fig. 3. Results of applying the Krymsky [1966] diffusion model to the cosmic ray flare on November 22, 1977. Circles represent experimental data from Tixie Bay; the solid curve denotes the theoretical amplitude-versus-time profile with $\alpha = 1$ and $t_0 = 1000$ UT.

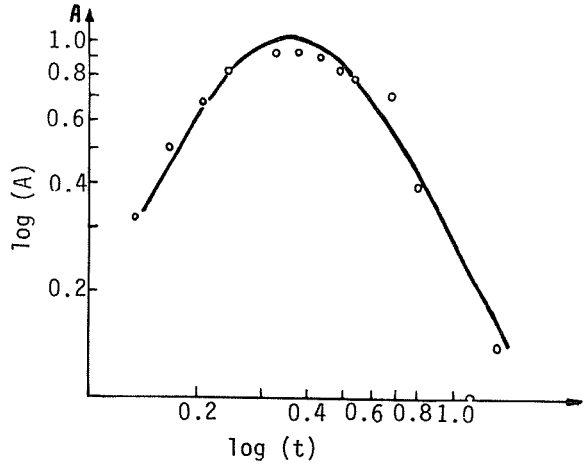

Figure 4 illustrates the dependence of the cosmic ray increase on geomagnetic cutoff rigidity. For rigidities R>1.8 and < 3.74 GeV the dependence has the form $R^{-\gamma}$, where $\gamma = 1.7$. Within the 1-2 GeV range the amplitude is practically independent of rigidity. Extrapolating the latitudinal dependence of this event's amplitude into the high energy region, we determined that the maximum energy of accelerated particles on the Sun was ~ 5.5 GeV.

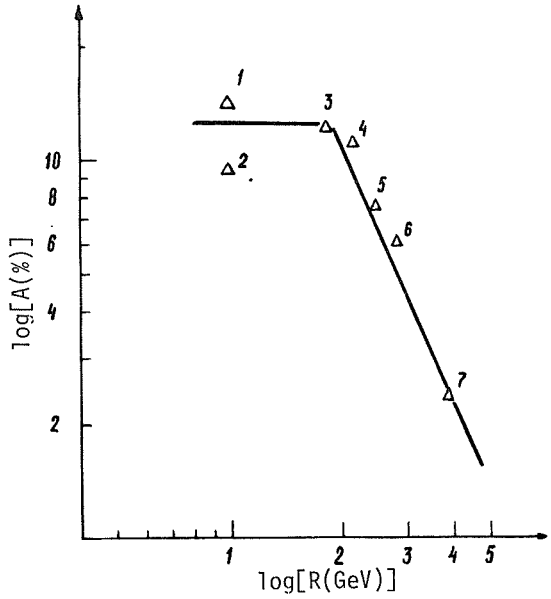

Fig. 4. Latitudinal dependence of the amplitude of the cosmic ray increase between 1045 and 1100 UT on November 22, 1977. Numbers near the experimental points correspond to the cosmic ray station numbers given in Table 1.

We also compared the computed longitudinal coordinate and time of particle injection on the Sun with observations of chromospheric flares. According to SGD [1977], a chromospheric flare of importance 2b was observed to begin at 0947 UT at W40. Because both of these values are in good agreement with our predictions, they confirm that the November 22, 1977 cosmic ray increase was indeed of solar origin.

REFERENCES

BURLAGA, L.F. 1967 Anisotropic Diffusion of Solar Cosmic Rays, *J. Geophys. Res., 72,* 4449-4466.

SGD 1977 *Solar-Geophysical Data,* 400 Part I, 10, December 1977, U.S. Department of Commerce (Boulder, Colorado, U.S.A. 80303).

FILIPPOV, A.T. 1975 "Issledovaniya po kosmofizike i aeronomii", izd-vo Yakut, Filiala SO AN SSSR, Yakutsk, 155 (in Russian).

KRYMSKY, G.F. 1966 "Issledovaniya po geomagnetizmy i aeronomii", izd-vo AN SSSR, M., 143 (in Russian).

Cosmic Ray Solar Flare Event of November 22, 1977

by

T. Mathews, D. Venkatesan and S.P. Agrawal*
Department of Physics
The University of Calgary
Calgary, Alberta, Canada

The Cosmic Ray Solar flare event of November 22, 1977, was recorded by the super neutron monitors at Calgary (114.1°W, 51.1°N, altitude 1,128 meters, vertical cut-off rigidity P_T 1.09 GV) and at Sulphur Mountain (115.6°W, 51.2°N, altitude 2,283 meters, P_T 1.14 GV). Increases observed, corrected to mean station pressures are shown in Figure 1. They began between 1015 and 1020 UT at both stations and reached a maximum value of 31.7 ± 0.5% at Calgary and 38.5 ± 0.5% at Sulphur Mountain at about 1050, making it the largest flare event recorded by ground level monitors since November 1960. Table 1 lists the 5-minute readings of the super neutron monitors.

The high energy particles recorded by ground based monitors were probably associated with the 2B flare in McMath plage region 15031 at N23 W40 with Hα maximum at 1007 UT. If the particle were released near the Sun at the time of Hα maximum, they reached our stations about 18 ± 3 minutes later. However, our stations were not in the most favored position to record prompt particles. Asymptotic directions of approach of particles in the 2-5 GV rigidity range, arriving at our stations, were about 60° west of the estimated direction of interplanetary magnetic field near the Earth.

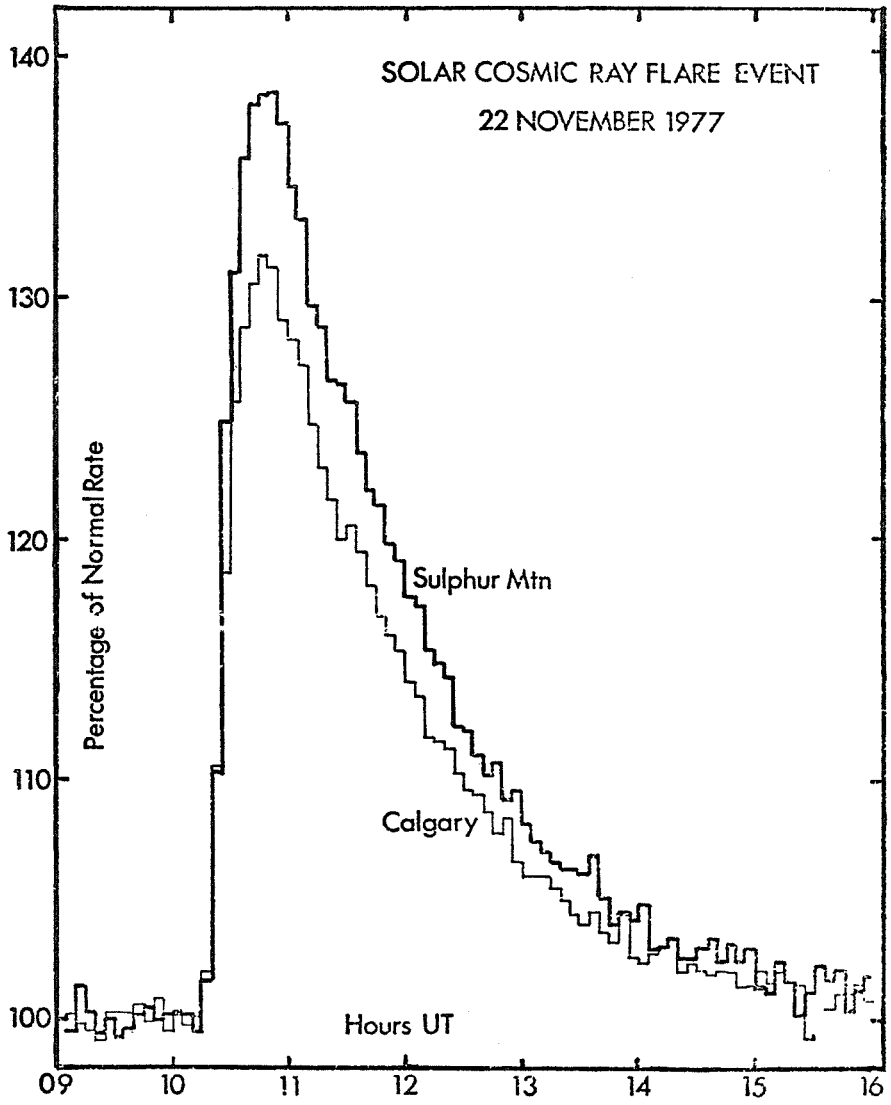

Fig. 1. Ground level event at Calgary and Sulphur Mountain.

*On leave of absence from Vikran Space Science Centre

Table 1. Five-minute values during the cosmic ray solar flare event of Nov. 22, 1977 at Calgary and Sulphur Mountain.

TIME HR.	MIN.	CALGARY UNCORR.	CALGARY PRESS.	CALGARY CORRECTED	SULPHUR MOUNTAIN UNCORR.	SULPHUR MOUNTAIN PRESS.	SULPHUR MOUNTAIN CORRECTED
9	05	9917	885.8	10134	846	754.4	774
	10	9934	885.8	10151	843	754.4	771
	15	9888	885.7	10096	860	754.3	786
	20	9875	885.7	10083	850	754.3	777
	25	9826	885.8	10041	842	754.3	770
	30	9952	885.7	10162	848	754.3	775
	35	9955	885.7	10165	841	754.3	769
	40	9946	885.7	10155	845	754.2	772
	45	9982	885.7	10192	849	754.2	776
	50	9912	885.7	10121	853	754.2	779
	55	10005	885.7	10216	847	754.2	774
10	00	9867	885.7	10075	850	754.2	776
	05	9945	885.7	10150	852	754.0	777
	10	9898	885.7	10106	851	754.0	776
	15	9931	885.7	10140	845	754.0	771
	20	10118	885.7	10331	863	754.1	788
	25	10983	885.7	11214	937	754.1	855
	30	11781	885.7	12029	1050	754.1	958
	35	12480	885.7	12743	1112	754.1	1015
	40	12771	885.8	13050	1153	754.1	1052
	45	12948	885.8	13231	1171	754.1	1069
	50	13056	885.8	13341	1175	754.1	1073
	55	13023	885.9	13318	1177	754.1	1074
11	00	12804	885.9	13080	1164	754.1	1063
	05	12729	885.9	13000	1143	754.0	1043
	10	12611	885.9	12896	1132	754.1	1033
	15	12371	885.9	12651	1101	754.1	1005
	20	12183	885.9	12459	1094	754.1	999
	25	12061	885.9	12334	1075	754.1	981
	30	11897	885.8	12157	1074	754.1	980
	35	11960	885.8	12221	1067	754.1	974
	40	11855	885.8	12114	1049	754.1	958
	45	11726	885.7	11973	1037	754.1	947
	50	11599	885.7	11843	1031	754.1	941
	55	11500	885.8	11751	1017	754.1	928
12	00	11435	885.8	11685	1012	754.0	923
	05	11310	885.8	11557	999	753.9	911
	10	11266	885.7	11503	996	753.8	908
	15	11107	885.6	11332	982	753.8	894
	20	11097	885.5	11313	977	753.8	890
	25	11063	885.5	11279	973	753.8	886
	30	10968	885.5	11182	954	753.8	869
	35	10892	885.4	11096	955	753.7	869
	40	10882	885.3	11077	945	753.7	860
	45	10821	885.3	11015	938	753.7	854
	50	10730	885.3	10922	944	753.6	858
	55	10801	885.2	10986	930	753.6	846
13	00	10634	885.1	10808	935	753.4	849
	05	10566	885.1	10739	924	753.4	839
	10	10579	885.0	10744	918	753.4	833
	15	10582	885.0	10747	914	753.4	830
	20	10538	884.9	10694	911	753.3	826
	25	10487	884.9	10642	911	753.3	825
	30	10437	884.7	10575	910	753.2	825
	35	10402	884.7	10539	908	753.2	822
	40	10453	884.7	10591	914	753.1	828
	45	10378	884.6	10507	899	753.1	814
	50	10344	884.6	10473	891	753.1	807
	55	10455	884.5	10577	894	753.1	810

Table 1. Five-minute values during the cosmic ray solar flare event of Nov. 22, 1977 at Calgary and Sulphur Mountain. (Continued)

TIME		CALGARY			SULPHUR MOUNTAIN		
HR.	MIN.	UNCORR.	PRESS.	CORRECTED	UNCORR.	PRESS.	CORRECTED
14	00	10273	884.6	10401	893	753.0	808
	05	10257	884.6	10384	897	753.0	812
	10	10294	884.6	10422	882	753.0	798
	15	10344	884.5	10464	883	752.9	799
	20	10368	884.5	10489	886	752.9	801
	25	10214	884.5	10333	880	752.8	795
	30	10275	884.5	10395	878	752.8	794
	35	10234	884.5	10353	882	752.8	797
	40	10207	884.5	10326	886	752.8	801
	45	10220	884.5	10339	878	752.8	794
	50	10254	884.5	10363	885	752.8	800
	55	10153	884.5	10271	878	752.8	794
15	00	10173	884.4	10284	883	752.8	798
	05	10229	884.4	10340	870	752.8	786
	10	10179	884.4	10290	869	752.8	785
	15	10218	884.5	10337	878	752.8	794
	20	10174	884.5	10292	872	752.8	788
	25	10166	884.5	10284	860	752.8	777
	30	9929	884.6	10052	867	752.8	784
	35	-	-	-	877	752.8	793
	40	10053	884.8	10194	873	752.8	789
	45	10102	884.8	10243	875	752.8	791
	50	10093	884.9	10242	860	752.9	778
	55	10122	885.0	10279	868	752.9	785
16	00	10052	885.0	10208	871	752.9	788
	05	10025	885.1	10189	864	752.9	781
	10	10065	885.1	10229	865	753.0	781
	15	10071	885.2	10243	863	753.0	781
	20	10081	885.2	10254	874	753.0	791
	25	10073	885.3	10230	861	753.0	779
	30	9906	885.3	10083	861	753.0	779
	35	9873	885.4	10058	861	753.0	779
	40	10012	885.4	10199	866	753.0	784
	45	10054	885.4	10242	855	753.2	775
	50	10033	885.5	10228	867	753.2	786
	55	10008	885.5	10203	861	753.2	781
17	00	9955	885.5	10149	864	753.2	783

Spectrum Variations of Solar Cosmic Rays Recorded on 22 November 1977 With the Sayan Spectrograph

by

Yu.Ya. Krestyannikov, A.V. Sergeev, V.I. Tergoev and L.A. Shapovalova
Siberian Institute of Terrestrial Magnetism, Ionosphere and
Radio Wave Propagation, Siberian Department of the USSR
Academy of Sciences, Irkutsk, USSR

In this paper data are given for the solar cosmic ray increase (SCR) on November 22, 1977, recorded with the cosmic ray spectrograph in Irkutsk (R_c=3.81GeV). The spectrograph consists of secondary cosmic ray detectors which record neutron and charge components. Table 1 gives the data at 5-minute intervals for the neutron component corrected to sea level ($\bar{P}$=965 mb) and at an altitude of 3000 m ($\bar{P}$=700 mb). Data are corrected for the barometer effect. In Fig. 1a the neutron component variations are shown, expressed in percent; the solid line is for sea level, the dashed line for an altitude of 2000 m, and the dash-dot line for an altitude of 3000 m. The period 0000-0500 UT on November 22, 1977, is taken for the background counting rate. Using the data of Fig. 1a, the intensity variations $\Delta D/D(R)$ of the primary cosmic rays with the rigidity R=4GeV were determined (see Fig. 1b and Table 2). The behavior of parameter γ, from $\Delta D/D(R) \approx BR^{-\gamma}$, is shown in Fig. 1c. The analysis of the 10-minute data $\Delta D/D(4GeV)$ and parameter γ gives the following interpretation recorded by the Sayan spectrograph. The cosmic ray increase started at ~1045 UT and ended at ~1145 UT. The total duration of the SCR increase is ~90 min. The maximum of the increase $\Delta D/D(4GeV) \approx 52\%$, is recorded at 1035 UT. The duration of the initial stage of increase is ~20 min. and the decrease phase is ~70 min. At the onset, 1035 UT, the parameter γ changed from 0 to minus 4 and remained at this value until the end of the event at 1145 UT. This means that for the observations at Irkutsk the additional current of SCR was changed through the power only.

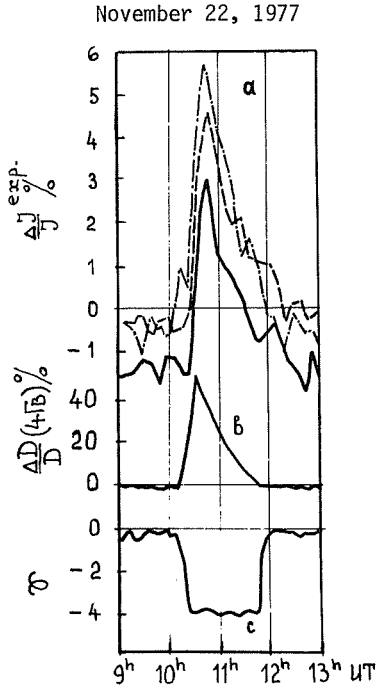

Fig. 1. Neutron component variations in (a)--solid line sea level, dashed line 2000 m, dash-dot line 3000 m; intensity variations of primary cosmic rays, R=4GV, in (b); and parameter γ in (c) at Irkutsk, November 22, 1977.

TABLE 2 10-minute values of $\Delta D/D(4GV)\%$ on Novemer 22, 1977.

hours / min	9h	10h	11h	12h
5	-0.9	-0.4	21.2	-0.8
15	-1.2	-0.6	14.5	-0.5
25	-0.9	36.5	10.1	-0.9
35	-1.1	52.0	6.5	-0.7
45	-1.2	37.7	0.5	-1.2
55	-0.8	28.2	0	-0.9

REFERENCE

SERGEEV, A.V. 1973 "The Spectrographic Method for the Study of Cosmic Ray Variations of Magnetospheric and Interplanetary Origin," *Thesis*, Moscow, 1973.

TABLE 1. The 5-minute values of the neutron component on November 22, 1977 (corrected for barometric pressure).

UT	Level $\bar{P}$ - 965 mb (scale factor 128)											
hour/min	5	10	15	20	25	30	35	40	45	50	55	60
0	385	386	384	383	386	384	385	384	386	383	386	386
1	385	383	383	386	384	388	385	383	387	387	387	388
2	387	386	386	389	386	388	384	386	385	390	391	389
3	390	387	385	392	385	387	384	388	390	390	392	387
4	386	386	392	385	390	389	389	386	389	384	384	383
5	382	381	388	381	385	385	385	383	386	381	381	380
6	382	378	379	383	385	384	383	379	383	381	381	386
7	384	386	384	385	382	387	381	384	383	385	381	380
8	380	382	383	381	382	381	382	377	385	383	385	383
9	382	380	380	375	378	381	379	380	381	376	382	381
10	379	382	380	379	388	395	400	396	392	394	390	389
11	385	393	389	386	388	383	385	381	385	382	384	384
12	381	382	379	383	380	377	384	381	379	375	380	381
13	379	377	379	377	377	376	382	375	379	380	376	377
14	380	383	380	381	383	379	379	380	379	378	380	382
15	380	377	373	382	379	378	378	381	377	376	378	373
16	384	378	380	379	382	387	381	380	380	381	382	383
17	382	378	378	381	381	380	382	380	380	378	379	377
18	378	381	380	382	381	381	379	374	379	379	382	375
19	379	380	376	379	381	381	385	379	382	373	380	381
20	376	379	381	382	383	378	381	374	386	380	380	378
21	379	381	374	384	374	377	380	384	382	382	382	381
22	382	381	376	383	381	376	377	379	379	377	381	380
23	378	380	378	380	382	379	380	382	380	377	378	378
	Level $\bar{P}$ = 700 mb (scale factor 1024)											
0	132	133	133	131	133	131	132	131	133	131	132	131
1	132	133	132	133	132	133	132	131	132	132	131	133
2	131	132	132	133	132	133	131	132	132	133	132	132
3	134	132	133	133	133	132	132	133	133	132	132	134
4	132	134	131	133	133	132	133	132	132	133	133	133
5	133	132	133	134	133	132	132	133	133	133	133	135
6	132	133	134	132	133	134	133	132	132	132	133	133
7	132	131	132	131	131	132	131	133	132	133	132	132
8	131	132	131	130	132	132	131	132	131	132	132	131
9	132	132	132	131	132	130	131	131	132	131	132	131
10	132	132	131	135	138	139	140	140	140	137	138	137
11	135	137	135	133	136	133	135	133	132	132	133	131
12	131	131	132	132	132	131	132	131	132	130	131	132
13	131	131	131	131	132	131	132	132	132	132	131	132
14	131	132	131	131	131	132	133	131	133	132	131	132
15	132	132	131	133	132	131	132	132	132	131	131	131
16	130	132	132	132	132	131	132	132	131	132	131	132
17	131	132	132	132	131	131	133	132	132	131	131	133
18	132	132	131	131	133	132	133	132	132	132	132	133
19	132	133	132	133	131	132	133	131	132	133	132	132
20	133	131	132	131	133	131	132	132	133	133	131	131
21	131	132	132	131	133	131	132	132	131	132	133	132
22	133	132	132	131	133	131	132	133	132	130	132	132
23	130	131	131	131	131	131	132	133	132	133	132	133

Lomnický Štít Neutron Supermonitor Data for the November 22, 1977 Ground Level Event

by

J. Ilenčík
Institute of Experimental Physics
Slovak Academy of Sciences
040 01 Kosice, Moyzesova 11, Czechoslovakia

The Lomnický Štít neutron supermonitor has geographic coordinates N49.11 E20.13, an altitude of 2634 m, a 4.00 GV cutoff rigidity and an average barometric pressure of 550.0 mm of mercury. Table 1 presents for the Nov. 22, 1977 ground level event the uncorrected and corrected 5-min total counts for each of the four single-counter units, their respective sums, and the various response ratios of the four monitors. The tabulation also includes the barometer height expressed in mm of mercury.

Table 1. Corrected and Uncorrected Counts/5 min

YEAR	DAY	TIME	UNCORRECTED VALUES					QUOTIENTS				CORRECTED VALUES					PRESSURE
	22 NOV	UT	A	B	C	D	SUM	A/B	B/C	C/D	D/A	A	B	C	D	SUM	(mm Hg)
1977	326	0900	18647	18821	19067	16836	71771	0.959	1.042	1.073	0.933	16289	16988	16307	15106	64780	540.6
1977	326	0905	18329	18540	19290	17203	73271	0.983	1.013	1.064	0.944	16453	16734	16516	15527	65230	540.6
1977	326	0910	18116	18615	19334	16865	71630	0.973	1.032	1.060	0.971	16351	16812	16277	15222	64662	540.6
1977	326	0915	18041	18746	19180	17078	72054	0.962	1.031	1.065	0.947	16266	16901	16309	15308	64964	540.5
1977	326	0920	18093	18680	19236	16884	71893	0.969	1.024	1.030	0.933	16330	16860	16460	15220	64880	540.6
1977	326	0925	18312	18955	19170	16710	72157	0.966	1.044	1.037	0.913	16528	17118	16400	15082	65128	540.6
1977	326	0930	17813	18953	19060	16930	71765	0.940	1.049	1.067	0.959	16078	17107	16309	15281	64775	540.6
1977	326	0935	18079	18918	19363	16954	72314	0.956	1.030	1.083	0.938	16318	17075	16574	15302	65269	540.6
1977	326	0940	18147	18911	19083	16944	72085	0.961	1.045	1.067	0.933	16307	17060	16321	15203	65071	540.6
1977	326	0945	18142	18796	19270	16931	72138	0.966	1.028	1.096	0.928	16357	16938	16480	15175	64950	540.5
1977	326	0950	18155	18846	19550	17152	72703	0.963	1.016	1.082	0.945	16369	16902	16725	15464	65550	540.5
1977	326	0955	18453	19165	19114	17143	72875	0.963	1.058	1.057	0.929	16637	17279	16332	15454	65704	540.5
1977	326	1000	18383	18817	19412	16908	72516	0.977	1.019	1.089	0.920	16556	16943	16592	15228	65309	540.4
1977	326	1005	18141	18691	19354	16885	72071	0.971	1.018	1.087	0.931	16338	16834	16530	15207	64909	540.4
1977	326	1010	18261	18948	19220	16961	73390	0.964	1.040	1.074	0.929	16446	17065	16409	15275	65195	540.4
1977	326	1015	18104	18900	19376	17173	72933	0.984	1.006	1.070	0.944	16326	16652	16550	15466	65054	540.4
1977	326	1020	18413	18870	19010	17100	72602	0.986	1.047	1.048	0.924	16763	16905	16228	15442	65548	540.4
1977	326	1025	18530	18876	19670	17523	73599	0.982	1.011	1.065	0.946	16689	17000	16815	15782	66286	540.4
1977	326	1030	18891	19168	19875	17742	74636	0.986	1.018	1.062	0.930	17014	17263	16963	15979	67219	540.4
1977	326	1035	18674	19444	19823	17559	74400	0.955	1.033	1.072	0.945	16728	17512	16952	15814	67006	540.4
1977	326	1040	19103	19457	19973	17767	75300	0.982	1.026	1.068	0.930	17205	17523	17088	16001	67817	540.4
1977	326	1045	18677	19480	19970	17580	74707	0.959	1.027	1.079	0.941	16821	17544	17085	15833	67283	540.4
1977	326	1050	18801	19390	19986	17723	74909	0.969	1.022	1.071	0.943	16933	17471	17099	15962	67465	540.4
1977	326	1055	18698	19278	19165	17543	74674	0.969	1.006	1.092	0.939	16831	17362	17250	15800	67253	540.4
1977	326	1100	19750	19249	19887	17555	74411	0.974	1.021	1.074	0.935	16887	17336	16993	15810	67016	540.4
1977	326	1105	18871	19402	19765	17746	74874	0.966	1.039	1.057	0.942	16960	17555	16900	15982	67397	540.4
1977	326	1110	18806	19408	19680	17656	74559	0.969	1.038	1.059	0.939	16937	17479	16832	15901	67149	540.4
1977	326	1115	18476	19246	19952	17417	74091	0.960	1.016	1.098	0.943	16640	17333	17069	15686	66728	540.4
1977	326	1120	18420	19312	19948	17409	74079	0.954	1.035	1.077	0.950	16589	17393	16975	15760	66717	540.4
1977	326	1125	18416	19286	19644	17406	73052	0.965	1.034	1.071	0.935	16766	17369	16791	15676	66602	540.4
1977	326	1130	18626	18992	19108	17511	73227	0.981	1.048	1.034	0.940	16775	17096	16308	15771	65950	540.4
1977	326	1135	18644	19186	18596	17119	73635	0.972	1.032	1.096	0.918	16773	17261	16721	15401	66156	540.3
1977	326	1140	18529	19004	18687	17550	73770	0.975	1.017	1.065	0.947	16688	17115	16830	15806	66439	540.4
1977	326	1145	18609	19125	19667	17268	73668	0.973	1.025	1.081	0.928	16759	17224	16812	15552	66347	540.4
1977	326	1150	18757	18641	19528	17131	72657	0.985	1.006	1.082	0.933	16533	16788	16687	15420	65437	540.4
1977	326	1155	18704	19070	19428	17229	73431	0.981	1.035	1.070	0.921	16827	17156	16579	15500	66062	540.3
1977	326	1200	18506	18823	19366	17216	73911	0.983	1.025	1.067	0.930	16649	16934	16523	15488	65594	540.3
1977	326	1205	18447	18874	19476	17086	73883	0.977	1.022	1.081	0.926	16596	16980	16622	15371	65569	540.3
1977	326	1210	18719	19193	19393	17089	73884	0.950	1.043	1.076	0.938	16791	17258	16547	15374	65570	540.3
1977	326	1215	18404	19031	18617	17330	73378	0.967	1.022	1.074	0.942	16557	17121	16745	15591	66014	540.3
1977	326	1220	18123	19440	19011	17284	73758	0.932	1.028	1.094	0.954	16304	17490	17013	15540	66355	540.3
1977	326	1225	19104	18831	19600	17195	73730	0.961	1.017	1.082	0.951	16287	16941	16741	15469	65438	540.3
1977	326	1230	18928	18938	19302	17132	72600	0.963	1.035	1.068	0.940	16309	17037	16445	15413	65314	540.3
1977	326	1235	18731	18959	19367	17122	72777	0.967	1.032	1.073	0.934	16491	17050	16524	15404	65469	540.3
1977	326	1240	18716	19137	19370	17088	73031	0.952	1.041	1.075	0.938	16388	17207	16526	15373	65494	540.3
1977	326	1245	19421	18977	19512	17358	73263	0.971	1.025	1.066	0.942	16672	17058	16654	15614	65910	540.3
1977	326	1250	18110	18834	19400	17176	72731	0.961	1.012	1.093	0.948	16202	16946	16741	15452	65431	540.3
1977	326	1255	18101	18767	19338	17272	72474	0.965	1.023	1.062	0.954	16284	16880	16498	15530	65201	540.3
1977	326	1310	18206	18761	19270	17169	73106	0.970	1.044	1.047	0.943	16379	16878	16167	15446	64870	540.3

Increase of Solar Cosmic Rays on November 22, 1977 and Determination of Their Ejection Phase

by

J. Dubinský, J. Ilenčík and M. Stehlík
Institute of Experimental Physics of the Slovak Academy of Sciences
Kosice, Czechoslovakia

and

L. Křivský
Astronomical Institute of the Czechoslovak Academy of Sciences
Ondrejov near Prague, Czechoslovakia

The neutron supermonitor 4-NM-64, situated at Lomnicky Stit (N49.20 E20.22) at an altitude of 2632 m above sea level recorded a cosmic ray intensity increase caused by a flux of solar particles. According to Shea et al. [1968], the site has a vertical cutoff rigidity (R_C) of 4.0 GV.

The time pattern of the superneutron monitor 5-min data is shown in Figure 1. The observations are corrected for air pressure, i.e., to a mean atmospheric level of 550 mm Hg (barometric coefficient 1.024% per mm Hg). The percent increases are computed with respect to the average counts (65124 pulses per 5 min) of the pre-flare level that extends from 0905-1000 UT. The error bar on the figure marks the height of 0.5 standard deviation above and below the average counting rate. From Figure 1 it can be seen that the counting rate of the neutron supermonitor began to increase between 1020 and 1025 UT and rose by 1025 UT to a value approximately 4 times as great as 1 standard deviation. Within 20 min the counting rate reached its maximum value of 4.1 $\pm$ 0.4% and then gradually decreased to its pre-flare level by about 1230 UT.

The increase in cosmic rays that began between 1020 and 1025 UT was caused by an importance 2n solar flare (position N24 W38), which according to the X-ray outburst, began at about 0948 UT. After two sharp onsets the flare reached its maximum X-ray emission between 1003 and 1006 UT. The SID in the D region, illustrated by the SEA on 27 kHz (Figure 1), roughly follows in course and duration the 2N flare in the H-alpha line.

The time of the particle acceleration or Y-phase [Krivsky 1963; 1972] was determined indirectly from the radio and X-ray emission profiles, since H-alpha photographs of the flare's development were not available. Indeed, the relationship between the radio and X-ray emissions and the Y-phase is known for a series of proton flares in the past: the particle acceleration and ejection phase of cosmic radiation being identified with the first maximum of the complex radio outburst in the centimeter and decimeter ranges and even occurring during a flare's initial radiation outburst. The 808 MHz (37 cm) solar radio noise record in Figure 1 shows that the first outburst, although not the largest, occurred at 0959, culminated at 1006 and ended at 1017 UT. In the range of longest wavelengths observed in solar radio astronomy, i.e., in the decameter range, the outburst also disclosed the simultaneous escape of cosmic radiation particles through the distant solar corona (Figure 1, 32.8 MHz record). Here the maximum outburst occurred between 1002 and 1009 UT (off scale), immediately after the sharp onset.

It is thus clear that the main phase of the acceleration and the escape of the fastest particles in the region of the flare took place between 1001 - 1006 - 1010 UT, i.e., in the interval 0953 - 0958 - 1002 UT, after correcting for the travel time of light. The fastest particles, therefore, arrived at Earth after 24 min $\pm$ 4 min.

REFERENCES

KRIVSKY, L. 1972 Prediction of Proton Flares and Forbush Effects, in Solar Activity Observations and Prediction, in *Progress in Astronautics and Aeronautics*, Vol. 30 (MIT Press, Cambridge, Mass.), 389-409.

KRIVSKY, L. 1963 Cosmic-Ray Flare of 1961 July 18 and Y-Shaped Stage of Flare Development as Phase Conditioning Ejection, *Nuovo Cimento, X-27*, 1017 - 1018.

SHEA, M.A., D.F. SMART, K.G. McCRACKEN and U.R. RAO 1968 Cosmic Ray Tables. Suppl. to IQSY Instruction Manual No. 10, AFCRL Spec. Rep. No 71.

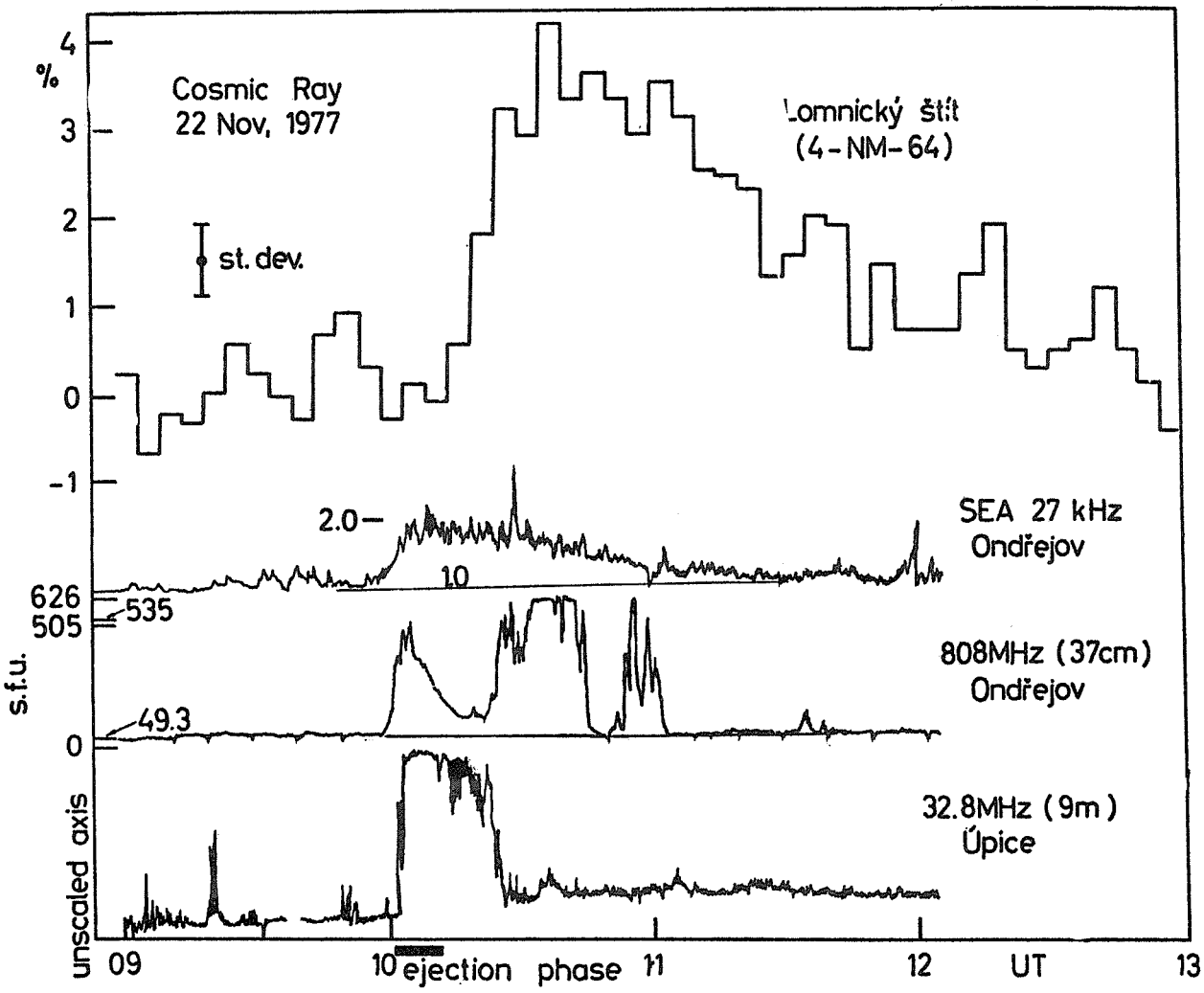

Fig. 1. Acceleration, ejection and arrival of solar cosmic rays from the importance 2n flare that began about 0948 UT on November 22, 1977. The SEA at 27 kHz roughly mimics the H-alpha light curve of the flare; the first maximum in the 808 MHz radio noise profile identifies the particle acceleration and ejection; the 32.8 MHz record reflects the escape of cosmic rays through the distant solar corona; and the 5-min superneutron monitor data depict the 24-min travel time of the most energetic solar corpuscles.

5. IONOSPHERE

Phase Anomaly of Trans-Antarctica VLF Signals During the PCA Event of November 1977

by

P.C. Ling

Ionospheric Prediction Service
Department of Science
Box 702 Darlinghurst, NSW, Australia

Omega signals transmitted from Golfo Nuevo, Argentina (43°03'S/65°11'W) are monitored continuously in Melbourne, Australia (37°29'S/144°34'E) at frequencies of 10.2 and 13.6 kHz. The great circle path is illustrated in Figure 1 which shows that a large portion of this path is within the auroral zone. Therefore, Polar Cap Absorption (PCA) events are expected to appear on the VLF records as phase anomalies with distinguishable characteristics.

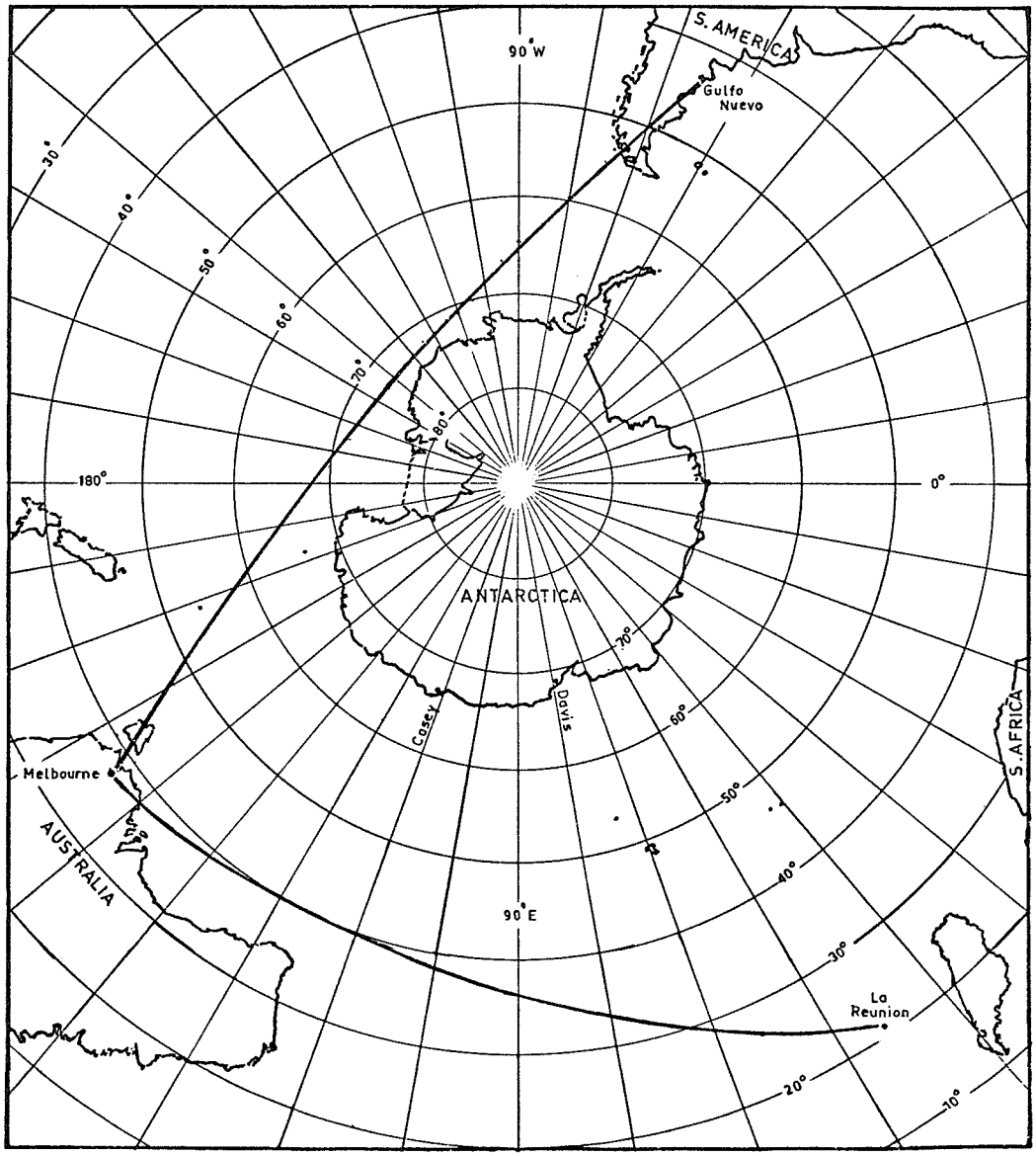

Fig. 1. Great circle paths from Gulfo Nuevo to Melbourne and from La Reunion to Melbourne.

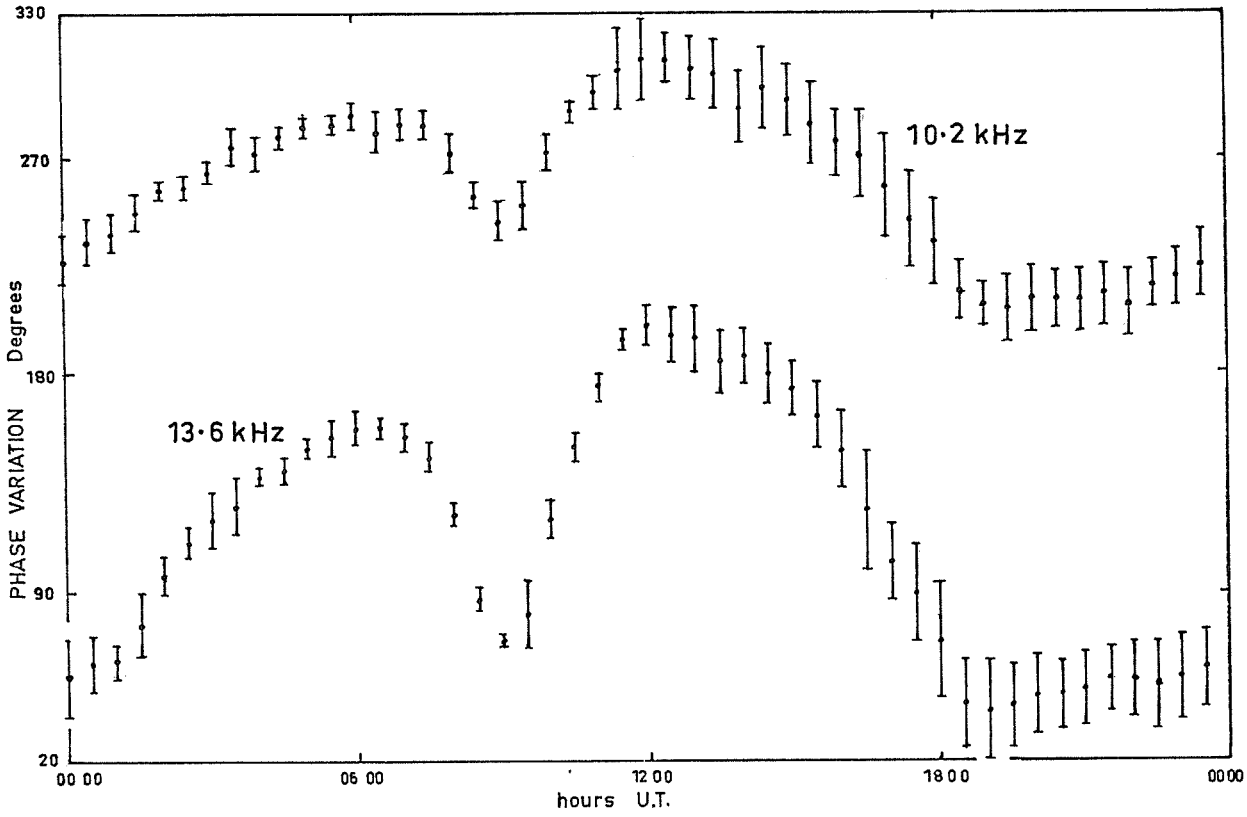

Fig. 2. Mean values of phase for each frequency during 15-21 November, 1977. Bars indicate the range of standard deviations.

From Figure 3 it is observed that during the early hours of November 22, the phase behaves normally until the onset of the solar flare. Then the phase delay decreases at a rapid rate and attains its maximum deviation of about half a cycle approximately three hours later. The phase remains retarded until late on November 25. By comparing it with the normal diurnal variation, we can see that the maximum deviation exceeds the normal range of diurnal variation. This means that the change in reflection height in the Antarctic region is much larger than that due to the diurnal variation. It is more obvious when we consider that the maximum phase deviation is obtained after the end of the solar flare. That is to say, the circuit is mainly affected by the PCA event which is localized at and around the Antarctic region. The cause of such a phase anomaly as due to PCA events was confirmed by its observation at Casey and Davis.

Contrary to this type of behavior of the phase, for the circuit from La Reunion (20°58'S/55°17'E) to Melbourne (see Figure 1) which is far from the Antarctic region, the phase records showed an immediate phase recovery at the end of the solar flare. Figure 3 also shows that the time of commencement of the phase anomaly is in accordance with the solar flare and PCA; but the phase recovers before the PCA ends. The PCA ended at Davis late on November 26.

Figure 4 shows a similar curve for the 10.2 kHz signal for the same circuit and during the same period. It displays the same characteristics as that of the 13.6 kHz signal with similar time scale. But it can be seen that the 10.2 kHz signal has a smaller maximum phase deviation than that of the 13.6 kHz signal. There was no reliable record for the 10.2 kHz signal from 1800 UT November 22 to 0200 UT November 23 due to its very low signal strength.

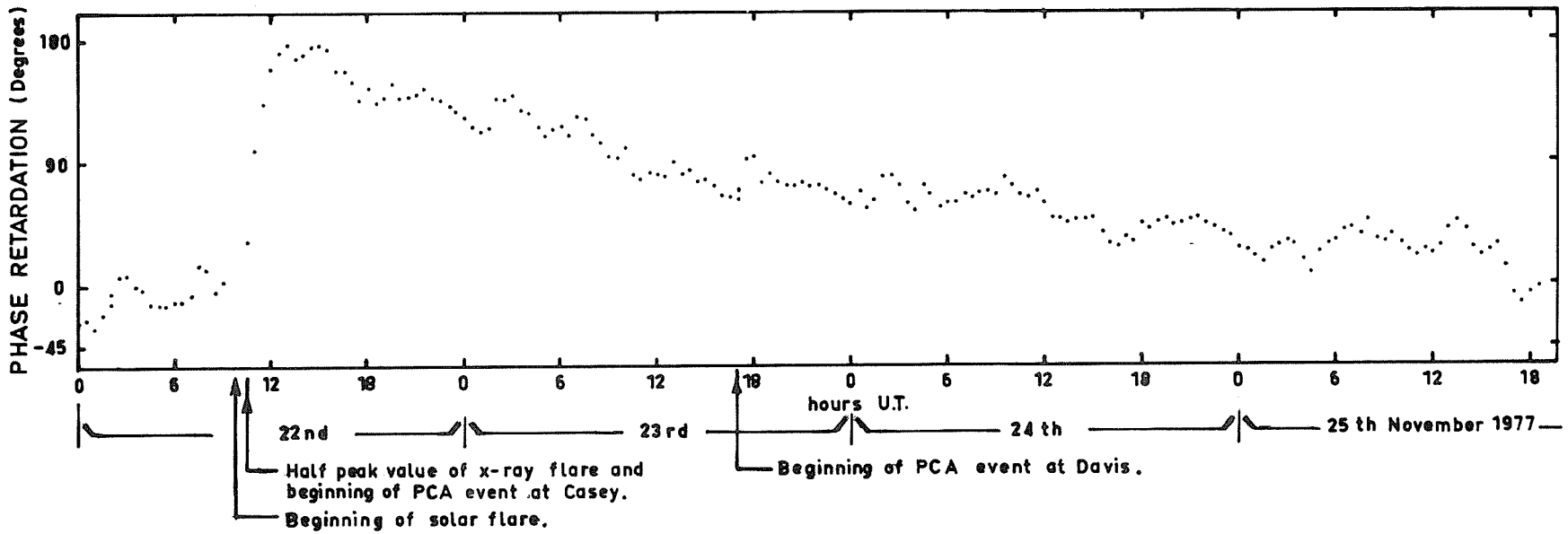

Fig. 3. Deviation of phase from reference for 13.6 kHz.

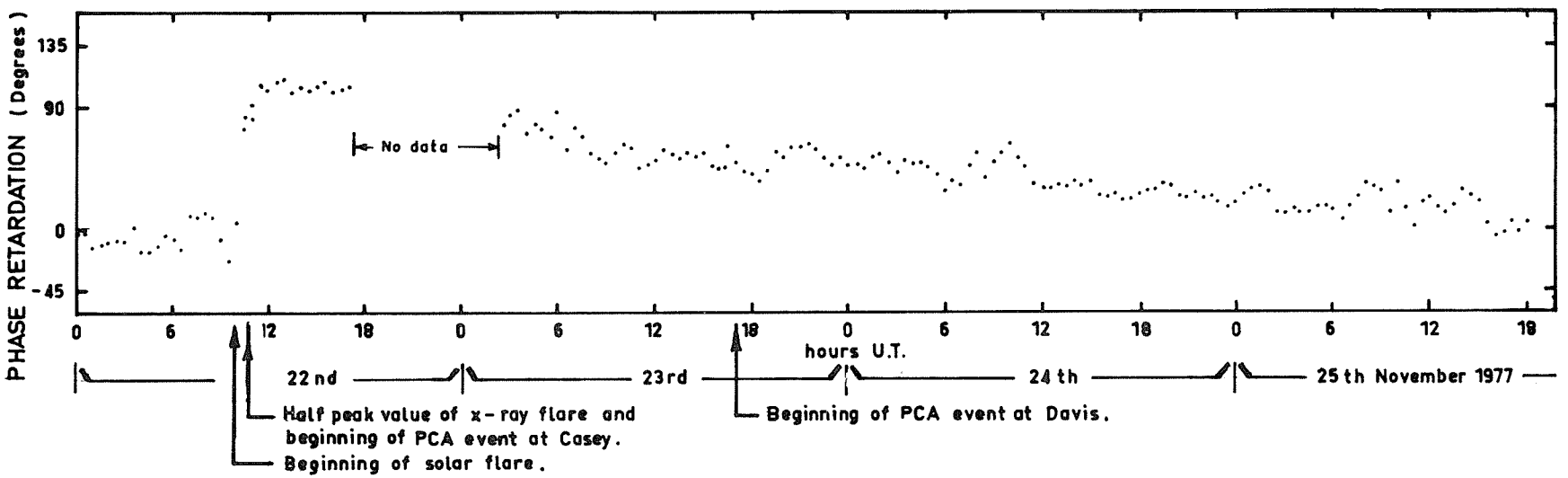

Fig. 4. Deviation of phase from reference for 10.2 kHz.

The records were supplied by the Department of Transport, Australia. Their assistance is gratefully acknowledged.

REFERENCES

Australian National Antarctic Research Expeditions (A.N.A.R.E.) 1977 *Preliminary Reports to IUWDS Regional Warning Centre*, IPS, Sydney, Australia.

SGD 1977 *Solar-Geophysical Data*, Part I, December 1977, NOAA, Boulder, Colorado 80303, USA.

Partial Reflections Observed on November 22, 1977 by the 2.75 MHz Radar at Tromso, Norway

by

A. Brekke and T. Hansen
The Auroral Observatory
Institute of Mathematical and Physical Sciences
University of Tromso
P.O. Box 953, N-9001 Tromso, Norway

Introduction

The auroral zone partial reflection radar at Ramfjordmoen, close to Tromso, Norway, is a high power (~50 kW peak power) radar operating at 2.75 MHz [Haug, 1977; Haug et al., 1977]. The antenna array, which is used both for transmitting and receiving, consists of 16 crossed half wavelength dipoles. The antenna beam width is about 17°, the gain 17 dB and the pulse repetition frequency 50 Hz.

The radar is computer controlled allowing for on-line variations of the pulse length, sampling window, gain control and averaging time. The echo amplitude is sampled by an 8-bit A/D converter and stored on magnetic tape for off-line analysis.

In the experiment described below we used a 20-μsec pulse transmitted alternatively on ordinary and extraordinary mode, a 100-km sampling window starting at 20-km height, and a sampling frequency of 150 kHz (1 km). The averaging time was 0.4 sec (10 pulses of each mode, ordinary and extraordinary).

Data

The radar was turned on at 1416 UT on November 22, 1977, and was operating for several 3.5-min periods until 2240 UT. The total amount of data in this period is 1.75 hours.

Throughout the 1416-2240 UT period rather strong and stable echoes were observed above 60 km altitude. In particular, the o-mode returns were quite spectacular, while the x-mode echoes gradually decreased in strength and disappeared at about 1800 UT.

In Figure 1 are shown typical echo recordings averaged for a period of 3.5 min. The echoes have sharp lower borders situated between 58 and 60 km in this example. The o-mode return is more than twice as strong as the x-mode, and the maxima are situated at 67.5 and 66.5 km, respectively. Recordings after 1800 UT do not show any x-mode echoes as already mentioned, but the shape of the o-mode echoes is quite similar to the one presented in Figure 1.

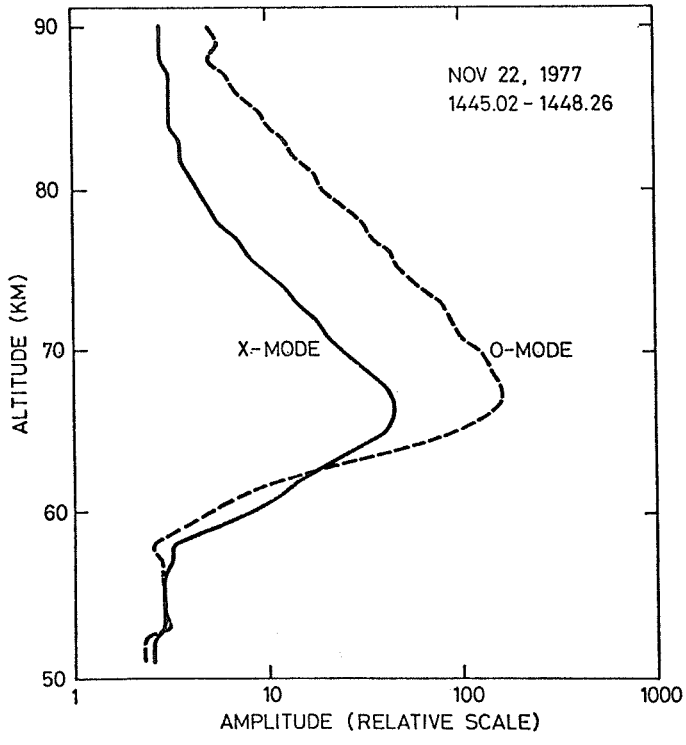

Fig. 1. o- and x-mode amplitude observations obtained by the partial reflection radar at Ramfjordmoen, Tromso, in the period 1445 to 1448 UT on Nov. 22, 1977. The amplitudes are plotted in relative scale versus altitude.

The echo moved slowly up in altitude during the 9-hour period of observation as indicated in Figure 2. On this panel the peak altitude of the lower border of the o-mode echo is plotted versus time. Starting from an altitude of 65 km at 1415 UT, the height of the echo peak slowly increased to about 77 km 9 hours later. In the same period the lower border of the echo moved up in altitude from 55 km to about 70 km.

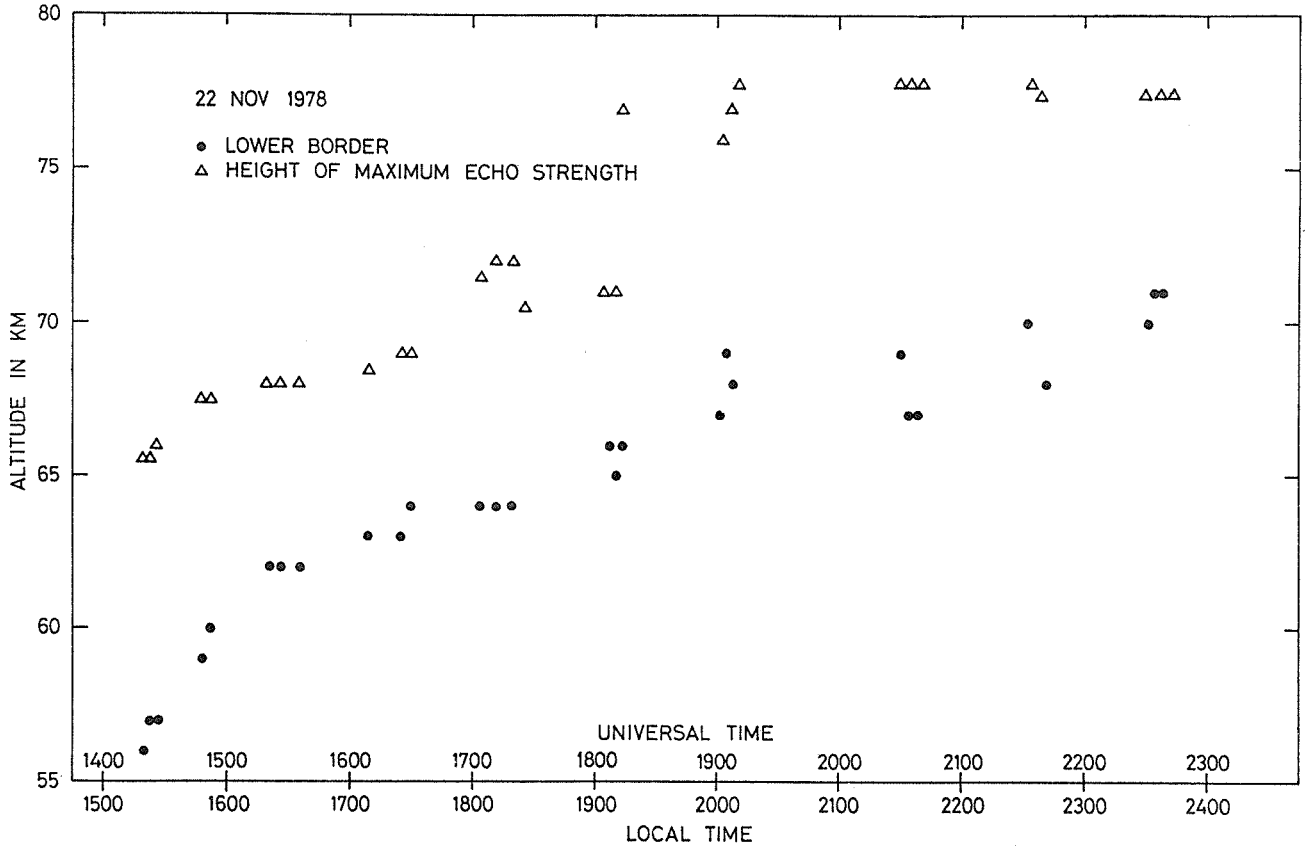

Fig. 2. The altitude of the peak amplitude and lower border of the o-mode echoes are plotted versus time for the whole observation period between 1415 and 2230 UT.

The amplitude of the echo went through some large variations during the observation period, as can be seen from Figure 3, where the maximum amplitude of the o- and x-modes are plotted on a relative scale versus time. At 1415 UT the amplitudes of the two modes were approximately equal; by 2230 UT the o-mode amplitude was almost 3 orders of magnitude stronger than the x-mode. Between 1700 and 1915 UT the o-mode amplitude decreased by as much as a factor of 5. The onset of this reduction appears to be related to the onset of a similar reduction in the cosmic noise strength at 30 MHz monitored at the Ramfjordmoen field site and presented in Figure 4. In this figure the riometer absorption on 40 MHz is also shown (lower trace). It appears that the higher frequency was influenced little between 1700 and 1800 UT. The strong reduction in the x-mode after 1800 UT can be related to a high electron density below the region of maximum o-mode echo.

The width of the time autocorrelation function at the altitude of maximum amplitude is less than 5 sec, and there is a weak tendency for the correlation time to decrease by altitude.

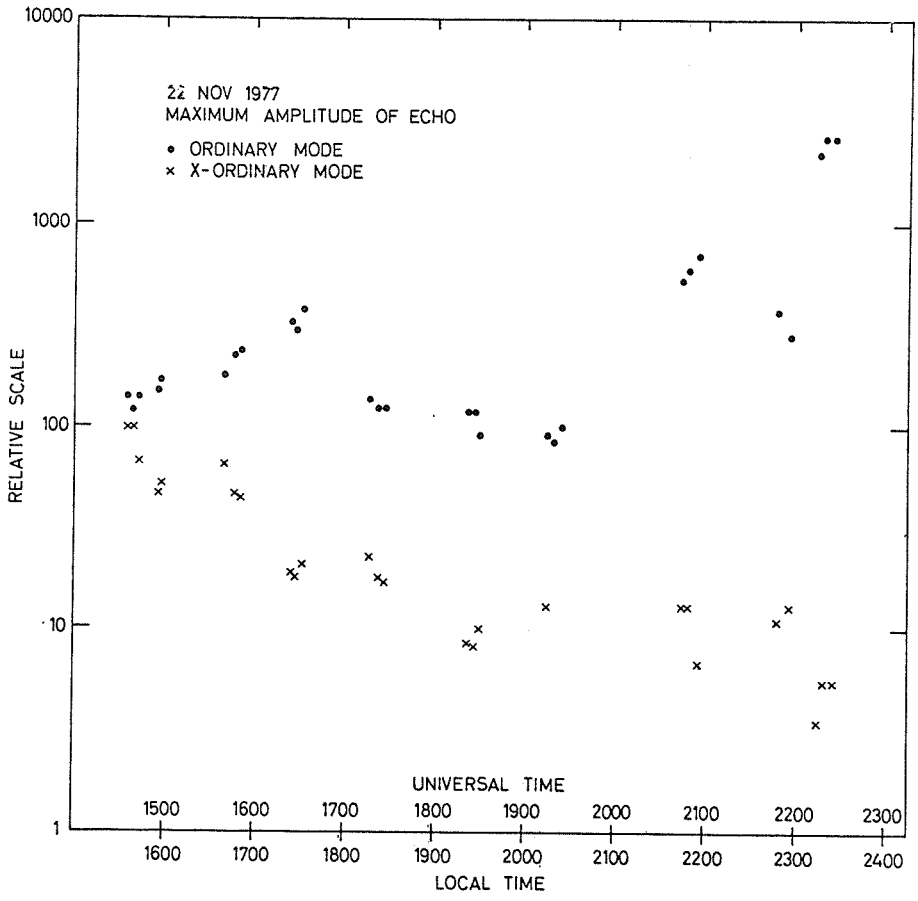

Fig. 3. The maximum amplitudes versus time for the experiment performed on Nov. 22, 1977.

From the observed ratio between the amplitudes of the x- and o-modes, an estimate of the D-region electron density can be derived by using models for the neutral atmosphere. According to the most simple theory, the electron density at height h is given by

$$N(h) = \frac{d}{dh}\left[\ell n(R_X A_X^o A_o / R_o A_o^o A_X)\right]\left[N/2(k_X - k_o)\right] \qquad (1)$$

where R_X and R_o are the theoretical values for the reflection coefficient of the x- and o-modes, respectively; A_X^o and A_o^o are the transmitted amplitudes; A_X and A_o the received amplitudes; and k_X and k_o the wave numbers. The last factor in Equation (1) is, according to simple theory, independent of the electron density N.

In Figure 5 the R_X/R_o model, which corresponds to the Committee on International Reference Atmosphere's (CIRA) 1972 equinox model of the neutral atmosphere, is plotted versus altitude. The A_X/A_o ratio derived from the amplitude observations presented in Figure 1 is also shown together with the electron density profile as derived by using Equation (1). Similar profiles have been derived for all the 3.5-min periods.

This preliminary analysis indicates that a layer in the electron density existed between 58 and 78 km with a peak density of about 10^3 electrons/cm^3. It is important to realize, however, that these electron density profiles are preliminary and therefore subject to great uncertainties.

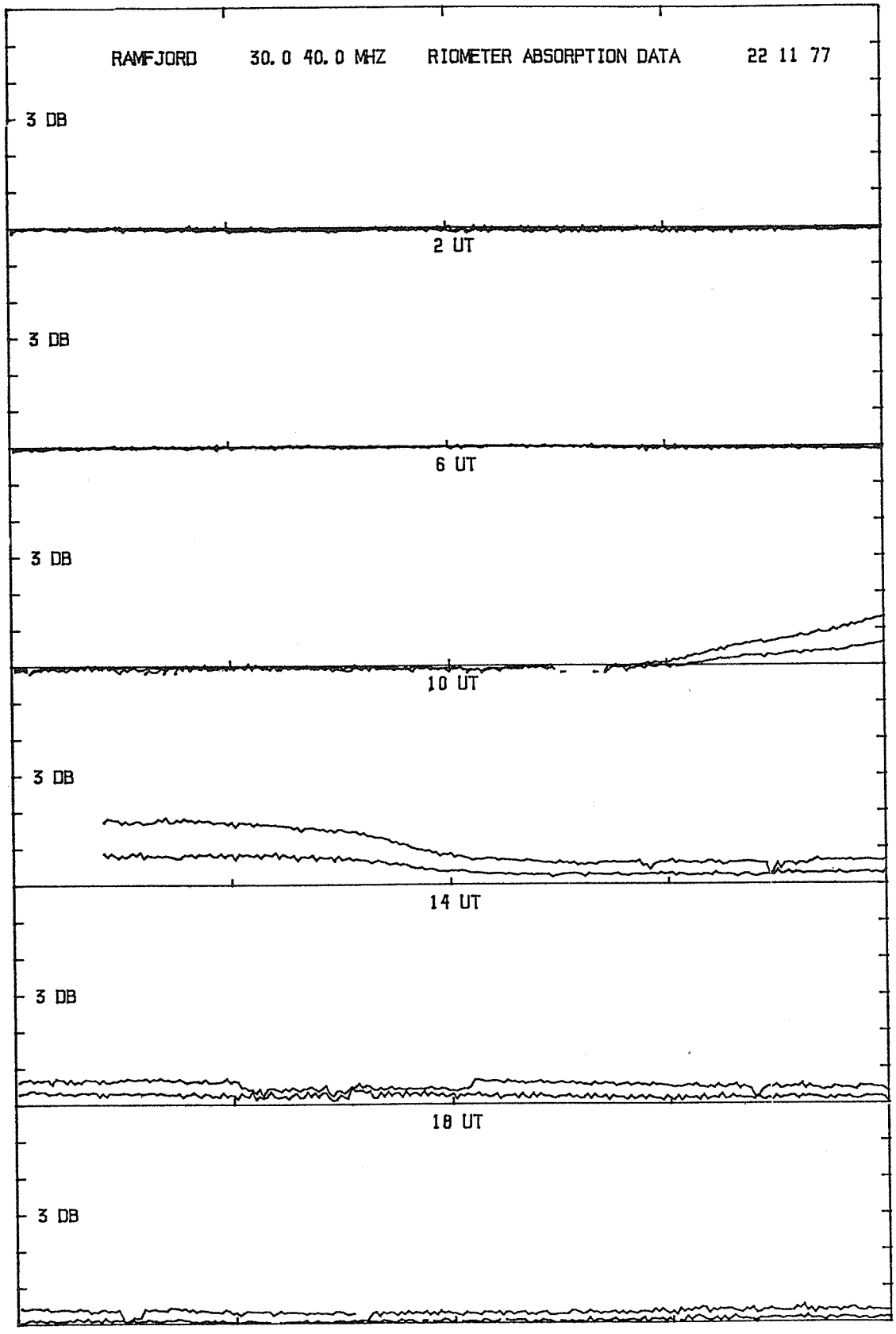

Fig. 4. Riometer recordings on 30 (upper trace) and 40 MHz (lower trace) at Ramfjordmoen, Tromso, for Nov. 22, 1977.

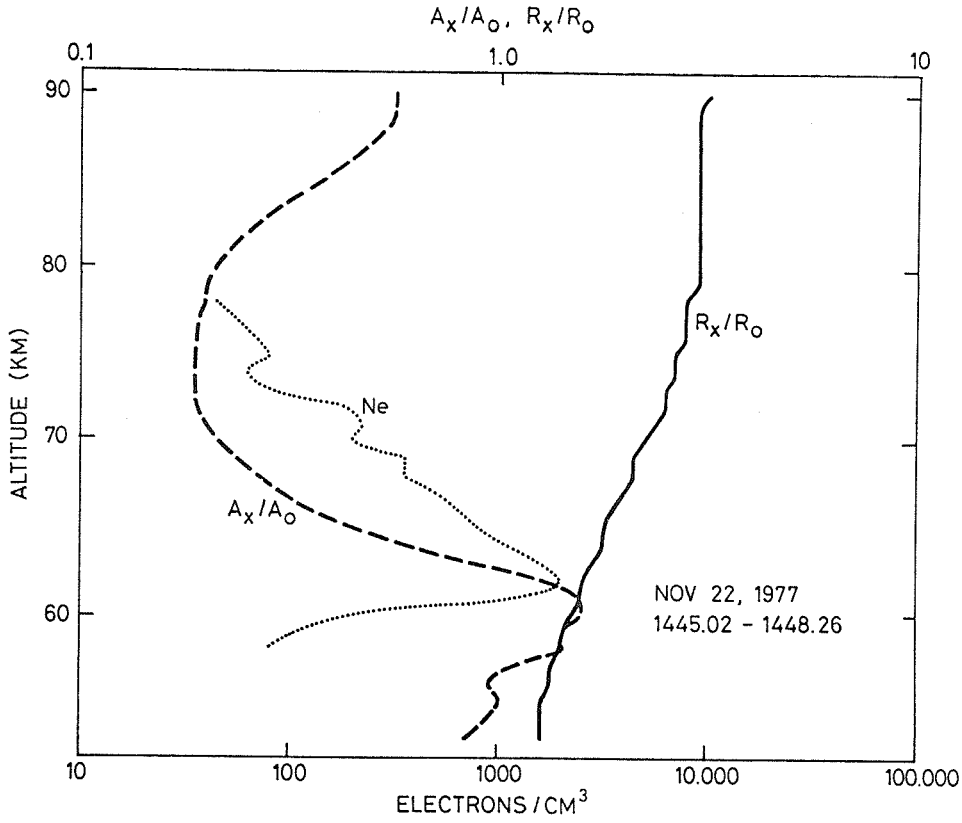

Fig. 5. Preliminary electron density profile obtained from the same data as presented in Figure 1.

Conclusion

During the whole observing period, the Sun was well below the horizon at a height of 70 km. Accordingly, the very pronounced D layer observed cannot be explained by effects from variations in the solar zenith angle. More likely the layer must have been caused by highly energetic particles.

On November 22 a solar flare occurred at 1000 UT and was accompanied by a Type IV radio burst, which is a strong indication of relativistic particles. At 1100 UT an extremely strong cosmic ray event was recorded at Climax and Kiel, and a PCA developed over parts of the polar region [Stauning, 1978]. The D layer reported here was probably caused by particles connected to this major solar-geophysical event.

Acknowledgment

We are greatly indebted to Prof. Olav Holt, Dr. Prabhat Rastogi, Dr. Eivind Thrane and Mrs. Kirsten Bjørnå for helpful comments and assistance. The kind cooperation of the engineers at the institute is much appreciated too. We also thank Dr. Peter Stauning of the Institute of Danish Meteorology who kindly supplied the riometer data.

REFERENCES

HAUG, A. 1977 Coordination of The Tromso Partial Reflection Experiment (PRE) and EISCAT in Radar Probing of the Auroral Plasma, A. Brekke, Ed., (Universitetsforlaget, Tromso, Norway), 429-450.

HAUG, A., E. V. THRANE, K. BJØRNÅ, A. BREKKE and O. HOLT 1977 Observations of Unusually Strong Partial Reflections in the Auroral D-region During an Absorption Event, *J. Atmos. Terr. Phys., 39,* 1333-1340.

STAUNING, P. 1978 *Polar Riometer Absorption Data September 5-28 and November 21-24, 1977* (Ionlab Report p. 76, May 1978, Ionosphere Laboratory, Danish Meteorological Institute, Copenhagen).

Predawn Ionospheric Disturbance on November 22, 1977, 1015-1300 UT

by

A.S. McWilliams and Chris Faust
Department of Physics and Astronomy, St. Cloud State University
St. Cloud, Minnesota 56301

VLF and LF radio transmissions are monitored at St. Cloud on a regular basis to detect sudden ionospheric disturbances (SIDs) and for other studies. SIDs produced by solar flare X-rays are routinely observed when the radio propagation path is located within the daytime hemisphere. The widely reported SID of November 22, 1977 (start 0948, maximum 1010, end 1152 UT), is an example of such an event. For this event all VLF and LF radio propagation paths west of St. Cloud's longitude were observed for these nighttime paths during the time of this flare.

Figure 1 shows the propagation path of the 18.6-kHz transmission from NLK, Jim Creek, Washington (geographic coordinates N48.2 W121.9) to St. Cloud, Minnesota (geographic coordinates N45.6 W94.2), and also the propagation path of the 37.2-kHz transmission from southern California (approximate geographic coordinates N34.5 W118) to St. Cloud. Ground sunrise times for November 22, 1977, are also shown, plotted as broken lines. As indicated by this Figure, both of the propagation paths were well within the dark hemisphere (even at the 200-km level) during the solar flare X-ray event prior to 1200 UT.

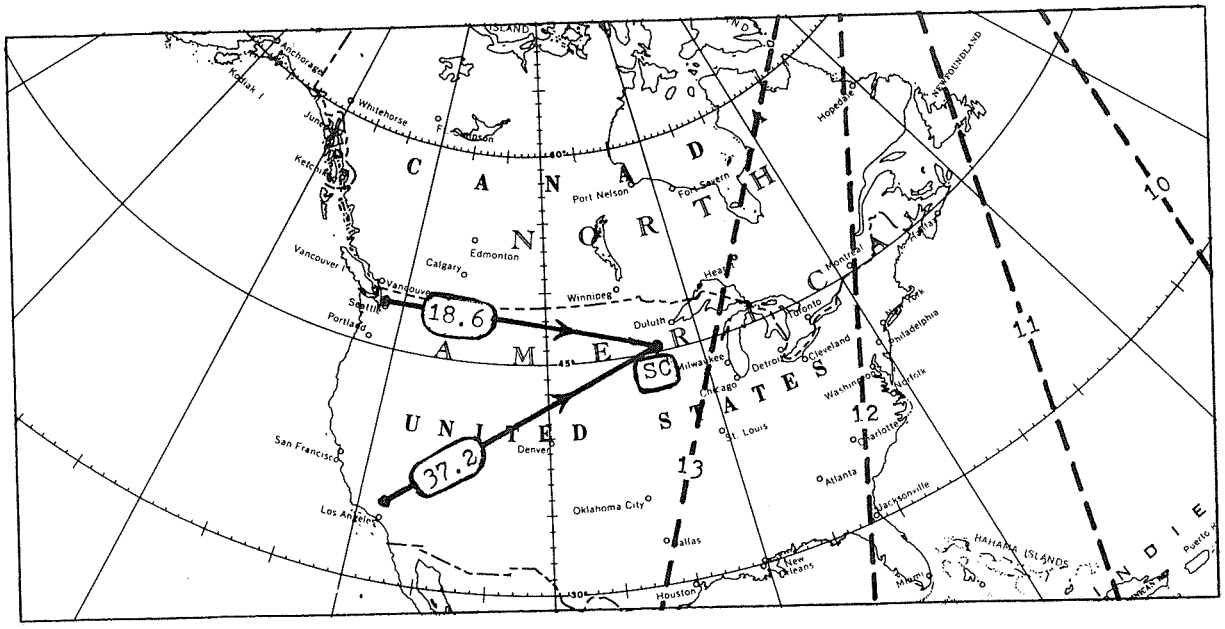

Fig. 1. Map showing the VLF (18.6 kHz) and the LF (37.2 kHz) propagation paths to St. Cloud (SC). Broken lines show November 22, 1977, ground sunrise, 1000, 1100, 1200 and 1300 UT.

For the 18.6-kHz transmission both the signal level and filtered signal level (filtered to separate out and display fluctuations in signal level with periods of the order of minutes) were recorded. Details of the methods used are given in McWilliams and Strait [1976]. For this northern path the overall signal level shows slowly varying changes from day to day, especially during nighttime in winter months. Therefore, unusual events marked by slowly varying changes in nighttime signal level are difficult to recognize. On the other hand, the rapidly varying nighttime fluctuations in signal level, with periods of the order of minutes, are always present to some degree and become relatively very intense during geomagnetic disturbances [McWilliams and Strait, 1976]. The horizontal component of the geomagnetic field is recorded with a sensitivity of 8 gamma/mm at St. Cloud and these recordings show the field to be very quiet for at least a few days before, during, and following November 22, and with no sign of any disturbance during the flare time. Figure 2 shows the 18.6-kHz signal level fluctuation recordings for November 21-23, 1977. They show typical quiet-time fluctuations which are normal for this geomagnetically quiet time period, except that the fluctuations were markedly reduced during the predawn period on November 22. Such reduced fluctuation activity can be interpreted as showing a tendency toward daytime behavior which is characterized by the lower ionosphere being uniformly and steadily bathed in direct solar ionizing radiation.

Fig. 2. VLF (18.6 kHz) amplitude fluctuation recordings for 0000-1500 UT, November 21-23, 1977. The recording for November 22 shows evidence of predawn quieting.

Figure 3 shows the signal level recordings for the more southerly 37.2-kHz path. For this transmission the signal level behavior is much more consistent on a day-to-day basis and therefore unusual behavior is easy to recognize. Only the signal level itself and not the filtered-out signal level fluctuations were recorded for this case. On November 22, 1977, the predawn trace took on a very unusual appearance beginning near 1015 UT. It was unusual for two reasons. First, the overall shape of the trace was markedly different from the usual trace as is evident from the recordings of November 20, 21 and 23. Second, the usual nighttime signal level fluctuations became very small. In this respect the trace had more the appearance of a daytime trace. Again, this unusual behavior may have been caused by uniform and steady ionizing radiation penetrating deep into the lower ionosphere. Direct solar electromagnetic radiation (such as flare X-rays) appears to be ruled out because the path was well into the dark hemisphere.

VLF and LF radio propagation disturbances due to ionization of the lower nighttime ionosphere soon after the start of a solar flare are apparently rare events and have been studied previously in connection with solar cosmic ray flux enhancements [e.g., Bailey, 1959]. We feel that the unusual VLF and LF radio propagation characteristics on November 22, described above, may well be related to the solar cosmic ray flux enhancement ground-level event reported for this date. It is significant that the unusual character of the 37.2-kHz signal level trace began within a few minutes of 1015 UT. This time coincides with the time at which the November 22 cosmic ray ground-level event began.

Acknowledgments

We thank Mr. Casper H. Hossfield of Mahwah, New Jersey; Mr. John B. Power of Trenton, New Jersey; and Mr. Keith L. Strait of Littleton, Colorado, for their helpful correspondence. In particular, we thank Mr. Power for submitting his VLF and LF recordings for inspection. We thank Mr. Strait for relaying to use the Mt. Washington and Durham 5-minute cosmic ray data provided by Mr. John A. McKinnon from data received from Dr. John Lockwood.

References

BAILEY, D.K. 1959 Abnormal Ionization in the Lower Ionosphere Associated with Cosmic-ray Flux Enhancements, Proc. IRE, 47, 255-266.

McWILLIAMS, A.S and K.L. STRAIT 1976 Recurrent VLF Amplitude Fluctuations: Detection Using a Filter and Correspondence with Geomagnetic Disturbances, J. Geophys. Res., 81, 2423-2428.

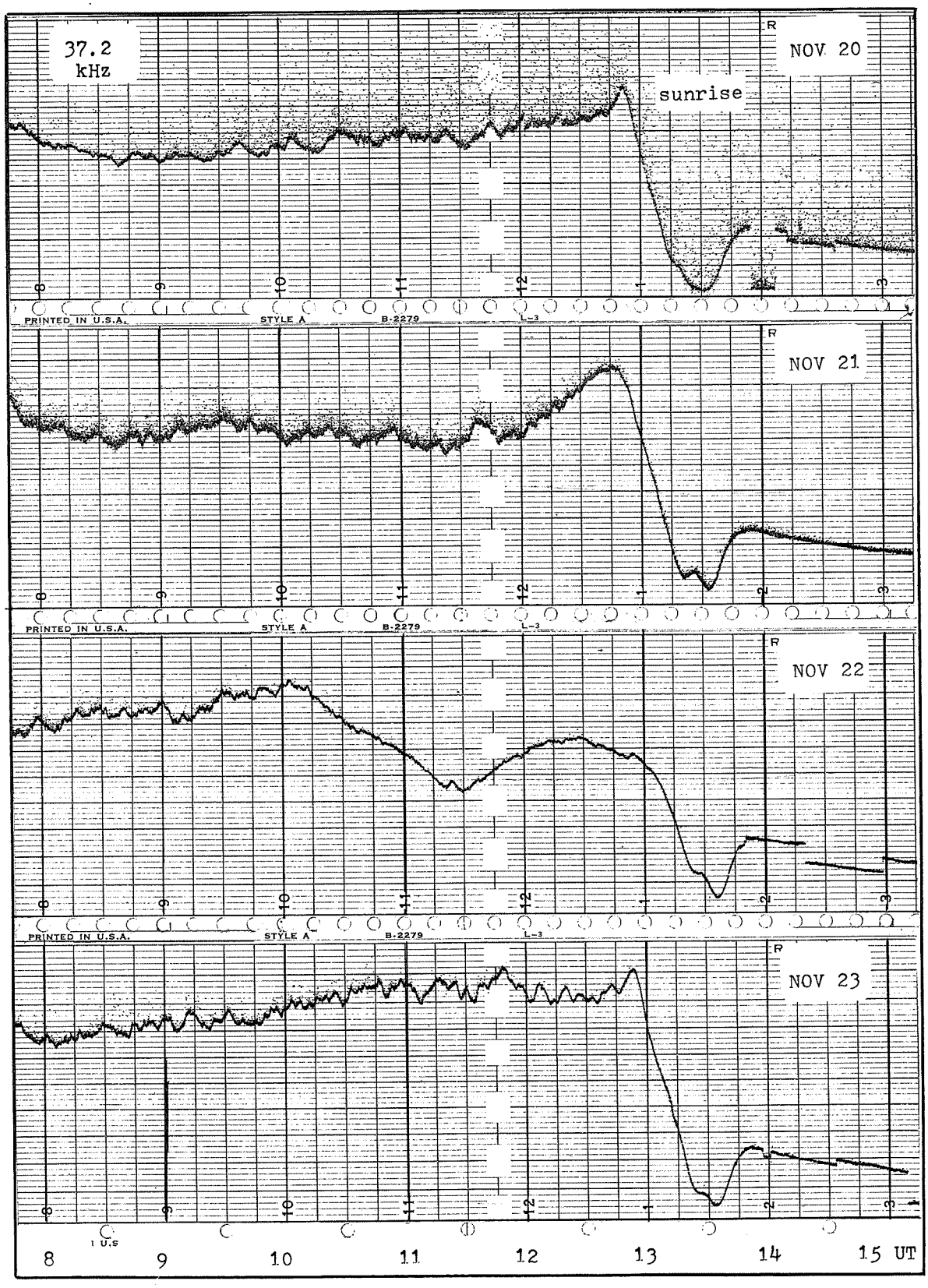

Fig. 3. LF (37.2 kHz) signal level recordings for 0800-1500 UT, November 20-23, 1977. The November 22 chart shows unusual nighttime propagation after 1015 UT, evidenced by a depressed signal level and a daytime-like smoothness.

Magnetic Activity in the Canadian Sector, November 22-26, 1977

by

E.I. Loomer, J.C. Gupta and G. Jansen van Beek
Earth Physics Branch, Energy Mines and Resources, Ottawa, Canada

ABSTRACT

An analysis of magnetic activity following the cosmic ray ground level event of November 22, 1977, has been carried out using magnetograms from Canadian stations. Except for the unusually long duration of the compression of the magnetosphere, lasting for 5 hours after the sudden commencement of November 25, no unexpected features were observed in the magnetograms of the Canadian sector during the 5 days following this very large cosmic ray event.

Introduction

A solar flare of importance 2B was observed at 0945 UT, November 22, 1977, in McMath region 15031. Subsequently, a very large cosmic ray ground level event occurred around 1300 UT. This paper describes the magnetic events recorded during the next 5 days at Canadian magnetic observatories.

Morphology of Disturbance

At the time of the ground level cosmic ray event, a small excursion with largest amplitude at Alert (ALE) (25nT in X component) and period about 7 min, was noted at all Canadian stations. The signature, especially at ALE, could be interpreted as a quiet-time Pc5 event or "Spacequake" [Gupta and Niblett, 1978]. On November 23 magnetic conditions were generally quiet throughout Canada. For the period November 22 to 26 inclusive, the inferred Interplanetary Magnetic Field was directed towards the Sun (negative sector).

On November 24 a double negative (-X) bay was observed at Yellowknife (YKC) beginning suddenly at 0850 UT, with maximum amplitude of -160 nT at 0900 UT. The equivalent westward electrojet was to the south of YKC. This storm was also clearly seen at Churchill (FCC), (-120 nT in X at 0925 UT), and with very much reduced intensity at Cambridge Bay (CBB), Great Whale River (GWC), Meanook (MEA), Victoria (VIC) and Ottawa (OTT). The intensity at College (CMO) was about -25 nT in X. Almost exactly 24 hours later, on November 25, another substorm was observed at 0855 UT which was again maximum at YKC, with amplitude of -180 nT in X (0900 UT) and with storm signatures at the stations listed for the storm of November 24. This coincidence may result from the collapsing of the lines of force in the same region of the magnetotail. The equivalent westward current associated with the November 25 storm moved from south of YKC to north of the station: it was most southerly at 0859 UT and most northerly at 0905 UT.

A sudden commencement was observed at all stations around 1225 UT November 25. The measured time of commencement was between 1223 UT and 1225 UT at all stations except St. John's (STJ), where it occurred at 1227 UT; the time shown in the IAGA listing is 1227 UT (Figure 1a,b). The observed differences in times of commencement appear to be real. The SC was not immediately followed by a storm, but there was generally some Pc5 activity for about 2 hours with maximum intensity (about 50nT in X) at FCC.

The lowest latitude Canadian station (VIC) showed a positive excursion of the H component (25 nT above the quiet level) which lasted for about 5 hours. A positive X(H) effect was also seen at MEA, Whiteshell (WHS), OTT and STJ over a shorter period. For these hours Dst was positive, indicating compression of the magnetosphere. The H, D, Z variations very clearly show that these stations were under the influence of an eastward current flow. However, variations to the north at YKC, FCC, Baker Lake (BLC) and CBB indicate a westward current flow in the oval between FCC and BLC at these hours. From the Dst indices the main ring current was established only after 20 UT, and persisted fo several days.

A sudden impulse (SI) was observed at Canadian stations at 1800 UT November 25. Current vectors were plotted (Figure 2) for 1910, 1930, 2000, 2030 and 2153 UT from the data given in Table 1. These times were determined from special features observed on the magnetograms. Current flows were consistent with those found by Loomer and Jansen van Beek [1971] for the day sector during magnetic substorms of December 5, 1968. In the polar cap, current flow was consistently westward and may be interpreted as the return current system of a westward electrojet inferred in the midnight sector of the auroral oval. A sequence of negative H bays began about 1800 UT at Tromso. Maximum perturbation was at 1848 UT (-440 nT in H). As early as 1910 UT a small eastward current vector is noted at GWC. As the earth rotated beneath the oval, the eastward current flow became apparent at FCC (2000 to 2153 UT). The maximum effect in X was observed at 2000 UT at GWC (260 nT). To the south of the auroral zone, current flow can be interpreted as return currents associated with the eastward current flowing in the auroral oval.

A new event was evident beginning about 2230 UT south of GWC, and current vectors were drawn (Fig. 2(b)) for the times 2218, 2335, 2347 UT, November 25, and 0100 UT, November 26 (not shown) from the data listed in Table 2. Although this was undoubtedly a new event, the interpretation is similar to

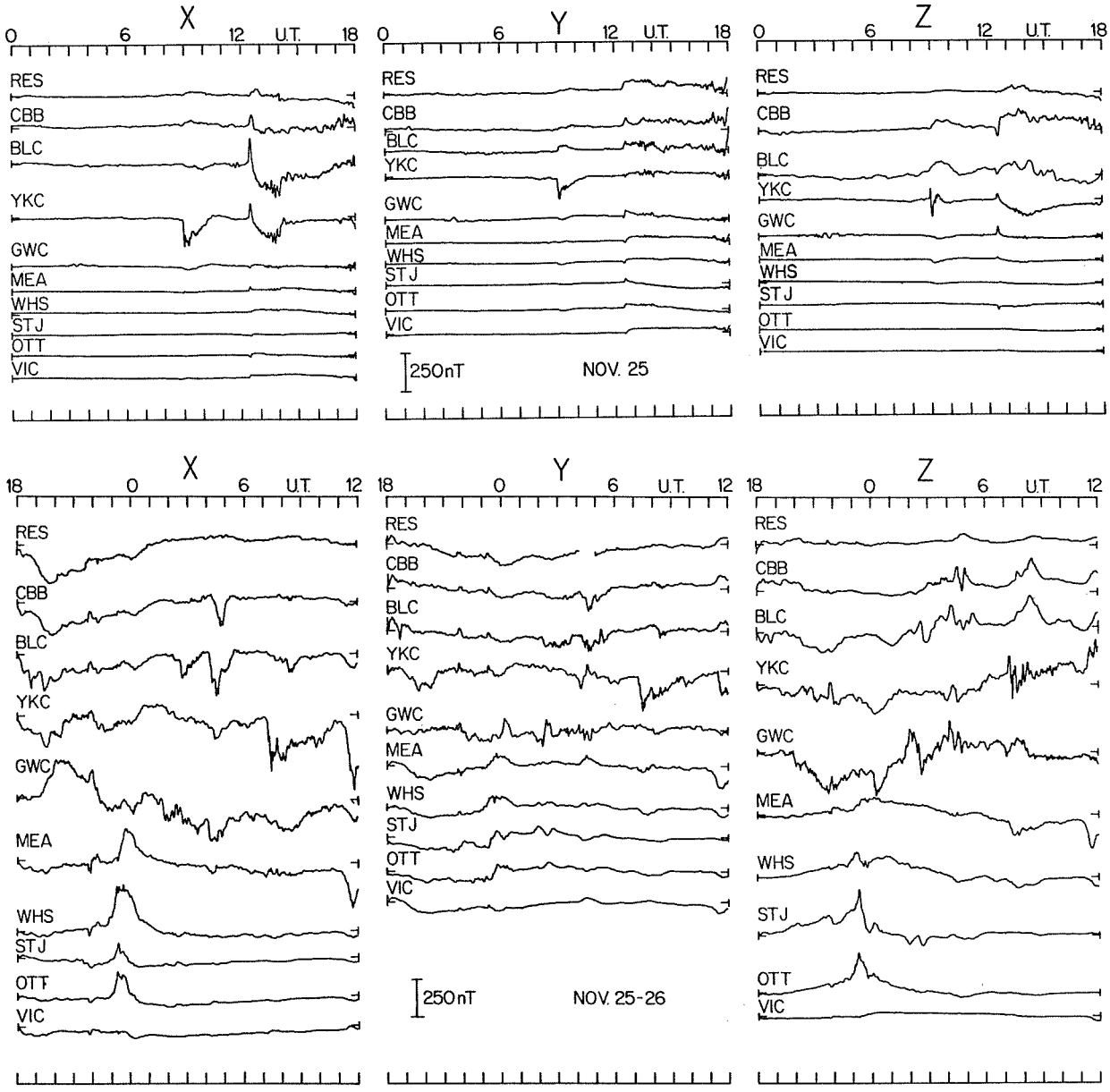

Fig. 1. Magnetograms plotted from 1-minute digital data for November 25-26, 1977.

that given for the event discussed above, except that now the eastward electrojet is further south and west, with maximum effect in X at WHS at 2318 UT (285 nT). This observed occurrence further west with time of the eastward current flow is consistent with the picture of the earth rotating beneath a fixed auroral oval.

The next suite of events were four well-defined polar substorms in the auroral oval in the midnight-morning, with maximum intensities near 0300, 0430, 0830 and 1200 UT, November 26 at BLC and FCC. The last storm was particularly intense at CMO (-550 nT in H) with westward current flowing between FCC and MEA in the Canadian sector and north of CMO in Alaska.

Table 1. Perturbations Measured from the Quiet Midnight Level (Nov. 23, 1977)

Station	Abbr.	X(H) nT Nov. 25				Y(D) nT Nov. 25				Z nT Nov. 25			
		1910	1930	2000	2030	1910	1930	2000	2030	1910	1930	2000	2030
Alert	(ALE)	-238	-355	-300	-116	0	+25	-13	-139	+13	+13	+26	+45
Resolute Bay	(RES)	-144	-240	-264	-197	+30	+43	+24	+6	+12	+24	+48	+24
Mould Bay	(MBC)	-156	-281	-310	-217	+56	+64	+77	+6	+24	+71	+101	+132
Cambridge Bay	(CBB)	-105	-185	-220	-160	+28	+10	0	0	+40	+70	+50	+10
Baker Lake	(BLC)	-104	-232	-168	-92	+16	0	0	-4	+8	+16	-40	+84
Yellowknife	(YKC)	-100	-195	-120	-10	-45	-80	-90	-35	-25	-40	-55	-35
Churchill	(FCC)	-40	-16	+80	+28	+20	+12	+36	+52	+16	-48	-72	-56
Great Whale River	(GWC)	+15	+100	+250	+240	-5	-30	-20	+5	0	-15	-80	-65
Whiteshell	(WHS)	-50	-40	-10	0	-30	-50	-70	-70	+5	+10	+20	+35
Meanook	(MEA)	-67	-85	-73	-45	0	-19	-25	-63	-5	-9	-5	+9
St. Johns	(STJ)	-10	-18	-15	-10	-45	-60	-82	-75	+20	+42	+80	+70
Ottawa	(OTT)	-25	-19	0	-9	-36	-56	-82	-56	0	0	+19	+30
Victoria	(VIC)	-59	-70	-48	-48	0	+26	-48	-3	-28	-32	-9	-30
College	(CMO)	-65	-234	-110	-104	-38	-76	-80	-51	-64	-154	-227	-206

Table 2. Perturbations Measured from the Quiet Midnight Level (Nov. 23, 1977)

Station	Abbr.	X(H) nT					Y(D) nT					Z nT				
		Nov.25				Nov.26	Nov.25				Nov.26	Nov.25				Nov.26
		2153	2318	2335	2347	0100	2153	2318	2335	2347	0100	2153	2318	2335	2347	0100
Alert	(ALE)	-12	-24	+49	+85	+49	-126	-75	-135	-158	-63	+18	+10	+27	+33	+26
Resolute Bay	(RES)	-120	-84	-96	-98	-30	-25	-30	-66	-81	-80	+18	+25	+12	+9	+24
Mould Bay	(MBC)	-105	-51	-64	-80	-13	-38	-26	-64	-82	-51	+12	+12	0	-12	-18
Cambridge Bay	(CBB)	-60	-70	-70	-70	-25	0	0	-40	-60	-45	-15	0	-15	-15	-30
Baker Lake	(BLC)	-48	-84	-48	-56	-12	0	-8	-48	-60	-40	-64	-44	-44	-44	-56
Yellowknife	(YKC)	+50	-30	-25	-35	+75	0	+40	-15	-15	+50	+25	-65	-105	-120	-80
Churchill	(FCC)	+56	-80	-36	-40	0	-8	0	-32	-48	-20	-104	-80	-64	-80	-96
Great Whale River	(GWC)	+170	-60	-10	-30	+25	+30	-70	-35	-40	-35	-205	-155	-120	-150	-105
Whiteshell	(WHS)	-20	+285	+260	+260	+25	-50	+20	+50	+50	+5	+60	+160	+80	+65	+130
Meanook	(MEA)	-45	+34	+150	+297	+38	-19	-19	-6	-13	-9	+28	+65	+103	+89	+87
St. Johns	(STJ)	-68	+100	+45	+10	-55	-105	-65	+5	+45	+30	+105	+305	+150	+40	+10
Ottawa	(OTT)	-30	+178	+153	+80	-56	-73	-26	+5	+57	+5	+45	+264	+191	+105	+52
Victoria	(VIC)	-34	-48	-44	-58	-58	-22	+5	-27	-33	-11	-20	-23	-9	-5	10
College	(CMO)	-78	-52	+21	+52	+5	-25	+25	-13	-19	-38	-90	-21	-6	-6	+25

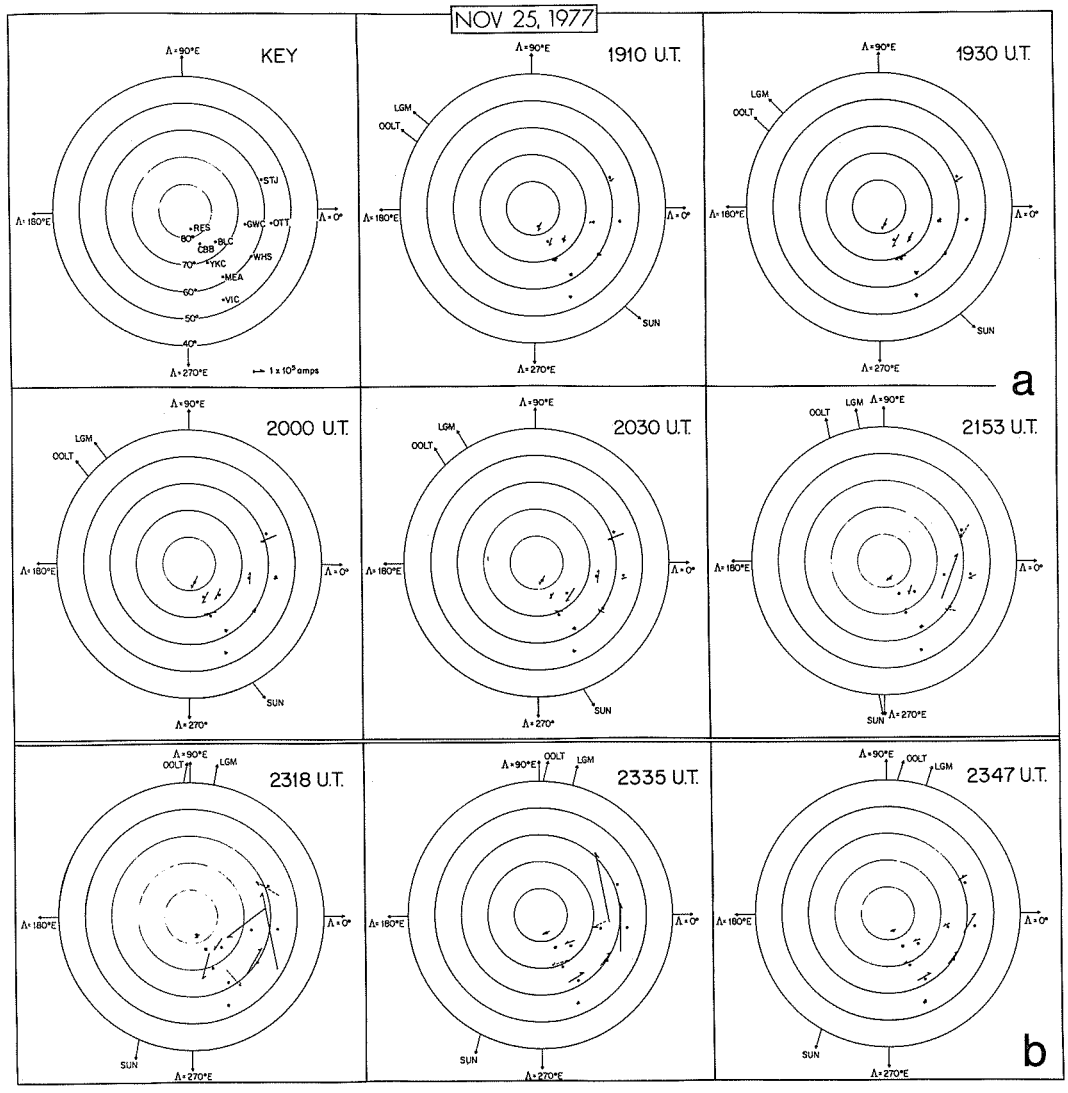

Fig. 2. Current vector plots for selected times on November 25, 1977.

Conclusions

An examination of magnetic records from Canadian stations has been carried out for the interval 0900 UT, November 25 to 1500 UT, November 26. Occasional reference has also been made to the College magnetograms published in the College preliminary geomagnetic data report for November. It was in this interval that magnetic activity was most apparent following the Ground Level Event (G.L.E.) of November 22.

Low latitude Canadian magnetograms, particularly VIC, indicated that the magnetosphere remains compressed for about 5 hours after the SC at 1227 UT, November 25. This is considerably longer than the usual duration of the first phase of a storm. Following this initial compression, a westward ring current developed, which, short-circuiting in the auroral zone, gave rise to eastward electrojets in the daytime sector and to westward electrojets in the midnight sector. These observations are consistent with the models of Crooker and McPherron [1972], Fukushima and Kamide [1973], and Gupta [1978].

The investigation of current flow in the daytime sector at the time of the beginning of the main phase of the storm (possibly originating from strong westward electrojets inferred in the midnight sector) showed that the development further to the west with time of an eastward electrojet can be adequately accounted for by the model of the earth rotating beneath a fixed auroral oval.

Acknowledgements

We would like to extend sincere thanks to Mr. J. Morris of the Computer Science Centre, Energy, Mines and Resources Canada for his valuable assistance in programming. These results have been published under Earth Physics Report Series as Contribution of the Earth Physics Branch, No. 729.

References

CROOKER, N.U. and R.L. MCPHERRON 1972 On the Distinction between the Auroral Electrojet and Partial Ring Current System, J. Geophys. Res., 77, 6886-6889.

FUKUSHIMA, N. and Y. KAMIDE 1973 Partial Ring Current Models for Worldwide Geomagnetic Disturbances, Rev. Geophys. Space Phys., 11, 795-853.

GUPTA, J.C. 1978 Geomagnetic Bays and Pc5 Pulsation Substorms at High Latitudes, J. Atmos. Terr. Phys., 40, 169-181.

GUPTA, J.C. and E.R. NIBLETT 1979 On the Quiet Time Pc5 Pulsation Events (Spacequakes), Planet. Space Sci., 27, 131-143.

LOOMER, E.I. and G. JANSEN VAN BEEK 1971 Magnetic Substorms December 5, 1968, Pub. Earth Phys. Br., 41, No. 10, 193-198.

Pamatai Geomagnetic Observatory Data During the November 1977 Event

by

H. G. Barsczus
Observatoire de Geophysique Pamatai Centre ORSTOM
B.P. 529, Papeete/Tahiti, French Polynesia

Introduction

Pamatai Geomagnetic Observatory is located on the island of Tahiti which lies in the Windward group of the Society Islands, and has geographic and geomagnetic coordinates as follows: (S17.57 E210.42) and (S15.35 E282.77). Standard geomagnetic data were obtained during the period under consideration from two sets of La Cour variometers (recording speed: 15 mm/hour; scale values: H=2.35 and 2.53 nT/mm; D=0.47 and 0.48 '/mm; Z=1.92 and 3.00 nT/mm) as well as from micropulsation sensors (quick run recording speed 6 mm/min and ultraquick run recording speed 60 mm/min).

The Data

Standard microfilms of magnetograms are available through WDC-A for Solar-Terrestrial Physics or from the observatory. For copies of selected quick run records please send your inquiries to the observatory, because even though the quick run records show a large amount of interesting phenomena, they are not processed on a routine basis.

Table 1 presents K indices for November 1977, Table 2 storm data, and Table 3 a special event for the same period. Figures 1 to 3 show the onsets of magnetic storms as recorded with the quick run system.

Table 1. Pamatai - November 1977 K Indices

Date			Sum	Date			Sum
(UT Day)	1 2 3 4	5 6 7 8		(UT Day)	1 2 3 4	5 6 7 8	
01	1 0 1 1	1 0 1 1	06	16	1 2 2 2	2 2 1 1	13
02	1 0 0 2	1 0 1 1	06	17	0 0 0 1	0 0 0 2	03
03	1 1 1 0	0 1 0 0	04	18	1 1 0 1	1 1 0 1	06
04	0 0 1 1	1 3 1 1	08	19	0 2 1 2	1 2 1 1	10
05	1 1 1 1	0 1 1 0	06	20	1 1 1 0	0 1 1 1	06
06	1 1 0 0	3 1 1 1	08	21	1 1 0 0	2 1 0 0	05
07	1 0 0 1	1 1 0 0	04	22	0 1 1 1	0 0 0 1	04
08	0 0 1 1	0 0 1 0	03	23	1 1 0 0	1 1 0 1	05
09	0 0 0 0	0 0 0 0	00	24	0 0 1 1	0 0 0 0	02
10	0 0 1 1	3 3 3 3	14	25	0 0 1 0	4 3 4 5	17
11	1 1 1 2	2 1 1 1	10	26	3 2 2 3	2 4 5 4	25
12	1 3 3 3	2 2 2 2	18	27	4 2 1 1	1 1 1 1	12
13	1 1 2 3	1 3 2 2	15	28	1 1 1 1	1 1 1 0	07
14	1 2 2 2	3 4 4 3	21	29	1 1 1 1	1 1 1 1	08
15	2 2 1 3	1 1 1 1	12	30	2 3 3 3	2 2 1 1	17

Note: At Pamatai K = 9 has a lower limit of 350 nT.

Table 2. Pamatai - Magnetic Storm Data from Normal Magnetogram

Date	Start		SC Amplitudes			Maximum 3-Hour Index	K	Ranges			UT End	
(1977)	UT	Type	D(')	H(nT)	Z(nT)	Day (3-Hour Period)	K	D(')	H(nT)	Z(nT)	Day	Hour
Nov 10	1309	SC		+6	-2	10 (5-8)	3				11	09
14	08..	Gradual				14 (6,7)	4				16	15
25	1225	SC	+0.4	+17	-2	25 (8)	5	2.9	73	9	26	06
26	1714	SC*	-1.3	+25*	-13*	26 (7)	5	4.8	61	25	27	15

*Sudden commencement in which main impulse followed small initial impulse. Values tabulated correspond to the main impulse.

Table 3. Pamatai - Special Event from Normal Magnetogram

(1977)	Start (UT)	Type	End (UT)	Amplitudes D(')	H(nT)	Z(nT)	Remarks
Nov 06	1916?	SFE?	1936	0	+4	-1	

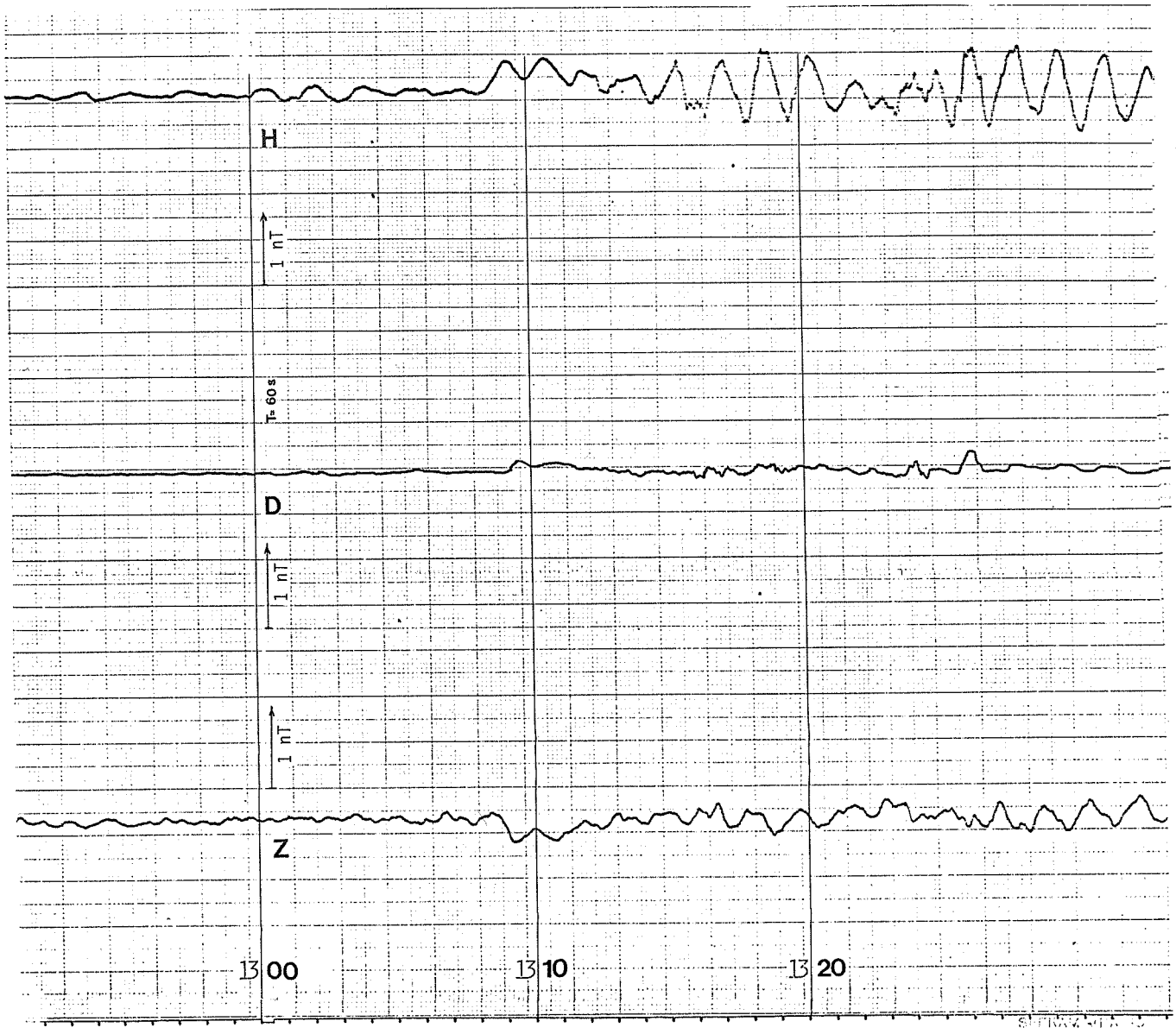

Fig. 1. Portion of rapid run record (6 mm/min) taken at Pamatai Geomagnetic Observatory on November 10, 1977. Heavy vertical lines mark 1300, 1310 and 1320 UT. The storm begins about 1309 UT.

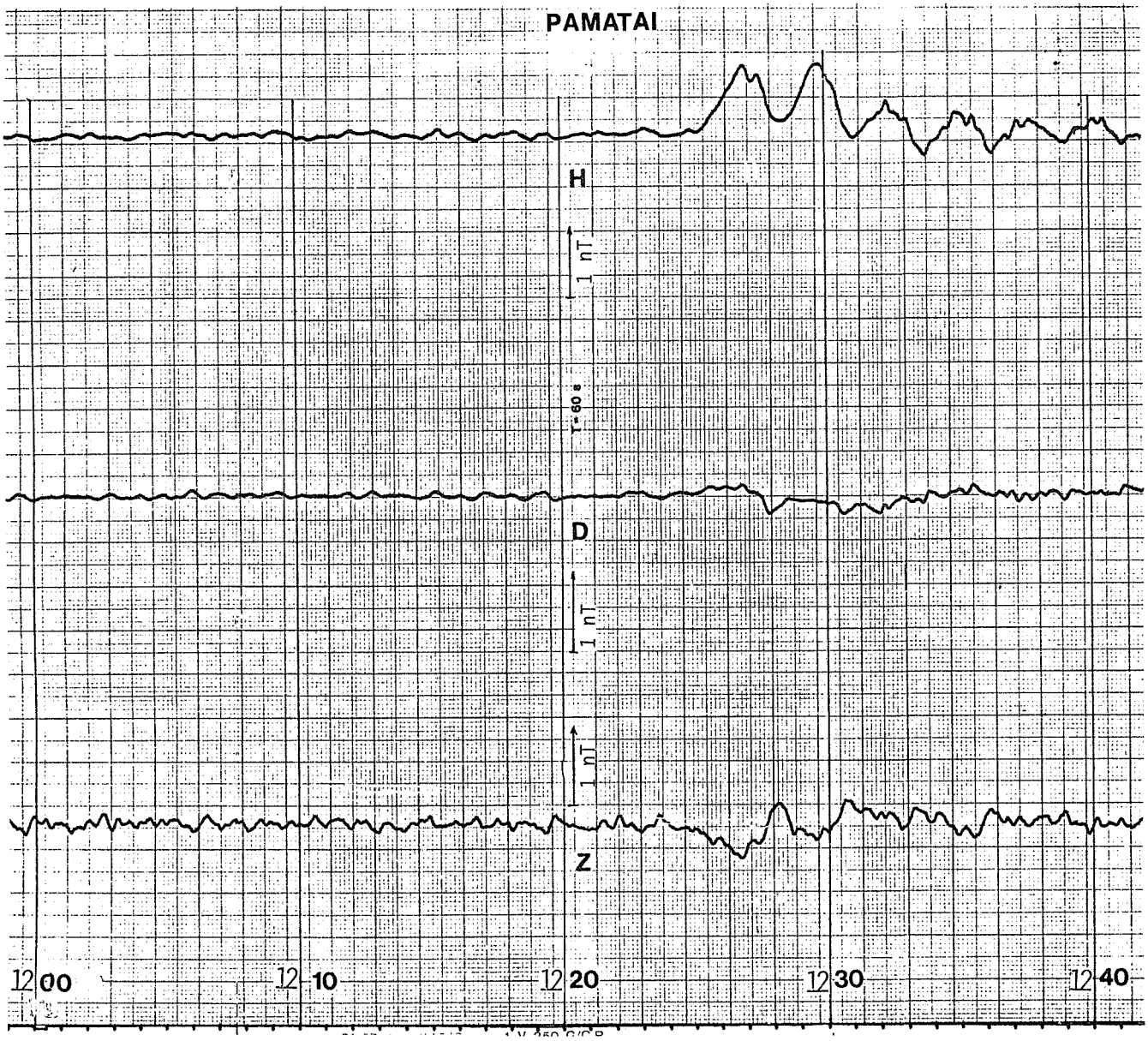

Fig. 2. Portion of rapid run record (6 mm/min) taken at Pamatai Geomagnetic Observatory on November 25, 1977. Heavy vertical lines mark 1200 to 1240 UT in 10-min intervals. The storm begins about 1225 UT.

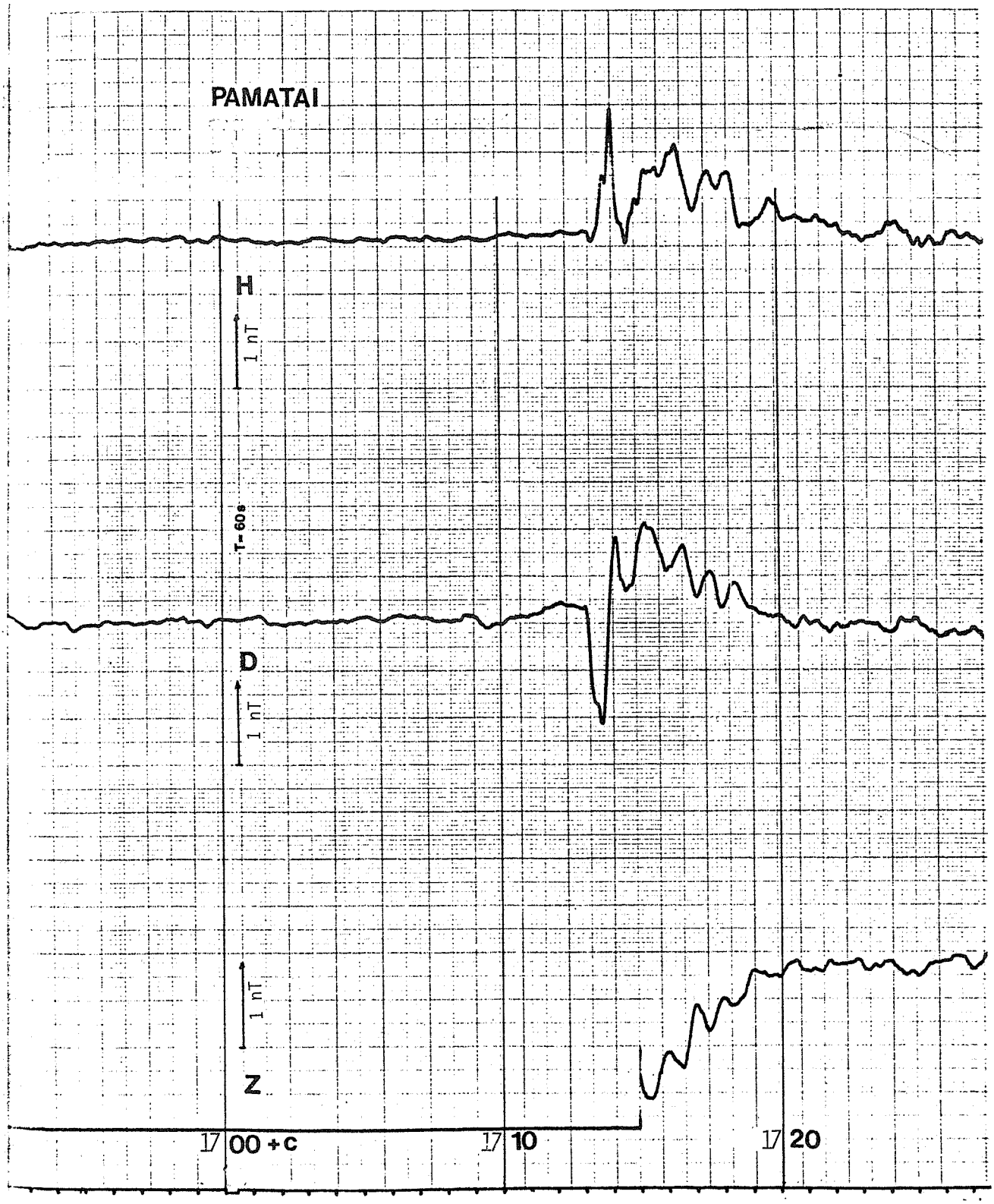

Fig. 3. Portion of rapid run record (6 mm/min) taken at Pamatai Geomagnetic Observatory on November 26, 1977. Heavy vertical lines mark 1700, 1710 and 1720 UT. The storm begins about 1714 UT.

AUTHOR INDEX

UAG SERIES OF REPORTS

Between 4 and 12 UAG Reports are published at irregular intervals each year. Subscriptions may be ordered through the National Geophysical and Solar-Terrestrial Data Center, Environmental Data and Information Service, NOAA, Boulder, CO 80303, USA. The subscription price for the calendar year only is $40.00 ($23.00 additional for foreign mailing). Each year the single copy prices total less than $40.00, the expiration date for all subscriptions will be extended. Back issues may be purchased at the prices shown below plus a $4.00 handling charge per order; some reports, though, are available only on microfiche. Orders must include check or money order payable in U.S. currency to the Department of Commerce, NOAA/NGSDC.

UAG-1 "IQSY Night Airglow Data," by L.L. Smith, F.E. Roach, and J.M. McKennan, ESSA Aeronomy Laboratory, Boulder, CO, July 1968, 305 pp, $1.75.

UAG-2 "A Reevaluation of Solar Flares, 1964-1966," by Helen W. Dodson and E. Ruth Hedeman, McMath-Hulbert Observatory, University of Michigan, Pontiac, MI, August 1968, 28 pp, $0.30.

UAG-3 "Observations of Jupiter's Sporadic Radio Emission in the Range 7.6-41 MHz, 6 July 1966 through 8 September 1968," by James W. Warwick and George A. Dulk, University of Colorado, Boulder, CO, October 1968, 35 pp, $0.55.

UAG-4 "Abbreviated Calendar Record 1966-1967," by J. Virginia Lincoln, Hope I. Leighton and Dorothy K. Kropp, ESSA now NOAA, Aeronomy and Space Data Center, Boulder, CO, January 1969, 170 pp, $1.25.

UAG-5 "Data on Solar Event of May 23, 1967 and its Geophysical Effects," compiled by J. Virginia Lincoln, World Data Center A, Upper Atmosphere Geophysics, ESSA now NOAA, Boulder, CO, February 1969, 120 pp, $0.65.

UAG-6 "International Geophysical Calendars 1957-1969," by A.H. Shapley and J. Virginia Lincoln, ESSA Research Laboratories, now NOAA, Boulder, CO, March 1969, 25 pp, $0.30.

UAG-7 "Observations of the Solar Electron Corona: February 1964 - January 1968," by Richard T. Hansen, High Altitude Observatory, NCAR, Boulder, CO, and Kamuela, HI, October 1969, 12 pp, $0.15.

UAG-8 "Data on Solar-Geophysical Activity October 24 - November 6, 1968," Parts 1 and 2, compiled by J. Virginia Lincoln, World Data Center A, Upper Atmosphere Geophysics, ESSA now NOAA, Boulder, CO, March 1970, 312 pp, $1.75 (includes Parts 1 and 2).

UAG-9 "Data on Cosmic Ray Event of November 18, 1968 and Associated Phenomena," compiled by J. Virginia Lincoln, World Data Center A, Upper Atmosphere Geophysics, ESSA now NOAA, Boulder, CO, April 1970, 109 pp, $0.55.

UAG-10 "Atlas of Ionograms," edited by A.H. Shapley, ESSA Research Laboratories now NOAA, Boulder, CO, May 1970, 243 pp, $1.50.

UAG-12 "Solar-Geophysical Activity Associated with the Major Geomagnetic Storm of March 8, 1970," Parts 1, 2 and 3, compiled by J. Virginia Lincoln and Dale B. Bucknam, World Data Center A, Upper Atmosphere Geophysics, ESSA now NOAA, Boulder, CO, April 1971, 466 pp, $3.00 (includes Parts 1-3).

UAG-13 "Data on the Solar Proton Event of November 2, 1969 through the Geomagnetic Storm of November 8-10, 1969," compiled by Dale B. Bucknam and J. Virginia Lincoln, World Data Center A, Upper Atmosphere Geophysics, ESSA now NOAA, Boulder, CO, May 1971, 76 pp, $0.90.

UAG-14 "An Experimental, Comprehensive Flare Index and Its Derivation for 'Major" Flares, 1955-1969," by Helen W. Dodson and E. Ruth Hedeman, McMath-Hulbert Observatory, University of Michigan, Pontiac, MI, July 1971, 25 pp, $0.30.

UAG-16 "Temporal Development of the Geophysical Distribution of Auroral Absorption for 30 Substorm Events in each of IQSY (1964-65) and IASY (1960)," by F.T. Berkey, University of Alaska, Fairbanks, AK; V.M. Driatskiy, Arctic and Antarctic Research Institute, Leningrad, USSR; K. Henriksen, Auroral Observatory, Tromson, Norway; D.H. Jelly, Communications Research Center, Ottawa, Canada; T.I. Shchuka, Arctic and Antarctic Research Institute, Leningrad, USSR; A. Theander, Kiruna Geophysical Observatory, Kiruna, Sweden; and J. Yliniemi, University of Oulu, Oulu, Finland, September 1971, 131 pp, $0.70 (microfiche only).

UAG-17 "Ionospheric Drift Velocity Measurements at Jicamarca, Peru (July 1967 - March 1970)," by Ben B. Balsley, NOAA Aeronomy Laboratory, Boulder, CO, and Ronald F. Woodman, Jicamarca Radar Observatory, Instituto Geofisico del Peru, Lima, Peru, October 1971, 45 pp, $0.55 (microfiche only).

UAG-18 "A Study of Polar Cap and Auroral Zone Magnetic Variations," by K. Kawasaki and S.-I. Asasofu, University of Alaska, Fairbanks, AK, June 1972, 21 pp, $0.20.

UAG-19 "Reevaluation of Solar Flares 1967," by Helen W. Dodson and E. Ruth Hedeman, McMath-Hulbert Observatory, University of Michigan, Pontiac, MI, and Marta Rovira de Miceli, San Miguel Observatory, Argentina, June 1972, 15 pp, $0.15.

UAG-21 "Preliminary Compilation of Data for Retrospective World Interval July 26 - August 14, 1972," by J. Virginia Lincoln and Hope I. Leighton, World Data Center A for Solar-Terrestrial Physics, NOAA, Boulder, CO, November 1972, 128 pp, $0.70.

UAG-22 "Auroral Electrojet Magnetic Activity Indices (AE) for 1970," by Joe Haskell Allen, National Geophysical and Solar-Terrestrial Data Center, Boulder, CO, November 1972, 146 pp, $0.75.

UAG-23 "U.R.S.I. Handbook of Ionogram Interpretation and Reduction," Second Edition, November 1972, edited by W.R. Piggott, Radio and Space Research Station, Slough, UK, and K. Rawer, Arbeitsgruppe fur Physikalische Weltraumforschung, Freiburg, GFR, November 1972, 324 pp, $1.75.

UAG-23A "U.R.S.I. Handbook of Ionogram Interpretation and Reduction," Second Edition, Revision of Chapters 1-4, edited by W.R. Piggott, Radio and Space Research Station, Slough, UK, and K. Rawer, Arbeitsgruppe fur Physikalische Weltraumforschung, Freiburg, GFR, November 1972, 135 pp, $2.14.

UAG-24 "Data on Solar-Geophysical Activity Associated with the Major Ground Level Cosmic Ray Events of 24 January and 1 September 1971," Parts 1 and 2, compiled by Helen E. Coffey and J. Virginia Lincoln, World Data Center A for Solar-Terrestrial Physics, NOAA, Boulder, CO, December 1972, 462 pp, $2.00 (includes Parts 1 and 2).

UAG-25 "Observations of Jupiter's Sporadic Radio Emission in the Range 7.6-41 MHz, 9 September 1968 through 9 December 1971," by James W. Warwick, George A. Dulk and David G. Swann, University of Colorado, Boulder, CO, February 1973, 35 pp, $0.35.

UAG-26 "Data Compilation for the Magnetospherically Quiet Periods February 19-23 and November 29 - December 3, 1970," compiled by Helen E. Coffey and J. Virginia Lincoln, World Data Center A for Solar-Terrestrial Physics, NOAA, Boulder, CO, May 1973, 129 pp, $0.70.

UAG-27 "High Speed Streams in the Solar Wind," by D.S. Intriligator, University of Southern California, Los Angeles, CA, June 1973, 16 pp, $0.15.

UAG-28 "Collected Data Reports on August 1972 Solar-Terrestrial Events," Parts 1, 2 and 3, edited by Helen E. Coffey, World Data Center A for Solar-Terrestrial Physics, NOAA, Boulder, CO, July 1973, 932 pp, $4.50.

UAG-29 "Auroral Electrojet Magnetic Activity Indices AE(11) for 1968," by Joe Haskell Allen, Carl C. Abston and Leslie D. Morris, National Geophysical and Solar-Terrestrial Data Center, Boulder, CO, October 1973, 148 pp, $0.75.

UAG-30 "Catalogue of Data on Solar-Terrestrial Physics," prepared by NOAA Environmental Data Service, Boulder, CO, October 1973, $1.50. Supersedes UAG-11, 15, and 20 catalogs.

UAG-31 "Auroral Electrojet Magnetic Activity Indices AE(11) for 1969," by Joe Haskell Allen, Carl C. Abston and Leslie D. Morris, National Geophysical and Solar-Terrestrial Data Center, Boulder, CO, February 1974, 142 pp, $0.75.

UAG-32 "Synoptic Radio Maps of the Sun at 3.3 mm for the Years 1967-1969," by Earle B. Mayfield, Kennon P. White III, and Fred I. Shimabukuro, Aerospace Corp., El Segundo, CA, April 1974, 26 pp, $0.35.

UAG-33 "Auroral Electrojet Magnetic Activity Indices AE(10) for 1967," by Joe Haskell Allen, Carl C. Abston and Leslie D. Morris, National Geophysical and Solar-Terrestrial Data Center, Boulder, CO, May 1974, 142 pp, $0.75.

UAG-34 "Absorption Data for the IGY/IGC and IQSY," compiled and edited by A.H. Shapley, National Geophysical and Solar-Terrestrial Data Center, Boulder, CO; W.R. Piggott, Appleton Laboratory, Slough, UK; and K. Rawer, Arbeitsgruppe fur Physikalische Weltraumforschung, Freiburg, GFR, June 1974, 381 pp, $2.00.

UAG-35 "Catalogue of Digital Geomagnetic Variation Data at World Data Center A for Solar-Terrestrial Physics," prepared by NOAA Environmental Data Service, Boulder, CO, July 1974, 20 pp, $0.20.

UAG-36 "An Atlas of Extreme Ultraviolet Flashes of Solar Flares Observed via Sudden Frequency Deviations During the ATM-SKYLAB Missions," by R.F. Donnelly and E.L. Berger, NOAA Space Environment Laboratory; Lt. J.D. Busman, NOAA Commissioned Corps; B. Henson, NASA Marshall Space Flight Center; T.B. Jones, University of Leicester, UK; G.M. Lerfald, NOAA Wave Propagation Laboratory; K. Najita, University of Hawaii; W.M. Retallack, NOAA Space Environment Laboratory and W.J. Wagner, Sacramento Peak Observatory, October 1974, 95 pp, $0.55.

UAG-37 "Auroral Electrojet Magnetic Activity Indices AE(10) for 1966," by Joe Haskell Allen, Carl C. Abston and Leslie D. Morris, National Geophysical and Solar-Terrestrial Data Center, Boulder, CO, December 1974, 142 pp, $0.75.

UAG-38 "Master Station List for Solar-Terrestrial Physics Data at WDC-A for Solar-Terrestrial Physics," by R.W. Buhmann, World Data Center A for Solar-Terrestrial Physics, Boulder, CO; Juan D. Roederer, University of Denver, Denver, CO; and M.A. Shea and D.F. Smart, Air Force Cambridge Research Laboratories, Hanscom AFB, MA, December 1974, 110 pp, $1.60.

UAG-39 "Auroral Electrojet Magnetic Activity Indices AE(11) for 1971," by Joe Haskell Allen, Carl C. Abston and Leslie D. Morris, National Geophysical and Solar-Terrestrial Data Center, Boulder, CO, February 1975, 144 pp, $2.05.

UAG-40 "H-Alpha Synoptic Charts of Solar Activity for the Period of Skylab Observations, May 1973 - March 1974," by Patrick S. McIntosh, NOAA Space Environment Laboratory, Boulder, CO, February 1975, 32 pp, $0.56.

UAG-41 "H-Alpha Synoptic Charts of Solar Activity During the First Year of Solar Cycle 20 October 1964 - August 1965," by Patrick S. McIntosh, NOAA Space Environment Laboratory, Boulder, CO and Jerome T. Nolte, American Science and Engineering, Inc., Cambridge, MA, March 1975, 25 pp, $0.48.

UAG-42 "Observations of Jupiter's Sporadic Radio Emission in the Range 7.6-80 MHz, 10 December 1971 through 21 March 1975," by James W. Warwick, George A. Dulk and Anthony C. Riddle, University of Colorado, Boulder, CO, April 1975, 49 pp, $1.15.

UAG-43 "Catalog of Observation Times of Ground-Based Skylab-Coordinated Solar Observing Programs," compiled by Helen E. Coffey, World Data Center A for Solar-Terrestrial Physics, NOAA, Boulder, CO, May 1975, 159 pp, $3.00.

UAG-44 "Synoptic Maps of Solar 9.1 cm Microwave Emission from June 1962 to August 1973," by Werner Graf and Ronald N. Bracewell, Stanford University, Stanford, CA, May 1975, 183 pp, $2.55.

UAG-45 "Auroral Electrojet Magnetic Activity Indices AE(11) for 1972," by Joe Haskell Allen, Carl C. Abston and Leslie D. Morris, National Geophysical and Solar-Terrestrial Data Center, Boulder, CO, May 1975, 144 pp, $2.10 (microfiche only).

UAG-46 "Interplanetary Magnetic Field Data 1963-1964," by Joseph H. King, National Space Science Data Center, NASA Goddard Space Flight Center, Greenbelt, MD, June 1975, 382 pp, $1.95.

UAG-47 "Auroral Electrojet Magnetic Activity Indices AE(11) for 1973," by Joe Haskell Allen, Carl C. Abston and Leslie D. Morris, National Geophysical and Solar-Terrestrial Data Center, Boulder, CO, June 1975, 144 pp, $2.10 (microfiche only).

UAG-48A "Synoptic Observations of the Solar Corona during Carrington Rotations 1580-1596 (11 October 1971 - 15 January 1973)," [Reissue of UAG-48 with quality images], by R.A. Howard, M.J. Koomen, D.J. Michels, R. Tousey, C.R. Detwiler, D.E. Roberts, R.T. Seal, and J.D. Whitney, U.S. Naval Research Laboratory, Washington, DC, and R.T. Hansen and S.F. Hansen, C.J. Garcia and E. Yasukawa, High Altitude Observatory, NCAR, Boulder, CO, February 1976, 200 pp, $4.27.

UAG-49 "Catalog of Standard Geomagnetic Variation Data," prepared by NOAA Environmental Data Service, Boulder, CO, August 1975, 125 pp, $1.85.

UAG-50 "High-Latitude Supplement to the URSI Handbook on Ionogram Interpretation and Rediction," edited by W.R. Piggott, British Antarctic Survey, c/o Appleton Laboratory, Slough, UK, October 1975, 294 pp, $4.00.

UAG-51 "Synoptic Maps of Solar Coronal Hole Boundaries Derived from He II 304A Spectroheliograms from the Manned Skylab Missions," by J.D. Bohlin and D.M. Rubenstein, U.S. Naval Research Laboratory, Washington, DC, November 1975, 30 pp, $0.54.

UAG-52 "Experimental Comprehensive Solar Flare Indices for Certain Flares, 1970-1974," by Helen W. Dodson and E. Ruth Hedeman, McMath-Hulbert Observatory, University of Michigan Pontiac, MI, November 1975, 27 pp, $0.60.

UAG-53 "Description and Catalog of Ionospheric F-Region Data, Jicamarca Radio Observatory (November 1966 - April 1969), by W.L. Clark and T.E. Van Zandt, NOAA Aeronomy Laboratory, Boulder, CO, and J.P. McClure, University of Texas as Dallas, Dallas, TX, April 1976, 10 pp, $0.33.

UAG-54 "Catalog of Ionosphere Vertical Soundings Data," prepared by NOAA Environmental Data Service, Boulder, CO, April 1976, 130 pp, $2.10.

UAG-55 "Equivalent Ionospheric Current Representations by a New Method, Illustrated for 8-9 November 1969 Magnetic Disturbances," by Y. Kamide, Cooperative Institute for Research in Environmental Sciences, University of Colorado, Boulder, CO; H.W. Kroehl, Data Studies Division, National Geophysical and Solar-Terrestrial Data Center, Boulder, CO; M. Kanamitsu, Advanced Study Program, National Center for Atmospheric Research, Boulder, CO; Joe Haskell Allen, Data Studies Division, National Geophysical and Solar-Terrestrial Data Center, Boulder, CO; and S.-I Akasofu, Geophysical Institute, University of Alaska, Fairbanks, AK, April 1976, 91 pp, $1.60 (microfiche only).

UAG-56 "Iso-intensity Contours of Ground Magnetic H Perturbations for the December 16-18, 1971, Geomagnetic Storm," Y. Kamide, Cooperative Institute for Research in Environmental Sciences, University of Colorado, Boulder, CO, April 1976, 37 pp, $1.39.

UAG-57 "Manual on Ionospheric Absorption Measurements," edited by K. Rawer, Institut fur Physikalische Weltraumforschung, Freiburg, GFR, June 1976, 302 pp, $4.27.

UAG-58 "ATS6 Radio Beacon Electron Content Measurements at Boulder, July 1974 - May 1975," by R.B. Fritz, NOAA Space Environment Laboratory, Boulder, CO, September 1976, 61 pp, $1.04.

UAG-59 "Auroral Electrojet Magnetic Activity Indices AE(11) for 1974," by Joe Haskell Allen, Carl C. Abston and Leslie D. Morris, National Geophysical and Solar-Terrestrial Data Center, Boulder, CO, December 1976, 144 pp, $2.16.

UAG-60 "Geomagnetic Data for January 1976 (AE(7) Indices and Stacked Magnetograms)," by Joe Haskell Allen, Carl C. Abston and Leslie D. Morris, National Geophysical and Solar-Terrestrial Data Center, Boulder, CO, July 1977, 57 pp, $1.07.

UAG-61 "Collected Data Reports for STIP Interval II 20 March - 5 May 1976, edited by Helen E. Coffey and John A. McKinnon, World Data Center A for Solar-Terrestrial Physics, Boulder, CO, August 1977, 313 pp, $2.95.

UAG-62 "Geomagnetic Data for February 1976 (AE(7) Indices and Stacked Magnetograms)," by Joe Haskell Allen, Carl C. Abston and Leslie D. Morris, National Geophysical and Solar-Terrestrial Data Center, Boulder, CO, September 1977, 55 pp, $1.11.

UAG-63 "Geomagnetic Data for March 1976 (AE(7) Indices and Stacked Magnetograms)," by Joe Haskell Allen, Carl C. Abston and Leslie D. Morris, National Geophysical and Solar-Terrestrial Data Center, Boulder, CO, September 1977, 57 pp, $1.11.

UAG-64 "Geomagnetic Data for April 1976 (AE(8) Indices and Stacked Magnetograms)," by Joe Haskell Allen, Carl C. Abston and Leslie D. Morris, National Geophysical and Solar-Terrestrial Data Center, Boulder, CO, February 1978, 55 pp, $1.00.

UAG-65 "The Information Explosion and Its Consequences for Data Acquisition, Documentation, Processing," by G.K. Hartmann, Max-Planck-Institut fur Aeronomie, Lindau, GFR, May 1978, 36 pp, $0.75.

UAG-66 "Synoptic Radio Maps of the Sun at 3.3 mm 1970-1973," by Earle B. Mayfield and Fred I. Shimabukuro, Aerospace Corp., El Segundo, CA, May 1978, 30 pp, $0.75.

UAG-67 "Ionospheric D-Region Profile Data Base, A Collection of Computer-Accessible Experimental Profiles of the D and Lower E Regions," by L.F. McNamara, Ionospheric Prediction Service, Sydney, Australia, August 1978, 30 pp, $0.88 (microfiche only).

UAG-68 "A Comparative Study of Methods of Electron Density Profile Analysis," by L.F. McNamara, Ionospheric Prediction Service, Sydney, Australia, August 1978, 30 pp, $0.88 (microfiche only).

UAG-69 "Selected Disturbed D-Region Electron Density Profiles. Their relation to the undisturbed D region," by L.F. McNamara, Ionospheric Prediction Service, Sydney, Australia, October 1978, 50 pp, $1.29 (microfiche only).

UAG-70 "Annotated Atlas of the H-alpha Synoptic Charts for Solar Cycle 20 (1964-1974) Carrington Solar Rotations 1487-1616," by Patrick S. McIntosh, NOAA Space Environment Laboratory, Boulder, CO, February 1979, 327 pp, $3.50.

UAG-71 "Magnetic Potential Plots over the Northern Hemisphere for 26-28 March 1976," A.D. Richmond, NOAA Space Environment Laboratory, Boulder, CO; H.W. Kroehl, National Geophysical and Solar-Terrestrial Data Center, Boulder, CO; M.A. Henning, Lockheed Missils and Space Co., Aurora, CO; and Y. Kamide, Kyoto Sangyo University, Kyoto, Japan, April 1979, 118 pp, $1.50.

UAG-72 "Energy Release in Solar Flares, Proceedings of the Workshop on Energy Release in Flares, 26 February - 1 March 1979, Cambridge, Massachusetts, U.S.A.," edited by David M. Rust, American Science and Engineering, Inc., Cambridge, MA, and A. Gordon Emslie, Harvard-Smithsonian Center for Astrophysics, Cambridge, MA, July 1979, 68 pp, $1.50 (microfiche only).

UAG-73 "Auroral Electrojet Magnetic Activity Indices AE(11-12) for January - June 1975," by Joe Haskell Allen, Carl C. Abston, J.E. Salazar and J.A. McKinnon, National Geophysical and Solar-Terrestrial Data Center, NOAA, Boulder, CO, August 1979, 114 pp, $1.75.

UAG-74 "ATS-6 Radio Beacon Electron Content Measurements at Ootacamund, India, October - July 1976," by S.D. Bouwer, K. Davies, R.F. Donnelly, R.N. Grubb, J.E. Jones and J.H. Taylor, NOAA Space Environment Laboratory, Boulder, CO, and R.G. Rastogi, M.R. Deshpande, H. Chandra and G. Sethia, Physical Research Laboratory, Ahmedabad, India, March 1980, 58 pp, $2.50.

UAG-75 "The Alaska IMS Meridian Chain: Magnetic Variations for 9 March - 27 April 1978," by H.W. Kroehl and G.P. Kosinski, National Geophysical and Solar-Terrestrial Data Center, Boulder, CO; S.-I Akasofu, G.J. Romick, C.E. Campbell and G.K. Corrick, University of Alaska, Fairbanks, AK; and C.E. Hornback and A.M. Gray, NOAA Space Environment Laboratory, Boulder, CO, June 1980, 107 pp, $3.00.

UAG-76 "Auroral Electrojet Magnetic Activity Indices AE(12) for July - December 1975," by Joe Haskell Allen, Carl C. Abston, J.E. Salazar and J.A. McKinnon, National Geophysical and Solar-Terrestrial Data Center, NOAA, Boulder, CO, August 1980, 116 pp, $2.50.

UAG-77 "Synoptic Solar Magnetic Field Maps for the Interval Including Carrington Rotations 1601-1680, May 5, 1973 - April 26, 1979," by J. Harvey, B. Gillespie, P. Miedaner and C. Slaughter, Kitt Peak National Observatory, Tucson, AZ, August 1980, 66 pp, $2.50.

UAG-78 "The Equatorial Latitude of Auroral Activity During 1972-1977," by N.R. Sheeley, Jr. and R.A. Howard, E. O. Hulbert Center for Space Research, U.S. Naval Research Laboratory, Washington, DC and B.S. Dandekar, Air Force Geophysics Laboratory, Hanscom AFB, MA, October 1980, 61 pp, $3.00.

UAG-79 "Solar Observations During Skylab, April 1973 - February 1974, I. Coronal X-Ray Structure, II. Solar Flare Activity," by J.M. Hanson, University of Michigan, Ann Arbor, MI; and E.C. Roelof and R.E. Gold, The Johns Hopkins University, Laurel, MD, December 1980, 43 pp, $2.50.

UAG-80 "Experimental Comprehensive Solar Flare Indices for 'Major' and Certain Lesser Flares, 1975-1979," compiled by Helen W. Dodson and E. Ruth Hedeman, The Johns Hopkins University, Laurel, MD, July 1981, 33 pp, $2.00.

UAG-81 "Evolutionary Charts of Solar Activity (Calcium Plages) as Functions of Heliographic Longitude and Time, 1964-1979," by E. Ruth Hedeman, Helen W. Dodson and Edmond C. Roelof, The Johns Hopkins University, Laurel, MD 20707, August 1981, 103 pp, $4.00.

UAG-82 "International Reference Ionosphere - IRI 79," edited by J. Virginia Lincoln and Raymond O. Conkright, National Geophysical and Solar-Terrestrial Data Center, NOAA, Boulder, CO, November 1981, 243 pp, $4.50.

UAG-83 "Solar-Geophysical Activity Reports for September 7-24, 1977 and November 22, 1977," Parts 1 and 2, compiled by John A. McKinnon and J. Virginia Lincoln, World Data Center A for Solar-Terrestrial Physics, NOAA, Boulder, CO, February 1982, 553 pp, $10.00.